CONCEPUT ÎN ROMÂNIA
Ministerul Cercetării și Inovării

25th edition

HERVEX

ISSN 1454 - 8003

Proceedings of International Conference on HYDRAULICS, PNEUMATICS, SEALING ELEMENTS, TOOLS, PRECISION MECHANICS, SPECIFIC ELECTRONIC EQUIPMENT & MECHATRONICS

HERVEX 2019

November 13-15 | Băile Govora, ROMANIA

November 2019
25th Edition

INTERNATIONAL CONFERENCE

HERVEX 2019

Hydraulics| Pneumatics|
Sealing Elements| Tools| Precision Mechanics|
Specific Electronic Equipment & Mechatronics

Baile Govora, ROMANIA | November 13 - 15, 2019

ORGANIZERS

HYDRAULICS AND PNEUMATICS RESEARCH INSTITUTE
BUCHAREST, ROMANIA

CHAMBER OF COMMERCE AND INDUSTRY VALCEA, ROMANIA

PARTNERS

WROCLAW UNIVERSITY OF SCIENCE AND TECHNOLOGY, POLAND

TECHNICAL UNIVERSITY OF MOLDOVA IN CHISINAU, REPUBLIC OF MOLDOVA

“POLITEHNICA” UNIVERSITY OF BUCHAREST, ROMANIA

NATIONAL INSTITUTE OF RESEARCH & DEVELOPMENT FOR MACHINES AND INSTALLATIONS DESIGNED TO AGRICULTURE AND FOOD INDUSTRY – INMA BUCHAREST, ROMANIA

“POLITEHNICA” UNIVERSITY OF TIMISOARA, ROMANIA

TECHNICAL UNIVERSITY OF CLUJ-NAPOCA, ROMANIA

MEDIA PARTNERS

HIDRAULICA
HYDRAULICS-PNEUMATICS-TRIBOLOGY-ECOLOGY-SENSORICS-MECHATRONICS

Partener European

CONFERENCE HELD UNDER HONORARY AEGIS OF

Comité Européen des Transmissions Oléohydrauliques et Pneumatiques
CETOP

Published by - Hydraulics and Pneumatics Research Institute, Bucharest, Romania
- Chamber of Commerce and Industry Valcea, Romania

INTERNATIONAL CONFERENCE

HERVEX 2019

IS SUPPORTED BY:

MINISTRY OF RESEARCH AND INNOVATION

NATIONAL PROFESSIONAL ASSOCIATION OF HYDRAULICS AND PNEUMATICS IN ROMANIA - “FLUIDAS”

Conference Proceedings is indexed by:

COMMITTEES

HONORARY PRESIDENT

PhD.Eng. Hubertus MURRENHOFF – Institute for Fluid Power Drives and Controls at Aachen University, Germany

HONORARY COMMITTEE

Dr. Stefan KÖNIG – President of European Fluid Power Committee – CETOP

Prof. PhD.Eng. Henryk CHROSTOWSKI – Wroclaw University of Technology, Poland

PhD.Eng. Petrin DRUMEA – President of National Professional Association of Hydraulics and Pneumatics – FLUIDAS, Romania

ORGANIZING COMMITTEE

Dipl. Eng. Gheorghe RIZOIU – General Manager of Chamber of Commerce and Industry Valcea, Romania

PhD. Eng. Gabriela MATACHE – Hydraulics and Pneumatics Research Institute in Bucharest, Romania

Prof. PhD. Eng. Viorel BOSTAN – Rector of Technical University of Moldova, Republic of Moldova

PhD. Eng. Krzysztof KEDZIA – Wroclaw University of Technology, Poland

Prof. PhD. Eng. Dan OPRUȚA – Technical University of Cluj-Napoca, Romania

Prof. PhD. Eng. Ilare BORDEAȘU – Politehnica University of Timisoara, Romania

Prof. PhD. Eng. Adrian CIOCĂNEA – Politehnica University of Bucharest, Romania

PhD. Phys. Mihai VARLAM - General Manager of National Research & Development Institute for Isotope & Cryogenics Technologies (ICSI) Râmnicu Vâlcea, Romania

PhD.Eng. Sergiu NICOLAIE – General Manager of R&D National Institute for Electrical Engineering ICPE-Advanced Researches, Bucharest, Romania

PhD.Eng. Nicolae-Valentin VLĂDUȚ – General Manager of National Institute of Research and Development for Machines and Installations Designed to Agriculture and Food Industry – INMA Bucharest, Romania

SCIENTIFIC PROGRAMMEE COMMITTEE

PhD.Eng. Mohamed HAJJAM – University of Poitiers – IUT Angouléme, France

PhD.Eng. Zygmunt DOMAGALA – Wroclaw University of Technology, Poland

Prof. PhD.Eng. Pavel MACH – Technical University of Praga, Czech Republic

Prof. PhD.Eng. Vasile JAVGUREANU – Technical University of Moldova, Republic of Moldova

PhD.Eng. Catalin DUMITRESCU – Director of Hydraulics and Pneumatics Research Institute in Bucharest, Romania

PhD.Eng. Ioan LEPADATU – Hydraulics and Pneumatics Research Institute in Bucharest, Romania

PhD.Eng. Wilhelm KAPPEL – Scientific Manager of R&D National Institute for Electrical Engineering ICPE-Advanced Researches, Bucharest, Romania

Prof. PhD.Eng. Gheorghe I. GHEORGHE – General Manager of National Institute of Research and Development in Mechatronics and Measurement Technique (INCDMTM), Bucharest, Romania

Dipl.Eng. Valentin CISMARU – President of Chamber of Commerce and Industry Valcea, Romania

PhD. Phys. Mihai VARLAM - General Manager of National Research & Development Institute for Isotope & Cryogenics Technologies (ICSI) Râmnicu Vâlcea, Romania

Prof.Dr.Ing. Andrzej SOBCZYK – Cracow University of Technology, Poland

Prof. PhD.Eng. Mihai AVRAM – Politehnica University of Bucharest, Romania

Prof. PhD.Eng. Cristian PAVEL – Technical University of Civil Engineering in Bucharest, Romania

PhD.Eng. Cornelia MURARU-IONEL – National Institute of Research and Development for Machines and Installations Designed to Agriculture and Food Industry – INMA Bucharest, Romania

PhD.Eng. Diana BADEA – National Institute of Research and Development in Mechatronics and Measurement Technique (INCDMTM), Bucharest, Romania

Prof. PhD.Eng. Alexandru MARIN – Politehnica University of Bucharest, Romania

Prof. PhD.Eng. Liviu VAIDA – Technical University of Cluj-Napoca, Romania

Prof. PhD.Eng. Doru Dumitru PALADE – National Institute of Research and Development in Mechatronics and Measurement Technique (INCDMTM), Bucharest, Romania

PhD.Eng. Andrei DRUMEA – Politehnica University of Bucharest, Romania

Prof. PhD.Eng. Sorin CĂNĂNĂU – Politehnica University of Bucharest, Romania

Prof. PhD.Eng. Ion DAVID – Technical University of Civil Engineering in Bucharest, Romania

Prof. PhD.Eng. Gheorghe VOICU – Politehnica University of Bucharest, Romania

Prof. PhD.Eng. Edmond MAICAN – Politehnica University of Bucharest, Romania

PhD.Eng. Mihai Gabriel MATACHE – National Institute of Research – Development for Machines and Installations Designed to Agriculture and Food Industry – INMA, Bucharest- Romania

PhD.Eng. Mircea PRICOP – S.C. HESPER S.A., Bucharest, Romania

PhD.Eng. Ioan Lucian MARCU – Technical University of Cluj-Napoca, Romania

Prof. PhD.Eng. Valeriu BANU – S.M.C. Romania

Dipl. Eng. Ioan CAMPEAN – S.C. HIDROSIB S.A. Sibiu, Romania

Dipl. Eng. Mircea DANCIU – PARKER HANNIFIN Corporation, Romania

CONTENTS

EDUCATION IN THE FIELD OF FLUID POWER TECHNOLOGY - CHALLENGES, OPPORTUNITIES AND POSSIBILITIES

Darko LOVREC[1]

[1]University of Maribor, Faculty of Mechanical Engineering, Slovenia, darko.lovrec@um.si

Abstract: *Education in the field of Fluid Power technology presents a huge challenge in terms of equipment, place, as well as adequate installed power, which enables the knowledge transfer under real operating conditions. In addition to this, it is necessary to add constant updating of the subject contents and adaptation to international guidelines and teaching approaches.*
The contribution presents the experiences gained over the years in providing knowledge within this field, for both regular full-time and part-time students, as well as for participants from industry at various courses and skills trainings. Various aspects were taken into account in the education process: Fundaments of knowledge, combining knowledge from different fields, integration into R&D and industrial practice, globalisation and internationalisation, as well as new methods and approaches, e.g. flipped, combined and project based learning in the field of Fluid Power technology and Systems.

Keywords*: Fluid power, education, practical work, equipment, approach, challenges*

1. Introduction

Teaching of Hydraulics and Pneumatics as a special branch of Technology in some countries dates back to the early 1950s of the last century. Most countries around the world are still engaged very intensively in transforming educational systems and learning content. Different views and experiences can serve as an incentive for the general public to begin to intensify their education, as well as to find appropriate methods and ways of educating professionals capable of meeting the challenges of today, including the digitisation of industry and society.
Countries with more and better potential for engineering and technical personnel in the future will clearly have the advantage. On the other hand, there is still not enough (desired) interest in the study of Engineering, which is not only a Slovenian specialty. It is a global phenomenon, reflecting the transition from industrial to post-industrial society, the age of Informatics, including Virtualisation and Virtual Reality.
Surveys among engineering students indicate that they complain of a "hard", tedious and old-fashioned study approach and poor teaching, often conditioned by equipment in practical work. In the list of shortcomings found by industry representatives, they draw attention to the modest ability to communicate, both written and oral, and insufficient practical experience, especially in design, which is more alarming. Additionally, they are worried that many graduates are unable to connect seemingly unrelated fields such as Politics, Social Sciences and Technology.
In the field of Higher Education of technology-related subjects, for example, Mechanical Engineering, we are faced with numerous challenges. This is especially true for the subjects concerning the operating principles of power drive systems and devices. Transmission of forces and motion based on the hydraulic principle definitely falls within this specific area: Fluid Power Drives and Systems.

How to satisfy different conditions, limitation and specifics in the knowledge transfer of these contents, where we are faced with:
- High energy density and realistic operating conditions,
- The interdisciplinarity of knowledge and skills,
- Diversity of equipment,
- Internationalisation of content,
- Integration into development technology trends like Industry 4.0,

Bearing in mind:
- The proposed, necessary and prescribed learning/teaching content, the pedagogical approach, industry needs on one side, and those suggested by the umbrella professional associations which relate to the subject matter, for example CETOP,
- The existing situation in the field of Higher Education at the national level,
- to ensure the safety within practical tests and experiments when using suchtype of equipment.

2. Forms of knowledge transfer and guidelines

Typically used forms of knowledge transfer in the field of Fluid Power engineering is shown in principle in Figure 1. They range from giving theoretical background in the oral way and in the form of equations and diagrams, which is, according the students' opinion, tedious and exhausting, but understanding the theoretical background is extremely important. Students prefer learning through simulation and visualisation (the so-called “click generation”) and independent practical work and experimentation (but not in the form of a demonstration and, of course, in a safe way).

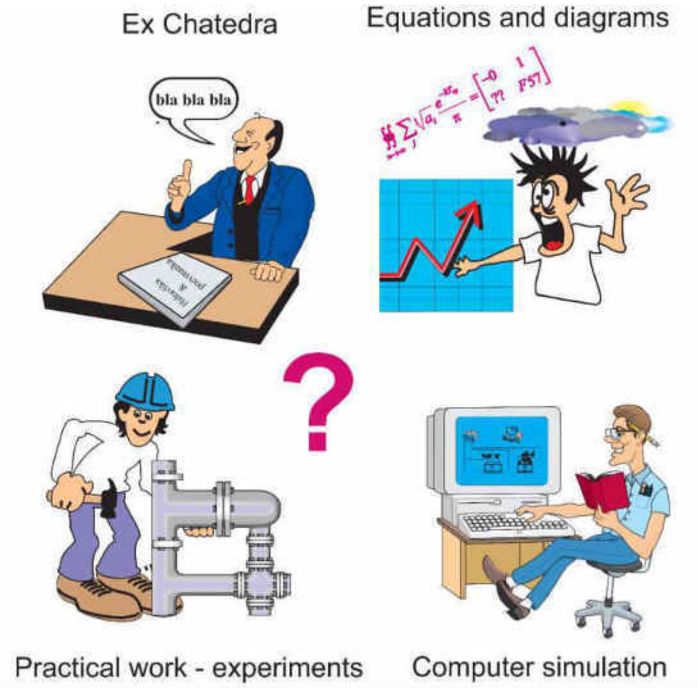

Fig. 1. Typical forms of knowledge transfer in the field of Fluid Power

In addition to all the methods and aspects mentioned, it is necessary to bear in mind (and of course also implement) the renovation, modernisation and adapting of learning contents to the education profile. The focus should be on use of newer approaches in the field of Education, taking into account the integration into the Bologna education system and internationalisation at the same time (e.g. Erasmus).
One of the tasks in order to stimulate and implement reforms of Study Programmes in Engineering effectively is undoubtedly a need for modernisation, introducing and testing new teaching methods and approaches.

These guidelines should also apply to the field of Fluid Power technology education process:
- *Emphasis on learning the basics (fundamentalisation of knowledge).* A modern engineer will have a good mastery of the basics, among which we consider, in addition to mathematics, computing, etc. The Natural Sciences and Social Sciences will contribute substantially to the

effective management of rapidly changing technologies in terms of the rapid obsolescence of knowledge and shorter time transfer of research results into industrial practice. *Understanding the physical interdependencies in the operation of hydraulic and pneumatic systems is a necessary starting point for the selection and sizing of components, commissioning these devices, maintenance and condition monitoring of these devices, including fault finding as one of the more difficult tasks – "hydraulic forensics".*

- *Combining the knowledge from different fields (synthesis).* It is of great importance to acquire and upgrade the ability to work with experts from other fields and teamwork, as well as the ability to integrate their work into larger systems. Today, Fluid Power technicians are closely associated with experts in Automation (control concepts, sensors, informatics, maintenance and remote control). Today, experts in the field of Fluid technology are closely associated with professionals engaged in automation (management concepts, sensors, information technology, maintenance and condition monitoring at a distance).
- *Integration into R&D and industrial practice (integration).* The focus of the education system only on classroom lectures and calculation exercises, without significant practical work and experiments in the laboratory, must be redirected to the integration of students into industrial practice and in Research and Development activities. Practical work can be in the form of student projects within a Study Programme (e.g. Mechanical Engineering, Mechatronics), in the form of students` projects on the national level in cooperation with an industrial partner, involving students in market-based applied projects for industry, topics for Bachelor's and Master's theses for industry, and a month long practice in the industry as a compulsory part of the educational programme.
- *Education as a "life-long" learning process.* Due to the increasing obsolescence of knowledge and professional skills, the term "life cycle of education" is, increasingly, being transformed into "education as a life process". Accordingly, universities, colleges (as well as secondary schools) are also expected to offer more continuing education programmes. In this sense, engineers who are already working under "pressure" in the field of Fluid Power engineering, or who have retrained in this field, should be offered longer or shorter seminars or training courses, whether of a general nature, or in-depth and thematically focused on a specific area of the technique (e.g. Tribology and Hydraulic Fluids, Servo Hydraulics, Hydraulic Safety Regulations, Hydraulic Pumps and the like, fluid power control circuits etc.).
- *Personality* development and ethics. In terms of personality development, a modern engineer must also, in a moral and ethical perspective, be brought up into a mature personality with a sense of responsibility to the environment – nature, society and the public, and to manifest himself with sacrificial work, e. g. knowledge and use of energy-saving components and drive concepts, use of environmentally friendly and sustainable hydraulic fluids.
- *Globalisation and internationalisation.* With the emergence of unified global markets and international cooperation, there are also needs for harmonisation of education systems that can no longer be restricted to individual countries or regions. As engineers and technicians, we need to possess internationally comparable professional qualifications and be familiar with the languages, (cultures and mentality, as well the circumstances and specificities) of other nations and areas, as well as the political, social and judicial systems of other countries.
- *Teaching with technology; new methods and approaches.* Implementing of ICT in flipped, combined and project-based learning, within the subject of Fluid Power technology, as well as e-learning and "forensic-case like learning".

The field of Technology, ranging from manufacturing and mobile machinery all the way to space technology, where hydraulic and pneumatic drive systems are used, is increasingly intertwined with knowledge of the control and monitoring of these systems, taking into account autonomous operation, far away from maintenance staff, and also the energy and environmental aspects – Automate-Monitor-Predict.

2.1 Introduction of changes and new approaches

How already today to accede to the changes in the field of Fluid Power technology education? What to preserve? What to improve? What to discard? The answers to these questions will be reached most quickly if we first determine the goals, work tasks, content and aids needed for education, and the population or target group at whom we are targeting the education. In order to formulate some general guidelines, it is necessary first to determine for whom the education is intended, and who are the populations in a country which will need essential knowledge in the field of Fluid Power engineering in their professional work. Are they countries that are more manufacturers of fluid power components and systems, or are they countries where they are mostly used?

Approximately 90 % of all those who are professionals in the field of Fluid Power are operators of already finished machinery. They should always intervene when the machine is no longer functioning properly. Their job is to find the causes of the disorders, to identify and correct them. Those who deal with the installation of hydraulic equipment are estimated roughly at around 10 %, but are faced with the same problem when commissioning the machine.
In the field of Research, Development, Construction and Design of fluid engineering components and devices, a relatively small percentage of experts are involved in the total number of all those involved in Fluid Power engineering.
Depending on their educational profile, they can be divided into:

- Maintenance profile or the fluid power machine operator and
- Engineer profile.

2.2 Necessary knowledge and skills of different professional profiles

Let us first turn to the profile of the maintainer, who represents the broadest interest group in the field of Education, with emphasis on practical instruction. In the event of a malfunction, they are forced to find the causes, to identify and remedy them, or to take preventative measures to prevent them from occurring at all.
Regarding the machines and appliances, it is crucial to know how they operate, how to find defects with the help of the available documentation (wiring diagram, technical data...) the functions of the individual components and the whole system. The operating functions of the individual components are generally valid, while the construction details vary from manufacturer to manufacturer. The maintainer must be able to understand the desired normal operation from the documentation, and then verify the actual status by means of measurements. Knowledge of appropriate measuring procedures and measuring equipment is certainly important. Based on the above, it is necessary to know basic expertise such as:

- The physical background,
- Knowledge of the control functions and performance of individual components and the system as whole, and
- As a continuation of these, in-depth – specialist training focused on user areas.

2.3 Scope of the Fluid Power professional

Depending on the activity area of a maintainer, his tasks can be extended to the in-depth phase of troubleshooting or fault finding. This phase, however, is usually followed by the phase of elimination of a malfunction. The following knowledge and skills required for the maintenance profile can be summarised in the following notes:

- Based on the real circuit, to design the circuit diagram of the hydraulic or pneumatic system properly, in accordance with the given technical requirements,
- Select the appropriate components optimally from the manufacturer's catalogue,
- Identify and localise the fault,
- Identify the causes of the fault reliably,

- Eliminate the fault in accordance with professional measures, and
- Select replacement components correctly from the manufacturers' data sheets.

Based on the above, we can go immediately to the educational profile of the engineer, and find that most of the skills described above can serve an engineer as a basis. This, however, must be supplemented with in-depth knowledge of the control techniques, as the increasing degree of automation of controlling and monitoring of modern machines is becoming more demanding and complex – Industry 4.0.
Without going into detail, it should be noted that, in addition to knowledge of the structure, function and operational properties of fluid power devices and measuring equipment, an engineer must also have an insight into the dynamic behaviour of fluid power systems, which is not only intended for development and design, but increasingly serves for efficient and prompt preparation of Tender documentation. In addition to this, it is necessary to have certain knowledge in other fields of engineering.
In the case of a general education programme that does not specify exactly where the future engineer will work, specialisation in a certain direction of the Fluid Power technology area is, on the one hand, due to over-specialisation too narrow for the general engineer profile, and, on the other hand , unfair to other areas. Each of the specific, narrow areas of the profession requires its own additional specialist knowledge. That's why it's more important and necessary to place emphasis on matters of general character/knowledge and importance. Undoubtedly, these are the physical basics of how the systems work, different types of components and their purpose, particularly of fluid power systems, the ability to interpret hydraulic or pneumatic circuits, and to identify the operation of the device on that basis.

2.4 Forms of knowledge transfer

The verbal way of imparting knowledge – especially theory, as the most widespread method of knowledge, cannot be avoided. The transfer of knowledge and topics should, of course, be adapted to the educational profile and level of education. Special care must be taken when the transfer of knowledge is underpinned or supplemented with equations and diagrams. Both methods provide a huge opportunity to adapt and keep up with changes in the technical field.
Nowadays, the theoretical application of the theory in this field – the so-called two-dimensional technique "on paper" – is a very widespread, practical education in teaching or training. Real hydraulic and pneumatic systems and assemblies (so-called three-dimensional technics), are, in many cases, due to barriers in the form of available equipment and a place for it, pushed more into the background. This is especially evident in areas where theoretical education is at the forefront, and the practical application of theoretically acquired knowledge usually draws the shorter end. Practical work is very important within the field of Fluid Power Engineering.
Practical training – learning about the control functions and performance characteristics of components and systems on learning devices (setups) is important, both in terms of educating the engineer, as well the maintainer. For the latter, the importance of practical work and experimentation is particularly important.
When selecting and designing the equipment and testing facilities for the practical part of the training, it is reasonable to select such devices that are, as much as possible, suited to real-world performance in industry in terms of actual pressures, fluid flows, circuit design...
Here, we must emphasise the possibility of using computers and appropriate software. For many years, computerised simulation of dynamic systems, designed primarily to educate the engineer profile, is an important tool for designing electrohydraulic and -pneumatic drives. Numerous insights into the physics of fluid power circuits` structures and innumerable technical improvements have made software more precise through extensive research in computer models. Nevertheless, many computer software packages are slowly making their way onto desks of Project and Development Departments. The reason for this may lie in the excessive scientific orientation and the long duration from learning about such a programme to its effective implementation in practice.

The real reason for this is probably the relatively high price of complex software packages. There are not so many lecturers who think they have no money so that "students could play". The money that they earn through research and projects for industry is invested in the necessary equipment for the further research, and the State, as the "official trustee" of official Study Programmes, has "no ear" for it. Thus, this aspect is often left to the individual holder of the object, often his ingenuity.
It is a misconception that most of the conditions for the effective use of a simulation programme are fulfilled only when colleagues or entire departments that prioritise this technique are nearby. The simulation technique can be used very effectively in daily design, except that the programmes must meet certain requirements:

- Flexibility in designing models,
- Simple use of the programme and usefulness of the simulation results,
- The appropriatemanageable amount of theoretical knowledge required to design the models.

When these requirements are met, the benefits offered by the simulation technique can be very effective, and, above all, because the "comfortable" simulation programmes allow for a significant reduction in both the time required for testing on the test sites and the time spent on developing components or systems, first start-up, or systems design. The development of user-friendly programmes and the reduction of fear of use, were some of the tasks of modernising educational systems years ago. Nowadays, such programmes are well adapted to the user, so, especially the young generation, is growing up in the age of Informatics and smart devices, so using them has no problems.
Thus, only the problem remains – their procurement. A Fluid Power engineering Institute or Laboratory requires quite a few different software packages: A programme or software package for drawing circuits using appropriate symbols, for simulating circuit operation including component dimensions and operating parameters, for drawing electrical control circuits, for programming controllers, and visualisation of operation, to simulate the dynamic behaviour of servo systems and some extras.

3. Spatial arrangement of topics

In principle, we can say that there are only two problems in the field of Fluid Power education: “Where to place / Where would I put it?” and “Where to take / Where would I get it from?” This is the space available to place the equipment and the financial means to purchase the equipment.
Real-world practical and experimenting equipment is expensive, heavy and large, and requires a fixed layout – fixed working places. As these are usually larger pieces of equipment, it is not sensible to re-install, re-connect and check operation before each lab work. In such a way, the constant setting and storing equipment again, equipment will definitely degrade, or a piece of equipment can be misplaced, or even lost. On the other hand, the appropriate time and staff – the “equipment-keeper”, is not available for such an approach. A further problem is a suitable equipment warehouse. A fixed layout is the only sensible solution from these points of view, and not just from that point of view. Hydraulic equipment also needs a proper power connection – a central pipe network distributed throughout the hydraulic part of the laboratory.
Such an approach, topic-dependent layout and installation of the equipment, is adhered to in accordance with CETOP recommendations related to hydraulic and pneumatic education (e.g. [1]). Unfortunately, the recommendations, no doubt this make sense, are one thing, and the reality another. The problem of spatial arrangement is always, and usually, present at universities and colleges, since there are a lot of other topics and subjects that also include lab work. The buildings are usually old and have their own spatial limitations, and there are only a few new buildings. Adequate space is a particular problem for hydraulics, since, apart from the easily accessible room (due to relatively heavy and large equipment), the available electricity is required for the hydraulic power trains. According to the CETOP recommendations, we should have separate rooms, sorted

by individual topics. Taking into account, or at least following this recommendation, we tried to implement it at the Faculty of Mechanical Engineering at the University of Maribor. Figure 2 shows the layout of the spatial arrangement of laboratory facilities intended for practical work, for a specific segment of Fluid Power and Automation, and Figure 3 shows the pipeline system for hydraulic and for pneumatic energy transfer.

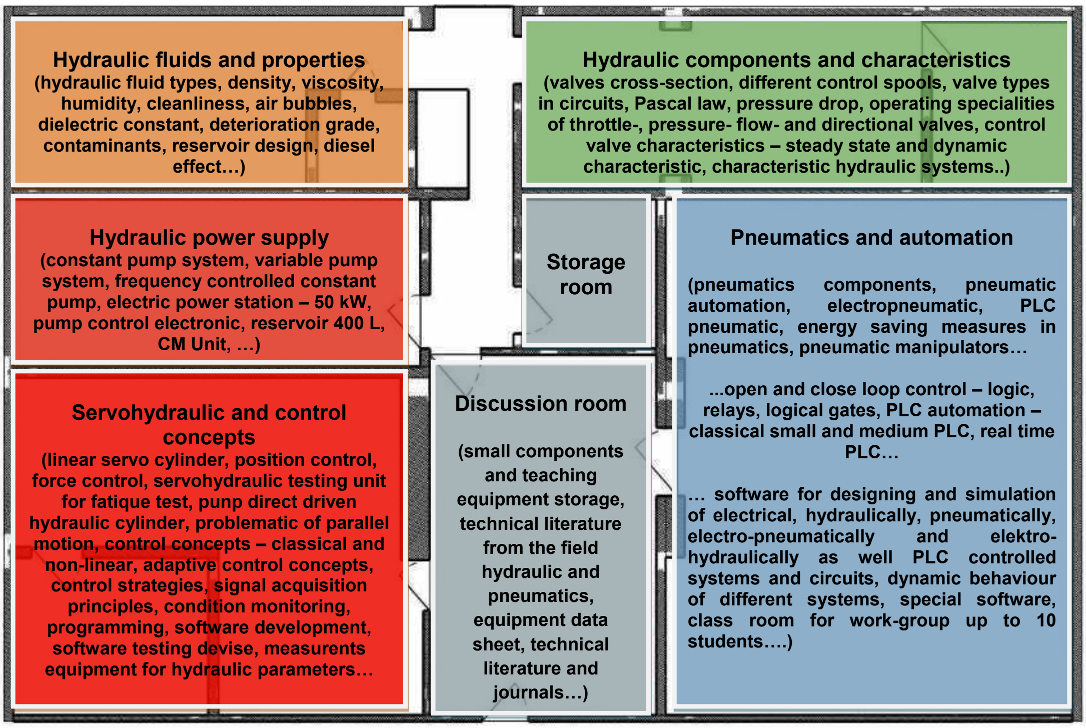

Fig. 2. Spatial arrangement of the laboratory facilities

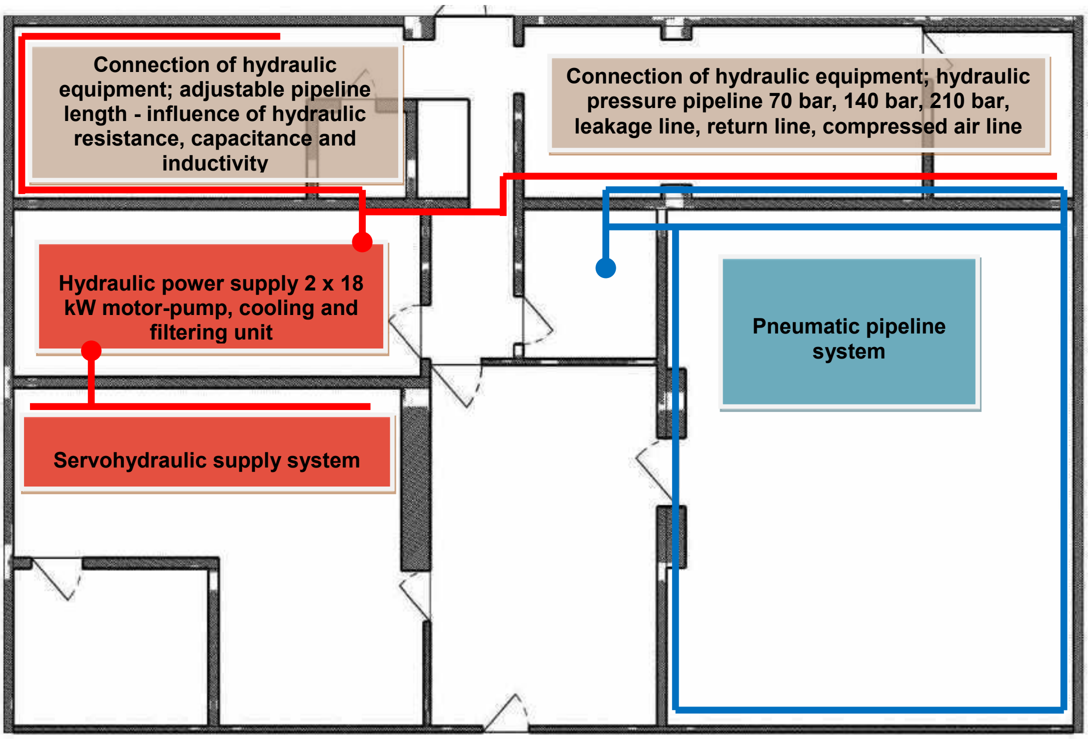

Fig. 3. Pipeline system arrangement

4. Contents related to the learning of hydraulic basics

According to the recommendations, for each topic, preferably in its own room, we also carry out individual sets of practical exercises and experiments. Exercises related to the determination of the density and viscosity of the hydraulic fluid is carried out in a place intended for the knowledge of the basic physicochemical properties of hydraulic fluids. Viscosity of a sample is measured at different rates, taking into account the influence of temperature, and understanding the viscosity values given by different Standards. Furthermore, the influence examination of different oil viscosity`s degree to resistances when the component parts move in the fluid.
The cleanliness level measurement is intended to understand the importance of cleanliness of a hydraulic fluid, the manner in which it is given in the literature, including search for information regarding the required cleanliness level of a particular hydraulic component, given in the component manufacturer's datasheets in the form of different Standards. Furthermore, the degree of chemical, thermal degradation (acidification) of the oil is determined by use of simple instruments, as well as by precision laboratory ones. Of great importance is also the issue of air bubbles inside hydraulic fluid, as well as the proper design of the inside of the tank – layout of the suction and return pipes, and measures for the better functioning of the tank (partition wall, diffuser on the return line etc.). Hydraulic oil compressibility is also discussed in relation to air issues - measuring the compressibility modulus for different types of hydraulic fluid inside different pipes (steel tube and hose). The effect of air (dissolved in oil or present in the form of air bubbles) is also visualised by a diesel effect test. One part of the space for learning about the properties of hydraulic fluids is shown in Figure 4.

Fig. 4. Basic properties of hydraulic fluid – detail from the experimental room

In this part of the laboratory, pressure drops at different fluid temperatures (cold start and operating temperature) are also measured, as well as the influence of the length of the pipeline on the size of the pressure drop (hydraulic resistance), and the effect of the pump flow size on the pressure drop (the latter can be achieved by an adjustable pump). Thus, it is also possible to determine the hydraulic capacitance and inductance of the pipe network.
In fact, this set of experiments is already related to the next set of experiments, to learn about the specificities of hydraulic power transfer. Part of this second set of experiments is conducted in the next laboratory room – Hydraulic components and characteristics. It is intended for experimenting about different types of valves (throttling valves, pressure valves, flow valves and directional valves), different designs of real hydraulic circuits, pressure drops on components and circuits, as well as experimenting regarding the operating specialities of individual valve designs. Each of the valve types is mounted at its own workstation. Two examples of experimental layout for this group of experiments are shown in Figure 5.

Experiments: Throttle vs. orifice, serial and parallel connection of hydraulic resistors and pressure drops, heat generation, Pascal Law, influence of pipeline design and the pressure drops, influence of flow amount on the pressure drop…

Experiments: Design form of pressure valves – one-stage pressure valve with and without damping piston, flow depended operational instabilities, pressure shock valve two-stage pressure valve, influence of back-pressure, adjusting principle…

Fig. 5. Setup for hydraulic basics and components experiments – pressure drops (left) and pressure valves (right)

Similarly configured are a test rig for the measurement of static and dynamic characteristics of the valves and a test stand for servo drives. The latter is located in its own part of the laboratory (see Figure 2). Figure 6 shows a part of the test setup for measuring the (control) valve characteristics and a linear servo drive.

Steady-state experiments: Δp-Q characteristic, flow-input signal, flow capacity, leakage, valve linearity, threshold, rated flow, flow gain, limiting power etc.

Experiments: Position control, force control – force sensor, pressure sensors, adaptive control concepts development, influence of accumulators and pipeline system etc.

Fig. 6. Setup for valve steady-state characteristic measurement (left) and linear servodrive (right)

As shown in Figure 3, the power supply to all rooms dedicated to the hydraulics is derived from the central power unit – see Figure 7). It is also used for many experiments at the same time: Except for the basic task of powering hydraulic working places, various types of pump control (variable pump, speed controlled constant pump), to know the importance of sensors for monitoring the condition of the power unit, CM of built oil, remote control and adjustment of all operating parameters, visualisation of operating parameters etc. as well as of special operating situations e.g. aeration of the system through a loose pipe connector and, consequently, noise and foaming.

Fig. 7. Central hydraulic power unit with control cabinet

5. Contents related to learning of Pneumatics and Automation

Pneumatic-related exercises are performed in a separate laboratory room – Figure 2. In contrast to the hydraulics experiments, the pneumatics has less emphasis on the physical background of the operation of the pneumatic systems. More emphasis is on the use of the pneumatics as a technique for products` manipulating – automation (handling and assembly). In this sense, the various pneumatic control circuits, from basic cases, through the electropneumatic to the PLC pneumatic, are at the forefront. Students build and test pneumatic controls or circuits at five workstations, where the exercises are upgraded, from simple ones to the more advanced. Workstations can be rearranged quickly and easily according to the subject under consideration – pneumatic controls or electrical controls, in various implementations and techniques (relay technology, semiconductor technology or PLC-programmable technique). Figure 8 shows the aforementioned multifunctional workstations for pneumatic circuits, and for automation basics with electrical components.

Fig. 8. Modular laboratory equipment – pneumatic and automation basics

A more advanced approach is to build pneumatic manipulators with the ability to reprogramme in terms of performing different sequence of actuator motions – automation of production processes.
Automation of production processes is the driving force of development of production-oriented companies. Thus, it is important that future technical personnel acquire specific skills in designing, implementing and managing automated devices and processes. Unfortunately, the didactic equipment used in educational institutions is usually of a simple nature (operation and control of individual components), so the transition of the trained technical personnel into a real industrial environment can be very demanding [2, 3]. A lot of related work was found in this field, yet the

work is more focused on developing single components, adding vision control [4], or developing higher level SCADA and manufacturing systems. However, closely related work on didactic pneumatic workstations was also found [5], which presents a more simple solution. We attempted to fill this gap with design and construction of a more complex didactic station, which is based entirely on real industrial components, and represents an automated workstation based on the use of pneumatic systems.
The workstation is based on a pre-designed work cycle. Workpieces are loaded into a container, from where a two-way cylinder pushes them to the pick-up point. The transfer of the workpiece from the pick-up point to the workplace is carried out by a 3-axis pneumatic manipulator, which can perform different movements of the workpiece – Figure 9.

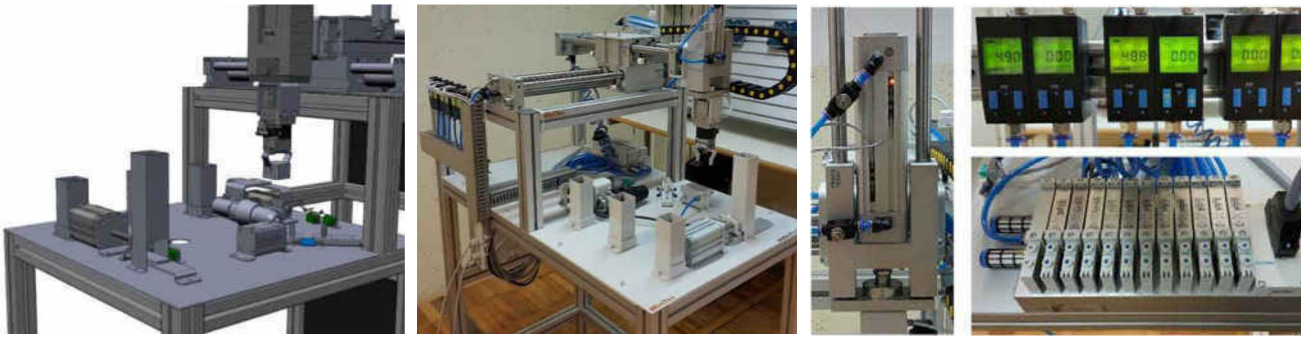

Fig. 9. Didactic workstation – 3D design (left), real appearance (middle), detail – industrial components (right)

The designed workstation provides a high level of flexibility in design using a PLC programmable pneumatic control system; from the simplest control cycles, where only three axes are managed; the user inserts the workpiece into the workplace manually, followed by clamping, drilling, stamping, un-clamping and manual removal of the workpiece; to very complex control cycles, where all 9 available axes are operated: Ejection of the workpiece from the container, pick-up and transfer to the workplace, both machining operations, clamping and turning of the workpiece by 180°, re-clamping and repeating the machining operations, and transfer to an appropriate container in respect to its current fill capacity.
The basic concept of the station and its operation was developed further and conceived in SolidWorks, where we created a simulation of movement through the work process, making it easier to reconcile the individual movements of all 9 axes. On the basis of the final 3D model, the drawings and plans were made for manufacturing and assembly.

Conclusions

In higher education courses that relate to the automation of individual machines, systems or entire industrial plants, including hydraulic and pneumatic components, we are faced constantly with rapid development of new technologies. The main challenges are not the basics, the basic background and concepts of industrial automation, but rather a vast number of technical innovations related to the design and use of automation building blocks: Sensors, programmable logic controllers and corresponding programming languages, as well as new fluid power components.
Students who complete a certain degree of education should not only have an appropriate basic knowledge, but they should also have an insight into the equipment used most commonly by their potential employers in the local and international areas. Since we are experiencing rapid technological advancement, we need to find a way to use the limited resources allocated for equipment, while following the development of new technologies, and providing students with the new, ever more powerful, flexible and versatile equipment that they will use tomorrow in industry. This problem began to stand out with the implementation of the internationally comparable Bologna

Process, and became even more demanding with the introduction of Industry 4.0 in our companies. In addition to theoretical and practical exercises the problem also involves mainly student projects.

We have been dealing with this problem successfully for more than two decades. As an example of good practices in teaching, we conform to the following principles – approaches:

- The main emphasis is on obtaining the basic knowledge.
- Concepts of exercises and content delivered is according to the principle: “Start with basics and add functions”. In this manner, we cover the minimal skills that everyone should understand fully. For those more interested students we have the possibility to upgrade the basic exercise. We use this well-proven and accepted concept for both full-time and part-time students, for student project work, as well as for participants from industry in various trainings and courses.
- The next approach is to teach how to use different equipment to solve the same problem.
- Solving the given task in various ways, including thinking "out of the box", where the creativity of students is particularly evident and leads to the desired target – an intelligent student or an expert. We also encourage students by enhancing common tasks and existing controls with hidden errors that they have to find, diagnose and repair.
- In parallel to the practical work, the students have to use modern e-tools for industrial automation planning and design, and, later, they have to switch from the virtual world to the real world.
- We incorporate the “self-service” concept, whereby students search for the necessary equipment in a box, as when purchasing it in a company. Then they have to read the instructions, install it, wire it and use it;
- Within the practical work, both in the field of Hydraulics and Pneumatics, we use real industrial components, and realistic operating conditions.

This approach also provides insight into the specificities of the operation of these systems. In addition, it provides a variety of already established and newer approaches to learning: Implementing of ICT in flipped, combined and project based learning, within the subject of Fluid Power Technology, as well as e-learning and “forensic-case like learning”.

References

[1] CETOP RE-2004.03/H, Industrial hydraulics programme (IH2), 2004.
[2] Skopis, V., I. Uteševs, and A. Pumpurs. “Advanced Control System Development on the Basic of FESTO Training Laboratory Compact Workstation." 54th International Scientific Conference of Riga Technical University. Section of Power and Electrical Engineering: Digest Book and Electronic Proceedings, Latvia, Rīga, 14-16 October, 2013. Riga: RTU Press, 2013, pp.38-40. ISBN 978-9934-10-470-1. 2013.
[3] Bustamante, M., G. Moreno, A. Pelaez, and C. Madrigal. "Design and implementation of an automation didactic module focused to machine vision and programmable logic control." 2014 III International Congress of Engineering Mechatronics and Automation (CIIMA), Cartagena, 2014, pp. 1-5. doi: 10.1109/CIIMA.2014.6983451, 2014.
[4] Krawczyk D., and K. Paweł. "Bottom-up approach for developing a tailor-made manufacturing execution system." 2016 11th France-Japan & 9th Europe-Asia Congress on Mechatronics (MECATRONICS) /17th International Conference on Research and Education in Mechatronics (REM), Compiegne, 2016, pp. 236-241. doi: 10.1109/MECATRONICS.2016.7547148, 2016.
[5] Stankovski, S., L. Tarjan, D. Skrinjar, G. Ostojic, and I. Senk. “Using a Didactic Manipulator in Mechatronics and Industrial Engineering Courses.” *IEEE Transactions on Education* 53, no. 4 (November 2010): 572- 579, doi: 10.1109/TE.2009.2036002.

EVALUATION OF TEMPERATURE OF THE AXIAL PISTON HYDRAULIC MOTOR BY INFRARED THERMOGRAPHY

Nicuşor BAROIU[1], Viorel PĂUNOIU[1],
Khaoula BERKAS[2], Mohamed Rafik SARI[2], Elena Felicia BEZNEA[3]

[1] Department of Manufacturing Engineering, ”Dunărea de Jos” University of Galaţi, Romania
Nicusor.Baroiu@ugal.ro, Viorel.Paunoiu@ugal.ro

[2] Mechanical Engineering Department, University Badji Mokhtar of Annaba, Algeria
berkaskhaoula@gmail.com, sari_rafik10@yahoo.fr

[3] Mechanical Engineering Department, ”Dunărea de Jos” University of Galaţi, Romania
Elena.Beznea@ugal.ro

Abstract: *When a hydraulic system has problems, it is common practice to first look at the pump or hydraulic motor. Obviously, when preliminary troubleshooting, the analysis focuses on the hydraulic motor, a series of steps can pinpoint the specific problem and lead to the cure. The monitoring condition of a hydraulic system can bring benefits, other than just reliability and improved safety.*

This paper aims to present a modern diagnosis method of specific malfunctions of the hydrostatic drive systems and the use of the equipment with an axial piston hydraulic motor. The diagnostic technique described is using the infrared thermography and can be considered a predictive maintenance.

Different operation modes of the axial piston hydraulic motor are simulated by changing the pressure in the hydraulic drive test system. Specific thermograms are obtained for each operation mode.

Keywords*: Maintenance, predictive maintenance, infrared thermography, axial piston hydraulic motor, hydraulic drive systems*

1. Introduction

Maintenance was an area that was often thought to not need much attention. However, with the greater focus on safety, environment, energy efficiency and profitability, maintenance has now become an area where there is renewed attention [1, 2, 3].

Hydraulic systems are becoming more complex in design and in function and the reliability of these systems must be supported by efficient maintenance regimes [4, 5]. There are three such regimes: breakdown maintenance (most expensive), time-based maintenance, and condition-based maintenance (least expensive). Choosing a maintenance regime depends on the hydraulic system - if the systems do not require high reliability or if economics or safety are not the issue, the breakdown maintenance approach may be sufficient. However, for maximum reliability and safety, the condition-based maintenance approach should be implemented. In general, most hydraulic systems do require high reliability and thus, the latter approach regarding the monitoring condition is most desirable [6, 7, 8].

The energy conservation involves the optimum use of resources and represents an imperative when it comes to the application of measures in order to develop an economy based on healthy growth. For this reason, it is necessary to obtain some accurate information on the energy performances of the equipment, installations or machinery. The information is obtained by drawing energy balances or developing an analysis based on data resulting from the inspection of selected aims. The evaluation of all energy losses susceptible to reduce the efficiency of a system requires a good vision on the thermal distribution of its components. This is achieved by thermography technique, which allows monitoring the temperature distribution on the equipment’s surface, by a method of measuring the infrared radiation [9].

Thermography (or thermovision) is a technique of measuring the thermal field of a physical object, which uses the infrared radiation, for recording and visualization of temperature distribution on the surfaces. Thermography is a non-destructive method that does not require direct contact with the analyzed surface and is particularly useful in malfunctions, diagnosing within industrial systems, because it is not necessary to interrupt the technological flow [10, 11, 12]. The industrial equipment presents energy losses, which depend on configuration, quality and sealing installation [13, 14, 15].

2. Theory of Thermography

2.1 Electromagnetic Spectrum

The electromagnetic spectrum is divided arbitrarily into a number of wavelength regions, called bands, distinguished by the methods used to produce and detect the radiation. There is no fundamental difference between radiation in the different bands of the electromagnetic spectrum. They are all governed by the same laws and the only differences are those due to differences in wavelength [16].

Thermovision or infrared visualization (IV) is a technique whereby a camera detects and displays a radiation intensity map on an electromagnetic spectrum field. The term "thermovision" defines the image obtained by the thermal camera and is used especially in military or civil surveillance applications, while thermography also involves temperature measurement, in industrial or scientific applications. It is known that any object, with temperature above 0 Kelvin, emits electromagnetic radiation. Substances considered cold and very cold: liquid nitrogen, ice and snow, emit infrared as well. The intensity of this radiation varies depending on the temperature of the object and its ability to emit energy.

The infrared occupies a wide portion of the electromagnetic spectrum, from 0.8 μm (micrometers) to 200 μm, but only a small part is usable by IV measurement and visualization equipment. For thermovision, only the domain raging between 0.75 μm and 15 μm presents interest. Basically, according to the manufacturer, 3 (or 2) sub-domains are recognized, Figure 1:

- SW – Short waves or near infrared: 0,8÷1,5μm;
- MW – Mid-waves: 2÷5μm;
- LW – Long waves: 7÷15μm.

Although wavelengths are given in μm (micrometers), other wavelength units are often used in this spectral region, e.g. nanometers (nm) and Ångström (Å) – 10000 = 1000 nm = 1 μm.

2.2 Equations of the Thermography Camera

When visualizing an object, the camera receives radiation, not only from the object itself, but also collects the radiation reflected in the surroundings of the object's surface. Both radiation are attenuated to some extent by the measurement atmosphere. In addition, a third radiation which must be considered, is the radiation from the atmosphere. This description is a real one, describing the measuring conditions.

What can be neglected, however, is sunlight and spreading in the atmosphere of uncontrolled radiation from intense radiation sources, outside the field of vision. Such disturbances are difficult to be quantified, but, however, in most cases, they are fortunately small enough to be neglected. If they are not neglectable, the measurement configuration is uncertain, even for a trained operator.

The operator is responsible for modifying situations where measurements can be disturbed: for example, by changing the direction of visualization, protection, etc., Figure 2.

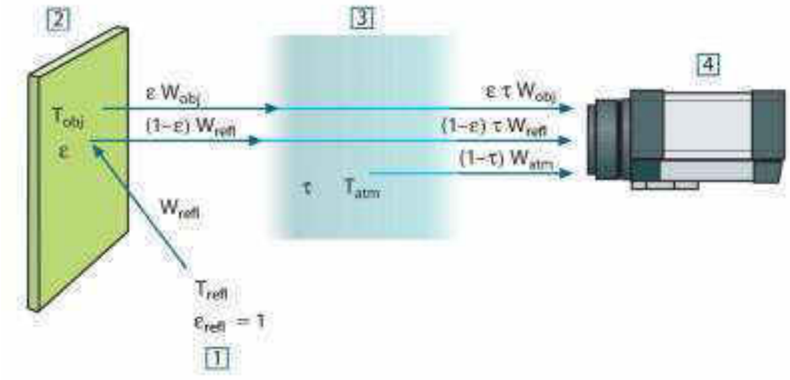

Fig. 2. Schematic representation of the method of thermography:
1-environment; 2-object; 3-atmosphere; 4-camera [16]

In order to obtain a formula for calculating the temperature of the object using the thermography calibrated camera, it is assumed that a power radiation W of a black object with a source temperature T_{source}, is received at a short distance. The camera will generate an output signal U_{source}, proportionately with the input power (linear power of the camera). Thus, the following equation can be generated:

$$U_{source} = CW\left(T_{source}\right) \tag{1}$$

or simplified:

$$U_{source} = CW_{source} \tag{2}$$

where: C – the constant.

If the radiation source is considered, for a grey object with an emissivity of ε, then the radiation received will therefore be the εW_{source}. Under these conditions, it can be defined:

1 – emissivity of the object = $\varepsilon\tau W_{obj}$,

where ε is the emissivity of the object, and τ atmospheric transmittance. The object's temperature will be T_{obj}.

2 – reflected emissivity of the external sources = $(1-\varepsilon)\tau W_{refl}$,

where $(1-\varepsilon)$ is the reflection coefficient of the object. The temperature of the external sources considered is T_{refl}. It is assumed that the temperature T_{refl} is the same for all surfaces emitting from the environment. This, of course, is for the case of the simplified hypothesis. It is also assumed that the emissivity of the environment is equal to 1. This is implied by the perspective of Kirchhoff's law.

3 – atmospheric radiation = $(1-\tau)\tau W_{atm}$,

where $(1-\tau)$ is the atmospheric emissivity. The atmospheric temperature is considered T_{atm}.
Total radiation can be written as:

$$W_{tot} = \varepsilon\tau W_{obj} + \left(1-\varepsilon\right)\tau W_{refl} + \left(1-\tau\right)W_{atm} \tag{3}$$

By multiplying each term with the constant C in the equation (1) and replacing the CW product, the corresponding output signal U, shall be obtained:

$$U_{tot} = \varepsilon\tau U_{obj} + \left(1-\varepsilon\right)\tau U_{refl} + \left(1-\tau\right)U_{atm} \tag{4}$$

Solving equation 3 for U_{obj}, we obtain:

$$U_{obj} = \frac{1}{\varepsilon\tau}U_{tot} - \frac{\left(1-\varepsilon\right)}{\varepsilon}U_{refl} - \frac{\left(1-\tau\right)}{\varepsilon\tau}U_{atm} \tag{5}$$

The formula resulting from the equation (5) is the measuring formula used in the FLIR System Series Thermographers [16].

The tensions used in the equation (5) are defined as: *U_{obj} – calculated output voltage of the thermovision camera for the black object's temperature, T_{obj}; U_{tot}* – the measured voltage of the thermovision camera for particular cases; U_{refl} – the theoretical output voltage of the thermovision camera for the black object's temperature, T_{refl}, according to the calibration; U_{atm} – theoretical output voltage of the thermovision camera for the black object's temperature, T_{atm}, according to the calibration.

3. Experimental equipment

The experiments were carried out on a hydrostatic plant (test bench) in a laboratory in the Department of Manufacturing Engineering, Faculty of Engineering, “Dunărea de Jos” University of Galați, Romania. Figure 3 shows the equipment needed to determine the recorded values.

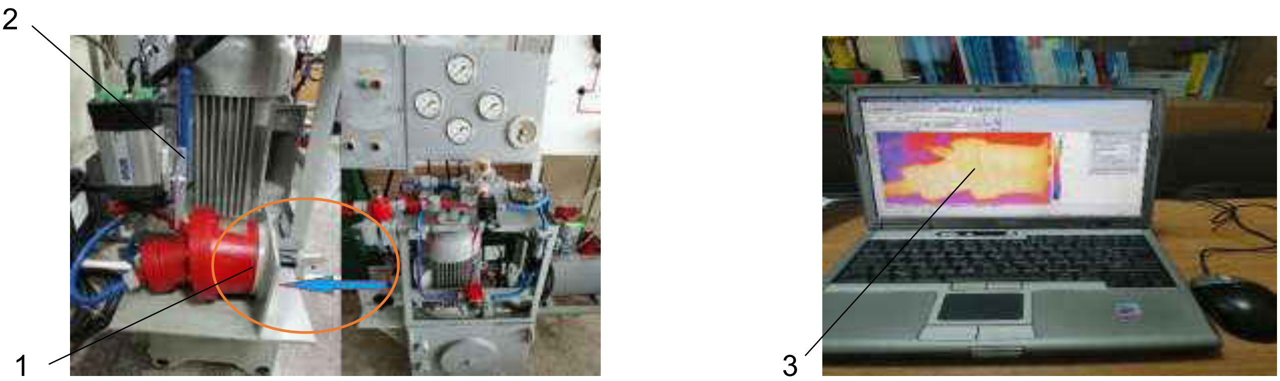

Fig. 3. Hydrostatic plant with camera thermography: axial piston hydraulic motor (1); FLIR ThermoVision A20M infrared thermal camera (2); ThermaCAM Researcher Professional specialized software for acquisition and processing of thermograms (3)

Infrared ThermoVision A20M from Flir Systems has been connected to a portable computer terminal, allowing it to be ordered from both the computer and an integrated keyboard (IK), in the forms of buttons placed accessible at the top of the camera. The most important features of the thermographic camera have been set: measuring range: 20 ÷ 900 °C; image frequency: 50 Hz; image resolution: 160x120 pixels; thermal sensitivity <0.1 °C; Digital Video Interface: FireWire;
- Spectrum wavelength: 7.5 ÷ 13 µm. In order to obtain a true infrared image, it is also necessary to consider the parameters describing the physical properties of the material to be processed (emissivity, reflected temperature), environmental temperature, relative humidity, distance from the lens of the camera to the hydraulic motor, Figure 4a and 4b.

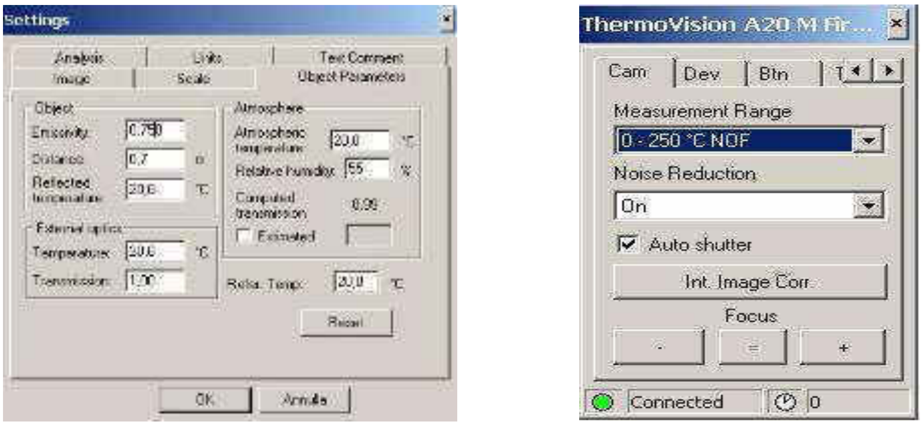

a. b.

Fig. 4. ThermoVision A20M ThermoVision Camera: the properties of the hydraulic motor material (a); choice of the temperature measurement range (b)

4. Specialized software ThermaCAM Researcher Professional

ThermaCAM Researcher Professional is the ThermoVision A20M ThermoVision thermo-imaging software - capable of measuring and capturing images of objects that emit infrared radiation. Due to the fact that radiation is a function which depends on the surface temperature of an object, the software allows the camera to make it possible to record the temperature in real time, but it can also be used for the acquisition and processing of thermograms that include the temperature range, recorded at the axial piston hydraulic motor, the images obtained showing the thermal state at a certain moment during the functioning process [17]. Using the ThermaCAM Professional software, the recordings of the thermography camera are captured and can be expressed numerically or graphically in the form of images, profiles, histograms etc. For the numerical analysis of the temperature and statistical information in the images, obtained either on the basis of the absolute measurements (the result is a real temperature) or the relative ones (the result is a difference in temperature), markers (evolution lines) were used on the image in infrared, which highlights the areas where the radiation of the object is equal. Markers can be punctual - temperature is measured in one place on the image, zonal - temperature, maximum, minimum, average and standard deviation, in a perimeter chosen in the image or linear - measuring the minimum temperature, maximum temperature, average and standard deviation, along a straight line within the image.

5. Results and discussions

In implementing the best predictive maintenance practices, a particular impact on the operation of industrial equipment, in general and hydraulic, in particular, is the way in which the operating temperature of the components of the installations is controlled. Thus, in experimental research it was measured, with the aid of an infrared thermal imaging camera FLIR ThermoVision A20M, the temperature recorded at the rotary hydraulic piston engine with axial pistons for two working pressure values: 20 bar and 50 bar. The registration with FLIR ThermoVision A20M was performed for 10 seconds after 15, 25, 35, 45 and 50 minutes of operation of the plant. The operating parameters of the rotary hydraulic engine with axial pistons are presented in Table 1.

Table 1: The parameters of the axial piston hydraulic motor

The parameters of the axial piston hydraulic motor	Value
p_n (nominal pressure) [daN/cm^2]	150
Q_n (nominal flow) [l/min]	17
n (rotation speed) [rpm]	1450

Test 1 - On the basis of the operating values of the pump n = 1275 rpm and p = 20 bar, images of the temperature variation with the infrared camera FLIR are presented in Figures 5, 7, 9, 11. In the present study, it was chosen to draw the evolution lines (L01, L02, ..., L05), Figures (6, 8, 10, 12), present graphs to plot from the recorded values opting for the maximum temperature.

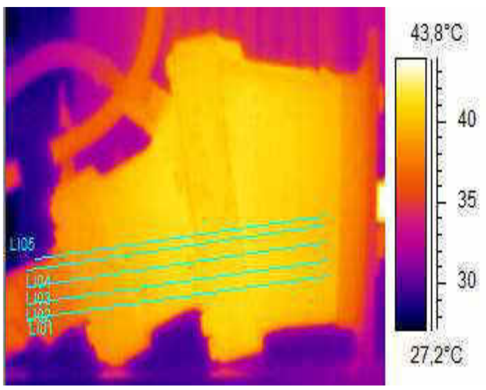

Fig. 5. FLIR camera frame-image after 15 min.

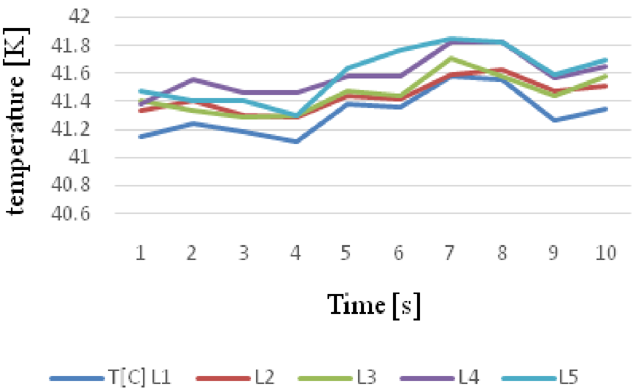

Fig. 6. Temperature variation for p = 20 bar after 15 min.

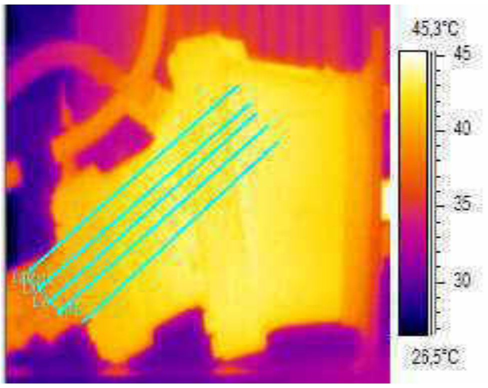

Fig. 7. FLIR camera frame-image after 25 min.

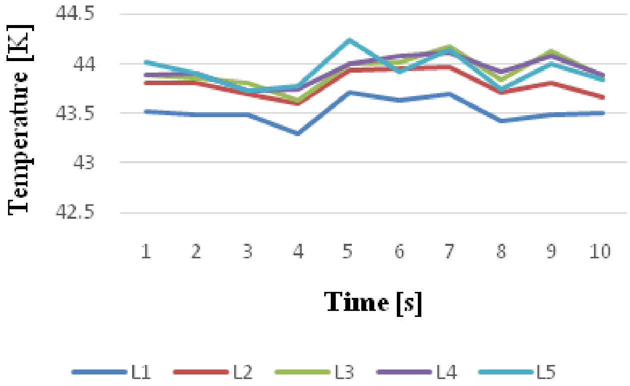

Fig. 8. Temperature variation for p = 20 bar after 25 min.

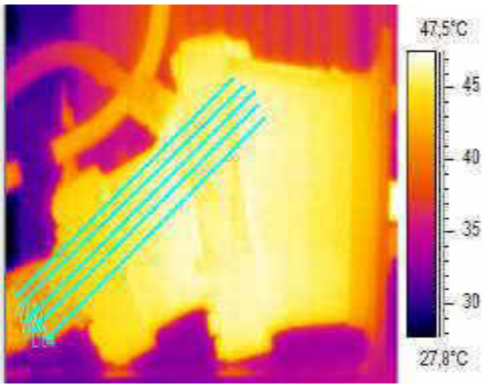

Fig. 9. FLIR camera frame-image after 35 min.

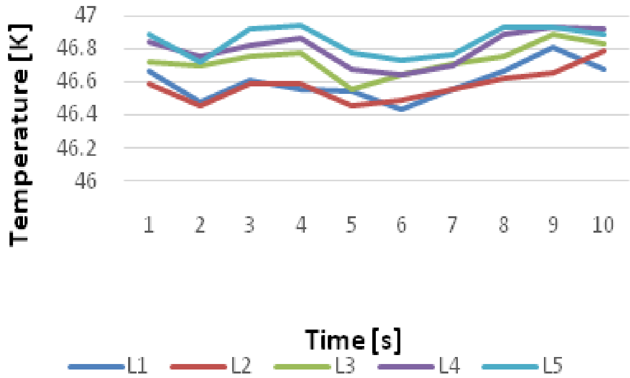

Fig. 10. Temperature variation for p = 20 bar after 35 min.

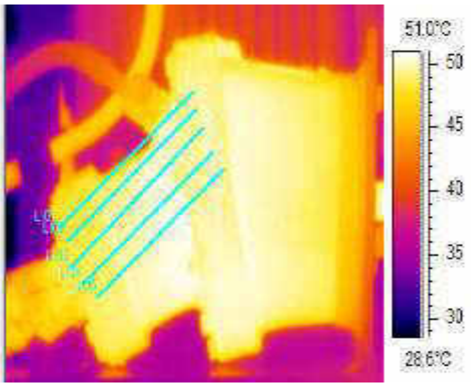

Fig. 11. FLIR camera frame-image after 50 min.

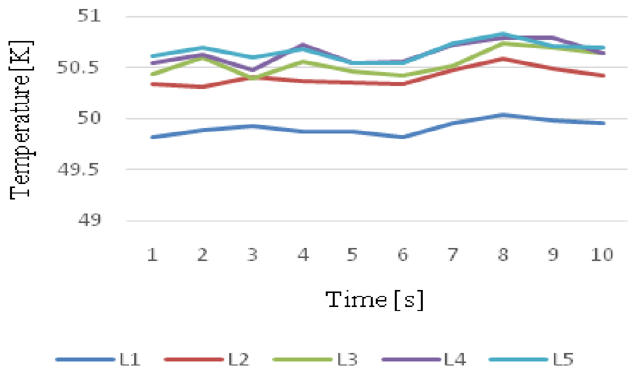

Fig. 12. Temperature variation for p = 20 bar after 50 min.

Test 2 - Figure 13 shows the hottest area of the axial piston hydraulic motor. The camera was fixed on this zone to see the variation of the temperature for p=50 bar and n=1700 rpm.

On the basis of the operating values of the pump n = 1700 rpm and p = 50 bar, images of the temperature variation with the infrared camera FLIR are presented in Figures 14, 16, 18, 20.

Figures 15, 17, 19, 21 present graphs to plot from the recorded values opting for the maximum temperature.

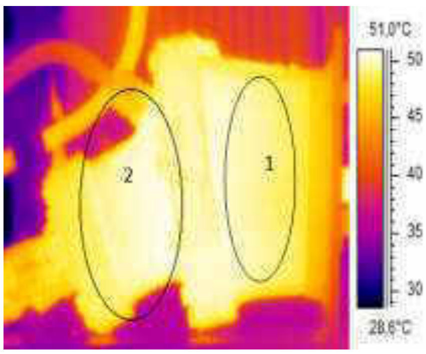

Fig. 13. The hottest area of the axial piston hydraulic motor

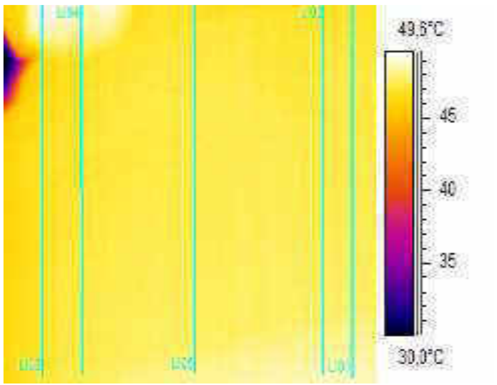

Fig. 14. FLIR camera frame-image after 10 min.

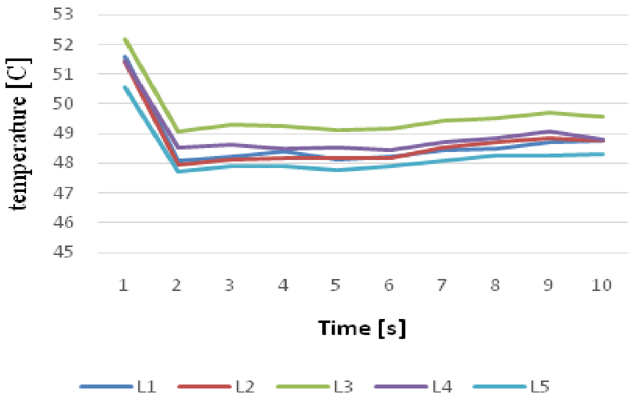

Fig. 15. Temperature variation for *p* = 50 bar after 10 min.

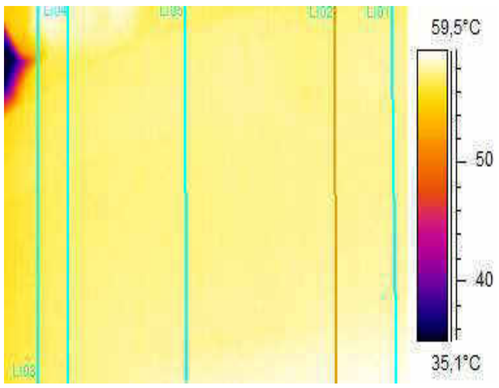

Fig. 16. FLIR camera frame-image after 15 min.

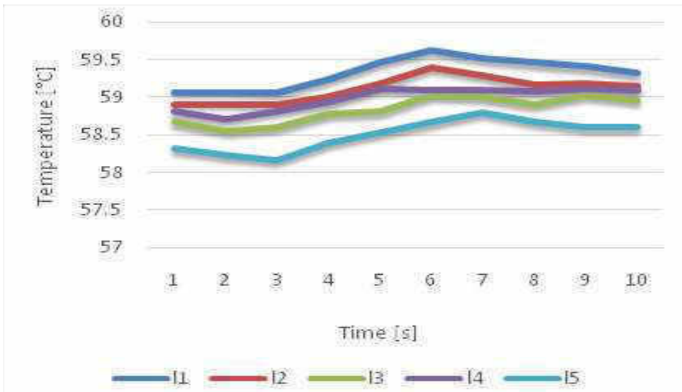

Fig. 17. Temperature variation for *p* = 50 bar after 15 min.

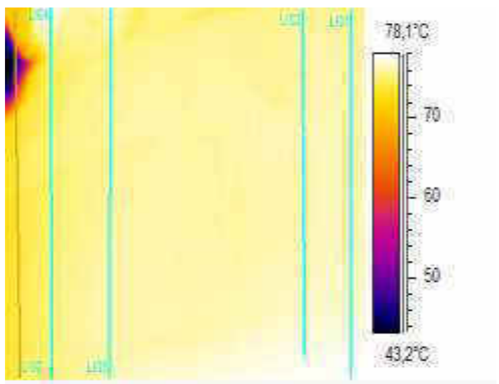

Fig. 18. FLIR camera frame-image after 30 min.

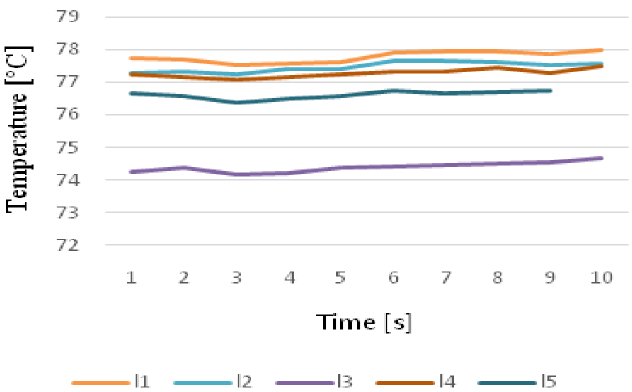

Fig. 19. Temperature variation for *p* = 50 bar after 30 min.

Conclusions

In mechanical and hydraulic drives, overheating is a general problem, which indicates breakdown in near future. Thermal imaging technology serves an important purpose for predictive maintenance of axial piston hydraulic motor and produces heat-based images, where the colors in the image show a relationship between every pixel of the hydraulic equipment image and a reference surface temperature. Following the experimental research presented on the demonstration of the possibility of using infrared thermography to predict the behavior of hydrostatic systems, to evaluate the state of wear and the operation of axial piston hydraulic motor, a series of numerical and graphics was obtained.

Regarding the test performed, the following punctual conclusions are appropriate:

- The first test was performed at p= 20 bar - the thermogram analysis presented in Figure 11 shows that the pump tested in Figure 3 is operating normally. Thus, we see that on the lower side of the pump, corresponding to the piston block (area 2 in Figure 13), the temperature is about 51ºC and on the upper side, where the pistons are located (area 1 in Figure 13), the measured temperature is about 46ºC. The temperature difference recorded at the pump heads is 5°C, which is below the critical value of 10°C.

- For the second test, concerning the hottest portion (1 in Figure 13) of the pump, the temperature rises to 78.1°C at p = 50 bar, after a 30 minutes-operation (Figure 18).

Acknowledgments

This work was supported by an ERASMUS+ grant 2017-3071/001-001, in Capacity Building in Higher Education, Project reference number – 586035-EPP-1-2017-1-DZ-EPPKA2-CBHE-JP: The Algerian National Laboratory for Maintenance Education (ANL MEd).

References

[1] Deepak Prabhakar, P., and A. Dharmaraj. “Modern plant maintenance and reliability management methods – A review.” *International Journal of Mechanical and Production Engineering Research and Development (IJMPERD)* 8, no. 3 (June 2018): 791-802.
[2] Cabral, J.S. “Pratical Guide to Facilities Maintenance Management.” ManWinWin Software. Accessed May 16, 2019. https://manwinwin.com/en/maintenance-management-software/, 2016.
[3] Abuzant, S.I. "Maintenance Management Model For Local Municipal Services." An-Najah National University, Faculty of Graduation Studies. Master’s Degree Thesis. 2011.
[4] Worldwide Hydraulic Professionals - Common platform for the hydraulic peoples. February 16, 2019. Accessed September 16, 2019. https://whyps.com/hydraulic-system-problems-and-solutions.
[5] Maintenance world. “Hydraulic Trouble Shooting.” February 27, 2014. Accessed September 14, 2019. http://www.maintenanceworld.com/2014/02/27/hydraulic-trouble-shooting/.
[6] Rochambeau, R. “Pop the Cavitation Bubble in Hydraulic.” Valin Corp., September 09, 2015. Accessed September 16, 2019. https://www.hydraulicspneumatics.com/hydraulic-pumps-motors/pop-cavitation-bubble-hydraulic-systems.
[7] Vision Engineers Process Equipment. “Maintenance of hydraulic oil”, 2012. Accessed August 10, 2019. http://www.visionengineers.nl/images/downloads/olie_reiniging/Maintenance-Eng.pdf.
[8] Lovrec, D., and V. Tič. “Determination and comparison between different hydraulic and turbine oils' lifetimes.” Paper presented at the 3rd Conf. „MAINTENANCE 2014“, Zenica, B&H, June 11–13, 2014.
[9] Chou, Y.C., and L. Yao. “Automatic Diagnostic System of Electrical Equipment Using Infrared Thermography.” Paper presented at the International Conference of IEEE Soft Computing and Pattern Recognition (SOCPAR'09), Malacca, Malaysia, December 4–7, 2009.
[10] Sambhi, S. “Thermal Imaging Technology for Predictive Maintenance of Electrical Installation in Manufacturing Plant-A Literature Review.” Paper presented at the 2nd IEEE Int. Conf. on Power Electronics, Intelligent Control and Energy Systems (ICPEICES), New Delhi, India, Oct. 22-24, 2018.
[11] Lopez-Perez, D., and J. Antonino-Daviu. “Application of infrared thermography to failure detection in industrial induction motors: case stories.” *IEEE Transactions on Industry Applications* 53, no. 3 (2017): 1901-1908.
[12] Łopata, S., and M. Kocot. “The conditions for thermographic testing of thermal power engineering installations.” *Technical Transactions* 10 (2017): 179-192.
[13] AFTIB - "Association Française de Thermographie Infrarouge dans le Bâtiment, Industrie, R & D". Accessed June 21, 2019, http://www.aftib.org/exemples-applications-thermographie-infrarouge.php.
[14] Manca, D., and M. Rovaglio. “Infrared thermographic image processing for the operation and control of heterogeneous combustion chambers.” *Combustion and Flame* 130, no. 4 (September 2002): 277-297.
[15] Bagavathiappan, S., B.B. Lahiri, T. Saravanan, J. Philip, and T. Jayakumar. “Infrared thermography for condition monitoring, A review.” *Infrared Physics & Technology* 60 (September 2013): 35-55.
[16] ThermoVision A20M. Operator's manual, Flir Systems, 2004. Accessed May 16, 2019, https://www.flir.com/.
[17] ThermaCAM Researcher. Stores, retrieves and analyzes infrared images, 2019. Accessed May 16, 2019, https://thermacam-researcher-pro.software.informer.com/.

POLISH, EUROPEAN AND WORLD FLUID POWER MARKET - AT THE TURN OF THE SECOND AND THIRD DECADES OF THE 21ST CENTURY

Krzysztof KĘDZIA[1], Jarosław PROKOPOWICZ[2]

[1] Department of Maintenance and Operation of Logistics, Transportation and Hydraulic Systems, Faculty of Mechanical Engineering, Wrocław University of Science and Technology, krzysztof.kedzia@pwr.edu.pl

[2] jaroslaw.prokopowicz@pwr.edu.pl

Abstract: *(The article describes the fluid power market in Poland, Europe and world. It contains historical and current data as well as a forecast related to the future of the industry. Due to the current policy of the European Union, especially in the field of ecology, fluid power drives and controls are increasingly being replaced by electric drives - commonly considered as ecological. The described situation forces a change in approach in many areas, mainly drive system design as well as management and marketing. The article ends with the authors' forecast for the future of fluid power in Poland, Europe and the world.*

Keywords*: Fluid power market, statistics, analysis, forecast.*

1. Introduction

The world hydraulics and pneumatics market in 2001 was as follows: the production of hydraulics and pneumatics was the domain of global companies and concerns located in six technologically and economically developed countries. Their total sales covered 88% of the global fluid power sector (Table 1) [1], including: - almost 70% in hydraulics, - almost 80% in pneumatics.

Table 1: Share of various countries in the hydraulics and pneumatics market in 2001 [1].

Country	Share in%	GDP at current prices per capita in thousand USD
USA	39	35,475
Japan	23	32,524
Germany	11,5	22,511
Italy	6,7	18,933
France	4,3	22,031
UK	3,8	23,918
Sweden	1,8	23,752
Spain	1,5	14,574
Others, including Poland	8,4 0,35-0,45	- 4,737

The largest producers of hydraulic and pneumatic drives and controls in 2001 were:

- PARKER HANNFIN - annual turnover around 6.6 billion USD [1]. 44 thousand employees in 44 countries.

- BOSCH - total turnover amounted to 35 billion EUR, including 0.5 billion EUR in Poland. 224 thousand employees, including 16 thousand in the area of R&D and production development.

- BOSCH – REXROTH - sales in the area of hydraulics and pneumatics approx. 3.9 billion EUR, over 20 thousand employees.

SAUER - DANFOSS, turnover amounted to approx. 950 million USD, approx. 7.2 thousand employees in 28 modern factories in 10 countries on 3 continents.

Countries associated in the CETOP- European Oil Hydraulic and Pneumatic Committee- 16 national associations of producers of hydraulics and pneumatics from 14 countries: Belgium, Czech Republic, Finland, France, Spain, the Netherlands, Germany, Norway, Slovenia, Switzerland, Sweden, Turkey, United Kingdom and Italy had a global market share of 35%.

The macroeconomic situation in the countries associated in CETOP is presented in Table 2. It can be clearly seen that expenditure on R&D in the countries that joined the EU are on average 3 times lower (0.5-0.6% of GDP) in relative to the average of the more prosperous countries (1.8% of GDP).

Table 2: Selected macroeconomic data for CETOP countries in 2014.

Country	Population (million)	GDP per capita (in current prices in thousands of EURO)	R&D expenditure to GDP in%	R&D employees per 1000 employees	Growth rate of expenditure on R&D in% (2011-2015)
Belgium	10,449	37,407	2,45	10,4	5,4
Czech Rep.	10,627	16,510	1.9	7,4	6,2
Finland	5,268	38,959	2,9	16	-4,1
France	66,259	33,431	2.2	10,3	1,9
Spain	47,737	23,970	1.2	7,1	-1,8
Netherlands	16,877	40,941	2,0	9,5	2,7
Germany	80,996	37,997	2.87	9,0	3,6
Norway	5,147				
Poland	38,346	11,041	$1,0^{2015}$	5,0	11,1
Romania	21,729	8,582	0.5	2.2	4,4
Slovakia	5,443	14,907	1,17	6,3	18,6
Slovenia	1,988	19,262	2,2	9,6	-1,2
Switzerland	8,061				
Sweden	9,723	46,564	3.25	14,5	2,6
Turkey	81,619				
UK	63,742	36,096	1.7	9,4	8,6
Italy	61,680	27,588	1.3	5,4	2,5

The shares of the associated countries in CETOP in the hydraulics and pneumatics market in 2009 are presented in Fig. 1.

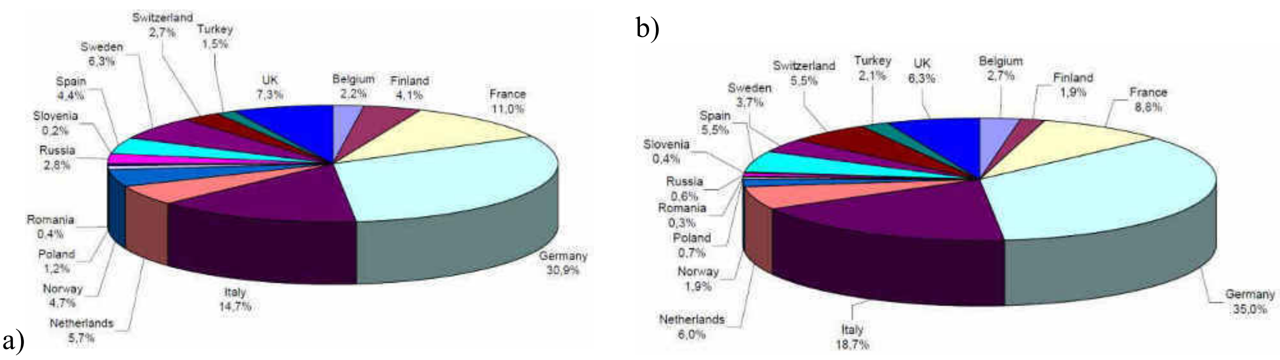

Fig. 1. Share of associated countries in CETOP a) in the hydraulics market with the value of domestic sales in 2009 around 6.1 billion EUR, b) in the pneumatics market with the value of domestic sales in 2009 2.2 billion EUR [3].

2. Global crisis 2008-2009

The situation on the hydraulics and pneumatics market in the years 1980–2009 in Germany is presented in Fig. 2. Until the global crisis of 2008–2009 one can notice a monotonic growth of the market. The largest decreases at that time concerned the fluid power industry and were respectively 44% for hydraulics and 33% for pneumatics. Due to the very strong links between the German economy and Poland (up to 70% of Polish exports go to Germany), this was a very big blow to this industry in Poland.

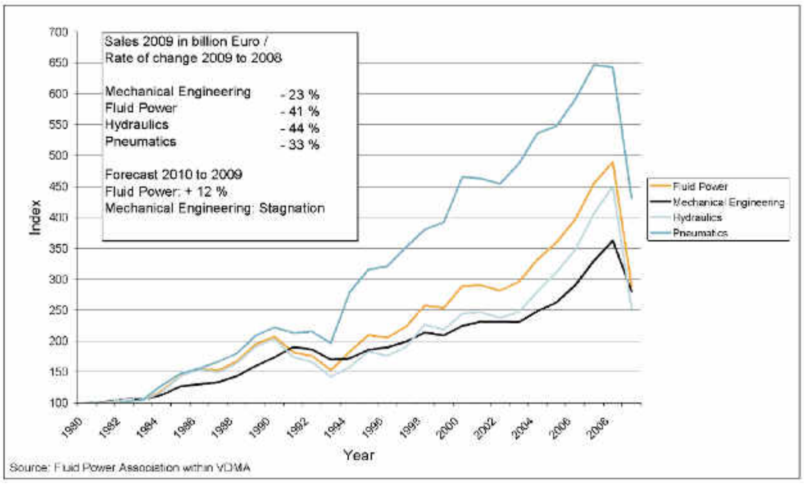

Fig. 2. Sales development of machinery and equipment for fluid power products (hydraulics and pneumatics) in Germany in the years 1980–2009 [3].

Other countries associated in CETOP had similar decreases - from 29% to even 55%, except China. China market growth was at the level of 5% (Fig. 3).

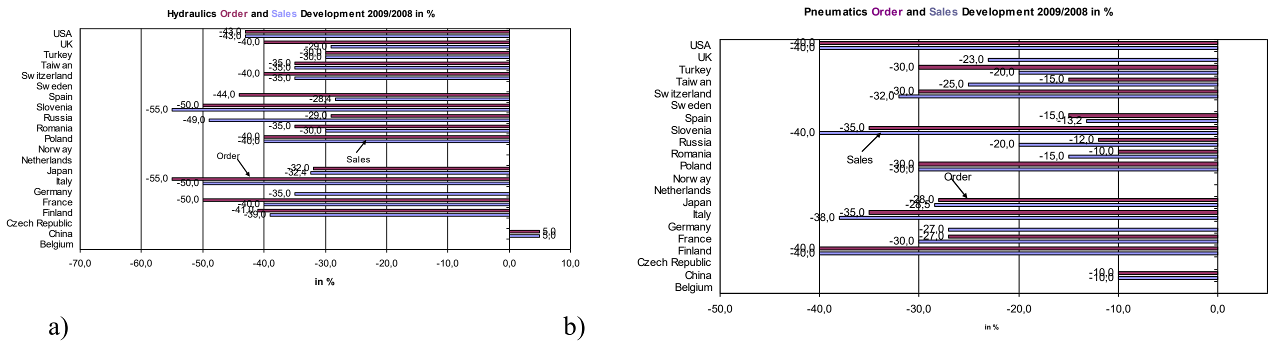

Fig. 3. Dynamics of product orders and sales 2009 to 2008: a) hydraulics, b) pneumatics [3].

3. Nowadays situation in fluid power market

The development of mobile hydraulics in the years 2000 - 2017 is shown in Figure 4.

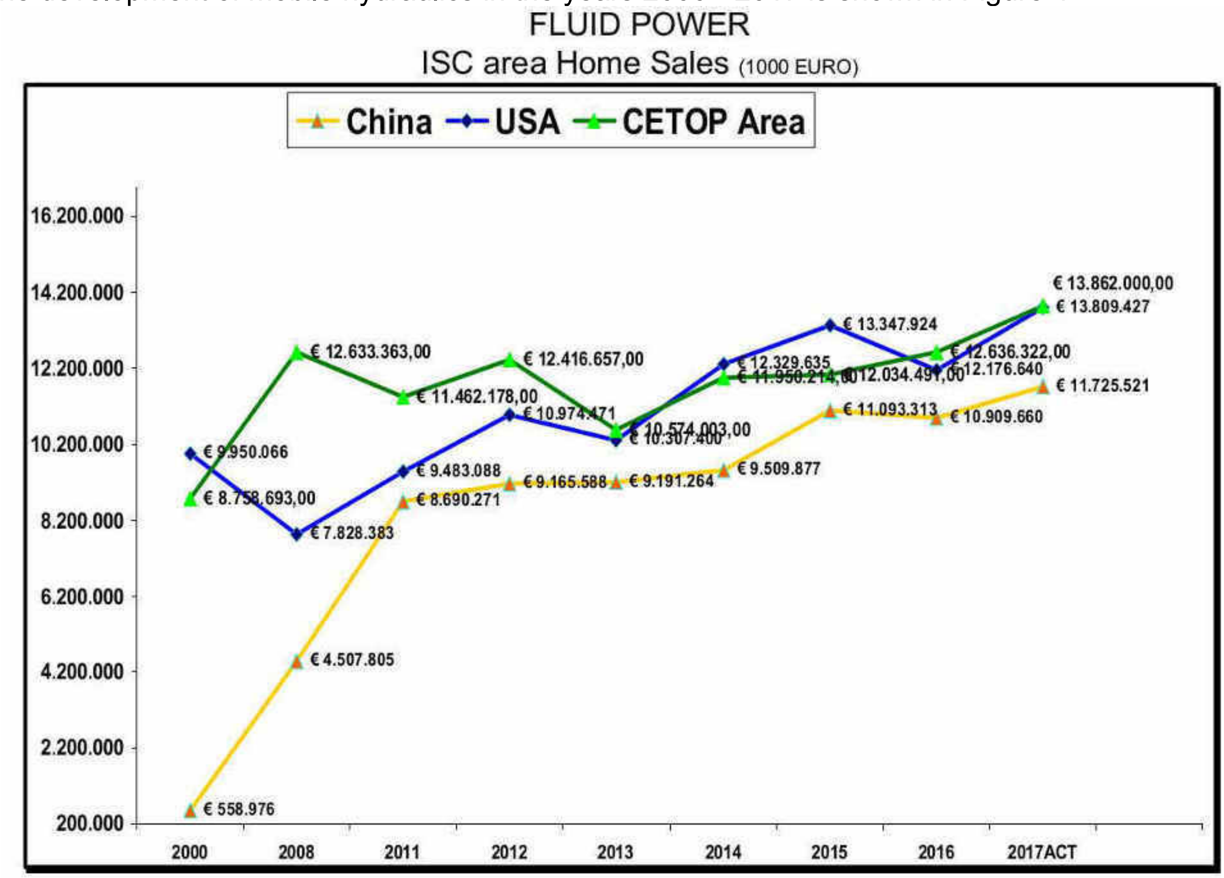

Fig. 4. The development of machine hydraulics market and its main shareholders [3].

A rapid increase in China's share in the hydraulics market in 2000-2011 is visible from 0.5 billion to 8.6 billion EUR. At that time, the US and European market has experienced a crisis, though balance has been restored and remains high today with a slight upward trend.
The years went by and the fluid technology market made up for the losses associated with the crisis and in 2017 the FP market increased from EUR 25.7 billion to EUR 43.6 billion. Figure 5 shows a global comparison of the situation in the field of hydraulics and pneumatics in 2000 and

2017. The graphs presented show that in the field of fluid technology the status quo was maintained by the CETOP countries and the USA. The Chinese market showed the highest increase (almost 14 times) (from 2 to 27%), while the Japanese market recorded a 3-fold decrease in market value (from 23 to 8%).
The years went by and the fluid technology market made up for the losses associated with the crisis and in 2017 the FP market increased from EUR 25.7 billion to EUR 43.6 billion. Figure 5 shows a global comparison of the situation in the field of hydraulics and pneumatics in 2000 and 2017. The graphs presented show that in the field of fluid technology the status quo was maintained by the CETOP countries and the USA. The Chinese market showed the highest increase- almost 14 times (from 2 to 27%), while the Japanese market recorded a 3-fold decrease in market value (from 23 to 8%).

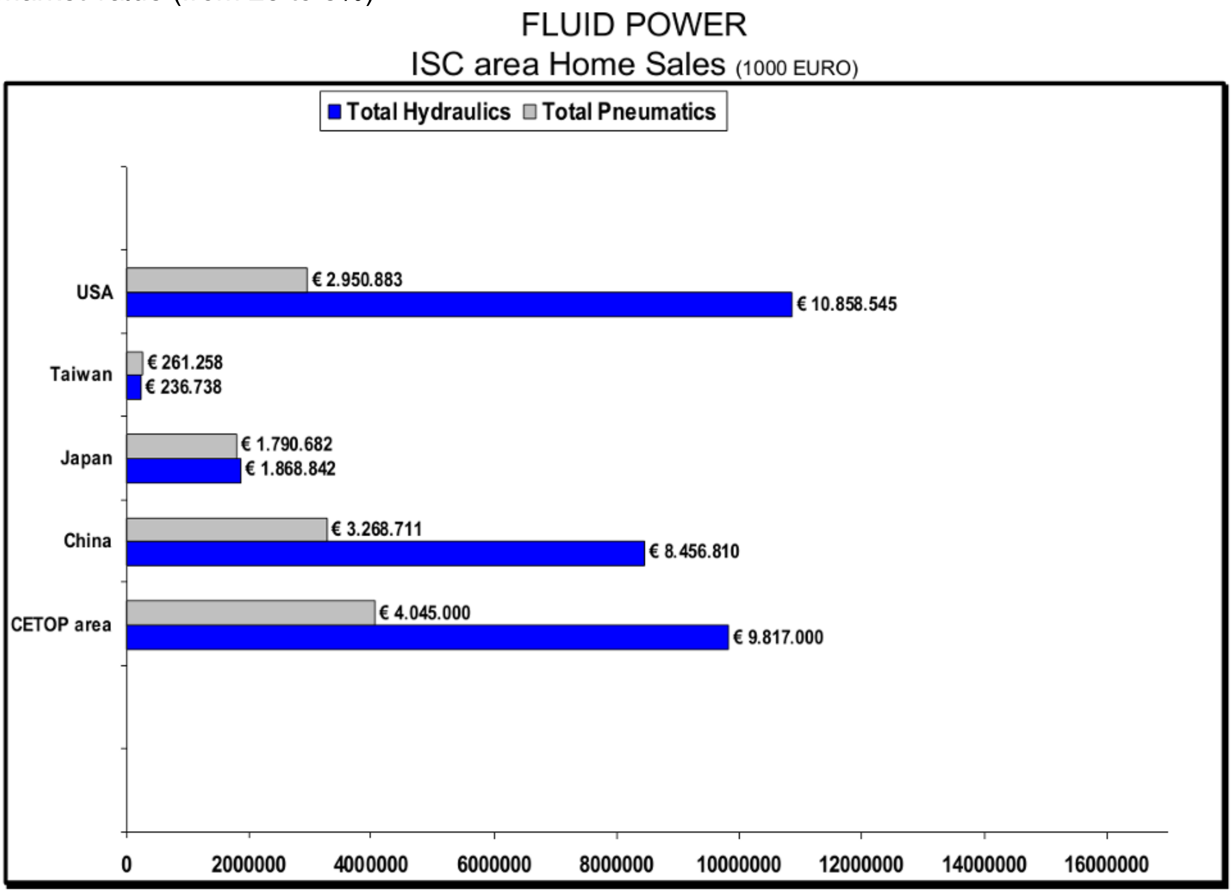

Fig. 5. Global domestic sales of fluid power products and services in 2017 [3].

Associated countries in CETOP have the largest share in the production of hydraulic and pneumatic drives and controls, they are matched by the United States with production worth 13.8 billion EUR. China's potential is 11.7 billion EUR, followed by Japan (3.66 billion EUR) and Taiwan (0.49 billion EUR).

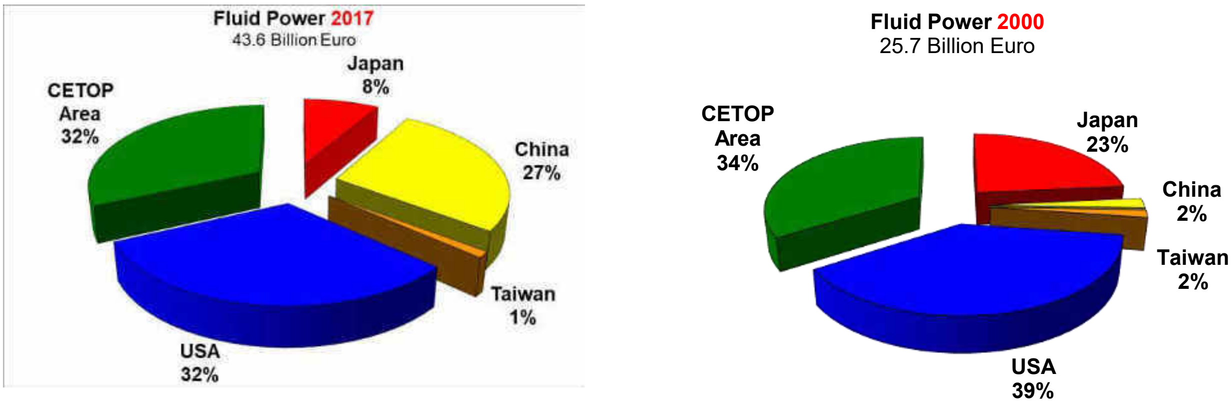

Fig. 6. Global Fluid Power Home Market 2017 and 2000 [3].

The global development of the hydraulics area is shown in Fig. 7, while pneumatics in Fig. 8.

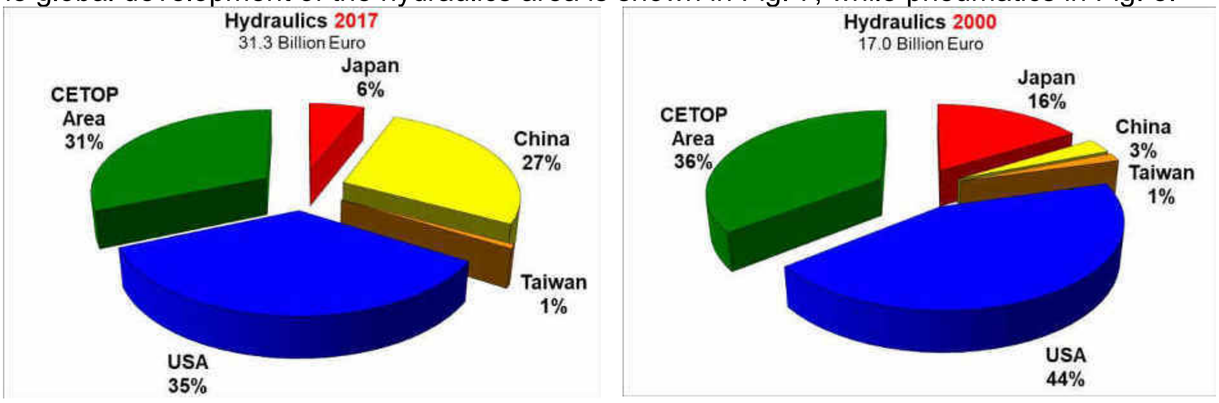

Fig. 7. Global Hydraulics Home Market 2017 and 2000.

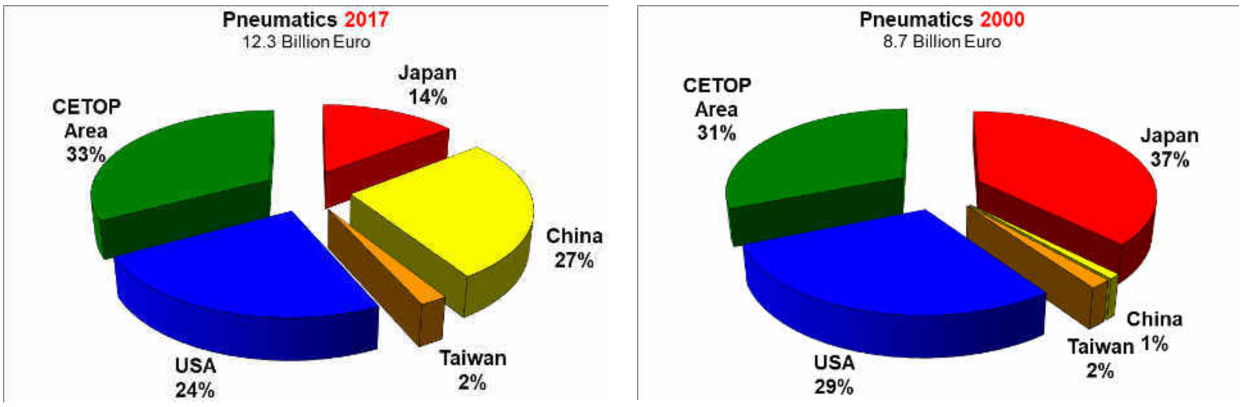

Fig. 8. Global Pneumatics Home Market in 2017 and 2000 [3].

On the European market, Germany still has the largest market share in the fluid technology market, with a 33% market share in 2017, followed by Italy (18%), France (10%) - Figure 9.

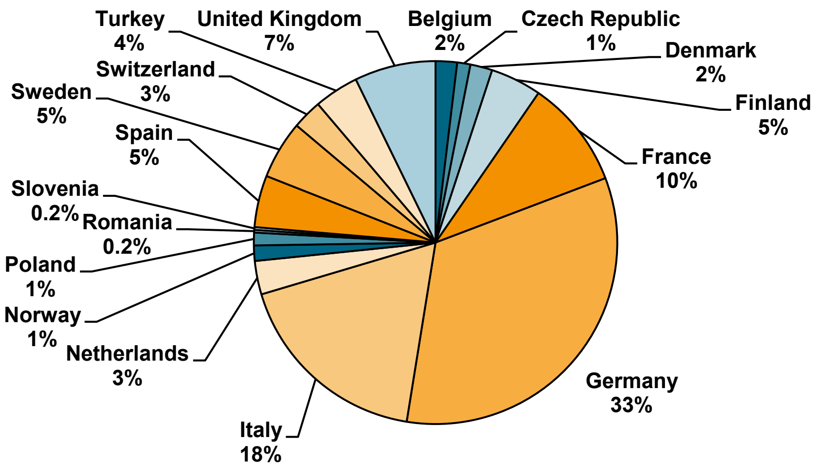

Fig. 9. European fluid power home market in 2017 (13.9 billion Euro) [3].

With a breakdown into hydraulics and pneumatics, the share of individual CETOP member countries is shown in Figure 10.

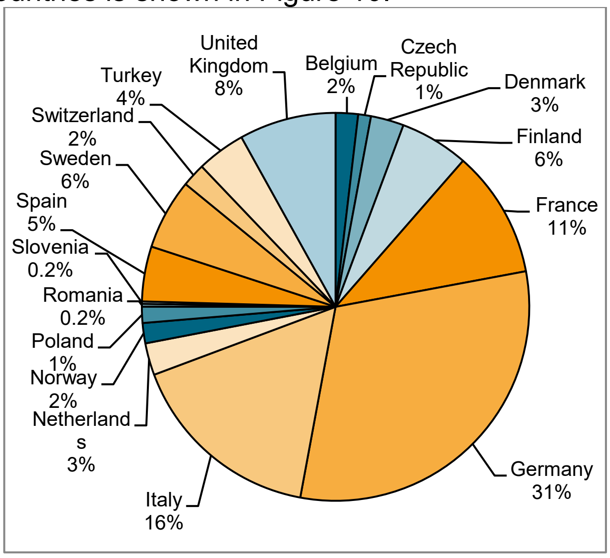

a) Hydraulics

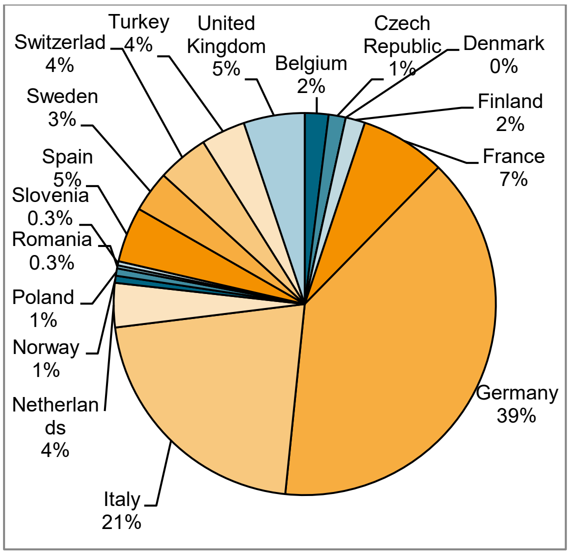

b) Pneumatics

Fig. 10. Home Market of European Fluid Power Industry in 2017 [3]

At present, patent applications are a very important factor influencing the assessment of the potential and possibilities of markets. For several years, the Polish government has been supporting the innovative activity of entrepreneurs and scientists through appropriate financial incentives. As a result of these activities, the number of patent claims increases every year (Fig. 11).

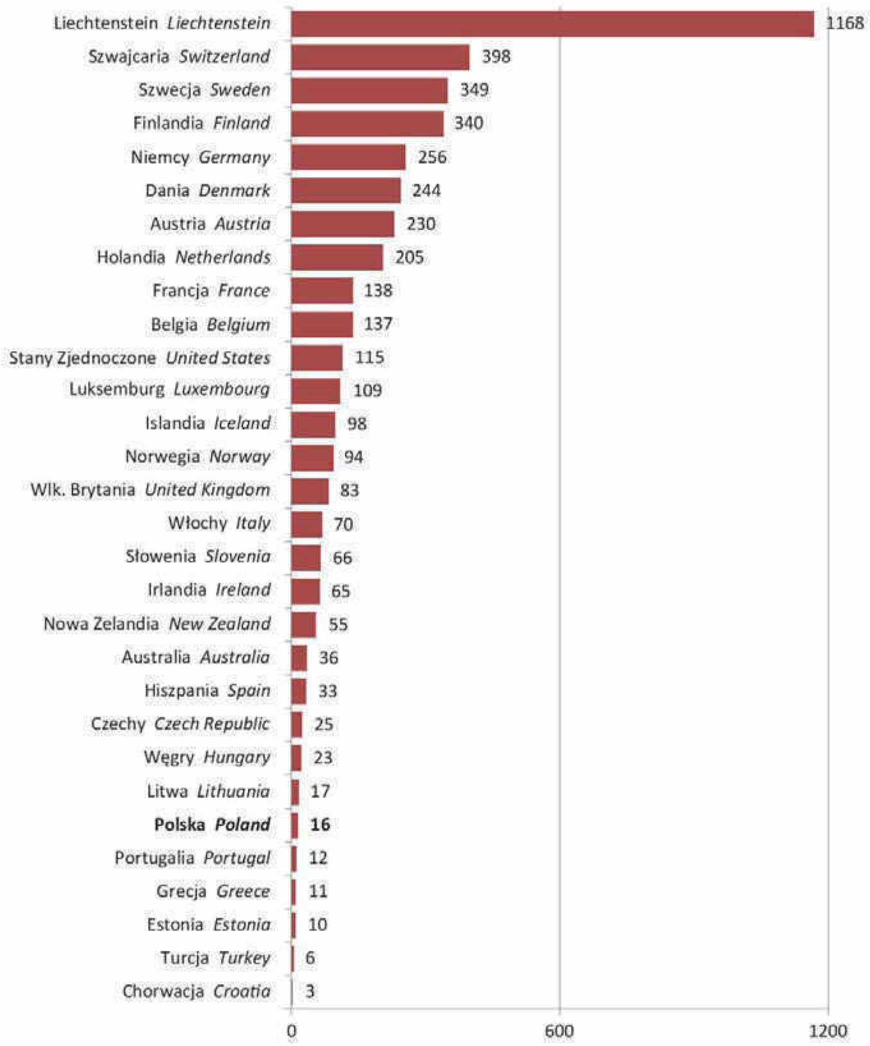

Fig. 11. Patent applications to the European Patent Office per million inhabitants in 2014 [2].

The highest number of applications for inventions per national sum of research and development expenditure was recorded in Finland (284.53 applications per 1 billion EUR), for Poland, according to the estimated data, the number of applications was 157.28 per 1 billion EUR of expenditure and placed Poland on 10th position. In the entire European Union, in 2014 this indicator amounted to 199.86 applications per 1 billion Euro of expenditure.

An analogous number of notifications per total research and development expenditure in the enterprise sector places Poland 9th among European Union countries with a value of 337.62 notifications per 1 billion EUR. The highest number of applications per total domestic research and development expenditure in the enterprise sector was recorded in the Netherlands - 469.57.

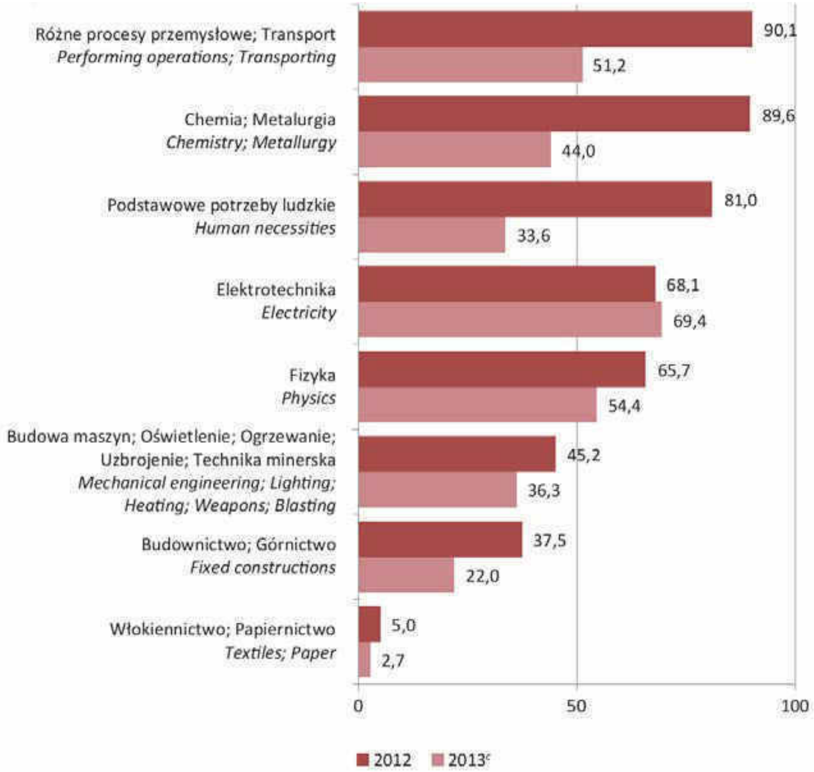

Fig. 12. Applications for inventions made by Polish entities in the European Patent Office by divisions of the International Patent Classification [2].

An interesting situation can be observed in the area of applications to the European Patent Office (Fig. 13), which shows that the number of applications for patent protection of inventions is decreasing each year. According to the authors, this is due to the increasing use of inventors by another form of intellectual property protection - **know how**.

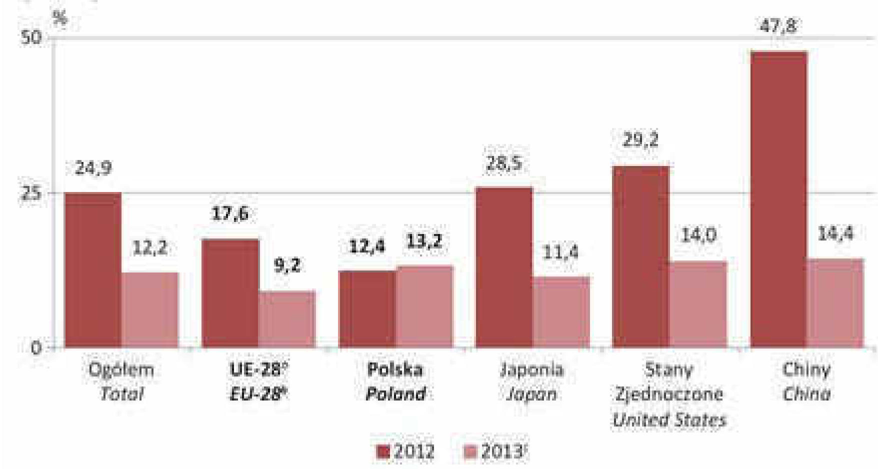

Fig. 13. Percentage of high-tech application to the European Patent Office in 2013 to 2012 [2].

4. Conclusions

The hydraulics and pneumatics market in the last two decades, despite the waves of crisis in 2009 and 2013, the displacement of fluid technology drives by electric drives and unfavourable pro-ecological policy, especially of European countries, is doing well. The reduction of market shares of countries such as Japan, the United States or Germany to China, Brazil or India is due to the globalization of the market and cheap labour. The interest of major players is shifting towards high-technology…

References

[1] Chrostowski, Henryk, Adam Młyńczak, Zygmunt Popczyk, and Jolanta Szadkowska. "Rynek komponentów maszyn roboczych – na przykładzie hydrauliki pneumatyki; Polska a Europa i świat." *Mechanik* 76, no. 8/9 (2004): 544-548.
[2] Roczniki Statystyczne Rzeczpospolitej Polskiej z lat: 2000 do 2018. GUS, Warszawa.
[3] http//www.cetop.org /leer.html.

ISSN 1454 - 8003
Proceedings of 2019 International Conference on Hydraulics and Pneumatics - HERVEX
November 13-15, Băile Govora, Romania

EXTENDABLE REMOTE CONTROLLED PORTABLE BARRIER FOR STOPPING VEHICLES BY CONTROLLED TIRE DEFLATION

Ioan PAVEL[1], Gheorghe ȘOVĂIALĂ[1], Ioan BĂLAN[1], Ana-Maria POPESCU[1]

[1] Hydraulics and Pneumatics Research Institute INOE 2000-IHP, Bucharest; pavel.ihp@fluidas.ro

Abstract: *The article presents equipment for efficient and safe stopping of vehicles with tires, by rapidly expanding a barrier with removable spikes on the transverse direction of the road on which the target vehicle moves, thus causing controlled puncturing and deflation of at least one of its tires, on crossing the barrier. Afterwards, the barrier is quickly retracted to clear the road and allow access for the vehicles of the intervention crews to the target vehicle. The equipment is provided with mechanical and electrical safety elements which prevent accidental extension of the barrier. The phenomenon of tire explosion is avoided by a special construction of the spikes, provided with controlled air outlet holes.*

Keywords*: Barriers, spikes, extendable barriers, controlled tire deflation*

1. Introduction

The National Strategy for Research, Development and Innovation 2014 – 2020 [1] stipulates that "Social security is based on the development of technologies, products, research capabilities and systems for local and regional security, protection of critical infrastructures and services, "intelligence'', cyber security, internal and citizen security, emergency management and management of security crises, as well as for fighting terrorism, cross-border threats, organized crime, illegal trafficking, and all this has as a background the development of a security culture "; the Strategy supports "increasing the role of science in society. To this end, research and innovation meet the actual needs of the economic environment and the public sector, especially the one to increase the quality of the services offered (such as the health or safety of citizens) ".

In the rapid intervention actions of the gendarmerie, police and army crews aiming to stop target vehicles, worldwide, portable equipment such as extendable spiked barrier is used; they pierce through the tires and produce controlled deflation, causing the vehicle to slow down and stop. Other solutions practiced are the bollards which are visible on the surface but other parts of them are buried 1-2 meters beneath the ground, with a solid foundation. Near them control systems, compressed air systems or hydraulic systems are installed to lift and lower them; they also require control cables, backup generators, monitoring systems, human protection. Such arrangements are expensive and have a permanent character; usually airports, embassies and other military targets are protected in this manner. For example, a post of 0.8 meters requires a foundation of 1.2 meters, as well as all the control piping, and the posts must be installed every meter. Barriers need a similar space beneath the ground and a solid foundation, depending on the retraction mode (electric, hydraulic, pneumatic). Installing them for temporary public events is practically impossible.

The presented equipment contributes to the increase of the operability of the intervention crews involved in public order and security missions, by developing specific modern and efficient equipment, creating optimal training conditions for the crew to accommodate with them and assimilate the operational procedures, resulting in implementing a high performance management of emergency situations.

Worldwide there are all kinds of systems for restricting access or forcibly stopping cars, generally at fixed points that require excavation and assembly work. This type of extendable / retractable spiked barrier does not require such work, and it is easy to install and use.

Interests in the field of this type of equipment date from 1986, when the American company Phoenix International Ltd produced the extendable / retractable ramp with puncturing spikes and manual operation, called MagnumSpike™ [2].

Other companies with activity in the field are: Dyna Systems, Stinger Spike [3] and Federal Signal Stinger (USA) [4], Gold Deer (China), Trakya (Turkey).
DynaSpike system patented in the United States (Fig. 1) consists of the extendable / retractable platform hinged scissors-type, equipped with tire puncturing elements (spikes), pneumatic extension / retraction system, compressor for compressed air supply, electronic remote control system, protection cover of the extendable platform.

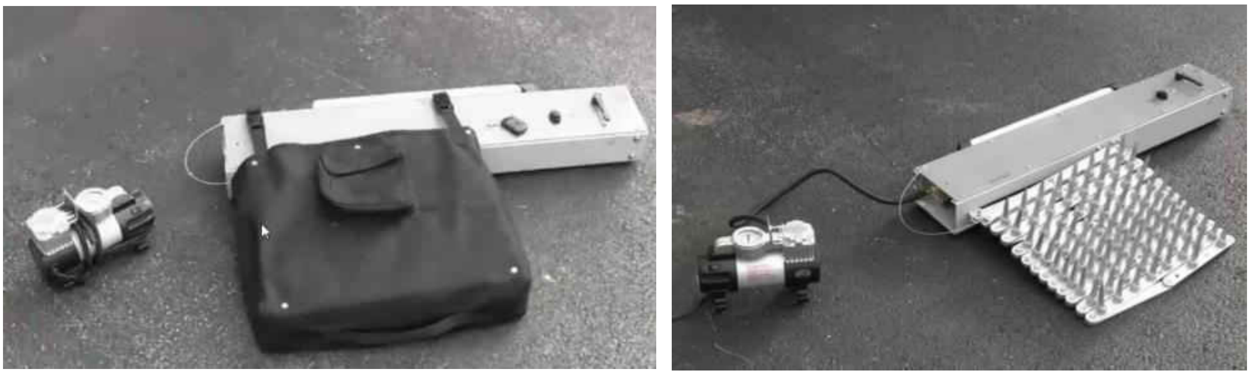

a. b.

Fig. 1. DynaSpike system patented in the United States [3]

At national level, the issue of producing a piece of equipment of type extendable / retractable spiked barrier, usable in public order and security missions, is raised for the first time.

2. The solution presented

The equipment presented is a novelty at the national level, as this product was not in the attention of the R&D entities or the productive industrial units, nor has it been manufactured so far in Romania.
In the presented version, the product “Extendable, remote controlled portable barrier for stopping vehicles by controlled tire deflation” is similar in purpose and principle of operation with the system DynaSpike, but it is based on own solutions regarding the actuation, shape and attachment of the spikes, the safety elements, etc.

Fig. 2. Extendable, remote controlled portable barrier for stopping vehicles by controlled tire deflation

The equipment is structured on three subassemblies:

1. Electro-pneumatic drive system
2. Extendable / retractable platform
3. Electronic control system

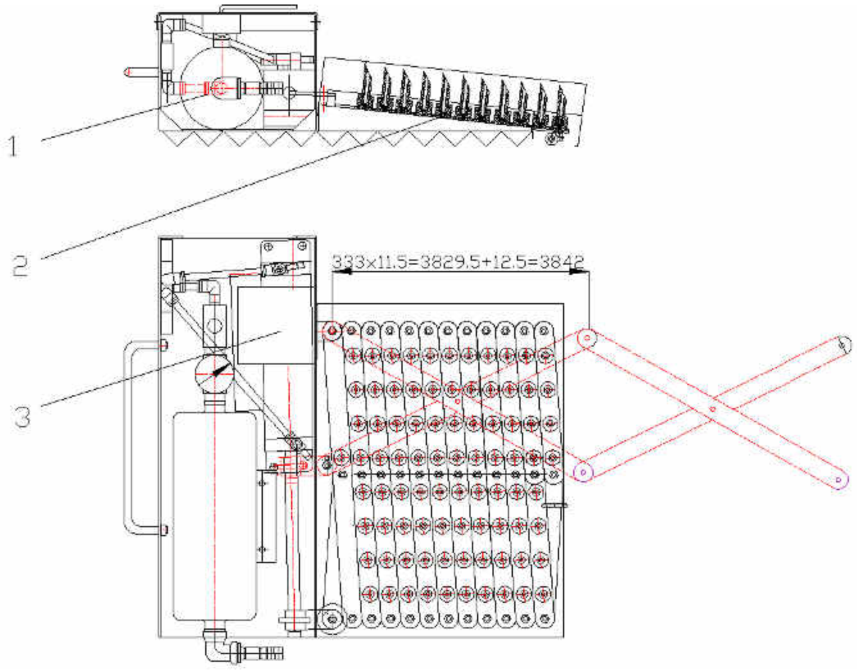

Fig. 3. Structure of the equipment type extendable, remote controlled portable barrier for stopping vehicles by controlled tire deflation

2.1 The electro-pneumatic drive system for extension / retraction includes the accumulator, the double acting pneumatic actuator, the safety valve, the solenoid valve, fast air discharge devices and loading valve [5]. The operating principle is shown in the pneumatic diagram in figure 4: valve (1) allows the accumulator (2) to be charged with compressed air at the pressure of 10 bar, registered on the pressure gauge (3). The safety tap valve (4) allows air supply to the solenoid valve (5) which drives the cylinder (7) to which one of the branches of the hinged bars of the extendable platform is connected. At maximum extension, the platform covers at least one traffic lane (3.5 m).

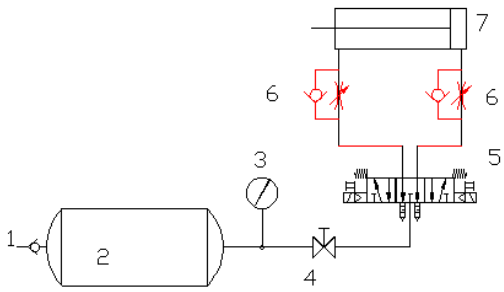

Fig. 4. Pneumatic diagram of extendable barrier [6]
1-valve; 2-compressed air tank; 3-pressure gauge; 4-safety tap valve; 5-solenoid valve; 6-throttles; 7-pneumatic cylinder

The pneumatic accumulator, initially charged at a pressure of 10 bar, stores enough air to perform a complete platform extension / retraction work cycle [7].

The double acting pneumatic actuator has the liner fastened to the housing and the rod - at the free end of one of the bars of the first deformable parallelogram. The rod stroke is correlated with the extension of the platform.
The solenoid valve, connected to the electric accumulator by an on / off safety button, provides pressurized air supply to the piston / rod chambers of the actuator, for the purpose of extension / retraction of the platform.
A safety valve type lever ball tap valve is mounted between the pneumatic accumulator and the solenoid valve on the pressure circuit to avoid accidental operation of the equipment.

2.2 The extendable platform

The hinged bars of the platform are made of spring steel, which gives them resistance and elasticity, avoiding the occurrence of remanent deformations at the impact with the tires of the target vehicle. On the upper bars of the parallelograms the penetrating spike bearing seats are arranged (8 on each bar, a total of 84 pieces). The free ends of the first deformable parallelogram are connected to the equipment housing - one, and to the pneumatic actuator rod – the other.

Fig. 5. Extendable platform

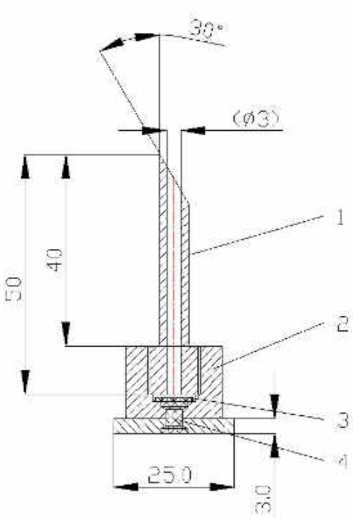

Fig. 6. Spike – spike bearing assembly

Inside the spike bearing seat (2) (Fig. 6) a neodymium magnet Ø 8x1 (3) is bonded; it has a power of about 410 g and keeps the spike (1) in position during transport and extending of the platform; when piercing occurs it is released without dragging the platform. The spike bearing seats (2) are fastened with bolts (4) to the hinged bars.

2.3 The electrical system provides the following functionalities:
Actuation of the electro-pneumatic directional control valve;

- Radio actuation, from a maximum distance of 200 m, of the electromagnets of the electro-pneumatic valve;
- Operation of the electrical system outdoors, at ambient temperatures in the range -20°C…+50°C.

The power supply of the electrical system is provided by an accumulator, which ensures a voltage of 12Vdc, at a capacity of 7Ah, type sealed accumulator with control valve (Valve Regulated Lead Acid – VRLA or Sealed Lead Acid – SLA) which can work in any position, since the electrolyte is of type gel absorbed in a porous material.
The radio actuation and operation of the electro-pneumatic directional control valves is provided by a radio control kit consisting of a receiver unit with two-channel antenna and a remote control with 2 buttons. The control outputs of the coils of the directional control valves are on the relay, with the possibility of programming each output for monostable or bistable type operation [8].
The components of the electrical installation, pneumatic installation and remote control system are located inside the equipment housing.

3. Sizing of the system [9]

The Fc force in the pneumatic cylinder rod breaks down into two forces: F_h force, which acts in the direction of the longitudinal axis of the platform, and F_b force, which acts in the direction of the bars (Fig. 7).

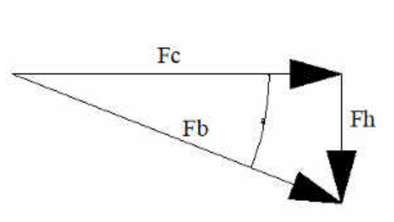

Fig. 7. Fc force in the pneumatic cylinder rod

F_h force, which is the useful force in the extension / retraction of the platform, is given by the equation:

$$F_h=F_c\cdot tg\alpha \quad (1)$$

where α is the angle formed by the bar with the housing, and it varies from the value of 4^0 for the retracted position (the bars completely folded) to the value of 62^0 for the extended barrier position.
The friction force required to extend the barrier, $F_{h\mu}$, is given by the equation:

$$F_{h\mu}=\mu\cdot G_b \quad (2)$$

where μ is coefficient of friction between steel and asphalt, and G_b is barrier weight (set consisting of bars, screws, washers, nuts, spikes and spike bearing seats).

$$G_b=m\cdot g \quad (3)$$

where m is mass of the barrier components, [kg], and g - gravitational acceleration, [m/s^2].
The friction force is determined by the equation:

$$F_{h\mu}=\mu\cdot m\cdot g=0.6\cdot 10.575\cdot 9.81=62.25\ N=6.225\ daN \quad (4)$$

1 [N]=1[kg·m/s^2]
Pneumatic cylinder with 50 mm piston diameter for 10 bar working pressure develops an axial force as calculated by (5)

$$F_c=p\cdot A=10\cdot\pi\cdot d^2/4=10\cdot 3.14\cdot 5^2/4=196.25\ daN \quad (5)$$

The force required to start the action of extending the barrier is:

$$F_h=F_c\cdot tg\alpha=196.25\cdot tg4^0=196.25\cdot 0.0699=13.71\ daN \quad (6)$$

$$F_h=13.71> F_{h\mu}=6.225 \text{ daN} \tag{7}$$

The point of articulation of the first parallelogram to the equipment housing can be placed in a favorable position to extend the barrier; the angle α has a decisive role in terms of the value of the useful force F_h.
For example, for an angle of 6^0, thought as acceptable when building the platform, the value of the useful force is 20.6 daN.
Capable force for a 50 mm cylinder:

$$F = p \cdot A = 10 \cdot \frac{\pi \cdot d^2}{4} = 10 \cdot \frac{\pi \cdot 5^2}{4} = 196.25\ daN \tag{8}$$

The air accumulator (compressed air tank)
For a 200 mm stroke, the volume of air required to drive the cylinder is:

$$V = A \cdot c = \frac{\pi \cdot d^2}{4} \cdot c = \frac{\pi \cdot 5^2}{4} \cdot 20 = 392.5\ cm^3 \tag{9}$$

4. Experimental results

The equipment (Fig. 8) was tested under real operating conditions, and the results were at the level of expectations.

Fig. 8. Equipment subjected to operational testing

At each passing of the car over the extendable remote controlled portable barrier for stopping vehicles by controlled tire deflation at least two tires were pierced through by at least 3 spikes (Fig. 9). Tire deflation was controlled through the holes in the spikes, and no danger of accident was noticed, either for the driver or for the car. On the other hand, penetration of the tires forced slowing down the speed of the car and stopping the car.

Fig. 9. Sequences from operational tests and the effect of using the extendable barrier

Fig. 9. Sequences from operational tests and the effect of using the extendable barrier (continuation)

The system has demonstrated its role and efficiency of use in emergency situations.

References

[1] https://www.edu.ro/sites/default/files/_fi%C8%99iere/Minister/2016/strategii/strategia-cdi-2020_-proiect-hg.pdf.
[2] https://magnumspike.com/nationalspikes/wp-content/themes/1e/pdf/tire-deflation-brochure.pdf.
[3] https://www.dynaspike.com/.
[4] https://www.fedsig.com/product/stinger.
[5] Avram, Mihai. *Actionari hidraulice si pneumatice. Echipamente si sisteme clasice si mecatronice / Hydraulic and pneumatic drives. Classic and mechatronic equipment and systems.* Bucharest, University Publishing House, 2005.
[6] Festo Romania – Products. https://www.festo.com/cat/ro_ro/products_MTR_DCI.
[7] INOE 2000-IHP. “Theoretical and experimental study on the improvement of dynamic and energy performance of pneumatic systems in various operating modes, driven with the computer.” <Nucleu> Programme.
[8] Tehno Electric. https://www.tehnoelectric.ro/200-telecomenzi_automatizari_2
[9] Radcenco, Vs., N. Alexandrescu, E. Ionescu, and M. Ionescu. *Calculul si proiectarea elementelor si schemelor pneumatice de automatizare / Calculation and design of pneumatic automation elements and schemes.* Bucharest, Technical Publishing House, 1985.

ISSN 1454 - 8003
Proceedings of 2019 International Conference on Hydraulics and Pneumatics - HERVEX
November 13-15, Băile Govora, Romania

NUMERICAL SIMULATIONS FOR HYDRODYNAMIC TORQUE DETERMINATION IN CASE OF FIXED OSCILLATING WAVE ENERGY CONVERTERS

Daniel Vasile BANYAI[1], Ioan Lucian MARCU[2], Dan OPRUȚA[3]

[1] Technical University of Cluj-Napoca, daniel.banyai@termo.utcluj.ro

[2] Technical University of Cluj-Napoca, lucian.marcu@termo.utcluj.ro

[3] Technical University of Cluj-Napoca, dan.opruta@termo.utcluj.ro

Abstract: *Due to their low impact and high power flux, wave energy converters have unrivaled potential. Studies and research are needed, that will lead to the development of more efficient and low maintenance equipment. The paper presents the mathematical model for determining the total torque (hydrodynamic plus inertial) respectively the forces and speeds that can be transmitted to an electric generator, from a wave energy converter of Fixed oscillating wave surge, type. The mathematical model was transposed into Matlab Simulink and simulated in this environment, and the results obtained will be compared with experimental results in another paper.*

Keywords: *Renewable energy; wave energy; mathematical model.*

1. Introduction

With a power flux of 2…3 kW/m^2 resulting from the action of wind energy (0.4…0.6 kW/m^2) which in turn comes from solar energy (0.1…0.3 kW/m^2), the wave energy capture (WEC) systems, have become increasingly studied in the last period, being part of the renewable energy sources [1]. There are several categories of wave energy converters classified according to their operating principles, into: attenuators, point absorbers, oscillating wave surge converters (OWSC), oscillating water columns (OWC), terminators or submersed pressure differential devices, according to [2,3]. The principle sketches are shown in Figures 1 and 2.

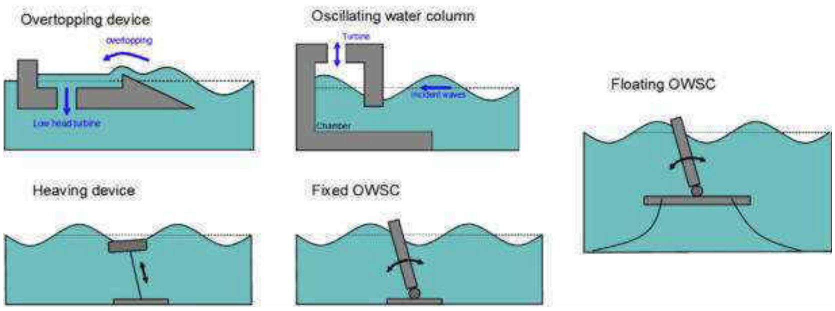

Fig. 1. Wave energy converters classification by [2]

Fig. 2. Wave energy converters classification by [3]

In figure 3 is presented the Capture Width Ratio (CWR), $CWR = \frac{Absorbed\ power}{Incident\ power \cdot Device width}$, for the existing wave energy converters.

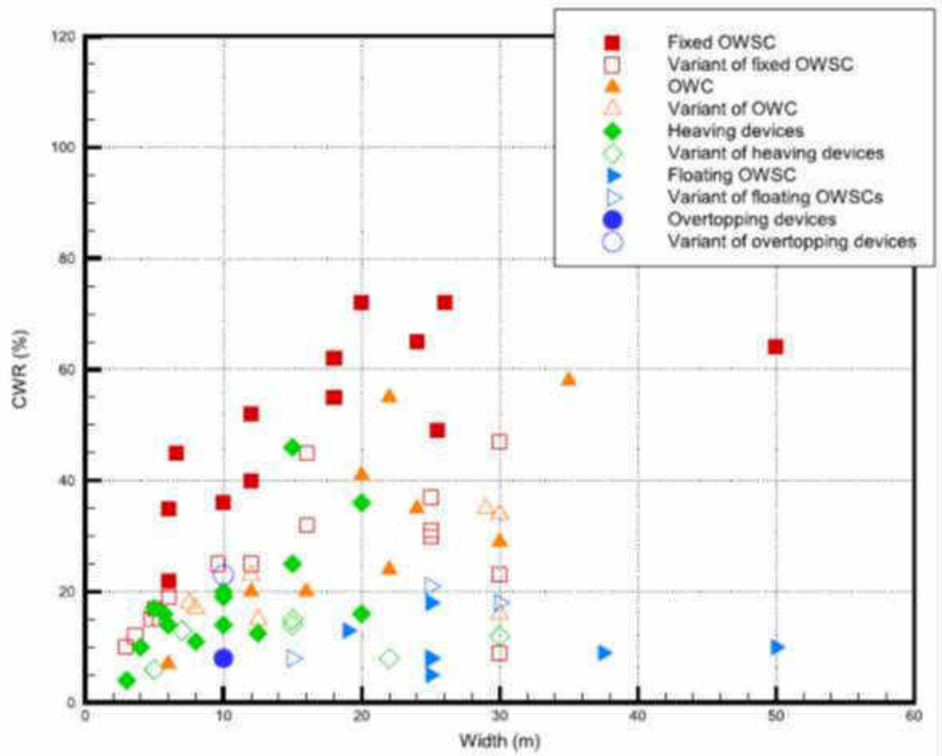

Fig. 3. Fraction of wave power flowing through the device that is absorbed versus Width of the WEC by [3]

However, wave energy technology is still in the research and development stage. Therefore, levelized energy cost for Wave Energy Converters designs is still high, compared to other renewable energy technologies, such as wind and solar [4].

To identify the devices of interest, eventually closest to commercial applicability, several are the aspects that need to be considered and to serve as basis to classify the existing devices, as several are the key aspects contributing to the technical and economic feasibility and success of a project. The main aspects are: the dynamics of the device and the principle according to which it interacts and extracts energy from waves (Power Take Off); the mooring and station keeping characteristics. Furthermore, aspects like building, installation and maintenance are also important for decision making. [5]

Because the Fixed OWSC systems have the highest CWR, the present paper refers to the development of a mathematical model for predicting the behavior of vertical flap structures in wave conditions, for this category of wave energy converters. Thus, being able to simulate, still at the concept level, the forces, respectively the power exerted by waves on the system. Power Take-Off (PTO) system, which can be: Hydraulic motor; Hydraulic turbine or Linear generator, is not the subject of the present work.

The theory of linear flow potential has proven to be successful in anticipating the behavior of devices under different practical conditions. This theory of potential linear flow can be used to describe fluid flow, by applying the conditions that exist at the boundary of the fluid domain. Thus, this theory is also applicable in the case of wave energy converter with vertical flap. When analyzing the waves, some assumptions are taken into account, namely that the fluid is incompressible and irrotational. Applying the law of mass conservation and Laplace's equation to the fluid imposes the incompressibility of the fluid. Due to the fact that the fluid is irrational, it allows simplifying the expression of the flow velocity as a gradient of a scalar potential, Φ, called velocity potential.

Another simplification is made by asserting that the radiated wave field can be described as the overlap of the waves created by each of the six degrees of freedom of an oscillating body.

2. Mathematical model

To design, analyze and optimize the wave energy converters, the mathematical model has an essential role, being able to develop and manipulate the configuration of the system at the virtual level with significantly lower costs compared to the physical prototype. The resulting virtual system can be analyzed and optimized, in this phase, until it meets the required criteria.
The sketch of the WEC studied in this paper, based on which the mathematical simulation model is developed for determining the forces, displacements and speeds, is shown in Figure 4.

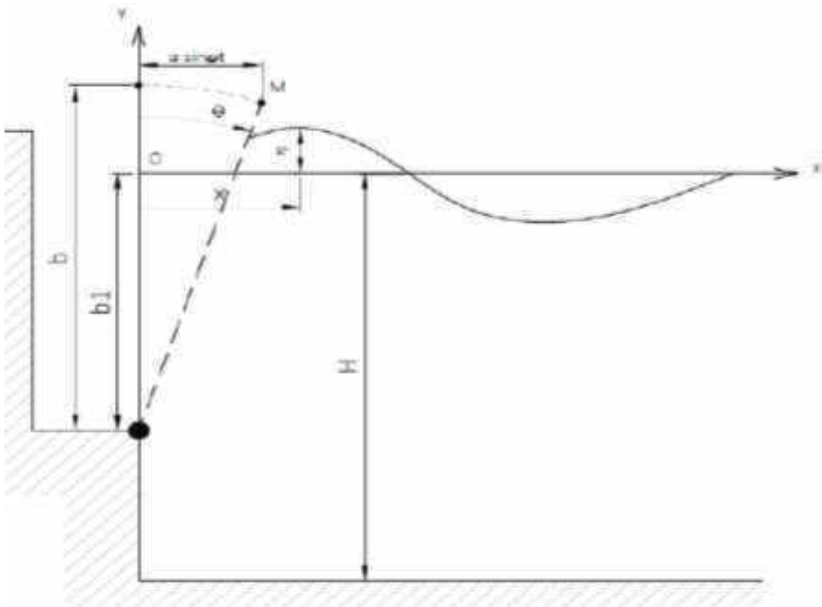

Fig. 4. 2D model for Vertical flap WEC

In order to determine the hydrodynamic moment, one starts from a function of potential of the water movement speed, Φ, which generates the movement of the flap, defined as follows:

$$\Phi = \frac{2a\omega}{b}\left\{\frac{\left(\frac{b_1\omega^2}{g}-1\right)\cosh k_0H+\cosh k_0(H-b_1)}{k_0^3\left(H+\frac{g}{\omega^2}\sinh^2 k_0H\right)}\sin(\omega t-k_0x)\cosh k_0(y+H)-\right.$$
$$\left.-\cos\omega t\sum_{m=1}^{\infty}\frac{\left(\frac{b_1\omega^2}{g}-1\right)\cosh k_mH+\cosh k_m(H-b_1)}{k_m^3\left(H-\frac{g}{\omega^2}\sin^2 k_mH\right)}e^{-k_mx}\cos k_m(y+H)\right\} \quad (1)$$

where: H-water depth; b - height of the flap; b_1 - the distance from the pivot point of the flap to the free surface of the water; a - the amplitude of the movement of the highest point of the flap; θ - angular displacement of the flap; ω - angular velocity of the flap; η - water elevation; B - the width of the flap; g - gravitational acceleration; k_0 and k_m are the roots of equations (2), respectively (3):

$$k_0 \tanh k_0H = \frac{\omega^2}{g} \quad (2)$$

$$-k_m \tan k_m H = \frac{\omega^2}{g} \tag{3}$$

The hydrodynamic force, F, is obtained by summing the forces given by the instantaneous pressure on each unit of area on the flap.
The hydrodynamic torque is obtained by multiplying by the force with distance.

$$M_H = \int_{-b_1}^{0} Bp(b_1 + y)dy \tag{4}$$

The value of the pressures is obtained from the relation:

$$p = \rho\left(\frac{\partial\phi}{\partial t}\right)\Big|_{x=0} - \frac{q^2}{2}\rho - \Omega\rho \tag{5}$$

where: q - the velocity of the water particle; Ω=g·y - the gravitational potential.

Substituting (5) into (4), we obtain: $\frac{M_H}{B\rho} = \int_{-b_1}^{0}(b_1 + y)\left\{\left(\frac{\partial\phi}{\partial t}\right)\Big|_{x=0} - \frac{q_{x=0}^2}{2} - \Omega\right\}dy$ (6)

$$\left(\frac{\partial\phi}{\partial t}\right)\Big|_{x=0} = \frac{2a\omega}{b}\{A\cosh k_0(y+H)\cos\omega t + \sin\omega t\sum_{m=1}^{\infty}B_m\cos k_m(y+H)\} \tag{7}$$

$$q_{x=0}^2 = \left(\frac{\partial\phi}{\partial x}\right)^2\Big|_{x=0} + \left(\frac{\partial\phi}{\partial y}\right)^2\Big|_{x=0} \tag{8}$$

$$\left(\frac{\partial\phi}{\partial x}\right)\Big|_{x=0} = \frac{2a\omega}{b}\{-Ak_0\cosh k_0(y+H) + \sum_{m=1}^{\infty}k_m B_m\cos k_m(y+H)\cos\omega t\} \tag{9}$$

$$\left(\frac{\partial\phi}{\partial y}\right)\Big|_{x=0} = \frac{2a\omega}{b}\{Ak_0\sinh k_0(y+H)\sin\omega t + \sum_{m=1}^{\infty}k_m B_m\sin k_m(y+H)\cos\omega t\} \tag{10}$$

where,

$$A = \frac{\left(\frac{b_1\omega^2}{g} - 1\right)\cosh k_0 H + \cosh k_0(H - b_1)}{k_0^3\left(H + \frac{g}{\omega^2}\sinh^2 k_0 H\right)} \tag{11}$$

$$B_m = \frac{\left(\frac{b_1\omega^2}{g} - 1\right)\cosh k_m H + \cosh k_m(H - b_1)}{k_m^3\left(H - \frac{g}{\omega^2}\sin^2 k_m H\right)} \tag{12}$$

Substituting (9) and (10) into (8) we obtain:

$$q_{x=0}^2 = \left(\frac{a\omega}{b}\right)^2\left\{(b_1 + y)^2\cos^2\omega t + b_1^2\,\mathrm{sech}^2\frac{\omega^2 H}{g}\sinh^2\frac{\omega^2(H+y)}{g}\sin^2\omega t\right\} \tag{13}$$

Thus, the expression for the hydrodynamic moment is obtained by replacing relations (7) and (13) in relation (6):

$$M_H = B\rho\frac{a}{b}\omega^2\left\{2A\left[\frac{b_1}{k_0}\sinh k_0 H - \frac{1}{k_0^2}(\cosh k_0 H - \cosh k_0(H - b_1))\right]\cos\omega t + 2\left[\sum_{m=1}^{\infty}B_m\left[\frac{b_1}{k_m}\sin k_m H - \frac{1}{k_m^2}(\cosh k_m H - \cosh k_m(H - b_1))\right]\right]\sin\omega t - \frac{a}{8b}b_1^4\cos^2\omega t + \frac{1}{6}\cdot\frac{gb_1^3}{\frac{a}{b}\omega^2} + \frac{a}{8b}b_1^2\,\mathrm{sech}^2\frac{\omega^2 H}{g}\left[b_1^2 - \frac{gb_1}{\omega^2}\sinh\frac{2\omega^2 H}{g} + \frac{1}{2}\left(\frac{g}{\omega}\right)^2\left(\cosh\frac{2\omega^2 H}{g} - \cosh\frac{2\omega^2(H - b_1)}{g}\right)\right]\sin^2\omega t\right\} \tag{14}$$

The moment of inertia is determined with the relation:

$$M_I = \frac{I}{g}\frac{\partial^2\theta}{\partial t^2} = \frac{I}{g}\frac{a}{b}\omega^2 \sin \omega t \quad (15)$$

where I - the mass moment of inertia.

3. Simulations results and Conclusions

For solving the equations numerically, it can be used Matlab / Simulink environment, with which it can easily model, simulate and optimize the mathematical system.
The input data for the type of wave energy converter studied in this paper (the dimensions are applicable to an experimental model):
a=1 m; b=3.892 m; b_1=2.897 m; B=0.7 m; ρ_{water}=1020 kg/m^3; b_y= 1,754 m;
g=9,8 m/s^2; H=3.892 m; ω_{max}= 10 °/s = 0.17453 rad/s.

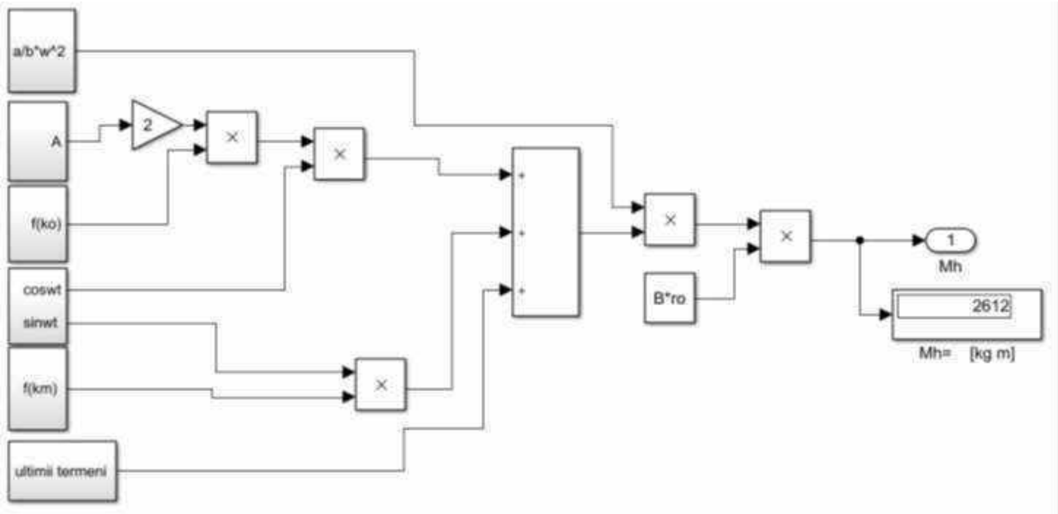

Fig. 4. Simulink model for Hydrodynamic moment (contains 6 subsystems)

The total resistive moment consists of the hydrodynamic moment and the moment of inertia of the entire flap assembly, as follows:

$$M_T = M_H + M_I \quad (16)$$

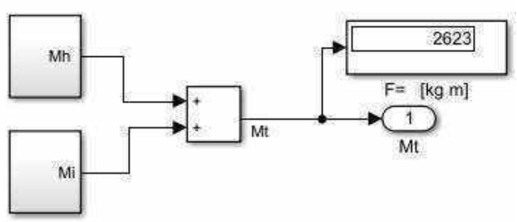

For these types of energy capture systems, the energy transfer can be done with hydraulic cylinders, so it is necessary to know the total resistance force that can act on the cylinder. From the expression of the total resistant moment, determine the resistant force using the equilibrium relation of the forces at the point of pivot of the pallet as follows:

$$F \cdot b_y = M_T \quad (17)$$

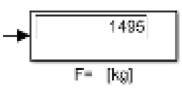

where F, is the resistive force and b_y - the distance between the pivot point of the flap and the center of the rotating coupling between the cylinder rod and the flap).

Due to the high speed with which the expected results are obtained, in the case of numerical modeling and simulation, it is also proved with these applications that when developing new systems, the possibility of optimization offered by numerically simulated mathematical models makes them a very favorable technical-economic solution.

It is further proposed to study the possibilities of energy transmission from the Fixed OWSC, through pressurized liquids, to hydraulic turbines or motors. For these systems, besides energy efficiency, the control strategy is very important, which must be able to transmit all the energy captured from the waves to the electric generator.

References

[1] Passoni, Giuseppe, Giambattista Gruosso, Silvia Bozzi, Renata Archetti, Adrià Moreno Miquel, and Alessandro Antonini. “Energia da onda nell'offshore italiano: tecnologie a confronto.” Paper presented at the “ENERGIA DAL MARE” University Parthenope, Napoli, Italy, 2016.

[2] Triasdian, B., Y.S. Indartono, N.S. Ningsih, and D. Novitasari. „Device Selection of the Potential Wave Energy Site in Indonesian Seas.” 3rd International Conference on Energy and Environmental Science, IOP Publishing. doi:10.1088/1755-1315/291/1/012040. 2019.

[3] ***https://wave-energies.weebly.com/types-of-wec.html#. Accessed September 2019.

[4] Yu, Yi-Hsiang, Nathan Tom, and Dale Jenne. “Numerical Analysis on Hydraulic Power Take-Off for Wave Energy Converter and Power Smoothing Methods.” Paper presented at the 37th International Conference on Ocean, Offshore, and Arctic Engineering, Madrid, Spain. NREL/CP-5000-71078. 2018.

[5] Pietra, L., M. Tello, J. Bhattacharjee, and C. Guedes Soares. “Review and classification of wave energy converters.” Centre for Marine Technology and Engineering (CENTEC), Instituto Superior Técnico, Lisboa, Portugal. doi: 10.1201/b12726-82. 2012.

ISSN 1454 - 8003
Proceedings of 2019 International Conference on Hydraulics and Pneumatics - HERVEX
November 13-15, Băile Govora, Romania

POSSIBILITIES AND CHALLENGES ON THE FIELD OF WATER HYDRAULICS

Franc MAJDIČ[1]

[1] University of Ljubljana, Faculty of Mechanical Engineering, franc.majdic@fs.uni-lj.si

Abstract: *A clean and healthy environment must be an increasing priority. Different kinds of hydraulic fluids are in use nowadays. Unfortunately, the majority of them are harmful. The use of tap water as a hydraulic-pressure medium is one of the possible solutions. This study presents the research and development of different hydraulics components. Every research of a new water-hydraulic component starts with basic tribological investigations of different material pairs and their surfaces. Then, the design and calculations of the hydraulics characteristics, the production of a prototype and its experimental investigations follow. The following water-hydraulic components were developed, researched and analysed in our laboratory: proportional control valve, hydraulic cylinder, piston pump, hydraulic accumulator, check valve and hydraulic motor.*

Keywords: *Water hydraulics, tribology, components, system*

1. Introduction

Water hydraulics is an old way of technical science, but it is still in beginning of development. Oil hydraulics is phenomen for use of mineral oil as a pressure medium. It is widely in use, more than 80 % of hydraulic system has mineral oil. In 1990's were some researches start to revive environmental friendly water hydraulics [1-3]. The main challenges to use water as a hydraulic pressure medium are right material pairs. A lot of tribological experts worldwide have investigated lubrication and wear properties of different material pairs in water [4-6]. For any research of water hydraulics in real-scale components, home-made components and test rigs are required, because they do not exist on the market. However, this is associated with costs and technical problems. The much lower viscosity of water compared to oil causes a high rate of leakage with clearances typical for oil, while reduced clearances result in excessive wear and high friction. Higher working temperatures, which are still common for oil hydraulics, i.e., around 70 or 80 °C, are hardly acceptable for water in hydraulic systems because of the evaporation at local contact spots [7]. In water, micro-organisms develop with time. This causes several problems with chemical changes to the water and the growth of algae, which results in sediments. The tribological properties of conventional materials (stainless steel) in water are unfavourable, while comparable material selection is poor, and their properties are unknown. For example, a new class of high-potential diamond-like-carbon materials [8-10] that showed excellent properties in a variety of conditions that are in many ways comparable to those in water hydraulics have not been investigated in detail for this application yet. Furthermore, another class of materials that has already confirmed excellent properties suitable also for water [11-13], i.e. ceramics, are probably too brittle for the required dynamic conditions in water hydraulics or are too expensive for precise manufacturing [14], but this has not been investigated either. Corrosion and cavitation are other well-known problems related to tribological performance and the life-time of components. Therefore, research into the chemical and tribological properties that affect the life and performance, as well as the dynamic characteristics, of water hydraulics, are required for the successful development of new components, which is necessary for the wider use of the water in power control hydraulics.

2. Tribological aspect of sliding contacts lubricated with water

As mentioned, special material pairs should be use in water hydraulics. Before we made prototypes of water hydraulics components, preliminary tribological tests of different material pairs have been done.

2.1 Test rigs

Different tribological test rigs are available. We have used two of them, pin-on-disc and ball-on-flat standard test rig.

Pin-on-disc

First tests were performed in a pin-on-disc apparatus (CSEM, Switzerland) with uni-directional sliding between the disc and the pin, see Figure 1.a. The relative sliding velocity was 0.1 m/s and a load of 1 N was applied (Fig. 1.b), which corresponded to 40-70 MPa of initial contact pressure, depending on the material pair. In the open literature [4-5], data are available for some selected polymeric materials at lower pressures, but our goal was to investigate the higher-end load-region of those materials. Tests were run for 370 m of total sliding distance. All the tests were performed in a cup with distilled water at around 21ºC, i.e. at room temperature conditions. These conditions correspond to a boundary lubrication regime, where hydrodynamic effects are negligible and the tribological performance depends primarily on surface and interface phenomena. Friction was monitored during the test and wear loss of the disc materials was subsequently calculated. The first empirical friction and wear results are presented in Figure 5 respectively. At present, detailed surface analyses, which would allow determination of wear and friction mechanisms and confident interpretation of the results, are still in progress.


a.

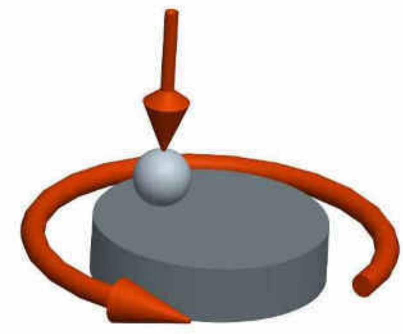
b.

Fig. 1. a) CSEM pin-on-disc, b) testing principle

The next tribological tests were performed using the ball-on-flat testing geometry in a commercially available reciprocating sliding device (Cameron Plint TE77, Figure 2). Loads of 14 N, 40 N and 112 N, simulating those in a hydraulic motor, were applied through a stationary loading system, and this resulted in about 614 MPa, 868 MPa and 1227 MPa of initial maximum Hertzian contact pressure. The stroke was 10 mm and the frequency 5 Hz, which provided 0.1 m/s of relative contact velocity. Prior to the test, the disc was submerged in oil or water before the ball was brought into contact. The calculated Tallian’s lambda value [15] suggested boundary lubrication. Every experiment lasted for 180 minutes. The total sliding distance in each experiment was 1080 m. Every test was repeated three times in a room at ambient temperature. Results of measurement is shown in Figure 6.b.

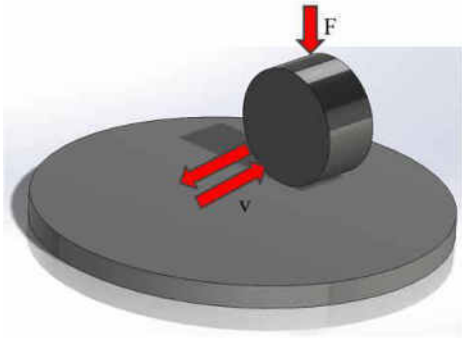

a. b.

Fig. 2. a) Cameron Plint TE77 ball-on-flat, b) testing principle

2.2 Polymer materials

Polymer materials are widely used in mechanical engineering. A wide range of different polymers are available on the market. Advantages of composite polymers are: wear resistance, self-lubrication, low coefficient of friction (COF), good chemical stability, low weight, an easy way to make, etc. Disadvantages of composite polymers are: water absorption, residual tension, less rigidity, higher temperature sensitivity, etc. In combination with steel materials, composites with different inclusions are used to enhance the properties of the base material. Carbon fiber composites are the most commonly used for industrial applications. Carbon based materials have a wide range of mechanical, thermal, electrical and tribological properties suitable for many different applications. Of these, carbon nanotubes, carbon fibers and graphite are the most widely used thermoplastic composites.

Potentially tribological useful polymer/composite materials for water hydraulics are: POM-C, PA66+GF30, PEEK, PEEK+CF30, PEEK+GF30, PTFE, PRFE+CF30, PI, etc. Figure 3 shows differences between water absorption for POM and PA 66 [16]. In this case, POM is much more useful for water hydraulics than PA 66.

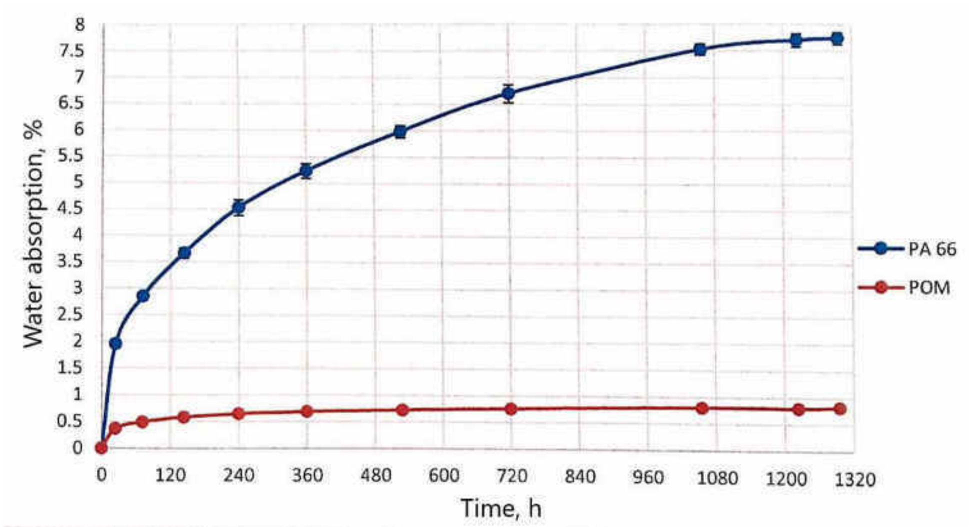

Fig. 3. Water absorption for POM and PA 66 [16]

The available results of wear and friction coefficients are difficult to compare because the authors use different measurement methods. Measurements are influenced by different measurement times, different loads, different applied loads, different temperatures, different sample shapes, different methods of sample preparation, different methods of manufacturing the materials themselves, and different ways of supplying water during the measurements. Figure 4 shows the coefficients of friction (COF) for the polymer materials presented as a function of velocity at different loads. The lowest COF 0,045 were authors [17] found out with composite PEEK450-FC30 against stainless steel AISI630 at 1,66 MPa contact pressure. The highest COF 0,33 were authors [18] found out with composite PPS in contact to Inconel 625 at 5 MPa contact pressure.

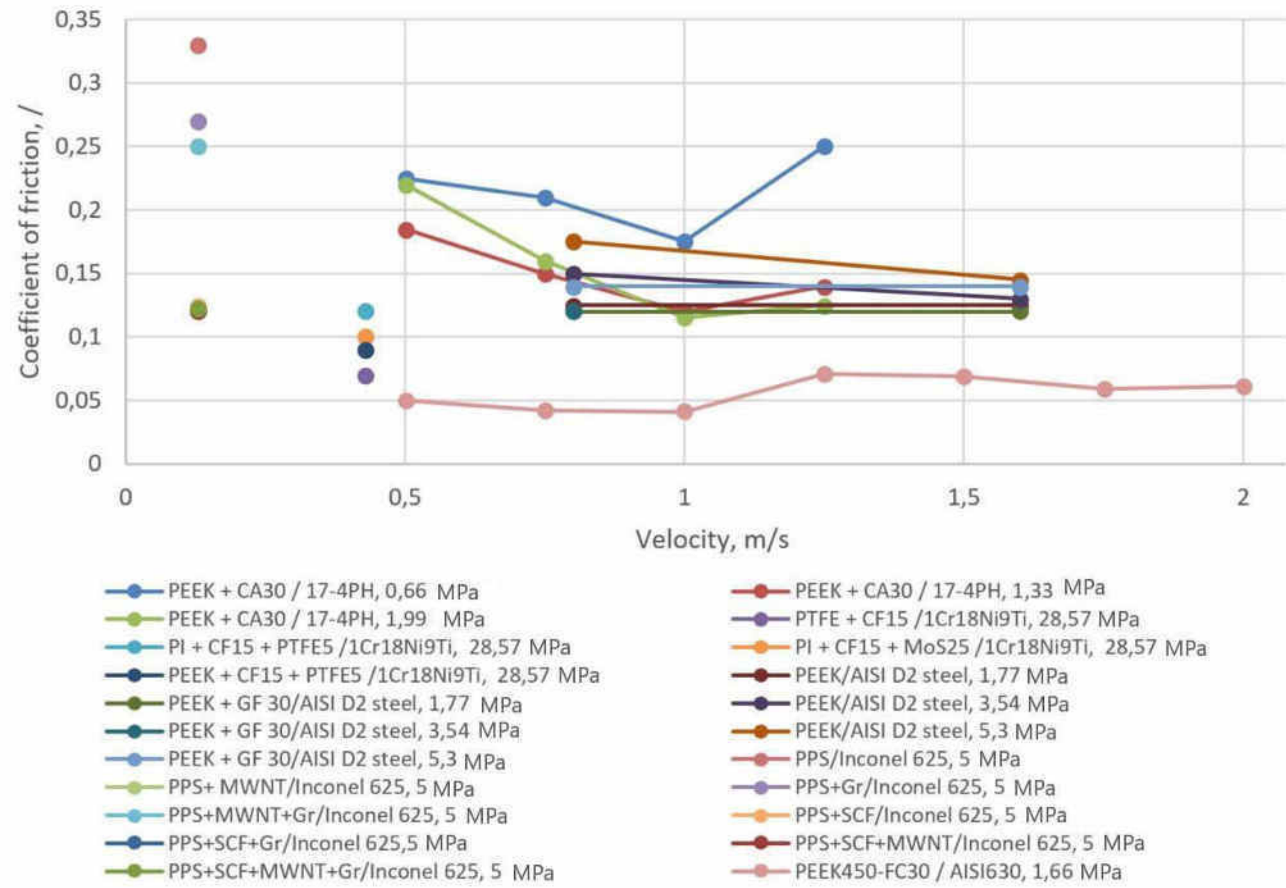

Fig. 4. An overview of tribological results for different polymers in water [17-21]

Our first preliminary results of COF in water on pin-on disc test rig are shown of figure 5. Compared to polymeric materials, significantly higher friction values were measured in contacts with stainless (SS) discs, which were in the range of 0.6-0.8. Other friction data show friction values between 0.13 and 0.28, which is 2-3 times less than with SS discs. With the exception of pure polyimide (SP1), with all other polymer discs, contacts with alumina pins resulted in lower friction than against SS pins. However, these differences were not very high. Nevertheless, it is to be noticed that friction in the polyimide SP1 / SS contact resulted in the second lowest friction – about 0.16. This is important, because the polymeric material contain no additional components and is thus simpler and cheaper. Moreover, the SS pin is also the most preferred counter-material from a practical point of view. The lowest friction in this study was, however, obtained with the PEEK CA30/Al2O3 combination, where friction was about 0.13.

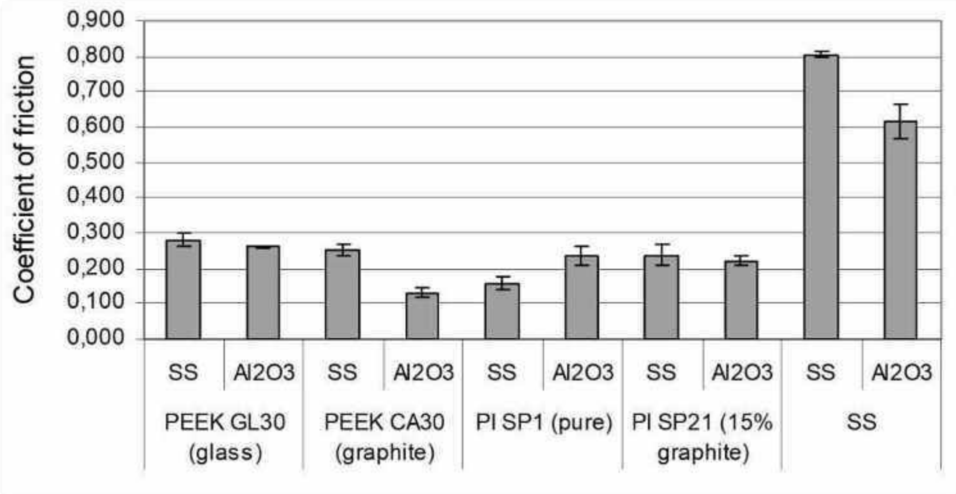

Fig. 5. Coefficient of friction for selected material pairs (SS and Al2O3 pins against four different disc materials is shown)

2.3 Metal materials and coatings

Polymers and even composite materials are not useful for higher loads. With this reasons we made tribological tests on TE77 standardised test rig (Figure 2) with metal materials in contact lubricated with pure water. Figure 6.a shows coefficient of friction (COF) for two similar stainless steels AISI 440C in contact at three different normal forces (14 N, 40 N and 112 N), two different roughness (0,05 µm an 0,2 µm) at hardness of 60 HRc of both materials in contact. The highest COF 0,47 was at load 112 N and roughness 0,05 µm, the lowest COF 0,32 obtained at the same load (112 N) and at roughness of 0,2 µm. Figure 6.b shows the obvious advantage of diamond like carbon coatings (DLC) lubricated with water. The lowest COF 0,058 obtained at maximum load 112 N. It is more than 5-times lower than in contact of AISI440C / AISI440C.

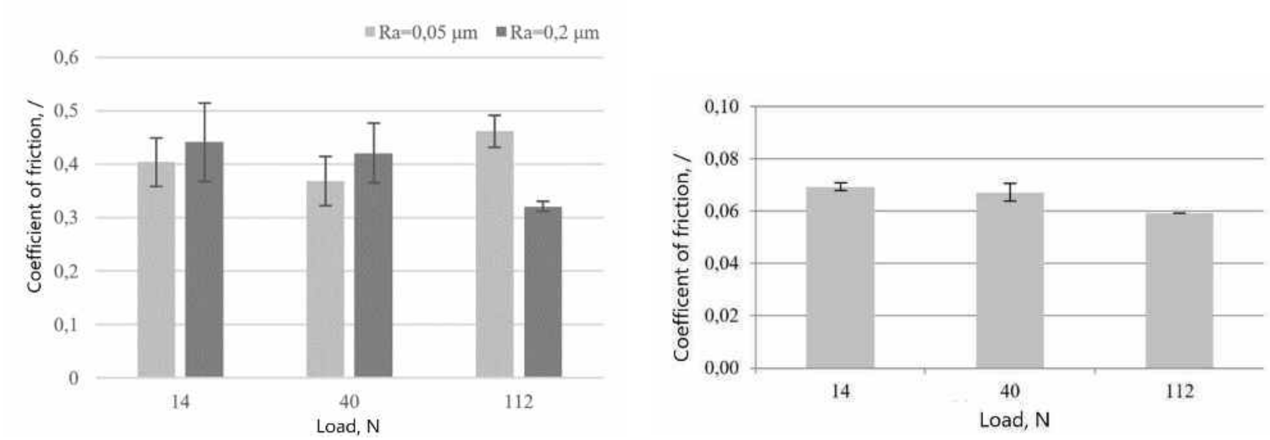

Fig. 6. Coefficient of friction in water a) AISI 440C/AISI440 , b) coating DLC / AISI 440C

3. Water hydraulics components

Laboratory for fluid power and controls from Faculty of Mechanical Engineering University of Ljubljana was start with researches and development on the field of water hydraulic in 2006. Since then, a lot of research and developed several prototypes of water-hydraulic components have been done. Some of them are presented below.

3.1 Directional proportional control valve

High-pressure proportional 4/3 directional spool-sliding control valves are moreover widely used in the oil PCH, but for water PCH they are still almost wholly missing from the market [22]. That was the basic reason for our decision for the research, investigations and development of the new water 4/3 proportional directional control valve (Fig. 7) of the spool-sliding type.

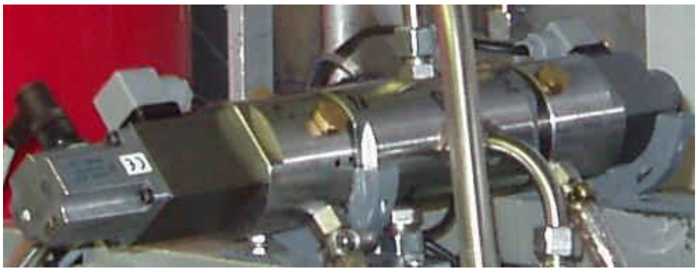

Fig. 7. Prototype of proportional directional control valve for water hydraulics

Fig. 8 shows the results of a long-term lifetime test of a proportional directional valve for water hydraulics. The situations were as follows: single, by-pass filtering, the pressure was 160 bar, the flow was 20 l/min, the frequency was 5 Hz and the water temperature was 40°C. The leakage measured during the lifetime test of the water 4/3 proportional directional control valve oscillated, probably owing to the different positions of the spool (centric/eccentric, turned at different angles inside the sleeve). The measured leakage at the end of the first testing procedure amounted to 0,0825 lpm. The calculated, predicted internal leakage of a similar, oil 4/3 proportional directional control valve should be 0.085 lpm after 2,5 million cycles.

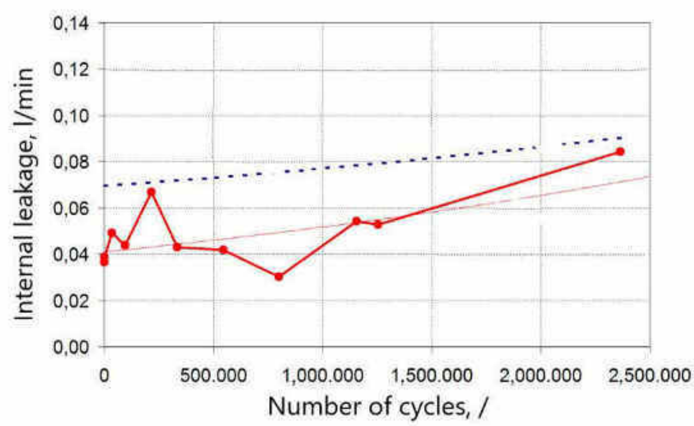

Fig. 8. Results of leakage during long-term tests of proportional water directional control valve

3.2 Light-weight hydraulic cylinder

The purpose of presented research was to find out the wear on the seals installed in a carbon water hydraulic cylinder tube, later referred as a specimen. It contains the results of measurements of the internal leakage (Figure 9.a) through the piston seals of the specimen and the pressures on both sides of the piston. After 30 km of sliding path first signs of wear – internal leakage was found (Fig. 9.a). After 40 km of sliding distance, cylinder was destroyed (Fig. 9.b).

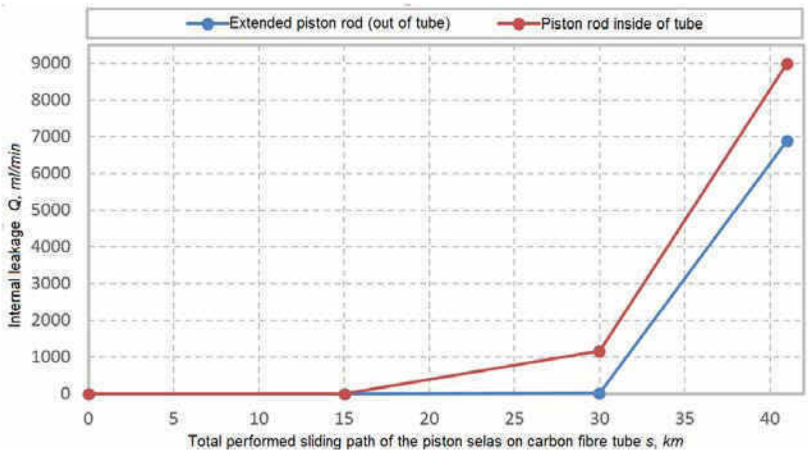

a.

b.

Fig. 9. Results of long-term tests of carbon-fibre hydraulic cyl. tube, a. internal leakage, b) wear

3.3 Hydraulic accumulator

The new water-hydraulic accumulator (Figure 10.a) was designed, manufactured and tested by the Laboratory for Power-Control Hydraulics. This water accumulator was constructed in such a manner that we could easily exchange its seals and/or study the tribological and hydraulic behaviour of the sliding contacts. The hydraulic accumulator with a 4-litres volume allowed a maximum working pressure of 390 bar. A prototype was manufactured and a certificate was acquired from the European Pressure Directive PED 97/23/EC. The piston type of water-hydraulic accumulator consists of the following parts: piston with special seals and guides for gas and water, tube, piston rod, two end-covers, two pressure and two temperature sensors and a displacement sensor for the detection of the piston's position. The necessary additional equipment is a pre-set pressure-relief valve and two manually operated ball valves [23]. Figure 10.b shows the pre-filling pressure effect of nitrogen on the efficiency of the accumulator measured in the water-hydraulic system. As can be seen, in all four cycles (different compression and expansion times) the efficiency rises with an increase of the nitrogen pre-filling pressure.

a.

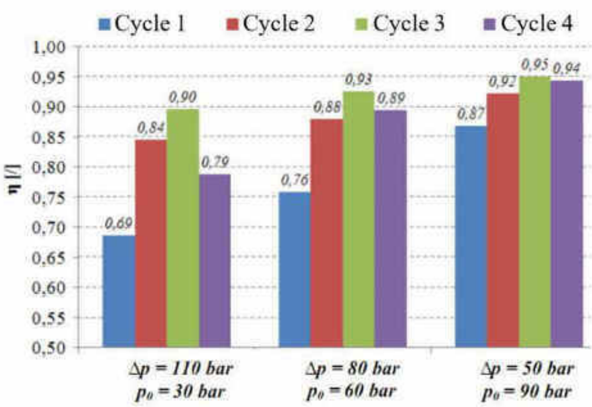

b.

Fig. 10. a) Prototype of a piston-type water-hydraulic accumulator, b) Influences of different nitrogen pre-filling pressures for all four cycles on the water-hydraulic accumulator efficiency

3.5 Check valve

The check valve was designed (Fig. 11.a) in such a way that it can be simply and quickly disassembled [24]. Check valves consist of a housing made from two pieces, seat, closing element, guidance element and spring. The design of the valve allows researchers to experiment with different closing elements (ball, different conical elements, etc.) and different numbers of flow channels (from 1 to 6). Figure 11.b shows the results of the experimental and numerical investigations of the water-hydraulic check valve for fully-opened slots. At a water flow of 60 lpm, 0.35 MPa of pressure drop was measured. The results of the numerical investigations show lower valves.

a.

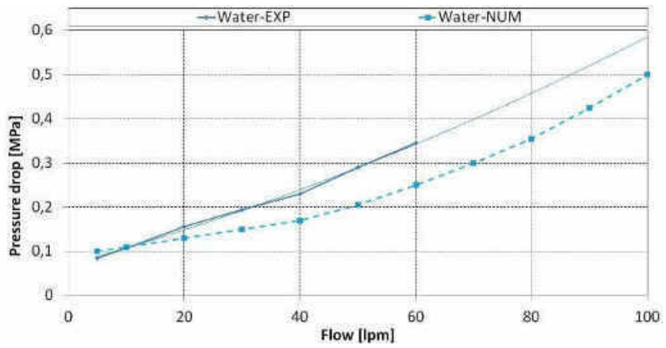

b.

Fig. 11. a) A prototype of the water-hydraulic check valve, b) Comparison between experimental measurement (EXP) and numerical (NUM) simulations for the water check valve

3.6 Hydraulic motor

A low-speed, high-torque, orbital hydraulic motor that converts the energy of a fluid under high pressure into the motion of a shaft of the hydraulic motor was developed. The important mechanical parts of the hydraulic motor are (1) the inner rotor, (2) the floating outer ring, and (3) the gerotor housing, as presented in Figure 12.a. The modified hydraulic motor (steel/DLC contacts) satisfactorily operated for a few hours. The relatively high average total efficiency (up to 12.1%-green field) was observed at the higher rotational speeds, as shown in Figure 12.b, where one circle represents the average total efficiency at a specific operating point regarding the rotational speed and the pressure difference. The measurement included four physical quantities (p, pressure; n, rotational speed; M, torque; Q, flow rate), which are needed to calculate the total efficiency of the orbital hydraulic motor [25].

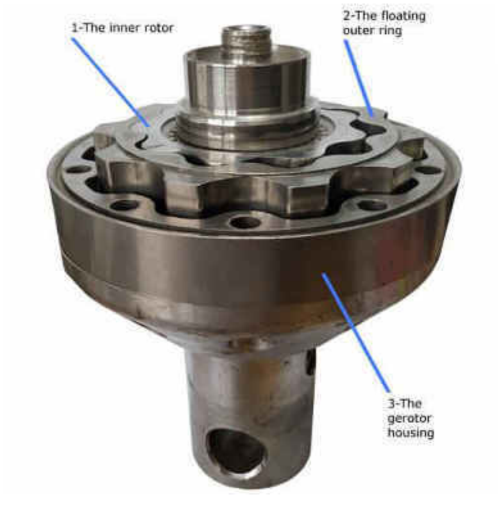

a.

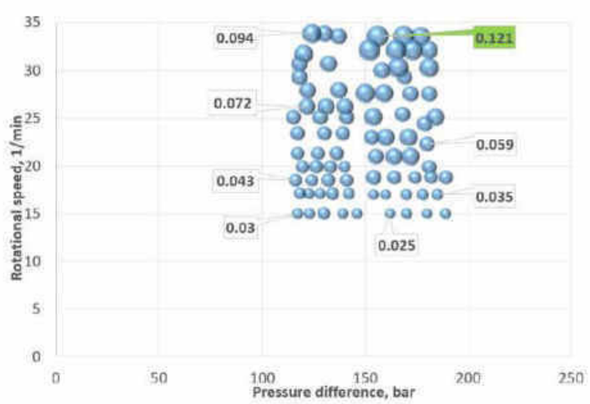

b.

Fig. 12. a) A prototype of a low-speed water-hydraulic motor b) Total efficiency (value in label) of the modified hydraulic motor for water

4. Conclusions

The paper deals with the tribological aspects of water hydraulics. The key results can be summarized as follows:
- the material pair PEEK CA30/AL23 had the lowest coefficient of friction among the tested samples. The coefficient of friction in water was close to 0.1;
- the diamond-like-carbon coating reduced the coefficient of friction in water significantly;
- in-depth research and understanding of the tribological behaviour in different contacts leads to the development of new components in hydraulics (e.g., proportional directional control valve, accumulator, cylinder, check valve, hydraulic motor).

Presented results show that water hydraulics has a lot of possibilities for the further researches and development.

Acknowledgments

For full support of this research author is sincerely grateful to Prof. Dr.Mitjan Kalin, Head of TINT. For technical support is author grateful to Ervin Strmčnik, Andreja Poljšak and Rok Jelovčan.

The authors are also grateful to the Slovenian company Tajfun, the largest producer of forestry machinery in Europe, for their financial and technical support. For the financial support of this research, we are grateful to the Slovenian Research Agency.

References

[1] Trostmann, E. *Water hydraulics control technology.* Lyngby, Technical University of Denmark, 1996.
[2] Bartz, W.J. “Lubricants and the environment.” *Tribology International* 31 (1998): 35-47.
[3] Backe, W. “Water- or oil-hydraulics in the future.” SICFP’99, Tampere, Finland, pp. 51–65, 1999.
[4] Yamamoto, Y., and T. Takashima. “Friction and wear of water lubricated PEEK and PPS sliding contacts.” *Wear* 253 (2002): 820-826.
[5] Yamamoto, Y., and T. Takashima. “Friction and wear of water lubricated PEEK and PPS sliding contacts Part 2. Composites with carbon or glass fibre.” *Wear* 253 (2002): 820-826.
[6] Davim, J.P., N. Marques, and A.M. Baptista. “Effect of carbon fibre reinforcement in the frictional behaviour of Peek in a water lubricated environment.” *Wear* 251 (2001): 1100-1104.
[7] Kalin, M. “Influence of flash temperatures on the tribological behaviour in low-speed sliding: a review.” *Mater. Sci. Eng. A* 374, no. 1/2 (2004): 390-397.
[8] Donnet, C., and A. Grill. “Friction control of diamond-like carbon coatings.” *Surface and Coatings Technology* 94-95 (1997): 456-462.
[9] Fontaine, J., C. Donnet, A. Grill, and T.L. Mogne. “Tribochemistry between hydrogen and diamond-like carbon films.” *Surface and Coatings Technology* 146-147 (2001): 286-291.
[10] Kalin, M., J. Vižintin, J. Barriga, K. Vercammen, K. Van Acker, and A. Arnšek. “The effect of doping elements and oil additives on the tribological performance of boundary-lubricated DLC/DLC contacts.” *Tribology Letters* 17 (2004): 679-688.
[11] Andersson, P. “Water lubricated pin-on-disc tests with ceramics.” *Wear* 154 (1992): 37-47.
[12] Zhou, F., K. Adachi, and K. Kato. “Sliding friction and wear property of a-C and a-CNx coatings against SiC balls in water.” *Thin Solid Films* 514, no. 1-2 (2006): 231-239.
[13] Novak, S., M. Kalin, and T. Kosmac. “Chemical aspects of wear of alumina ceramics.” *Wear* 250, no. 1-12 (2001): 318-321.
[14] Kalin, M., and S. Jahanmir. “Influence of roughness on wear transition in glass-infiltrated alumina.” *Wear* 255, no.1-6 (2003): 669-676.
[15] Strmcnik, E., F. Majdic, and M. Kalin. “Water-lubricated behaviour of AISI 440C stainless steel and a DLC coating for an orbital hydraulic motor application.” *Tribology International* 131 (2019): 128-136.
[16] Breskvar, K. *Absorpcija vode pri polimernih materialih*, / *Water absorption in polymeric materials* Graduate thesis. Univerza v Ljubljani, Fakulteta za strojništvo, Ljubljana, 2016.
[17] Linjama, M., and M. Vilenius. “Digital hydraulics-Towards perfect valve technology.” In: Vilenius, J. & K.T. Koskinen (eds.) The Tenth Scandinavian International Conference on Fluid Power SICFP'07, Tampere, Finland, May 21-23, 2007.

[18] Park, S.H. "Development of a proportional poppet-type water hydraulic valve." Proceedings of the Institution of Mechanical Engineers, Part C: Journal of Mechanical Engineering Science, 2009, 223.9: 2099-2107.
[19] Linjama, M., K.T. Koskinen, and M. Vilenius. "Pseudo-Proportional Position Control of Water Hydraulic Cylinder Using On/Off Valves.: In: Proceedings of the JFPS International Symposium on Fluid Power. The Japan Fluid Power System Society, 2002. pp. 155-160.
[20] Linjama, M., J. Tammisto, K. T. Koskinen, and M. Vilenius. "Two-way solenoid valves in low pressure water hydraulics." In: McLain, T. and D. Kim (ed.), Fluid Power Systems and Technology 2000 (IMECE2000), ASME, New York, 2000, pp.55-60.
[21] Yang, H., and M. Pan. "Engineering research in fluid power: a review." *Journal of Zhejiang University SCIENCE A* 16, no. 6 (2015): 427-442.
[22] Koskinen, K.T., T. Leino, and H. Riipinen. "Sustainable development with water hydraulics – possibilities and challenges." Paper presented at the 7th International Symposium in Fluid Power, JFPS'08, Toyama, Japan, September 15-18, 2008.
[23] Majdič, F., and A. Bombač. "Piston-Type Accumulator for Water Power-Control Hydraulics." Paper presented at The 9th International Fluid Power Conference, 9. IFK, Aachen, Germany, March 24-26, 2014.
[24] Majdič, F. "Water hydraulic check valve researches." Paper presented at The Fourteenth Scandinavian International Conference on Fluid Power, Tampere, Finland, May 20-22, 2015.
[25] Strmčnik, E., F. Majdič, and M. Kalin. "Influence of a Diamond-Like Carbon-Coated Mechanical Part on the Operation of an Orbital Hydraulic Motor in Water." *Metals* 9, no. 4 (2019): 466.

ISSN 1454 - 8003
Proceedings of 2019 International Conference on Hydraulics and Pneumatics - HERVEX
November 13-15, Băile Govora, Romania

MANAGEMENT OF TIME AND HUMAN RESOURCES FOR WEEE RECYCLING LINE MONITORING

Irina RĂDULESCU[1], Alexandru Valentin RĂDULESCU[1], Mihai CORNEA[1]

[1] University POLITEHNICA of Bucharest, e-mail address: irina.radulescu@upb.ro

Abstract: *In this paper we report on our experience in WEEE recycling monitoring; authors present problems and solutions of recycling of waste from electrical and electronic equipment and they focused on the analyse of an Eldan S1000 shredder recycling line.*
Concerning the European Union's environmental policy, there are three aspects about: conservation, protection and improvement of the quality of the environment, protection of population health and the correct and rational use of natural resources with their reuse. Waste electrical and electronic equipment (WEEE) represents a domain with the fastest growing, both national and international level; Romania held the European Union last place in electronic and electrical equipment waste collecting in 2016, 1.6 kg per inhabitant, below the 8.9 kilograms European average, as it is shown in European Bureau for Statistics published data.
Electronics recycling provides precious and special metals to be recovered, it reduces the environmental impact associated to the electronics manufacture from raw materials and it ensures that electronics hazardous substances are treated properly. The reused products must be accordingly and efficiently recycled at the end of their useful life.
The WEEE components recycling process is a very complex one, each stage having its own importance, timing and steps required for recycling need to be respected according to national and European rules.
The Eldan S1000 shredder recycling line consists of many equipment and it has approximately 4 tonnes / hour processing capacity, function the type of material to be processed.
To solve the desired recycling problem by using Eldan line represents a possibility by a modular approach flexibility, which means that a number of combinations can be obtained, with variations from a single machine to complete systems. The WEEE Eldan recycling plants and lines are designed for automatic processing, with specialized personnel for supervision. They can be easily adjusted to reduce the material size, depending on its type and in accordance with the market requirements.
High performance, low processing and maintenance costs, low energy consumption, minimal metal losses and the appropriate mechanical technique for reducing and separating components recommend these equipment type for successful WEEE recycling, with a modern and flexible technology.
This type of modern WEEE recycling system solutions offers an innovative character, paying attention to main factors – human resources and time – their good management being important to the proper functioning of the Eldan recycling line.

Keywords*: Waste electrical and electronic equipment (WEEE), Environment, Recycling, Shredder recycling line*

1. Introduction

The aim of the paper is to analyse and report on Romanian experience in recycling monitoring, by considering problems and solutions of electrical and electronic equipment waste recycling, using an Eldan S1000 shredder recycling line.
Waste electrical and electronic equipment (WEEE) represents a domain with the fastest growing, both national and international level. Concerning the European Union's environmental policy, there are three aspects about: conservation, protection and improvement of the quality of the environment, protection of population health and the correct and rational use of natural resources with their reuse.
Waste is a major problem, but EEE has an impact on the environment during all stages of their life cycles: production, use, end-of-life. The WEEE components recycling process is a very complex one, each stage having its own importance, timing and steps required for recycling need to be respected according to national and European rules.

Since 2003, when it was published the Directive 2002/96 /EC, EuropeanUnion managed WEEE by the principle of producer extended responsibility, ensuring that producers can fulfill their obligations either individually or collectively. After numerous changes during the voting process, the final text of the new Directive (2012/19 / EU) was published in the Official Journal of the European Union on July 24, 2012 and it has been transposed in Romania by the Government Emergency Ordinance no.5 / 2015, [1-2].
One of the main changes introduced by the new Directive concerns the redefinition of the collecting target for the Member States. Table 1 provides a planning of the evolution of WEEE collection targets at country level, based on the provisions of the new WEEE Directive. Romania, together with other countries, due to the lack of necessary infrastructure and the low level of EEE consumption, has the possibility of derogating from the initial deadlines.

Table 1: Planning of the evolution of WEEE collection targets at country level, [3]

<table>
<tr><th>Year</th><th>2012</th><th>2013</th><th>2014</th><th>2015</th><th>2016</th><th>2017</th><th>2018</th><th>2019</th><th>2020</th><th>2021</th></tr>
<tr><td>Target initially set by the WEEE Directive</td><td colspan="4">Minimum 4 kg. per capita or the average quantity expressed in kg per capita annually collected in the previous 3 years.</td><td colspan="3">Minimum 45% of the quantity placed on the market (annual average of the previous 3 years)</td><td colspan="3">65% of the quantity placed on the market (annual average of 3 previous years) or 85% of the amount of generated WEEE.</td></tr>
<tr><td>Target for România</td><td colspan="4">Minimum 4 kg. per capita or the average quantity expressed in kg per capita annually collected in the previous 3 years.</td><td colspan="5">Minimum 40% of the quantity placed on the market (annual average of the previous 3 years)</td><td>65% of the quantity placed on the market (annual average of 3 previous years) or 85% of the amount of generated WEEE.</td></tr>
</table>

In Europe there were produced around 9 million tonnes of WEEE in 2005 and the estimated data show that by 2020, the quantity generated will exceed 12 million tonnes.
Romania held the European Union last place in electronic and electrical equipment waste collecting in 2016, with 1.6 kg per inhabitant, below the 8.9 kilograms European average, as it is shown in European Bureau for Statistics (Eurostat) published data.
Electronics recycling provides precious and special metals to be recovered, it reduces the environmental impact associated to the electronics manufacture from raw materials and it ensures that electronics hazardous substances are treated properly. The reused products must be accordingly and efficiently recycled at the end of their useful life.
Within the manufacturing process, there are a number of dangerous and toxic substances that are used for integrated circuits, capacitors, screens. For the manufacture of a computer there are required 22 kg of chemicals products, 1.5 tonnes of water and a significant amount of lead, cadmium and mercury; these substances can have adverse effects on human health and environmental factors, in general,
The WEEE recycling is an important subject from the point of view of the waste treatment and from the point of view of the valuable materials recovery, being divided into 3 major phases:

- the disassembly, that can be selective and manual,
- the improvement using mechanical, physical and / or metallurgical processes, in order to mend the content of unwanted materials.
- the refining - the recovered materials return to their life cycle.

The large number of Electric and Electronic Equipment and their waste variety complicate the treatment and the management of WEEE. Technological development and more new equipment constantly provide more services and encourage consumers to quickly replace their old devices.
As a result, the quantities of Electric and Electronic Equipment waste are increasing every year, around 20 to 50 million wastes are worldwide generated (non-ferrous and ferrous metals, inert-glass, wood,

concrete, plastics, dangerous parts-batteries, cathode-ray tubes, capacitors, liquid crystal displays, mercury switches). These wastes can pose major risks to human health and to the environment, [3].
Also, electric and electronic equipment are high energy users, requiring a considerable amount of electricity during their lifetime. Their improper usage can increase energy consumption. Every year, in the field of computers, it is consumed an amount of electricity as a 155 million inhabitants country consumes.
WEEE contains a number of useful materials: metals and non-metals, precious metals (gold, silver, platinum), plastics, other materials. By their recycling important raw materials and energy savings are made, their treatment being carried out in specialized and authorized centers. Recycling procedures that are not based on best practices waste precious metals and recyclable plastics, generating energy consumption and environmental damage as a result of the pure materials production. The benefits concern the environment, also, the WEEE ecological treatment brings significant social benefits by increasing the number of jobs in this treatment sector, [4-5].

2. About treatment, recovery, recycling and revaluation techniques

The electrical and electronic equipment waste recycling represents an important subject, considering the waste treatment point of view and also, considering the valuable materials recovery.
The major phases of WEEE are:
• the disassembly, that can be selective and manual;
• the improvement, by using mechanical, physical and /or metallurgical processes in order to improve
the content of undesirable materials;
• the refining - the recovered materials return to their life cycle.
Considering the electronic waste management for life, this one includes:
• The reuse of functional electronics;
• The rehabilitation and repair of electronics;
• The reuse and the recovery of electronic components;
• The processing for metal recovery
• The elimination.
Electronics recycling provides precious and special metals to be recovered, it reduces the environmental impact associated with the electronics manufacture from raw materials and it ensures that hazardous substances from electronics are properly treated. The reused products must be properly and efficiently recycled at the end of their useful life. According WEEE Directive, the systems available for the WEEE treatment must use the best techniques of treatment, recovery and recycling, but there is no reference document for the best techniques available for their treatment, recovery and recycling (according to the procedures in Directive 96/61/EC), [1].
To give an example for the treatment of small and large household appliances, the steps to follow are:

- Preparation of the devices for treatment - it consists in removing the external electrical cables and the elements with dangerous contents.
- Primary seeding - the primary grinder performs the devices fractionation, for easier manual sorting of the resulting materials and components.
- Manual sorting - there are sorted certain components to be treated on other lines (capacitors, coils and transformers, printed circuit boards) etc.
- Secondary milling - it has the role of bringing the fractions to smaller dimensions.
- Fraction separation
  a) magnetic separation: the ferrous metal fractions are separated from the obtained fractions;
  b) inductive separation: from the remaining fractions, the non-ferrous metal fractions (e.g. aluminium and copper) are separated from the non-metallic fractions (e.g. plastic, wood, rubber).

As a result of the complex treatment operations, different fractions with positive economic value are obtained, such as:
• ferrous and non-ferrous metals (aluminium, copper, brass)

• various types of plastic:
  o ABS / PS mixes from small electronic refrigerators;
  o PVC and PE from cables, monitor housings, TVs or printers;
  o ABS and PP from washing machines.

• various electrical and electronic components (motors, transformers, compressors, coils).

These fractions are carefully sorted and traded, both at home and abroad, [4-5].
They are considered secondary raw materials and re-enter in the industrial circuit for the new products manufacture, saving a large amount of the natural resources. They can also be used as an alternative fuel (the wood from dismantling, the pelletized polyurethane foam).

2.1 Functional scheme of waste recycling line

The Eldan S1000 shredder recycling line (Figure 1) has the processing capacity about 4 tonnes / hour, function the type of processed material and it consists in modern equipment, as: a load conveyor belt (1), a S1000 chopper (2), a vibrating conveyor belt to eliminate waste, an electromagnet (an electromagnetic separation band) type 451-60 / 140-290-S0, which separates the iron particles from the material stream (4), a discharge conveyor belt (5), a load conveyor belt with magnetic cylinder (6), an Eddy separator (non-ferrous metal separator) 0428-25 / 90 (7), a conveyor belt (8), a reverse rotary distributor for supplying the multifunctional scraper with a controllable quantity of materials (9), a MPR120 multifunctional scraper (10), a service platform used during the operation and scraper's maintenance operations (11), a vibrating discharge conveyor (12), a magnetic strip for separating the ferrous fraction (13), a conveyor belt to load, with magnetic cylinder (14), an Eddy non-ferrous metal separator, type 0428-25 / 90 (15), a conveyor belt (16), a loading conveyor belt (17), a SMV silage 1m3 volume (18), a HG169 industrial granulator (19), a pneumatic transport system (20), a pneumatic transport system (21), a SMV silage 1m3 volume (22), a C22 separation table (23), a flexible helical conveyor (24), a PC12 sorter (25), a power supply unit for positions 1-7 and 28 (26), an electrical and control panel for positions 8-25 and 29 (27), JM 21 / 45-06 4TR T3 type air filter (28 - 30), JM 70 / 40-06 4TR T3 type air filter (31 - 33).
As it is seen the main equipment used in waste recycling line consist in:

- the S1000 chopper (2),
- the Eddy separator (non-ferrous metal separator) 0428-25 / 90 (7),
- the MPR120 multifunctional scraper (10),
- the Eddy non-ferrous metal separator, 0428-25 / 90 type (15),
- the HG169 industrial granulator (19) and
- the C22 separation table (23).

The conveyor belts are used to transport the material, to charge or to discharge it, also the transport pneumatic systems.
The C22 separation table (23) has the role to separate the metal fraction from the rest of the insulation materials.
The sorter (25) will effectively remove the fine copper and aluminium particles from the plastic fraction. It consists of two layers of griddles and a tray at the bottom.
The purpose of the silages (18 and 22) is to balance the flow from the granulator by the maximum feed rate of the separation table, thus ensuring the quality of the separation, [6].

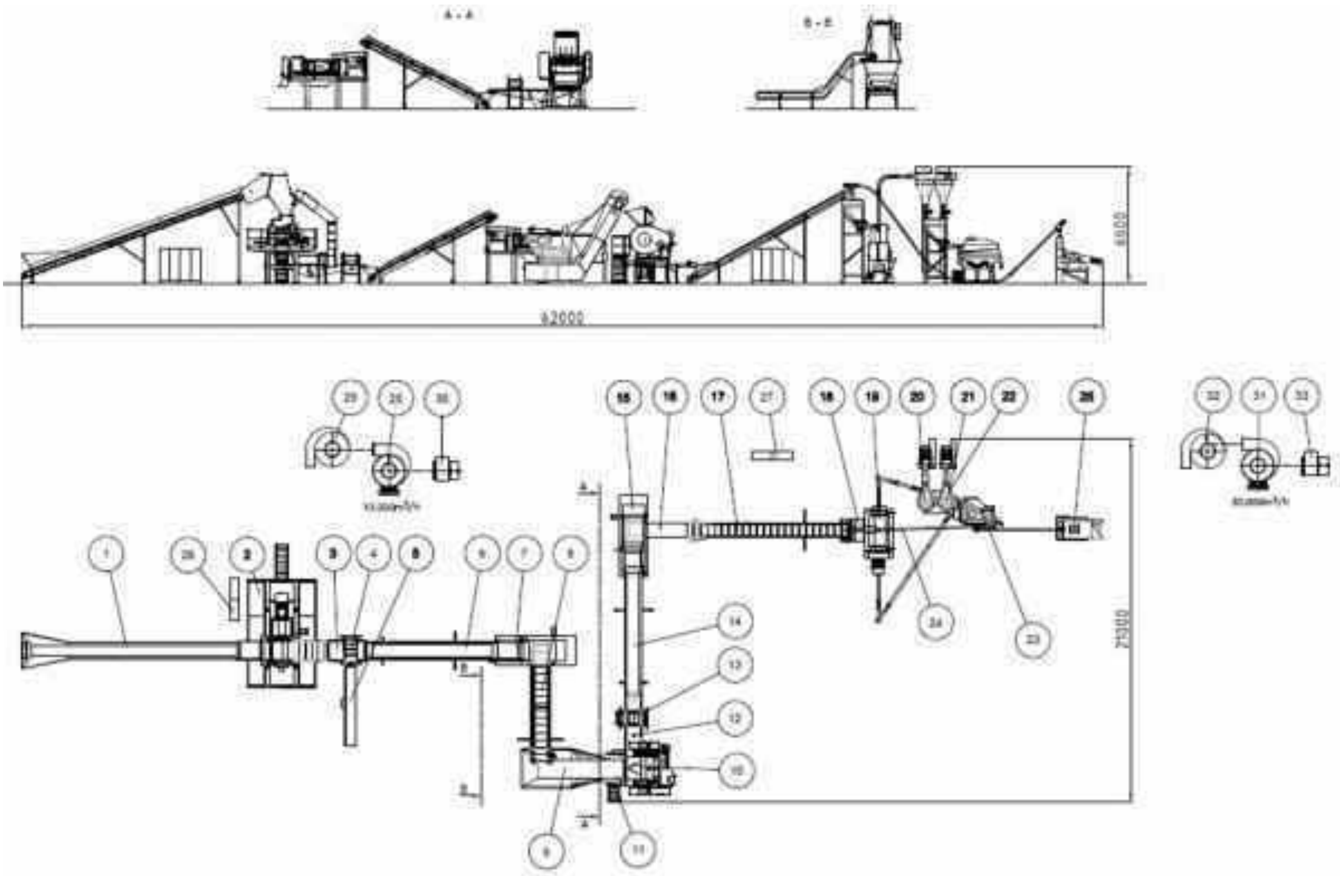

Fig. 1. Eldan Shredder S1000 WEEE Recycling Plant, [6]

2.2 Main components of the waste recycling line

The main components involved in waste recycling line and their utility are presented in next descriptions.

The S1000 shredder (Figure 2) is the first line equipment and it performs the main operation – the WEEE material size reduction. Components are reduced to a size that allows most ferrous materials to be separated from non-ferrous or plastic fractions. After reducing the dimensions by cutting with a chopper, the resulting mixture is transported under a magnetic strip, achieving separation of the metal fraction from the rest of the contents, [6].

For the separation of non-ferrous metals, Eldan firm incorporated two Eddy separators (ECS) (Figure 3) at different points in the line. The first equipment is responsible for separating the non-metalliferous fraction from the rest of the heavy mixture. After reducing the mixture size in the multifunctional scraper, the second Eddy separator separates the non-metalliferous fraction from the rest of the light mixture, [6].

The MPR120 multifunctional scraper (Figure 4) is responsible for the second step of WEEE material shredding. It is an effective medium-speed granulation device, a dual processing unit, specially designed for WEEE recycling. The multifunctional scraper ensures the individual reduction of the material size up to about 12 mm. The material is passed under another magnetic strip where the metal component is again separated. The second Eddy separator ensures the separation of the medium size non-ferrous fraction from the remaining organic fraction, [6].

The HG169 industrial granulator (Figure 5) is responsible for the last step of material dimensions reduction. The device is a high speed granulator, with a single axis, capable of reducing the material size with values between 6 mm to 10 mm, depending on the material type. After processing in the industrial granulator, the material is passed into separation table for the final separation process, [6].

The C22 separation table (Figure 6) is used in the separation process of the final mixture into an organic (plastic) fraction and a complex metalliferous fraction. The exit of the separation table includes four fractions, [6]:

Powders	- eliminated through the suction system
Metallic fraction	- Is present at the top of the collection area. - At this point, the metallic fraction purity is almost 100%
Plastic fraction	- is eliminated through the bottom of the collection area
Mixing fraction	- is present in the middle part of the collection area. This fraction is sent back in the separation process.

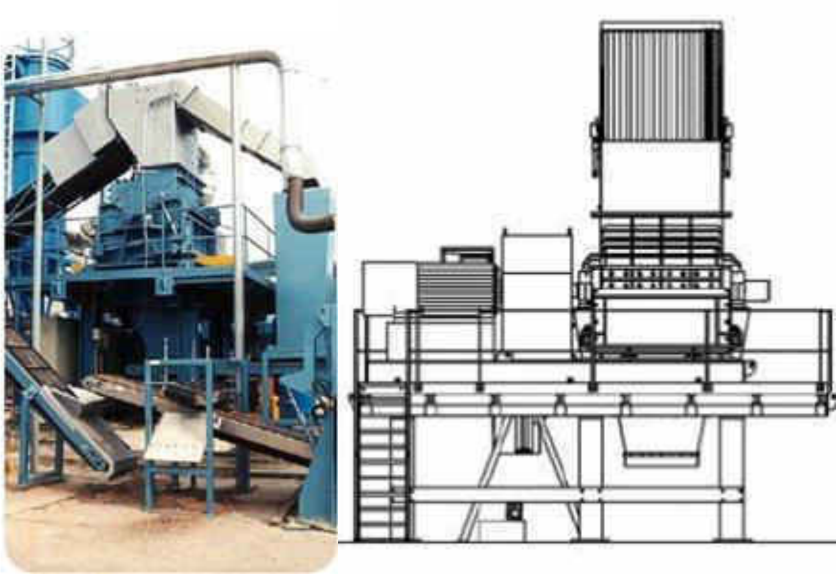

Fig. 2. Shredder S1000, [5]

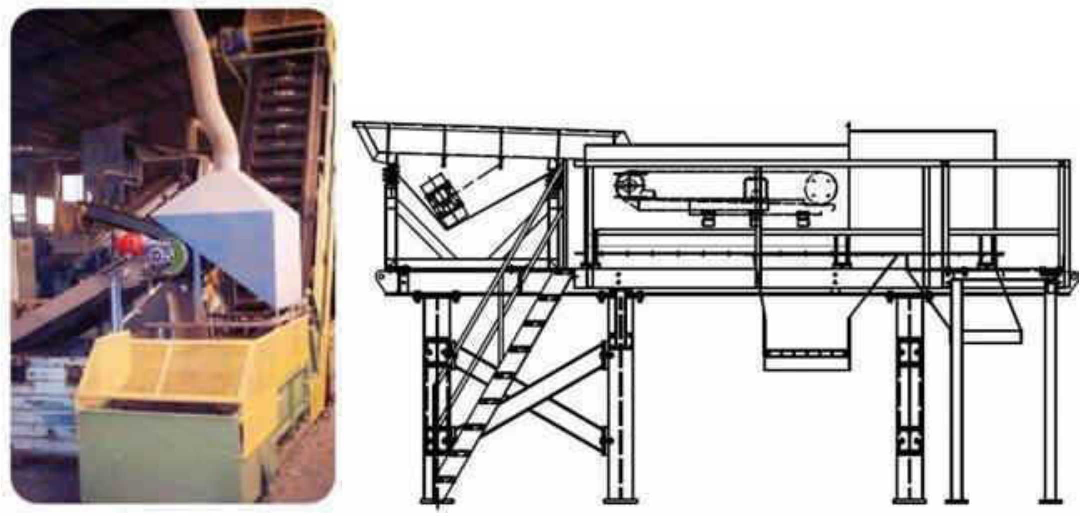

Fig. 3. Eddy Separator, [5]

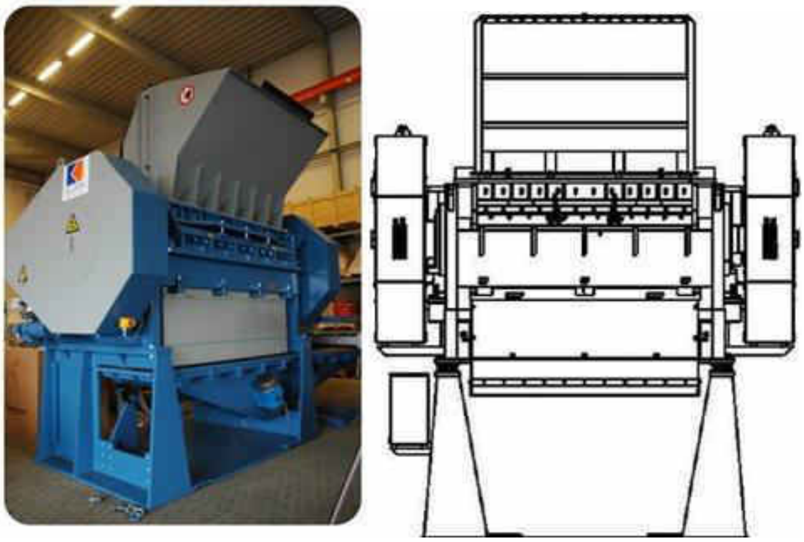

Fig. 4. MPR120 Multifunctional scraper, [5]

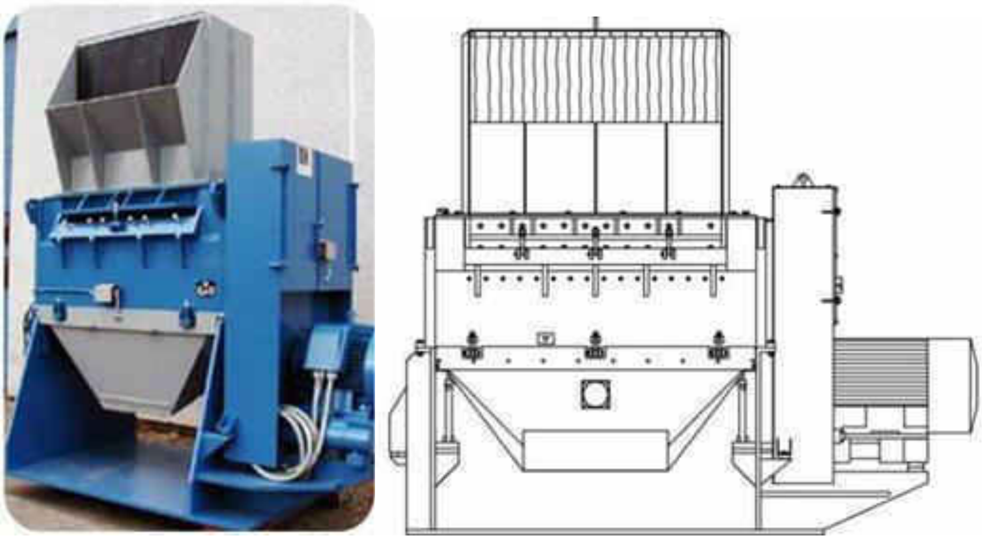

Fig. 5. HG169 Industrial granulator, [5]

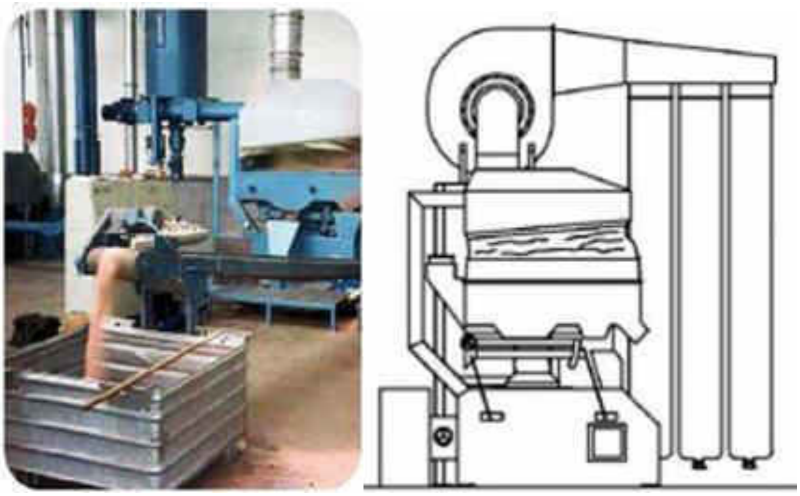

Fig. 6. C22 Separation table, [5]

3. Management of time and human resources for WEEE recycling line monitoring

The WEEE components recycling process is a very complex one, each stage has its own importance, that is why all times and steps required for recycling need to be respected, according national and European standards.

The first step of Eldan recycling line is to reduce the WEEE materials size on the S1000 chopper; this operation takes about 2 hours and it needs to be supervised by a qualified person, who knows very well the process and the machine.

The second step is equally important and it involves the non-metalliferous fraction separation from the rest of the heavy mixture, on the Eddy separator; this operation lasts 1 hour and it is also performed by a specialized person.

After this step, the second shredding of the WEEE material is made on the MPR120 multifunctional scraper; this operation leads to obtaining a finer and easier to process WEEE material. The action takes approximately 2 hours and it is performed by another qualified worker.

The fourth stage is very similar to the second stage, as the third one was similar to the first one. It aims a more detailed sorting of the WEEE material, by passing onto the magnetic stripe and separating the medium size non-ferrous fraction from the organic fraction, that remained on the second Eddy separator, all operation lasts 1 hour.

The fifth operation works to reduce the dimensions of the materials to be processed on the HG169 industrial granulator; this stage lasts 2 hours and it is performed by trained personnel.

The last step is the most detailed one because it involves the separation of the final mixture into organic fraction and complex metalliferous fraction, on C22 separation table, this action is lasting 2 hours.

It is very important that every step is supervised by qualified personnel, who respect the process and equipment specifications.

The Gantt chart for the WEEE recycling line is presented in Figure 7, where there are figured the duration of components size reducing and separation process and the operation persons in charge for each activity.

Gantt chart for the WEEE recycling line

						Timings										
No.	Activity	Time in (hour)	Time out (hour)	Duration	Operation person in charge	8:00	9:00	10:00	11:00	12:00	13:00	14:00	15:00	16:00	17:00	18:00
1	Reducing the size of WEEE materials on the S1000 chopper	8:00	10:00	2:00	Qualified Worker Workstation 1											
2	Separating the non-metalliferous fraction from the rest of the heavy mixture on the Eddy separator	10:00	11:00	1:00	Qualified Worker Workstation 2											
3	The second step of the WEEE material grind on the MPR120 multifunctional scraper	11:00	13:00	2:00	Qualified Worker Workstation 3											
4	The material displacement on a magnetic strip, with the separation of the medium size non-ferrous fraction from the organic fraction remaining on the Eddy separator 2	13:00	14:00	1:00	Qualified Worker Workstation 4											
5	Reduction of the dimensions of the processing materials on the HG169 industrial granulator	14:00	16:00	2:00	Qualified Worker Workstation 5											
6	Separation of the final mixture into organic fraction and complex metalliferous fraction on C22 separation table	16:00	18:00	2:00	Qualified Worker Workstation 6											
	Total hours			**10:00**												

Fig. 7. The Gantt chart for the WEEE recycling line

4. Conclusions

Electronics recycling provides precious and special metals to be recovered, it reduces the environmental impact associated with the electronics manufacture from raw materials and it ensures that electronics hazardous substances are properly treated.
The recycling using the Eldan lines complies with the elements mentioned in the WEEE Directives of European Union. The existence of standard recycling facilities, as those presented in the paper, represents the starting point in factories adjustment, to meet the customers' specific requirements.
To solve the desired recycling problem represents a possibility by a modular approach flexibility, which means that a number of combinations can be obtained, with variations from a single machine to complete systems. The WEEE Eldan recycling plants and lines are designed for automatic processing, with specialized personnel for supervision. They can be easily adjusted to reduce the material size, depending on its type and in accordance with the market requirements.
High performance, low processing and maintenance costs, low energy consumption, minimal metal losses and the appropriate mechanical technique for reducing and separating components recommend these equipment type for successful WEEE recycling, with a modern and flexible technology.

References

[1] Directive 2002/96/EC.
[2] Directive 2012/19/EU.
[3] https://ec.europa.eu/eurostat/web/waste/key-waste-streams/weee.
[4] Crowe, M. et al. "Waste from Electrical and Electronic Equipment (WEEE)- quantities, dangerous substances and treatment methods. " European Topic Center on Waste, European Environment Agency, 2003.
[5] Lifeng, Zhang. "Recycling of electronic wastes: Curent Perspective." *JOM, The Journal of The Minerals, Metals & Materials Society* 63, no. 8 (August 2011).
[6] https://www.eldan-recycling.com/.

ISSN 1454 - 8003
Proceedings of 2019 International Conference on Hydraulics and Pneumatics - HERVEX
November 13-15, Băile Govora, Romania

THEORETICAL AND EXPERIMENTAL RESEARCH REGARDING THE WATER OXYGENATION THROUGH PIPES

Constantin Remus VOICU[1], Rasha CUSMA[1], Iulian Alexandru GRIGORE[1], Nicolae BĂRAN[1], Nicoleta ALBU[1], Francesca ȘELEA[1], Mihaela PETROȘEL[1]

[1] University Politehnica of Bucharest, Faculty of Mechanical and Mechatronic Engineering, remus.voicu@yahoo.com

Abstract: *The research paper in the area of water oxygenation through the introduction of a new type of fine bubble generator. By the realization of 0.1mm holes, water insufflation is ensured by air bubbles with the diameter <0.1mm, such that the transfer of the oxygen into the water is intensified. Presenting an experimental equipment which highlights the growth of the dissolved oxygen into the water.*

Keywords: *Water oxygenation, transfer of the oxygen into the water, fine bubble generator.*

1. Introduction

Through water oxygenation is understood the transfer of the oxygen from the atmospheric air into the water, which is in fact a phenomenon of transfer of a gas into a liquid. The most common method for removing organic impurities under the action of an aerobic bacterial biomass is the introduction of the oxygen gas into the wastewater. The oxygen comes most commonly from the atmospheric air, in this case the process bearing the name of water aeration. [1][2]
Aeration can be done through several methods, respectively: by using mechanical aerators (e.g. turbine type) or pneumatic aerators (e.g. injection of the air at the base of the water volume), the latter being the most commonly used. Also, the oxygen needed for the aeration process can also be introduced into the water by the mixed method (mechanical and pneumatic)
To increase the concentration of the dissolved oxygen from the wastewaters, several types of air diffusion devices have been developed. These devices can be found as simple holes (they generate large air bubbles – most usually used in pipes), or as fine bubble generators. Due to the generators which can be made of different materials, of different shapes and sizes, the air diffusion devices are classified according to the diameter of the produced bubbles. Thus, there exist fine, medium and large bubbles generators. [3][4][5]
At the moment the aeration is done using three methods: with mechanical aerator, with pneumatic aerators, and mixed aerators. Pneumatic aerators are most often used. After the introduction of the oxygenation processes with active mud, different types of air diffusion were created, tried and developed in order to increase the dissolved oxygen concentration from the wastewaters. These devices are either in the form of simple holes in pipes that generate large air bubbles or in the form of fine bubble generators. Due to the fact that the shape, material, and the material used to build the fine bubble generators differs, the air diffusion devices are classified and reported to the relative diameter of the produced bubbles. Thus there are fine bubble generators, medium bubble generator and large bubble generators. Fine bubble aeration is more efficient than large bubble aeration, because the specific area interfacial area between the two systems (air – water) is larger. For the intensification of the phenomenon of mass transfer of the oxygen from the air, the realization of a maximum interphase surface is needed as a result of air bubbles with the minimum diameter. Theoretical and experimental research has been carried out for various constructive forms of fine bubble generators (G.B.F.) [6][7][8].

2. Presentation of a fine bubble generator

A F.B.G. is proposed where the dispersion holes of the air into the water are processed by micro-drilling. 152 holes of Ø 0.1 mm were realized in the plate. Figure 1 shows the plate with the holes.

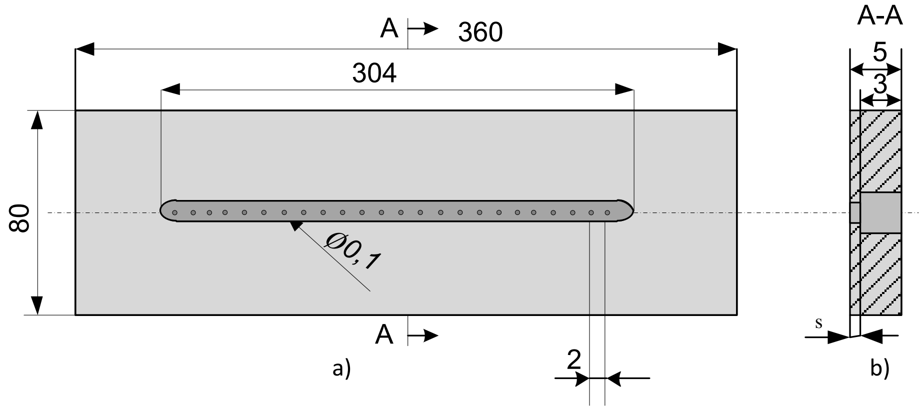

Fig. 1. Plate with holes as F.B.G.
a) Top view; b) cross section

To make the holes in the plate, a channel deep of 3mm, and a length of 304mm was created; a hole where the air comes out has a thickness of 2mm. Later with the help of a C.N.C (Computer Numerical Control), 152 holes with a diameter of Ø 0.1 mm were made in the channel.
The CNC equipment has a precision of ±0.5 μm, which assures the creation of an original F.B.G. solution
Figure 2 shows the constructive solution of F.B.G.

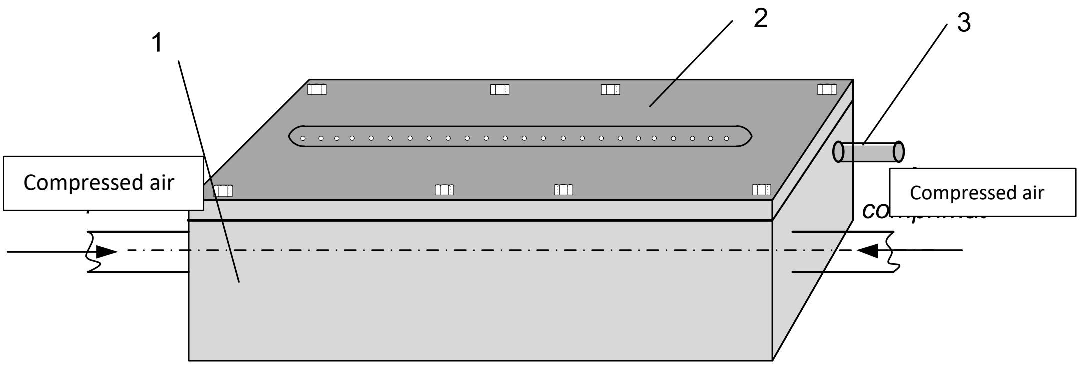

Fig. 2. Fine bubble air generator
1 – tank filled with compressed air; 2 – plate with holes;
3 – coupling for the measurement of the air pressure

When introducing an air stream into the water, the following aspects should be taken into account [9][10]:

- The kinetic energy of the gas stream is consumed to move the water particles.
- The outlet of the jet may have a circular or rectangular shape (square, rectangle);
- After leaving the initial section, the jet tents to retain its original section shape. [11][12]
  Thus:
- If the outlet is circular we will obtain a symmetrical axial jet;
- If the output section is a rectangle, the result will be a plane jet.

3. The experimental equipment

The same experimental equipment will be used for researches regarding the functionality of different types of fine bubble generators (F.B.G.)

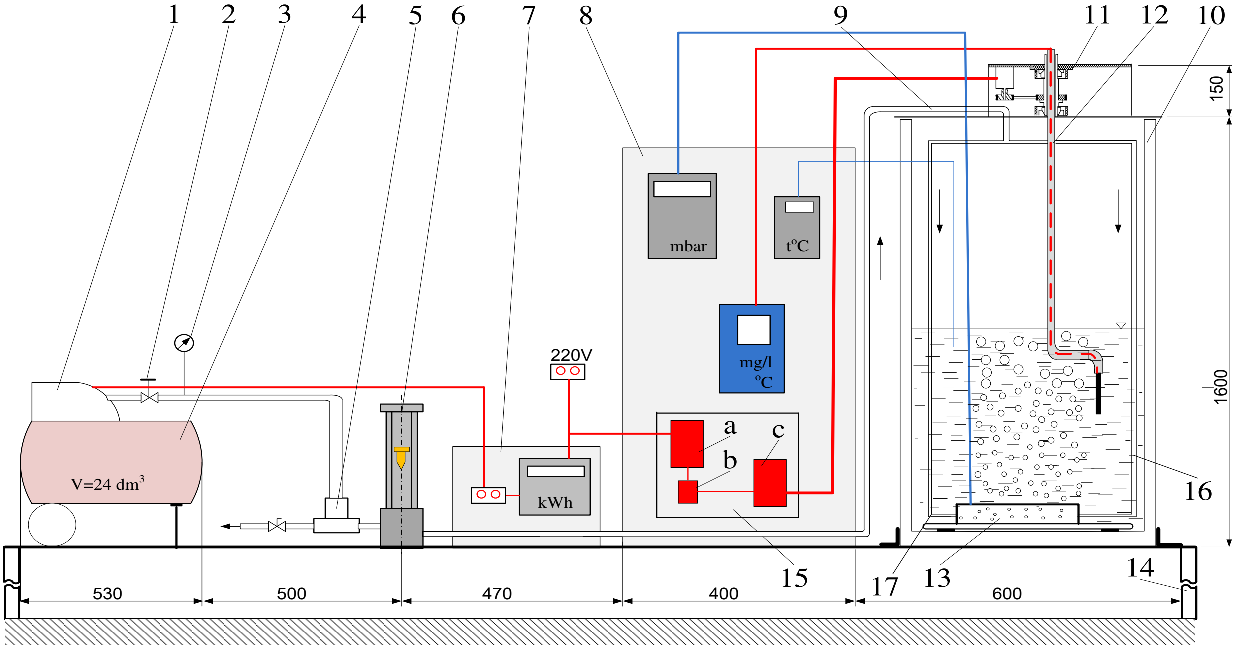

Fig. 3. Drawing of the experimental equipment for researches regarding the water oxygenation
1 – compressor with air tank; 2 – pressure reducer; 3 – pressure gauge; 4 – tank with compressed air V = 24 dm3; 5 – T coupling; 6 – flowmeter; 7 – electrical cabinet; 8 – panel with measuring devices; 9 – pipe for compressed air transportation; 10 – water tank; 11– probe drive mechanism; 12– Oxygen meter probe; 13 – F.B.G.; 14– equipment's stand; 15 – electronic command device: a – power supply, b – switch, c – command device; 16, 17 – compressed air pipes

4. The purpose and methodology of the research

Research objectives:
For a certain working regime, the concentration of dissolved oxygen into the water will be monitored as a function of time
The duration of the water aeration process will be established until the saturated concentration of dissolved oxygen in the water is reached.
Measurement involves the following steps [13][14][15]:
1. The 152 holes are checked if are working properly
2. The tank is filled with water la H = 500 mm H_2O;
3. CO, t_{H2O}, t_{aer} are measured;
4. The fine bubble generator (F.B.G.) is placed in the water, and the time (τ) is written down
5. Every 15 minutes, the F.B.G is pulled out of the water and the concentration of dissolved oxygen in the water is measured; [17][18]
6. When a horizontal line of the function (C = f (τ)) is reached, the measurements stops, with the condition that:
$C \approx Cs$;
7. From the previous researches [16][18], the concentration of the dissolved oxygen into the water tends towards concentration at saturation after a duration of two hours. The measurement of the oxygen's concentration will take place after 15 minutes; 30 minutes...120 minutes.
8. At the end of the measurements, the oxygen meter's probe is washed, and the water from the tank is flushed.

5. Experimental results

In the experimental equipment from figure 3, was mounted in position (13), F.B.G. mentioned above.
In figure 4 a fine bubble generator with 152 holes of Ø 0.1 mm each in diameter can be seen working.

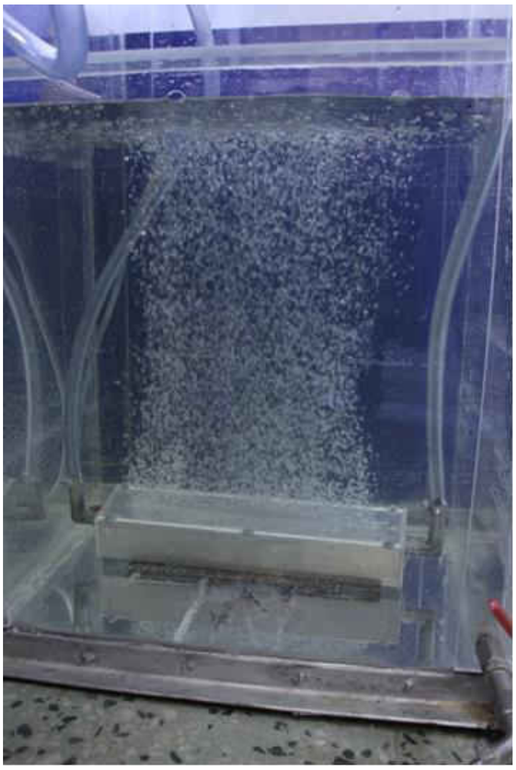

Fig. 4. F.B.G. with 152 holes

For experimental research, initial data is specified:

- The air flow introduced in F.B.G.: $\dot{V} = 600 dm^3/h$;
- Height of the water in the tank: H = 0.5 m;
- Air pressure in F.B.G.: p = 573 mm H_2O;
- Water temperature: t = 24 ºC;
- Value of the concentration of dissolved oxygen into the water as initial value: C0 = 5,48 mg/ dm^3;
- Value of concentration at saturation: Cs=8,4 mg/ dm^3.

The data obtained after the experimental research can be found in table 1
OD – Dissolved oxygen in the water

Table 1: Experimental data obtained with F.B.G. of rectangular shape with 152 holes

Nr.crt	0	1	2	3	4	5	6	7	8
τ [min]	0	15	30	45	60	75	90	105	120
t_{H2O}[ºC]	23.7	23.7	23.7	23.7	23.7	23.7	23.7	23.7	23.7
t_{aer}[ºC]	24.1	24.1	24.1	24,1	24.1	24.1	24.1	24.1	24.1
OD[mg/dm^3]	5.48	7.39	7.85	8.01	8.26	8.30	8.35	8.37	8.39

Based on the data from table 1, the function was created: $C_{O_2} = f(\tau)$ from figure 5.

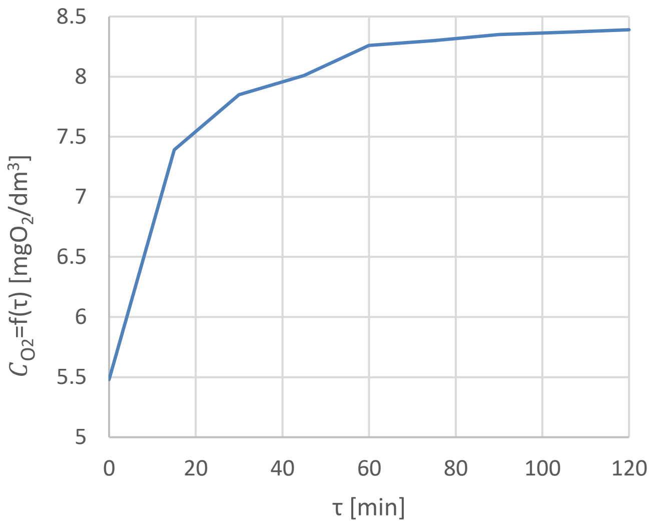

Fig. 5. Change of dissolved oxygen's concentration in the water, as a function of time

The experimental data obtained is similar with other results from the specialized literature [16][17][18].

6. Conclusions

This paper is of interest to a number of research engineers, PhD students, etc. who study in the field of water aeration.
The new findings consist of:
The F.B.G. which has very small holes (Ø 0.1 mm), is mounted, ensuring an efficient interfazic contact (air-water)
After functioning for two hours, the curb $C_{O_2} = \mathrm{f}(\tau)$ is build, which shows that after the time interval, the saturation of concentrations of the dissolved oxygen into the water is reached Cs=8,4 mg/ dm^3 for a temperature of the water of 24^{0}C.

Acknowledgements

This article was supported by a grant of the European Social Fund, part of the project „Burse pentru educația antreprenorială în rândul doctoranzilor și cercetătorilor postdoctorat" (Be Antreprenor) – Contract no. 51680/09.07.2019POCU/380/6/13 – Code SMIS: 124539)

References

[1] Howe, K.J., D.W. Hand, J.C. Crittenden, and R.R. Trussell, G. Tchobanoglous. *Principles of Water Treatment.* John Wiley & Sons, Inc., 2012.
[2] Crittenden, J.C., R.R. Trussell, D.W. Hand, K.J. Howe, and G. Tchobanoglous. *Water Treatment–Principles and design* – Third Edition. Hoboken, New Jersey, John Wiley & Sons, Inc., 2012.
[3] Oprina, G., I. Pincovschi, and Gh. Băran. *Hidro-Gazo-Dinamica Sistemelor de aerare echipate cu generatoare de bule / Hydro-gas-dynamic of aeration systems equipped fine bubbles generator*. Bucharest, Politehnica Press, 2009.
[4] Tănase, E.B., N. Băran, and R. Mlisan. "An Efficient Solution for Water Oxygenation." *Asian Engineering Review* 1, no. 3 (2014): 36-40.
[5] Pătulea, Al.S. "Influence of the functional parameters and the fine bubble generators architecture on the efficiency of aeration installations." PhD thesis, University Politehnica of Bucharest, 2012.
[6] Călușaru, I. "Physical properties influence of the liquid on the efficiency of oxygenation processes." PhD thesis. University Politehnica of Bucharest, Faculty of Mechanical and Mechatronic Engineering.
[7] Mateescu, G.M. "Hydro-gas-dynamic of fine bubbles generators." PhD thesis. University Politehnica of Bucharest, Faculty of Mechanical and Mechatronic Engineering, 2011.

[8] Tănase, E.B. “Influence of the composition of the gas introduced into the water on the content of dissolved oxygen.” PhD thesis. University Politehnica of Bucharest, Faculty of Mechanical and Mechatronic Engineering, 2017.
[9] Constantin, M., N. Băran, and B. Tănase. “A New Solution for Water Oxygenation.” *International Journal of Innovative Research in Advanced Engineering (IJIRAE)* 2, no. 7 (2015): 49-52.
[10] Mlisan (Cusma), Rasha. “Influence of the fine bubble generators architecture on the concentration’s growth of dissolved oxygen into the water.” PhD thesis. University Politehnica of Bucharest, Faculty of Mechanical and Mechatronic Engineering, 2017.
[11] Dobrovicescu, Al., N. Băran, and Al. Chisacof. *Technic thermodynamic basis, Elements of technic thermodynamics*. Bucharest, Politehnica Press, 2009.
[12] White, F.M. *Fluid mechanics*. New York, McGraw Hill Inc., 2011.
[13] Pătulea, Al., I. Căluşaru, and N. Băran. “Researches regarding the measurements of the dissolved concentration in water.” *Advanced Materials Research* 550-553 (2012): 3388-3394.
[14] Căluşaru, I. M., A. Costache, N. Băran, G.L. Ionescu, and O. Donţu. “The determination of dissolved oxygen concentration in stationary water.’ *Applied Mechanics and Materials* 436 (2012): 233-237.
[15] Pătulea, Al., N. Băran, and I. M. Căluşaru. “Measurements of Dissolved Oxygen Concentration in Stationary Water.” *World Environment* 2, no. 4 (2012): 106-109.
[16] Căluşaru-Constantin, M., E.B. Tănase, N. Băran, and Rasha Mlisan-Cusma. ‘Researches Regarding the Modification of Dissolved Oxygen Concentration in Water.” *IJISET - International Journal of Innovative Science, Engineering & Technology* 1, no. 6 (2014): 228-231.
[17] Constantin, M., N. Băran, and B. Tănase. “A New Solution for Water Oxygenation.” *International Journal of Innovative Research in Advanced Engineering (IJIRAE)* 2, no. 7 (2015): 49-52.
[18] Căluşaru, I., N. Băran, and Al. Pătulea. “The influence of the constructive solution of fine bubble generators on the concentration of oxygen dissolved in water.” *Advanced Materials Research* 538-541, (2012): 2304-2310.

ISSN 1454 - 8003
Proceedings of 2019 International Conference on Hydraulics and Pneumatics - HERVEX
November 13-15, Băile Govora, Romania

CHALLENGES AND RESEARCH IN THE INNOVATION OF DIGITAL ENTERPRISE AND SMART INDUSTRY (4.0)

Gheorghe GHEORGHE[1], Univ. Prof. PhD. Eng. EurEng.

[1] General Manager - INCDMTM Bucharest,

Prof. Univ. assoc. UPB, UVT and UTM

Correspondent Member - Academy of Technical Sciences Romania

Doctor Honoris Causa at Valahia Univ. of Targoviste

Abstract: *The scientific paper "Challenges and Research in the Innovation of the Digital Enterprise and the Intelligent Industry (4.0)",* ***states focused****, the scientific and technological concerns at the highest level, on the construction and development of the digital enterprise and the intelligent industry (4.0), through the results of the research and innovation in the specialized field of intelligent mechatronics and cyber-mechatronics, intelligent products and integrated and cobotic platforms.*
The scientific paper also presents the paradigm of research and innovation regarding the new advanced digital transformation of the enterprise and the intelligent industry corresponding to the integration of cyber-physical systems with the Internet of Things (IoT).

Keywords*: Digital enterprise; smart industry (4.0); mechatronic & cyber-mixmechatronic; intelligent and cobotic technological platforms.*

1. Introduction

The development of mechatronics, cyber-mechatronics and information and communication technology generates more and more things / objects that become integrated (with sensors) and have the ability to communicate with other objects, which **transforms the physical world itself into a systemic information and knowledge.**
Mechatronics, Cyber-Mix Mechatronics and the Internet of Things (IoT) allow things / objects in our environment to be active participants, i.e. they share information with other actors or members of the network; cable / wireless, which often uses the same Internet Protocol (IP) that connects the Internet.
Thus, objects / things are able to recognize events and changes around them and act and react in a quasi-autonomous way without human intervention.
In this exposed context, challenges in research, development and innovation create an "intelligent planet," where physical, digital and virtual worlds converge to create smart environments that can make energy, transport, cities and many other intelligent domains.
The development of some generic technologies such as "nano electronics", "communications", "sensors", "smart phones", "embedded systems", "cloud computing and software" (fig. 1), will be among the key to supporting future innovations of IoT and cyber – mechatronics products, which affects many industrial sectors.
Today, many national and especially European projects and initiatives address technologies and knowledge about mechatronics, cyber-mixmechatronics and Internet of Things. Given that topics can be highly diversified and specialized, there is a strong need to integrate individual results.
The integration of knowledge, in this context in general, is conceptualized as the process by which disparate, specialized, localized knowledge in several projects throughout Europe are combined, applied and assimilated.
The national and European research on the Internet of Things aims at defining IoT technology and developing research challenges at national and European level for global development.

ISSN 1454 - 8003
Proceedings of 2019 International Conference on Hydraulics and Pneumatics - HERVEX
November 13-15, Băile Govora, Romania

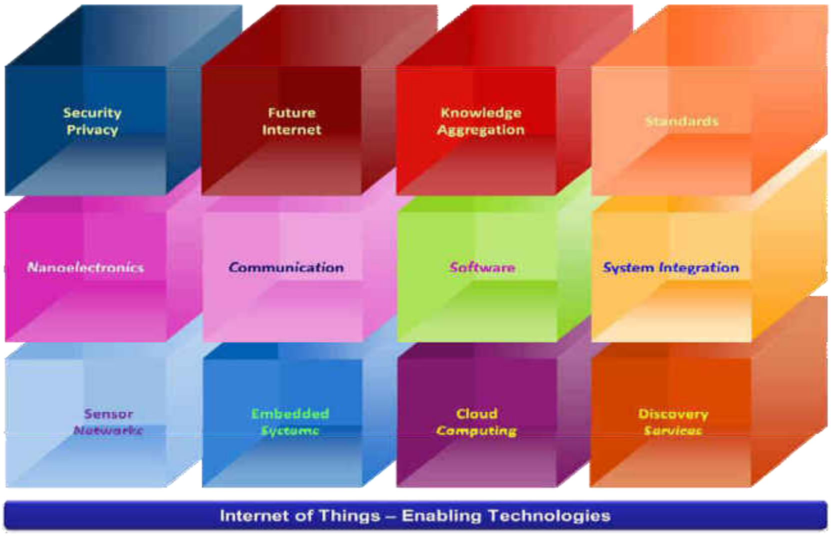

Fig. 1. Internet of Things – Enabled technologies

The research brings together national and European projects in the field of IoT technology, thus supporting the basic multidisciplinary science. The motivation for the Internet of Things is to address the great potential of IoT-based capabilities in Europe - to coordinate / encourage the convergence of ongoing activities on the most important issues - to build a broad consensus based on the ways to achieve IoT in Europe and Romania.
The perspective of the future is the emergence of a network of interconnected, uniquely identifiable objects, and their virtual representations in a similar Internet structure, which is positioned over a network of interconnected computers, which allows the creation of a new platform for economic growth (fig. 2).

Fig. 2. Internet of Things –technology platforms

The major areas of application of the street Internet are the creation of intelligent environments / spaces and things of their own (for example, intelligent transport, cities, buildings, energy, life, etc.) for climate, food, energy, mobility, health applications.

2. Common framework at national – European level

The common framework will contribute to the efforts of the researchers involved in these projects to generate new ideas, to transmit their knowledge and to translate them into marketable products / services / concepts of mechatronics, cyber-mixmecatronics and IOTs, with all the circumstances of the research and innovation in that area.
This common framework and the integration concept for mechatronic, cyber-mixmechatronics and IoT activities at national and European level are in line with the global European research strategy in the field.
The Horizon 2020 Research and Innovation Framework Program shows how the Framework Program could support the research and innovation objectives of the Europe 2020 Strategy and the Research and Innovation Framework Program and connects / coordinates the new Framework Program with national initiatives.
The concept creates a true integrated financing system and the coordination of the technical activities.
The research and innovation activities in the field of mechatronics, cyber-mixmechatronics and IoT must be interconnected and integrated into the Horizon 2020 Research and Innovation Framework Program.
These innovation activities must address important advances in the fields of mechatronics, cyber-mixmechatronics and IoT, such as infrastructure development, standardization, educational programs, and measures to support important industrial sectors or that foster innovation such as smart cities or regions.
Integration and coordination between European programs and national initiatives in the field of mechatronics, cyber-mixmechatronics and IoT offers the innovation-oriented, industry-oriented approach as an integral part of the Horizon 2020 Research and Innovation Framework Program, involving SMEs as well as drivers of innovation are assured.
This facilitates the dissemination of knowledge and the transfer of IoT technology, including applications that respond to social and societal challenges.
The common framework and the integration concept for mechatronic, cyber-mechatronic and IoT activities at national and European level generate programs for innovative actions to develop international networks and to support national programs, programs on knowledge and technological innovation.
It makes better use of and enhances the knowledge generated and enhances the ability to interact with SMEs and to enable them to enter new market niches and gain a high level of knowledge. This will generate cooperation in the development of clusters and business networks; innovative projects of SMEs with universities and technology centers; financing innovation, investments, venture capital, start-ups and spin-offs.
The common framework and the concept of integration for mechatronic, cyber-mixmechatronics and IoT activities at national and European level are expected to:

- Diversification and consolidation of research and innovation in the field at European level in partnership with national programs by improving innovation systems.
- Improving the capacity for elaboration and cooperation with the national innovation strategies.
- Building and sustaining new partnerships with Member States.
- Improving the quality of national / European partner programs.
- Assisting EU and national policies with new examples of good practice.
- A new framework for SMEs and the cluster of mechatronic, cyber-mixmechatronics and IoT technologies.
- Creating new transnational links between the companies operating in the field of mechatronics, cyber-mixmechatronics and IoT.
- Exchange of good applications and technological development practices for business networks.
- The transfer of mechatronic, cyber-mixmechatronics and IoT technology between scientific institutions and SMEs.

- New measures through venture capital for financial support for start-ups and spin-offs for new Internet developments.
- Testing innovative pilot measures for mechatronics, cyber-mixmechatronics and IoT.

3. The structure and dimensions of Industrial Internet

Industrial Internet refers to the integration of machines through sensors and network software. It does not just mean a substantial transformation of the global industry, but it has an impact on many aspects of daily life, including how many of us work. The industrial Internet will bring increased speed and efficiency in a variety of industries, such as aviation, rail, electricity, oil and gas and medical care. It brings the promise of stronger economic growth, more and better jobs, as well as improved living standards, regardless of geographic location.
The industrial Internet combines the improvements brought about by the two previous revolutions: the machines, factories, fleets and networks born from the industrial revolution and the innovations in computers, information and communication systems introduced by the much more recent Internet revolution.
Three elements constitute the essence of the industrial internet:
Smart machines: in the form of new ways to connect machines, plants, fleets and networks through sensors, control systems and complex software applications.
Advanced analysis: use of notions such as analytical ability, forecasting algorithms, automation and ultra-specialized experience in materials science and electrical engineering, to understand how large-scale machines and systems work.
People at workplace: connecting people wherever they are - in industrial factories, offices, hospitals, on the move and at any time, to promote smarter design, operations and maintenance and to generate superior quality service, alongside a improved safety.

4. Structural schemes of Digital Enterprise from Smart Industry (4.0)

Connecting smart devices, enterprises, fleets and networks with people in the workplace and on the move opens up new possibilities for process optimization and the potential for increased productivity and efficiency. In addition, it will alter the competitive balance and force the rest of the industry to adapt quickly, if it wants to survive. The pace of this process will differ from industry to industry, but the effects will be amplified in the economy as adoption grows. Thus, they are designed and presented:

- in figure 3, the structural scheme of a digital enterprise from Smart Industry (4.0) is presented, with the identification of the related physical-cybernetic systems.

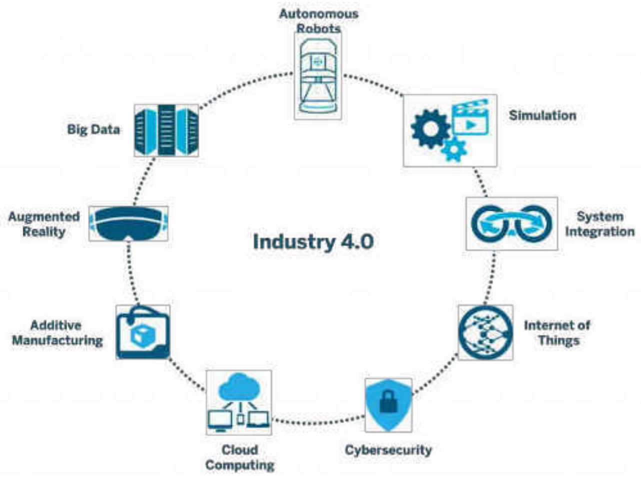

Fig. 3.

Figure 4 shows the optimization of real-time operations from a smart factory.

Fig. 4.

In the Intelligent Factory of the future, centralized control mechanisms are replaced by intelligent networks. Enhancing automation and digitization allows machines to independently organize, monitor and control processes.
For manufacturing companies, this provides many opportunities for intelligent use of analytical methods to generate added value from machine and production data and build new data-driven business models.
Figure 5 shows the COBOT technology platform used in the intelligent manufacturing of the automobile industry.

Fig. 5.

Figure 6 shows "a structure of industrial robots in a digitized factory".

Fig. 6.

In figure 7, there is presented "a robotics structure of parts supplying a CNC machine tool", in a smart factory.

Fig. 7.

Figure 8 shows the "connections of a telemedicine pilot center in Romania".

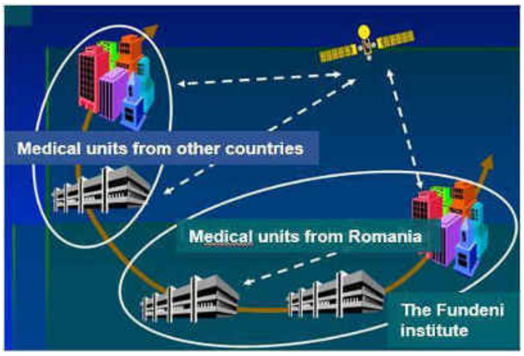

Fig. 8.

Figure 9 shows "an integrated telemedicine network that also includes patient telemonitoring".

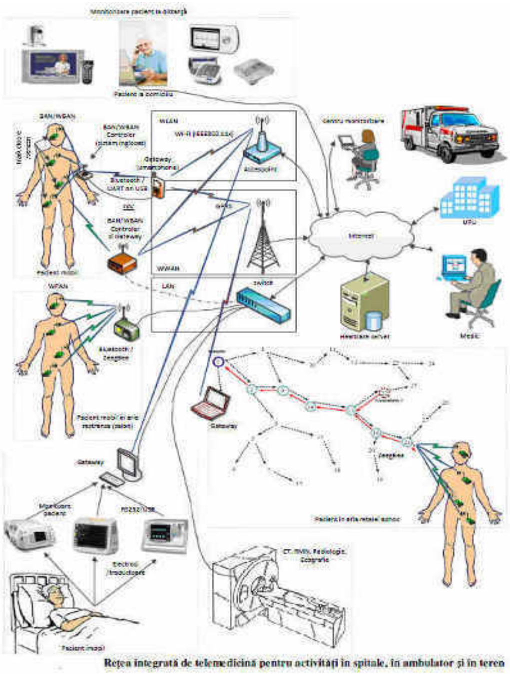

Fig. 9.

Figure 10 shows "an example of a workstation on the automotive manufacturing line", from the smart industry (4.0).

Fig. 10.

5. Structural schemes of Smart Agriculture

The evolution of agriculture is based on a number of decision-makers, important conditions for intelligent agriculture and intelligent food supply chains. Some of them are:

• Innovative technologies: machining hardware (robotics), RFID, sensors, wireless networks, including broadband in rural areas, web technology, cloud computing, big data, predictive analytics tools.

• Standardization: fast, error-free and efficient exchange of digital data within and between companies, based on information standards.

• Skills: knowledge, adoption and knowledge of digital information systems and standards and their ability to use them.

• Governance: organizational implementation and business models, including agreements on property rights and decision rights, remuneration, risk management, etc. (see the section on data ownership below).

Figure 11 shows the "IT effects on business models in the food chain".

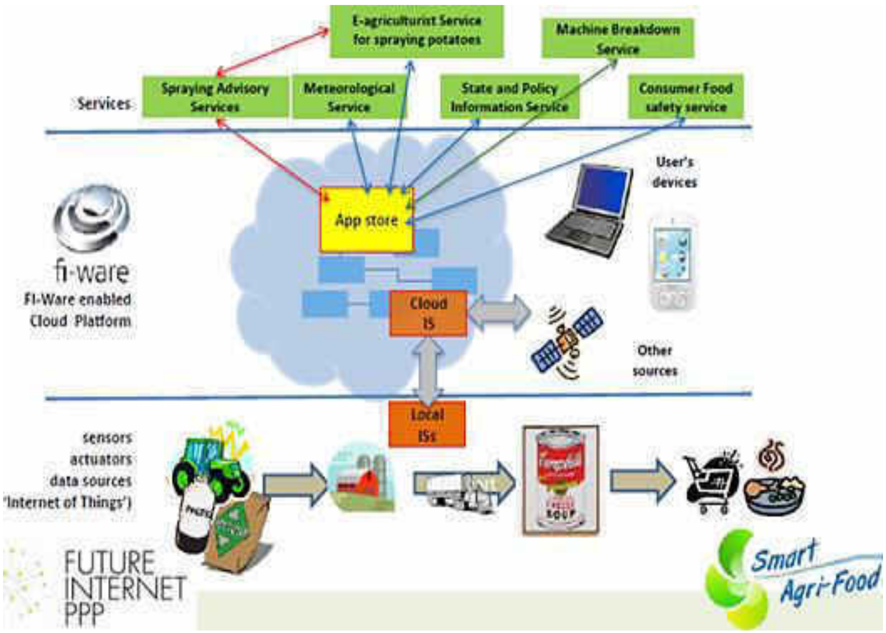

Fig. 11.

The digitization of agricultural processes continues to expand and intensify. The supply and demand of agricultural data is growing rapidly. There is an increase in market data tools and even more in the decision making process. Data-driven initiatives are growing in the agri-food chains. Agriculture becomes a booming business of data collections, in which many players take bites in the data generated by agriculture. Many data-driven initiatives continue to explore viable business models to capture the value of data. A variety of business models are used and developed with different value propositions for different actors.
Figure 12 shows the "use of drones to support agriculture".

Fig. 12.

While some sectors seem to be resisting digital implementation, others are in the process of transformation. In general, this refers to the sectors that face the most constraints (money, time and / or workload). These sectors use digital technology to increase productivity, but also to innovate. Agriculture has seen in digital a way to overcome many difficulties inherent in this sector. If the development of a country goes through industrialized agriculture, it is possible that in the next few years the development will take place through digital agriculture.
Figure 13 shows "an example of precision treatments in agricultural crops using smart drones".

Fig. 13.

Figure 14 shows "an example of agricultural digitization through the use of robots".

Fig. 14.

6. Concepts of technological and cobotics platforms for Digital Enterprise and Smart Industry (4.0)

The development of the technical and technological concepts of type "COBOT" for Enterprise and Industry 4.0, is based, on the one hand, the concepts, the advanced technical sciences, the technological paradigms, the cognitive treasures, the scientific strategies, and on the other hand, the scientists and world strategies, regarding the construction of industry, economy and society at high competitive levels and of excellence, optimum efficiency and maximum productivity.
The holistic architectural structure of the technical and technological concepts of COBOT type for Enterprise and Industry 4.0, includes new approaches embraced by the paradigms of new organizational cultures, in an evolution towards modern practices, still being defined, all subject to digital transformations. A digital transformation, in general, involves a change of leadership style, traditional ways of thinking, in favor of innovation and new business models. Thus, by incorporating the latest digital technologies, the aim is to improve the experience of the employees of the company and of the clients, suppliers, partners and shareholders of that company.
In summary, digital transformation represents the integration of digital technologies in absolutely all areas of a company and has the effect of fundamentally changing the operating mode and the way in which the surplus value is created / delivered to the clients of that company.
Changes and digital transformation are not only reflected in the way business is conducted, but also in the whole of society.
Almost everyone is talking about digital transformation today (or digitizing human activity, as everyone prefers). But is this digital transformation just a trendy word or a phenomenon that has the wave of change that will affect everyone in the years to come?
The attempt to give a relatively unanimously accepted definition would say something like this: Digital transformation represents the profound transformation of business, organizational activities, processes, competencies and working models to fully exploit the changes and opportunities created by a mix of new technologies and the impact on their full acceleration on human society.
Even though the term "digital transformation" is predominantly used in business contexts, it has profound impact on other organizations such as governments, public sector agents and organizations involved in responding to societal challenges such as pollution and aging, precisely by trying to leverage one or more of the existing and emerging technologies. In some countries, such as Japan, digital transformation aims to generate an impact on all aspects of life in that society (hence a beautiful generic name, namely the 5.0 Business Initiative), which is far beyond the limited vision called Industry 4.0 from other countries.
And as Romania is in Europe, and countries such as Japan are far from many points of view, the focus on digital transformation must remain, for the time being, on the business dimension of the term. In this context, the aforementioned development of new skills revolves around the capabilities of companies to increase their agility, to be more people-oriented, to be innovative, to be consumer-centered, efficient and capable of taking advantage of opportunities to change. the

state of affairs and to open the taps for new sources of income fed by information and services. It is certain that efforts and strategies related to digital transformation are more present and imperative in markets with a high degree of commoditization.
The present and future changes and changes, which lead to the necessity of a digital transformation strategy, can be induced by several causes, often simultaneously, at the level of consumer behavior and expectations, of new economic realities, of changes among populations (such as the aging phenomenon), disruptive events in the ecosystem and industry and the accelerated adoption of digital technologies. In practice, optimizing customer experience, increasing business operational flexibility and innovation are essential drivers of digital transformation, along with the development of new revenue sources and new value ecosystems fueled by the power of information. And all of this leads to major changes in business models.
Many are currently asking whether digital transformation is a goal in itself. However, the most correct one would be, in my view, for digital transformation to be considered a journey with many intermediate goals interconnected, the aim, if we can talk about it, being that of a continuous optimization of business processes and ecosystems. an era of hyper-connectivity, in which the key to success is the construction of the right bridges between the various functions.
A digital transformation strategy aims to create the capabilities to fully exploit the possibilities and opportunities offered by the new technologies and to correct, faster and more innovative management of their impact in the future. Any journey of digital transformation requires a step-by-step approach with a clear roadmap, involving many stakeholders in the process. Such a map must take into account the fact that the final objectives are extremely fluid, because digital transformation itself is a perpetual journey, as are digital change and innovation.
Digital technologies, and the ways we use them in our personal lives, at work and in society, have changed the way business looks and will continue to do so. This has happened permanently in history, but the pace at which things are going now is unprecedented. Yes, more. is in full acceleration, threatening to speed up the pace of internal transformations of organizations, resulting in a huge danger of cleavage between the two phenomena. This is because digital transformation does not refer only to disruptive phenomena or technology.
Digital transformation means new business ecosystems. These are evolutions of partner networks as well as contextual factors that affect the company, such as regulations or priorities and economic developments. Digital transformation means building new ecosystems between companies with diverse backgrounds based on the same digital information network, in which tradable data and information become innovative assets.
Another important node of the digital transformation "network" is business asset management. Certainly, the focus area will continue to be that of traditional assets, but digital transformation will involve increasingly focusing on less "tangible" assets, such as information and customers. Why? Improving customer experience is a leading goal for many digital transformation projects, and information is becoming more and more the "blood" of business, technological developments and inter-human relationships. As such, both clients and information will need to be treated as real assets from all points of view.
Another essential point is the organizational culture. Such a knot means, in a digital context, a clear customer-focused, agile and aware goal for all company staff, an objective that can be achieved by acquiring key personnel skills such as digital maturity, leadership, knowledge of points weak mental ones who have to undergo transformations, and so on.
An important area of transformation is also that of the business ecosystem of the company and of the partnership models. This requires increasing the degree of cooperation, collaboration and collaborative creation, as well as new approaches to business ecosystems, which will lead to new business models and, consequently, to new sources of income.
Last but not least, another important point is the approaches towards clients, employees and partners. Digital transformation puts people and strategies ahead of technology. As such, changing the behaviors, expectations and needs of all stakeholders is essential. This is expressed through many smaller change projects (sub-projects) within which focus on the customer, user experience, employee empowerment, new job models, changing the dynamics of the partner channel, etc.

It is important to note that digital technologies are never the only solution to tackle all these aspects of business and people. People mean respect and empower other people first and foremost, technology is an additional catalyst and part of the equation of fundamental choices and needs.

In the following are presented, in original concepts, examples of COBOT technology platforms:

- In the figure 15, COBOT technology platform for verification and integrated control processes in the Enterprise and Smart Industry (4.0)

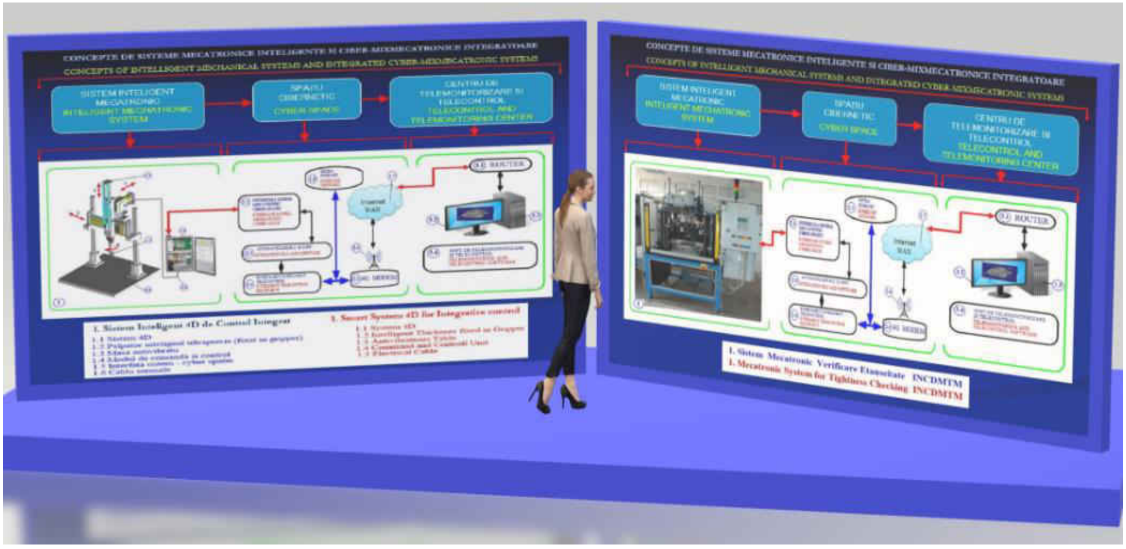

Fig. 15. COBOT technology platform for verification and integrated control processes in the Enterprise and Smart Industry (4.0)

- in the figure 16, COBOT technology platform for measuring and intelligent control processes in the Digitized Enterprise and Smart Industry (4.0) in the field of Technological Equipments

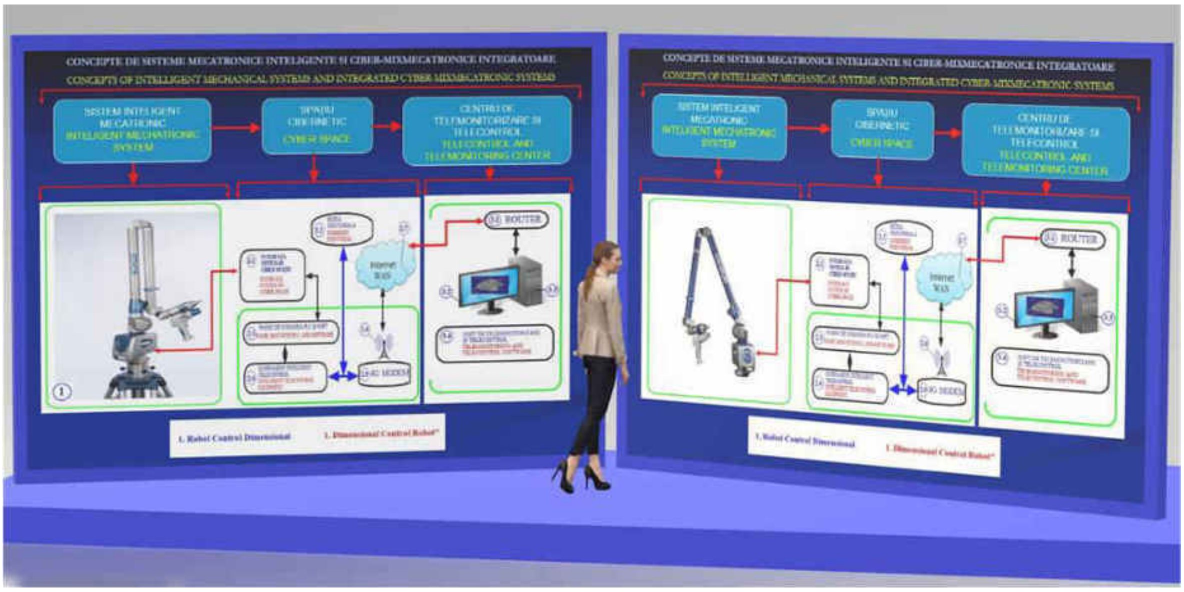

Fig. 16. COBOT technology platform for measuring and intelligent control processes in the Digitized Enterprise and Smart Industry (4.0) in the field of Technological Equipments

- in the figure 17, COBOT technology platform for assembly processes and industrial parts from Enterprise and Industry 4.0, in the field of Machine Construction

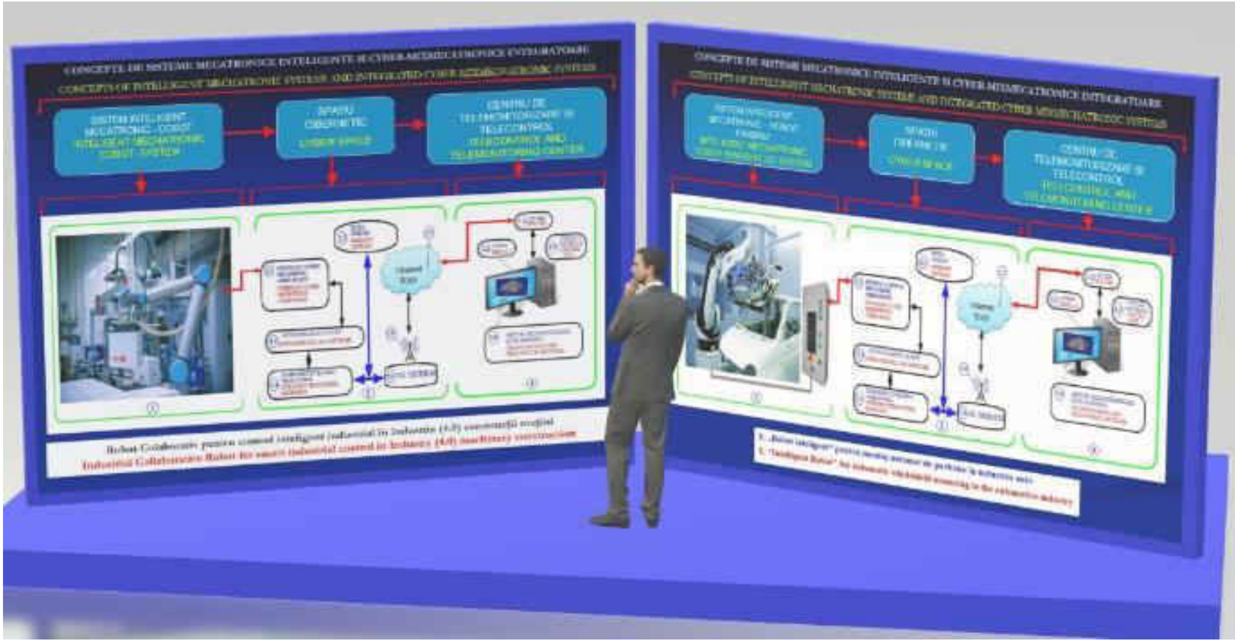

Fig. 17. COBOT technology platform for assembly processes and industrial parts from Enterprise and Industry 4.0, in the field of Machine Construction

- in the figure 18, COBOT technology platform for positioning processes in metrology laboratories in the Enterprise and Intelligent Industry (4.0) in the field of Intelligent Metrology.

Fig. 18. COBOT technology platform for positioning processes in metrology laboratories in the Enterprise and Intelligent Industry (4.0) in the field of Intelligent Metrology

7. Conclusions

The scientific paper shows that industrial digitization will have an impact both horizontally and vertically on the value chain, which means that, on the one hand, companies must integrate and digitize their vertical data flow much better, in the development of products and procurement up to the processing and logistics of transport, and on the other hand, implies a horizontal collaboration with key suppliers, customers and other partners in the value chain.
Companies, businesses and industry in general 4.0 must be involved in the development and implementation of complex digital solutions, and all staff are confident that industrial digitalization is the most appropriate and necessary choice for the future.
The scientific work also synthesizes the beginnings of industrial digitization, by presenting intelligent concepts and solutions proposed by the author, for integrating mechatronic and cyber-mixmechatronics mechatronic systems that are or are to be implemented in different industrial sectors (automotive, aerospace, agriculture, medicine, etc.) from Romania.
The digitization strategy of Enterprise and Industry 4.0 is synthesized, for national and European level in the following diagram:

Pillar 1

Single Digital Market - Free cross-border access to online services and information

Pillar 2

Interoperability and standards - integration, devices, applications, data and services in the code of social ethics

Pillar 3

Trust and security - Increase Internet users' trust in electronic services and online transactions through transparency and security

Pillar 4

Fast and ultrafast access to the Internet - aims to invest in infrastructure in broadband equipment

Pillar 5

Research and Innovation in ICT - Stimulates adequate funding for increased competitiveness

Pillar 6

Increasing the digital literacy of skills and inclusion - Creating a bridge to the digital divide

Pillar 7

ICT benefits for EU society - ICT's ability to reduce bureaucracy, support elderly care, improve health services, and deliver public services

Goals to be achieved by 2020:

- Employment (75% of people between 20 and 65 years should be employed)
- Research / Development (3% of GDP should be allocated to R / D)
- In the field of education (40% of people between 30 and 34 years to complete the third level of education)
- Combating poverty and social exclusion.

References

[1] Noble, B.D., and J. Flinn. 2007. “Wireless, self-organizing cyber-physical systems.” NSF Workshop on Cyber-Physical Systems. Austin, TX.

[2] Busse, M., and F.-J. Wostmann. “Intelligent Cast Parts - Application of Adaptronic Components with Cast Parts.” Proc. Adaptronic Congress, Gottingen, Germany, May, 2006.

[3] Barros, C., C.P. Leão, F. Soares, G. Minas, and J. Machado. “RePhyS: A multidisciplinary experience in remote physiological systems laboratory.” *International Journal of Online Engineering* 9, no. 5 (2013): 21-24, DOI: 10.3991/ijoe.v9iS5.2756.

[4] Pereira, C.E., S. Paladini, and F.M. Schaf. “Control and Automation Engineering Education: Combining Physical, Remote and Virtual Labs.” Proceedings of the 9th International Multi-Conference on Systems, Signals and Devices – SSD 2012, Chemnitz, Germany, 20-23 March, 2012.

[5] ***. "Digital Transformation Monitor – Key lessons from national Industry 4.0 policy initiatives in Europe." https://ec.europa.eu/growth/tools-databases/dem/.
[6] Gheorghe, Gh. *Mecatronica și Cyber-MixMecatronica în Industria 4.0*. Bucharest, CEFIN Publishing House, ISBN: 978-606-8261-28-7, 2018.
[7] Gheorghe, Gh. *Ingineria Cyber-Mecatronică și Clatronică*. Bucharest, CEFIN Publishing House, ISBN 978-606-8261-26-3, 2017.
[8] Gheorghe, Gh. *Elaboration of new scientific and technological concepts and new virtual mechatronics and adaptronics models and cyber-mechatronics and cyber-adaptronics*. Bucharest, CEFIN Publishing House, 2016.
[9] Gheorghe, Gh., A. Constantin, I. Ilie. "Scientific Evolution from Mix – Integrating Mechatronics to Cyber-Intelligent Mechatronics and to Claytronics Science." Proceedings of International Conference on Aerospace, Robotics, Manufacturing Systems, Mechatronics and Neurorehabilitation OPTIROB 2016, Jupiter, Romania, June 29- July 2, 2016.
[10] Gheorghe, Gh., A. Constantin, I. Ilie. "Mechatronics and Cyber Mechatronics in Intelligent Applications from Industry and Society." Proceedings of International Conference on Aerospace, Robotics, Manufacturing Systems, Mechatronics and Neurorehabilitation OPTIROB 2016, Jupiter, Romania, June 29- July 2, 2016.
[11] Machado, J., F. Soares, and L. Celina. "A virtual Workbench applied to Automation Students Response Analysis." Proceedings of 11th Portuguese Conference on Automatic Control - Controlo 2014, Porto, Portugal, July 21-23, 2014.
[12] Varela, M.L.R., G.D. Putnik, V.K. Manupati, G. Rajyalakshmi, J. Trojanowska, and J. Machado. "Collaborative manufacturing based on cloud, and on other I4.0 oriented principles and technologies: A systematic literature review and reflections." *Management and Production Engineering Review* 9, no. 3 (2018): 90--99.
[13] Gheorghe, Gh. *Micro-nano-ingineria inteligentă integronică*. Bucharest, CEFIN Publishing House, ISBN: 978-973-720-538-4, 2014.
[14] Gheorghe, Gh. *Study and analysis regarding the concepts of mechatronics and adatronics virtual models and cyber-mechatronics and cyber-adaptronics*. Bucharest, CEFIN Publishing House, 2016.
[15] Bruns, F.W., H.H. Erbe, and M. Faust. "Engineering Future Laboratories." *Marvel – A Leonardo da Vinci Pilot Project– Mechatronics Training in Real and Virtual Environments*. Bremen, 2005.
[16] Noble, B., and J. Flinn. "Wireless, self-organizing cyberphysical systems." Proc. of the NSF Workshop on CyberPhysical Systems, Austin, TX., 2007.
[17] Pop, I.G., and V. Matiec. "Transdisciplinary Approach of the Mechatronics in the Knowledge-based Society. Advances in Mechatronics." H. Martinez-Alfaro (Ed.), InTech, 2011.
[18] Gharavi, H., K.V. Prasad, and P. Ioannou. "Scanning advanced automobile technology." Proc. IEEE 95 (2007): 328–333.

ISSN 1454 - 8003
Proceedings of 2019 International Conference on Hydraulics and Pneumatics - HERVEX
November 13-15, Băile Govora, Romania

MODELLING AND SIMULATION OF A CLOSED LOOP PUMP HYDRAULIC CIRCUIT FOR NEUTRAL PRESSURE VARIATION STUDY

Himanshu PRABHAT[1], Venkateswaran KRISHNASAMY[1], Nitin HANDE[1], Anil KHARPAS[1]

[1] Eaton India Innovation Center;
HimanshuPrabhat@eaton.com, VenkateswaranKrishnasamy@eaton.com, NitinJHande@Eaton.com, AnilKharpas@eaton.com

Abstract: *Closed loop pump circuits are used in hydrostatic transmission (HST) which combines variable displacement piston pump and fixed displacement motor. This paper studies one of the most important parameters i.e. 'neutral pressure variation' which is safety critical element to prevent the unexpected vehicle movement. The HST system has been modelled using MATLAB Simulink tool with meticulous modeling efforts on the axial piston motor, relief valves, check valves, shuttle valves, charge pump circuit along with pump swash controls. The closed loop system model has been validated with test bench result. Further, neutral pressure variation as predicted by model is correlated with test data. The study of dynamical behavior of such system is very significant for accurate estimation of closed loop system performance parameters like motor starting torque, system pressure, motor speed characteristics and their dynamic fluctuations. The detailed system model proposed here enables simulation of the dynamic behavior of closed loop pump circuit, facilitating prediction of the dynamic performance of system, which can be used to improve the design parameters through parameters sensitivity analysis.*

Keywords: *Hydrostatic Transmission, Axial Piston pump, Axial Piston Motor, Neutral Pressure, Simulation*

1. Introduction

Hydrostatic transmission (HST) have been widely used in the mobile machines and off-road vehicles such as wheel loaders, fork lift, tractors, harvesters etc. Hydraulic power transmission bears several advantages such as higher efficiency, variable speed & torque control, step less speed change with easy forward/backward movement, capable to transfer over longer distance, hydrostatic braking, handling heavy loads and smooth operation [1]. Hydrostatic transmission utilizes a variable displacement axial piston pump and fixed displacement axial piston motor connected in closed loop system. Figure 1 shows the simple closed loop pump circuit of hydrostatic transmission with control. Oil is circulated by the pump to the motor and then returned directly back to the pump. A charge supply is used to supplement the closed loop system with oil as well as to avoid cavitation and the charge flow is supplied external source. The pump is driven by the prime mover, which generates flow to drive the hydraulic motor.

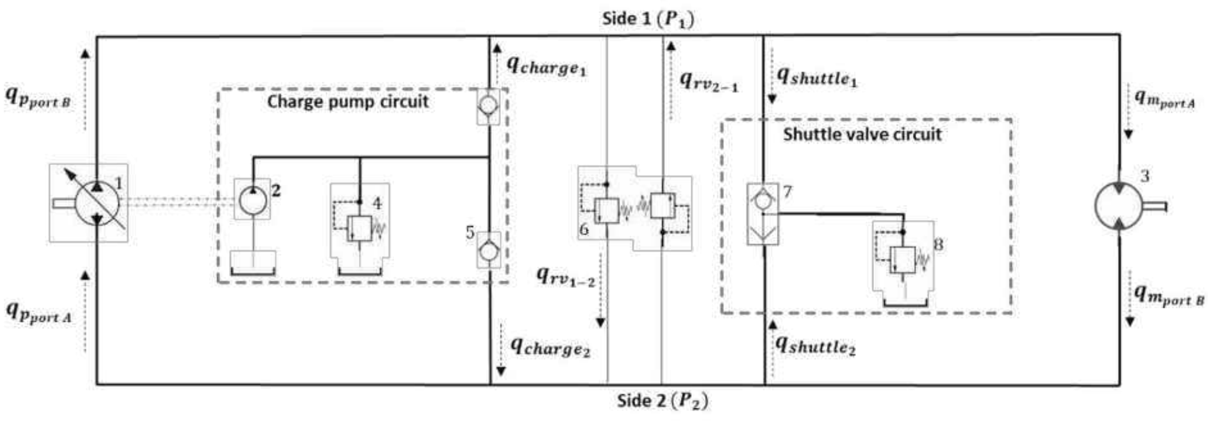

Fig. 1. Hydraulic schematic diagram of closed loop circuit in HST
1.Bidirection piston pump; 2. Charge pump; 3. Hydraulic motor; 4. charge pump relief valve; 5. Check valve; 6. IPOR relief valve; 7. Shuttle Valve; 8. Relief valve

The motor is connected to the gear box which transmits the power. Pressure is generated in the system due to the load connected to the hydraulic motor. The system pressure relief valve is used to maintain the maximum pressure in the forward and reverse direction of pump rotation. Check valves are provided to distribute the additional flow from the charge pump based on the direction of rotation of the pump. Direction and rotation of the motor depends of the output flow of the pump. Pump flow depends on the speed and displacement of the pump. The displacement of the pump is controlled by the swashplate position.

Several CTQ's can be addressed by developing a mathematical model for the closed loop pump circuit system and one of the CTQ in the current paper study is neutral pressure variation. When pump is in closed loop circuit and is brought back from full load, full stroke to no load and no stroke condition, ideally it is expected that pressure differential between pump port A and B should also fall back to zero. However, because of frictional losses and leakages, some pressure differential may occur which is called neutral pressure variation. Neutral pressure variation can be summed up as difference in pressure between two ports of closed loop circuit piston pump at no stroke and no-load condition. This is very critical when the vehicle or any machine application needs to stand at neutral i.e. without driving the external load, unexpected hazardous movement will occur when the pressure exceeds more than certain limit. Usually that limit is set to be around 30 psi. So, in any hydrostatic transmission this is very important in meeting the requirement and a mathematical model of closed loop pump circuit will help in evaluating the situation better before pump testing. Also modelling and simulating the entire closed loop circuit represent a strong and reliable approach and allow the better understanding of the baseline system, influence of design parameters on the system performance.

The aim of the paper is to show the modelling effort to develop the system level closed loop pump circuit model and to predict the neutral pressure variation CTQ. As part of this system CTQ, subsystem CTQ's like motor starting pressure, torque, torque ripple was established and verified. The model started with 49cc piston pump with 49cc fixed displacement piston motor configuration, the methodology can be scaled up to higher displacement motor/pump combination. The mathematical model was developed from first principle using MATLAB Simulink software. The system model consists of several subsystems like pump, motor, swash controls, charge pump, relief valve, check valves etc and there is complexity associated at bigger system level integration. Hence a holistic step by step approach with sub system modelling and verification of each subsystem was carried out on the flow, pressure characteristics. The model was validated with dynamic test data for the pressure, speed performance and predicted the variation of neutral pressure.

2. System Modelling of CC circuit components

This section addresses modelling aspects of various hydraulic components involved in cc circuit as shown in figure (1). Primarily, we have two main hydraulic lines, one going from pump to motor and other from motor to pump. Accordingly, hydraulic components not explicitly connected to these lines are grouped into single unit from modelling perspective, as shown in schematic diagram in figure (1) with dashed border. Thus, major components which have been modelled in following sections are bidirectional variable displacement axial piston pump with electric proportional swash control, fixed displacement axial piston motor, IPOR valves, charge pump circuit and shuttle valve circuit. Each component either supply or extract fluid from both hydraulic lines. This idea is crucial for integration of all components to generate cc circuit model.

2.1 Bidirectional Variable Displacement Axial Piston Pump Model

Mathematical modelling of axial piston pump has been addressed before in [2,3,4,5]. However, the modelling approach and conventions followed, doesn't ensures bidirectional nature of the pump model. The pump model developed in [1] has been modified to inculcate bidirectional nature in pump model. Similar approach has then been carried on for motor model as well. Axis sign convention chosen in this model is as per figure (2).

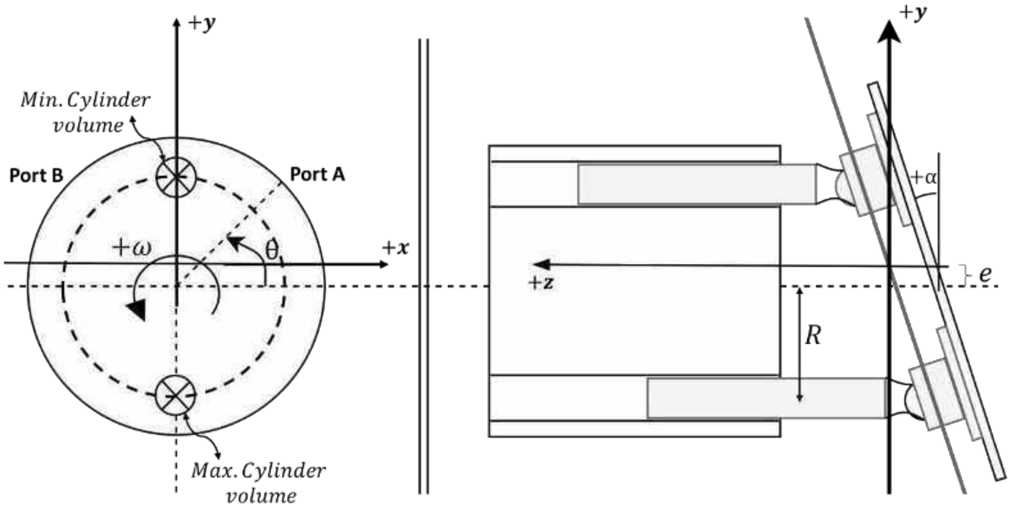

Fig. 2. Schematic diagram of pump RG kit with assigned sign convention

Port A & B side of pump as function of piston angular position, θ is defined as follow:

$$Port\ A\ Side: \theta \in \left[0, \frac{\pi}{2}\right) U \left(\frac{3\pi}{2}, 2\pi\right) \tag{1}$$

$$Port\ B\ Side: \theta \in \left[\frac{\pi}{2}, \frac{3\pi}{2}\right] \tag{2}$$

By convention, when swash angle and pump rotation are positive, port B and A are pump outlet & inlet, respectively. Bidirectional nature of pump is enabled by allowing swashplate to move in both directions.

2.1.1 Piston Kinematics & Pressure Dynamics

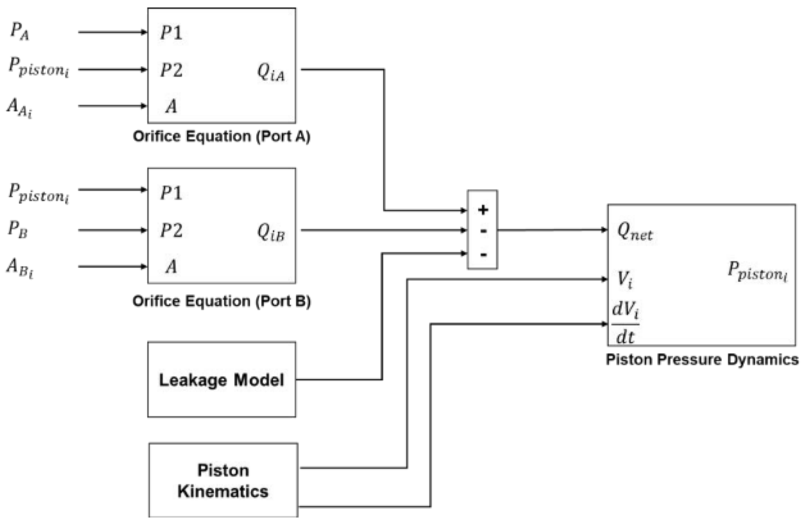

Fig. 3. Piston pressure dynamics model for pump

Flow going in and out of piston-barrel interface can be modelled using classical orifice equation based on Bernoulli's principle. [5] Thus, flow through an orifice, Q_i having pressure, P_1 and P_2 on either side and orifice area A, is given as:

$$Q_i = sign(P_1 - P_2) C_d A \sqrt{\frac{2}{\rho} |P_1 - P_2|} \tag{3}$$

At any instant, piston could be located on either port A or port B side. Depending on swash angle sign, port A & B can be inlet and outlet respectively or vice versa. Flow entering or leaving the piston through piston valve plate overlap area can be obtained using orifice equation. Figure (3) presents the schematics of piston pressure dynamics model. It's evident from geometric model that at any instant piston would be located either on port A or port B side. Depending on piston location and swash angle sign, instantaneous flow contribution of piston on either side is described in table (1).

Table 1: Piston flow contribution on pump port A & B

Swash Angle Sign (α)	Pump Port A	Pump Port B	Piston Location	Q_{A_i} (Sign)	Q_{B_i} (Sign)
+	Inlet	Outlet	A	Q_{A_i}(+)	0
+	Inlet	Outlet	B	0	Q_{B_i}(+)
-	Outlet	Inlet	A	Q_{B_i}(-)	0
-	Outlet	Inlet	B	0	Q_{B_i}(-)

When swash angle is positive, flow entering or leaving piston as obtained from port A & B, i.e. Q_{A_i} & Q_{B_i} are either zero or positive. On contrary, for negative swash angle, they are either negative or zero. Thus, the sign change in flow contains the information of inlet and outlet switching. Q_{A_i} & Q_{B_i} can be obtained by substituting relevant information from schematic diagram shown is figure (3) into equation (3):

$$Q_{A_i} = sign(P_A - P_{piston_i}) C_d A_i \sqrt{\frac{2}{\rho} |P_A - P_{piston_i}|} \tag{4}$$

$$Q_{B_i} = sign(P_{piston_i} - P_B) C_d A_i \sqrt{\frac{2}{\rho} |P_{piston_i} - P_B|} \tag{5}$$

A_i is instantaneous piston-valve plate overlap area through which fluid enters or leaves. It is a function of piston angular position θ_i. As per convention, for pressure dynamics in piston-barrel control volume, flow entering the CV is considered positive and vice versa. Multiplying port B piston flow to negative sign, ensures that net flow input to pressure dynamics block comes with correct sign irrespective of inlet and outlet change. Piston pressure, P_i is obtained by solving pressure dynamics equation for control volume shown in figure (4), obtained by applying the fundamental law of the conservation mass as discussed by Zeiger and Akers [6]:

$$\frac{dP_i}{dt} = \frac{\beta}{V_i}\left(Q_i - Q_{leak} - \frac{dV_i}{dt}\right) \tag{6}$$

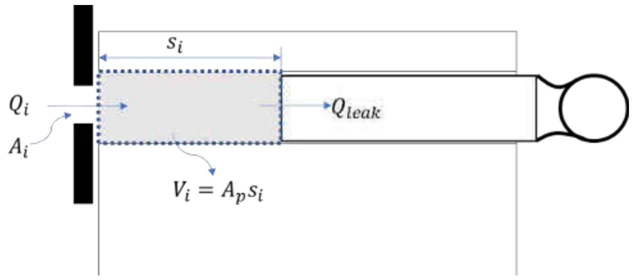

Fig. 4. Piston-barrel control volume

Control volume length, s_i is given as:

$$s_i = s_o - (Rsin\theta - e)\tan(\alpha) \tag{7}$$

Derivative of control volume dV_i/dt is obtained as:

$$\frac{dV_i}{dt} = -\frac{\pi d_p^2}{4}\left\{\left((Rsin\theta - e)\sec^2\alpha\right) * \frac{d\alpha}{dt} + Rcos\theta\tan(\alpha)\,\omega\right\} \tag{8}$$

Combining equation (6), (7) and (8), we get:

$$\frac{dP_i}{dt} = \frac{\beta\left(Q_i - Q_{leak} + \frac{\pi d_p^2}{4}\left\{\left((Rsin\theta - e)\sec^2\alpha\right) * \frac{d\alpha}{dt} + Rcos\theta\tan(\alpha)\omega\right\}\right)}{\frac{\pi d_p^2}{4}\{s_o - (Rsin\theta - e)\tan(\alpha)\}} \tag{9}$$

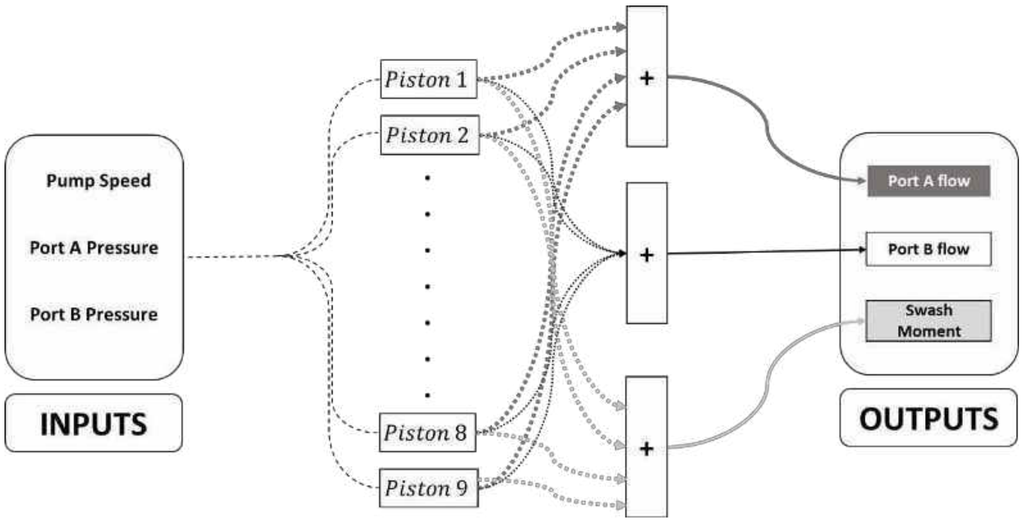

Fig. 5. Schematic overview of bidirectional pump mathematical model

Figure (5) presents an overview of bidirectional pump model. Pump speed, port A and B pressure goes as input to each piston. Each piston contributes either towards port A or port B flow which is summed up to obtain net flow through pump ports. Also, each piston produces a moment on swash plate which is discussed in next section. Likewise, each piston moment is added to obtain pump swash swivel torque.

2.1.2 Pump Swash Moment

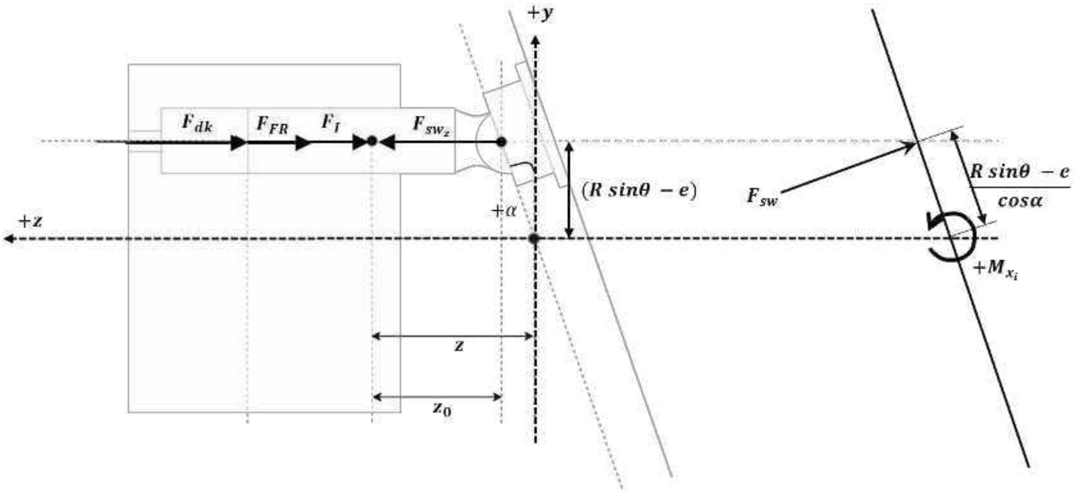

Fig. 6. Piston free body diagram for pump swash moment

Swash-piston reaction force F_{SW_i} generates a moment M_{x_i}, which produces tilting moment on swash plate. This moment needs to be countered by swash control mechanism. To obtain moment contribution of each piston, i.e. M_{x_i}, force balance on piston is done in z direction. Swash-Piston reaction force z-component, $F_{sw_{i_z}}$ is given as:

$$F_{sw_{i_z}} = F_{di} + F_{FR_i} + F_{i_I} \tag{10}$$

Where, F_{di} is pressure on piston and is described as [5]:

$$F_{di} = \frac{\pi d_k^2}{4}(P_{piston_i} - P_{case}) \tag{11}$$

Inertia force, F_{i_I} is given as:

$$F_{i_I} = -\ m_i \omega^2 R\ sin\ \theta_i\ tan\ \alpha \tag{12}$$

Modelling of friction force acting on piston barell overlap is quite complex in nature because of hydrodynamic effects involved and a huge topic of research. Friction models based on mechanical efficiency estimation [7] and empirical relation considering stribek and hydrodynamic friction as well as pressure dependant term [8] has been developed. For the sake of simplicity, friction force has been assumed to be negligible. However, suitable friction models [7,8] can be included to improve model physics. Swash reaction force, F_{sw} , perpendicular to swash plate can be obtained as:

$$F_{sw_i} = \frac{F_{sw_{i_z}}}{\cos\alpha} \tag{13}$$

Moment arm for piston location θ_i is shown in figure (6). Considering axis sign convention, M_{x_i} is given by:

$$M_{x_i} = -\frac{(R\sin\theta_i - e)}{\cos\alpha}\{F_{dk} + F_I + F_{FR}\} \tag{14}$$

Considering 9 pistons, net pump swash moment is given as:

$$M_x = \sum_{i=1}^{9} M_{x_i} \tag{15}$$

M_x is essentially an internal disturbance which must be counteracted by swash plate control mechanism to ensure smooth operation.

2.1.3 Electric-Proportional Swash Displacement Control

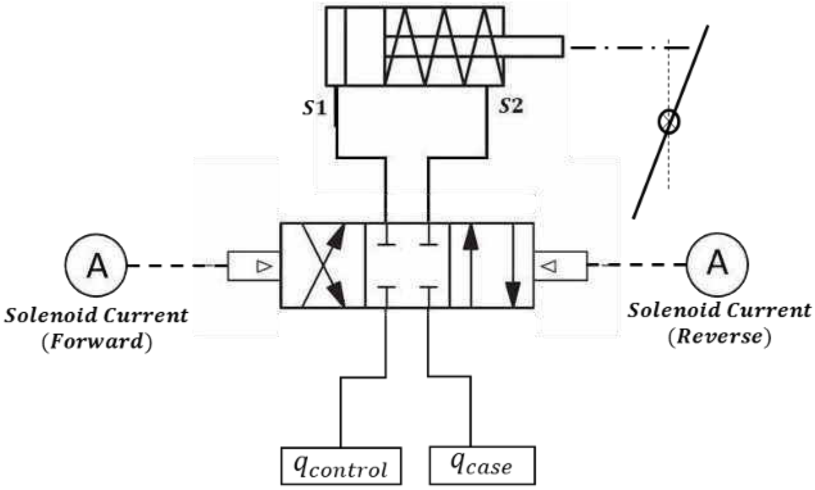

Fig. 7. Electric Proportional Pump Swash Control

Swash control circuit broadly consists of 4-way 6-position solenoid actuated directional control valve and double acting cylinder actuator which is connected to swash plate by mechanism suitable to particular pump design as shown in figure (7). Control flow, $q_{control}$ is extracted from flow supplied by charge pump to cc circuit. Under ideal circumstance, i.e. pressure drop across valve orifice is small and valve is completely shifted either of forward or reverse position, pressure on high pressure side of cylinder will nearly be equal to charge pressure. Flow drained out of control adds to case flow, q_{case}. Physical model of direction control valve has been developed following the principles discussed by Manring [9]and Merrit [10]. Forces acting on control piston can be listed as spring force, Swash reaction force, pressure force and viscous damping force. Swash swivel force acting on control pison, F_{swivel} can be obtained by multiplying swash moment M_x as described in previous section with moment arm of linkage mechanism. Pressure force is given as:

$$F_{pressure} = A_{Piston}(P_{S1} - P_{S2}) \tag{16}$$

Spring force as a function of spring displacement, x is given as:

$$F_{spring} = K(x + x_{preload}) \tag{17}$$

Likewise, viscous damping force, F_d is given as:

$$F_d = c\frac{dx}{dt} \tag{18}$$

Force balance on control piston yields:

$$M_p\frac{d^2x}{dt^2} + c\frac{dx}{dt} + K\left(x + x_{preload}\right) = F_{pressure} + F_{swivel} \tag{19}$$

At equilibrium, preload force, $Kx_{preload}$ cancels out swivel force. Pressure force is generated based on the soenoid signal input to DCV. Thus, indirectly it is control input in above dynamics. In present work, open loop control of pump is considered where predetermined forward and reverse solenoid signals are provided to DCV and accordingly control piston changes position as per dynamic equation discussed in eq. (19) thus changing swash angle.However, this can be modified to feedback controls depending on application.

2.2 Bidirectional Fixed Displacement Axial Piston Motor Model

Empirical model of axial piston motor as a part of hydrostatic transmission has been developed in [11,12] from control design perspective. Gao et. al. [13] presents physics-based model considering geometric parameters of motor from design and performance perspective. However, the bidirectional nature of motor hasn't been ensured. Thus, like bidirectional pump model, similar approach has then been carried on motor model allowing it to swing both ways. Sign convention for motor model has been adopted as per figure (8).

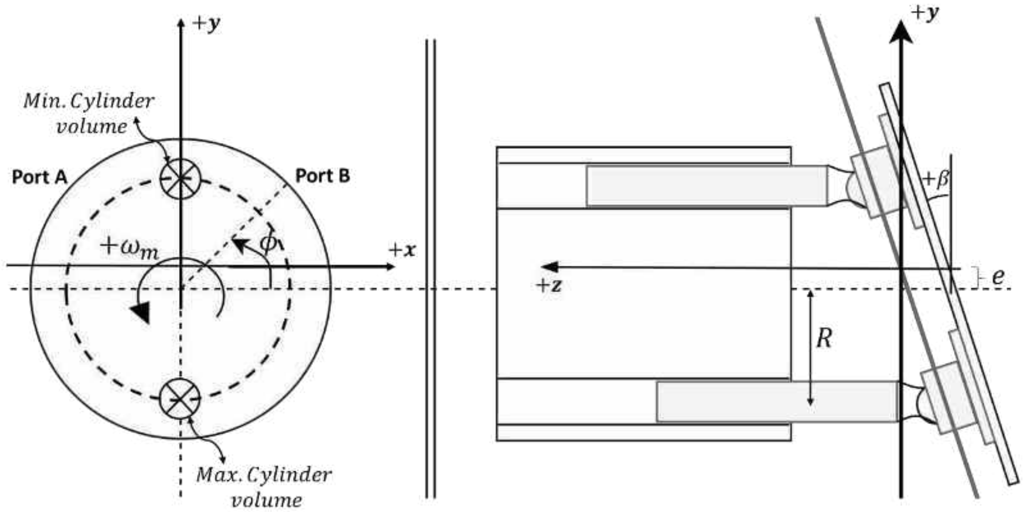

Fig. 8. Schematic diagram of motor RG kit with assigned sign convention

Port A & B side of axial piston motor as function of piston angular position, ϕ is defined as follow:

$$Port\ A\ Side: \phi \in \left[0, \frac{\pi}{2}\right) U \left(\frac{3\pi}{2}, 2\pi\right) \tag{20}$$

$$Port\ B\ Side: \phi \in \left[\frac{\pi}{2}, \frac{3\pi}{2}\right] \tag{21}$$

Being a fixed displacement motor, swash angle is fixed however motor can rotate in both senses depending on pressure at port A and B. By convention, motor would acquire positive angular velocity when port B and A are low & high-pressure side, respectively. In other word, port A will be motor inlet whereas port B will be motor outlet.

2.2.1 Piston Kinematics & Pressure Dynamics

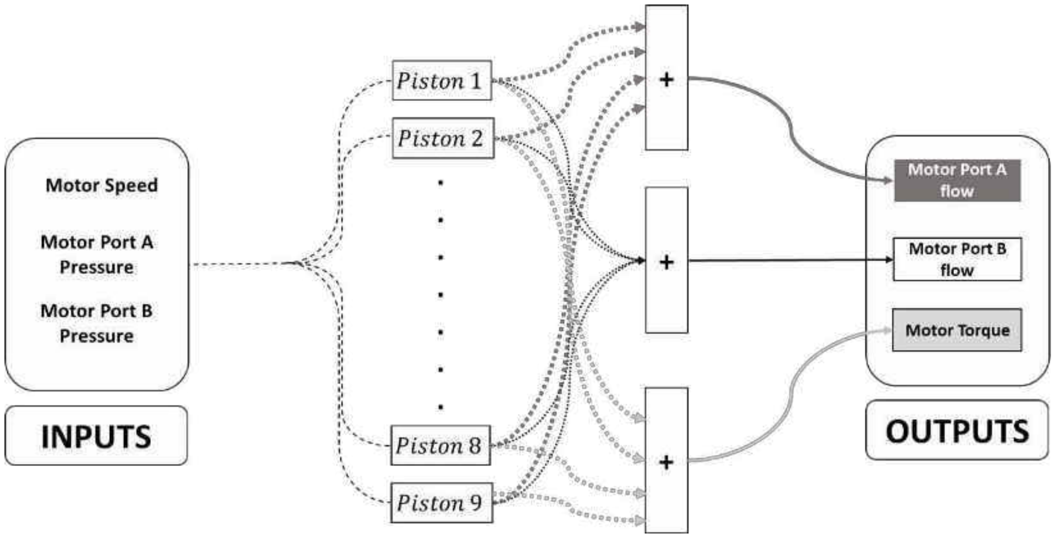

Fig. 9. Schematic overview of bidirectional motor model

Schematic of piston kinematics and dynamics for axial piston motor is like the one made for pump as shown in figure (3) with P_A & P_B being motor port pressures. Likewise, instantaneous flow contribution from each piston depending on piston location and sign of angular velocity is given below:

Table 2: Piston flow contribution on motor port A & B

Motor Angular Velocity Sign (ω)	**Motor Port A**	**Motor Port B**	**Piston Location**	Q_{A_i} **(Sign)**	Q_{B_i} **(Sign)**
+	Inlet	Outlet	A	Q_{Am_i}(+)	0
+	Inlet	Outlet	B	0	Q_{Bm_i}(+)
-	Outlet	Inlet	A	Q_{Bm_i}(-)	0
-	Outlet	Inlet	B	0	Q_{Bm_i}(-)

Just like in pump model, chosen sign convention for flow ensures that pressure dynamics behaves in correct fashion. Schematic overview of motor model is shown in Figure (9). Motor speed and pressure at motor port A, B goes as inputs to each piston. Port A and port B flow is determined by summing up flow output coming from each piston. Each piston will have individual contribution in net motor torque as described in following section. Motor speed is thus, determined by doing torque balance on motor shaft.

2.2.2 Motor Torque and Speed

Torque produced by motor is essentially net torque acting on the cylinder block along axis of symmetry. Since piston reaction force on cylinder contributes to cylinder torque, force balance on piston needs to be done. To obtain swash reaction force, we need pressure force, inertia force and friction force. For the sake of simplicity, friction force between piston barrel interaction has not been considered. Formula for pressure force and inertia force computation is same as eq. (11) and eq (12) respectively, with each variable bearing sense in context with motor**.** Thus component of swash reaction force in xy-plane, F_{sw_y} & F_{sw_x} as per sign convention are:

$$F_{sw_{i_y}} = -\left\{\frac{F_{dk}+F_{FR}+F_I}{\tan\beta}\right\} \tag{22}$$

$$F_{sw_{i_x}} = 0 \tag{23}$$

Slipper reaction force magnitude, F_{TG} is given by: [4]

$$F_{TG_i} = \frac{\mu\omega R}{h_g}\pi(R_g^2 - r_g^2) \tag{24}$$

R_g and r_g are slipper shoe inner and outer land radius. h_g is film thickness formed slipper shoe and swash plate. For simplicity sake, it has been assumed to be constant and of the order of $8\ \mu m$. [13] As per chosen sign convention, slipper reaction force has been resolved into x, y components, F_{TG_x} & F_{TG_y} as follow:

$$\begin{aligned} F_{TG_{i_x}} &= F_{TG}\sin\phi_i \\ F_{TG_{i_y}} &= -F_{TG}\cos\phi_i \end{aligned} \tag{25}$$

Centrifugal force, acting on piston is given as:

$$F_{\omega_i} = m_i\omega^2 R\ \frac{l_{s1}-l_{f/2}}{l_{km}} \tag{26}$$

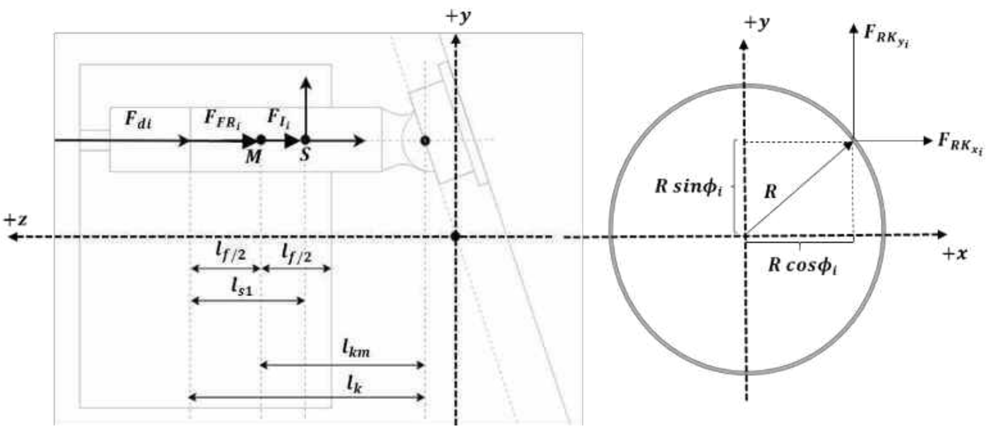

Fig. 10. Piston free body diagram for motor torque computation

ls_1 is piston's centre of mass distance measured from it's tip, as shown in figure (10). Other length, $l_{f/2}$ & l_{km} is given as:

$$\begin{aligned} l_{f/2} &= (l_{fa0} + R\tan\beta(1+\sin\phi_i))/2 \\ l_{km} &= l_k - l_{f/2} \end{aligned} \tag{27}$$

Resolving F_{ω_k} into x, y components,we get:

$$F_{\omega_{ix}} = F_{\omega_k} \cos \phi_i \\ F_{\omega_{iy}} = F_{\omega_k} \sin \phi_i \tag{28}$$

Net xy-plane piston reaction force F_{RK_i} can be resolved into $x - y$ component, $F_{RK_{i_x}}$& $F_{RK_{i_y}}$, which are obtained in terms of forces mentioned in equations (21), (22), (23), (24), (25), (26), (28) as:

$$F_{RK_{i_x}} = F_{\omega_{k_x}} + F_{TG_x} \\ F_{RK_{i_y}} = F_{\omega_{k_y}} + F_{sw_y} + F_{TG_y} \tag{29}$$

Contribution to motor torque from i_{th} pistion, M_{x_i} is given as:

$$M_{z_i} = R \cos \phi * F_{RK_{iy}} - R \sin \phi * F_{RK_{ix}} \tag{30}$$

Net torque M_x, would be summation all those contribution and can be expressed as:

$$M_z = \sum_{i=1}^{9} M_{z_i} \tag{31}$$

Motor speed is obtained by newton's second law as:

$$\omega(t) = \frac{1}{J} \int_0^t (M_z - T_{load})\, dt \tag{32}$$

2. 3 Sub component modeling

The component like internal pressure override relief valves (IPOR), shut off valves was modeled based on the pressure difference logic established on the port line pressure A, B which exceeds the critical pressures. charge pump is modelled as constant flow source. All interconnecting ducts has been lumped into a single volume, thus neglecting pressure drop in pipes. Considering the complexity level, the details of the modeling is not considered much.

2.4 Integrated Closed Loop Circuit

A generic cc circuit schematic diagram has been shown in figure (1). Flow directions through each hydraulic line, as indicated in the figure correspond to case when swash angle is positive, i.e. pump is discharging flow from port B and hence, side 1 is high pressure side. Since pressure loses in Intermediate pipes have not been considered, pipes and flow ducts on each side in cc circuit, has been lumped together as one volume, $V_{side_1}$and V_{side_2} on each side.

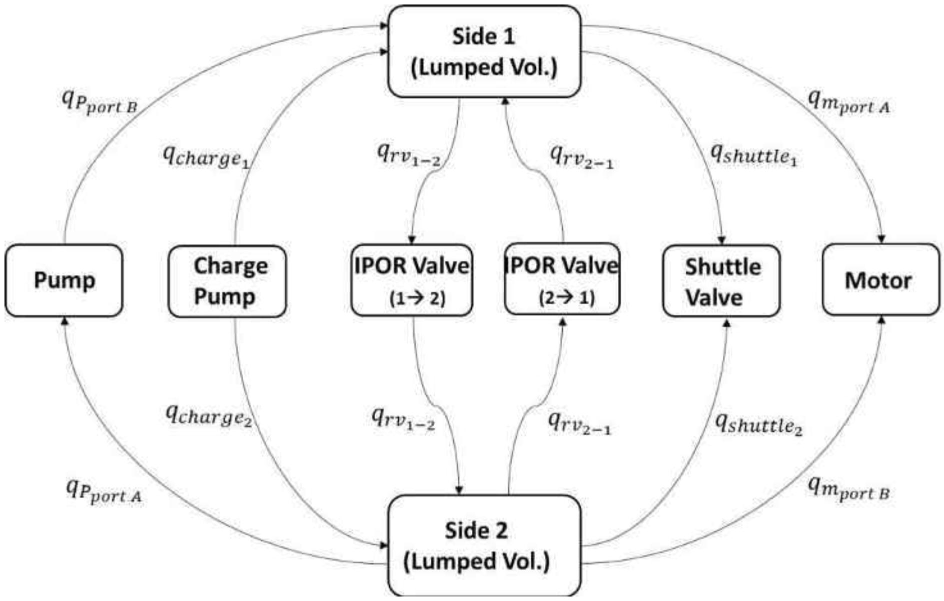

Fig. 11. Schematics of integrated CC circuit system model

The same has been done for integrated circuit modelling as shown in figure (11). Pressure on each side is computed on solving pressure dynamics equation in each volume. Following same sign convention, flow entering the volume is considered positive and vice versa. As discussed in respective subsection, sign of flow coming from each sub-component has been carefully assigned to ensure system's bidirectionality.

3. Model Validation

Developed model has been validated using test data conducted for examining motor characteristics in closed loop circuit. 49 cc motor attached with flywheel, subjected to negligible external load torque, is connected with other cc circuit components. Motor speed is brought up to around 3000 rpm in one direction, back to zero and then, up to same speed in other direction. Predefined solenoid current input to electric proportional pump swash control is used to achieve this behavior. Pressure on each side of cc circuit, motor speed and torque are some of characteristics that has been recorded in real time test data. Major parameter pertaining to cc circuit components used in simulation has been listed in table (3).

Table 3: CC circuit parameters

Parameters	Values
Main pump displacement	49 cc
Charge pump displacement	13.8 cc
Charge pump relief valve cracking pressure	16 bars
IPOR valve cracking pressure	320 bars
Shuttle valve cracking pressure	10 bars

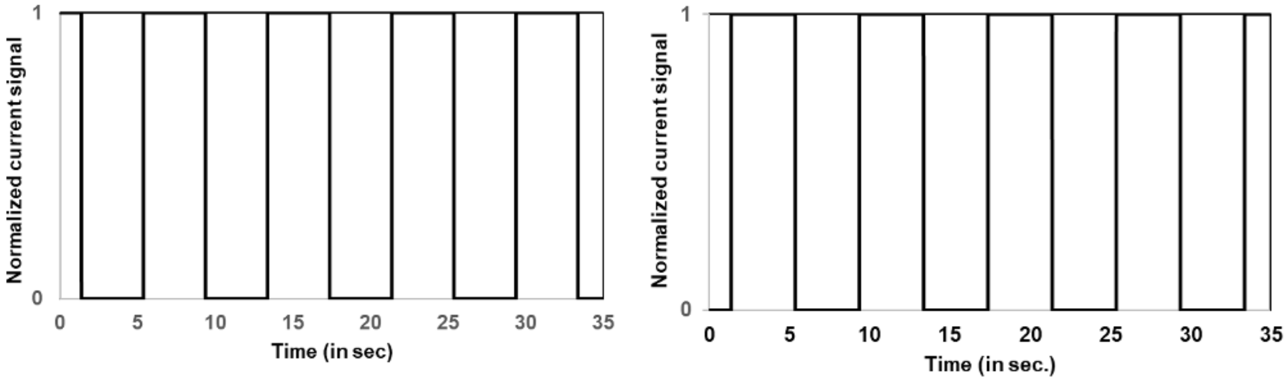

(a) (b)

Fig. 12. Forward solenoid current signal (a) and reverse solenoid current signal (b)

Solenoid current signal input in forward and reverse as provided to pump swash control is shown in figure (12). Data has been normalized with nominal value of each parameter without any loss of trend. Figure (13) present plots of motor torque and speed in real time as predicted by model, compared with test data. Except for occasional overshoot in torque, we observe good correlation trend wise with test data. This is expected since frictional torque losses in the model has not been considered. Subsequently, same is observed for side 1 and side 2 pressure, P_1 and P_2 as shown in figure (14).

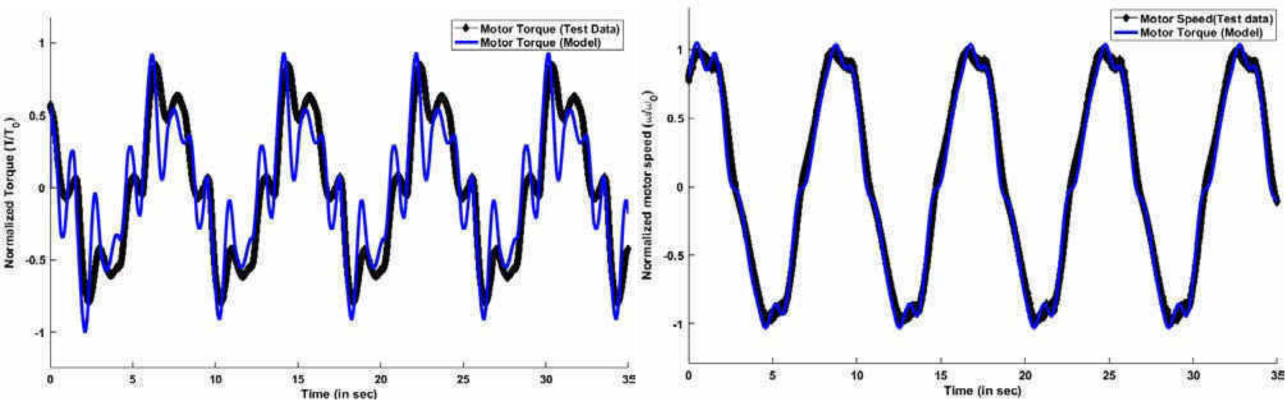

(a) (b)

Fig. 13. Normalized motor torque (a) and motor speed (b) validated with test data

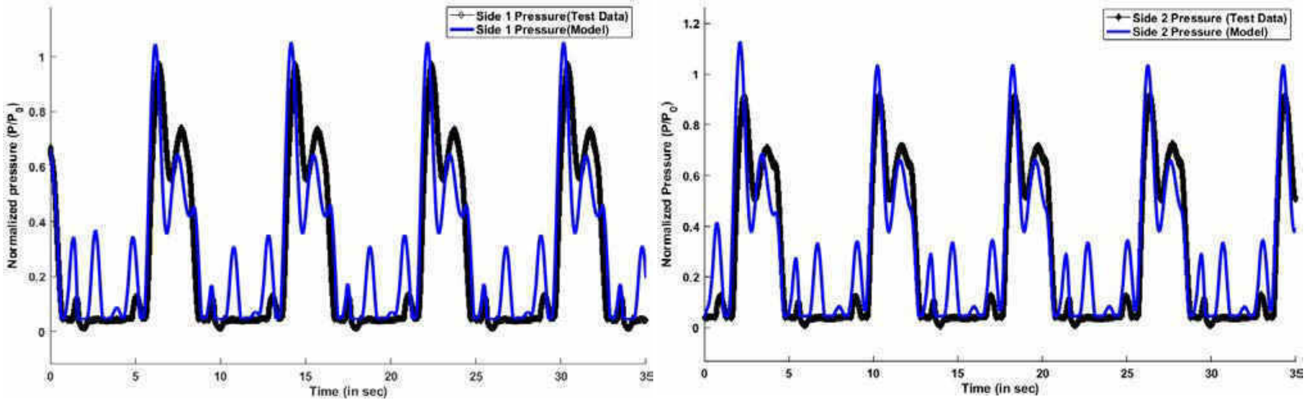

(a) (b)

Fig. 14. CC circuit side 1 pressure (a) and side 2 pressure (b) validated with test data

4. CTQ Prediction

To overcome load and frictional torque, motor needs high initial torque called starting or breakaway torque to start rotation. This high starting torque is physically generated when initially, pump is supplying full flow and motor is static, leading to pressure rise in high pressure line resulting in high torque produced. The same has been observed Qualitatively in figure (16). Forward and reverse solenoid signal to swash control is given in figure (15). Thus, Pump will supply flow in forward direction for some time and then flow direction will reverse. Initially motor is at rest, which leads to high pressure in port 1 side and torque as seen in figure (16a), (16b) respectively. The same is observed when pump reverses the flow, resulting in high port 2 pressure and torque in opposite sense.

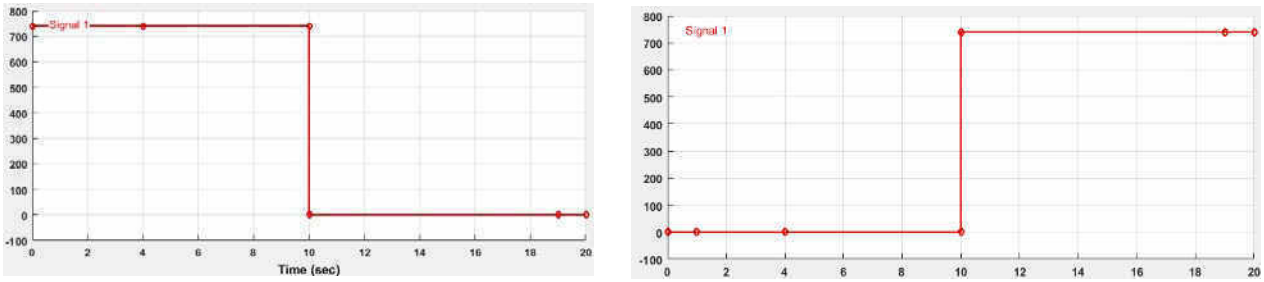

(a) (b)

Fig. 15. Forward (a) and reverse (b) solenoid current

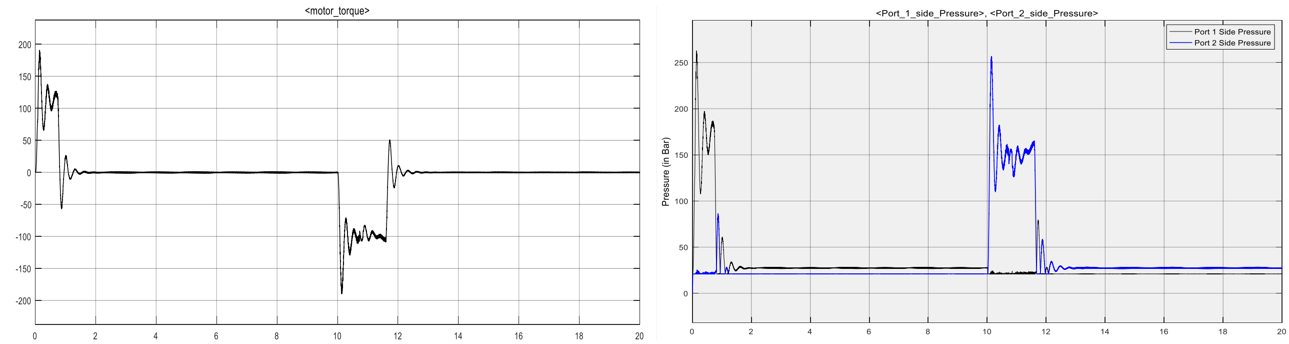

(a) (b)

Fig. 16. Motor Torque (a) and Port 1 Port 2 side pressure (b)

Pressure and torque ripple is inevitable phenomenon observed in axial piston machines. It is fluctuation in torque observed at designated operating condition. Figure (17) exhibits torque ripple as predicted by model in no load condition. This has been qualitatively verified with Ivantysyn et. al. [4].

Neutral pressure variation study has been done for the pump and is correlated with test data. During test, pump was brought to full stroke and full load condition with load pressure being around 1000 psi and then stroked back to neutral condition. This was performed in both senses i.e. forward-neutral-reverse and reverse-neutral-forward and averaged data was recorded. Simulation scenario has been set in similar fashion. Neutral pressure variation is observed while pump is going from forward to neutral as well as reverse to neutral. Two test cases have been simulated. In test case 1, pump angular speed is 710 rpm where as in test case 2, pump rotates at 1525 rpm. Figure (18a), (18b), (18c) and (18d) present model prediction of neutral pressure variation for test case 1 in forward to neutral and reverse to neutral cases respectively. Likewise, the same has been for test case 2 in figure (19). Averaged neutral pressure as obtained from model and as seen in test has been listed in table (4). The neutral pressure variation is within 30 psi for both test data as well as model prediction. Also, Model prediction accuracy can be said to be more than 95 percent given the available amount of test data. This can be further be refined if we consider a detailed and more complex motor torque loss model as given by Moslått [14].

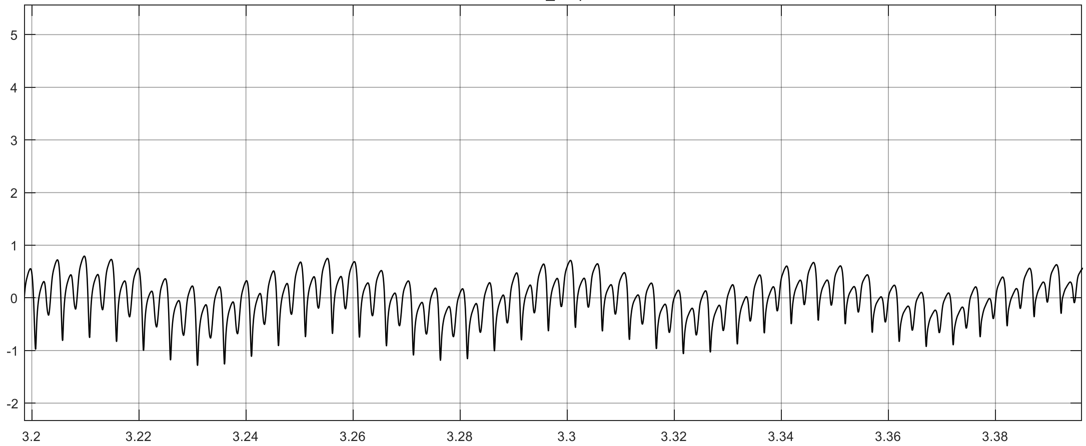

Fig. 17. Torque Ripple

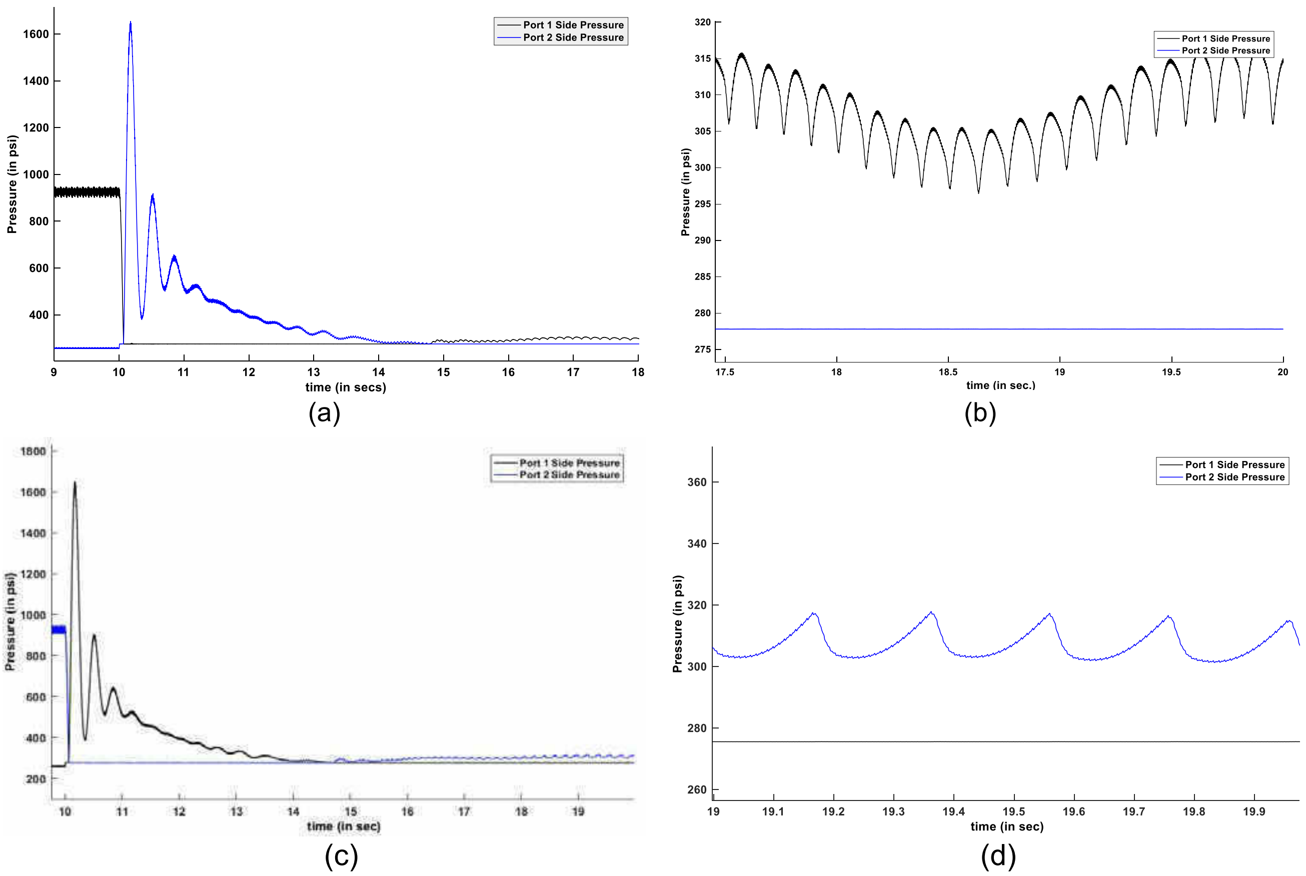

Fig. 18. Test Case 1: Model Prediction

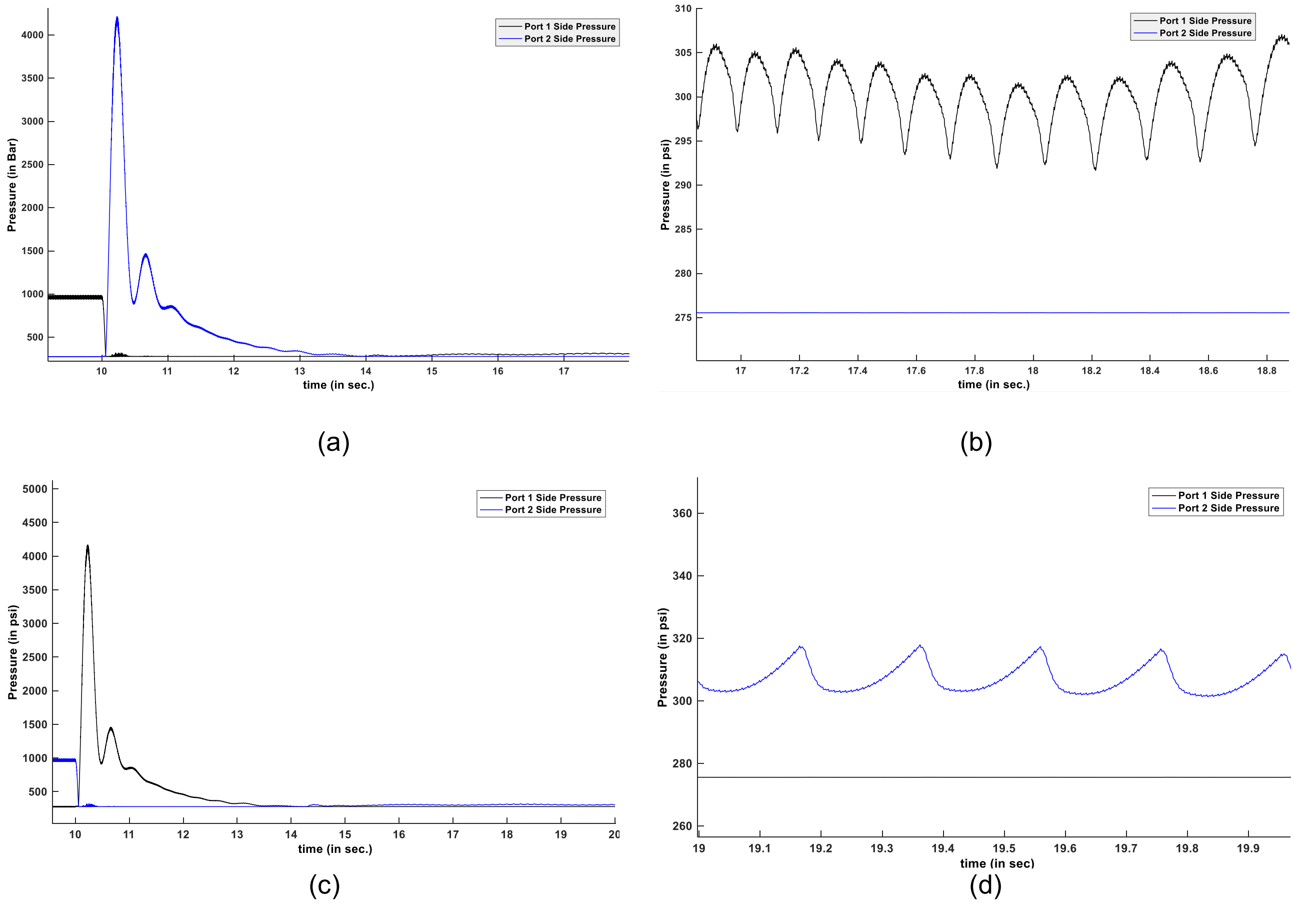

Fig. 19. Test Case 2: Model Prediction

Table 4: Neutral Pressure Correlation with Test Data

	Test Data-psi (avg.)	**Model-psi (F to N)**	**Model-psi (R to N)**
Test Case 1	28.6	28.5	29.5
Test Case 2	27.5	27.8	27.2

5. Conclusions

Current literature does not mention effects of system level interactions on closed-circuit piston pump’s performance (e.g. Motor torque variation due to pump swash fluctuations), however individual details are available for few components. The major contribution of this study is the development of detailed mathematical model of closed-circuit pump with variable displacement pump, fixed displacement motor, swash controls by first principle physics knowledge and predictable accuracy on the neutral pressure variation. The experimental results are found to be consistent with the model predictions; hence the methodology developed here can be used for higher displacement machines and different applications of hydrostatic transmission. The model is useful for concept evaluation, component sizing and selection & optimization of system level performance. Future scope can be to refine the model further by inclusion of possible leakages in components, pressure drop across valves based on test data and friction dynamics for each interface.

References

[1] Limon, S.M., O.P. Yadav, J. Muscha, and B. Nepal. ”Hydrostatic Transmission System Failure Analysis and Utilization of FailureKnowledge: A Case Study.” Proceedings of the 2015 IEEE International Conference on Industrial Engineering and Engineering Management (IEEM), Singapore, December 6-9, 2015.
[2] Degaonkar, Chandrashekhar, and Richard Lyman. “Digital prototyping of axial piston pump load sense dynamics.” Paper presented at 11th Asian International Conference on Fluid Machinery and The 3rd Fluid Power Technology Exhibition, Chennai, India, November 21-23, 2011.
[3] Kaliafetis, P., and T. Costopoulos. "Modelling and simulation of an axial piston variable displacement pump with pressure control." *Mechanism and Machine Theory* 30, no. 4 (May 1995): 599-612.
[4] Ivantysyn, Jaroslav, and Ivantysynova, Monika. *Hydrostatic Pumps and Motors: Principles, Design, Performance, Modelling, Analysis, Control and Testing*. Tech Books International, 2003.
[5] Manring, N.D. "The Discharge Flow Ripple of an Axial-Piston Swash-Plate Type Hydrostatic Pump." *ASME J. Dyn. Sys., Meas., Control* 122, no. 2 (June 2000): 263–268.
[6] Zieger, G., and A. Akers. "Torque on the swashplate of an Axial Piston Pump." *ASME J. Dyn. Sys., Meas., Control* 107, no. 3 (September 1985): 220-226.
[7] Manring, N.D. "Friction Forces Within the Cylinder Bores of Swash-Plate Type Axial-Piston Pumps and Motors." *ASME J. Dyn. Sys., Meas., Control* 121, no. 3 (September 1999): 531–537.
[8] Nouri, B.M.Y., F. Al-Bender, J. Swevers, et al. "Modelling a pneumatic servo positioning system with friction." Proceedings of the 2000 American Control Conference, Chicago, IL, USA, June 28-30, 2000.
[9] Manring, N.D. *Hydraulic Control Systems*. New Jersey, USA, John Wiley and Sons, 2005.
[10] Merrit, H. *Hydraulic Control Systems*. New York, USA, John Wiley and Sons, 1967.
[11] Dasgupta, K. "Analysis of a hydrostatic transmission system using low speed high torque motor." *Mechanism and Machine Theory* 35, no. 10 (October 2000): 1481-1499.
[12] Manring, N.D., and Greg R. Luecke. "Modeling and Designing a Hydrostatic Transmission With a Fixed Displacement Motor." *ASME J. Dyn. Sys., Meas., Control* 120, no. 1 (March 1998): 45-49.
[13] Gao, Y., W. Huang, L. Quan, Y. Lan and J. Huang. “The distributed parameter model of hydraulic axial piston motor and its application in hydraulic excavator swing system.” Proceedings of the Institution of Mechanical Engineers, Part I: Journal of Systems and Control Engineering, 231(5), 395–413, 2017.
[14] Moslått, Geir-Arne, Michael R. Hansen, and Nicolai Sand Karlsen. "A model for torque losses in variable displacement axial piston motors." *Modeling, Identification and Control* 39, no. 2 (2018): 107-114.

**Credit to the authors and Eaton Intelligent Power Limited*

ISSN 1454 - 8003
Proceedings of 2019 International Conference on Hydraulics and Pneumatics - HERVEX
November 13-15, Băile Govora, Romania

CONSIDERATIONS REGARDING THE USE OF HYDROSTATIC TRANSMISSIONS IN WIND TURBINES

Teodor Costinel POPESCU[1], Ionaș-Cătălin DUMITRESCU[1]

[1]Hydraulics and Pneumatics Research Institute / INOE 2000-IHP Bucharest, popescu.ihp@fluidas.ro, dumitrescu.ihp@fluidas.ro

Abstract: *Starting from some general considerations regarding the use of hydrostatic transmissions for increasing the efficiency of high power wind turbines, the authors present some basic schemes for hydrostatic transmissions, with and without pneumatic energy storage, for medium and small power wind turbines.*

Keywords*: Hydrostatic transmissions, wind turbines, pneumatic energy storage*

1. Introduction

In 2018, the electricity obtained from the conversion of wind power covered 5.5% of the total consumption worldwide, using capacities of energy production of 591 GW. Of the 181 GW representing new capacities installed in 2018 for electricity generation, 51 GW are wind turbines of various sizes. Romania has a total installed capacity of 3,029 MW, covering in 2018 approximately 10.2% of the country's electricity consumption. Most of this energy production is obtained with horizontal axis wind turbines. For this type of turbine, the location of the electric generator in the turbine platform leads to a significant increase in the mass of the platform, and implicitly the mass of the pillar supporting the turbine. In addition, the maintenance of the turbine becomes more difficult with the increase of the rotor diameter and the height of placement.
The platform (excluding the rotor) represents between 20 ... 35% of the total weight of a large turbine reaching in some cases the order of hundreds of tons. In the case of the VESTAS V90 turbine, the platform weighs 75 tons, the rotor 40 tons, and the tower 152 tons. [1]. In the case of small turbines, even if we do not have such heavy weights, the same values are kept as a percentage.
Other research has shown that in current offshore turbines, one of the main issues is gearbox failure, with current designs requiring replacement or capital intervention every 4 years. With the gearbox contributing to around 10% of turbine cost [2], such frequent replacements are very detrimental to the overall viability of offshore wind energy conversion. Danop Rajabhandharaks of San Jose State University states in his thesis [3] that it is not uncommon for a gearbox to fail on average every 5 years while the designed lifetime of a wind turbine is typically about 20 years.
On the other hand, there are wind turbines that have appeared in the last decades that differ from the classic solutions, and fall into the category of unconventional wind turbines; they have different shapes, are arranged vertically or horizontally at different heights, and in terms of power they usually fall into the category of low power turbines (below 100 kW), Figure 1. Regardless of their type and structure, in most of these turbines the generator is located near the rotor, at height.



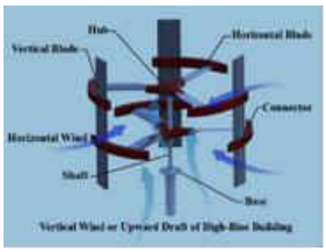

Fig. 1. Unconventional wind turbines

Reducing the weight of the platform, and implicitly the weight of the support pillar, would be easy to achieve if the electric generator were located on the ground and the tower would support only the rotor and a few other auxiliary elements. Maintenance would also be much easier to achieve. As for the unconventional turbines, they are located in the most diverse places, and the reduction of the suspended mass and reduction of the gauge is likely to simplify the construction and improve the visual impact. While in the turbines with vertical axis located on the ground or near the ground, the generator has small dimensions and weight, in those placed on buildings or bridges, the location on the ground of the generator significantly simplifies the construction.
For all these problems ***the solution is the hydrostatic transmission*** of energy from the rotor to the generator, also giving up the gearboxes that multiply the reduced rotor speed (5 ... 40 rpm) to make it compatible with that of the generator (1500 ... 3000 rpm); by an intelligent use of some classic, modern hydraulic components, a high performance hydrostatic transmission can be achieved.

2. Examples of use of hydrostatic transmissions for wind energy conversion

Research on the hydraulic transmission of energy to wind turbines began as early as the 1970s. We mention the 3 MW turbine, model SWT-3, produced by Rybak company and put into operation on December 16, 1980. The movement of the rotor is taken over by a hydrostatic transmission with 14 fixed capacity pumps, located in the platform, and 18 engines with variable displacement. The pumps are connected to the rotor by a speed multiplier. The variable motors were connected to the generator by another multiplier [4].
In 2010, in Germany, the RWTH Aachen University developed an experimental platform that simulates a variable speed wind turbine and carried out experimental research with modeling and simulation. In this model, the fixed displacement pump supplies the variable motor, which drives the synchronous generator to obtain electricity. The results indicated that this hydraulic transmission of wind power can compensate the influence of the fluctuation of the wind speed on the output power, but also achieve an optimal efficiency of 85% [5,6,7,8].
In the same year, the American company EATON studied the technology of hydraulic energy transmission and proposed a hydraulic solution based on the use of a pump with radial pistons and axial piston engines. About 90% of the system was placed on the ground [9].
The fundamental principle of all the wind turbines mentioned above is shown in Figure 2. In this, the speed multiplier in the dotted area may be missing, depending on the type of pump.

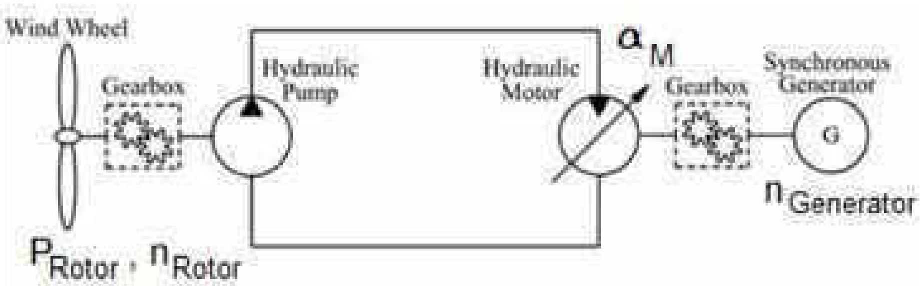

Fig. 2. Fundamental principle of hydrostatic transmision (HST).

Basically, the HST transfers the rotor power P_{Rotor} to the generator while transforming the variable rotor speed n_{Rotor} into the required constant generator speed n_{Gen}. The rotor speed is regulated using the motor's displacement setting α_m. Low wind speeds require low displacement settings as less flow is generated by the rotor, while higher wind speeds generate more flow and require larger motor displacements.
As a result of this variable power input, the system's efficiency will change according to the wind speed. Below the rated speed all the components will operate at part load conditions leading to decreased efficiency.

To ensure good efficiency throughout the wind speed range a switched displacement hydrostatic transmission (HST) for a 1 MW turbine has been developed at IFAS, see Figure 3(a). The new architecture allows individual pumps and motors to be switched on and off depending on the current operating point [10]. Two fixed displacement pumps convert the wind power into hydraulic power in the form of pressurized fluid. Two sets of motors are then used to drive two generators. Each component, except for the smallest pump, can be switched to idle mode, which allows different pump-motor combinations for different operating points. By allowing individual pumps and motors to be switched on and off depending on the current operating point the new architecture leads to an improved system efficiency throughout the operating range, see Figure 3(b).

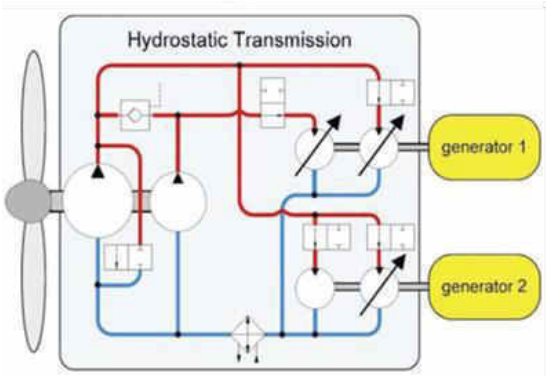

a)

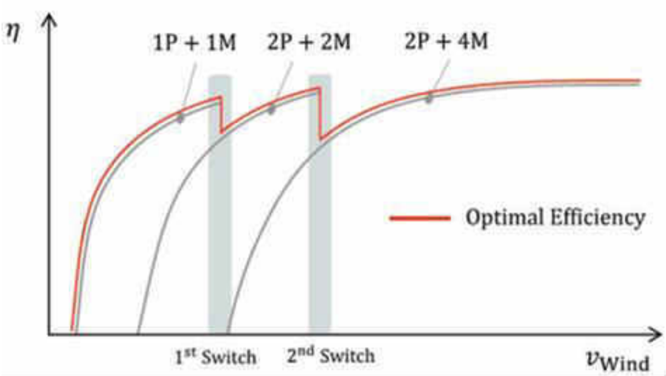

b)

Fig. 3. HST for a 1 MW turbine has been developed at IFAS: **a)** Structure of the hydraulic scheme; **b)** Diagram of system efficiency.

As time has passed and technological advancement occured in the fields of wind turbine construction and hydraulics, the research has progressed in 2 seemingly divergent directions: on the one hand towards the implementation of hydrostatic transmissions to turbines of increasing power, in agreement with the increase of the installed power of the of commercial turbines, and on the other hand towards smaller power turbines, as the interest for the local production of energy from wind sources increases.

The stochastic nature of wind makes it difficult to integrate into a grid and causes frequent wind power curtailment [11]. The utilization of a storage system is a better solution to reduce or alleviate these problems.

The wind energy storage can not only solve the problem of randomness and volatility of the wind power, but also has the function of peak regulation and frequency modulation, which can greatly improve the reliability and economic efficiency of the power system [12].

In 2009, the Scottish Artemis Intelligent Power company applied a new digital hydraulic variable pump to the 1.5 MW hydraulic variable speed wind turbine aimed at storing wind energy and obtaining higher efficiency. Experimental results proved that the efficiency of the wind turbine can reach over 90% under most wind speed, which was equivalent to the efficiency of traditional wind turbines. However, ***this digital hydraulic variable pump design is strictly confidential and unavailable for others.***

Artemis Digital Displacement drivetrain [13] is formed by a hydrostatic transmission followed by two parallel synchronous generators as presented in Figure 4. The hydrostatic transmission is given by a high efficiency - low speed ring cam radial piston pump driving a high speed radial piston motor; dimensions, number of cylinders and configuration might be different between pump and motor. In general, the Artemis Digital Displacement machines can be considered as an optimized radial piston machines. The optimization consist in reducing slipping surfaces; but most important, by making the valve's operation independent of the angular displacement of rotor shaft. This unconstrained dependence allows individual operation of each cylinder. Discrete operation of cylinders helps to dramatically reduce leakage losses in preselected cylinders (those cylinders that are not required to fit the current load condition, are just idled). Also, effects due to transition regions (regions 2, 3, 5 and 6) are minimized by means of careful software tuning. Optimization is reduced to intelligent control of suction and discharge valves, which are triggered by electric solenoids.

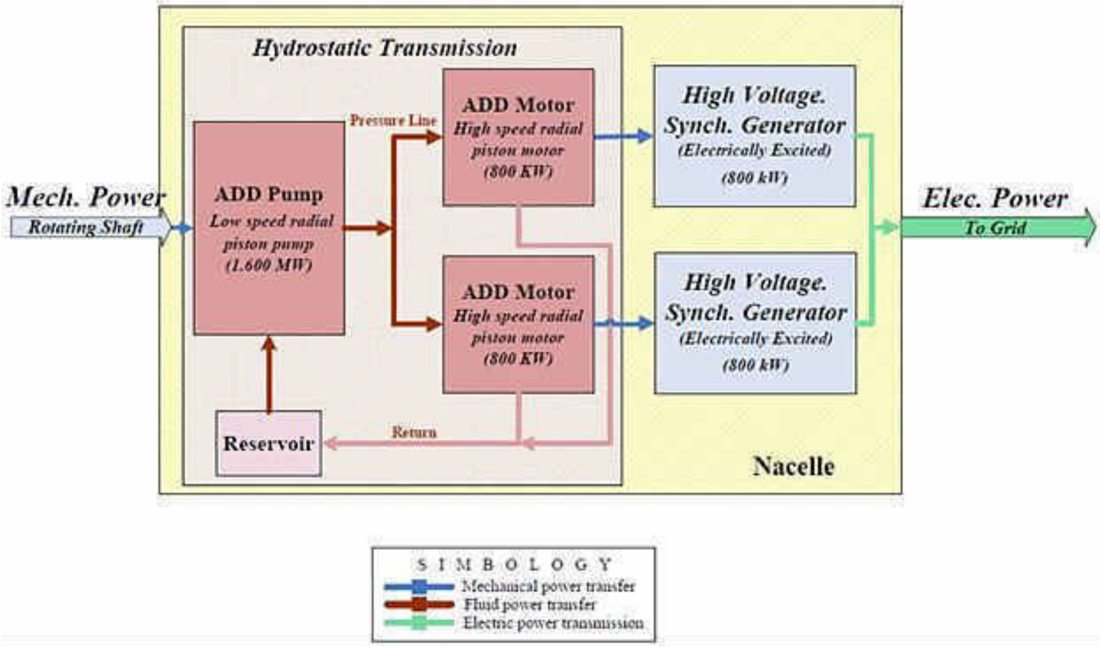

Fig. 4. Artemis 1.6 MW drivetrain system.

Software control makes possible to implement, and tune up, any kind of machine behavior (idling, braking, pumping or motoring) within the same hardware. For instance, it is possible to idle some cylinders (aimed to reduce leakage losses on those cylinders) while the rest works at rated power, making possible to fit any partial load condition with the minimum number of cylinders working at rated power.

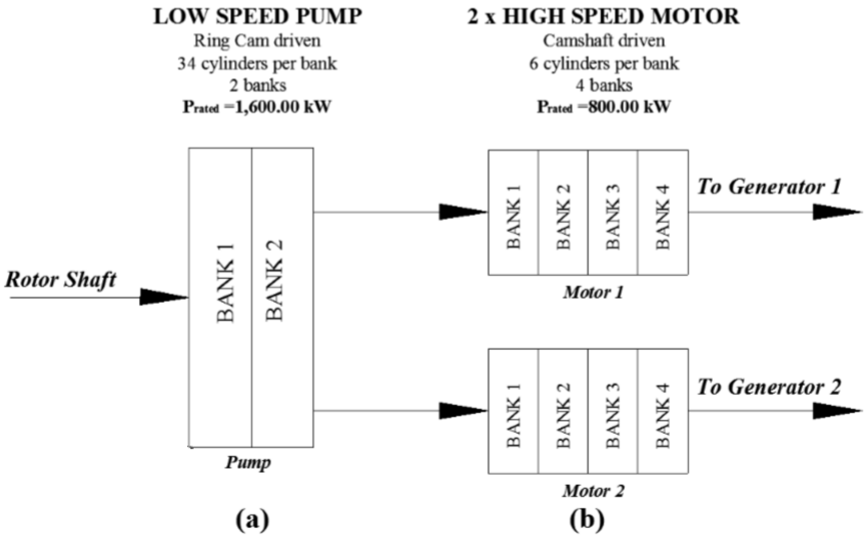

Fig. 5. Schematic representation of the ADD pump (**a**) and ADD motor (**b**).

Artemis drivetrain uses a low rotating pump driving a high speed hydraulic motor (s). For the 1.6 MW system (rated power), one low speed pump drives two 800 kW hydraulic motors. The hydraulic motors drive one electrically excited high voltage synchronous generator each one.

Artemis Digital Displacement motor has in total ***24 cylinders*** of same geometry. They are distributed in ***4 banks***. Each bank contains ***6 cylinders*** equally radially distributed. The banks are stacked over each other. One single camshaft drives the 24 cylinders so each cylinder had one full stroke any single revolution. A schematic view of the motor is presented in Figure 5(b).
On the other hand, the ADD ***low speed pump has a total of 68 cylinders*** contained in ***two parallel banks***, Figure 5(a). Although the principle of operation is similar to the motor, the ADD pump uses a different mechanism to drive the cylinders up and down: a ring cam. A ring cam is a large rotating piece concentric to the main axis of rotation. It does not have any kind of eccentricity. Instead, a ring cam had a sequence of specially shaped lobes over the all external cylindrical surface. The combination between lobes and rotation of the ring cam makes possible to drive the cylinder stroke. In the case of the ADD 1.6 MW pump, the 24 lobes drive up and down all cylinders 24 times per single revolution of the ring cam. The shape of the lobe determines the motion characteristics of radial coordinate r.
Figure 6 presents a simplified cross section of the ADD low speed radial piston pump. In there, the springs were removed to allow a clearer perspective. For a detailed view of the employed components for each cylinder, refer to Figure 7, where the cross section of a cylinder for a motor is presented. The components employed for piston and cylinder only differ in dimensions.

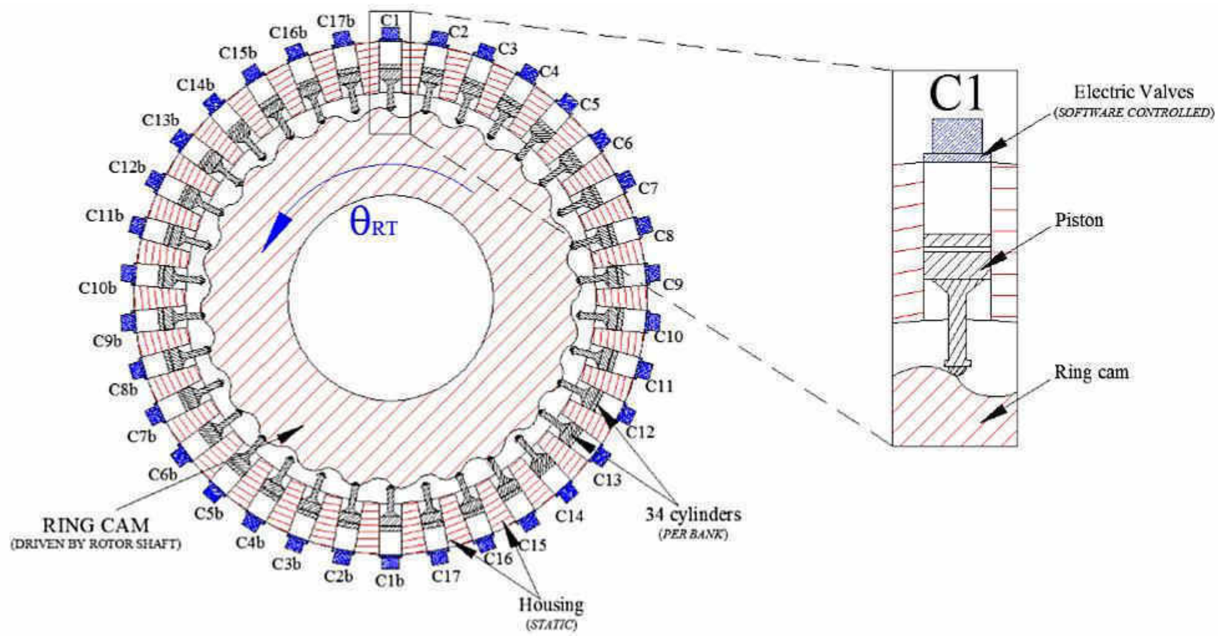

Fig. 6. Simplified cross section for one bank of low speed ADD pump.

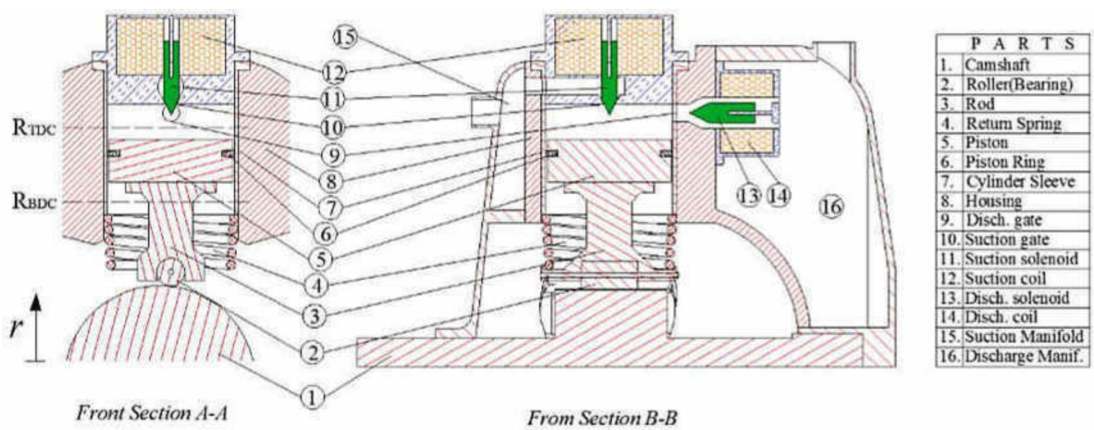

Fig. 7. One single cylinder set with electric valves.

Furthermore, the topic of digital pumps is addressed through theoretical and experimental research in other research units, as well; in Romania, in ***Politehnica University of Timișoara*** and ***Hydraulics and Pneumatics Research Institute in Bucharest***, there are current interests regarding this type of pump, which is studied also in doctoral theses. Also, in ***ICPE-CA Bucharest*** there have been researches and achievements for high frequency electromagnets, which are found to be key elements in the operation of the digital pump valves.
As a proof of the interests as to implementing hydraulic transmissions in low power wind turbines, there is also the research carried out in a thesis at ***Delft University of Techology***, which considered the implementation of a hydraulic transmission for a 10 kW offshore turbine [14]. The energy transmission system has 2 circuits as main components (Figure 8.a):

- a closed hydraulic circuit, which consists of a fixed hydraulic pump connected to the wind rotor, and transmits hydraulic energy to a high speed rotary hydraulic motor; this circuit uses hydraulic oil as a working fluid;
- an open hydraulic circuit, in which a hydraulic water pump, driven by the engine of the first circuit, sends pressure water to a Pelton type turbine; this circuit works with seawater.

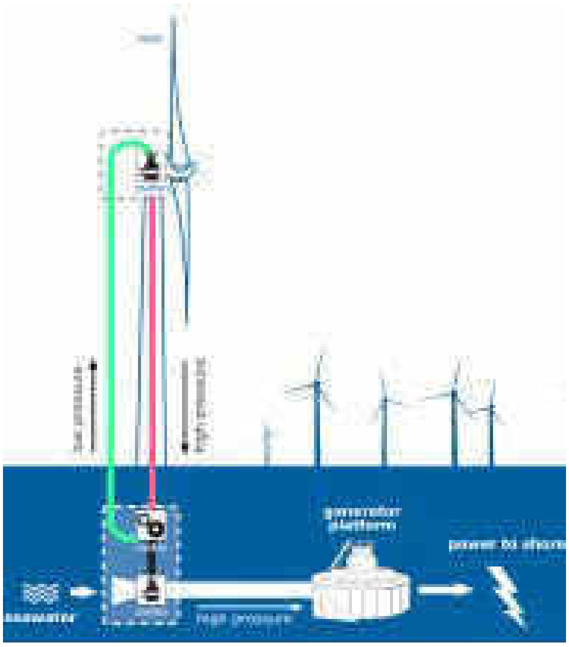

a)

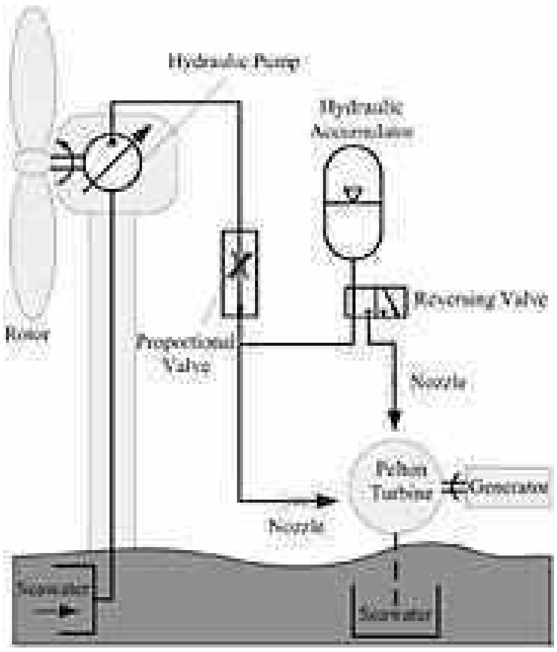

b)

Fig. 8. Offshore wind turbine with sea water: **a)** The principle works; **b)** Structure of the HST.

Another approach, also for an offshore turbine, is that in which the hydraulic pump driven by the wind turbine is the water pump itself, which sends pressure water to a Pelton turbine, driving a generator (Figure 4.b). As in the case above, a hydraulic accumulator is provided to supplement the flow that drives the turbine, as the wind speed decreases. This accumulator performs energy storage and reuse, but the idea has limited applicability due to the small volume of the accumulator, and the stored energy is mainly used to reduce the variation in the drive speed of the generator. [15]. As in the previous case, the system uses seawater as a working fluid.
One of the current trends in the field of renewable energy is the emergence of hybrid systems, which combine 2 or more systems to obtain a type of energy (mainly electricity), with storage in various forms. We mention the paper [16], which presents a system of energy pneumatic storage in the floats of an offshore turbine, thus assuming a dual role. Electricity is obtained from wind energy combined with wave energy.

3. Hydrostatic transmissions for low power wind turbines

The authors propose that, in addition to developing a hydrostatic transmission for a low power turbine (10 kW), to develop a pneumatic storage system, where the compressor is also driven by a hydraulic motor. After compression, the air is stored in a pressure tank, to be used for electricity generation using a pneumatic engine. The electricity thus obtained can be combined with that obtained in the main branch (hydrostatic transmission), but can also be used for auxiliary purposes (for example for auxiliary systems of the closed-loop hydrostatic transmission: cooling, additional pump drive, etc.). The diagram of the entire proposed installation, in parallel with the principle diagram of a classical wind turbine, is presented in Figure 9. The pneumatic storage facility was approached at theoretical level and by physical realization within INOE 2000-IHP in 2016. Following these researches, a patent application was filed.

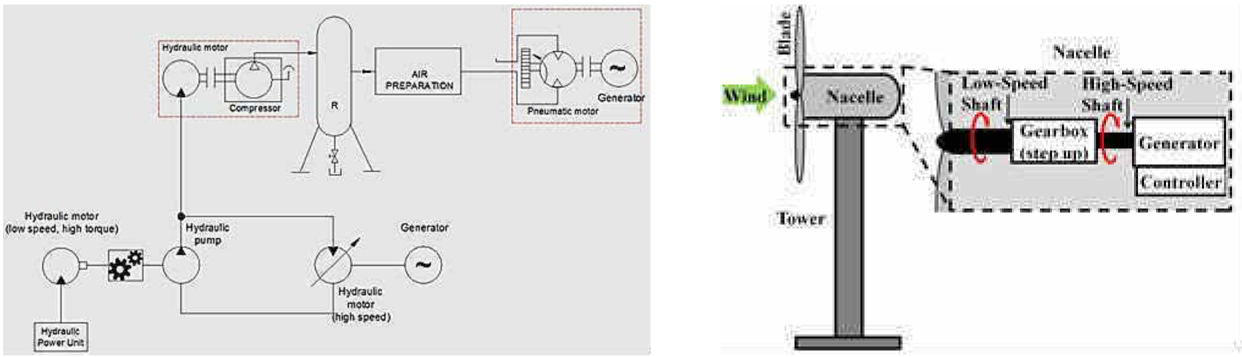

a) **b)**

Fig. 9. HST combined with energy pneumatic storage system (**a**), compared to a classical turbine (**b**).

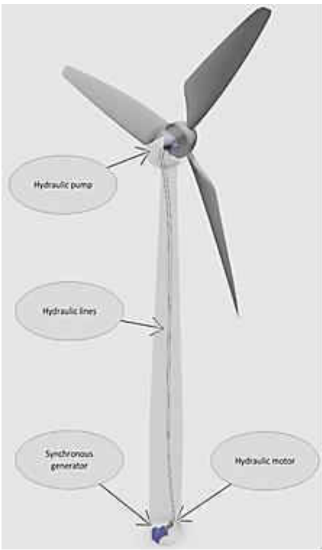

Fig. 10. The main components of the wind turbine equipped with HST, mounted in the nacelle, tower and base of the tower.

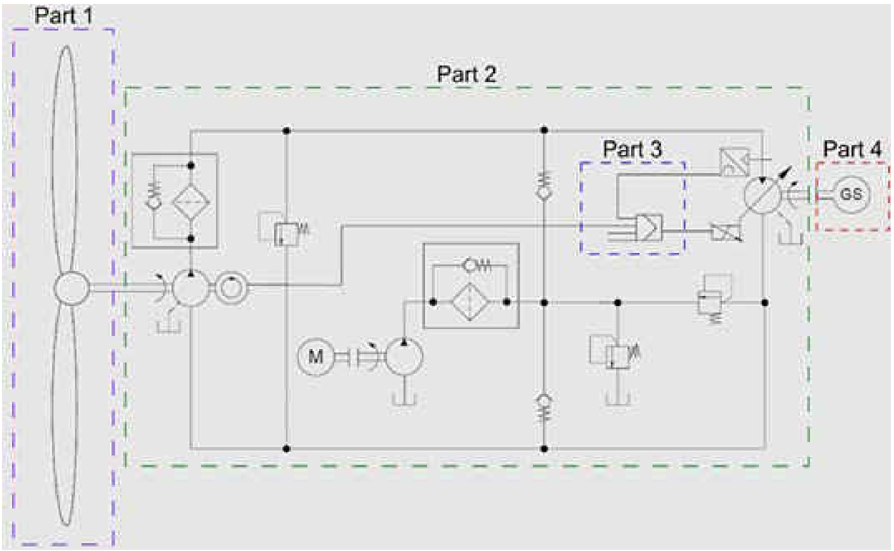

Fig. 11. The subassemblies of the HST testing bench:
Part 1 = wind turbine simulated with variable electric/ hydraulic motor;
Part 2 = HST for low-power turbines; **Part 3** = HST controller; **Part 4** = synchronous generator.

Figure 10 shows the location of the main components of the wind turbine equipped with HST: the rotor and the main pump - in the nacelle; the hydraulic lines - inside the tower; the electric generator and the rest of HST components at the base of the tower. Figure 11 shows the main subassemblies of the stand where the hydrostatic transmission will be tested. The stand will be

made by INOE 2000-IHP. The transmission will be executed in a closed circuit (excluding the volume loss recovery system). It will contain a fixed capacity main pump, a variable-capacity main motor, hydraulic circuits, hydraulic accumulators, safety valves, sensors, filters, heat exchanger, anti-cavitation volume loss compensation pump, hydraulic motor capacity controller with hydraulic circuit with feedback from the high pressure hydraulic circuit, aerodynamic rotor speed and wind speed.
This project comes to meet the energy efficiency improvement requirements of these small wind turbines (whose number is constantly increasing today), in the sense of extracting a greater quantity of the available energy of the wind, even at low wind speeds, by promoting a new solution. It is based on two main component systems: a classical hydraulic transmission (HST), containing two standard rotary volumetric machines (pump and motor), combined with a system of wind energy pneumatic storage (EPS). Consequently, it is proposed to develop a demonstrator, type experimental model, that is a 10 kW test platform, on which this technical solution, designed to ensure simultaneously energy efficiency and economic benefit of lowering to the ground components of the low power wind turbines, will be evaluated, experimentally validated and promoted.

Conclusions

The project aims to promote a hydrostatic transmission for low-power wind turbines in order to increase the extraction of electricity from the available wind energy and also to demonstrate the following advantages:
- the possibility of practical implementation of a transmission for low-power wind turbines, from standard and specially designed components, with a continuous variable ratio in the capacity adjustment range of variable hydraulic machines;
- increasing the efficiency of wind turbines equipped with HST by using control strategies dedicated to the wind turbine system comprising the wind rotor, the hydrostatic transmission and electric synchronous generator;
- the possibility of maintaining a predetermined constant rotational speed of the electric generator when braking or acceleration loads occurs at the wind rotor;
- the possibility of obtaining a faster response to sudden wind speed variations compared to mechanical or electromechanical transmissions;
- the possibility of low-maintenance of the turbine with reduced costs by placing some components on the ground.

Acknowledgments

This paper represents a proposal for an experimental demonstration project, developed by INOE 2000-IHP and ICPE-CA, Bucharest, within the PED 2019 project competition.

References

[1] www.wind-watch.org - Presenting the facts about industrial wind power, Accessed August 08, 2019.
[2] Buhagiar, Daniel, and Tonio Sant. “Analysis of a stand-alone hydraulic offshore wind turbine coupled to a pumped water storage facility.” Paper presented at Sustainable Energy 2013: the ISE Annual Conference, 21st March 2013, Dolmen Hotel, Qawra, Malta.
[3] Rajabhandharaks, Danop. “Control of Hydrostatic Transmission Wind Turbine.” In Partial Fulfillment of the Requirement for the Degree Master of Science. San Jose State University, December 2014.
[4] Rybak, S.C. “Description of the 3 MW SWT-3 Wind Turbine at San Gorgonio Pass, California.” Bien Wind Energy Conference Workshop; Bendix Corp., Environment and Technology Office: Sylmar, CA, USA, 1982; Volume 1, pp. 193–206.
[5] Mortensen, K.A., and K.H. Henriksen. “Efficiency Analysis of a Radial Piston Pump Applied in a 5MW Wind Turbine with Hydraulic Transmission.” Master Thesis in Electro-Mechanical System Design. Aalborg University, Aalborg, Denmark, 2011.

[6] Schmitz, J., N. Vatheuer, and H. Murrenhoff. “Development of a hydrostatic transmission for wind turbines.” Paper presented at the 7th International Fluid Power Conference, Aachen, Germany, March 22–24, 2010.
[7] Schmitz, J., N. Vatheuer, and H. Murrenhoff. “Hydrostatic drive train in wind energy plants.” RWTH Aachen Univ. IFAS Aachen Germany 2011.
[8] Vukovic, Milos, and Hubertus Murrenhoff. “The Next Generation of Fluid Power Systems.” *Procedia Engineering* 106 (December 2015): 2 – 7. DOI: 10.1016/j.proeng. 2015.06.002.
[9] Eaton. Microgrid Content Journey [EB/OL], 2010, https://doi.org/10.3390/pr7070397, Accessed November 06, 2019.
[10] Eriksen, P.B., T. Ackermann, H. Abildgaard, P. Smith, W. Winter, and J.M.R. Garcia. “System operation with high wind penetration.” *IEEE Power Energy Mag.* 3 (2005): 65–74.
[11] Vaezi, M., and A. Izadian. “Energy storage techniques for hydraulic wind power systems.” Paper presented at the 2014 International Conference on Renewable Energy Research and Application (ICRERA), Milwaukee, WI, USA, October 19–22, 2014.
[12] Whitby, R.D. ‘Hydraulic fluids in wind turbines.” *Tribol. Lubrication Technol.* 66 (2010), 72.
[13] https://pdfs.semanticscholar.org/d9f6/a743a5c28fb6ee324817ce289b865b09d2bc.pdf Accessed November 06, 2019.
[14] Kempenaar, A.S. “Small Scale Fluid Power Transmission for the Delft Offshore Turbine. Design, Modeling, Construction and Testing of a Small Scale Fluid Power Transmission.” Thesis for the degree of Master of Science in Sustainable Energy Technology at Delft University of Technology, March 14, 2012.
[15] Fan, Y., A. Mu, and T. Ma. “Study on the application of energy storage in offshore wind turbine with hydrostatic transmission.” *Energy Convers and Management* 110 (2016): 338-346.
[16] Sant, T., D. Buhagiar, and R.N. Farrugia. “Modelling the dynamic response and loads of floating offshore wind turbine structures with integrated compressed air energy storage.” Paper presented at ASME 2017 36th Int. Conf. on Ocean Offshore and Arctic Engineering, Trondheim, Norway, June 25-30, 2017.

ISSN 1454 - 8003
Proceedings of 2019 International Conference on Hydraulics and Pneumatics - HERVEX
November 13-15, Băile Govora, Romania

EFFECT OF TEMPERATURE ON THE LUBRICATION PROPERTIES OF DIESEL-SESAME OIL BLENDS

Alireza SHIRNESHAN[1]

[1]Department of Mechanical Engineering, Najafabad Branch, Islamic Azad University, Najafabad, Iran

Abstract: *Injectors and fuel pumps of diesel engines are lubricated by the fuel itself. So, the lubricity is very important issue for the engines. In this research, the effect of temperature variation on the friction coefficient as the lubrication property of diesel-Sesame oil blends was investigated by using four ball wear testing machine. The tests were conducted for fuel blends D90S10 (90% diesel and 10% Sesame oil by volume contained), D85S15, D80S20 and D100 according to ASTM D4172 and at temperatures of 25, 50, 75°C for 1500 and 3600 seconds. The results showed that the lubricity increases as a consequence of increasing Sesame oil in the fuel blend. The effect of temperature on the friction coefficient for test duration of 3600 seconds is more than that of test duration of 1500 seconds as a result of fuel degradation and losing fuel film stability between the balls.*

Keywords: *Friction, Four-ball Wear Testing Machine, Temperature, Sesame oil, Diesel*

1. Introduction

Injectors and fuel pumps of diesel engines are lubricated by the fuel itself. So, the lubricity is very important issue for the engines. Temperature of the fuel inlet can effect on lubrication of the engine fuel system, injectors and fuel pumps [1, 2]. There is not appropriate lubricating properties for conventional diesel fuels [3]; Recently there has been an increased concern in enhancing the use of biodegradable vegetable oils in lubricants because of environmental, economic and supply issues. Moreover, vegetable oils are also the alternative fuels that can blended with diesel fuel and used in CI engines[4]. In recent years, there are some studies about wear and lubrication properties of diesel blended with biofuels especially biodiesel[5]. Anastopoulos et al. [6] reported improved lubrication performance for blend levels with as little as 1% biodiesel. In Haseeb et al. [3] research, the authors found that with an increase in temperature, both friction and wear were higher slightly. Masjuki and Maleque [7] reported corrosion and oxidation in the lubricant after using more than 5% biodiesel derived from palm oil. Maru et al. [8] studied frictional properties of biodiesel according to Stribeck curves and demonstrated animal fat biodiesel lubrication has lower friction coefficient compared to soybean methyl ester oil. Fazal et al. [9] indicated that there were other relevant parameters (auto-oxidation, moisture absorption, viscosity and density of fuel) which significantly affect friction and corrosion in biodiesel and tribological properties. Lacey et al. [10] noted that sulphur included compounds in diesel fuel provided natural lubricity and that this helped to improve frictional and lubricity properties in the fuel. Habibullah et al. [11] studied the tribology characteristics of Calophyllum inophyllum biodiesel as lubricity enhancer by applying four ball tribometer. The result showed that diesel fuel has 16% and 40% higher friction coefficient and wear scar diameter than pure biodiesel respectively. Dhar and Agarwal [12] investigated the tribological properties of Karanja biodiesel blends compared to mineral diesel in the long term test. The results showed that that there is significant deterioration of lubricating oil because of higher concentration of wear trace metals in the oil of the engine fuelled with biodiesel compared to mineral diesel. According to the literature, it can be observed there is a lack of research to find lubrication properties of diesel-vegetable oils blends under various temperature conditions. Since Sesame oil is a conventional vegetable oil in Iran so in the present study, the effect of temperature variation on the friction coefficient as the lubrication property of diesel-Sesame oil blends was investigated by using four ball wear testing machine. The tests were conducted for fuel blends D90S10 (90% diesel and 10% Sesame oil by volume contained), D85S15, D80S20 and D100 according to ASTM D4172 and at temperatures of 25, 50, 75°C for 1500 and 3600 seconds.

2. Methods

Friction characteristics of fuel mixtures were studied under steady-state condition by using the four-ball wear testing machine according to ASTM D4172 standard. Fig. 1 shows the four-ball wear testing machine with the temperature control system. The test balls and prepared fuel blend according to the Table 1. The HMI controller records the friction torque and calculated the friction coefficient by following the Eq. (1). The test conditions in the present study are described in Table 1.

$$\text{Coefficient of friction}(\mu) = \frac{T\sqrt{6}}{3Wr} \quad (1)$$

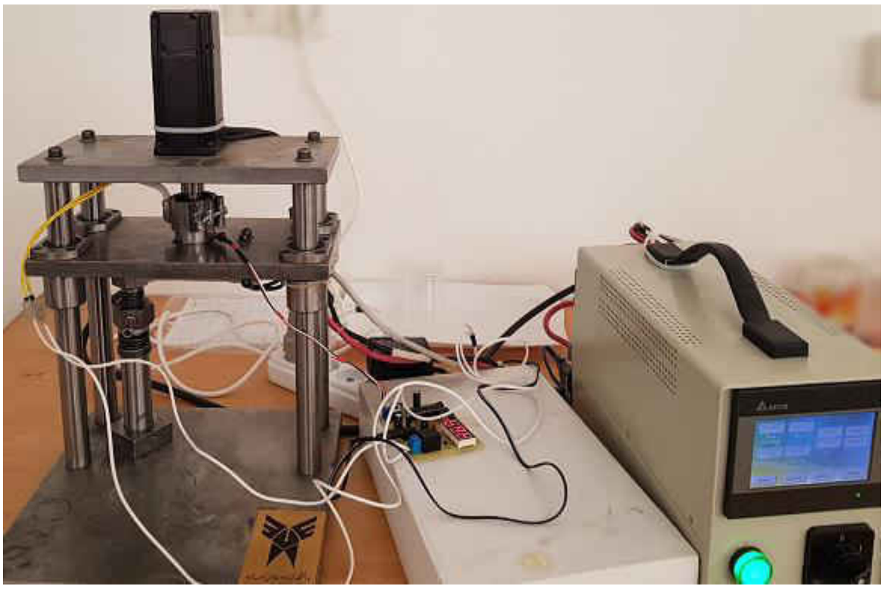

Fig. 1. The four-ball wear testing machine

Table 1: Tests conditions

Item	Value
Applied load (N)	392
Rotation (rpm)	1200
Test duration (s)	1500, 3600
Fuel blends	D90S10, D85S15, D80S20,D100

2.1 Results and discussion

Steady state friction coefficient averaged over the last 1500 seconds was calculated from the recorded torque and is plotted in Fig. 2 as a function of test temperature. Fig. 3 shows the friction coefficients versus test temperature for test duration of 3600 seconds.

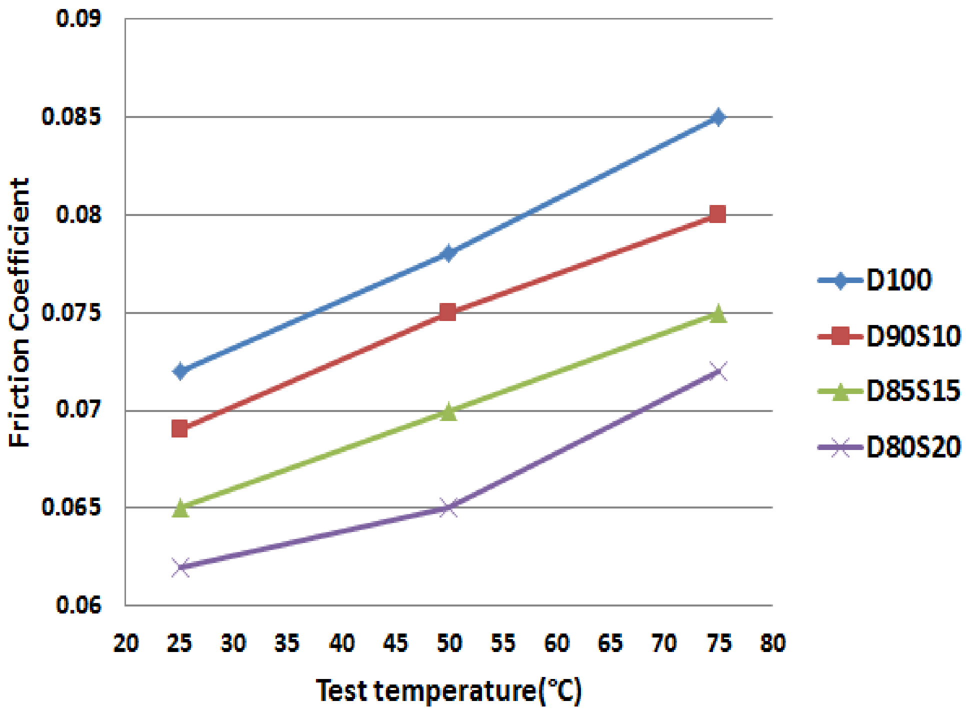

Fig. 2. The friction coefficients versus test temperature for test duration of 1500 s

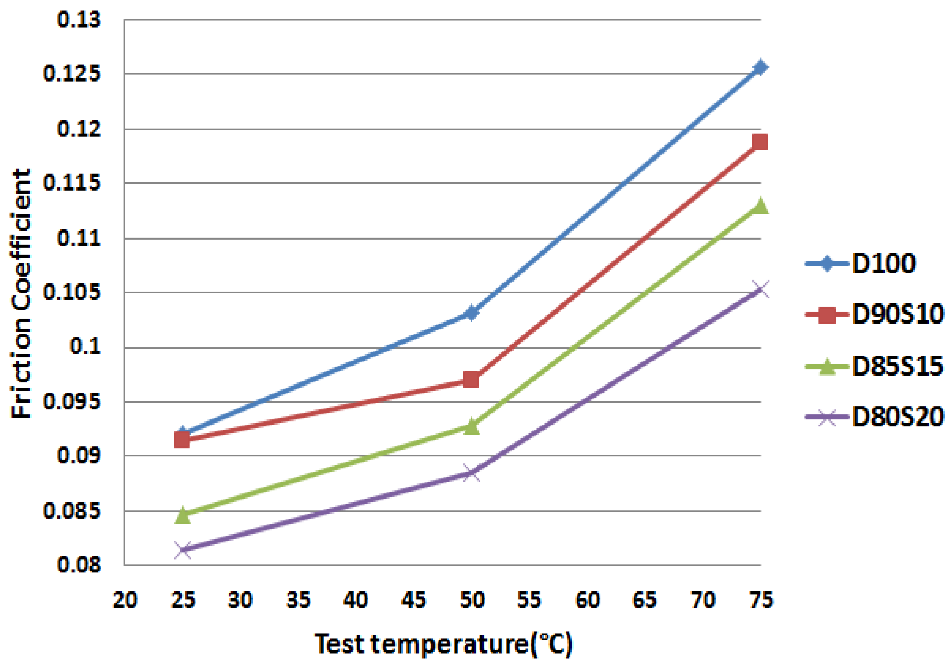

Fig. 3. The friction coefficients versus test temperature for test duration of 3600 s

The results showed that the lubricity increases as a consequence of increasing Sesame oil in the fuel blend. The reason could be due to the trace components in Sesame oil including free fatty acids, monoglycerides, diglycerides that improve the lubricity of the oil. In addition, the protective films can reduce thermal energy in sliding contact and thereby improve lubricity.

The results also indicated that the effect of temperature on the friction coefficient for test duration of 3600 seconds is more than test duration of 1500 seconds because of fuel degradation and losing fuel film stability between the balls. According to Clark et al. [13], viscosity of the fuel decreases with increasing of temperature. Another possible interpretation given by Masjuki et al. [14] is that the breakdown of boundary lubrication is due to the lower viscosity. In the other words, the stability of fuel film is depended on operating conditions such as load, temperature, speed as well as fluid viscosity and composition [15]. The present results suggest that at higher temperatures, these films seem to be less stable and thereby cause comparatively higher friction.

Acknowledgments

The author would like to thank the Aerospace and Energy Conversion Research Center at Najafabad Branch, Islamic Azad University for partly supporting this study.

References

[1] Sarvi, A., C.-J. Fogelholm, and R. Zevenhoven. "Emissions from large-scale medium-speed diesel engines: 2. Influence of fuel type and operating mode." *Fuel Processing Technology* 89, no. 5 (2008): 520-527.
[2] Nwafor, O.M.I. “The effect of elevated fuel inlet temperature on performance of diesel engine running on neat vegetable oil at constant speed conditions.” *Renewable Energy* 28, no. 2 (2003): 171-181.
[3] Haseeb, A.S.M.A., et al. "Effect of temperature on tribological properties of palm biodiesel." *Energy* 35, no. 3 (2010):1460-1464.
[4] Oğuz, H., et al. "Investigation of engine performance and kit design for the usage of safflower oil as in diesel engine." *Renewable Energy* 143 (2019): 692-702.
[5] Fazal, M.A., A.S.M.A. Haseeb, and H.H. Masjuki. "Investigation of friction and wear characteristics of palm biodiesel." *Energy Conversion and Management* 67 (2013): 251-256.
[6] Anastopoulos, G., et al. "Lubrication Properties of Low-Sulfur Diesel Fuels in the Presence of Specific Types of Fatty Acid Derivatives." *Energy & Fuels* 15, no. 1 (2001): 106-112.
[7] Masjuki, H.H., and M.A. Maleque. "Investigation of the anti-wear characteristics of palm oil methyl ester using a four-ball tribometer test." *Wear* 206, no. 1-2 (1997): 179-186.
[8] Maru, M.M., et al. "Assessment of the lubricant behaviour of biodiesel fuels using Stribeck curves." *Fuel Processing Technology* 116 (2013): 130-134.
[9] Fazal, M.A., A.S.M.A. Haseeb, and H.H. Masjuki. "A critical review on the tribological compatibility of automotive materials in palm biodiesel." *Energy Conversion and Management* 79 (2014): 180-186.
[10] Lacey, P.I., et al. "Lubricity of Volatile Fuels for Compression Ignition Engines." *SAE Transactions* 109 (2000): 980-988.
[11] Fazal, M.A., A.S.M.A. Haseeb, and H.H. Masjuki. "Corrosion mechanism of copper in palm biodiesel." *Corrosion Science* 67 (2013): 50-59.
[12] Xue, J., T.E. Grift, and A.C. Hansen. "Effect of biodiesel on engine performances and emissions." *Renewable and Sustainable Energy Reviews* 15, no. 2 (2011):1098-1116.
[13] Clark, S.J., L. Wagner, M.D. Schrock, and P.G. Piennaar. "Methyl and ethyl soybean esters as renewable fuels for diesel engines." *Journal of the American Oil Chemists’ Society* 61 (1984):1632–8.
[14] Masjuki, H.H, M.A. Maleque, A. Kubo, and T. Nonaka. "Palm oil and mineral oil based lubricants – their tribological and emission performance." *Tribology International* 32 (1999):304–14.
[15] Maleque, M.A, H.H. Masjuki, and A.S.M.A. Haseeb. "Effect of mechanical factors on tribological properties of palm oil methyl ester blended lubricant." *Wear* 239 (2000):117–25.

ISSN 1454 - 8003
Proceedings of 2019 International Conference on Hydraulics and Pneumatics - HERVEX
November 13-15, Băile Govora, Romania

S-CURVE MOTION PROFILES GENERATOR FOR HYDRAULIC ACTUATORS

Ioana ILIE[1], Marian BLEJAN[1], Robert BLEJAN[2]

[1] INOE 2000- IHP, ilie.ihp@fluidas.ro
[2] University POLITEHNICA of Bucharest, student, robertblejan@yahoo.com

Abstract: *Position control is usually achieved using a position controller and a profile generator. The profile generator establishes the desired trajectory based on reference position and predefined profiles, and the position controller forces the actual position to traces the generated position trajectory. The proposed profile generator allows control for maximum values of speed, acceleration and jerk, using S-curve motion, it uses an original solution of point to point movement with feedback. When profile position value reaches the value of final point position, the generator sends a signal to the set-point generator to move on to next desired point of motion profile, and so on. This motion profile generator will be implemented as a software sequence on a PLC.*

Keywords: *S-curve motion, profile generator, hydraulic actuator*

1. Introduction

The motion profiles generator, used in hydraulic actuator, allows the load movement from point A to point B in minimum time, while controlling the maximum values imposed for speed, acceleration and jerk. These values are imposed by the hydraulic actuation limitations regarding the flow rate, the response to the step signal or because the payload may be damaged when exceeding the critical acceleration and jerk values.
The material aims to analyze the motion profile for the hydraulic actuator that simultaneously controls: speed *v[m/s],* acceleration *a[m/s²]* and jerk *J[m/s³]*. The paper presents an original S-curve motion profile generator of "point to point motion profile" type. There are presented some principles of design of the hydraulic actuators proportional to the limitation of speed, acceleration and shock. The generator implementation on *PLC* hardware support is realized using Ladder Diagram programming language.

2. Theoretical assumptions

The equations describing the rectilinear motion (straight-line motion), for which velocity, acceleration and jerk are controlled, are the following (S-curve profile) [1]

$$J[\tfrac{m}{s^3}] = constant \tag{1}$$

$$a(t)\left[\frac{m}{s^2}\right] = \int_0^t J\,dt = a_0 + Jt \tag{2}$$

$$v(t)\left[\frac{m}{s}\right] = \int_0^t a(t)dt = v_0 + a_0\,t + Jt^2/2 \tag{3}$$

$$p(t)[m] = \int_0^t v(t)dt = p_0 + v_0 t + a_0\,t^2/2 + Jt^3/6 \tag{4}$$

where *p(t)* is the actuator position, *v(t)* is speed, *a(t)* is acceleration and *J* is jerk.
Determining the value of the flow required for a linear hydraulic actuator is done according to the considerations presented below.

- Calculation of the actuator cylinder area [2]

$$A[m^2] = 1.3F_R[N]/p_s[Pa] \tag{5}$$

where A is the cylinder area, F_R is the load force in cylinder rod and p_s the supply pressure of the hydraulic drive.
In order to compensate for the unknown forces that may occur at the level of the hydraulic cylinder rod, is chosen a factor of 1.3 (30% more than the desired force).

- Calculation of the flow required to reach a required speed of actuation of the load [2].

$$Q_L[\frac{m^3}{s}] = A[m^2]V_L[\frac{m}{s}] \tag{6}$$

$$p_L[Pa] = F_R[N]/A[m^2] \tag{7}$$

where Q_L is the flow required to reach a required speed V_L maximum velocity of the rod, and p_L the pressure drop required by the load.

- The maximum actuation speed (velocity) V_{max} of the hydraulic cylinder rod is

$$V_{max}[\frac{m}{s}] = Q_R[\frac{m^3}{s}]/A[m^2] \tag{8}$$

where Q_R is the nominal flow rate of the proportional electro-hydraulic device, servo valve or proportional valve.

- The maximum acceleration a_{max} of the hydraulic cylinder rod can be estimated by knowing the response time at the step signal t_{SR}, jump from zero to maximum flow rate, of the electrohydraulic device, such:

$$a_{max}\left[\frac{m}{s^2}\right] = V_{max}\left[\frac{m}{s}\right]/t_{SR}[s] \tag{9}$$

3. Implementation of the motion profiles generator

The motion profiles generator in the functional block diagram of the proportional hydraulic actuation, fig. 1, is placed between the input of the position set-point (desired position) and the input of the hydraulic actuator controller. The generator adapts the reference position signal to the hydraulic limitations, regarding the maximum speed and maximum acceleration of the hydraulic cylinder rod. These limitations are imposed by the maximum rated flow and the response time at the step signal, specific to the proportional electro-hydraulic device with which the hydraulic drive is built.

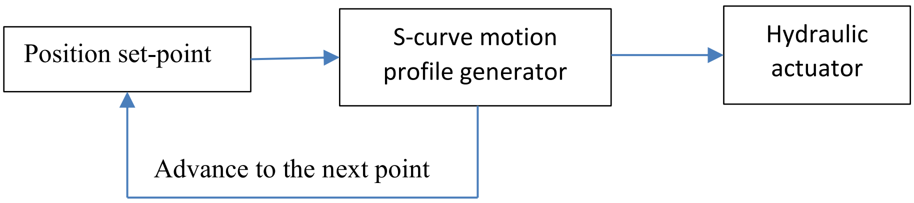

Fig. 1. Hydraulic unit with generator of motion profiles

The motion profiles generator is "point to point motion profile" type. Its operation is as follows, see fig. 1:

- „Position set-point” generates a value of the position set-point, the current point in the motion profile;

- „S-curve motion profile generator” generates a motion profile, from the previous point to the actual value of the position set-point, according to the equations of motion (1)…(4);

- Reaching value of set-point position, the current point in the motion profile, trigger the control block "Position set-point " to advance to the next point in motion profile;

- The operating sequence is repeated.

Motion profile generator can be implemented as a software module running on PLC program that controls hydraulic drive. The signals processed by the motion profile generator are processed numerically according to equations (1), (2), (3) and (4) with the limitations of the speed and acceleration values given by the equations (8) and (9).

The numerical processing of the signals involves the writing of equations (1) ... (4) in the discrete form as:

$$J_T = J = constant \tag{10}$$
$$A_T = A_T + J \tag{11}$$
$$V_T = V_T + A_T + J/2 \tag{12}$$
$$P_T = P_T + V_T + A_T/2 + J/6 \tag{13}$$

where P_T , V_T , A_T , J_T are the values of position, speed of acceleration and shock at time *T*.
Given the limitation of speed and acceleration values, the equations of the motion profile will become

$$J_T = J = constant \tag{10}$$
$$A_T = \min\left(A_T + J, a_{max}\right) \tag{11}$$
$$V_T = \min\left(V_T + A_T + J/2, V_{max}\right) \tag{12}$$
$$P_T = P_T + V_T + A_T/2 + J/6 \tag{13}$$

Figure 2 shows the S-curve motion profiles for position, speed, acceleration and jerk [3], and in figure 3 are presented the formulas that define the motion parameters for the time intervals that compose the motion profile.

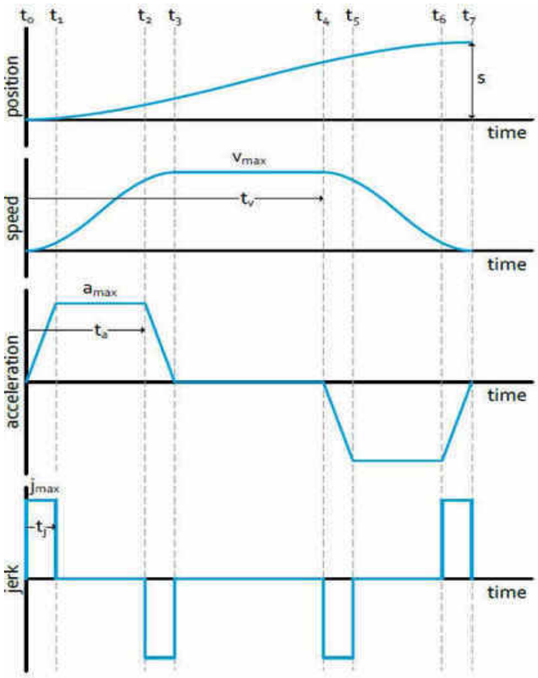

Fig. 2. S-curve motion profiles – motion parameters variation

The implementation of the S-curve motion profile generator for hydraulic actuators using the PLC „M221 Logic Controller” [4] will be exemplified. It will set an execution as "Periodic tasks" at a time of *1ms* or a thousand times per second, thus the time for integration and derivation is Δt = *1ms*. Formulas (10) ... (13) written using the "Ladder Diagram" are shown in figure 4.

<table>
<tr><th colspan="8">Motion parameters</th></tr>
<tr><th></th><th>jerk</th><th>acceleration</th><th colspan="2">velocity</th><th colspan="3">position</th></tr>
<tr><td>$t_0 \ldots t_1$</td><td>j_{max}</td><td>$j_{max} \cdot (t - t_0)$</td><td colspan="2">$\frac{1}{2} \cdot j_{max} \cdot (t - t_0)^2$</td><td colspan="3">$\frac{1}{6} \cdot j_{max} \cdot (t - t_0)^3$</td></tr>
<tr><td>$t_1 \ldots t_2$</td><td>0</td><td>$a_1 = a_2$</td><td colspan="2">$v_1 + a_1 \cdot (t - t_1)$</td><td colspan="3">$p_1 + v_1 \cdot (t - t_1) + \frac{1}{2} \cdot a_1 \cdot (t - t_1)^2$</td></tr>
<tr><td>$t_2 \ldots t_3$</td><td>$-j_{max}$</td><td>$a_2 - j_{max} \cdot (t - t_2)$</td><td colspan="2">$v_2 + a_2 \cdot (t - t_2) + \frac{1}{2} \cdot -j_{max} \cdot (t - t_2)^2$</td><td colspan="3">$p_2 + v_2 \cdot (t - t_2) + \frac{1}{2} \cdot a_2 \cdot (t - t_2)^2 + \frac{1}{6} \cdot -j_{max} \cdot (t - t_2)^3$</td></tr>
<tr><td>$t_3 \ldots t_4$</td><td>0</td><td>0</td><td colspan="2">$v_3 = v_4$</td><td colspan="3">$p_3 + v_3 \cdot (t - t_3)$</td></tr>
<tr><td>$t_4 \ldots t_5$</td><td>$-j_{max}$</td><td>$-j_{max} \cdot (t - t_4)$</td><td colspan="2">$v_4 + \frac{1}{2} \cdot -j_{max} \cdot (t - t_4)^2$</td><td colspan="3">$p_4 + v_4 \cdot (t - t_4) + \frac{1}{6} \cdot -j_{max} \cdot (t - t_4)^3$</td></tr>
<tr><td>$t_5 \ldots t_6$</td><td>0</td><td>$a_5 = a_6$</td><td colspan="2">$v_5 - a_{max} \cdot (t - t_5)$</td><td colspan="3">$p_5 + v_5 \cdot (t - t_5) + \frac{1}{2} \cdot a_5 \cdot (t - t_5)^2$</td></tr>
<tr><td>$t_6 \ldots t_7$</td><td>j_{max}</td><td>$a_6 + j_{max} \cdot (t - t_6)$</td><td colspan="2">$v_6 + a_6 \cdot (t - t_6) + \frac{1}{2} \cdot j_{max} \cdot (t - t_6)^2$</td><td colspan="3">$p_6 + v_6 \cdot (t - t_6) + \frac{1}{2} \cdot a_6 \cdot (t - t_6)^2 + \frac{1}{6} \cdot j_{max} \cdot (t - t_6)^3$</td></tr>
<tr><td colspan="2">$t_1 = t_j$</td><td>$t_2 = t_a$</td><td>$t_3 = t_a + t_j$</td><td>$t_4 = t_v$</td><td>$t_5 = t_v + t_j$</td><td>$t_6 = t_v + t_a$</td><td>$t_7 = t_v + t_j + t_a$</td></tr>
</table>

Fig. 3. S-curve motion profiles – motion parameters formula's over time

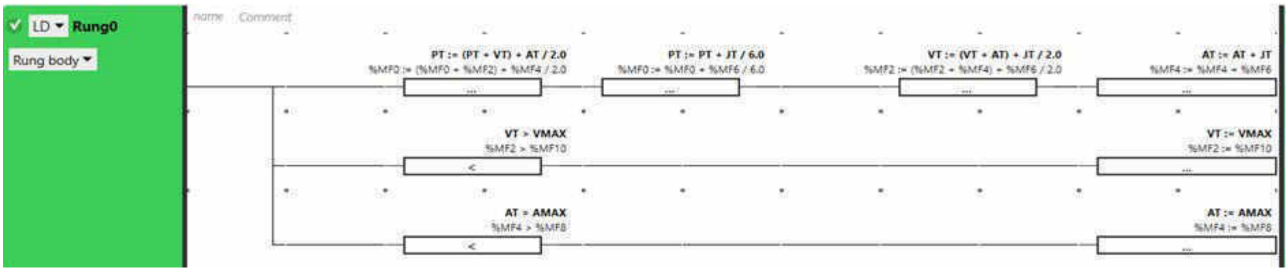

Fig. 4. Implementation example of S-curve motion profiles in language „Ladder Diagram”

4. Conclusions

The design of an optimal motion profile generator for hydraulic actuators, to achieve a "point to point" movement in a minimum time, taking into account the limitations imposed by the hydraulic actuation parameters, allows to obtain a more efficient actuator.

There were presented some considerations for the design of the hydraulic drive in order to ensure an imposed motion profile; thus the choice of the proportional electro-hydraulic device with which the actuation is equipped is made according to the value of the maximum speed and the value of the maximum acceleration that is desired to be obtained in the actuating rod.

An S-curve type motion profile generator was presented having an original conception in the sense that the event of ending a movement between two points triggers a new movement between next two points. This type of generator allows the realization of a movement profile, described by successive points, which is executed in minimum time, respecting the limitations regarding the maximum values imposed for speed, acceleration and jerk.

Finally, the generator implementation principles were presented as the software module written in the programming language specific to the programmable controller.

References

[1] www.pmdcorp.com.
[2] www.moog.com.
[3] Mu, Haihua, Yunfei Zhou, Sijie Yan, and Aiguo Han. "Third-order trajectory planning for high accuracy point-to-point motion." *Frontiers of Electrical and Electronic Engineering in China* 4, no.1 (March 2009): 83–87.
[4] www.schneider-electric.com.

ISSN 1454 - 8003
Proceedings of 2019 International Conference on Hydraulics and Pneumatics - HERVEX
November 13-15, Băile Govora, Romania

CONSIDERATIONS REGARDING THE SHOCK ABSORBERS STATIC PERFORMANCES ACCORDING TO HYDRAULIC FLUID WEAR DEGREE

Alexandru Valentin RĂDULESCU[1], Irina RĂDULESCU, Radu Florin MIRICĂ, Daiana Georgiana IVAN

[1] University POLITEHNICA of Bucharest, alexandru.radulescu@upb.ro

Abstract: *The purpose of this paper is to determine the performance of hydraulic shock absorbers in static conditions and to correlate the experimental results with the rheological parameters of the specific fluid, considering its wear degree. The study was performed on two used hydraulic shock absorbers, that were part of a car suspension system. One of them was disassambled, in order to design the component parts and to recuperate the used hydraulic working fluid, and the other one was kept whole, for experimental testing in static conditions. The rheological properties of the used hydraulic fluid were determined, using a Brookfield rotating viscometer CAP 2000+, with cone and plate geometry. Finally, it can observe that the analytical relation for the variation of the static load versus velocity is quite appropriate at low velocities (until 25 mm/s), with the assumption of Newtonian or power law rheological model validity. At higher velocities, the model must be refined, taking into account the real geometry of the hydraulic shock absorber valve.*

Keywords*: Rheology, shock absorber, static test, fluid wear*

1. Introduction

Hydraulic shock absorbers utilize liquid fluid to convert mechanical energy into thermal energy. The dampening is facilitated by the shock absorber's fluid being moved by a piston displaced by mechanical action that forces the flow of the fluid through orifices or restrictors. The orifices which the fluid passes through limits the velocity or volume flow and converts the mechanical energy of the fluid into thermal energy. The heat energy is then transferred through the fluid and out the devices mechanical mass to the ambient air or environment. These types of absorbers are utilized within automobile, agriculture equipment, motorcycle suspensions, heavy truck, aircraft landing gear, conveyor systems, structural engineering applications and many other custom industrial applications [1 – 3].
Determining the correct hydraulic shock absorber size and performance characteristics requires a complete understanding of the dynamic and static requirements of the mechanical system involved. Performance requirements of a shock absorber system should be accurately estimated, so a functional test should be performed to verify the main technical characteristics: static and dynamic force at hydraulic shock absorber, velocity and stroke of target application, kinetic energy, deceleration rate of shock absorber etc. [4 – 7].
The study was performed on two used hydraulic shock absorbers [8], that were part of a car suspension system. One of them was disassambled, in order to design the component parts and to recuperate the used hydraulic working fluid [9], and the other one was kept whole, for experimental testing in static conditions.
The rheological properties of the used hydraulic fluid were determined, using a Brookfield rotating viscometer CAP 2000+, with cone and plate geometry [10]. It was observed that the used hydraulic fluid segregates in two fractions, according to their density: light fraction and heavy fraction.
A simple analytical expression for the static load of the hydraulic shock absorber was determined, performing also a comparison between theoretical and experimental variation of the static load versus velocity of the piston rod.

2. Theoretical model

The theoretical model is based on the geometry of a hydraulic shock absorber (Figure 1) [8], but assuming a simplified approach of the working area, with the main dimensions presented in Figure 2.

a) General view [8]

b) 3D model

Fig. 1. Hydraulic shock absorber

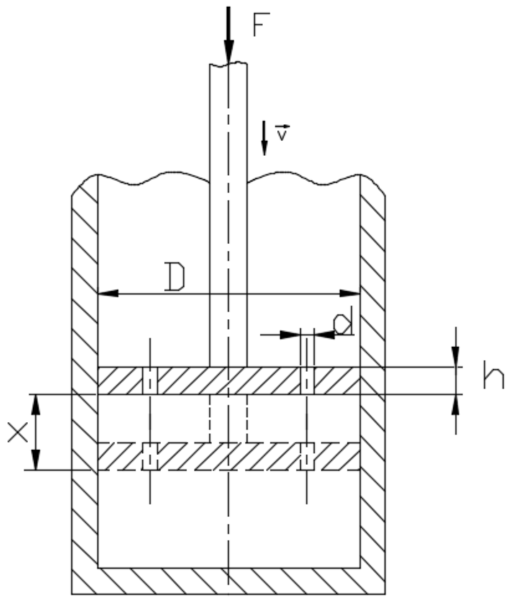

Fig. 2. Detail of the working area

The working area is characterized by piston diameter *D* = 40 mm, holes diameter in the piston *d* = 1 mm, number of holes *N* = 9 and holes length *h* = 10 mm.
In order to obtain the static load of the hydraulic shock absorber, it was assumed that at a downward displacement of the hydraulic piston at distance *x*, the volume of expelled working fluid is forced to flow through the *N* holes in the piston. So, the flow conservation equation has to written, taking into account the flow into the cylinder and the flow through the holes.
The flow of the working fluid into the cylinder, for a displacement *x* of the hydraulic piston, is expressed as:

$$Q = \frac{\pi D^2}{4} v \tag{1},$$

where: Q – working fluid flow into the cylinder;
v – velocity of the hydraulic cylinder rod;
D – piston diameter.
The flow through the piston holes is calculated with the assumption that the working fluid is modelled with the power law rheological model [11]:

$$\tau = m \left(\frac{du}{dy}\right)^n \tag{2},$$

where: τ – shear stress;
m – consistency index;
n – flow index;
u – fluid local velocity;
y – local coordinate;
The advantage of using this general model is that when flow index *n* is equal to one, the power law model reduces to the Newtonian fluid model and consistency index *K* has the unit of viscosity.
With assumption, the flow through the piston holes becomes [12]:

$$Q = \frac{\pi\left(\frac{d}{2}\right)^3}{\frac{1}{n}+3}\left[\frac{\Delta p\left(\frac{d}{2}\right)}{2hm}\right]^{\frac{1}{n}} \cdot N \tag{3},$$

where: Q – working fluid flow through the piston holes;
d – holes diameter;
h – holes lenght;
N – number of holes;
Δp – hydraulic cylinder pressure drop;
The hydraulic cylinder pressure drop can be calculated with the following relation:

$$\Delta p = \frac{F}{\frac{\pi D^2}{4}} \tag{4},$$

where: F – static load of the hydraulic shock absorber.
The final expression for the static load of the hydraulic shock absorber can be obtained from the flow conservation equation, namely by equalization of the equations (1) and (3) and considering the expression of the pressure drop given by equation (4):

$$F = \frac{2\pi h m D^{2n+2}\left(\frac{1}{n}+3\right)^n}{4^{n+1}\left(\frac{d}{2}\right)^{3n+1} N^n} v^n \tag{5}$$

If the working fluid is a Newtonian fluid (*n* = 1), the static load of the hydraulic shock absorber will be calculated with a simplified relationship:

$$F = \frac{\pi h \mu D^4}{2\left(\frac{d}{2}\right)^4 N} v \qquad (6),$$

where: μ – fluid viscosity.

3. Experimental stand and methodology

The rheological measurements were performed on a Brookfield viscometer CAP2000+ equipped with four cone-and-plate geometry and using a Peltier system for controlling the temperature. The CAP 2000+ Series Viscometers are medium to high shear rate instruments with Cone Plate geometry and integrated temperature control of the test sample material [10].
A typical view of the viscometer is presented in Figure 3, with a detail of the working cone number 8 fixed in the coupling device.

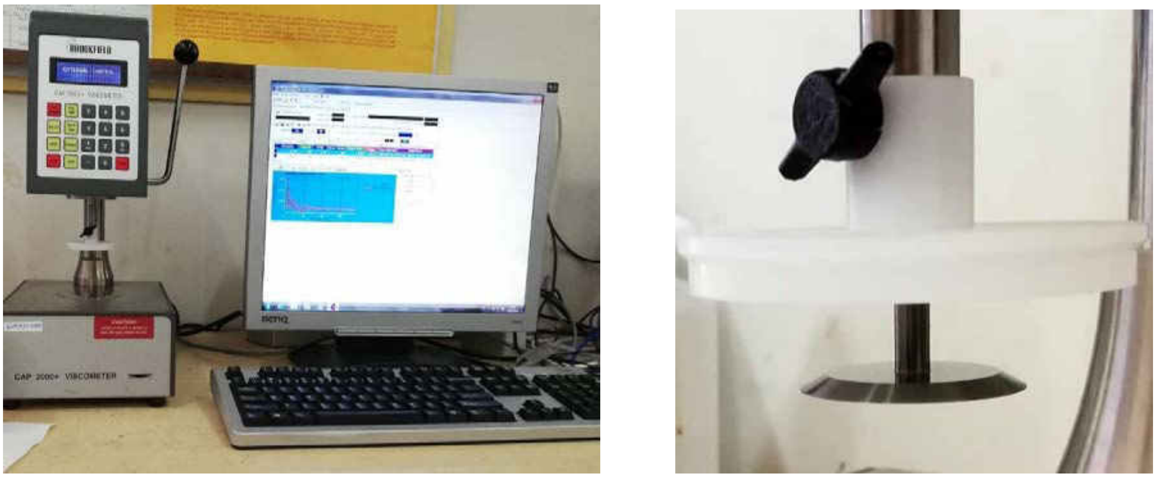

a) General view b) Cone no. 8

Fig. 3. Brookfield viscometer

Concerning the technical parameters of the viscometer, rotational speed selection ranges from 5 to 1000 rpm. Viscosity measurement ranges depend upon the cone spindle and the rotational speed (shear rate). Viscosity is selectively displayed in units of centipoise (cP), poise (P), or Pascal seconds (Pa•s). Temperature control of sample is possible between either 5°C (or 15°C below ambient, whichever is higher) and 75°C or 50°C and 235°C, depending on viscometer model. The viscometer uses a CAPCALC32 software for complete control and data analysis. The tested lubricant is an used hydraulic working fluid, with physical and chemical properties presented in Table 1 [9].

Table 1: Physical and chemical properties of the hydraulic working fluid [9]

Characteristic parameter	Hydraulic working fluid
Colour	light yellow
Odor	characteristic
Flash point [^{0}C]	152 (EN ISO 2592)
Density at 15°C [g/ml]	0.87 (DIN 51757)
Viscosity at 40°C [mm^2/s]	17.1 (DIN 51562)

Concerning the experimental determination of the static load of the hydraulic shock absorber, it was used an worn-out shock absorber, which was fixed in a vise (Figure 4). For the measurement of static load, a range of marked masses were placed on a flange mounted on the end of the shock absorber rod. There were used successively marked masses of 5, 10, 15, 20, 25 and 30 N.

The displacement time of the rod was established by timing, the timing starting from the moment when the flange was released. Knowing the shock absorber stroke and observing that the movement is uniform, the velocity of the hydraulic cylinder rod can be easily calculated.

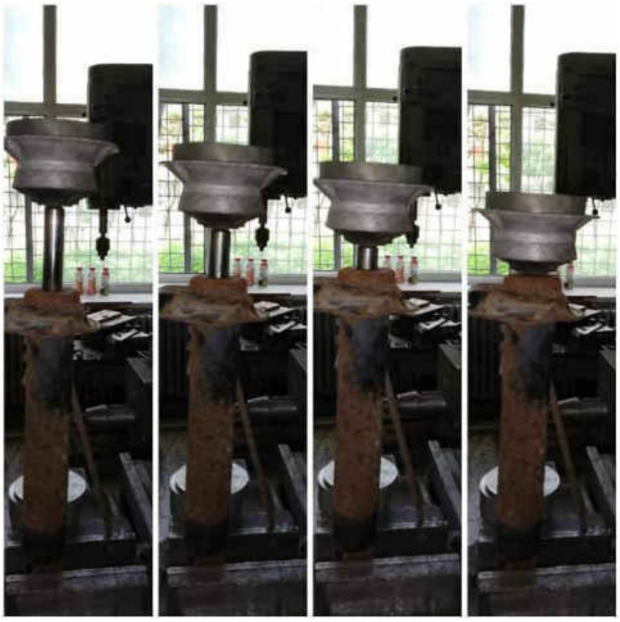

Fig. 4. Experimental setup for shock absorber testing

Using the rheological parameters determined for the working fluid with Brookfield viscometer, the theoretical values of the static load for the shock absorber were obtained. These values were compared with the experimental ones, measured on the real worn-out shock absorber.

4. Results and discussions

The experimental rheological tests were performed in two stages:

- tests for fluid stability - determination of the homogenization time (soaking time) of the samples, at five different shear rates: 200, 400, 600, 800 and 1000 s^{-1}
- tests for rheological parameters - consist of a load from 200 s^{-1} to 1200 s^{-1} shear rate gradient and measuring the shear stress, at a constant temperature of 20 ^{0}C.

During the experimental tests, it was observed that the used hydraulic fluid segregates in two fraction, according to their density: light fraction and heavy fraction. So, the results will be presented for these two fractions, and also for the mixture between them, called mixed fraction.
Figures 5, 6 and 7 present the results from the stability tests, where from it can determine the soaking time. This time represents an input data for the data acquisition program, request by Capcalc 32 software specific for the viscometer. Analysing these results, it can observe that working fluid viscosity decrease with the increasing of shear rate, for all three types of fractions: light, heavy and mixed. Regarding the soaking time (the time after which the fluid flow stabilizes), the curves presented in Figures 5, 6 and 7 show the stabilization of the movement after time intervals depending on the type of analyzed working fluid fraction (Table 2).

Table 2: Soaking time for different fraction of the hydraulic working fluid

Type of fraction	Soaking time [s]
light	50
heavy	70
mixed	60

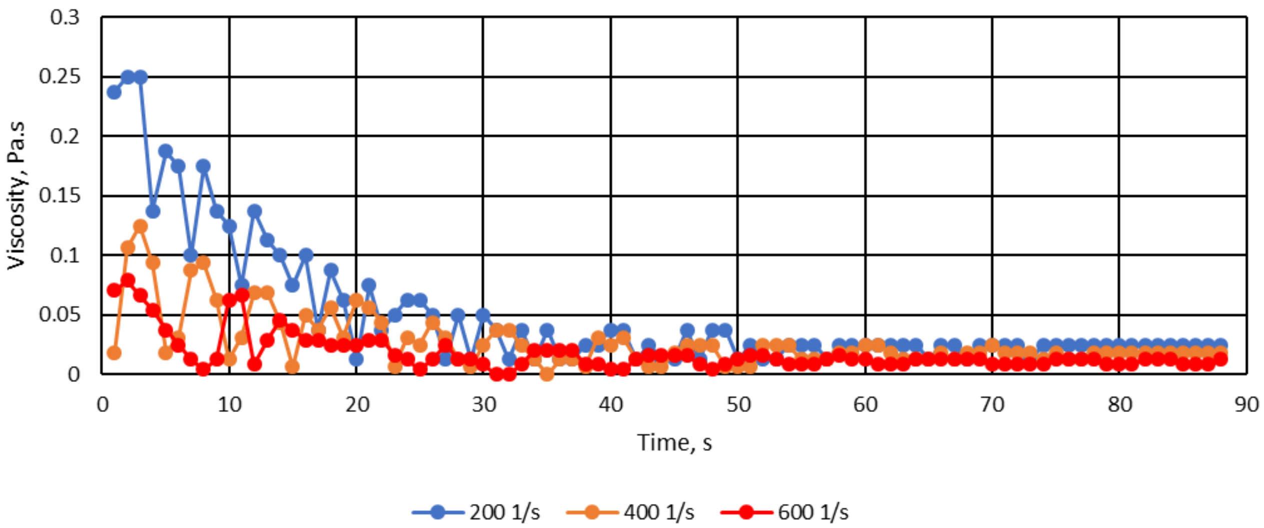

Fig. 5. Variation of the viscosity versus time for light fraction of the working fluid, at different shear rates

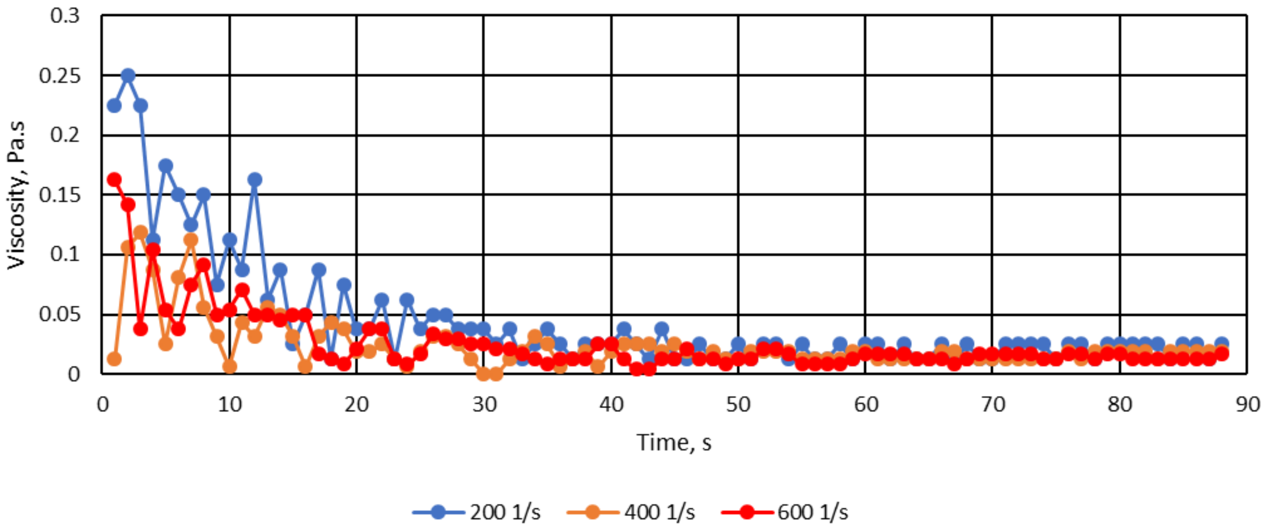

Fig. 6. Variation of the viscosity versus time for heavy fraction of the working fluid, at different shear rates

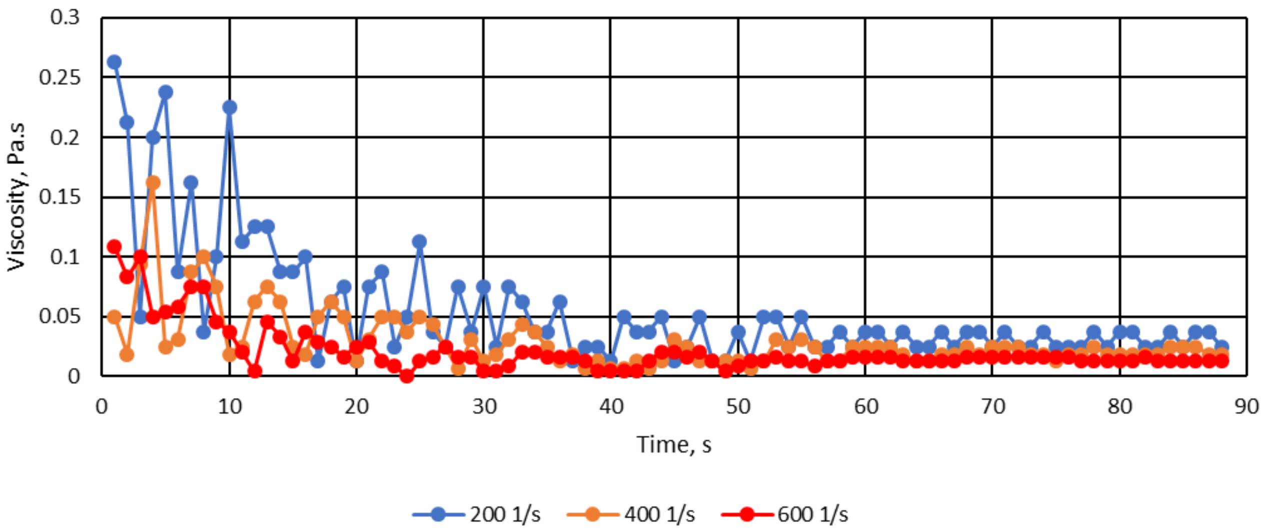

Fig. 7. Variation of the viscosity versus time for mixed fraction of the working fluid, at different shear rates

Figure 8 presents the specific rheograms for the hydraulic working fluid, corresponding to those three type of fractions (light, heavy and mixed). Based on these results, the rheological models of the analyzed fractions can be obtained, using the regression analysis method with MathCAD software.

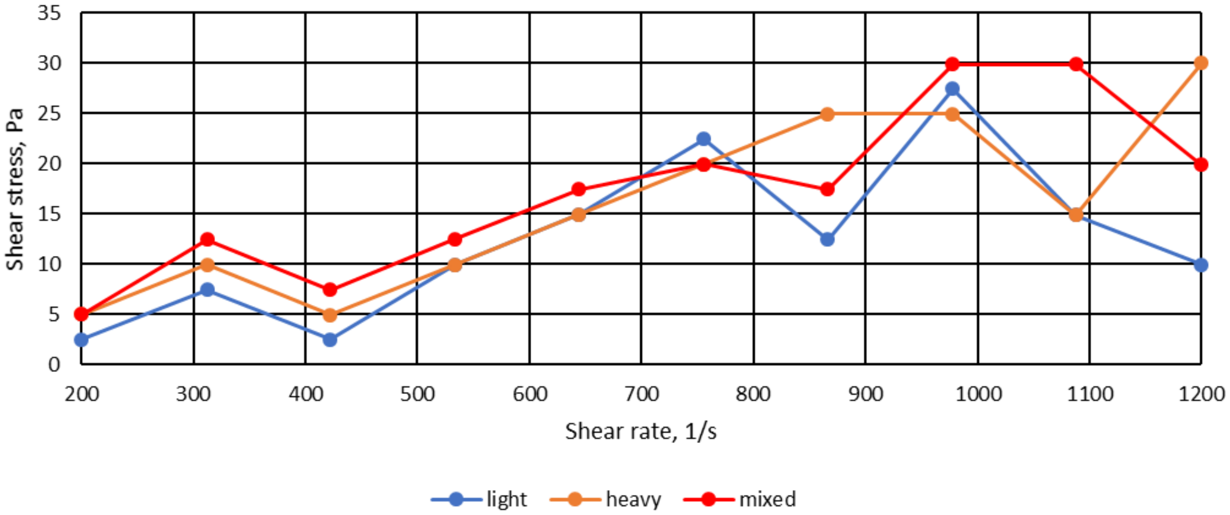

Fig. 8. Rheograms for different fractions of the working fluid, at 20 ^{0}C

Table 3 presents the values of the rheological parameters for the three types of working fluid fractions. Analyzing these results and considering the magnitude of the correlation coefficient, it can observe that power law rheological model is more appropriate for light fraction, while Newtonian model corresponds better for heavy and mixed fraction.

Table 3: Rheological parameters of hydraulic fluid different fractions

Lubricant	Newtonian model		Power law model		
	Viscosity, Pa·s	Corr. coeff., %	Consistency index, Pa·s^n	Flow index	Corr. coeff., %
Light fraction	0.0172	33.55	0.010	1.07	51.41
Heavy fraction	0.0227	73.70	0.029	0.96	72.23
Mixed fraction	0.0240	80.43	0.053	0.88	78.80

The results concerning the experimental determination of the static load of the hydraulic shock absorber are presented in Table 4.

Table 4: Experimental results for static load

G [N]	12.8	17.8	22.8	27.8	32.8	37.8	42.8
t [s]	25.60	14.26	9.49	6.96	4.98	4.13	2.75
v [mm/s]	3.75	6.73	10.12	13.79	19.28	23.25	34.91

Finally, the comparison between theoretical and experimental variation of the static load versus velocity of the piston rod, for all three fractions of the hydraulic working fluid, is presented in Figure 9.

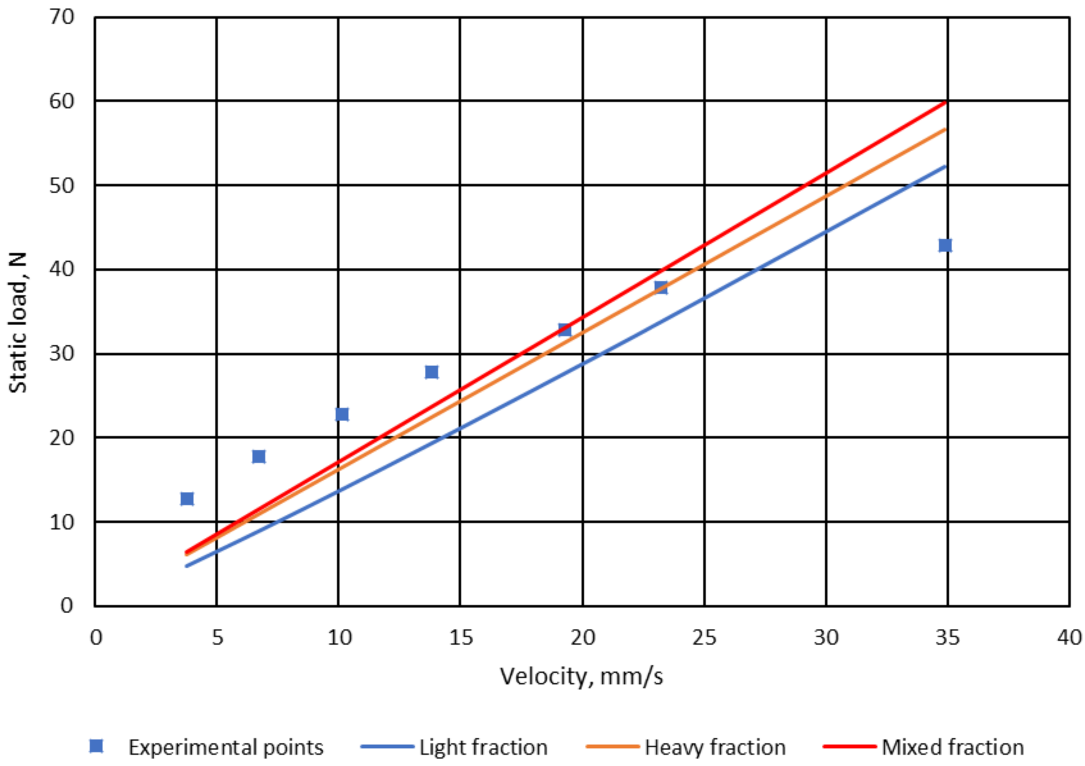

Fig. 9. Variation of static load versus velocity of the piston rod: comparison theory - experiment

5. Conclusions

The purpose of this paper was to determine the performance of hydraulic shock absorbers in static conditions and to correlate the experimental results with the rheological parameters of the specific fluid, considering its wear degree.
During the experimental tests, it was observed that the used hydraulic fluid segregates in two fraction, according to their density: light fraction and heavy fraction. From rheological point of view, it was found that power law rheological model is more appropriate for light fraction, while Newtonian model corresponds better for heavy and mixed fraction.
Finally, a simple analytical relation was proposed, for the variation of the static load of the shock absorber versus velocity of the piston rod. This calcul relation is quite appropriate at low velocities (until 25 mm/s), with the assumption of Newtonian or power law models validity.
At higher velocities, the theoretical model has to be refined, taking into account the real geometry of the hydraulic shock absorber valve.

References

[1] Singh, Manpreet, Singh, Jasvinder and Singh, Gurpreet. “Review on shock absorbers & suspension system”. *International Research Journal of Engineering and Technology,* Vol. 4, No. 4 (Apr. 2017): 1521-1527.
[2] Morettini, Giulia, Bartolini, Nicola, Astolfi, Davide, Scappaticci, Lorenzo, Becchetti, Matteo and Castellani, Francesco. “Experimental diagnosis of cavitation for a hydraulic monotube shock absorber”. *Diagnostyka*, Vol.17, No. 3 (2016):75-80.
[3] Czop, Piotr and Gnilka, Jacek. “Reducing aeration and cavitation effect in shock absorbers using fluid-structure interaction simulation”. *Computer Assisted Methods in Engineering and Science,* Vol. 23 (2016): 171-189.
[4] Wieckowski, Dariusz, Dabrowski, Krzysztof and Slaski, Grzegorz. “Adjustable shock absorber characteristics testings and modelling”. *IOP Conf. Series: Materials Science and Engineering,* 421 (2018) 022039: 1-10.

[5] Titurus, Branislav, du Bois, Jonathan, Lieven, Nick and Hansford, Robert. “Model uncertainty in identification of the static characteristics of the hydraulic damper”. *10th International Conference RASD 2010*, Southampton (12-14 July 2010): 170-180.
[6] Ferdek, Urszula and Luczko, Jan. “Modeling and analysis of a twin-tube hydraulic shock absorber”. *Journal of Theoretical and Applied Mechanics,* Vol. 50, No. 2 (2012): 627-638.
[7] Krakov, Mikhail. “Influence of rheological properties of magnetic fluid on damping ability of magnetic fluid shock-absorber”. *Journal of Magnetism and Magnetic Materials,* Vol. 201, No. 1-3 (Julay 1999): 368-371.
[8] https://www.engineersedge.com/hydraulic/hydraulic-shock-absorbers.htm (accessed on 26.09.2019).
[9] https://cdn.partsfinder.bilsteingroup.com/pf-document/CLP02615_GB.PDF (accessed on 03.10.2019).
[10] http://www.brookfieldengineering.com/-/media/ametekbrookfield/manuals/ lab%20viscometers/cap2000%20instructions.pdf?la=en (accessed on 29.09.2019).
[11] Balan, Corneliu. *The rheology of lubricating greases.* NLGI ed., 2000.
[12] Chhabra, Raj and Richardson, John, Francis. *Non-Newtonian flow and applied rheology: engineering applications.* Butterworth-Heinemann ed., 2011.

ISSN 1454 - 8003
Proceedings of 2019 International Conference on Hydraulics and Pneumatics - HERVEX
November 13-15, Băile Govora, Romania

RAPID PROTOTYPING AND ADDITIVE MANUFACTURING OF FLUID POWER COMPONENTS - SUITED FOR SPECIAL APPLICATION

Darko LOVREC[1]

[1]University of Maribor, Faculty of Mechanical Engineering, Slovenia, darko.lovrec@um.si

Abstract: *Additive Technology has already established itself as an important manufacturing technology to shorten the time from idea to product marketing, while reducing development costs and raising the quality of finished products. The prototypes thus created were considered to have a high geometric accuracy, and the mechanical properties of the materials from which they were made did not meet the requirements of the final product. Therefore, they were intended primarily for presentations of finished products, concept visualization, design and matching analyses, tool engraving and foundry moulding, and easier functional tests.*
The paper presents the possibilities of using Additive Technology in the field of Fluid Power and practical experiences: From simple parts of components, to high load valves of special shapes and requirements, and special cases in the field of Pneumatic Components. Each case presented illustrates the path of product development, and the limitations and specifics that dictated the use of layered technologies, right down to the end product effectively used in practice.

Keywords: *Fluid power, Additive Manufacturing, hydraulic valves, special components, accessories*

1. Introduction

Advances in materials and technologies, however, have led to the increasing use of these technologies to produce finished, functional products. That's why we are talking more and more about Rapid Manufacturing and not Rapid Prototyping. Essentially, rapid prototyping processes are ancillary procedures – the processes of adding materials that differ from each other, depending on how the material is added. The process is chosen according to the intended use of the end product, the product range being extremely wide: From housings, internal components of machines, bottles, tools..., to medical applications, e.g. surgical implants, hearing aids...
Fluid Power products represent a specific area, since the components are exposed to high internal pressure and to external mechanical stresses. The latter applies to hydraulic valve housings. However, in the field of Fluid Power technology, it is possible to apply modern technology to many other components, both hydraulic and pneumatic. Some examples of this will be discussed in more detail in the following Sections.

2. Rapid Manufacturing of hydraulic valves

The valve body, or valve housing, is usually the most basic part of the hydraulic valve, and, at the same time, the part that largely determines the characteristic and physical properties of the valve as a whole. In the classical valve housing manufacturing, there are two approaches. Manufacturing of housing from a raw, metal rod material, and manufacturing of a housing by using casting technolgy. Manufacturing of housing from metal rods is suitable for individual pieces or for smaller series, due to the costs associated with machining at machining centres and long technological processing times. Also, the designer, in this case, is relatively limited, since he has to adjust the construction more often in the direction of the possibility of the manufacturing process than in the direction of the best functionality of the component.
In the case of hydraulic valve housings made from metal rods, compared to the cast housing, the outer dimensions of the valve and, consequently, the weight of the valve, are larger, although both valves have comparable performance. Also, the internal shape of the channels is not optimal – Figure 1.

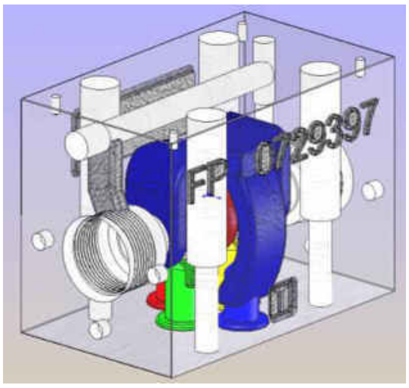

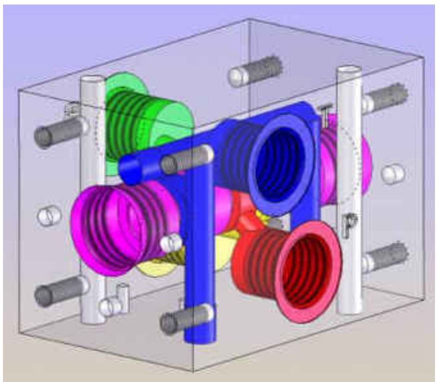

Fig. 1. Valve housing as a cast product (left) and as made from metal rods (right)

In view of its complex design and required mechanical properties, manufacturing of a valve housing by using rapid manufacturing, is very challenging. On the one hand, there is the rather complex internal geometry of the valve, and on the other hand, the product must be able to withstand all dynamic pressures and forces. There are two options for using the RM valve manufacturing method: Either to make only the casting core of the valve after the RP procedure and then cast it according to the classical procedure (saving the time and cost of prototype tooling, as well as the cost of subsequent corrections), or use the direct process, where the valve is literally "printed" using the appropriate material.

2.1 Rapid Manufacturing – RM of valve housings

The development of additive technology already enables the production of homogeneous materials that can withstand high pressure loads, which are characteristic for hydraulic components. Selective deposition of metal powders by means of a laser or an electron beam is available for the direct, rapid manufacture of valve housings. Regardless of the energy source, we get a product of full material density from original engineering materials.

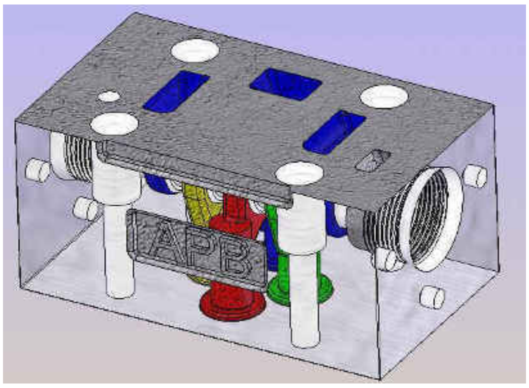

Fig. 2. Housing of a directional control valve size NG 6; CAD model (left) and finished product manufactured by the EBM process (right)

Materials include a variety of steels, from maraging tool steel, super alloy (e.g. inconel), to medical stainless (e.g. CoCr), and special metals such as titanium. The Selective Laser Melting (SLM) process allows for a rather high precision workmanship, making it possible to produce a valve in a final or near-final shape (near net shape) with all accessories such as threads and centring holes. Unfortunately, the process is quite lengthy and, therefore, disadvantageous in price. The Electron Beam Melting (EBM) Electron Beam Deposition Process has a significantly higher energy supply, making it significantly faster, and at least 5 times cheaper than the SLM process. Unfortunately, due to the huge energy input, the surface is quite rough, which makes it impossible to produce details such as threads – Figure 2.

2.2 Rapid tooling – RT for casting housings

In the field of Rapid Tooling, casting with a lost core and making sand moulds using layered technologies are available as representatives of indirect RT processes. A casting process with a lost core requires a casting model made of material with a relatively low melting point. The process is known in goldsmithing, where models are serially made from wax in rubber moulds.
For valve housings, this process is not appropriate, because it requires a tool to produce wax valve housings. Rapid Prototyping (RP) procedures using suitable materials are appropriate. For this purpose, there are a few printers which can produce models of synthetic wax, SLS – Selective Laser Sintering and stereolithography polystyrene with special photopolymers for this purpose. The model thus obtained is inserted into a special frame – coat, and filled with special reinforced plaster in a liquid state. When the plaster solidifies the resulting mould is heated appropriately so that the wax melts and drains from the mould. Liquid metal is then poured into the resulting mould. This gives a functional casting of the desired material. This is very advantageous, because the resulting model can be made of the same material as the castings will be made in series, making it easy to check the technological procedures and functions of the valve. The appearance of the molten core casting model is shown in Figure 3.
For this purpose, there are several printers making synthetic wax models, SLS – selective laser polystyrene sintering, and stereolithography with special photopolymers.

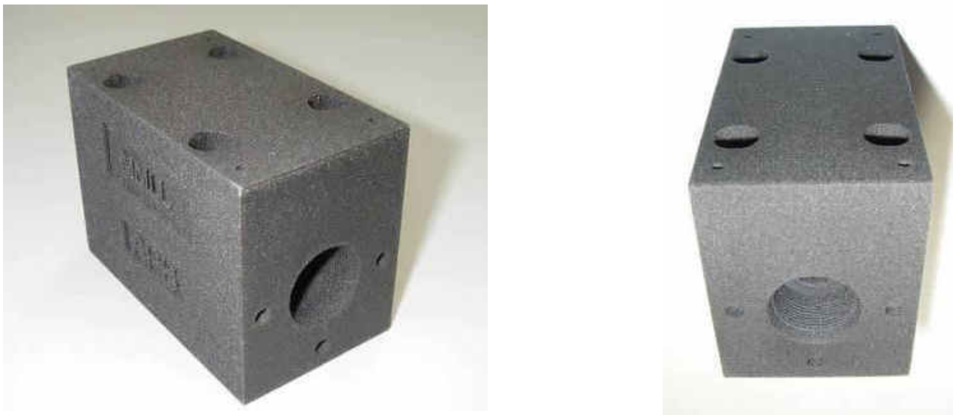

Fig. 3. Model for core casting made of polystyrene with the SLS process. The threads and other details are clearly visible

The production of sand moulds with layered technologies has evolved due to the requirements of the Foundry industry for the rapid production of complex moulds for small batches of products. There are some printers in this area that operate under the patented 3DP process. In this process, a layer of foundry sand is applied to the carrier tray, and the print head, as known from the ink-jet printers, injects a furon into the sand layer in the form of a single cross-section of an emerging foundry mould or core. The tray is then pulled down and repeated with the next layer – see Figure 4.
An alternative is the process of Selective Laser Sintering of foundry sand. The process is the same as sintering plastic or metal deposition, except in this case, the sintering powder has been pre-treated – mixed with furon. The laser thus "melts" or activates the furon, thereby causing the sand to adhere.

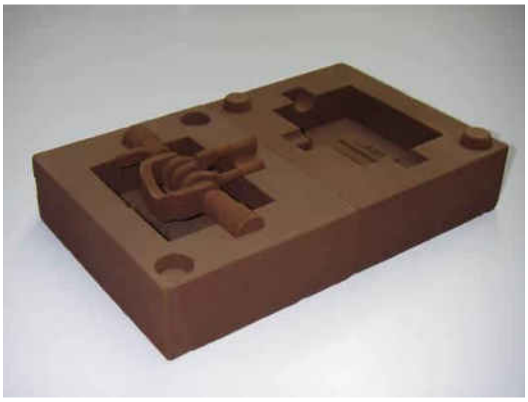


Fig. 4. Sand form and core made with Selective Laser Sintering

In both ways a relatively large series of cores and shapes can be obtained fairlyquickly and inexpensively, which is especially important in the production of prototype products. The moulds formed in this way are then used in exactly the same way as conventional ones, on moulding machines` manufactured moulds.

Manufacturing a valve for a known client is a fairly common process that has "inked" additive technologies. The usual procedure in these cases starts with reconciling the documentation between the buyer and the manufacturer, and then proceeds to produce some prototype products that the buyer tests, and orders the first batch of products if they meet his requirements. The problem is some prototype pieces that usually need to be made according to the casting process described above with the production of all casting tools. Price and time of manufacture of prototype products are, therefore, very large, and usually go at the expense of the manufacturer. Prototype pieces can be produced with the proper fast manufacturing process, and, in the case of small batches, the entire series of valves can be manufactured at relatively low cost and in a short time. In this case, each valve may have some specific design characteristics, but this does not affect the price or time of manufacture.
In addition to all the advantages of Rapid Manufacturing in the field of Hydraulic Components` Manufacturing, all other possibilities offered by Rapid Prototyping and products are not negligible. Rapid production of products in Hydraulics is also useful in the Marketing field, when the design and construction of a component is made, but it cannot be produced in a short time. In such a case, the addition of a non-functional physical model of the valve can be created quickly with the addition technology processes, which can then be presented to clients or used as an exhibit at a Trade show.

3. Compressor air consumption and RM technology

Also, in the field of Pneumatics, these technologies are very useful in the production of pneumatic components. As an example of the use of layered technology in the field of Pneumatics, two unconventional solutions will be presented which relate to savings in the consumption of compressed air.
Approximately 70 % of all manufacturers are using compressed air systems. These systems can power a variety of equipment, or can be used for cleaning, drying or cooling diverse products, using diverse blow-guns or blast nozzles. A significant reduction in compressed air consumption can be achieved by using energy-saving nozzles characterised by a very complex geometry that is based on CFD geometry optimization. However, such complex geometries cannot be produced by conventional manufacturing processes. The solution is to use RM technology.
Usability of RM technology will be shown on an example of an energy-saving blow off nozzle, which was produced with use of the Rapid Manufacturing process. Upgrading this approach represents the energy-saving cooling unit of plastic products with a much more complex geometry.

The designed nozzle-system was used for cooling purposes in plastic canister manufacturing. The previously used conventional cooling system presented the largest share of compressed air consumption in the company. The newly designed air-efficient cooling system, with increased capacity of the cooling air, allows enormous energy savings of compressed air – up to 50 %.

3.1 Energy-saving blow-nozzle

The most commonly used "pneumatic component" is the simple blow-nozzle. This small component is an integral part of any blow-gun, which is, without a doubt, one of the major consumers of compressed air. In order to achieve the highest efficiency of such a nozzle (minimum quantity of air at the inlet and maximum at the outlet), the inside of the nozzle must be designed appropriately to optimise the air-flow amplification principle, which allows air to accelerate, entraining the free surrounding air as it exits. Thus, on the basis of known physical processes, the nozzle-system is designed and optimised based on CFD simulation, and then produces using RP/RM (Rapid Prototyping / Manufacturing) manufacturing technology.
Energy-saving nozzles work on the “Venturi nozzles” principle with side inlets. The operating principle is based on the Bernoulli and Continuity equation. By reducing the cross-section, the speed increases, and if the speed is increased, the pressure is reduced all the way to the vacuum, so that the surrounding air is sucked through the side openings. We do not need to compress this additional air that is sucked from the ambient area. This means we are actually blowing more air out of the gun than we are providing to the gun – Figure 5. Example Type A shows the air consumption of a conventional blow-gun with classical nozzles, example Type B shows air consumption by using an energy-saving nozzle. Savings in compressed air consumption are approximately 40 %, in some cases, even more.

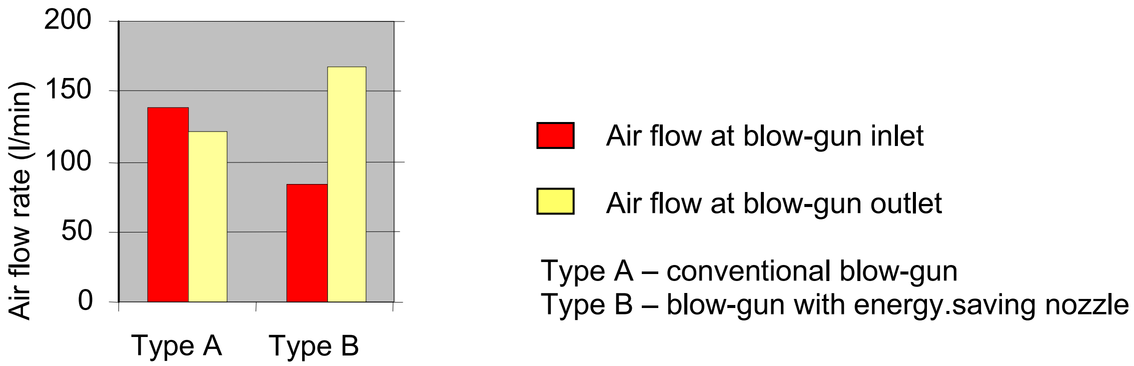

Fig. 5. Air consumption of different blow-guns types at an operating pressure of 4.5 bar

To achieve maximal efficiency of such a nozzle (the smallest amount of air entering and maximal leaving) the inside of the nozzle must be designed appropriately: Flow conditions must be optimised to ensure maximal suction effect. The optimal nozzle geometry, in terms of most effectively sucking the surrounding air, was designed based on a corresponding mathematical model and numerical simulations of air flow through the nozzle. Simulation was carried out in the program package ANSYS Workbench, based on the Finite Volume Method (FVM).
The mathematical background for a more complex two-phase homogeneous model is based on the current use of the following laws and equations:
- Mass continuity equation. The continuity equation results from the fundamental physical principle that mass is conserved.
- Momentum equation. The resulting force on the volume element is equal to the time increment of the momentum in the volume and the flux across the element surface.
- Conservation of turbulent kinetic energy and turbulent kinetic energy dissipation. The two-equation model for the turbulent kinetic energy k and the dissipation of turbulent kinetic energy ε

or the *k*-ε model, is the most important two-equation turbulent model that is based on the turbulent viscosity principle.

More details of the equations can be found in the literature, for example [2] [3]. The equations represent the basis for carrying out numerical simulation of fluid flow. Numerical simulations in Computer Fluid Dynamics are divided into four phases: Design and meshing of the geometry – modelling the physics` phenomenon – numerical equation solving – processing of results.
The result of this approach is the optimal internal nozzle geometry, which enables extremely efficient use of compressed air. The internal geometry of the nozzle was optimised based on the simulations, and it is shown in Figure 6.

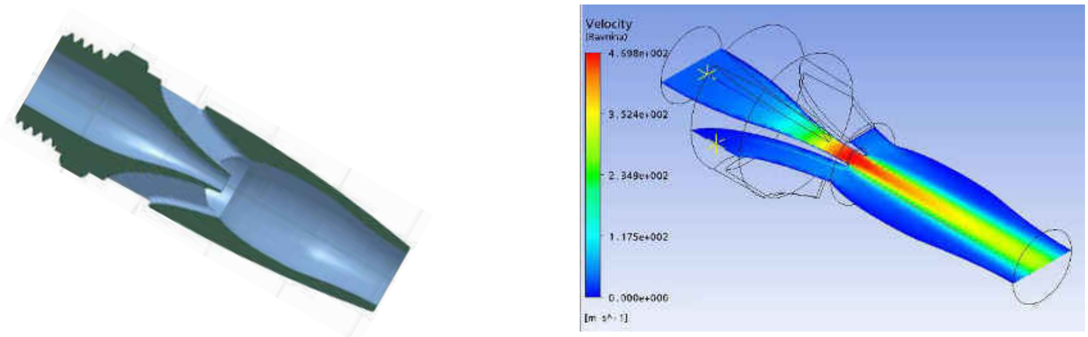

Fig. 6. Computer-based optimised nozzle geometry (left) and simulation result (right)

The external shape and internal geometry of the nozzle are, thus, determined. The problem that remained was the construction of such forms. It is usually where things come to standstill, as complex forms require the use of complex and expensive manufacturing procedures. But, if not, and we use simpler forms and construction, and, thus, lower the costs, the effect of nozzles is not optimal. Combine two good things: To maintain the complex geometry of the nozzles with low cost manufacture is possible using the Rapid Manufacturing technology.
For experimental verification of its effectiveness, the energy-saving nozzle was produced by the Rapid Prototyping method with SLS technology (Selective Laser Sintering). The material PA2200 with 30 micrometres` granulation was used, while the high power laser (CO_2 laser) sticks together fine particles of plastic, metal or ceramic powder into layers, that finally form a 3D object. The final product made from this material has sufficient strength, is thermally stable and has low weight. The effectiveness of the energy-saving nozzle is shown in Figure 6 – blow nozzle Type B.

3.2 Energy saving cooling block

Compressed air is also used on the plastic blow moulding machine. Blow moulding, also known as blow forming, is a manufacturing process by which hollow plastic parts are formed. In general, there are three main types of blow moulding: Injection blow moulding, stretch blow moulding and extrusion blow moulding. The blow moulding process begins with melting down the plastic and forming it into a parison or preform.
After the extrusion processes it is only necessary to remove the residues from the bottom of the plastic canister, or residue from the throat, and, in the case of canisters, the plastic rests under and above the handle. The cooling process is performed using compressed air via a simple cooling block with multiple nozzles, as shown in Figure 7. The cooling process causes a large consumption of compressor air – the cooling phase lasts cca 15 s, by consumption of compressed air in the amount of 48 m^3/h. Figure 7 shows the appearance of a discuses plastic canister as the end-product, with areas of hot plastic above and below the handle, which must be removed, showed in the infra red spectrum (as seen using a thermal camera). The Figure also shows the existing cooling block.

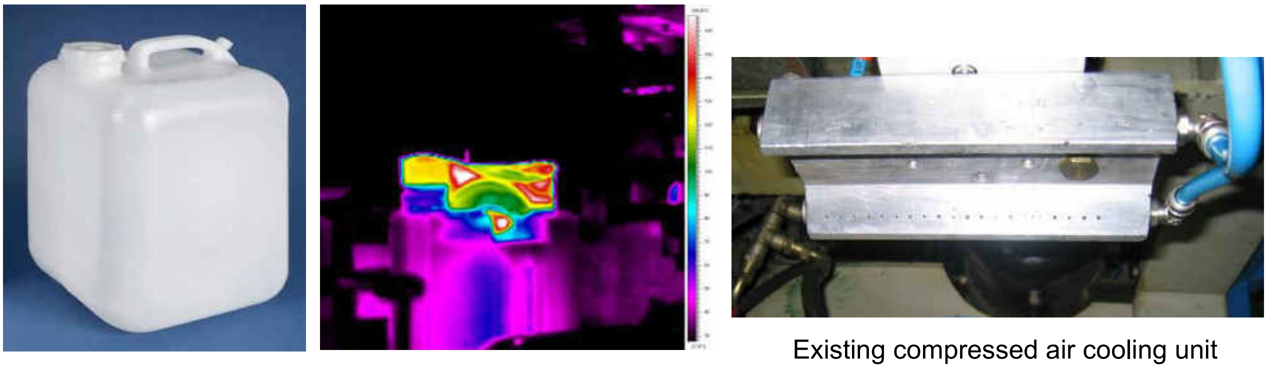

Existing compressed air cooling unit

Fig. 7. Plastic canister, areas of hot plastic during the cooling process and existing cooling unit; temperature scale: 28 °C to 166 °C

A similar approach was used, as in the case of the energy-saving nozzle, to design an energy-saving cooling-block. Compared with the relatively simple geometry of the nozzle, the geometry of the cooling block is definitely more complicated and complex. The base idea in block design was to place a series of nozzles into line, with a single outlet joint to a common outlet manifold. A cross-section of the geometry at the nozzle location is shown in Figure 8.

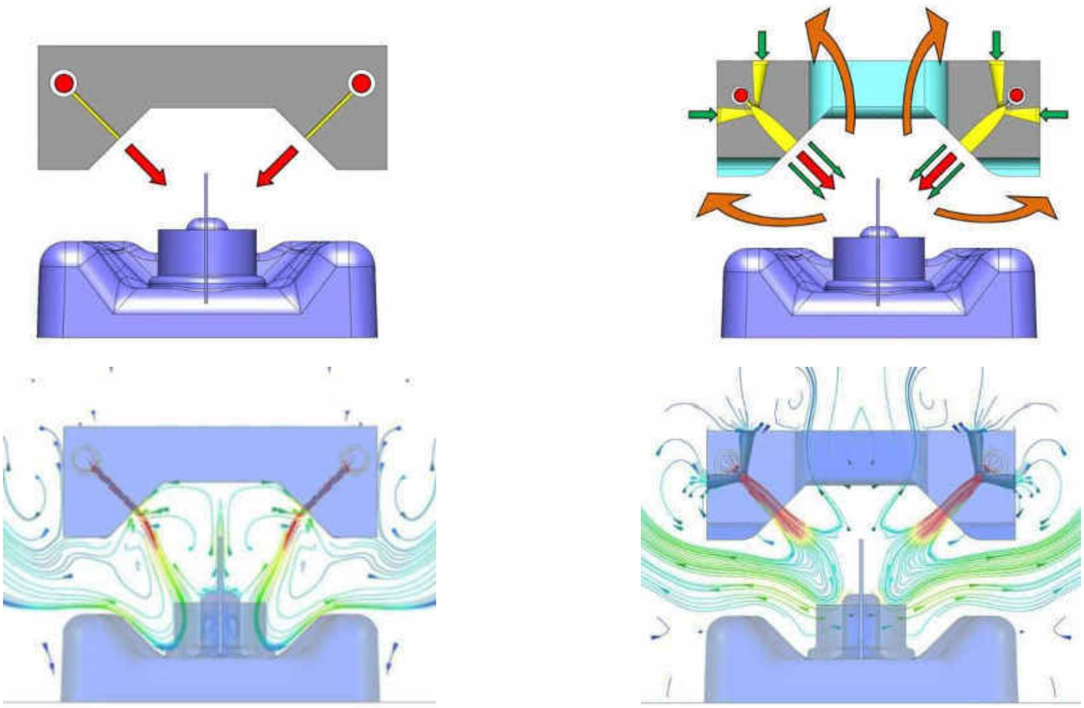

Fig. 8. Existing cooling block (left) and new optimised energy-saving design with additional openings to provide better warm air disposal (right) and, correspondingly, CFD flow stream lines

The results of air flow based on CFD simulations show 2D forward velocity streamlines starting from vertices on a cutting plane with a time limit of 0,01 s. A rainbow colour range is used, from blue 0.0 m/s to red 100 m/s. Air flow in the cooling phase is shown in Figure 8: Flow of fresh air from the cooling nozzles in place, sucking surrounding air through side inlets and disposal of warm air after cooling. Simulation results show 45 % increase of air mass flow at the outlet manifold compared to the existing block.
The existing cooling block, without optimization of nozzle geometry and without the possibility of sucking surrounding air, uses 48 m^3/h of compressed air, while the temperature of the cooled

material ranged between 134 °C and 135 °C. At higher temperatures, which may arise due to lack of cooling efficiency, e.g. due to lower input quantities of compressed air, the plastic is not cooled sufficiently and may lead to bad material cut – an unusable product.

The key factor of the product quality is, therefore, a sufficiently low temperature of the plastic before cutting surpluses, with minimum consumption of compressed air, whether it is fully provided from a pneumatic network, or the amount provided from the network is smaller and an additional quantity is sucked from the block`s surroundings. Temperature conditions at the given measured flow rates of compressed air at the inlet of the cooling-block are shown in Figure 9. In all cases, the temperature fields were recorded at the end stage of cooling, immediately before cutting waste material.

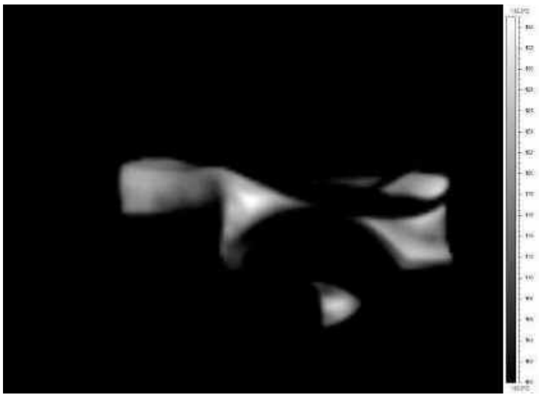

Existing cooling block; 48 m^3/h

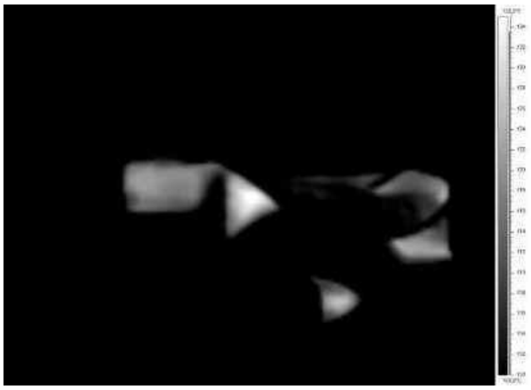

Energy-saving cooling block; 48 m^3/h

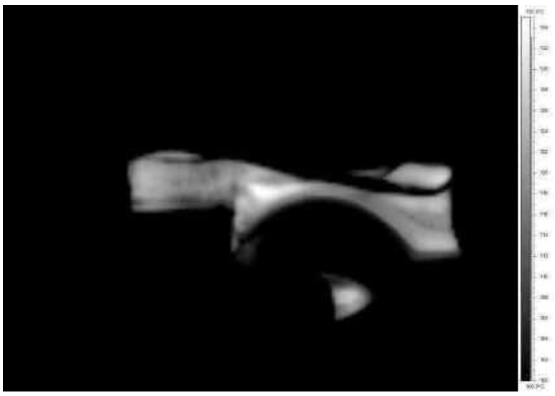

Existing cooling block; 25 m^3/h

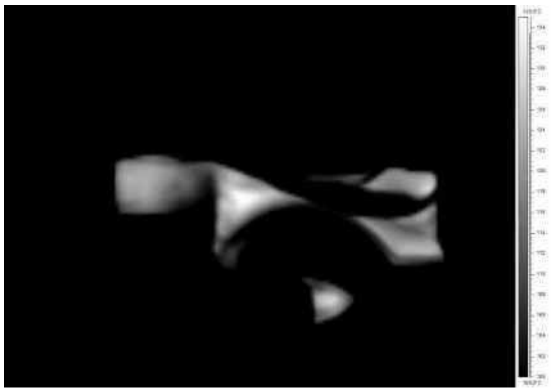

Energy-saving cooling block; 25 m^3/h

Fig. 9. Comparison of temperature fields of existing and new energy-saving cooling block (temperature scale: 100 °C to 140 °C)

From the comparison of thermal images of the temperature fields of waste materials, it is pretty clear that cooling with an energy-saving cooling block is much more effective than with the old one – Figure 9 above left and right.

In other words: A new cooling block allows equal effective cooling as the existing one with almost half of compressed air used – Figure 9, top left and bottom right. The remaining amount of air involved in the cooling was sucked “free” from the surroundings.

Despite the high performance achieved, there are many possibilities for further development of this system in the way of its higher efficiency, e.g. concentrated cooling at points with large amounts of material, cut-line aimed cooling instead of cooling the whole waste, production of light-weight unit in honeycomb-like design with possible significant material savings etc. The latter is only achievable through the use of layer technologies, with the faster and cost-effective RP/RM manufacturing process: Higher efficiency at lower product price.

Conclusions

Rapid Manufacturing processes are still believed to be expensive, and, in some environments, they may even be a fashion fly or an unnecessary toy. This paper demonstrates that this is not the case, and that additional procedures are indeed an important tool for shortening both development and standby times. The reason for their relatively modest use in certain environments can be found primarily in poor knowledge of these technologies, limited experience in conventional manufacturing technologies, and the use of relatively expensive machines.
Some high-speed devices are actually expensive and often overpriced. This is due partly to the demand-driven market, and partly to the fact that the processes are still very young and, therefore, underdeveloped, necessitating continued investment in development and a correspondingly high price of products. However, some processes (particularly SLS and SLA) have already reached some maturity, which is reflected in the falling equipment prices.
However, this is not a reason for the low use of add-on technologies, as more companies could join forces and invest in this technology together. They are completely superfluous to competitively coloured fears – on the contrary! With this kind of cooperation, companies can only gain from the exchange of experience and their involvement in new problems.
It could even be said that add-on technologies are not just a new technological process, they are leading to a small industrial revolution. With the development of Rapid Manufacturing, not only the course of action changes, because the idea and knowledge, instead of technology, are at the forefront, but completely new solutions are enabled.

References

[1] Drstvenšek, Igor, Darko Lovrec, Vito Tič, Anton Burjek, and Luka Jelovčan. “Implementation of rapid manufacturing techniques for fluid power products.” *Ventil* 14, no. 5 (2008).
[2] Lovrec, Darko, and Vito Tič. *Energy saving cooling-unit for plastic moulding machine*. Strojniški vestnik, ISSN 0039-2480, feb. 2011, vol. 57, no. 2, pp. 83-90, ilustr., doi: 10.5545/sv-jme.2010.082, 2011.
[3] Lovrec, Darko, and Vito Tič. “Reduction in air consumption when air-blowing using an energy-saving nozzle.” Efficiency through fluid power: workshop proceedings, 7th International Fluid Power Conference (7th IFK), 22-24 March 2010, Aachen, Germany; 7. Internationales Fluidtechnisches Kolloquium (7. IFK), Vol. 4, pp. 303-316, 2010.

ISSN 1454 - 8003
Proceedings of 2019 International Conference on Hydraulics and Pneumatics - HERVEX
November 13-15, Băile Govora, Romania

RADIO CONTROLLED HYDRAULIC PILLAR

Alexandru HRISTEA[1], Bogdan TUDOR[1], Ștefan-Mihai ȘEFU[1]

[1] INOE 2000- IHP, hristea.ihp@fluidas.ro

Abstract: *In today's modern world, the problem of protecting the associated spaces of some constructions of public interest is becoming more and more frequent. Mobile terminals protect the streets with limited access, sidewalks, parks or spaces around apartment blocks, or hotels.*
The device described above is in principle a cylindrical pillar mounted on the road, which must be able to be lowered and raised as needed.

Keywords*: Hydraulic pillar, remote control, public safety*

1. Introduction

In recent years, the necessity to protect public spaces such as squares, parks, streets with limited or prohibited access, paid parking, parking of certain institutions or private areas, etc. has emerged. Due to the considerable proliferation of cars, the authorities have taken measures to systematize the access spaces. The locking solution with movable pillars offers the advantage of a more elegant appearance and can provide a higher resistance to unauthorized penetration by an auto vehicle. It also allows the unrivaled passage of cyclists and pedestrians.

The areas where this device is used are the following:

- the automatic gates protect the halls and the courts of the institutions or private domains
- the automatic barriers allow access, usually, in the paid parking spaces for public use
- mobile terminals protect the streets with limited access, sidewalks, parks or spaces around apartment blocks or hotels.

Such a retractable pole has as an element of resistance, a movable cylinder, which slides vertically into a fixed one, reinforced in the roadway. The two cylinders are constructed of strong steel pipe, and can withstand an attempt to force the access. In some cases, even the use of a barrier and a mobile terminal is used in parallel, having the main role in preventing the forced access (Fig. 1).

To protect a larger area, several movable poles can be fitted (fig. 2). These poles are operated electro hydraulically, from an electrical panel or via a remote-control device. The vehicles unauthorized to access are blocked with the most discreet solution possible.

They can be lowered to the level of the road, to allow the access of the authorized vehicles, with the help of a remote control, in the possession of the driver, which can be operated on the road, near it. Also, from the remote control the pole can be raised in place, after passing the vehicle. These products are accepted by the road authority, as they are also visible at night, being marked with reflective elements, or with LED lights. These poles are operated electro hydraulically, from an electrical panel or via a remote control.

2. Construction of the hydraulic pillars

The following figures illustrate two situations of using the remote-control posts.

Fig. 1. Pillars to prevent the forced access to the barrier

Fig. 2. Covering a larger opening with more retractable posts

They can be lowered to the road level, to allow access of the authorized vehicles, with the help of a remote control, which can be operated inside the vehicle or near it. Also, from the remote control the pole can be raised in place, after the vehicle has pass. These products are accepted by the road authority, as they are also visible at night, being marked with reflective elements, or with LED lights.

Because they are mounted in concrete roadway, they become secure and robust, and cannot be pulled or broken by vehicles or by malicious persons. With installed power below 350 W, it has low power consumption, mobile poles are economical and easy to maintain.

From a constructive point of view, the pillar assembly is composed of three distinct parts:

- fixed outer shirt, which is inserted into a concrete pit, buried in the road surface;

- movable cylindrical pole, which is inserted into the fixed outer shirt;

Fig. 3. Commercial Hydraulic pillar made by Fardini

2.1 Hydraulic diagram

An example of a hydraulic drive diagram is as follows:

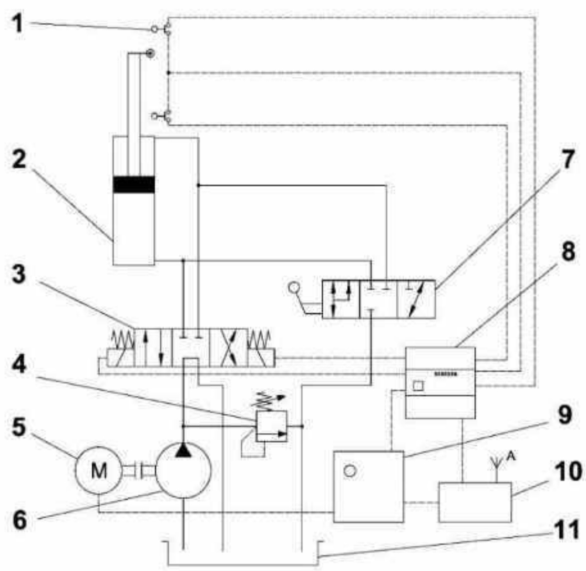

Fig. 4. Hydraulic scheme

1-Position limiter, 2-Hydraulic cylinder, 3- 4/3 hydraulic directional valve, 4-Pressure limiting valve, 5-Electric motor, 6-Gear pump, 7-Fault withdrawal valve, 8-PLC, 9-Electric box, 10-Radio remote control receiver, 11-Oil tank

2.2. The construction of the hydraulic pillar

The electro-hydraulic drive for pillar is a compact mechanism, with the following components, as in the example from fig. 5.

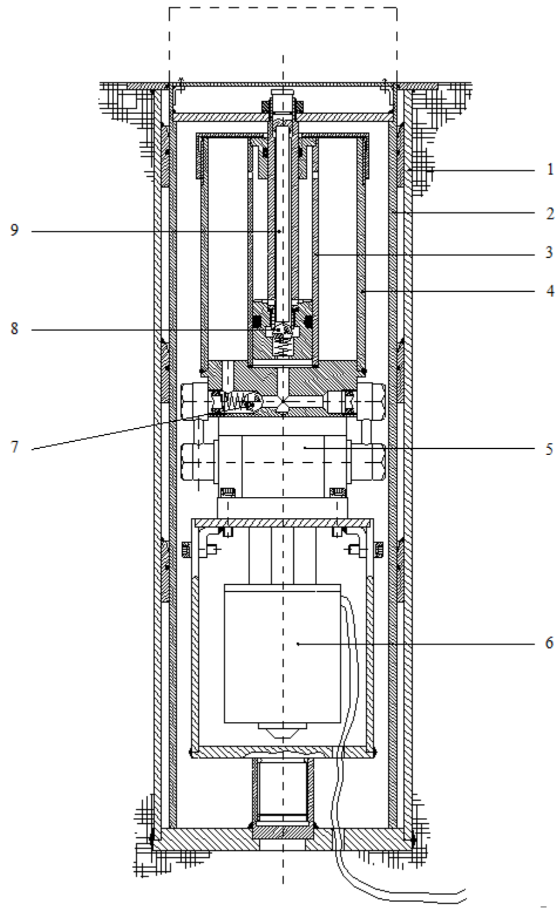

The numbers have the following meanings:
1- fixed cylindrical jacket, which is buried in the roadway surface,
2- movable cylindrical pipe with lid, which rises on a hight of 500 mm
3- hydraulic cylinder
4- sealed container
5- reversible, gear pump
6- electric motor
7- protection valve
8- relief valve
9- unlocking rod

Fig. 5. Constructive sketch of the electro hydraulic pillar

3. Functional performance

Its technical characteristics are:

Electric motor	Hydraulic Electro-pump	Hydraulic power	Performances
• Power: 0,25 kW • Supply voltage: 230 V • Frequency: 50 Hz • Current absorbed: 1,8 A • RPM: 2800 r.p.m. • Intermittent service: S3	• Hydraulic pump: P10 • Pomp flow: 4,45 l/min • Nominal pressure: 20 bar • Maximal Pressure: 40 bar • Work temperature: - 20 ÷ 80 °C • Oil type: A 15 Agip • Weight: 10 kg • Standard protection: IP54	• Piston diameter: 30 mm • Rode diameter: 16 mm • Stroke time: 4 sec • Pretensioner: 15 daN • Piston stroke: 500 mm	• Service operation: 6s raise - 30s stationary - 6s – lower - 30s stationary • Complete weight: 86 kg • Protection class: IP57

Mobile locking systems can be equipped with the following safety accessories:
- Pair of Photocells for safety
- Flashing lamp
- Detector for police or ambulance sirens for automatic lowering of the pole.

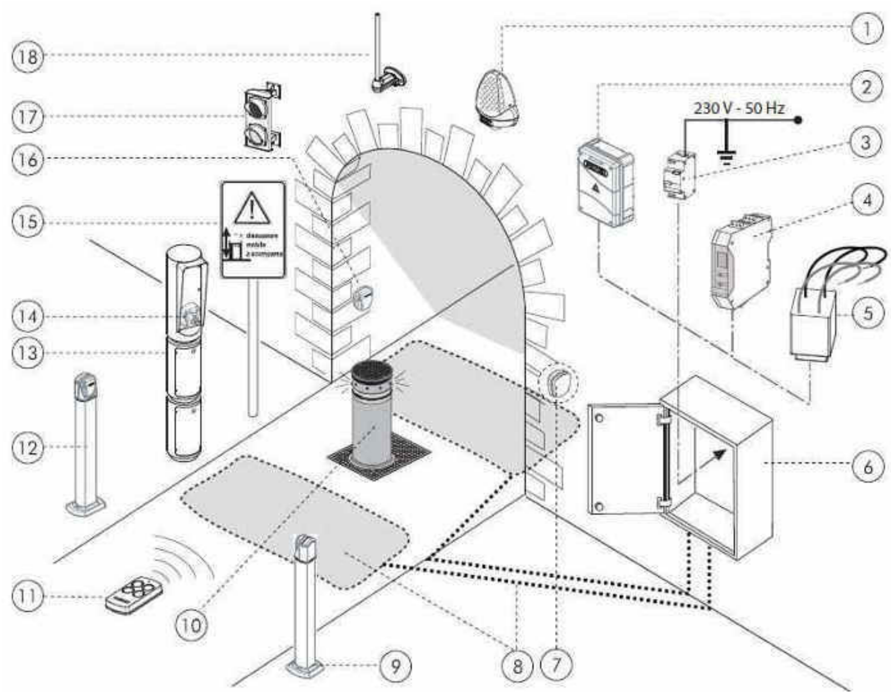

Fig. 6. Optional Accessories that can be equipped [7]

1 –LED flashing lamp
2 – Electronic controller with radio receiver
3 – Electrical safety relay
4 – Two channels for detecting mass metal
5 – voltage stabilizer
6 –Anti vandalism metal box
7 – Photocell receiver
8 – Pre-assembled loop with power cord
9 – Pole with light barrier transmitter
10 – Pole with hydraulic drive
11 – Remote controlled
12 – Pillar with photocell receiver
13 – Pillar with control
14 – Key switch
15 – Warning indicator for post existence
16 – Photo barrier emitter
17 – Traffic light
18 – Antenna for remote control receiver

The pillar is equipped with a remote control system. The remote control unit contains three buttons, namely:

- a button for rising the pole

- a stop button

- a button to lowering the pole

With a very small table and dimensions, it can be kept i pocket.

4. Conclusions

Most concerned about the pillars mobile remote-controlled areas are public administrations of the municipalities and the hotel industry.

The public administrations and the governmental institutions show an increased interest for the use of these protection systems, for the efficiency of the traffic in the areas of interest, for avoiding the blockages generated by the presence of the unauthorized vehicles or for securing some roads.

A growing demand for temporary access restriction systems are observed and privately-owned businesses. Thus, major shopping malls, supermarkets tend to acquire such systems. These systems are a modern and effective way of ensuring the flow of supply of these units, while traffic congestion that characterizes cities generally perimeters near the premises in particular.

References

[1] Sfarlea, I., L. Marcu, and D. Banyai. “Flow through command hydraulic resistance.” *Hidraulica Magazine* no. 3 (2015): 59-64.
[2] Rădoi, R., M. Blejan, I. Ilie, and A. Hristea. “Electro hydraulic installation for actuating the brush of a machine for washing PV panels.” Paper presented at TE-RE-RD 2015, Posada Vidraru – Romania, June 4-6, 2015, pp. 119-124.
[3] Radoi, R., A. Hristea, and A. Mirea. “Operational maintenance and testing of an electrically operated 3 stage directional servo-valve with on board electronics.” Proc. of 23rd Conf. CYLINDER 2015, Kliczków Castle, Poland, Sept 23-25, 2015, pp. 238-244.
4] Drumea, P., R. Rădoi, B. Tudor, and I. Bordeasu. “Digital hydraulics solutions.” Paper presented at HERVEX 2016 International Conference on Hydraulics and Pneumatics, Baile Govora, Romania, November 9-11, pp. 73-79.
[5] Drumea, P., R. Radoi, B. Tudor, A. Hristea, and I. Balan. “Normally closed switching valve for high frequency.” Paper presented at HERVEX 2016 International Conference on Hydraulics and Pneumatics, Baile Govora, Romania, November 9-11, pp. 92-97.
[6] Lepadatu, I., C. Chiriță, M. Blejan, L. Dumitrescu, and P.A. Chiriță. “Technology and computerized stand for proofing reversible hydrostatic pumps.” Paper presented at HERVEX 2016 International Conference on Hydraulics and Pneumatics, Baile Govora, Romania, November 9-11, pp. 248-255.
[7] http://www.fadini.net/prodotto.asp?language=ENG&id=36.
[8] http://www.securitybollardsdirect.co.uk/automatic-rising-bollards.html.
[9] http://www.quantum.com.eg/english/products/product.aspx?pid=28&cid=31&productid=22.

ISSN 1454 - 8003
Proceedings of 2019 International Conference on Hydraulics and Pneumatics - HERVEX
November 13-15, Băile Govora, Romania

MECHANICAL TESTING EQUIPMENT FOR PELLETS AND BRIQUETTES

Gheorghe ȘOVĂIALĂ[1], Gabriela MATACHE[1], Alina Iolanda POPESCU[1], Carmen NECULA[1]

[1] Hydraulics and Pneumatics Research Institute INOE 2000-IHP, sovaiala.ihp@fluidas.ro

Abstract: *The article analyzes and presents a methodology and equipment for mechanical testing of briquettes and pellets from biomass in general and from sawdust in particular. Most of the time the buyers of briquettes or pellets face the situation in which the transport does not take place on flat roads and as a result there is a destruction of the pellets or briquettes due to the mechanical shocks that appear. In order to eliminate these problems, the technology and the production equipment must ensure a physical stability of the product, which is why at the approval and periodically, mechanical tests must be carried out in accordance with ISO 17831 defining both the technology and the materials introduced. The article presents a solution of equipment made by the authors, which can be used by researchers and manufacturers and users of briquettes and pellets to verify the durability of these types of products.*

***Keywords**: Pelletizing, mechanical testing equipment, mechanical durability*

1. Introduction

In the last few decades, the use of biomass instead of fossil fuels has transformed from an interesting and possible solution into a necessity and more recently into an obligation of the countries, at European and global level. Biomass whether agricultural or forestry tends to be used more and more in the form of briquettes or pellets. It seems that both the manufacturing technology and the quality of the raw material and the final product are well established by international standards and norms. Since renewable energies are generally more expensive than conventional ones, the great advantages of the energy obtained from biomass must be emphasized. Only if we refer to the CO_2 balance and to the fact that the raw material is composed of vegetal residues, including forestry, and plants that produce energy of high yield, we realize the utility in perspective of this type of energy. The most interesting solution for the processing of biomass for its use in energy is its transformation into briquettes and pellets. The big differences between the two products are related to size, density and ash content, but also the possibilities of including them in automatic combustion equipment. The compaction methods have as a common element the pressing operation, through which the thickening of the particles of the primary material is produced, resulting in the increase of the density of the finished product (tablets, pellets, briquettes, etc.).

The pellets are produced by chopping sawdust, wood chips, splints, tree shells, fodder, etc. and pressing of the material obtained through a mould. The heat resulting from friction is sufficient for softening the lignin. By cooling, the lignin becomes rigid and binds the material. The pellets have a cylindrical or spherical shape with a diameter of less than 25 mm (usually 6 ... 8 mm). The briquettes are rectangular or cylindrical in shape and are obtained by pressing together the sawdust, chips, splints or tree shells in a piston or screw press. The energy content of pellets and briquettes is about 17 GJ / ton, with a moisture content of 10% and a density of about 600-700 kg / m3.

The main advantages of wood biomass densification are:

- Increased density of compressed material (from 80-150 kg / m^3 for straw or 200 kg / m^3 for wood sawdust up to 600-700 kg / m^3 for final products);
- Higher caloric power and a homogeneous structure of compressed products;
- A low moisture content (less than 10%).

The raw material used for the production of pellets and briquettes must meet certain physical characteristics, important during the densification process:

• Material fluidity and adhesive capacities (different additives, such as lubricants or binders, may be used to provide the respective characteristics);

Fig. 1. a- Pellets b- Briquettes

- Predetermined dimensions of the particles of the raw material (too thin a choppers can increase the cohesion properties, causing a reduced flow of the material);
- Material hardness (too much hardness of the particles creates difficulties during the densification process) [1].

2. Description of the biomass pelletizing process

The process of producing pellets involves subjecting the biomass to high pressures and forcing it to pass through the cylindrical holes of a mould. When exposed to appropriate conditions, the biomass "fuses" into a solid mass. This process is called extrusion.
The pellets are manufactured by pressing without binders the wood waste or from the secondary agricultural production (straw, sunflower strains, soybean and rape, stalk and corn cobs, cereal residues, ropes of vine, branches resulting from maintenance work from orchards, leaves, seeds and peels of seeds from the food industry).
The material subjected to the pelletizing process must meet two essential conditions: the size of the pellets between 30-50 mm and the maximum humidity 15%. In this regard, a pellet manufacturing line will include equipment for drying the raw material, chopping and pelletizing.

2.1 Equipment for biomass pelletizing

The most important equipment for pelletizing biomass are presses, with active moulding organs and pressing rollers. There are several constructive variants of the pelletizing equipment, in fig. 2 a, b, are presented those: with annular mould and press rolls, respectively with flat mould and press rolls. For each of the mentioned variants, the pressing moulds / rollers can be rotary or fixed [2].
The usual system for making pellets is the extrusion of the chopped material through a mould provided with a series of holes.
In general, pellet presses are the main equipment in a pellet production line. The technical characteristics of a pellet press greatly influence the quality and productivity. These characteristics are generally the size of the mould, the speed of the mould and the distance between the working elements. The material, with the help of rollers, is pressed through the mould, thus forming the pellets. On the outside of the mould a knife cuts the pellets to the desired length. After extrusion the pellets reach the temperature of 90-100°C and are transported to the refrigerator, where their temperature drops to 25°C. It fixes lignin and strengthens the product, helping to maintain its quality in storage and transport. Finally, they are sieved so that the residual debris is separated and reused in the process. Dust-free pellets are ready for storage, transported to packing equipment and stored.

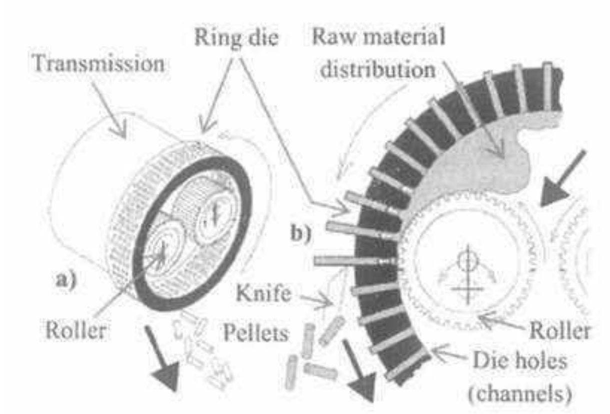

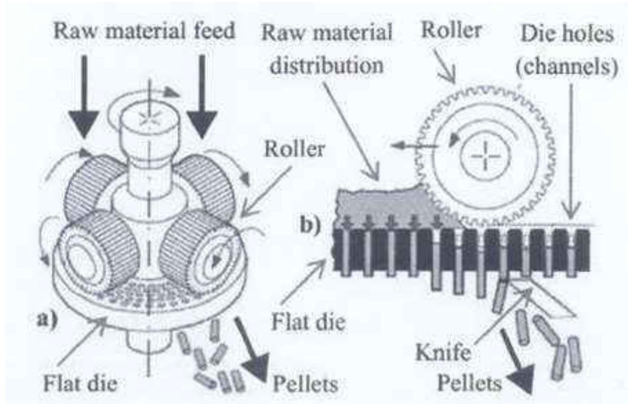

Fig. 2. a Pelletizing chamber with rotating annular mould and fixed press rollers [3]   b. Pelletizing chamber with fixed flat mould and rotary press rollers [3]

A pelletizing equipment, fig. 2 is composed of:
- helical feed system with dosing role of the compaction material;
- funnel for directing the compaction material;
- pellet press;
- drive gear motor;
- control cabinet.

The most common devices used for pelletizing are those with mould and one or more pressing rollers. These are available in two constructive variants:
- with fixed mould and movable rollers
- with rotary mould and fixed rollers (with rotation movement only around its own axis).

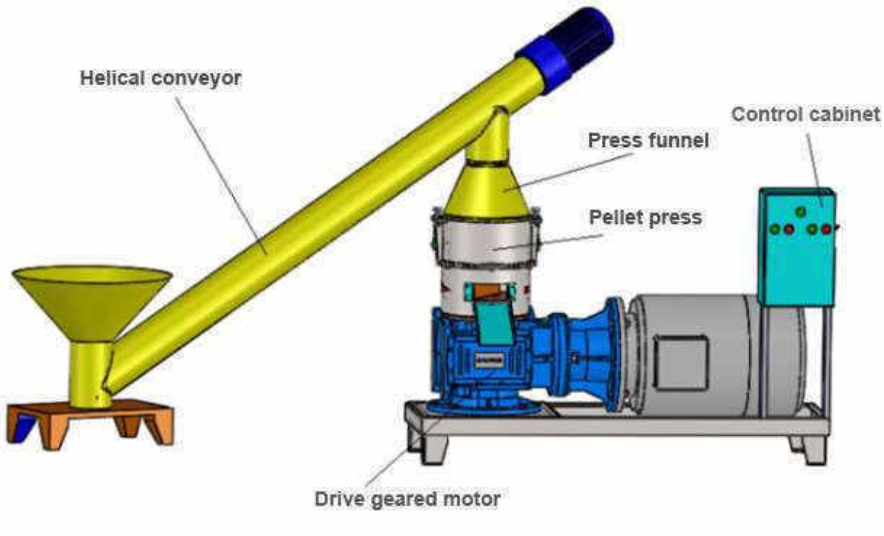

Fig. 3. Pellet press with feed and dosing with helical conveyor

2.2. Determination of the technical-functional parameters of pelletizing presses

On the stands destined for the experimentation of the active parts of the pelletizing presses made worldwide, for each type of biomass 4 parameters are monitored:
- the force required to extrude the biomass in the mould with a single hole, respectively with multiple holes;

- static and dynamic friction forces generated at the contact between the active piece of the press (die or press roller, depending on the constructive variant) with the material of high density and small thickness formed between them in the extrusion process;
- the compressive strength of the pellets obtained;
- pellet density.

In fig. 4 is presented the multifunctional test stand made at Danish Technological Institute in Denmark, with which it is followed the variation of the parameters of compressive strength and extruded material density along the extrusion hole (diagram in fig. 5), respectively the mechanical resistance of the pellets under the action of a compressive force, fig.6, fig. 7. [4]

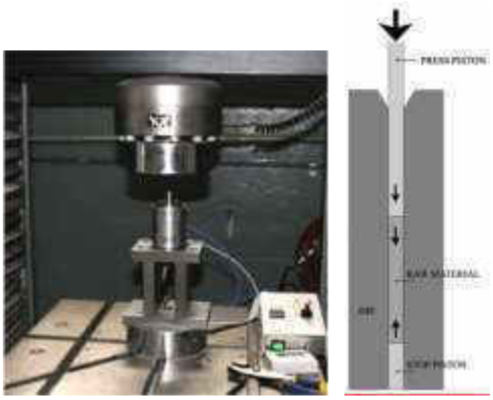

Fig. 4. Stand for determining the extrusion force (single hole mould) [4]

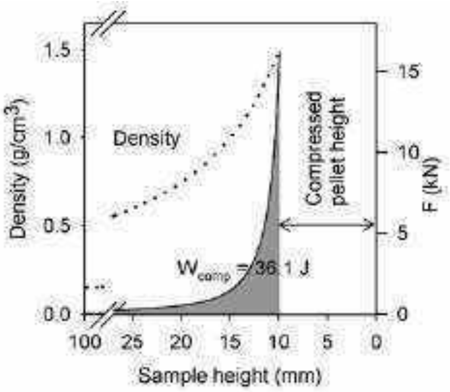

Fig. 5. Variation of the compressive strength and density of the pellets along the extrusion hole [4]

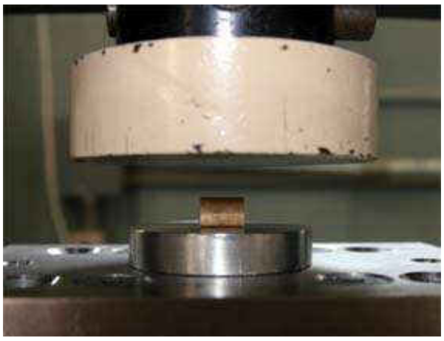

Fig. 6. Stand for determining the mechanical strength of the pellets when applying a compressive force [4]

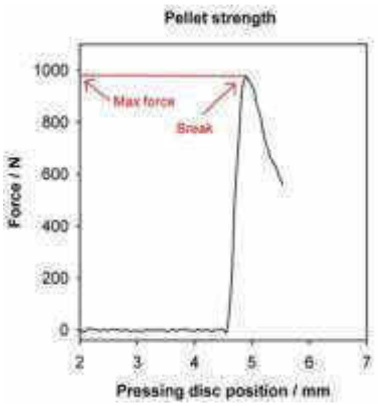

Fig. 7. Determining the quality of the pellets by compression [4]

The density of the pellets is determined by measurements (length, diameter and weight) and application of the known calculation formula [2].

3. Testing of briquettes and pellets

The testing of briquettes and / or pellets is done in the introduction phase, in the manufacturing reception phase and in the use phase of the products. It is possible that some tests and verifications may be carried out in one or more phases, the verification method and equipment being the same or different.

A stand was created to determine the extrusion force of pellets. Considering the above considerations, it was considered necessary to perform it in order to perform the extrusion force determinations for several types of biomass.
The overall drawing of the device for determining the pellet extrusion forces is shown in Fig. 8.

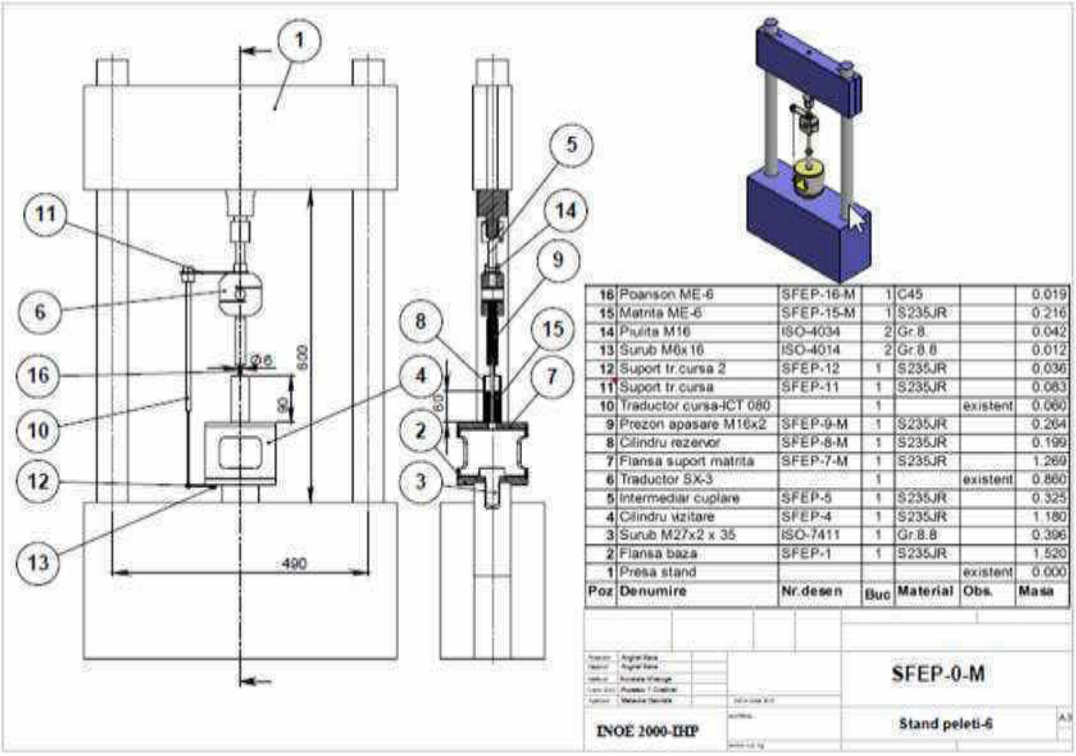

Fig. 8. Overall drawing of the device for determining pellet extrusion forces

The stand made by IHP, fig. 9, fig. 10, is composed of a rigid resistance frame, integral with the linear of the hydraulic drive cylinder 5, a cross that can be moved on two columns and fixed in the desired working position, a pressing device 3, in solidarity with the rod of the hydraulic cylinder. The force transducer 1 and the piston for pressing the extruded material into the mould are mounted on the cross member.
The hole in the mould and the pressing piston are perfectly coaxial, so as to avoid the occurrence of moments generated by the eventual release.
The pressing of the material is done by moving the pressing device vertically towards the pressing piston.
Between the pressing device (mobile) and the cross member, which by fixing with screws on columns, closes in the upper part of the test enclosure 4, a resistive displacement transducer 2 is mounted.
The hydraulic power supply of the drive cylinder is made from a hydraulic unit, consisting of an oil tank, electric pump 12, return filter 11, safety valve 10. The pressure gauge 9, mounted on the discharge circuit of the pumping group indicates the pressure value hydraulic oil when entering the working fluid distribution apparatus. Servovalve 8 allows very precise control of the value of the flow / pressure working parameters for the execution element (hydraulic cylinder), by the size of the electrical control signal; by their values, the flow rates and pressures regulated by the servo valve determine the values of the speeds and forces of the cylinder rod, imposed by the experiments performed on the stand.
The pressure transducer 6, mounted on the feed circuit of the piston chamber of the hydraulic cylinder, provides information on the pressure value during the biomass compression process. Hydro-pneumatic accumulators 7, have the role of attenuating the pulsations and maintaining at

constant value the pressure in the rod / piston chambers of the hydraulic cylinder during the working sequences compressing extruded material in the mould / piston retraction. The compressive strength of the biomass in the extrusion process is determined on a single hole mould with a diameter of 6 mm and a depth of 60 mm.
The data that are the subject of the experiments are acquired with the help of a data acquisition system.
Fig. 10 shows the block diagram of the stand for determining the extrusion force of pellets.

Fig. 9. Physical realization of the research stand

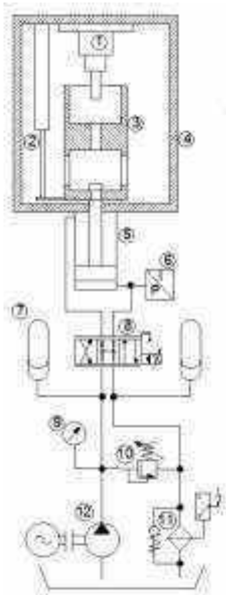

Fig. 10. Pellet stand hydraulic diagram1-strong translator; 2-position translator; 3-pressing device; 4-metal frame; 5-hydraulic cylinder; 6-pressure transducer; 7-hydropneumatic battery; 8 servovalve; 9-gauge; 10-safety valve; 11-return filter; 12 electropump

4. Conclusions

Research on the integration of mechatronic components and systems in biomass compaction equipment for the purpose of extending compaction applications to various types of biomass from agricultural or forestry is of great interest for pellet and briquette producers. Within the INOE 2000-IHP institute, the researches in this direction aim to establish the parameters (mainly the compaction pressure, temperature, humidity of the material, working speed, shape and dimensions of the final product depending on the material, etc.). Providing sensors and transducers for these sizes will allow a machine to expand its range of use, by adapting the working parameters to the material to be compacted. The adjustment of the working pressure and the feed rate of the material in the area of the briquette / pellet formation will be done by the variation of the hydraulic pressure and flow parameters, in the case of the machines with main hydraulic drive.

Acknowledgments

This paper has been developed in INOE 2000-IHP, supported by a grant of the Romanian Ministry of Research and Innovation, under the National Research Programme NUCLEU, project title: ‘Research in optoelectronics and related fields regarding the creation and dissemination of new knowledge, technologies, infrastructures for promoting "open science"’ and contributions to addressing global challenges’, Phase 11: ‘Experimental research for increasing the efficiency of conversion of energy from biomass by advanced compacting with mechanical-hydraulic equipment’, Financial agreement no. 18N/08.02.2019, Add. no. 2/2019, Research theme no. 1.

References

[1]. Study under Nucleu 2019; 'Research in optoelectronics and related fields regarding the creation and dissemination of new knowledge, technologies, infrastructures for promoting "open science"' and contributions to addressing global challenges', Phase 11: 'Experimental research for increasing the efficiency of conversion of energy from biomass by advanced compacting with mechanical-hydraulic equipment', Financial agreement no. 18N/08.02.2019, Add. no. 2/2019, Research theme no. 1.
[2]. Scientific-technical report under Nucleu 2019; 'Research in optoelectronics and related fields regarding the creation and dissemination of new knowledge, technologies, infrastructures for promoting "open science"' and contributions to addressing global challenges', Phase 11: 'Experimental research for increasing the efficiency of conversion of energy from biomass by advanced compacting with mechanical-hydraulic equipment', Financial agreement no. 18N/08.02.2019, Add. no. 2/2019, Research theme no. 1.
[3] Pencic, Marko, Maja Cavic, and Miodrag Zlocolica. "Analysis of the conceptual solutions of biomass pellet mill." The 9th International Symposium KOD 2016, Balatonfured, Hungary, June 9-12, 2016.
[4] Stelte, Wolfgang, Jonas Dahl, Niels Peter K. Nielsen, and Hans Ove Hansen. "Densification concepts for torrefied biomass." Torrefaction workshop. 20th European Biomass Conference and Exhibition, Milan, Italy, June 18-22, 2012.
[5]. Popescu, Alina Iolanda, and Carmen Necula. "Determination of the Calorific Power of Densified Solid Biofuels." *Hidraulica Magazine*, no.3 (September 2019): 68-75.
[6]. Marian, Grigore. *Solid biofuels - production and properties - Manual for the use of solid biofuel producers*. Chisinau, 2016.
[7] Matache, Gabriela, Gheorghe Sovaiala, Valentin Barbu, Adrian-Mihai Alexe, and Mariana Epure. "Hydraulic stand for research of the correlation between pellet quality, raw material quality and physical-mechanical parameters of manufacturing equipment." *Hidraulica Magazine*, no.4 (December 2018): 76-83.
♦ ISO 17828: Solid biofuels - Determination of bulk density.
♦ ISO 17829: Solid Biofuels - Determination of length and diameter of pellets.
♦ ISO 17831-1: Solid biofuels - Determination of mechanical durability of pellets and briquettes - Part 1: Pellets.
♦ ISO 18122: Solid biofuels - Determination of ash content.
♦ ISO 18125: Solid biofuels - Determination of calorific value.
♦ ISO 18134: Solid biofuels - Determination of moisture content.
♦ ISO 18846: Solid biofuels - Determination of fines content in quantities of pellets.
♦ ISO 9001: Quality Management Systems – Requirements.

ISSN 1454 - 8003
Proceedings of 2019 International Conference on Hydraulics and Pneumatics - HERVEX
November 13-15, Băile Govora, Romania

MARKET POTENTIAL OF UNCONVENTIONAL WIND TURBINES. A TECHNOLOGY REVIEW

Rareș-Andrei CHIHAIA[1], Sergiu NICOLAIE[1], Gabriela CÎRCIUMARU[1], Andreea EL-LEATHEY[1], Dumitru CONSTANTIN[1]

[1] National Institute for R&D in Electrical Engineering ICPE-CA Bucharest, office@icpe-ca.ro

Abstract: *The paper presents an in-depth analysis regarding the market potential of unconventional wind turbines from a technological perspective. The envisaged solutions were identified in literature and are currently in different development stages. The aim of the analysis is to estimate which types of wind turbines are suitable for further development and have the potential to replace someday the traditional vertical axis wind turbines with three blades that currently represent the best solution for onshore and offshore wind farms. The development of wind power conversion solutions is a current topic due to low carbon energy policies and presents several challenges. Essentially, it needs to be cost competitive compared with fossil fuels technologies and other renewable energy sources, especially photovoltaic (PV) power plants that recently gained ground due to a continuous reduction of manufacturing costs. Both the PV and wind turbines must have a complementary approach for a good energy mix. The technology of the wind turbines of today is continuously improved in order to increase their competitiveness on the market. Further developments are expected both for large capacity wind turbines and for low power concepts while the reliability over time will determine the best solution that will be adopted and maintained for years to come. Not all the solutions can have future development potential, but some results and approaches can be applied in the industry having a positive impact in terms of production cost and energy conversion efficiency.*

Keywords: *Wind power, emerging technology, counter rotating turbines, future development*

1. Introduction

The continuous development of wind power conversion systems has a significant impact on their use on large scale. Due to stringent measures, policies and regulations regarding the use of fossil fuels across the world, clean and renewable energy sources must be better harnessed. The purpose of this paper is to gather, organise and analyse wind turbine solutions currently in use or future emerging technologies in order to point out the advantages and disadvantages of each system and determine the current trend in research of wind power energy conversion. A large number of the solutions identified originate from academic work within universities and research institutes. Some of the technologies identified are being developed by university spinoffs or start-up companies [1].
The wind energy industry has gone through intensive technological advancement in terms of aerodynamic design, mechanical systems, electric generators, power electronic converters, integration to power systems and control theory.
From the electrical engineering perspective, the electric generators and power electronic converters are two major components in the operation of wind energy conversion systems (WECS). Since the beginning of grid-connected operation in 1980s, various combinations of electric generators and power electronic converters have been developed in commercial wind turbines to achieve fixed-speed, semi-variable-speed and full-variable-speed operation [2],[3].
The most common type of wind turbine used worldwide is the three-bladed upwind horizontal-axis wind turbine (HAWT), where the turbine rotor is placed in front of the nacelle, facing the wind upstream of its supporting tower. Another popular technology type is the vertical-axis wind turbine (VAWT), with blades extending upwards in a vertical position, strengthen by a frame consisting of two circular plates. Besides these two established solutions, many wind turbine designs are available in different stages of technological readiness level (TRL). The variety of designs reflects ongoing commercial, technological, and inventive interests in harvesting wind resources more efficiently.

Due to the fact that the Betz law cannot be exceeded, certain designs have been developed to maximize the energy conversion efficiency by raising the power coefficient as much as possible. In this category, we mention the diffuser-augmented wind turbine (DAWT) with a cone-shaped wind diffuser and counter rotating wind turbines, described in a separate chapter of the paper. Some unconventional designs have entered commercial use, while others have only been demonstrated through experimental models or by numerical simulations. Unconventional designs cover a wide range of innovations, including different rotor types, electric generators, blade types, rotational speed and movement principle.

2. Unconventional wind turbines
2.1. Airborne wind energy

Airborne wind energy (AWE) defines all the concepts that convert wind energy into electricity with the common feature of autonomous kites or unmanned aircraft, linked to the ground by one or more cables [4]. AWE systems offer several potential advantages over conventional wind turbines. They require less material than tower based turbines, have the potential to be manufactured at lower cost, can be deployed faster and can harness stronger and steadier winds by flying at higher altitudes. Several concepts presented in Fig.1 are currently being pursued and convergence towards the best architecture has not yet been achieved [1].

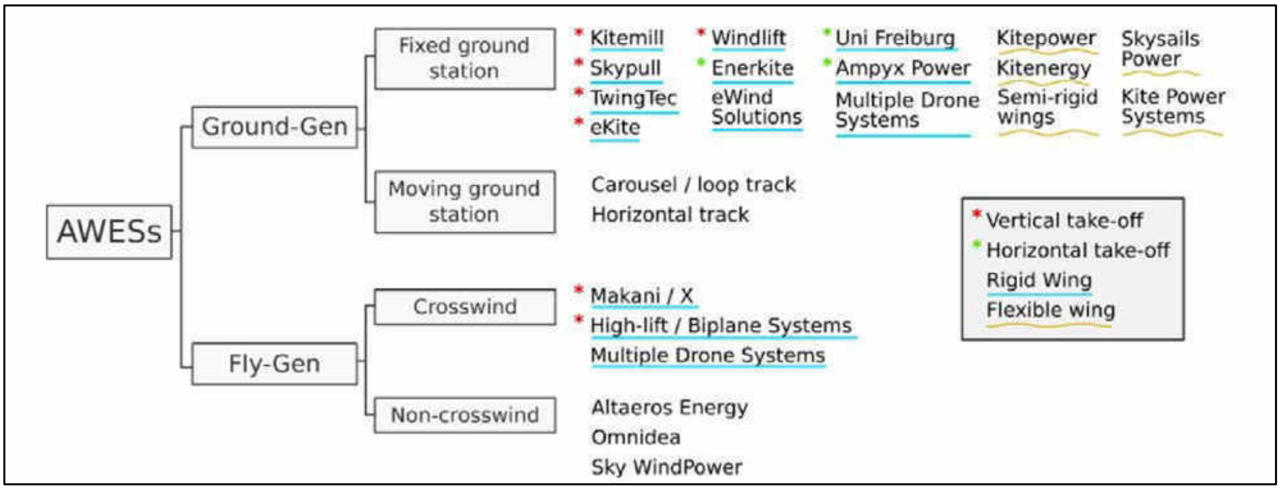

Fig. 1. Classification of AWE systems [1]

According to the above classification, the ground-gen concepts are based on the conversion of mechanical energy into electrical energy at ground level, while fly-gen concepts are based on the conversion in the air, on board the airborne unit. Most ground-gen concepts drive a drum-generator module in pumping cycles, alternating between traction and retraction phases to generate electricity. Fly-gen concepts use on board wind turbines with continuous electrical energy output and a conducting tether to deliver this energy at ground level. Of the fly-gen solutions, crosswind systems can generally produce more power (1-2 orders of magnitude higher) than non-crosswind systems [5]. The main advantages claimed by these concepts are low capital costs, due to the small amount of material used, a relatively simple construction, installation and a higher capacity factor, due to stronger and more consistent high-altitude winds prevalent above 200m altitude.
A potential reduction in weight could reduce the capital expenditure (CAPEX) of platforms and subsea structures; also the reduced size of the devices allows for rapid installation at a lower cost [1]. Important technical challenges of AWE systems are [6]:

- High complexity of the control system since the operation of AWE depends on a fast-feedback control algorithm based on the information gathered by sensors that must ensure precise actions that allows fully autonomous flight, reducing the crash risks.

- Early stage of development. The existing technology demonstrators still rely on supervised operation, especially in the take-off and landing phases. Certain technologies currently developed, can achieve up to 24 h of autonomous flight.

- Limited knowledge. For this type of systems is difficult to predict the economic potential and environmental benefits of AWE based only on the results obtained during supervised flight. For the moment, it is not certain that after full development, the technology will provide the promised energy conversion performance. Therefore, the impact and feasibility of scaling up such systems has not been rigorously assessed so far. The Makani kite system is presented in Fig. 2a. Makani is developing energy kites that use a wing tethered to a ground station to efficiently harness energy from the wind, generating electricity at utility-scale. As the kite flies autonomously in loops, rotors on the wing spin as the wind moves through them, generating electricity that is sent down the tether to the grid. In Fig. 2b, the Kite Power Systems (KPS) technology is presented. While the Makani system is based on an aircraft with rotors for generating electricity, the KPS system uses kites that tension a 100-200m line to be spooled out from a drum on the ground, which is connected to a generator – thus creating electricity. The working principle is based on strong aerodynamic lifting forces which are produced by the wing of the kite, and exerted against its cable.

Fig. 2a. Makani energy kite [7]

Fig. 2b. Kite Power Systems (KPS)

There is a need for more research on wind potential at high altitudes and how the wind energy can be transformed using on flight sustainable energy systems. The concept is still in its early development stage and there are still several technical problems to address such as: the durability of materials, the complexity of the management system (take off, landing, in flight operation). Another aspect to take into consideration is the space restrictions (a restricted zone is necessary given the altitudes in which these devices would operate), regulation, social acceptance, safety and the risks due to lightning strikes and storms. Broken cables could send the aircraft on a randomly trajectory with the possibility of crashing in inhabited areas. Additional research and improvement is needed to perfect this concept until the commercial version becomes available.

2.2. Multi-rotor wind turbines

Such type of turbines implies the use of more than one rotor in a single and compact assembly. Thus, to improve efficiency and reduce overall loads on a wind turbine, it is possible to replace a large single rotor with a multiple-rotor system (MRS), as shown in Fig. 3. This solution allows a large power system (20MW or more) to be installed on a single pole by using few standardised rotors. Scaling up is seen as a key factor in overall cost reduction for this design. Possible advantage of the MRS is to avoid structural and material problems associated with the scaling up to a large device. In some cases, there is the possibility of yawing without the requirement for a dedicated mechanism. Overall design optimisation is interactive with aerodynamic, electrical, loading considerations and other factors. The main disadvantage for this design is represented by the higher cost because it involves the use of more components. Although the size for each turbine is reduced, the total price could be higher compared to a single turbine. The main advantage of this solution is the fact that there is already a commercial demonstrator of this technology as mentioned below in Fig.3 and there is potential for industrial funding of research to bring this technology to maturity, supported by public funding to tackle some of the more fundamental challenges associated with aero elastic design and control [1].

Fig. 3. Vestas multi-rotor wind turbine

Fig. 4. Turbine with tip rotors [1]

Another interesting approach for multiple rotor turbines is the wind turbine with tip rotors. This conceptual technology consists of wind turbines where the traditional gearbox and generator is substituted by a fast-rotating rotor/generator mounted on the tip of each blade (see Fig. 4). While conventional turbines extract power at a direct wind speed of around 10 m/s by conversion of torque, the tip-rotor converts power at around 70 m/s, being placed at the tip where the tangential speed is higher. The concept can be designed for both two- or three-bladed turbines [8]. The concept is more suitable to very large wind turbines, since larger turbines have fewer challenges related to the centrifugal forces on the rotors. This technology may be more appropriate for the offshore environment, given the additional noise and visual impact compared with conventional single rotor turbines. Regarding the degree of development of this technology, no prototype has yet been constructed or tested. The TRL of such a concept is thus 1–2 with a possible scalability of the same order of magnitude as for a conventional 10 MW offshore turbine. A slow TRL trend is anticipated since investors are reluctant to fund the technology due to its radical and high-risk nature. This form of technology is clearly at a very fundamental level of development with only very basic concepts elaborated. There is the need for detailed concept studies in order to assess the challenges and potential for this system before any industrially-led developments can be expected [1].

The counter rotating turbines are also a dual rotor type of wind turbine. Such systems are most promising, due to sufficient data available regarding their operation, energy conversion efficiency and reliability. This design and the research carried so far, will be detailed in a separate chapter.

2.3. Diffuser augmented wind turbines

A diffuser-augmented wind turbine (DAWT) is a wind turbine with an added cone-shaped wind diffuser used to increase the efficiency of converting wind power to electrical power.

The increased efficiency is possible due to the increased wind speeds that the diffuser can provide. In traditional bare turbines, the rotor blades are vertically mounted at the top of a support tower or shaft. In a DAWT, the rotor blades are mounted within the diffuser, which is then placed on the top of the support tower. Additional modifications can be made to the diffuser in order to further increase efficiency though the structure of the diffusers remains a challenge.

DAWT devices are at a semi-commercial level of development in Japan, with power ratings of the order of tens of kW. The most advanced projects have been developed by Kyushu University, who have studied several configurations, from single DAWT to multi rotor systems [9]. In addition, tests on floating platforms were performed in Hakata bay.

Multi-rotor DAWTs appear to display convincing performance with the typical challenges of MRS, enhanced by complex interactions with the diffusers.

Fig. 5. Different types of DAWT wind turbines

Another interesting solution is the INVELOX technology. The turbine works like a wind injection system. A large intake captures wind and funnels it to a concentrator that ends in a Venturi section and finally wind exits from a diffuser. The turbine is placed inside the Venturi section of the INVELOX. Inside the Venturi the dynamic pressure is high while the static pressure is low. The Turbine converts dynamic pressure or kinetic energy to mechanical rotation and thereby to electrical power using a generator [10]. Although this technology is not likely to be significantly cheaper than the non-ducted technology, it could be suitable for a niche-market. The TRL is around 5–6, with a scaling up target of 1 MW. The TRL evolution is expected to be average [1]. This type of technology will be more suitable for smaller scale applications and it is not expected that there will be major industrial investment in associated research in the near future.

2.4. Magnus effect turbine

One type of wind turbines that can harvest wind energy at lower wind speed is the horizontal-axis Magnus Wind turbines (MWT) [11]. The main difference is the replacement of airfoil-shaped blades with rotating cylinder blades, thus harvesting wind energy at low wind speed condition. Additionally, the performance of MWT can be increased by enhancing the surface of the rotating cylinder blades. There are several innovations for increasing the performance of MWT rotating cylinder blades such as using different shapes for dimple and fins to ensure the rotation. Figure 6 shows the MWT with spiral fins coiled around the rotating cylinder blades that has been developed in Japan.

Fig. 6. Magnus wind turbine with fin-like on rotating cylinder blades [11]

2.5. Vertical axis wind turbines

Darrieus's patent from 1927 covers practically any possible arrangement using vertical airfoils. One of the more common types is the H-rotor (fig. 7), also called the Giromill or H-bar design, in which the long curved blades of the common Darrieus design are replaced with straight vertical or twisted blade sections attached to the central tower with horizontal supports.

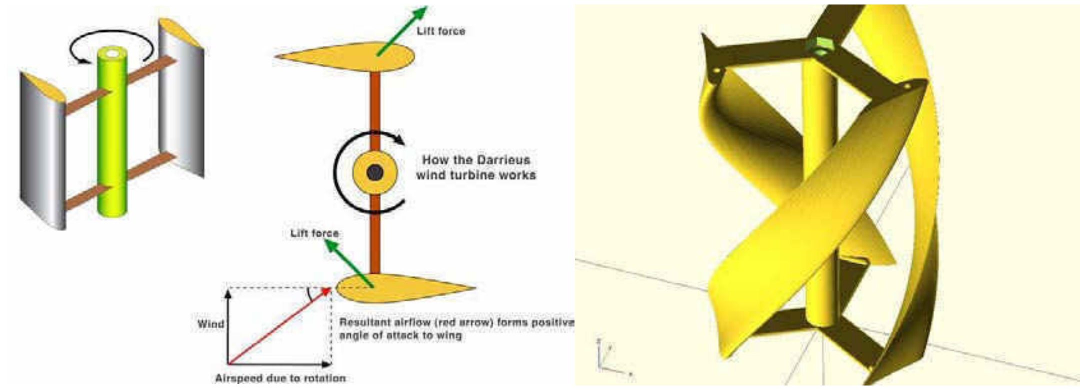

Fig.7. Darrieus vertical axis turbines variations [12]

Another variation of the Giromill is the Cycloturbine, in which each blade is mounted so that it can rotate around its own vertical axis. This allows the blades to be "pitched" so that they always have some angle of attack relative to the wind. The main advantage of this design is that the generated torque remains almost constant over a wide angle, so a Cycloturbine with three or four blades has a fairly constant torque. Over this range of angles, the torque itself is near the maximum possible, meaning that the system also generates more power. The Cycloturbine also has the advantage of being able to self-start, by pitching the "downwind moving" blade flat to the wind to generate drag and start the turbine spinning at a low speed. On the downside, the blade pitching mechanism is complex and generally heavy and some sort of wind-direction sensor needs to be added in order to pitch the blades according to the wind direction.

These types of wind-turbines are suitable for building roofs. Examples include Marthalen Landi-Silo in Switzerland, Council House 2 in Melbourne, Australia. Ridgeblade in the UK is a vertical wind turbine on its side mounted on the apex of a pitched roof. Another example installed in France is the Aeolta AeroCube. Discovery Tower is an office building in Houston, Texas, that incorporates 10 wind turbines. Rooftop wind turbines may suffer from turbulence, especially in cities, which reduces power output and accelerates turbine wear. Due to structural limitations of buildings, limited space in urban areas, and safety considerations, building turbines are usually small (with capacities in the low kilowatts). This technology can be used as an alternative for low power energy system and has many challenges when scaling up for large wind farms. The main disadvantage is the low starting torque. This can be improved using J-shaped straight-blades or incorporate a Savonius rotor to provide a quick start even at low wind speeds.

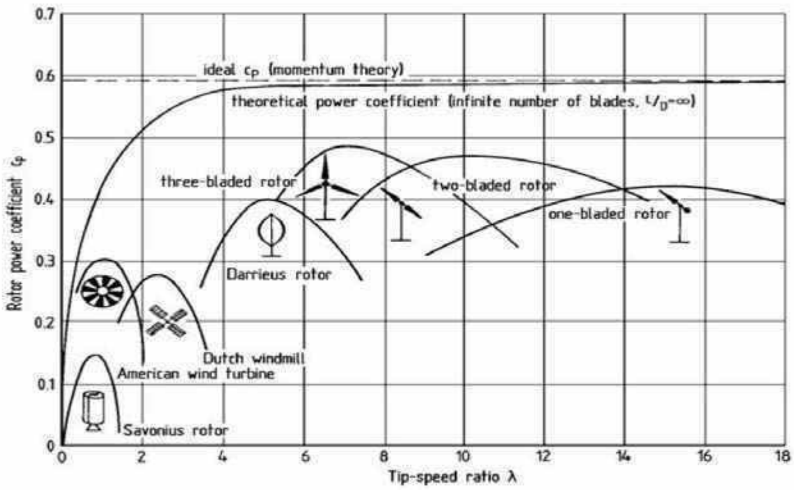

Fig. 8. Power coefficient for a wide range of wind turbines

Although over the years some improvements were made to increase the efficiency of vertical wind turbines, their power coefficient is still reduced compared to classical 3 blade horizontal axis, as shown in figure 8.

2.6. Bladeless wind turbines

Air flow-induced vibrations of mechanical systems can be exploited to extract energy, when specifically designed to experience large-amplitude oscillations. The mechanical system has to be combined to work with suitable energy-conversion apparatus, such as electromagnetic or piezoelectric transducers. This type of technology will not be used for large-scale generation, but for applications where a small amount of autonomous power is required, e.g. wireless sensors or structural health monitoring. These energy harvesting devices have possible applications in urban settings and for energy harvesting at small and micro-scales [1]. Flutter-based devices involve a rigid, streamlined model (a simple flat plate or aerofoil) of finite length, which is elastically suspended to oscillate along two degrees of freedom: heaving (cross-flow translation) and pitching (rotation). The energy extraction is activated in the heaving motion component, being less sensitive to a damping increment. Linear generators, typically solenoids, are used (see Fig. 9). Depending on the application, different governing parameters can be selected. The design configuration can be adapted to specific operating ranges of flow speed. [13], [14].

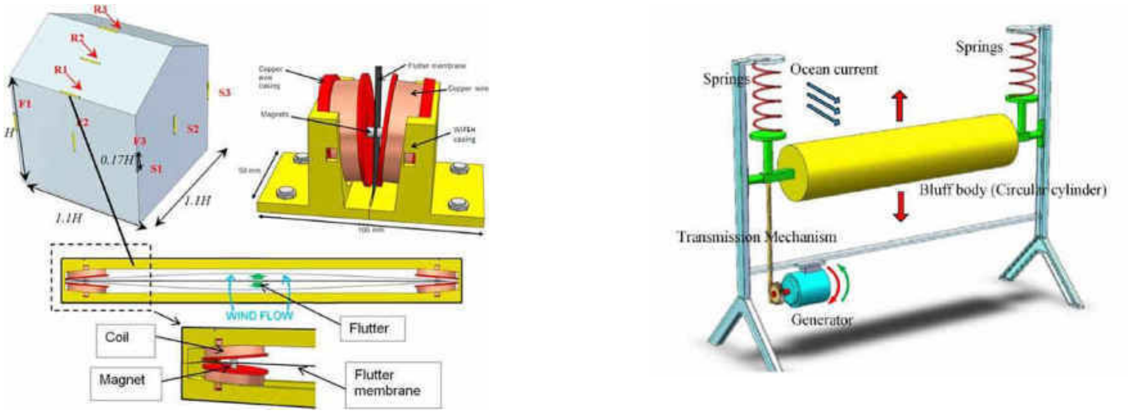

Fig. 9. Devices exploiting the induced vibration [13], [14]

Another new concept is the Saphonian turbine which implements a patented system called “Zero-Blade Technology” in order to harness the wind’s energy. This is said to involve channelling the wind then produce hydraulic pressure, which can be instantly converted to electricity via a hydraulic motor and a generator, or stored in a hydraulic accumulator (fig.10).

Fig. 10. Saphonian turbine

The Saphonian, invented by Anis Aouini, promises to offer an efficient, reliable and eco-friendly way to harness wind and generate Green Energy. The creators stated that Saphon Energy is in process of building its 1st industrial design Saphonian machine in partnership with Microsoft Corporation.

3. Analysis of the performance and development stage of counter rotating turbines

Counter-rotating wind turbines (CRWT) represent a system of two rotors which rotate in opposite directions. For horizontal axis wind turbines, the rotors are placed at a certain distance, either both in the front of the generator, or one in front and one in the rear of the generator. The performances of the counter-rotating wind turbines have been intensively approached recently. Some research is focused on numerical investigations of counter-rotating wind turbines, while others approach the study of CRWT both numerically and experimentally [15]. The investigated systems enclose different generators' concepts: one generator for each wind rotor [16], one electric generator coupled to the rotors using a differential planetary system [17] or a single permanent magnets generator, with mechanical coupling of the wind rotors [18]. Beside the other two solutions, the last one presents some advantages such as: decreasing the overall size of the electric generator, increasing the rotational speed, eliminating the mechanical power losses induced by the use of a gearbox.
Promising results were obtained by the research team of ICPE-CA [15] when testing a CRWT experimental model in a wind tunnel. The experimental model of 1 kW rated power shown in fig. 11 consists of:
- Up-wind rotor (Diameter D = 2.66 [m]): chord at the hub level cr0 = 0.1 [m]; chord at the blade's tip level cR = 0.1 [m]; the blade's torsion angle 0 [°] (the blade has no torsion);NACA 6409.
- Down-wind rotor, (Diameter D = 2.46 [m]): chord at the hub level cr0 = 0.15 [m]; chord at the blade's tip level cR = 0.044 [m]; the blade's torsion angle Δβ = 15 [°];EPPLER 664
- Electric generator with counter rotating armatures.

Fig. 11. Experimental model of the counter rotating wind turbine [15]

Fig.12. Prototype of the CRWT

The obtained results were centralized in table 1, as a comparative power output of the counter-rotating wind turbine vs. single rotor wind turbine. It can be seen that the contribution of the second rotor is significant compared to a single rotor turbine.

Table 1: Comparative power output of the counter-rotating wind turbine vs. single rotor wind turbine

Wind velocity [m/s]	*5,5*	*6,3*	*6,88*	*7,74*	*8,7*	*10*
P_{max} - Single rotor (up-wind rotor) [W]	98,12	148	192	275	388,84	591,13
P_{max} - Counter rotating turbine [W]	179,1	245	305	461,8	614,9	939,3

Detailed studies on the model revealed that the low power coefficient (Cp) of the first rotor (around 0,2) allows a better output for the second rotor. The experimental model was also tested in situ [19] in order to validate de experimental data. The results are presented in Fig.13.

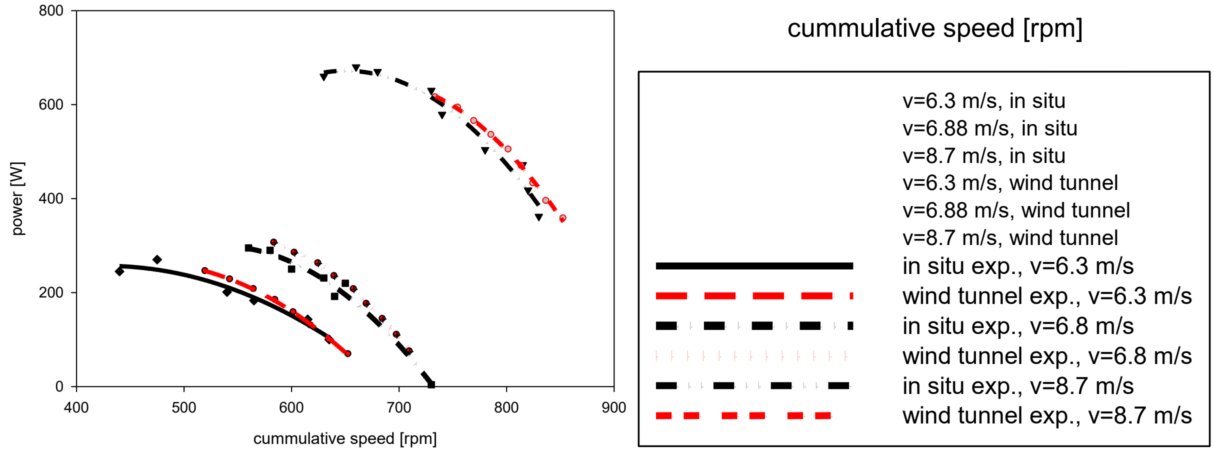

Fig. 13. Power curves at constant wind velocity – comparison between wind tunnel and in situ [19]

Analyzing the plots shown in Fig.13, it can be noticed that there is a good consistency between the two series of curves. Generally, the power characteristic obtained as a result of in situ testing is slightly lower than the one obtained in the wind tunnel. This might be explained by the numerous sudden changes in winds' velocity and direction. Encouraged by the results obtained on the experimental model, the research team from ICPE-CA developed a 10 KW prototype of the counter rotating wind turbine presented in fig.12. Currently, functional tests are being performed and specific parameters are registered for a good characterization of the wind turbine and for further analysis.

4. Conclusions

The wind turbines of today have constant developments in technology in order to increase their competitiveness on the market. Further developments are expected both for large capacity wind turbines and for low power concepts and the reliability over time will determine the best solution to be adopted and maintained for years to come.
From the multitude of the solution analysed in this paper, the counter rotating turbine is within reach and has the potential for developing to large scale installations since it can use the technology already validated in the case of classical three-bladed horizontal axis turbines. However, additional studies and testing are required to establish the technical reliability and also a cost/efficiency analysis is needed to attract investments for this type of wind turbines. Beside the presented solutions, many other wind energy conversion devices can be found in different development stages (simulation, experimental models, patents). Not all the solutions can have future development potential but some results and approaches can be applied in the industry having a positive impact in terms of production cost and energy conversion efficiency.

References

[1] Watson, Simon, Alberto Moro, Vera Reis, et al. "Future emerging technologies in the wind power sector: A European perspective." *Renewable and Sustainable Energy Reviews* 113, 2019, 109270, ISSN 1364-0321, https://doi.org/10.1016/j.rser.2019.109270.
[2] Blaabjerg, F., Z. Chen, and S. Kjaer. ''Power electronics as efficient interface in dispersed power generation systems''. *IEEE Trans. Power Electron*. 19, no. 5 (Sep. 2004): 1184–1194.
[3] Chen, Z., J. Guerrero, and F. Blaabjerg. ''A review of the state of the art of power electronics for wind turbines.'' *IEEE Trans. Power Electron.* 24, no. 8 (Aug. 2009): 1859–1875.
[4] Ahrens, U., M. Diehl, and R. Schmehl (editors). *Airborne wind energy*. Berlin Heidelberg, Springer-Verlag, 2013. https://doi.org/10.1007/978-3-642-39965-7.

[5] Cherubini, A., A. Papini, R. Vertechy, and M. Fontana. “Airborne wind energy systems: a review of the technologies.” *Sustain Energy Rev* 51 (2015): 1461–76.
[6] Hussen, K van, E. Dietrich, J. Smeltink, K. Berentsen, M. van der Sleen, R. Haffner, et al. ”Study on Challenges in the commercialisation of airborne wind energy systems.” Draft Final Report. Brussels: European Commission. 2018. https://doi.org/10.2777/87591.
[7] https://makanipower.com/.
[8] De Vries, O. ”Fluid dynamic aspects of wind energy conversion.” Natl aerosp lab rep AGARD-AG-243, publ by NATO, pg.156.
[9] Göltenbott, U., Y. Ohya, S. Yoshida, and P. Jamieson. ”Aerodynamic interaction of diffuser augmented wind turbines in multi-rotor systems.” *Renew Energy* 112 (2017): 25–34. https://doi.org/10.1016/j.renene.2017.05.014.
[10] McKenna, Phil. "Ducted Wind Turbines: An Energy Game Changer?". MIT Technology Review.
[11] Bychkov, N.M., A.V. Dovgal, and V.V. Kozlov. „Magnus wind turbines as an alternative to the blade ones.” *J. Phys. Conf. Ser.* 75 (2*007*): 12004.
[12] ***.”Design of an Alternative Hybrid Vertical Axis Wind Turbine” Qualifying Report Submitted to the Faculty of the WORCESTER POLYTECHNIC INSTITUTE, E-project-032714-164435 - PPM MQP 1342.
[13] Aquino, AI., J.K. Calautit, and B.R. Hughes. “Evaluation of the integration of the wind induced flutter energy harvester (WIFEH) into the built environment: experimental and numerical analysis.” *Appl. Energy* 207 (2017):61–77.
[14] Zhang, B., B. Song, Z. Mao, W. Tian, and B. Li. “Numerical investigation on VIV energy harvesting of bluff bodies with different cross sections in tandem arrangement.” *Energy* 133 (2017):723–36. https://doi.org/10.1016/j.energy.2017.05.051.
[15] Mituleț, L.A., G. Oprina, R.A. Chihaia, S. Nicolaie, A. Nedelcu, and M. Popescu. “Wind tunnel testing for a new experimental model of counter-rotating wind turbine.” *Annals of DAAAM International 2014* 25, no. 1 & Collection of Working Papers for 25th DAAAM International Symposium, ISBN 978-3-901509-99-5.
[16] Debleser, Y. (Jeumont Industrie). “Wind turbine with counter rotating rotors.” US Patent No. 6504260, 2003.
[17] Jung, S.N., T.-S. No, and K.-W. Ryu. “Aerodynamic performance prediction of a 30 kW counter-rotating wind turbine system.” *Renewable Energy* 30 (2005): 631–644.
[18] Shinn, C., and M.C. Hur. (Kowintec Corp.) “Over–drive gear device.” US Patent No. 5222924, 1993.
[19] Oprina, G., L.A. Mituleț, S. Nicolaie, R. Cîrnaru, and D. Cuciureanu. „Comparative Analysis of a Counter Rotating Wind Turbine Testing Results.” 15th International Multidisciplinary Scientific GeoConference & Expo SGEM 2015, 18-24 June 2015, Albena, Bulgaria, pp. 115-122, ISBN 978-619-7105-38-4, ISSN 1314-2704, DOI: 10.5593/sgem2015B41

ISSN 1454 - 8003
Proceedings of 2019 International Conference on Hydraulics and Pneumatics - HERVEX
November 13-15, Băile Govora, Romania

VIBROACOUSTIC PREDICTIVE INVESTIGATIONS ON NORMAL OR DEFECTIVE OPERATION OF HYDROSTATIC PUMPS

Alexandru-Daniel MARINESCU[1], Nicolaie ORĂȘANU[2], Carmen-Anca SAFTA[2], Corneliu CRISTESCU[1]

[1]Hydraulics and Pneumatics Research Institute INOE 2000-IHP, marinescu.ihp@fluidas.ro

[2] University "Politehnica" of Bucharest, norasanu62@yahoo.com

Abstract: *In industrial predictive maintenance, as well as in many practical situations, it is necessary to measure the noise and vibrations produced by machines and equipments in order to evaluate their state of functionality or malfunction. In this paper, the results of the experiments of a group of engineers from INOE 2000-IHP Bucharest and from the University Politehnica of Bucharest are presented, which aimed to show the effects of the cavitation phenomenon in hydraulic gear pumps on the frequency spectra resulting from the vibration signals processing.*

Keywords: *Predictive maintenance, noise measurement, vibration analysis, hydrostatic pumps, hydraulic drives*

1. Introduction

In predictive industrial maintenance, but also in many other practical situations, noise measurement is required. A noise is defined by the specific physical parameters, namely: intensity, frequency spectrum or time variation of its level. If the noise refers to a certain source of sound, such as an electric motor, a fan, a textile machine or a pneumatic hammer, then the parameters that characterize the source from an acoustic point of view must be determined, regardless of the environment in which they are working. These are: *acoustic power*, *directivity*, *frequency spectrum* or the *noise variation over time*. In order to obtain appropriate values for each physical parameter mentioned, in addition to a specific measurement technique, a suitable equipment must be used. With regard to noise of the same nature, it can be said that only by observing certain measurement conditions, the resulting data can be accurate and approved for publication. In this way a comparative database from different laboratories can be made.[1]
Also, the maintenance operators determine the proper functioning of a machine, or detect the symptoms of a malfunction appearance within it and by vibration analysis. Two measurements can be made by which the state of a vibrating body can be defined. The first one determines the state of motion of the body by measuring one of the following parameters of vibration: displacement, speed or acceleration, usually the acceleration is measured. The second measurement indicates the state of tension but also of deformation that the body or the surrounding element of construction undergoes as a result of the action of the vibrations that lead to smaller or greater deformations. These can be recorded by *electrical tensometry*, the deformations producing variations of an electrical parameter, such as *resistance*, *capacity or inductance*.[1] This type of method can be used not only for the measurement of vibrations caused by mechanical forces but also for actions of electrical or hydraulic nature. In order to identify the imminently destructive cases of the analyzed equipment, the vibration signal is processed. This results in a signal of the frequency spectrum which is a good indicator by which the cases of faults can be identified between them.[2] As the support technology of the mechanical equipments in the predictive maintenance system and the management of their maintenance advances, it is recommended to measure the mechanical vibrations as an indicator of attention [2,3], and in the large installations, where the danger caused by possible failures can be a major one, a permanent vibrations monitoring and the automatic shutdown of the operation take place if the vibrations level exceeds certain limits.

2. Noises and vibrations in hydraulic installations

In tools and equipments that have moving parts, such as hydraulic equipments, shocks and vibrations occur, which on the one hand are transmitted to the whole system, and have a negative effect on the machine as a whole. On the other hand, vibrations and shocks generate air oscillations, producing unwanted noises. These effects, sometimes fatal, can in many cases be prevented, provided that the involved specialists establish clear relationships between the type of noise and the state of functionality of the equipments [4]. In many cases, *the abnormal noise* is caused by cavitation or by air entering the oil. The noise of the air in the system is given by the compression and decompression of the air, during the movement in the system, together with the working fluid. The aeration results in the foaming of the hydraulic oil that it destroy. Lubrication and sealing are also destroyed, and finally the hydraulic equipments. Sometimes the air enters in system through the suction line of the pump, which may have mechanical defects, or when the oil level in the tank is below of the normal level. The air may also penetrate the pump shaft if its sealing is improper. [4] When the volume of oil required for the hydraulic circuit exceeds the volume received from the pump, the *cavitation* phenomenon occurs. Due to this, there is a drop in pressure in that area of the circuit under the vaporization pressure of the working fluid. As a result, bubbles (cavities) are formed which break down during compression, resulting in a characteristic noise. The consequences in the system may be of the nature of the metal erosions that contaminate the fluid and damage the hydraulic components. Often the defects caused by cavitation are found in the pumps, and for this reason the specialists must take into account that their suction line is free. The introduction of suction filters or valves must be done carefully, with the consent of the designers.[4] Among the processes that strongly influence the occurrence of malfunctions of hydraulic equipments and systems, the vibrations, self-vibrations and shocks caused by the pulsations of pumps, pressure valves and distributors are detached, together with the nonlinearities that appear in dynamic regime .[4]

3. Assessment of the hydrostatic pumps behavior using flow charts

In the predictive maintenance, in the last years, the authors of the paper have made numerous attempts to evaluate the behavior of hydrostatic pumps in operation by specific non-invasive methods, of which two main methods are detached: namely, the investigation with the help of infrared thermography or the method of vibration analysis, which have led to interesting results and conclusions published in various articles, such as those indicated in the Bibliography in the positions, [5,6]. Because it is almost impossible to attempt the quickly establish of the cause and to correct any errors that have occurred, even in the simplest hydraulic system, it is advisable to adopt a logical approach of the maintenance in order to locate an occurred fault during in the shortest possible time and in the most precise way (Fig. 1). In the industry, the outcome time of modern machines is very expensive, because an allocated hour for detecting a fault can mean a very large amount of money. In the recent years, hydraulic systems became more and more complex and, accordingly, the control methods of machines became more and more sophisticated. Therefore it is essential that the manufacturer's equipments or service information keep up with the used hardware. In this paragraph are presented procedures for logical approach of the maintenance operations that can be extended to certain machines in all industrial fields. The basis of these procedures, related to the control of excessive noise and vibration in hydraulic installations, find their support in numerous examples and applications in the industry. A flowchart (*Algo 0.3*), proposed by ***EatonVickers (USA)*** for testing hydrostatic pumps, when excessive operating noise appears, is shown in Fig. 2. Similarly, another flowchart for testing hydrostatic pumps at the occurrence of excessive vibrations in operation is shown in Fig. 3. In this case the FAULT, CAUSE, REMEDY (F.C.R) charts can be used to locate the problem area [7].

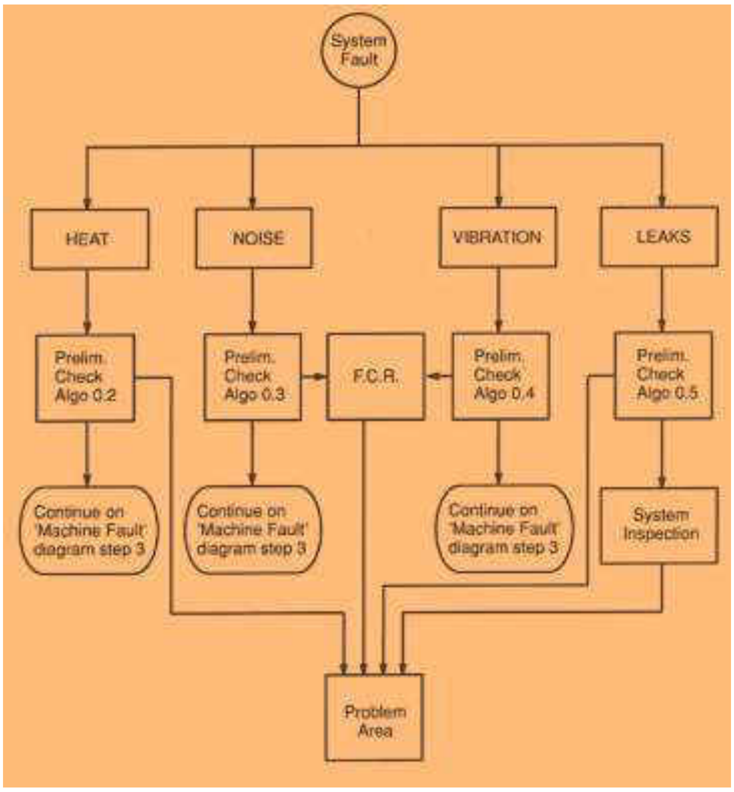

Fig. 1. Flowchart for faults that may occur in a hydraulic system, [7]

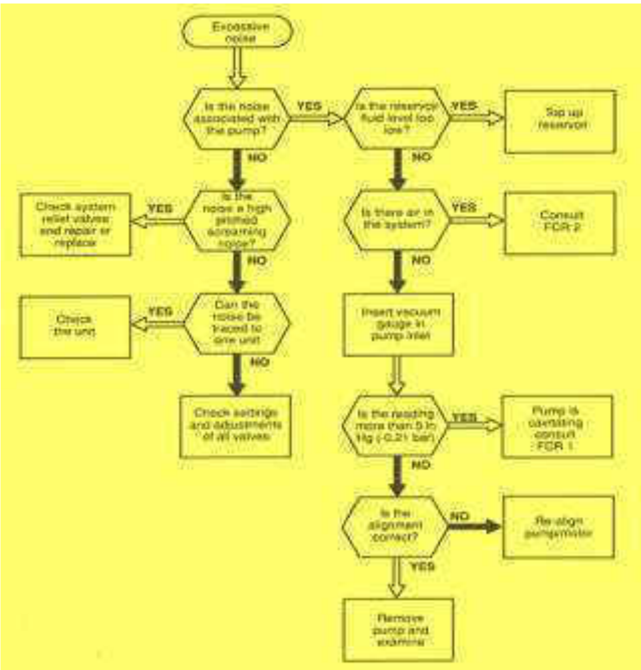

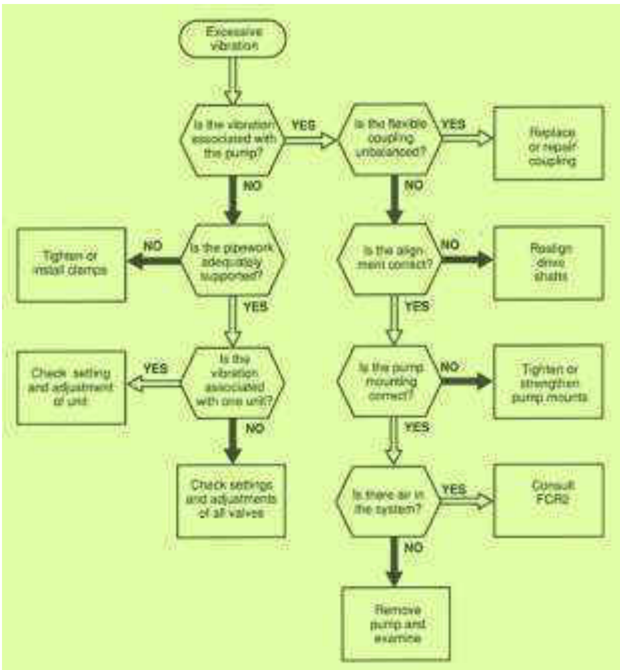

Fig. 2, Fig. 3 (from left to right) Hydrostatic pumps tested for excessive noise and for excessive vibration [7]

ISSN 1454 - 8003

4. Assessment of the measured vibration spectra in operation of certain hydraulic gear pumps in normal and cavitational mode

Inside of Hydraulics Laboratory of INOE 2000-IHP, an experimental stand was created (Fig. 4), on which two hydraulic gear pumps model **Vivoil XV 2P-DC (Italy)** were separately tested in normal and cavitational mode (Fig. 5, Fig. 6), having the displacements of **9 cm^3 /revolution** , respectively **6 cm^3 / revolution.**

Fig. 4. Experimental stand

Fig. 5. Pump with a displacement of 9 cm^3/rev

Fig. 6. Pump with a displacement of 6 cm^3/rev

The hydraulic diagram of the experimental stand and its components are shown in Fig.7 and Fig.8

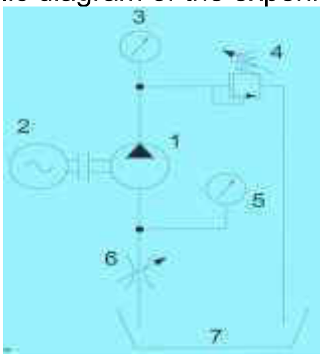

Fig. 7. Hydraulic diagram of the stand

No	Component	Technical characteristics	Manufacturer
1	Hydraulic gear pump	Tip XV 2P-D/C , V_g = 9 cm^3	Vivoil, Italy
2	Electric motor	Tip D63110, 2,65 kW, 1420 rot/min, 50Hz	AG Motoren GmbH, Rodgau, Germany
3	Gauge with glycerin	P = (0-160) bar, precision class 1,5	Hansaflex, Germany
4	Pressure valve	Tip SPP 6-04, Pmax= 315 bar	Hidrosib, Romania
5	Vacuummeter	P = (0-1) bar, precision class 1,5	Afriso, Germany
6	Throttle valve	FT 257/2-12, 400 bar	F.lli Tognella, Italy
7	Oil basin	V= 79, 3 l	INOE 2000-IHP, Romania

Fig. 8. Hydraulic components

4.1 - Vibration analysis of a hydraulic gear pump with a displacement of 9 cm^3/revolution in normal and cavitational mode operating

In order to produce the **cavitation** phenomenon, on the suction hose of the pump, with a nominal diameter Dn = 40 mm, an adjustable way throttle was installed, through which several vacuum steps were generated, in a range from -0.2 bar (first measurement) to -0.7 bar (last measurement). Simultaneous, all performed measurements were made by generating through an adjustable valve of three pressure steps, respectively: 50 bar, 75 bar and 100 bar. Recording of the system vibrations under normal operating conditions and under cavitational mode was made using three **Bruel & Kjaer (Denmark)** type accelerometers, **model 4507 B** (Fig. 9), fixed in three different points of the test stand, respectively: on the pump housing. , on the electric motor and on the oil tank (Fig.10,11,12).

Fig. 9. Accelerometers

Fig.10. Accelerometer mounted on pump

Fig.11. Accelerometer mounted on motor

Fig. 12. Accelerometer mounted on oil tank

Accelerometer signal processing was performed using a **National Instruments** data acquisition plate model **NI 9233**, (**USA**), connected to a laptop.(Fig. 13, Fig. 14).

Fig. 13. Data acquisition plate

Fig. 14. Laptop

Note: Due to the installation of the pump on the stand, but also of the dimensions of the hydraulic hoses, at the start of the electric motor, without throttling, the pump has in suction a vacuum of -0.2 bar, registered by the vacuum meter. In the experiment, it was agreed that this value should be considered as a reference for the normal operating mode of the pump, while all measurements corresponding to the throttling steps starting from -0.3 bar to -0.7 bar will be associated of its cavitational operating mode.

4.1.1. Obtained results

As a result of the measurements, **90 vibration signals** resulted. By means of **Matlab** software, all vibration signals were then converted into frequency spectra. For the paper, of a special interest are the vibration signals generated spectra, taken by the accelerometer **A1** mounted on the pump, at different pressures measured respectively by the manometer and the vacuum meter (Table 1).

Table 1: Vibrations signals

Accelerometer signal A1 - pump	Pressure [bar]	
	at vacuummeter	at gauge
01 dB_wave_114.mat	-0,20	100
01 dB_wave_159.mat	-0,50	100
01 dB_wave_177.mat	-0,60	100
01 dB_wave_195.mat	-0,70	100

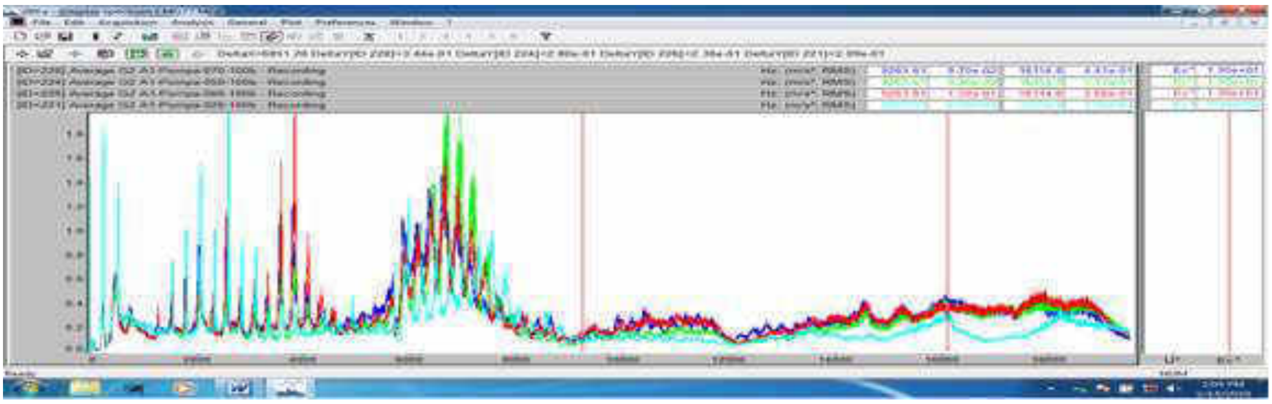

Fig. 15. The overlayed spectra analysis

4.1.2. Discussions

It can be seen from Fig. 15 on the overlayed spectra that in the high frequency band, **9000-16000 Hz**, the acceleration level is higher at big cavities (-0.7 bar; -0.6 bar) and lower at small values (-0.2 bar and -0.5 bar)

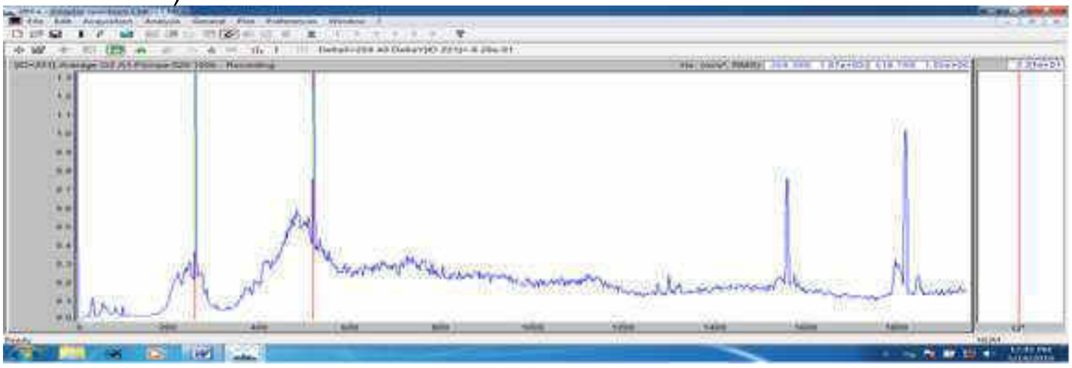

Fig. 16a. Spectrum analysis for Pv = -0.20 bar; Pm = 100 bar

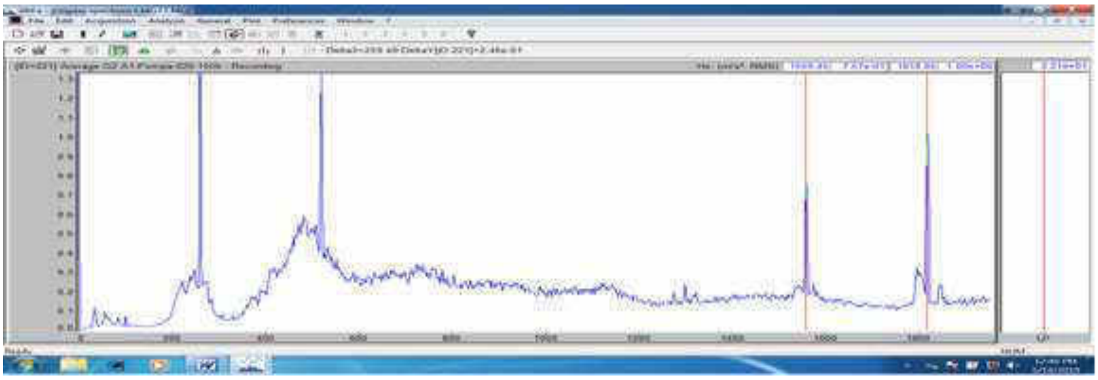

Fig. 16b. Spectrum analysis for Pv = -0.20 bar; Pm = 100 bar

In the spectrum of Fig.16a it is observed that a frequency of about **259.4 Hz** appears, having a harmonic of **518.8 Hz**, and in the spectrum of Fig. 16b it is observed that this frequency is then repeated with higher harmonics of **1559 Hz (6x 258.4 Hz)**, then of **1818 Hz**, etc. (Pv = vacuum meter measured pressures; Pm = manometer measured pressures).

4.2 - Vibration analysis of a hydraulic gear pump with a displacement of 6 cm^3/revolution in normal and cavitational mode operating

For the resulting vibrations analysis following the 6 cm^3/revolution displacement pump testing in the normal and cavitational mode, the same working scenario was followed as in the case of the pump with displacement of 9 cm^3/rev. In contrast to the experiments described above, in this case, for vibration recording, accelerometers were mounted at three different points of the pump(Fig. 17). Thus, the vertical, horizontal and axial vibrations are recorded respectively by the accelerometers **A1**, **A2** and **A3**.

Fig. 17. Positioning of the accelerometers on the pump

4.2.1. Obtained results

Following measurements, **90 vibration signals** resulted. By means of **Matlab** software, all vibration signals were converted into frequency spectra. Two of these are shown in (Fig.18-19). P are the pressures and C are the cavities.

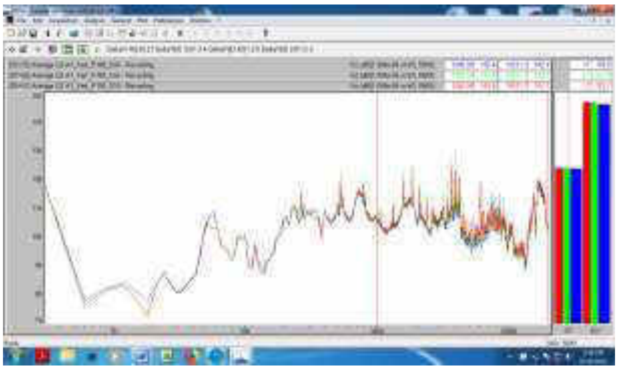

Fig. 18. A1-vertical /P=100bar C=(-0.40;-0.45; -0.50)bar

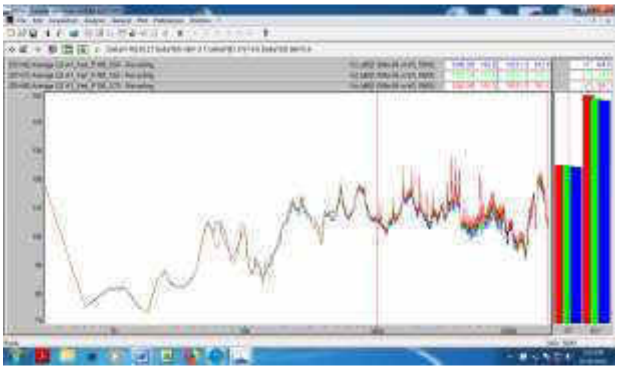

Fig. 19. A1-vertical /P=100bar C=(-0.60;-0.65; -0.70)bar

4.2.2. Discussions

From the vibration spectra analysis indicated in Fig. 18 and Fig.19 it is observed that in the 3000-6000 Hz band, the vibrations are increasing as the cavitation increases (Fig. 20 and Fig. 21).

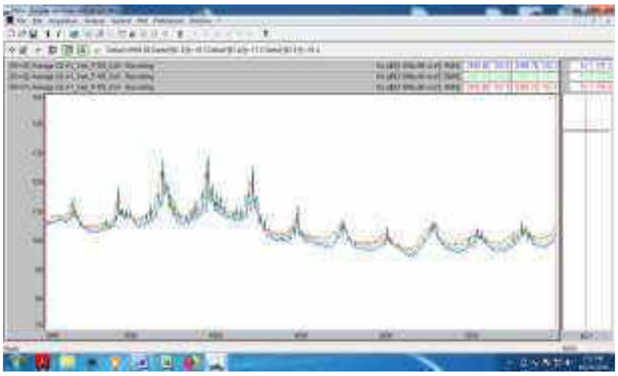

Fig. 20. A1-vertical /P=100bar C=(-0.40;-0.45; -0.50)bar

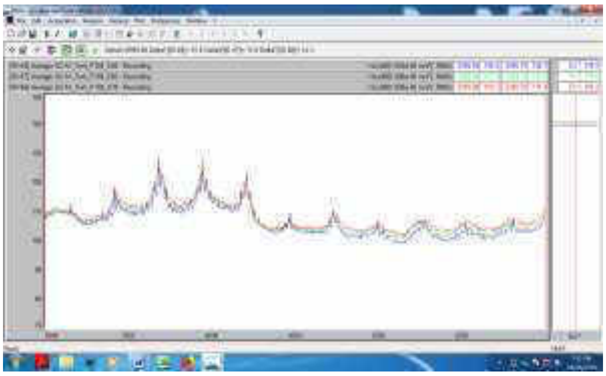

Fig. 21. A1-vertical/P=100barC=(-0.60;-0.65; -0.70)bar

-As the pressure increases on the pump discharge, the amplitude of the vibrations decreases and in some areas, it is greatly reduced.
-The more vacuum on the pump suction is more pronounced, the amplitude of the vibration increases.

5. Conclusions

- By pump testing with displacement of **9 cm^3/rev** the following conclusions could be detached:
  - Although the cavitation phenomenon should have been detected at high frequencies, this thing has been obstructed due to the occurrence of certain higher harmonics of very large amplitudes which are more important especially at low pressures.
  - Clearer determination of how the cavitation is reflected in the frequency spectra could be makes it simpler in the event that these defects would not manifest themselves so obviously.

- By the method of vibration analysis, although surprising results have been obtained, they indicate a state of abnormal operation of the tested pump on the stand, explained by the internal losses suffered of this as a result of the grinding.
- Because the authors wished to obtain more conclusive results, another one Vivolil hydraulic gear pump, with a displacement of **6 cm^3/rev** was subsequently tested, action which resulted in the following conclusions:
- The experiments must focus on signals analyzing at narrower frequency intervals, in order to accurately identify the area where the cavitation is found in the signal.
- By comparing with the normal operating spectrum of the pump, the degree of its wear because of cavitation can be estimated. This will trigger a predictive maintenance alert by re-evaluating /repairing of the suction circuit, or even installing the pump on a checking stand an/or sending it into service in repair procedure. If necessary, the pump will be replaced.

References

[1] Grumăzescu, M., A. Stan, N. Wegener, and V. Marinescu. *Combaterea zgomotului și vibrațiilor / Suppressing noise and vibration*. Bucharest, Technical Publishing House, 1964.
[2] Hajianto, M.R., and A. Yulianto. ”Vibration analysis for monitoring the condition of hydraulic powerpack for underground mining supporting simulation at education and training unit of underground mining (Etuum).” *American Journal of Engineering (AJER)* 6, no. 5 (2017): 123-129.
[3] Kelly, S.G. *Fundamentals of Mechanical Vibration.* Second Edition. Mc Graw Hill, 2000.
[4] Assofluid Italian Association of Manufacturing and Trading Companies in Fluid Power Equipment Components. *Hydraulics in Industrial and Mobile Applications*. Brugherio (Milano), Grafiche Parole Nuove srl, 2007.
[5] Marinescu, A. D., C. Cristescu, T.C. Popescu, and C.A. Safta. ”Assessing the opportunity to use the infrared thermography method for predictive maintenance of hydrostatic pumps.” Proceedings of the International Conference of Energy and Environment (CIEM), Bucharest, Romania, October 19-20, 2017. ISI indexed paper.
http://ieeexplore.ieee.org/xpl/tocresult.jsp?isnumber=8120754.
[6] Marinescu, A. D., C.A. Safta, T.C. Popescu, and C. Cristescu. ”Maintenance of hydraulic drive systems via vibroacoustic diagnosis.” Proceedings of XVIII Multidisciplinar International Conference “Professor Dorin Pavel – the founder of the Romanian Hidropower ”, Cluj-Napoca, Romania, June 1-2, 2018. IDB indexed paper.
https://stiintasiinginerie.ro/34-29-mentenanta-sistemelor-de-actionare-hidraulica-prin-diagnoza-vibroacustica/
[7] Vickers Eaton. SM4 and SX4 Servovalves. ”Installation and Troubleshooting Guide”.
http://www.eaton.eu/ecm/groups/public/@pub/@eaton/@hyd/documents/content/ct_233700.pdf.

ISSN 1454 - 8003
Proceedings of 2019 International Conference on Hydraulics and Pneumatics - HERVEX
November 13-15, Băile Govora, Romania

USE OF 3D PRINTING TECHNOLOGY FOR PROTOTYPING IN MECHANICAL ENGINEERING

Alexandru-Polifron CHIRIȚĂ[1], Liliana DUMITRESCU[1], Ștefan-Mihai ȘEFU[1], Ionela-Mihaela BACIU[1]

[1] Hydraulics and Pneumatics Research Institute INOE 2000 - IHP, Bucharest; chirita.ihp@fluidas.ro

Abstract: *The article presents a brief history of the processes of additive production (3D printing), describing and classifying them. At the same time, two prototypes are presented in the material, a vertical axis wind turbine and the body of a piston of a fertigation pump that were successfully produced at IHP with the help of this technology.*

Keywords*: Additive manufacturing, 3D printing, FDM, vapor smoothing, FFF.*

1. Introduction

The 3D printing process builds a three-dimensional object from a computer-aided design (3D CAD) model, usually by successively adding material layer by layer, which is why it is also called additive manufacturing, unlike conventional machining, casting and forging processes, where material is removed from a stock item (subtractive manufacturing) or poured into a mold and shaped by means of dies, presses and hammers.

2. Brief history of 3D printing

David E.H. Jones was the first who laid out the concept of 3D printing in the journal “New Scientist”, in 1974. [1]

In 1981, Hideo Kodama of Nagoya Municipal Industrial Research Institute invented two additive methods for fabricating three-dimensional plastic models with photo-hardening thermoset polymer, where the UV exposure area is controlled by a mask pattern or a scanning fiber transmitter.[1] On 16 July 1984, Alain Le Méhauté, Olivier de Witte, and Jean Claude André filed their patent for the stereolithography process. Three weeks later in 1984, Chuck Hull of 3D Systems Corporation filed his own patent for a stereolithography fabrication system, in which layers are added by curing photopolymers with ultraviolet light lasers. Hull defined the process as a "system for generating three-dimensional objects by creating a cross-sectional pattern of the object to be formed”. Hull’s contribution was the STL (Stereolithography) file format and the digital slicing and infill strategies common to many processes today. [1]

The technology used by most 3D printers to date—especially hobbyist and consumer-oriented models—is fused deposition modeling, a special application of plastic extrusion, developed in 1988 by S. Scott Crump and commercialized by his company Stratasys, which marketed its first FDM machine in 1992.[1] By the mid-1990s, new techniques for material deposition were developed at Stanford and Carnegie Mellon University, including microcasting and sprayed materials. Sacrificial and support materials had also become more common, enabling new objects geometries.[1]

The term 3D printing originally referred to a powder bed process employing standard and custom inkjet print heads, developed at MIT by Emanuel Sachs in 1993 and commercialized by Soligen Technologies, Extrude Hone Corporation, and Z Corporation. The year 1993 also saw the start of a company called Solidscape, introducing a high-precision polymer jet fabrication system with soluble support structures. [1]

In 1995 the Fraunhofer Institute developed the selective laser melting process. Fused Deposition Modeling (FDM) printing process patents expired in 2009. As the various additive processes matured, it became clear that soon metal removal would no longer be the only

metalworking process done through a tool or head moving through a 3D work envelope transforming a mass of raw material into a desired shape layer by layer.
In 2008 Shapeways, a 3D printing service is launched in the Netherlands. A bit like RepRap, Shapeways makes 3D printing available to a wider audience. Rather than giving people their own 3D printers, however, Shapeways lets users submit their own 3D files, which the company then 3D prints and ships back. Shapeways rapidly expands to a factory in Queens, New York, and raises substantial venture funding. It also becomes a marketplace for 3D printed objects, which the company will then print on demand. Shapeways makes 3D printing accessible to a non-tech crowd, including artists, architects and other creative individuals. [2]
The 2010s were the first decade in which metal end use parts such as engine brackets and large nuts would be grown (either before or instead of machining) in job production rather than obligated being machined from bar stock or plate. As technology matured, several authors had begun to speculate that 3D printing could aid in sustainable development in the developing world.
In 2012 Filabot develops a system for closing the loop with plastic and allows for any FDM or FFF 3D printer to be able to print with a wider range of plastics. 2014: Georgia Institute of Technology Dr. Benjamin S. Cook and Dr. Manos M. Tentzeris demonstrate the first multi-material, vertically integrated printed electronics additive manufacturing platform (VIPRE) which enabled 3D printing of functional electronics operating up to 40 GHz.

3. Technologies in 3D Printing [3]

- Stereolithography (SLA) – This 3D printing method is the first method in the history of 3D printing. It is the oldest but is still being used today. Most printing techniques use a CAD file to process the object, which is then converted to a format that a printing machine can understand. In this technology, a software processes the CAD model and generates the STL file that contains the information for each layer. The whole process includes a consequent printing layer by layer. There could be up to ten layers per each millimeter. Once all layers are printed, the object needs to be rinsed with a solvent and placed in an ultraviolet oven to finish the process.
- Digital Light Processing (DLP) is similar to stereolithography. Larry Hornbeck of Texas Instruments created this technology in 1987. This is popular in the production of projectors and is applicable for cell phones and 3D printing as well. DLP technology uses digital micromirrors laid out on a semiconductor chip. Although DLP and SLA both work with photopolymers, they use different sources of light. DLP uses more conventional sources like arc lamps. Moreover, DLP uses a liquid crystal display panel that is being applied to the whole surface of the building material. The material for printing is a liquid plastic resin placed in the transparent resin container. The resin quickly hardens when exposed to a large amount of light. The printing speed is fast. Compared to SL, DLP produces more robust 3D objects with excellent resolution. It also uses lesser material that results in lower cost and reduced waste.
- Fused deposition modeling (FDM) is the most popular technology in 3D printing. It allows you to print concept models and final end-use products with engineering-grade thermoplastic. FDM is the only 3D printing technology that builds parts with production-grade thermoplastics that produces excellent mechanical, thermal and chemical qualities making it very useful and appealing to manufacturers and engineers. FDM Technology builds a 3D object layer by layer from the bottom to the top by heating and extruding thermoplastic filament. The whole process is similar to stereo lithography but slower. This technology uses a special software to cut the CAD model into layers and calculate the way the printer extruder will build each layer. The printer will heat the thermoplastic up to its melting point and extrudes throughout the nozzle onto the base to build platform along the calculated path. A computer will translate the dimension of the object into X, Y and Z coordinates and controls the nozzle and the base, so that it follows the calculated path during printing. This technology is used in automobile companies like Hyundai and BMW and food

companies including Nestle and Dial. FDM technology is simple to use, and it can build complex geometries and cavities. Moreover, it is environment-friendly.

- Selective Laser Sintering (SLS) This technology uses a laser as a power source to form 3D objects. Carl Deckard, a student of Texas University and his professor Joe Beaman discovered this technology in 1980. SLS has some resemblance with SLA but they differ in the material used. SLS uses powdered material instead of liquid resin. In addition, SLS does not use any support structures because the object being printed is already surrounded by unsintered powder. Similar to other technologies, SLS starts with the creation of the CAD file, which is then converted into a .stl format using special software. This technology allows nylon, ceramics, glass and metals like aluminum, steel or silver. Due to its wide variety of materials, SLS is popular for customizing 3D objects.
- Selective laser melting (SLM) This technique also uses CAD data and builds a 3D object through a high-power laser beam that fuses and melts metallic powders. Several sources consider SLM as a subcategory of SLS but the two technologies have major differences. The SLM processes fully melt the metal into solid 3D parts, unlike selective laser sintering. SLM also uses a CAD file, and special software to slice the CAD file into 2D layers. When the file is loaded, the printing machine's software will assign parameters and values for construction of the path. The fine metal powder is evenly distributed onto the plate and a high laser energy will be directed into it to fuse each slice of 2D layer image. The energy is so strong that the metal powder melts and forms a solid object. The process repeats for the next layer until the product is complete. SLM uses the following metals: stainless steel, titanium, cobalt chrome, and aluminum. SLM is widely used in objects with complex geometries and structures with thin walls and hidden voids or channels. This technology is used in aerospace manufacturing and orthopedics but it is not widely distributed among households.
- Electronic Beam Melting (EBM) This technology is another type of additive manufacturing for metal parts. It is similar to SLM as it also uses a powder bed fusion technique. However, instead of using a high-power laser beam as its power source, it uses an electron beam. This is the main difference between the two; the rest of the process is the same. EBM is slow and expensive compared to SLM. Also, the materials are limited. Most materials used are commercially pure titanium, Inconel 718 and Inconel 625. This technology focuses on medical implants and aerospace area.
- Laminated Object Manufacturing (LOM) Helisys Inc., a California-based company, develops this rapid prototyping system. During LOM process layers of adhesive-coated paper, plastic or metal laminates are fused together through heat and pressure. Then, they are cut into shapes with computer-controlled laser or knife. The post-processing of 3D printed parts includes machining and drilling. This technology also starts with a CAD file that is later converted into an STL or 3DS format. LOM printers use continuous sheet coated with adhesive and laid down cross substrate with a heated roller. The heated roller is passed over the material sheets on substrate melts the adhesive and the laser or knife will then trace it to its desired dimension. When the layer is finished, it will move down and a new sheet will be processed. The process is repeated until the 3D object is fully printed. LOM is not that popular but it is one of the most affordable and fastest 3D printing technology. Moreover, printing is low cost because it does not use expensive materials.
- Binder Jetting (BJ) Technology. The Massachusetts Institute of Technology invented BJ 3D printing. This is called by many other names such as: Powder bed printing, Inkjet 3D printing, Drop-on-powder, Binder Jetting (BJ) – the most popular name. BJ uses two types of materials a powder-based material and a bonding agent. The "bonding" agent acts as a strong adhesive that holds the powder layers together. The printer nozzles extrude the binder in a liquid form similar to a regular 2D inkjet printer. After completing each layer, the build plate lowers slightly to allow for the next one. The process is repeated until the process is finished. This 3D printing technology doesn't give you high-resolution or overly rugged 3D objects. But it allows you to print parts in full color. BJ is

being used in aerospace, automotive and medical industries. Material Jetting (MJ) Polyjet and Wax Casting Technology Material Jetting is also called wax casting. Unlike the other 3D printing technologies no one invented MJ. This is considered more of a technique than an actual printing process. Jewelers have used this for centuries to produce high-quality customizable jewelry. MJ starts with a 3D model (CAD file). Once this is uploaded to the printer, the system does all the rest. The printer adds molted (heated) wax to the aluminum build platform in controlled layers. It will be sweep evenly across the build area. As soon as it lands on the build plate, it begins to cool down and solidify (UV light helps to cure the layers). As the 3D parts build-up, a gel-like material helps support it. Once it's done, you can easily remove the object by hand or by using powerful water jets. Once the part is complete, it can be used right away. No need for further post-curing.
This produce objects with good resolution. Polyjet MJ 3D printers are used mainly in the dental and jewelry industries.

4. Prototypes made at IHP with the help of 3D printing technology

This chapter presents two of the prototypes produced at the Research Institute for Hydraulics and Pneumatics INOE200-IHP.
The prototyping process of vertical axis wind turbines (1:5 scale). [4]
Figure 1 shows the 3D model of the wind turbine, realized in the CAD modeling software SOLIDWORKS.

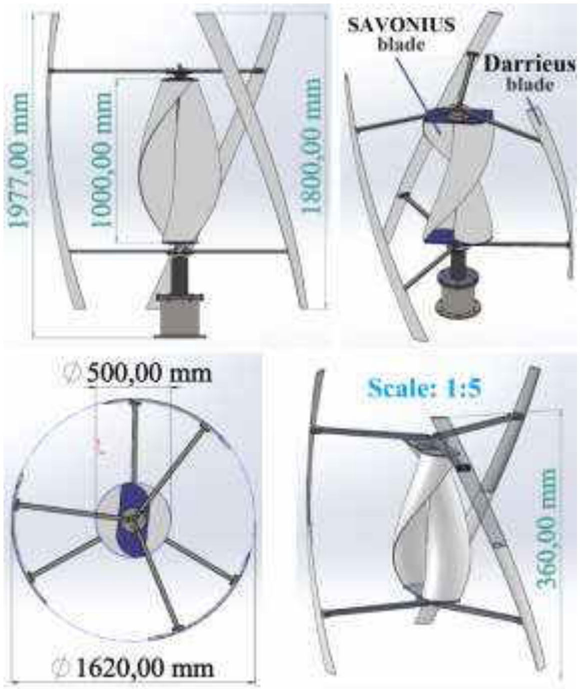

Fig. 1. 3D CAD models from the SolidWorks software

Printing was done on the BCN3D SIGMA R19 Printer (FFF) with the following facilities:
•Architecture: Independent Dual Extruder (IDEX);
•Printing volume: 210 mm x 297 mm x 210 mm;
•Heated bed maximum temperature: 100 °C;
•Positioning resolution (X/Y/Z): 1.25μm/ 1.25μm/ 1μm;
•Firmware: BCN3D Sigma - Marlin;
•Extruder system Extruder Bondtech ™ high-tech dual drive gears; Hotends: Optimized and manufactured by e3D ™;
•File preparation software: BCN3D Cura.
Both the printer and the slicing software of the 3D models are shown in figure 2.

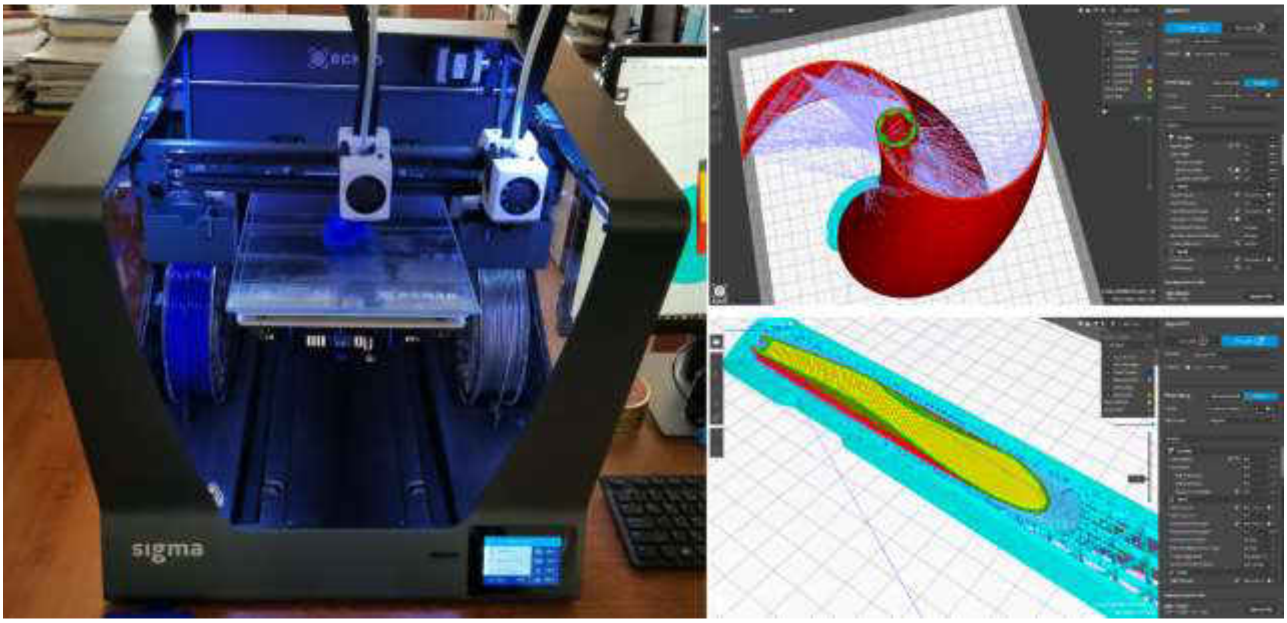

Fig. 2. SIGMA R19 Printer and BCN3D Cura software

All the parts of the functional model were printed with PLA and for the parts that needed support PVA was used, which dissolves easily in water.
Parameters of the 3D printing process: the filament diameter was 2.85 mm, 0.4 mm hotend diameter, 0.2 mm layer height, 35% or 100% infill density, 205°C printing temperature, 60°C build plate temperature and a conservative print speed of 50 mm/s.
Because the blades of the Darrieus turbine are larger than the printer can produce, they were divided into two pieces, and due to their curvature, in two planes, it was necessary to print with support material. Figure 3 shows the parts that needed support material, including the arms for the purpose of supporting the Darrieus turbine; they have practiced 2 through-holes that are necessary for the assembly with screws.

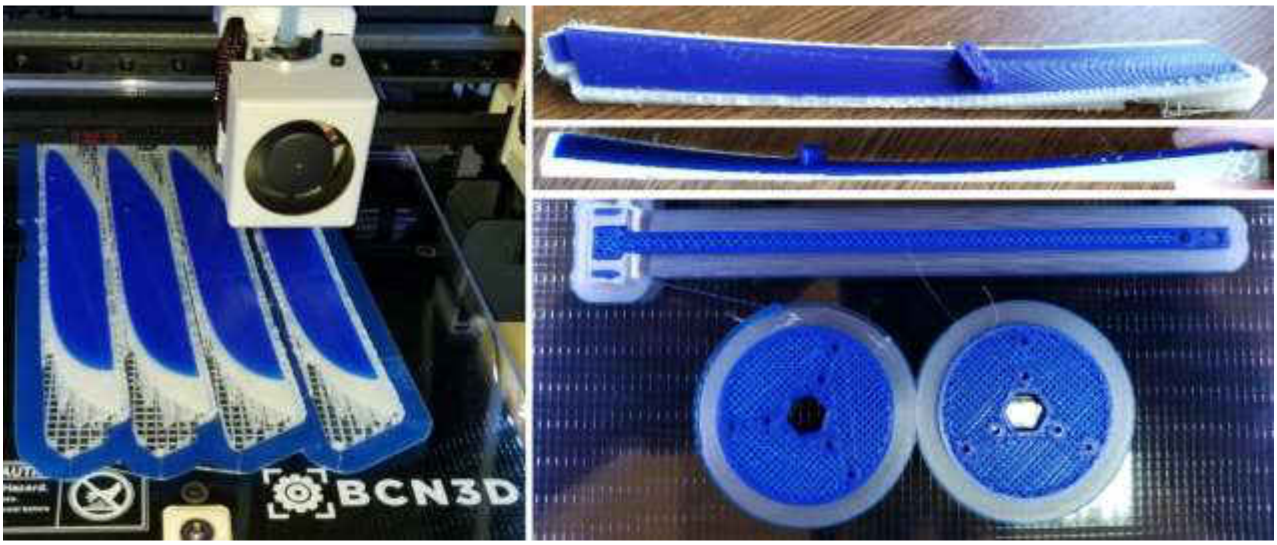

Fig. 3. The printed parts that needed support material.

Figure 4 shows the parts that did not need support material during the printing process; they are: the covers of the Savonius turbine, which have practiced a channel that rigidifies the whole sub-assembly, the Savonius turbine itself, as well as the bearing base, which has the role of support for hexagonal shaft and turbine.

Fig. 4. Components that did not need support material during the printing process.

And in Figure 5 is presented the prototype of the wind turbine with vertical axis, on a small scale.

Fig. 5. The prototype of vertical axis wind turbines (1:5 scale)

The prototyping process of the injection device piston used for fertigation. [5]

This section presents the 3D printing process of the piston and the process of improving surface quality. Figure 6 shows the 3D model made in the SolidWorks modeling software, as well as a section of it.

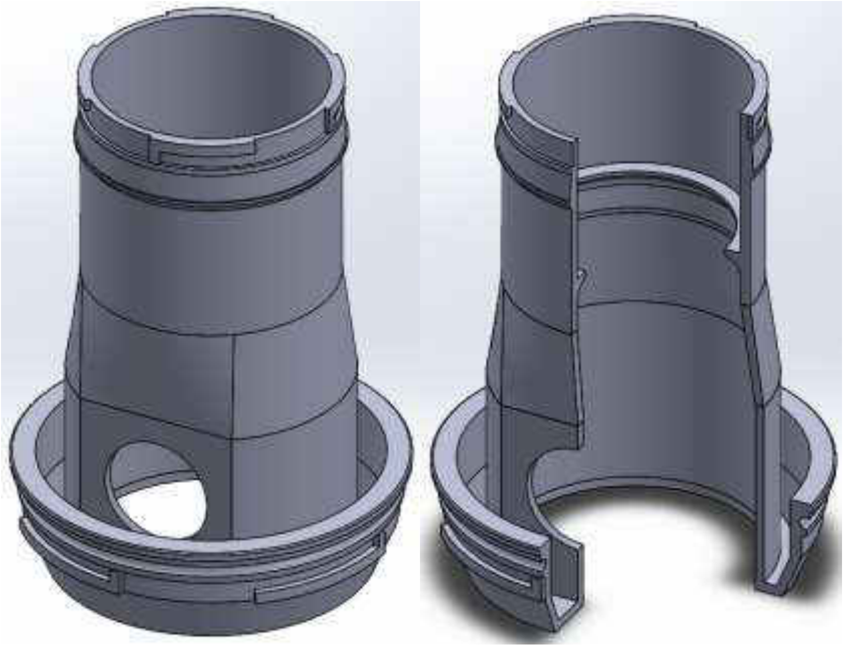

Fig. 6. 3D CAD models from the SolidWorks software

The piston body was made of ABS filament and the support structure was intended to support the layers with an angle greater than 45°.

Parameters of the 3D printing process: the filament diameter was 2.85 mm, 0.4 mm hotend diameter, 0.2 mm layer height, 99% infill density, 250 °C printing temperature, 95 °C build plate temperature and a conservative print speed of 55 mm/s.

The 3D model was converted to STL format and was imported into the Cura slicer (Figure 7) where the printing parameters were set.

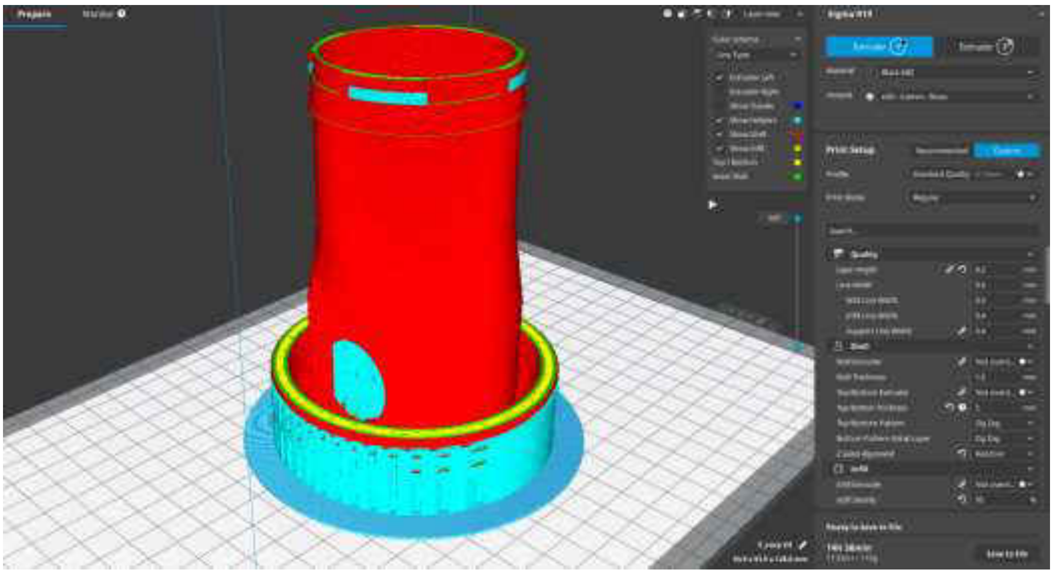

Fig. 7. The 3D model of the piston from the Cura slicer

The piston resulted at the end of printing can be seen in figure 8, as well as the fact that a closed enclosure was used during printing to prevent the deformation of the part and the delamination of the layers.

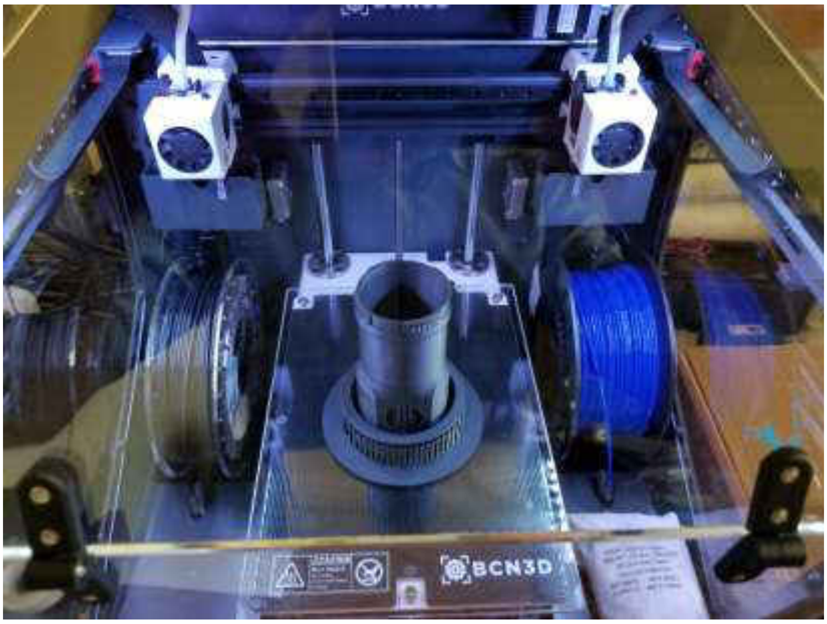

Fig. 8. 3D printer and piston body at the end of the printing process

Due to the fact that the fertigation pump operates at a maximum pressure of 6 bar and for a smoother flow of the liquid through the pump body, the piston has been applied the "vapor smoothing" process (figure 9). This process consists in the superficial melting of the surface of the ABS part with the help of an acetone vapor bath. The piston was placed in a tightly sealed vessel that has a sieve high up against the bottom of the vessel on which the piece sits. On the bottom of the vessel there is acetone and a piece of metal embedded in the glass that is driven by a device that heats the vessel and at the same time rotates the metal piece. Stirring the acetone as well as increasing the temperature increases the rate of acetone evaporation and finally the duration of the entire process.

Fig. 9. Vapor smoothing process installation

After about 15 minutes, the piece was removed from the vessel and left for the molten acetone surface to harden. The final quality of the surface can be seen in figure 10.

Fig. 10. Surface quality after vapor smoothing process

5. Conclusions

With the help of rapid prototyping technology, both the wind turbine and the piston body of the irrigation pump were produced quickly and cheaply.

Due to the additive nature of this technology, complex parts that could not be made with classical processes (milling, turning, casting ...), can easily be achieved.

Acknowledgments

This paper has been funded by the Romanian Ministry of Research and Innovation under Programme I - Development of national R&D system, Subprogramme 1.2 – Institutional performance – Projects financing excellence in R&D+I, Financial Agreement no. 19PFE/17.10.2018.

References

[1] 3D printing, 2019, https://en.wikipedia.org/wiki/3D_printing.
[2] Shapeways enables businesses, 2019, https://www.shapeways.com/.
[3] Types of 3D Printing Technology, 2019,https://all3dp.com/1/types-of-3d-printers-3d-printing-technology/
[4] Chiriță, Alexandru Polifron, Paul Bere, et al. "Aspects regarding the use of 3D printing technology and composite materials for testing and manufacturing vertical axis wind turbines." *Materiale Plastice* 56, no. 4 (December 2019).
[5] Sovăială, Gheorghe, Alexandru Polifron Chiriță, et al. "Rapid prototyping of the injection device piston used for fertigation using 3D printing technology." *Materiale Plastice* 56, no. 4 (December 2019).

ISSN 1454 - 8003
Proceedings of 2019 International Conference on Hydraulics and Pneumatics - HERVEX
November 13-15, Băile Govora, Romania

MULTIPASS HYDRAULIC FILTER TESTS

Franc MAJDIČ[1]

[1] University of Ljubljana, Faculty of Mechanical Engineering, franc.majdic@fs.uni-lj.si

Abstract: *Engineers in industry meet daily with various machines; their operation depends on hydraulic systems. In order to operate the machines smoothly it is necessary to pay special attention to the hydraulic liquid. By selecting the appropriate filter elements, we improve the filtration process and thus the condition of the hydraulic liquid, which in the long term helps to extend the useful life of hydraulic components and reliability of hydraulic systems. In order to select the most suitable filter cartridge, various methods of their evaluation and testing have been developed, including the Multiple Transition Test according to ISO 16889:2008 standard. Work will present development and validation of multipass filter test rig. Some results of the filter tests with standard MTD dust will be shown. ß valve and filter capability will be introduced on the end.*

Keywords*: Multi−pass test, filter element, hydraulic fluid, filtration ratio, cleanliness*

1. Introduction

Cleanliness of hydraulic fluid is extremely important for useful life of hydraulic components and the whole system. Filtering quality is very important [1]. The ISO 16889 [2] is in use to evaluate the quality of filters. Mentioned standard describe test rig and procedure to do appropriate and comparable filter tests. The standard also specifies a calculation procedure for determining the tested parameters and for evaluating the obtained experimental results. Standard test dust MTD by ISO 12103-1-A3 should be used [3-5].

First we calculate predicted test time of the tested filter element (equation 1). Desired upstream gravimetric level (c'_b) should user choose from the table in standard. There are three possibilities: 3 mg/L, 10 mg/L or 15 mg/L. Estimated filter element contaminant capacity (m_e) is a parameter of tested filter which should be known by the producer. Test flow rate (q) should be chosen by user.

$$\boldsymbol{t_{pr} = \frac{1000 \times m_e}{c_b{'} \times q}} \tag{1}$$

Minimum required operating injection system volume is calculated by equation (2).

$$\boldsymbol{V_{min} = (1,2 \times t \times q'_i) + V_v} \tag{2}$$

Desired gravimetric level is calculated by equation (3).

$$c'_i = \frac{c'_b \cdot q}{q'_i} \tag{3}$$

Quantity of contaminant is calculated by equation (4).

$$m = \frac{c'_i \cdot V_{ii}}{q'_i} \tag{4}$$

After test of filter element, it is necessary to calculate upstream (equation 5) and downstream (equation 6) particle counts.

$$\boldsymbol{\overline{N}_{u,x,t} = \frac{\sum_{j=1}^{n} N_{u,x,j}}{n}} \tag{5}$$

$$\boldsymbol{\overline{N}_{d,x,t} = \frac{\sum_{j=1}^{n} N_{d,x,j}}{n}} \tag{6}$$

Using equation (7), filtration ratios $ß_{x,t}$ can be determined for each of 10 reporting times of the test.

$$\overline{\boldsymbol{\beta}}_{\mathbf{x(c)}} = \frac{\overline{N}_{u,x,t}}{\overline{N}_{d,x,t}} \tag{7}$$

2. Test rig

Standard ISO 16889 describe test rig and protocol how to test hydraulic filters. Figure 1 shows hydraulic circuit of recommended test rig. It contains two subcircuits, A and B. Subcircuit **A is contamination injection system**. It consists of conical (60°) reservoir (a), injection pump (b), shut-off valves (c), clean-up filter (g) for preparing system before entering the test dust, check valve (m), particle counting system (e), flow meter (h) and oil cooler (j). **Filter test system (B)** consists conical (60°) reservoir (a), positive displacement system pump with drive (n), tested filter (d), differential pressure sensor, shut-off valves (c), two (one on input and one at output of tested filter) particle counting system (e), pressure sensor (l), back pressure valve (f), clean-up filter (g) for preparing system before entering the test dust, check valve (m), flow meter (h) and oil cooler (j).

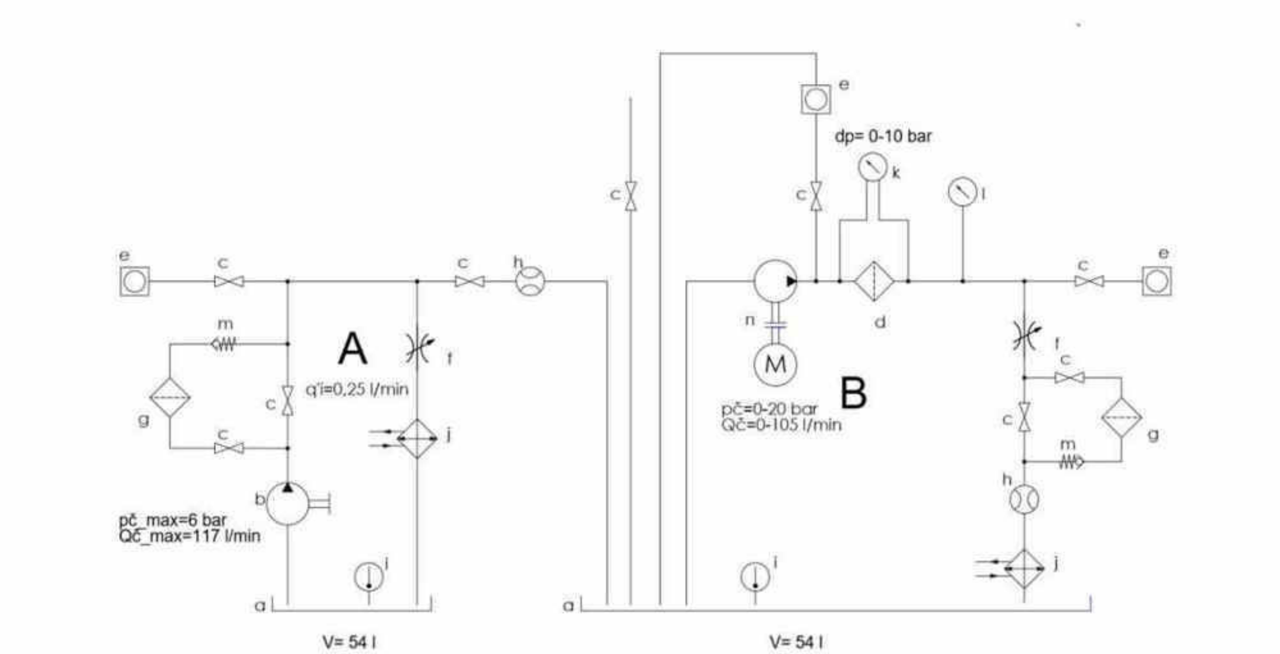

Fig. 1. Hydraulic circuit of multi-pass test rig [VIR = ISO 16889]

Figure 2 shows frame of new multipass filter test rig in development phase. We tested different construction type of pumps (Fig. 1, pos. b and n). Problem is with wear and cavitation, so in this way is very important to find correct construction of the pump.

Figure 3 shows two on-market accessible filters tested in the context of this research. Both filters have nominal filterability 20 µm.

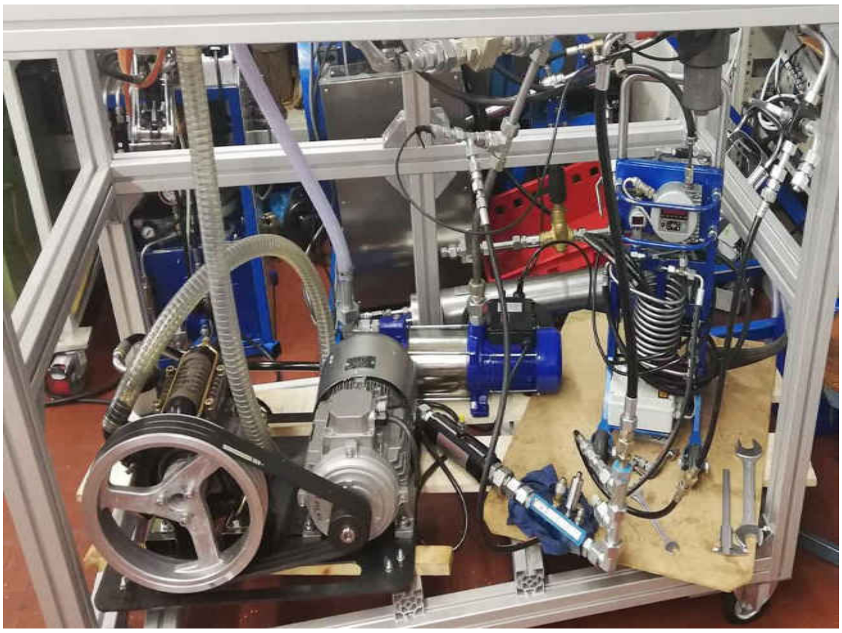

Fig. 2. Hydraulic test rig (in development phase)

Fig. 3. Tested hydraulic filters

3. Results and discussion

Two different standards, on market accessible filter element have been tested (Fig. 3).
Figure 4 shows results of filtration ratio ß for the first filter element. It is obvious that the smallest changes are seen in the particle size of 4 µm. Cleanliness in size of 4 µm was better just on start for 1 class of ß filtration ratio. At particle size of 6 µm was ß ratio 4 on the start, on the end it has fallen on ratio 2. The best result with the first filter element was for particle size of 14 µm. The best ß ratio, 9 was at the second period. On the end of the test was ß ratio 4 for particle size of 14 µm and more.
Figure 5 shows results of filtration ratio ß for the second filter element. It is also obvious, that the smallest changes are seen in the particle size of 4 µm. ß ratio for particle size of 4 µm was 2 just in third and fourth measurement in other measurement it was 1. At particle size of 6 µm was ß ratio 4 in six measurements, on the end it has also fallen on ratio 2. The best result with the second filter

element was for particle size of 14 µm. The best ß ratio, 11 was at the eight period. On the end of the test was ß ratio 10 for particle size of 14 µm and more. The second tested filter element (Fig. 5) was better than the first one (Fig. 4) in the way of filtration ration ß.

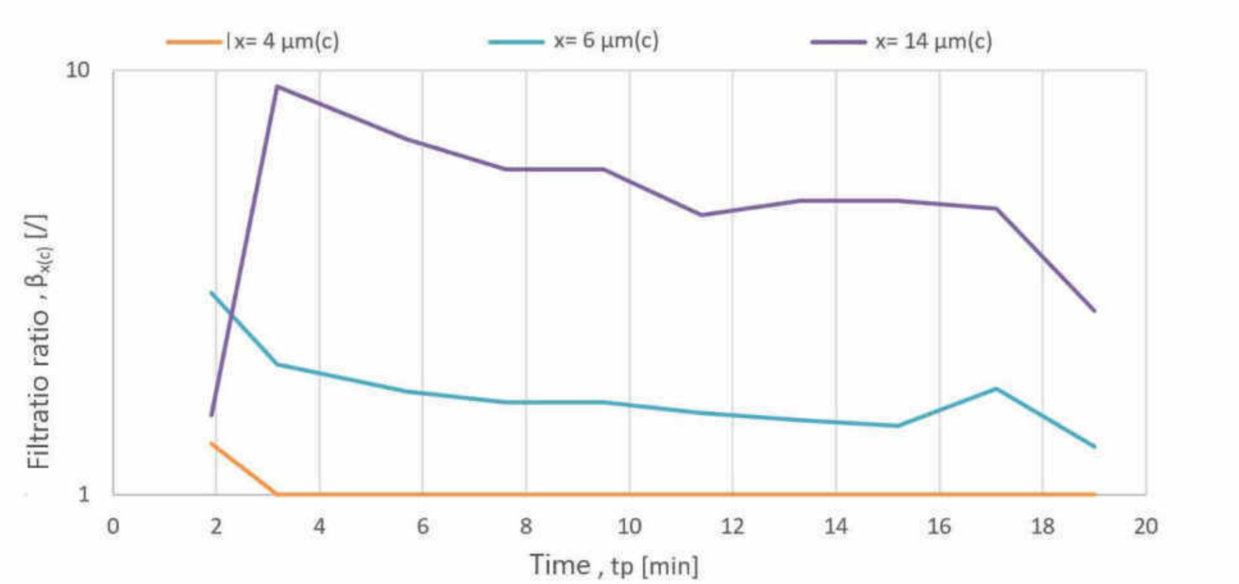

Fig. 4. Measuring results of the first tested filter

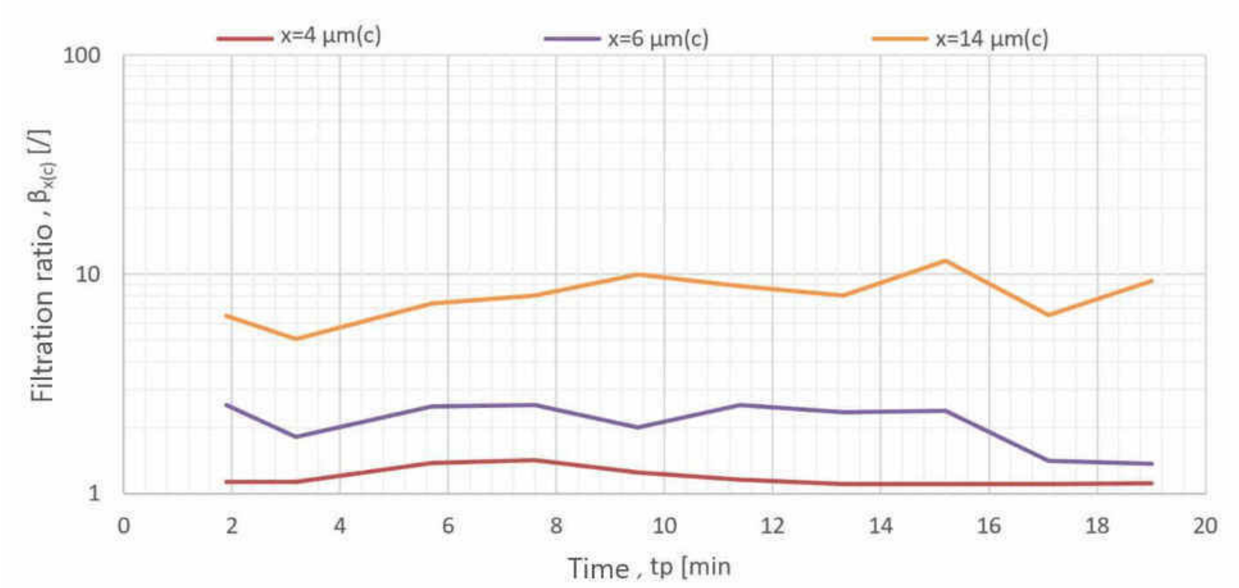

Fig. 5. Measuring results of the second tested filter

In addition to the filtration ratio, the quantitative absorption of the filter is also very important. Both filter elements have been weighed very carefully before and after the test. Results are shown in table 1.

Table 1: Results of weighing filters before and after the test

	Mass before test [g]	Mass after test [g]	Difference [g]	Calculated mass, m_R [g]
Filter element 1	189.807	193.527	3.720	5.02
Filter element 2	245.072	246.73	1.658	4.85

4. Conclusion

The ISO 16889 multi-pass test were examined and found out all the requirements for successful testing of hydraulic filter elements.

We designed and built a test rig with all the appropriate hydraulic components and measuring instruments that made it possible to test hydraulic filter elements.

We have found that, despite the recommendations of the standard, some hydraulic components are not available or are not suitable for testing under the conditions prescribed by the standard.

We successfully implemented configurations that improved the test conditions and did not affect the distribution of the test dust in the hydraulic fluid. The hydraulic pump pressure oscillations were reduced to the tolerable limit, ± 10%.

Testing of hydraulic filter cartridges was performed and the results obtained were analyzed according to the procedure prescribed by the standard. The measured final pressure drops on the filter elements were 2.57 bar in the first case and 3.55 bar in the second case. We have filled in all the necessary tables and plotted all the corresponding graphs.

We have found that hydraulic fluid must be handled carefully to prevent foaming, as air bubbles in the liquid affect the measured number of particles in the liquid. The average filtration ratio β had a value of 1 for the first test, for particles larger than or equal to 4 μm, due to the air bubbles in the hydraulic fluid resulting from foaming.

The results show that the test rig is suitable for testing according to ISO 16889. The average filtration ratio β for particles larger than or equal to 6 μm in the first test was 1.63 and 2.09 in the second. For particles larger than or equal to 14 μm, it was 4.65 in the first test and 7.4 in the second test, which makes sense given the nominal permeability of the filter cartridge.

We have identified the shortcomings of the test facility, especially in measuring equipment, which in some cases does not meet the requirements of the standard. Better measuring equipment would provide more accurate results, especially results related to filtration efficiency.

The multi-pass test can effectively evaluate the hydraulic filter elements. The test is suitable for testing all types and sizes of filter elements and shows us enough data to select the hydraulic element properly. A properly performed test gives a better idea of the effectiveness of the filter elements, and consequently it is easier to select the appropriate filter element that will ensure proper filtration of the hydraulic fluid and thus contribute to a better functioning of the hydraulic system.

Acknowledgments

The author is grateful to Slovenian company TRM PRO d.o.o for their financial and technical support. For technical support is author also grateful to Nejc Čegovnik and Rok Jelovčan.

References

[1] Zoeb, Heinz. *Filtrationstechnik*. Renningen-Malmsheim: expert –Verlag, 1996.
[2] SIST ISO 16889:2008. “Hydraulic fluid power – Filters –Multi-pass method for evaluating filtration performance of a filter element”.
[3] *O+P Fluidtechnik.* Filtration in hydraulischen systemen, Konstruktions-jahrbuch 2016.
[4] Peterlin, A. *Testiranje hidravličnih filtrov po standard*. Diploma thesis. Ljubljana, 2016.
[5] Čegovnik, N. *Preizkušanje hidravličnih filtrov po standard*. Master thesis. Ljubljana, 2018.

FLUID POWER, INDUSTRY 4.0 AND CIRCULAR ECONOMY

Petrin DRUMEA[1], Ana-Maria POPESCU[1], Cătălin DUMITRESCU[1]

[1] Hydraulics and Pneumatics Research Institute INOE 2000-IHP Bucharest, ihp@fluidas.ro

Abstract: *This article seeks to define some modern concepts regarding the economic and industrial development and make some general assessments on the framing of hydraulic drives in these approaches. The main connection of sustainable development with the circular economy and the 4th industrial revolution is highlighted, with arguments as close as possible to the engineering acceptation of social development. The material takes the basic elements of the definition of the three directions of analysis and makes brief remarks regarding some possible ways of aligning our area of activity with the current global trends.*

Keywords*: Sustainable development; circular economy; Industry 4.0; scientific research; development*

1. Introduction

In recent years, scientists have noticed some wrong directions that mankind, in its chaotic and, above all, mercantile development of the 20th century and the beginning of the 21st century, is going in. It is a good thing that there is a massive increase in production and consumption with no regard to costs, but isn't it true that lack of control leads to more serious problems and with irreparable consequences on medium and long term? The first serious warning occurred in 1970 and 1972 in Sweden and continued especially through the work of the World Commission for Environment and Development led by Gro Brundtland. In course of time, it has been accepted that sustainable development is the development that seeks to meet the needs of the present, without compromising the possibility of future generations to meet their own needs. In 1974 Lester R. Brown showed that there is a tendency to deplete natural energy resources, raw materials and even food, that mankind consumes renewable resources at a rate higher than their regenerative capacity and there can be noticed a physical deterioration and an accentuated pollution of some vital factors such as water, air and soil. One of the answers is the emergence of the circular economy model which involves first and foremost the idea of reducing waste and recycling materials, possibly subassemblies. It is necessary to give up the habit of throwing away the products that have reached the end of their lifespan and move to re-introducing them into the economy as assemblies or parts. An essential role in the change of mind is played by sustainable scientific research (and technical-scientific development) which must address the problems at global level, possibly only at a regional level, but in a way that will lead to smart growth. The spectacular increase of the scientific and technological level of the production has led a new form of development, known in our country as Industry 4.0. This industrial revolution also started from the fact that for several decades the manufacturing was transferred to Asia, so today the question of Europe's re-industrialization is posed for sustainable development. The problem of the technical-economic development of the countries is not just Europe's problem; it is felt in many countries of the world where it got all kinds of names, of which we mention IIC in USA, Industrial Value-Chain Initiative in Japan, Industrie de futur in France, and also a similar initiative in China.

2. Circular economy

In 1976 Walter Stahel and Genevieve Reday au elaborated for the European Commission a report called "The Potential for Substituting Manpower for Energy" in which they sketched the first model of circular economy through which the connection is made between design, manufacture, consumption of products and waste management process when these products exceed their lifespan. This signal was one of the first warnings regarding the need to give up the economic model of waste disposal in exchange for a system promoting the reuse, repair, reconditioning and recycling of seemingly outdated materials and products and the need to turn waste into raw material. This new concept helps the economy use fewer new materials and raw materials and create a new closed loop system through which existing products to be reused. While for technical and industrial products things are almost clear, for food, textiles, pharmaceuticals, etc. there is no repair, reconditioning, reuse, but there is the variant of recycling and extraction of special elements such as metals from household or biological waste. Many times, the question arises why so many complications are needed for something that seems unimportant. To give the correct answer we need to see that the global population grows, that the waste of materials also grows, while the essential raw materials are limited and already many countries no longer have them at their discretion. Early since 2015 the European Commission has adopted an action plan with 54 measures for the transition to the circular economy, through which to proceed to the correct management of waste.

There are a few things that should become principles of life for mankind, such as the idea that waste is raw material and not garbage, or energy should be obtained mainly from renewable sources, or to understand that it is important to use long-lifespan objects and reject disposable ones. In order to go in the direction of "zero waste" we must act from the design stage. In the field of hydraulic drives for a long time there are elements that can be included in the working methodologies of the concept of Circular Economy. In this regard, the maintenance, remanufacturing and metallizing practices can be analyzed.

Maintenance is defined as a combination of all technical, administrative and managerial actions that are taken during the life cycle of an equipment in order to maintain or restore its ability to perform the desired function (acc. to the European standard EN 13306). On this line, maintenance includes measurement activities, operation control, testing, fault detection, repair, adjustment, replacement of elements or subassemblies and service. It is obvious that repair or service activities are part of a complex action called maintenance and they can be included as part of the circular economy as well, given that they already exist in industrial practice and with ancient and widespread applications in hydraulic drives.

For example, as a result of the wear of the mobile equipment of the directional control valves, of the impurities of the oil or of other accidental causes, during the service life of the device the following failures were found by Italian specialists [1] and specialists of our institute; they, in principle, can be prevented by maintenance, can be repaired, parts can be remanufactured and only finally, when there are no resources, one shall obtain the residual waste (Table 1).

Table 1

Ref. no.	Failure	Cause	How to fix it
1	The directional control valve with electric control does not switch	- Electromagnet is out of order	- Check the functionality of the slide valve movement by pressing the operation button of the magnetic core - Check the coil voltage - Replace the coil or the entire electromagnet, as suited - Replace the push rod if it is battered
		- Slide valve is stuck	- Remove the slide valve from the body, wash both parts with oil, blow with air, lubricate the surfaces in contact and reassemble, and then test
		- The spring does not return to the starting position when the command is terminated	- Replace the broken or battered spring

2	The directional control valve or the pilot valve has large internal oil leaks	- Highly normal wear and tear due to exceeding the service life	- Replace the directional control valve
		- Accidental wear as a result of abrasive particles penetrating the directional control valve because of improper filtration	- Replace the oil, clean the installation, install new filter cartridges and then replace the hydraulic directional valve
3	Shocks (water hammer) on the system	- Throttling (timing) plate is out of order	- Disassemble the throttling plate and check the stroke of the one-way valve and the qualities of the spring - Replace the spring or the entire throttling plate
4	External oil losses	- O-rings, sealing cuffs are out of order	- Disassemble the directional control valve, the component parts, and replace the static and dynamic seals
5	Manual controls are not kept in the indexed position	- Springs are not strong enough, circular index notches have rounded edges	- Disassemble the manual control cover, ascertain the appearance of the spring, increase the prestressing force, or replace the piece and execute a new one with index notches

Maintenance ensures the continuity of production for as long as possible without interruptions that can cause a significant decrease in productivity, with the natural consequence of reducing the consumption of raw materials. In the case of complex equipment such as rotary hydraulic pumps and motors, when major failures occur, they are repaired and put back into use by replacing the totally compromised parts. This process of refurbishment, known and used for a long time, is a part of circular economy. The big difference between refurbishment and traditional reconditioning is that through refurbishment a complete disassembly of the complex hydraulic equipment takes place, a total check is made and all subassemblies and parts with problems are replaced [2]. Even the replaced components do not become garbage, but enter into a process of analysis and then restoration to the level of acceptability, in order to be reused in other situations of equipment failure.

There is a technology which, for a long time has been included among the hydraulic equipment repair technologies, especially hydraulic cylinders and hydraulic directional control valves. It is a simple technology, defined at the level of Wikipedia as a process through which coating is made with the necessary materials to some components such as rods or distribution slide valves undergoing significant wear and serious consequences. Metallizing - the technology in question - is suitable for medium and large dimension pieces, being ideal in covering their surfaces with zinc, aluminium, chromium, tungsten and other metals. Thickness of the coating layers which cover pieces for anticorrosive purposes, or restore the rubbed and worn layers, usually varies between 50-200 μm, but there are also much thicker coatings. Coating by metallizing is done according to international standards, ensuring a much longer life to the processed parts, compared to other processes similar as to their purpose.

Metallizing is not advantageous if one desires to process small parts (of the order of several millimeters).

Finally, Circular Economy can be visualized as in figure 1.

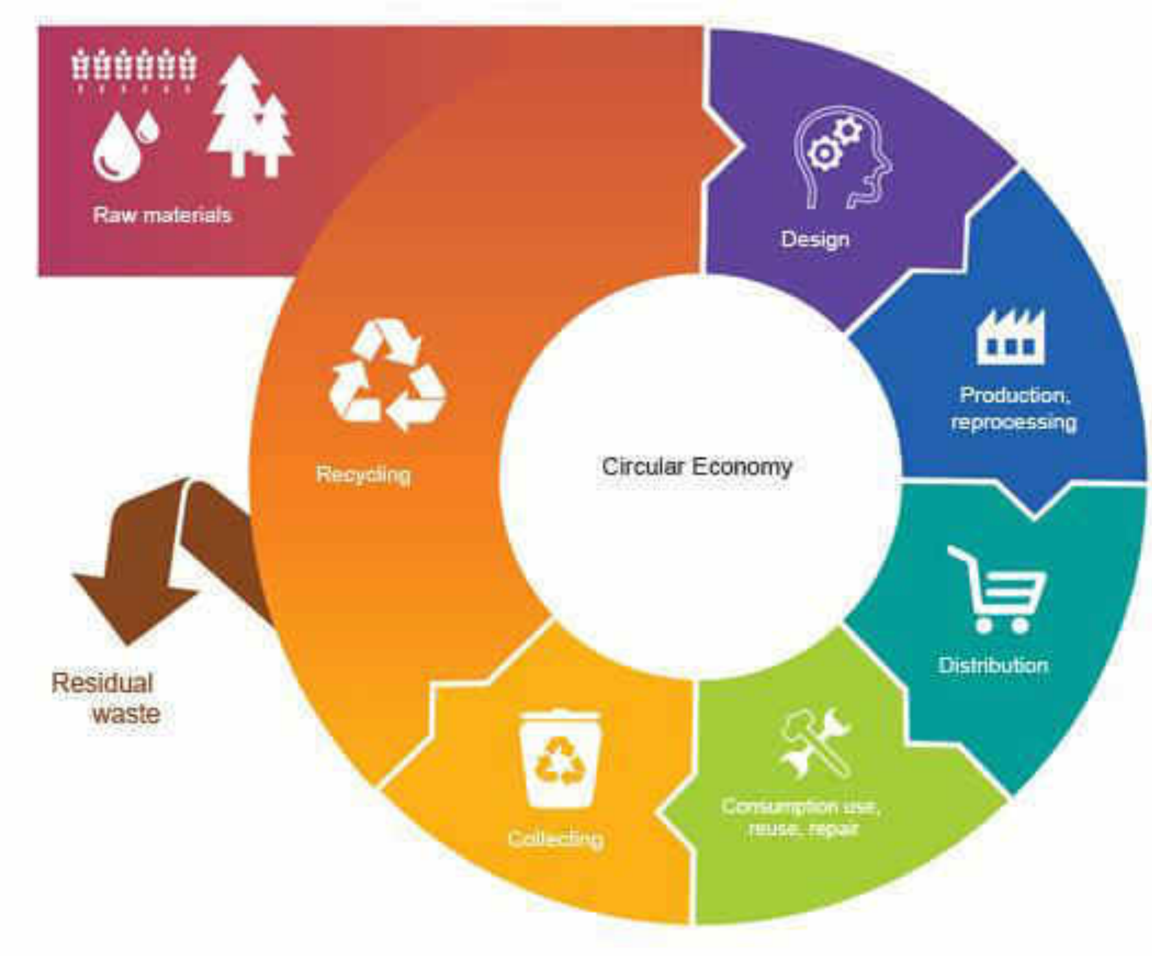

Fig. 1.

Source: [3]

Circular economy is a model of production and consumption that involves all stages, from design to consumption and then to recycling, resulting in only a small amount of waste comparable to raw material and initial materials.

3. Industry 4.0

The idea of Industry 4.0 is recent and was presented for the first time in 2011 at the exhibition in Hanover by a group of specialists from Germany (Henning Kagermann, Wolf-Dieter Lukas and Wolfgang Wahlster). While the label concepts of industrial revolutions were assigned to some stages of development of the world economy after their course was completed, the concept of Industry 4.0 has appeared and come into focus ever since the emergence of some components that we can categorize as small technological revolutions, such as the application of information and telecommunications technology, or new software technologies for modeling and simulation, or the development of cyber-physical systems for controlling physical processes and even the involvement of 3D printers in manufacturing. If the advances of the previous revolutions were taken readily and at an acceptable pace by most countries, transition to Industry 4.0 is fast and can be

performed only by the countries that have prepared their economy for such progress. For the first revolution, when the switch from the exploitation of animals to the use of water and steam in the engines of complex machines took place, mankind adapted quickly. The second industrial revolution allowed people to create physical connections through rail networks and connections of ideas through the telegraph, but also to improve the manufacturing process on modernized production lines through the special contribution of electricity. This technological revolution has been quite easily assimilated by most countries of the world and has been a great progress in the development of mankind.
At the end of the 20th century, the third industrial revolution took place, the digital one, which is quite difficult to be assimilated by mankind, already establishing noteworthy differences between countries.
The fourth industrial revolution, according to many specialists, is ongoing, and given the extremely high technical and scientific level special training is required for all countries.

An intuitive presentation of the course of these revolutions is shown in Fig. 2, taken from [4].

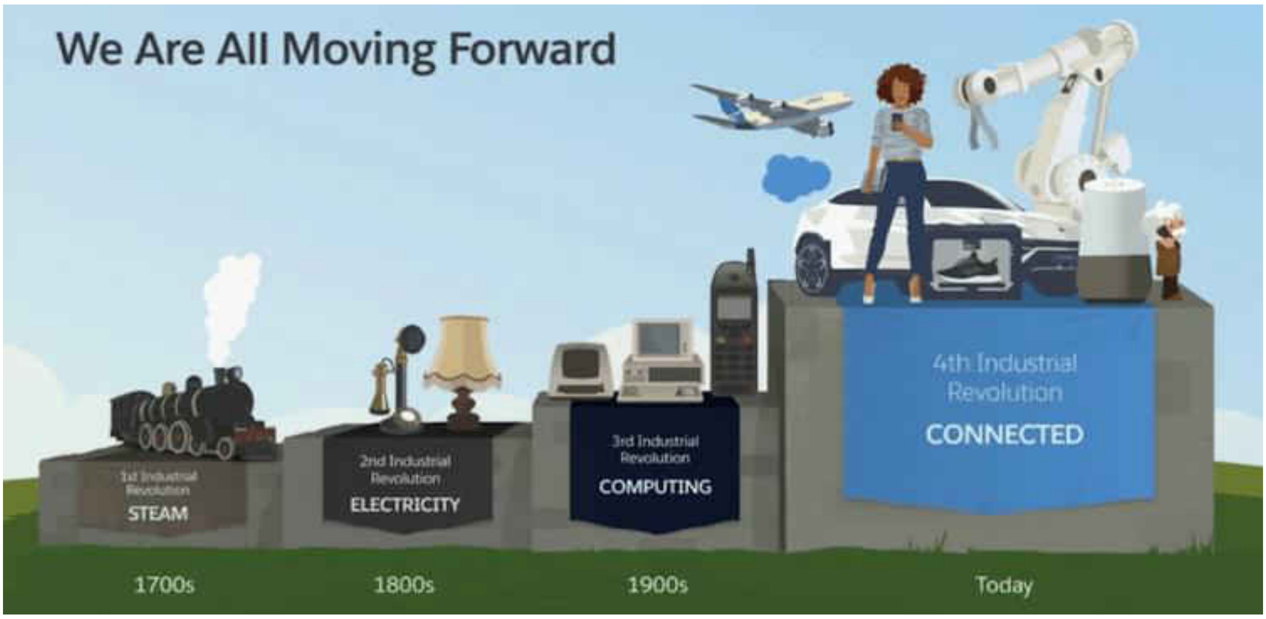

Fig. 2.

A country where notions like cyber-physical systems, the Internet of Things (IoT), the industrial Internet of Things (IIOT), cloud computing, etc. are not known well enough and mastered will have major problems in the process of framing in the progress implied by the new revolution Industry 4.0. The key to the success of this revolution seems to be the digitization process that applies in all industries and in all fields. In order for the economy of a country or a company to move on the road to Industry 4.0 it is absolutely mandatory for employees to be trained in understanding and applying the idea of digitization. The factory of the future becomes an intelligent factory that creates a convergence between the Internet and computerization, laying data and connectivity at the foundation of development. It is becoming increasingly clear that at this stage people and organizations alike need to transform and adapt to new technologies. The production will be full of interactions and connections, easy to fit into this industry of the future, but difficult to achieve given the problems that arise as a result of the many reorganizations and disruptions of resources and organizations. Another question that is often asked, besides the one that requires defining the concept in plain words, is the one that seeks the benefits of this industrial revolution. The first advantages are related to improved efficiency and increased productivity, both relating to

automation and increased professional performance of employees, and both raising the quality of products and services [5].
The problem that arises, unexpectedly, is that there are some disadvantages, too, among which there are some drawbacks related to the staff that see their creativity limited by technology, see the increase of the level of unemployment, and also sees the necessity and the difficulty of raising the level of initial and lifelong training. Although the technological level is in full growth, there can be noted an unexpected increase of the initial costs, an increase in efforts related to security of IoT, but especially an increase in the implementation time. In the paper of the specialists from Aachen [6] there is an interesting solution for structuring the manufacturing of a linear electro hydraulic actuator within the concept of Industry 4.0.
When analyzing the ways in which factories approach Industry 4.0, besides several expected possibilities, such as flexible production, manufacturing oriented to the consumer's demands, or increasing the role of data usage in manufacturing, there is also the need for a design capable of meeting the requirements of the circular economy with regard to recycling of raw materials.

4. Research and development

From what has been presented so far, it turns out that the support for Romania's involvement in the new global development trends is sustainable research and development which should use a cross-disciplinary systemic approach to processes and products, combining applied technical research with environmental research and social research.
This new research model engages besides specialized units such as universities and institutes also SMEs with specific research and development activities. Europe as a whole is trying to transform its standard economy into an economy based on innovation, through which to ensure competitiveness with the other economies in the world and to move to the sustainable development solution which takes into account the environment and resources. In March 2000 in Lisbon a target of 3% of GDP for research was set for European countries; this target has never been reached in Romania; on the contrary, it has decreased year by year. This has led to an alarming decline in the number of scientific research specialists, at the same time with an increase of their age. The attempts to develop the degree of innovation by increasing the number of patents did not produced the expected results, and the causes can easily be found in the absence of the real and steady forms of involvement of the researchers, but also in the complicated and expensive bureaucracy of studying and developing applications. Too many people without patents have become patent experts, advisors and school creators. Many ideas that emerged during this period were inefficient as neither the Technological Transfer Centers, nor the islands of excellence, nor other solutions initiated without a serious analysis carried out by specialists in the field proved to be useful or at least economical. Because applied research conducted by companies is possible where there are large, financially powerful companies it is clear that the best solution for Romania will be to maintain dedicated research units able to collaborate with SMEs. It is estimated that a large number of young people who will enter the research will work in areas that today do not exist and they will become a great added value in the management of new technologies. The natural conclusion is that the initial training, education and continuous professional development will become essential, as they will provide the basis for future development.

5. Conclusions

Industry 4.0 and Circular Economy represent two modern development trends, resulting from a serious, multidisciplinary analysis regarding the future of human society in general and Europe’s future in particular. The two research directions are essential for our future; they are not the fancies of guys posing as specialists, but represent probably the most important elements of perspective research, with direct and unfortunately very fast impact on life on the planet. These two areas are part of the general idea of sustainable development and come upon us with or without our will. Our country is involved in both topics and has managed to overcome the theoretical phase, moving to the implementation of many of the basic principles of these directions, without deconcentrating at the level of companies and specialists the elements that are generally discussed at global and national level.

Acknowledgments

This paper has been funded by the Romanian Ministry of Research and Innovation under Programme I - Development of national R&D system, Subprogramme 1.2 – Institutional performance – Projects financing excellence in R&D+I, Financial Agreement no. 19PFE/17.10.2018.

References

[1] ASSOFLUID. *Hydraulics in Industrial and Mobile Applications*. Brugherio (Milano), Grafiche Parole Nuove s.r.l. Publishing House, 2007.
[2] Prodan, Dan, and Sorin Marinescu. *Refabricarea si modernizarea masinilor-unelte: sisteme hidraulice / Remanufacturing and modernization of machine tools: hydraulic systems*. Bucharest, Technical Publishing House, 2005.
[3] https://www.europarl.europa.eu/news/ro/headlines/economy/20151201STO05603/economia-circulara-definitie-importanta-si-beneficii. Accessed October 8, 2019.
[4] https://www.salesforce.com/blog/2018/12/what-is-the-fourth-industrial-revolution-4IR.html. Accessed October 10, 2019.
[5] Marin, V., et al. *Sisteme hidraulice de actionare si reglare automata. Probleme practice. Proiectare, executie, exploatare / Practical problems. Design, execution, operation*. Bucharest, Technical Publishing House, 1981.
[6] Alt, Raphael, Hubertus Murrenhoff, and Katharina Schmitz. “A survey of „Industry 4.0” in the field of Fluid Power- challenges and opportunities by the example of field device integration.” Paper presented at the 11th International Fluid Power Conference, Aachen, Germany, March 19-21, 2018.

ISSN 1454 - 8003
Proceedings of 2019 International Conference on Hydraulics and Pneumatics - HERVEX
November 13-15, Băile Govora, Romania

RESEARCHES REGARDING THE DESIGN AND CONSTRUCTION OF AIR DISPERSION DEVICES IN THE TRANSPORTED WATER THROUGH PIPES

Octavian DONȚU[1], Rasha CUSMA[1], Constantin Remus VOICU[1], Iulian Alexandru GRIGORE[1], Francesca ȘELEA[1], Nicolae BĂRAN[1], Mihaela PETROȘEL[1], Titu-Cătălin CIOIENARU[1]

[1] University Politehnica of Bucharest, Faculty of Mechanical and Mechatronic Engineering, remus.voicu@yahoo.com

Abstract: *The research paper presents three devices for the dispersion of the air into the water:*
1) Device realized with the help of a 3D printer;
2) Device based on the construction of „ARHIMEDE's" spiral, which has 18 holes for the dispersion of the air in the transversal section of the tube;
3) Device which places a number of 17 holes generated by syringe needles into the transversal section. Each device (needle) that disperses the air into the wastewater transported inside of the tube, has the purpose to increase the concentration of the dissolved oxygen into the water.

Keywords: *Wastewater treatment, dissolved oxygen into the water.*

1. Introduction

Water aeration represents a process of mass transfer of the oxygen from the atmospheric air to a volume of water; resulting in an increase of the concentration of the dissolved oxygen into the water.
The water aeration systems constitute a certain energy consumption; which through the usage of modern technology construction of these systems it can obtain a reduction of energy consumption.
In the research papers [1], [2], [3] it shows the fact that pneumatic aeration is far more superior to the mechanical aeration systems.
The most developed aeration systems are the ones that produce fine air bubbles [4], [5] in which the aeration of the wastewaters is done through the introduction of compressed air into the water pipes used to transport the wastewaters.
Through this constructive solution, the aeration tanks filled with hundreds of m^3 are eliminated, thus the investment is reduced and a cost saving is made from the operating costs of the wastewaters treatment.
In stagnant systems, the transfer of one molecular species in the interior of the system is realized through a process of mass transfer which is called molecular diffusion.
In the case where we have a displacement of the fluid which contains a certain component the result is a convective diffusion.
The component is transferred due to the difference in concentration; the flow rate of the fluid is determined by the intensity of the mass transfer [6].
In table 1, mass transfer in specialty technic is presented.

Table 1: Classification of the diffusion processes

The environment in which the process takes place	**The nature of the flow**	**Flow regime**	**Nature of the diffusion phenomenon**
A-Stagnant Fluid ($w = 0$)	-	-	Molecular diffusion
B-Fluid in motion ($\mathrm{w} > 0$)	B1-free movement	-	Natural convective diffusion (Natural mass convection)
	B2-forced movement	Laminar flow	Forced convective diffusion (Forced mass convection)
		Turbulent flow regime	Forced convective diffusion (Forced mass convection)

2. Flow spectrum and the establishment of the flow regime of the biphasic fluid (air + water)

The structure of the biphasic flow regime, respectively how the geometric form and the phases are arranged is important for the thermodynamic interplay between the two phases

- Liquid phase: water;
- Gaseous phase: air.

The biphasic flow can take place in horizontal and vertical pipes.
In horizontal pipes case, a stratified flow can occur due to the difference in density $\rho_{apă} > \rho_{aer}$ (figure 1.a).
In vertical pipes case, the air bubbles are dispersed in the liquid mass (figure 1.b).

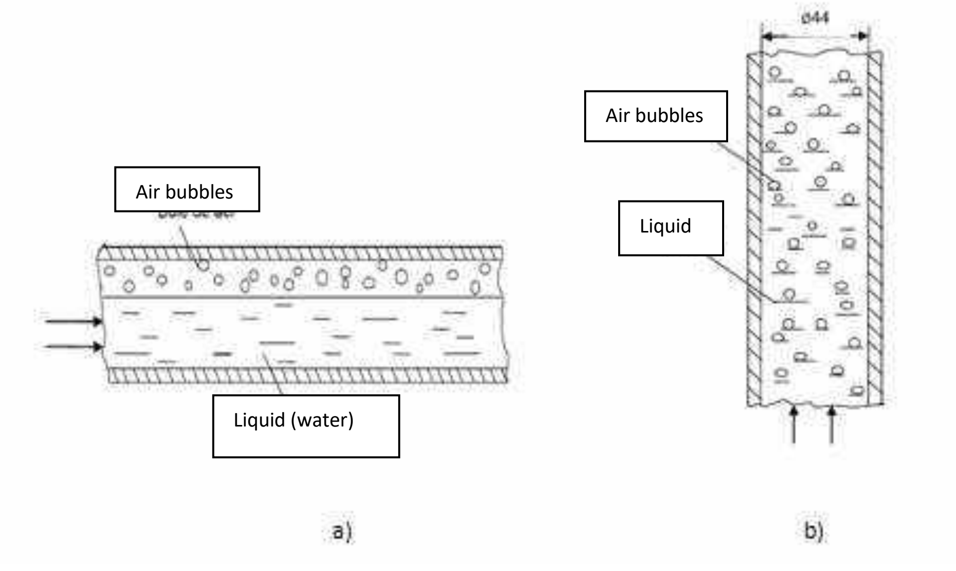

Fig. 1. Biphasic flow spectrum in horizontal (a) and vertical (b) pipes

Establishment of the flow regime of the biphasic mixture (water + air) is done as follows: the water volume that needs to be aerated in half is $0.125\ m^3$.

This volume will be pumped through a pipe of $\emptyset 50 \times 3$, as a result, the water flow (V) and the speed of the water (w) in the pipe will be [7], [8]:

$$\dot{V} = \frac{V}{\tau} = \frac{0,125}{2 \cdot 3600} = 0.01736 \cdot 10^{-3}\ m^3/s \tag{1}$$

$$\dot{V} = A \cdot w = \pi \cdot \frac{d^2}{4} \cdot w = 0.01736 \cdot 10^{-3}\ m^3/s \tag{2}$$

$$w = \frac{\dot{V}}{0.785 \cdot d^2} = \frac{0.01736 \cdot 10^{-3}}{0.785 \cdot (0.044)^2} = 0.0114\ m^3/s \tag{3}$$

For water at $20℃$ cinematic viscosity:

$$\nu = 1 \cdot 10^{-6}\, m^2/s \tag{4}$$

$$R_e = \frac{w \cdot d}{\nu} = \frac{0.0114 \cdot 0.044}{1 \cdot 10^{-6}} = 501.6 \tag{5}$$

The flow regime for the water is $(R_e < 2320)$, a laminar flow.
The air flow introduced into the water [9], [10]:

$$\dot{V} = \frac{0,6}{3600} = 0.0001666\ m^3/s \tag{6}$$

The low result value does not modify the flow regime established before.

3. Construction of the air dispersion device into the water with the help of a 3D printer

The pipe $\emptyset 50 \times 3$ has an inner diameter of 44mm; three circles with the diameters of 11mm, 22mm and 33mm are chosen, so that the holes created on the circles will assure an equal distribution of the air in the pipe.

The length of the circles will be:

$$\begin{aligned} L_1 &= \pi \cdot d_1 = \pi \cdot 11 = 34.56\, mm \\ L_2 &= \pi \cdot d_2 = \pi \cdot 22 = 69.12\, mm \\ L_3 &= \pi \cdot d_3 = \pi \cdot 33 = 103.67\, mm \end{aligned} \tag{7}$$

Total length $L_t = 207.35\, mm$.

A number of 17 holes will be placed at a distance of l equal to:

$$l = \frac{L_t}{n} = \frac{207.35}{17} = 12.19\, mm \tag{8}$$

On the first circle (figure 2) a number of holes will be determined:

$$n_1 = \frac{34.56}{12.19} = 2.8 \cong 3\, holes \tag{9}$$

The number of holes is determined for the second and third circle:

$$n_2 = \frac{69.12}{12.19} = 5.6 \cong 6\, holes \tag{10}$$

$$n_3 = \frac{103.67}{12.19} = 8.5 \cong 8\, holes \tag{11}$$

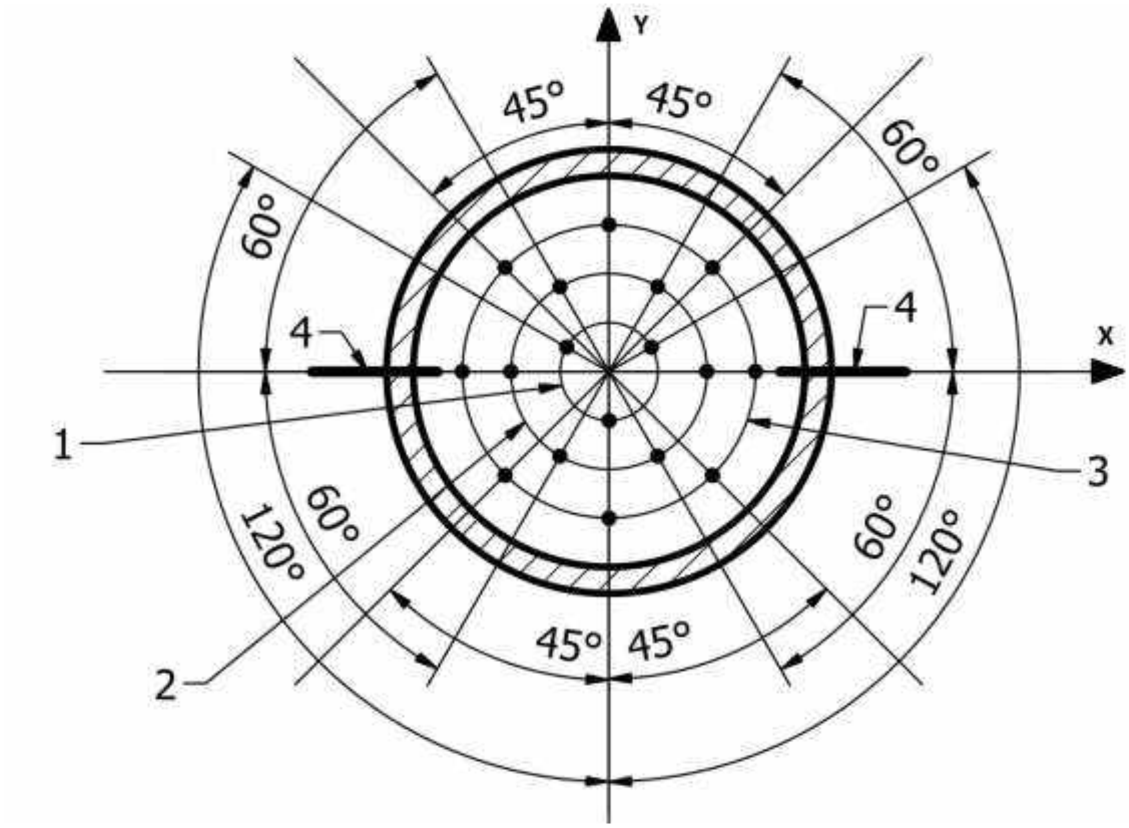

Fig. 2. The location of the three circles inside the pipe with $\emptyset 50 \times 3\ mm$
1-circle with $\emptyset\ 11\ mm$;2-circle with $\emptyset\ 22\ \mathrm{mm}$;3-circle with $\emptyset\ 33\ \mathrm{mm}$;4-coupling for compressed air.

On the first circle (1) 3 holes of $\emptyset\ 0.3\ mm$ are located at 120°; on the second cirle (2) 6 holes of $\emptyset\ 0.3\ mm$ are located at 60°; on the third circle (3) 8 holes of $\emptyset\ 0.3\ mm$ are located at 45°.
An uniform distribution of the air in the transversal section of the pipe is acquired by having an equal distance between the circles equal to 5mm. [11], [12].
The compressed air is introduced in through the air coupling 4 in the circle 3 and then in the circle 2 and 1 (figure 3).

Fig. 3. Compressed air dispersion device build on the 3D printer

The circles were materialized through $\emptyset\ 3\ mm$ pipes build on a 3D printer.

4. Construction of a device based on the construction of Spiral of Archimedes

The spiral is provided with 17 holes of $\emptyset\, 0.3\, mm$ located at an equal distance along the spiral (figure 4).

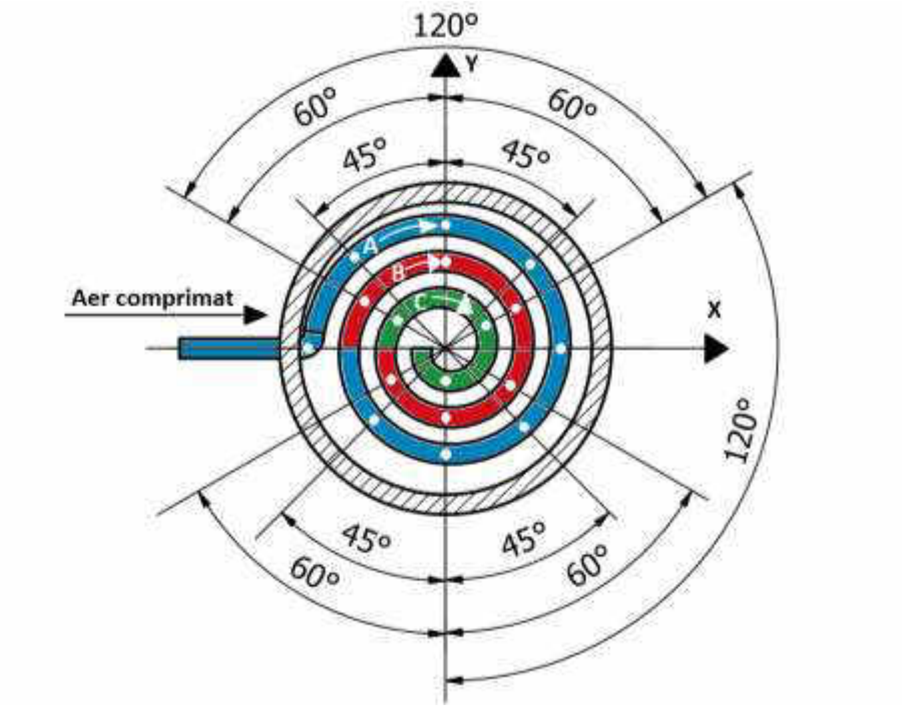

Fig. 4. Location of the 17 holes on the coper pipe $\emptyset\, 3 \times 1$ spiral

- on the first section of the spiral (green color) 3 holes at 120˚ are located [13];
- on the second section (red color) 6 holes at 60˚ are located;
- on the last section of the spiral (blue color) 8 holes at 45˚ are located.

The compressed air follows the ABC path. At a scale of 1:1 the spiral can be seen in figure 5.

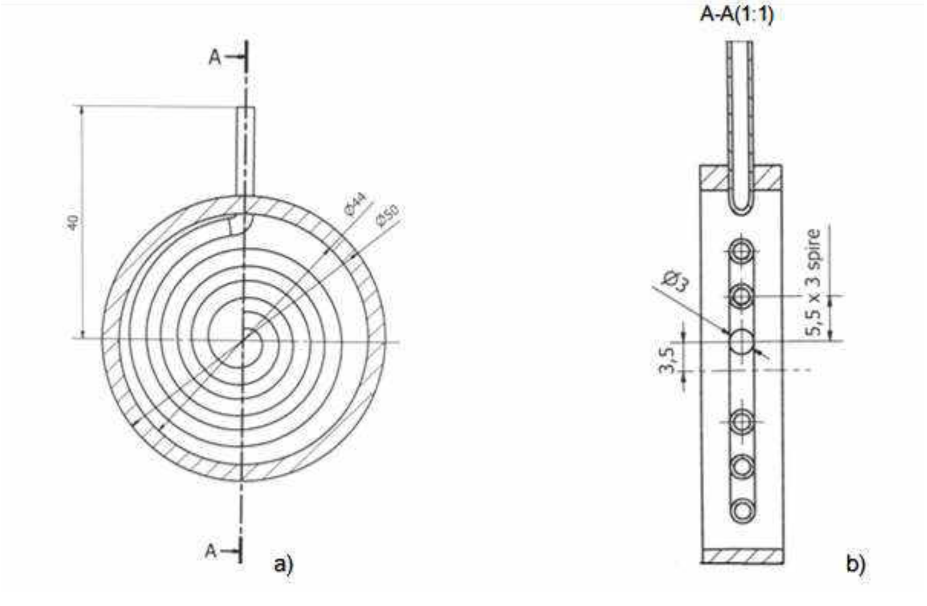

Fig. 5. Plan view (a) and a section view (b) of the spiral

An axonometric view of the spiral can be seen in figure 6.

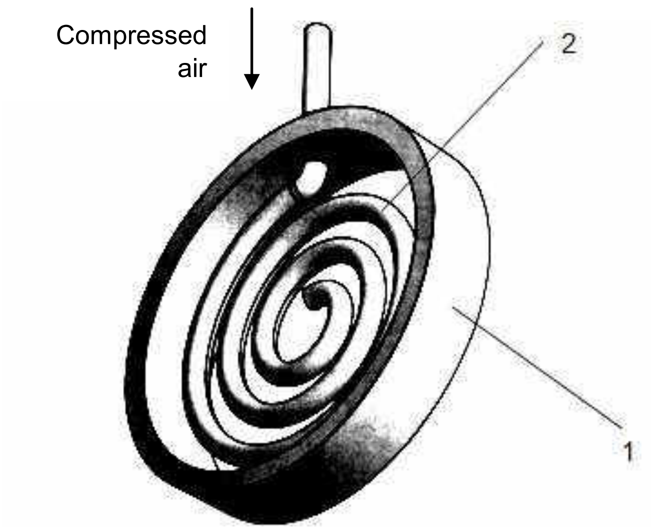

Fig. 6. Axonometric view of the spiral
1-pipe $\emptyset 50 \times 3$; 2-pipe spiral $\emptyset\ 3 \times 1$.

The water flows in the interior of the pipe through the spaces between the constructive elements of the spiral; the compressed air gets out of the holes of the spiral and flows in same direction as the water flow does.

5. Construction of a device where 17 syringe needles $\emptyset\ 0.25\ mm$ are located in the pipe's section

In the 7th figure it can be observed that the compressed air from the tank (1) is assigned to the 17 syringe needles that generate holes where the air is introduced into the water; the air jets generate a movement into the water that creates meaningful turbulence [14].

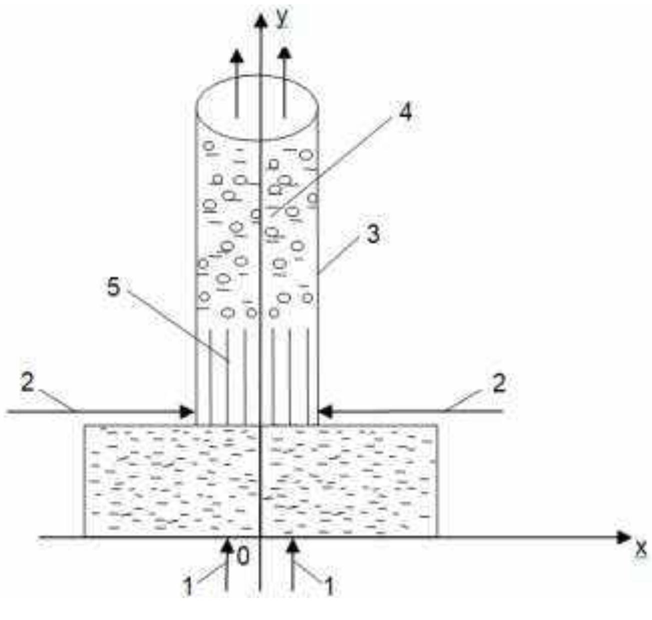

Fig. 7. Air dispersion device into the water

1-coupling for compressed air; 2-water inlet; 3-pipe $\emptyset 50 \times 3$; 4-biphasic mixture (air+water); 5-syringe needles with $\emptyset\ 0.25\ mm$.

The air gets in the tank through the inlet couplings (1), then in the syringe needles and flows in the same direction with the water flow in vertical direction.

6. Conclusion

All three devices assure the immersion into the water of fine air bubbles which in fact can be translated as transfer of the oxygen into the water.
The devices can be mounted on vertical pipes as well as on horizontal pipes.
In the experimental researches that will be presented in a future paper the following points will be taken into account:

- Measurement of the concentration of dissolved oxygen into the water at different lengths along the pipe
- Air flow or water flow's influence on the variation of the concentration of dissolved oxygen into the water

Acknowledgements

This work was supported by a grant of the Romanian National Authority for Scientific Research and Innovation, CCDI – UEFISCDI, project number Manunet – MNETI/ENER2307-CEBIOTREAT within PNCDI.

References

[1] Oprina, Gariela. “Hydro-gas-dynamic contributions of porous diffusers.” PhD thesis, University Politehnica of Bucharest, 2007.
[2] Mateescu, Gabrilea Maria. “Hydro-gas-dynamic of fine bubbles.” PhD thesis, University Politehnica of Bucharest, 2011.
[3] Law, C.N.S., and B.C. Khoo.“Transport across a turbulent air-water interface.” *AICHE Journal* 48, no. 9 (2002): 1856-1868.
[4] Băran, Nicolae, Mihaela Călușaru, and Gabriela Mateescu. “Influence of the architecture of fine bubble generators on the variation of the concentration of oxygen dissolved in water.” *Scientific Bulletin of University Politehnica of Bucharest*, *D series, Mechanical engineering* 75, no. 3 (2013): 225-236.
[5] Tănase, Betrice Elena. “Influența compoziției gazului insuflat în apă asupra conținutului de oxigen dizolvat.” PhD thesis, University Politehnica of Bucharest, 2017.
[6] Marinescu, Mircea, et al. *Mass and Heat Transfer*. Bucharest, Politehnica Press, 2000.
[7] Dobrovicescu Alexandru, Nicolae Băran et al. *Elements of Technic Thermodynamic*. Bucharest, Politehnica Press, 2009.
[8] Isbășoiu, Gh. C.E. *Fluid mechanics treaty*. Bucharest, AGIR Publishing House, 2011.
[9] Rasha (Cusma), Mlisan. “Influence of the fine bubble generators architecture on the concentration's growth of dissolved oxygen into the water.” PhD thesis, University Politehnica of Bucharest.
[10] Vlăsceanu (Banu), Mihaela, Dan Robescu, and Mihaela Călușaru (Constantin). “Theoretical and experimental research concerning the modification of dissolved oxygen concentration in aeration tanks equipped with surface aerators.” *Scientific Bulletin of University Politehnica of Bucharest, D series, Mechanical Engineering* 77, no. 1 (2015): 177-184.
[11] Chansonn, Hubert. “Air-Water Interface Area in Self-Aerated Flows.” *Water Res*. 28, no.4 (April 1994): 923-929.
[12] Pătulea, Alexandru. “Influence of the functional parameters and the fine bubble generators architecture on the efficiency of aeration installations.”,PhD thesis, University Politehnica of Bucharest, 2012.
[13] Radu, Constantin. *Linear algebra, Analytic and differential geometry*. Bucharest, Fair Partners Publishing House, 2008.
[14] Albu, Nicoleta, Nicolae Băran, Mihaela Petroșel, Daniel Besnea, and Mihaela Constantin. “Research Regarding the Execution of a Flat Jet Generator used for Water Aeration.” *Hidraulica,* no. 2 (June 2019): 23-28.

ISSN 1454 - 8003
Proceedings of 2019 International Conference on Hydraulics and Pneumatics - HERVEX
November 13-15, Băile Govora, Romania

BIOMASS CONVEYOR BELTS IN MICROWAVE FIELD

Alexandru HRISTEA[1], Adrian PEREBICIANU[2], Gabriela MATACHE[1], Ștefan-Mihai ȘEFU[1]

[1] INOE 2000- IHP, hristea.ihp@fluidas.ro

[2] S.C. LAMBDA MAT, prebiceanu@yahoo.com

Abstract: *An important component in the use of biomass is the transport system, as part of the machinery or equipment specific to a certain type of processing. Thus, a transport system is a mechanical system used to move materials from one place to another and is found in most processing and production industries, such as the chemical, mechanical, auto, mineral, pharmaceutical, electronic, etc. The paper presents a solution developed by INOE 2000 - IHP in partnership with a production company S.C LAMBDA MAT Bucharest.*

Keywords*: Biomass, transportation system, microwave*

1. Introduction

Biomass, the main fuel in rural area, can be used for heating livable spaces, water and for cooking. The maximum exploitation potential of the biomass implies the total use of the residues from the logging, the sawdust and other wood residues, the agricultural waste resulting from cereals or maize stalks, the vegetal residues of the vine as well as the urban waste and household residues.

From the point of view of the resources at least, bioenergy can make a decisive contribution due to the significant unexplored potential, coming from the available surface of agricultural area that Romania have. During the consultations that took place within the G2G European project, the Romanian experts in biomass energy agreed that biomass will make a major contribution to achieving the objectives set by the European Directive. A compromise must be made between the market potential and political objectives, which is in fact the role of strategic documents, such as the Biomass Action Plan. There are been made estimates regarding the other renewable sources of energy outside the biomass, the values ` being close to those presented in the PNAER.

The use of biomass has a great benefit for the atmosphere, which leads to a favorable balance of CO2, because the organic matter is able to retain more CO2 than that released by its combustion. Biomass can be obtained in a sustainable and renewable way, where the consumption speeds of these residues are not faster than their production speeds, giving a favorable balance for CO2 [3].

An important component in the use of biomass production is the transportation system, as part of the specific machinery or equipment to a certain type of processing. Thus, a transport system is a mechanical system used to move the materials from one place to another, and is found in most processing and production industries, such as the chemical, mechanical, auto, mineral, pharmaceutical, electronic, etc.

2. 2. Types of transporters used in the biomass transport system

The transport of biomass, as in any field, is a very an important activity, being sometimes determinant for establishing the speed of a technological process. This ensures the mechanization for lifting and transportation operations in the individual production, from small series to mass production, between the different machines and installations that make up the technological lines, automated lines or flexible processing systems [4].

Continuous transport equipment according to their construction characteristics include conveyors, which ensure a continuous flow of individual or bulk loads.

The conveyors, depending on the construction, are divided into two large groups:

● conveyors with flexible traction member: - conveyors with belt;

● conveyors without flexible traction member: - oscillating conveyors;

Conveyor belts

The lifting and transporting machines are made up of components of general use such as components of assembly, transmission of movement, bearings, couplings, etc.

The construction of conveyor belts is basically the same, even if the flexible traction component is a rubber band with textile, steel or wire mesh inserts. The main parts of a belt conveyor are shown in Fig. 1

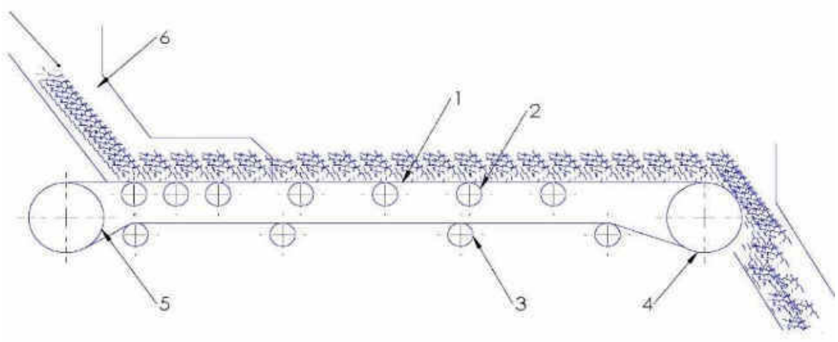

Fig. 1. Belt conveyor: 1- conveyor belt; 2- upper support rollers; 3- lower support rollers; 4- reel drive; 5- tensioning drum; 6- charging device; 7 device unloading.

Depending on the working conditions, the conveyor belts can also be provided with different devices for cleaning the belt suface, weighing, braking or blocking, etc.

The conveyor may be horizontal, or it may also be inclined over the entire length or portion of it.

From the point of view of the use of the belt, the conveyors can be:

► with flat surface, when used for the transport of individual loads (Fig. 2.a);

► with gutter-shaped tape, the surface being bent only on the loaded branch, in which case more material is transported than to the flat tape and usually loose material (Fig. 2.b).

The support components ensure the support of the conveyer belts on both sides, load branch and the return branch. The conveyer surface may be supported on boards, rollers or combinations of roller boards, but due to the frictional heating with the panels, the rollers are most commonly used in the construction of conveyors.

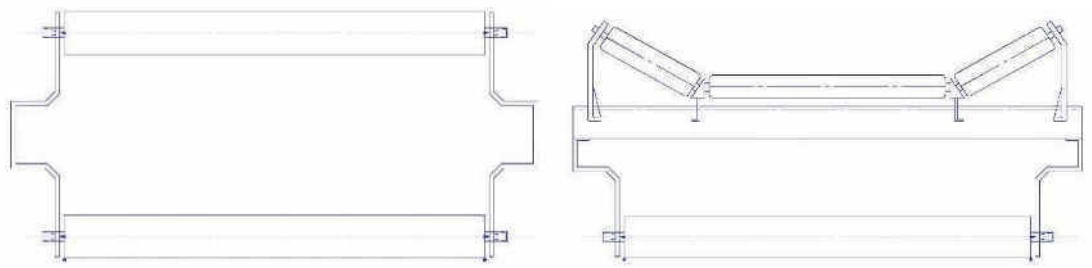

Fig. 2. Conveyor: a- with flat surface; b- with gutter-shape surface

Conveyor belts must meet specific requirements such as:

- high tensile strength in order to assure the traction force;
- sufficient elasticity to be able to withstand a large number of bends, when passing over rollers;
- not to lengthen much during operation;
- be resistant to abrasion from the material and to moisture, possibly weathering;
- to resist the chemical action of foodstuffs;
- be easy to repair and repair in case of breakage.

3. Conveyor belt in microwave field

When using the microwave as a biomass drying system, the selection of the material for fabrication the conveyor belt must also take into account the properties of the material in contact with the microwave. In this case, the selection of a plastic material that not influence the microwave field favors the life exploitation, the thermal influence being caused only by the contribution of the material (biomass) that will be heated under the action of the microwave.

Microwave heating is related to the polarization effect in the material with dielectric load, exposed to high frequency electromagnetic energy through waveguides. As a result of polarization, the electromagnetic waves are refracted and attenuated in dielectric material.

During microwave penetration into the resonant cavity, the electromagnetic waves undergo attenuation inside the microwave exposed material. If an electromagnetic wave of a certain density power reaches the surface of the dielectric (P_{in}), part of its density is reflected (P_{out}), while another part is absorbed by the dielectric material (P_{abs}).

The depth of penetration (Dp) in the material is an important parameter in the design of the heating systems in the radio frequency field because it gives information about the heat distribution in the material subjected to the heating. This parameter is defined as the depth material at which the power flow decreases to 1 / e (= 0.368) relative to the surface value and is described by the expression:

$$D_p = \frac{\lambda_0}{2\pi\sqrt{2\varepsilon'}} * \frac{1}{\sqrt{\{1+\left(\frac{\varepsilon''}{\varepsilon'}\right)^2\}^{0.5} - 1}}$$

In the case of ε '' ≤ ε ', the above equation is simplified in the form equation leading to values with an error of up to 10%:

$$D_p \approx \frac{\lambda_0\sqrt{\varepsilon'}}{2\pi\varepsilon''}$$

In the case of a semi-infinite layer of ideal material (eg having constant temperature values of the parameters ε 'and ε' ') on which a plane wave acts at the normal incidence, the temperature increase in the material with the depth follows an exponential function. In Fig. 3 the temperature variation with the depth of penetration into the material is represented graphically.

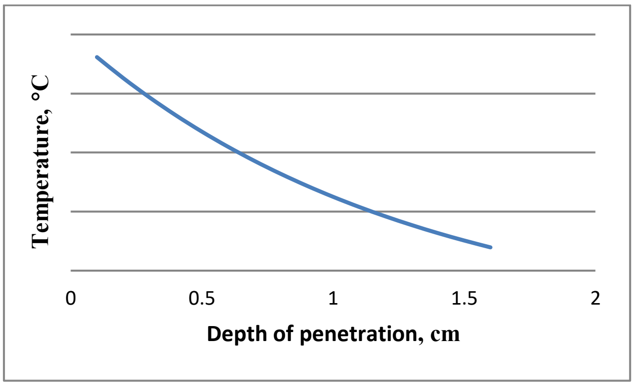

Fig. 3. Temperature variation with the depth of penetration into the material

An approximation of the heat distribution in a thin plate, heated consecutively on each face, can be made by overlapping two such exponential distributions having the origins in the two surfaces. It should be mentioned that the existence of this parameter does not limit the mass heating of the material beyond the penetration depth. The effect of the penetration depth is based on the dielectric loss factor ε '', which causes the power dissipation. As a result of this power dissipation, the density of the power flow decreases as the wave propagates into the material. It is interesting to note that, at a constant value of the loss factor ε '', the penetration depth increases with the relative permittivity ε '. This behavior is due to the fact that, as ε 'increases, the characteristic impedance Z0 of the medium decreases (as 1 / √ε'), therefore the stress of the electric field. They also decrease where the density of the power flow remains constant. Since the power dissipated on the volume unit is proportional to Ei^2, and it will decrease, therefore less energy will be taken from the wave as it advances in the material, the depth of penetration being thus greater [8].

It should be noted that the relative dielectric permittivity of a material is not constant, as it varies depending on the electrical parameters and the frequency of the electromagnetic wave. In addition, it is affected by the temperature, the degree of packaging, the humidity and the conductivity of the materials [1].

In the case of Teflon, for the relative electrical permittivity of 2.10 at 22ºC, the depth of field penetration at a frequency of 3 GHz is 146.44 m. For the frequency of 2.45 GHz, the depth of penetration at 20ºC is 32.56 m.

In addition, the maximum operating temperature of the Teflon being 260ºC, it recommends it as a material that can be used under the conditions of the drying process of the biomass for which the maximum working temperature can reach 150ºC.

4. The main technical parameters for the transportable installations

They are:

1. Productivity, expresses the quantity of material transported in the unit of time and is given by the relation:

$$Q = 3.6 \cdot q \cdot v, \text{ in t / h}$$

wherein q is the linear load, in kg / m; speed of material advancement, in m / s.
In the calculations a productivity will be taken that depends on the degree of unevenness:
Q calculation = average Q ·k
where k is the coefficient of nonuniformity, (k = 1,1….1,25).

2. The granulation of the spilled material is determined by means of the diagrams and depends on its nature.

3. The volumetric weight, represents the weight of the material spilled from a unit volume and is expressed in kN / m3.
4. The angle of the natural slope, at rest or in motion of the material, represents the angle between the generator of the cone of spilled material, which is deposited freely on a horizontal flat surface and that surface. This angle is equal to the interior friction angle of the material and depends on the nature of the bulk material [5].

Conveyor belt testing

The main conditions that the conveyor belts must meet are the following:
• high longitudinal resistance to breaking;
• both longitudinal (when winding on the drums) and transversal (to take the shape of the gutter) flexibility;
• limited cross stiffness so as not to open too much between two roller supports;
• puncture resistance (for sharpened wood type);
• high wear resistance given by the material being transported;
• reduced hygroscopicity;
• maximum stability at temperature increases;
• anti-flammability;
• not to charge electrostatically.

The characteristics of the conveyor belts regarding the fireproof are also very important. The material handling systems are often the most important component of a modern complex machine, knowing that without efficient transportation, production can be severely affected. The conveyor efficiency depends largely on the working conditions, the life of the belt itself, but the conditions under which it must operate can be extremely difficult, given the resistance, impact, abrasion, bacteria, water, fire and general mechanics damages. When constructing a conveyor belt, we must assume that the conveyor belt used is not a fire generator and should not help on propagate the fire.

The sawdust deposited on different installations can ignite from sparks generated from friction, welding or cutting with flame and incandescent burn. One solution to reduce the impact of fire is to use PVC coating on the conveyor belt.

Figure 4 shows the conveyor belt that was designed within the POC project "Eco-innovative technologies for the recovery of biomass waste - ECOVALDES" together with the beneficiary company S.C. LAMBDA MAT Bucharest.

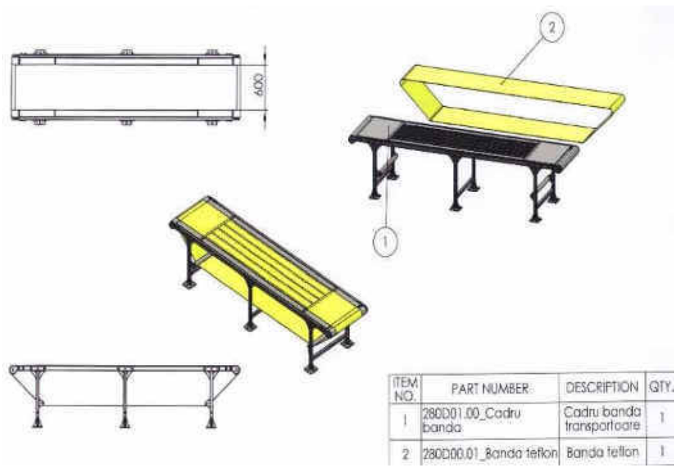

Equipment components:

• Rubber band
• Conveyor belt drive motor (direct drive or drive belts)
• Turning drum - rubber
• Rollers with inclination of approximately 20 degrees
• Metal frame for rubber band - with wheels for transport
• Reception bunker
• Rubber band alignment rollers
• Transport bar
• Electrical installation

Fig. 4. The conveyor belt

Once completed the design of the conveyor belt the partner company in the project will proceed to the physical realization of the equipment, in the next stage of the project.

5. Conclusions

Information regarding the operational conveyors that can be used within the biomass drying equipment under the action of microwaves was reviewed.
In this regard, the main technical parameters as well as the characteristics of the transported materials were scored.
Between those conveyors, the conveyor belt is an equipment that can be used in the microwave field, in the conditions of the selected material is for the belt that corresponds to the requirements of the process.
In order to select the material for the conveyor belt, in addition to the general conditions, it must meet the condition of transparency in the microwave field at the frequency of 2.45GHz. A suitable candidate is the Teflon material which, at the frequency of 2.45 GHz, the penetration depth at 20ºC is 32.56 m.

Acknowledgments

This paper has been developed in INOE 2000-IHP, as part of a project co-financed by the European Union through the European Regional Development Fund, under Competitiveness Operational Programme 2014-2020, Priority Axis 1: Research, technological development and innovation (RD&I) to support economic competitiveness and business development, Action 1.2.3 –Partnerships for knowledge transfer, project title: Eco-innovative technologies for recovery of biomass wastes, project acronym: ECOVALDES, SMIS code: 105693, Financial agreement no. 129/23.09.2016.

References

[1] Bagiu, L. *Tolerane si masurtori tehnice / Tolerances and technical measurements*. Vol. 1 and 2. Technical University of Timisoara, 1992.
[2] Dragu, D.,et al. *Tolerante si masuratori tehnice / Tolerances and technical measurements*. Bucharest, Didactic and Pedagogical Publishing House, 1982.
[3] Militaru, C. *Masurari pneumatice în tehnologia constructiilor de masini / Pneumatic measurements in the machines construction technology*. Bucharest, Technical Publishing House, 1987.
[4] Tarau, I., C. Georgescu, and D. Otrocol. *Precizia si calitatea la prelucrarea materialelor / Precision and quality in processing of materials*. Galati, Scorpion Publishing House, 2002.
[5] Ctr. no. 108/2007 – Tehnologie si echipament compct de extrudare si vulcanizare a amestecurilor de elastomeri, cu controlul computerizat al parametrilor pentru etansari hidraulice – INOE 2000.
[6] Ctr. no. 226/1997 – Cercetari privind determinarea regimurilor de intensitate si frecventa a fasciculelor de microunde folosite la polimerizarea cauciucului izoprenic – Studiu teoretic al modelelor de interactiune microunde – material – INOE 2000.
[7] Ctr. no. 1288/2001 – Tehnologii de vulcanizre cu microunde a elementelor de etansare – Elaborare DE pentru tehnologie prototip dispositive de vulcanizat cu microunde si elemente de etansare – INOE 2000.
[8] Ctr. no. 129/2016 - "Tehnologii eco-inovative de valorificare a deseurilor de biomasa – ECOVALDES", Subsidiary ctr. no. 95 – Banda transportoare pentru biomsa uscata.
[9] Habasit, A.G. *Fabric Conveyor Belts Engineering Guide*, www.habasit.com.
[10] Anath, K.N., and V. Rakesh. (2013). "Design and Selecting Proper Conveyor Belt." *Int. Journal of Advanced Technology* 4, no. 2 (2013): 43-49.
[11] Khan, Ahmad Shahid. *Microwave Engineering Concepts and Fundamentals*. CRC Press Taylor & Francis Group, 2014.

ISSN 1454 - 8003
Proceedings of 2019 International Conference on Hydraulics and Pneumatics - HERVEX
November 13-15, Băile Govora, Romania

LOW POWER ENERGY SYSTEM FOR GENERATING ELECTRICITY FROM SOLAR AND WIND SOURCES

Gheorghe ȘOVĂIALĂ[1], Radu RĂDOI[1], Gabriela MATACHE[1], Alina Iolanda POPESCU[1], Valentin BARBU[1]

[1] Hydraulics and Pneumatics Research Institute INOE 2000-IHP, ihp@fluidas.ro

Abstract: *The article refers to the presentation of a technical solution for combining two renewable sources from which to obtain the electricity needed to supply a low power consumer. The system was developed at the demonstration model level and has as generating elements a solar panel and a wind turbine. The novelty of the system is not only that it uses two different energy sources, but also that the wind power was realized from an original idea of the specialists of the institute, which contains 2 rotors, which work at different wind speeds (the internal rotor at low speeds, and the outside at higher speeds).*

Keywords: *Energy, renewable sources, solar; wind, combined system*

1. Introduction

In recent years, there has been a significant increase in energy consumption, well above the level of discovering new traditional resources, which has made specialists to pose the problem of replacing fossil fuels, in an extremely short term. As mankind always had at hand, renewable sources such as solar power, wind power, biomass, etc., the transition to their industrial exploitation became an absolute priority. In this regard, it was decided at EU level that by 2020 it will reach a share of energy obtained from renewable sources at 20% of total consumption, and by 2030 at a weight of at least 27%. One of the areas of interest for the use of energy obtained from renewable sources has been established at EU level as rural areas.

Energy security is, in short, the capacity of a country to provide the necessary energy resources for the well-being of the population, at stable prices. Currently, conventional methods of heating and lighting of homes are not only disappearing due to overcrowding, but also harmful to the environment, and this phenomenon is beginning to make its presence felt in Romania. The definition of green energy or renewable energy is based on the fact that it is non-polluting, that it is within the reach of man and especially it is restored due to natural processes, thus becoming inexhaustible at the historical level from the immediate or medium term perspective. It should be noted that there are periods when the share of renewable energy in general consumption and as a result and in the development of new production units slows noticeably, either for technical-financial reasons, or for political reasons or often for eco-technological reasons. However, it is found that the sector of wind energy and photovoltaic solar energy currently have the largest share in the production of electricity from renewable sources. According to a map prepared by the National Meteorological Administration, Romania's energy potential is zoned, as follows:

Danube Delta - solar energy; Dobrogea - solar and wind energy; Moldova - micro-hydro, wind power and biomass; Carpathian Mountains - high potential for biomass and micro-hydro; Transylvania - high potential for micro-hydro; Western Plain - opportunities for harnessing geothermal energy; Subcarpathians - potential for biomass and micro-hydro; Romanian Plain - biomass, geothermal energy and solar energy.

This map shows that there is a very large potential of solar, wind and plant biomass sources in large areas, so we only have to find the technical-economic solutions to use. For the communities that have the wood biomass resource, the solar-biomass hybrid systems represent a feasible solution for providing thermal energy in the community for the two main functionalities: domestic hot water and heating. The design of the solar-biomass system for the total use of the thermal energy obtained by the solar-thermal conversion and the use of the biomass for filling the thermal energy requirement in the community ensures the optimal functionality of the system by using only the solar energy during the warm period and using the biomass only when the energy solar does not provide the necessary thermal energy in the community. However, the strongest combination solution is the one in which a mixed solar-wind system is realized, as in fig.1.

Fig. 1. Mixed solar-wind system [5]

2. The demonstration model of electric combined system

Within the IHP, a mixed solar-wind panel has been designed and realized at the functional model level, which has 4 main components (fig.2):
1. Solar panel with axis orientation system
2. Wind turbine with rotors Darrieus (outside) and Savonius (inside)
3. Industrial fan
4. Addition electric block

Fig. 2. Demonstrative model of electric combined system

The demonstration model of the combined electric system has the role of highlighting the advantages arising from the combination of the two sources of renewable energy, solar energy and wind energy. For this purpose, the system can present both the amount of energy produced by each of the sources and in the combined system. The small photovoltaic panel 1 (0.5 A) is provided with a system of orientation and indexing on an axis (rotating around the horizontal axis); with the help of this guidance system the influence of the angle of incidence on the power of the panel can be highlighted. The wind turbine 2, made according to the idea patented by the IHP specialists, contains 2 rotors, which work at different wind speeds (the internal rotor at low speeds and the external rotor at higher speeds). The wind energy is provided by an industrial fan 3. The summing block 4 adds up the current from the 2 sources.

3. Wind turbine construction

To make the wind turbine within the demonstration model, a 3D printer was used to print the blades of the Darrieus rotor and the Savonius rotor after a geometry designed using SolidWorks

software.
Printing was done with the BCN3D SIGMA R19 (FFF) printer with the following facilities:
• Architecture: Two independent extrusions (IDEX);
• Print volume: 210 mm x 297 mm x 210 mm;
• Maximum temperature of the heated bed: 100 ° C;
• Positioning resolution (X / Y / Z): 1.25 um / 1.25 um / 1 um;
• Firmware: BCN3D Sigma - Marlin;
• Extruder system Extruder Bondtech ™ high technology double gears; Hotends: optimized and manufactured by e3D ™;
• File preparation software: BCN3D Cura.

In fig. 3 and 14 show the 3D printer and 3D drawings for the wind turbine made in SolidWorks.

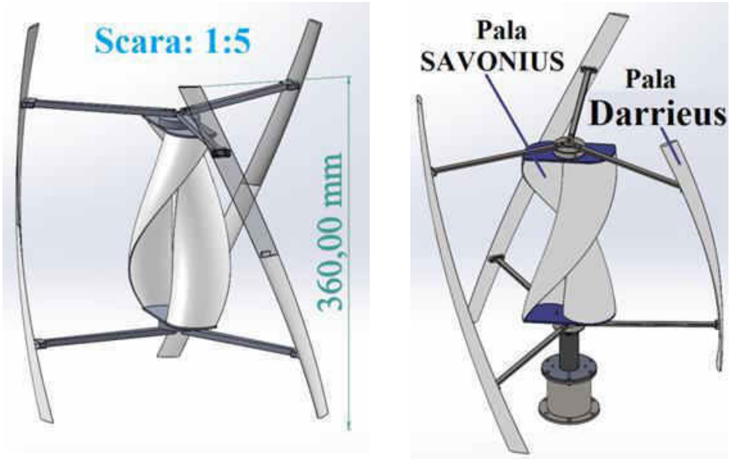

Fig. 3. SIGMA R19 printer and BCN3D Cura software

Fig. 4. 3D drawings for the wind turbine

Most of the components of the wind turbine were printed with PLA and for the parts that needed support was used PVA, which dissolves easily in water.
3D printing process parameters: filament diameter was 2.85 mm, casing diameter 0.4 mm, layer height 0.2 mm, filling density of 35% or 100%, printing temperature 205 ° C, temperature 60 ° C plate and a conservative print speed of 50 mm / s.
Because the blades of the Darrieus turbine are larger than the printer can produce, they were divided into two pieces and, due to their curvature, in two planes, it was necessary to print with support material. Fig. 5 shows the parts that needed support material, including the arms to support the Darrieus turbine; 2 holes were necessary for screw assembly.
Fig. 6 presents the parts that did not need support material during the printing process; they are: the covers of the Savonius turbine, which have practiced a channel that rigidifies the entire subassembly, the Savonius turbine itself, as well as the bearing base, which has the supporting role for the hexagonal shaft and the turbine.

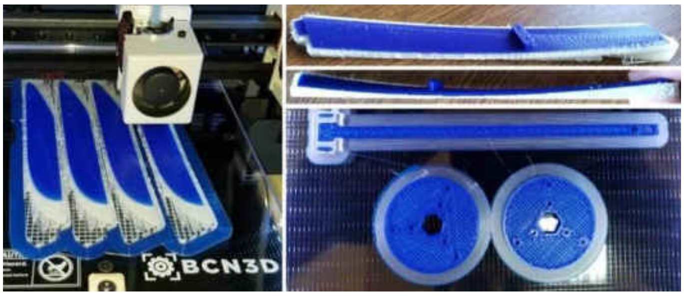

Fig. 5. Printed pieces that needed support material

Fig. 6. Components that did not need support material during the printing process

The physical object resulting from the wind turbine of the demonstration model of electric combined system is presented in fig.7:

Fig. 7. The wind turbine of the demonstration model of electric combined system

The wind turbine made as a component of the demonstration model consists of:
1. Darieus rotor (outside)
2. Savonius rotor (inside)
3. Rotor support axis, which also has the role of transmitting the movement
4. Speed multiplication system
5. Minigenerator
6. Supporting framework

The outer rotor Darrieus - item 1 - has 3 blades that have in section NACA 0018 profile, and ensures the operation of the turbine at speeds over 5 m / s.
The inner rotor Savonius - item 2 - has the role of putting the turbine in motion at lower wind speeds, starting from approx. 3 m / s; In this way, at wind speeds over 5 m / s, both rotors work to convert the kinetic energy of the air into mechanical energy.
The 2 rotors are mounted on the support shaft 3, which is widened at the bottom by means of 2 radial-axial bearings; the shaft has a large diameter wheel end, which together with another smaller diameter belt wheel, mounted on the minigenerator shaft 5, forms the speed multiplication system. This system combines the reduced axle speed with the 2 rotors (50 ... 200 rpm) with the minigenerator (1000 ... 1500 rpm). The wind turbine components are mounted on the supporting metal frame 6. The main components, the 2 rotors, were made by 3D printing. The wind turbine of the demonstration model is a small (1: 5) copy of the turbine of the experimental model.

4. The solar panel and the summing electric block

The solar panel with an axis guidance system (fig.8) has the following characteristics:
• Voltage at maximum power: 17.49V
• Current at maximum power: 580mA
• Maximum power: 10W
• Short circuit current: 610mA
• Material: polycrystalline silicon
• Outside dimensions: 290 x 330 x 25mm
• Mass: 1.5kg
• Panel adjustment angle 0… 90°

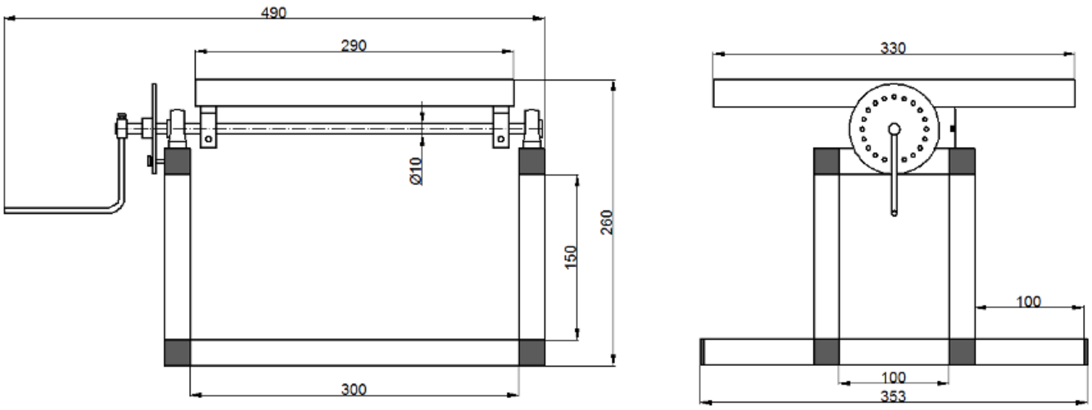

Fig. 8. Overall drawing of the photovoltaic panel with guidance system

The characteristics of the industrial fan used in the model are:
• Power supply voltage: 230 V
• Power: 1.1 kW
• Air flow: 7850 m3 / h

The summing electric block (fig. 9) consists of:
- 1 solar controller with maximum power point tracking (MPPT) with the output voltage 3.4 V;
- 1 voltage regulator with output voltage 3.4 V;
- 2 Schottky diodes;
- 1 bulb or LED consumer.

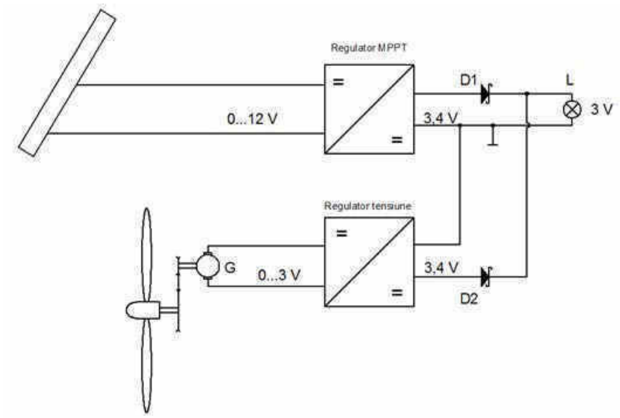

Fig. 9. Diagram of the summing electric block

5. Conclusions

For the most part, small communities rely on wood biomass and fossil fuel consumption. The official trend, but even the particular one, is the shift to energy production systems green, from renewable resources that are usually solar wind and plant biomass. Given that usually the resources listed above are not available 24 hours a day, it is necessary to make some combinations, especially between the 3 sources that are available longer and especially at different times of the day such as solar-wind.
The demonstration block realized by IHP allows obtaining important data necessary for the manufacture of composite (mixed) systems.

Acknowledgements

This work was supported by a grant of the Romanian Ministery of Research and Innovation CCDI - UEFISCDI, Project INNOVATIVE TECHNOLOGIES FOR IRRIGATION OF AGRICULTURAL CROPS IN ARID, SEMIARID AND SUBHUMID-DRY CLIMATE, project number PN-III-P1-1.2-PCCDI-2017-0254, Contract no. 27PCCDI / 2018, within PNCDI III.

References

[1] INOE 2000-IHP. Technical study on the production of combined low power systems within the project "Establishing a high level proficiency nucleus in the field of increasing renewable energy conversion efficiency and energy independence by using combined resources”, Financial agreement no. 37/02.09.2016.
[2] Brooks, A. "Solar Energy: Photovoltaics." In *Future Energy: Improved, Sustainable and Clean Options for our Planet.* London, London Elsevier, 2013.
[3] Dragomir S., and E. Vasilescu. "High performance wind energy systems for renewable electricity production." *AGIR Bulletin*, no. 3.
[4] Maican, Edmond. *Renewable energy systems*. Bucharest, Printech Publishing House, 2015.
[5]https://editiadedimineata.ro/romania-este-pe-primul-loc-in-europa-de-est-la-productia-de-energie-regenerabila-exclusiv-institutul-verde/.
[6] Ilie, Constantin Adrian. “Hybrid systems based on renewable sources to ensure the need for thermal energy in small communities.” PhD thesis 2019.
[7] Vișa, Ion, Anca Duță, Macedon Moldovan, and Bogdan Burduhos. “Implementing renewable energy systems in nearly zero energy communities.” Paper presented at the Conference for Sustainable Energy (CSE), Brasov, Romania, 2017.
[8] Ilie, Adrian, Ion Visa, and Anca Duță. “Solar-Thermal Systems for Domestic Hot Water Production Implemented in Communities of Collective Households.“ *Journal of Energy Engineering* 143, no. 6 (December 2017).
[9] Dulgheru, Valeriu. *Combined wind turbine with vertical axis and helical blades*. Patent MD 3817B1 on 2009.01.31.

ISSN 1454 - 8003
Proceedings of 2019 International Conference on Hydraulics and Pneumatics - HERVEX
November 13-15, Băile Govora, Romania

THE TECHNOLOGY OF THE FURROW DIKER AT SUNFLOWER

"WATER⁺ FURROW DIKER" name under which it is known machine + technology in the BRIGAID project

Ilie BIOLAN[1], Ioana DRĂGAN[1], Nicu CONSTANTIN[2], Cătălin POPESCU[1]

[1] S.C. AQUAPROIECT S.A., iliebiolan@gmail.com

[2] National Institute for Development Research for Machinery and Installations for Agriculture and Food Industry

Abstract: *Furrow diker is a method of water and soil conservation and it is used on uneven land with small slopes. This technology reduces soil erosion, it uses a greater amount of water from rainfall and achieves a better distribution of water at the surface of the soil. By storing water in micro basins, better soil moisture is achieved in the root zone and can be applied in arid areas and semi-arid. The work was carried out within the BRIGAID project, Horizon 2020.*

Keywords*: Furrows dike, soil and water conservation, micro basins*

1. Introduction

The soil modeling machine runs furrow dike in aggregate with the tractor with 35-80 HP. The soil modeling machine was made in two constructive variants for: Row crops and vines / fruit trees respectively.
In row crops, soil modeling with furrow dike is performed when the plants have 30 - 60 cm height.
In vineyards and orchards, soil modeling can be done from spring to autumn, on lands with a slope of up to 5%, concurrently with the soil works.
The article presents the variant for row crops (used in sunflower).

Side view device for making furrows dike for row crops

Front view device for making furrows dike for row crops

2. Material and research method

By using the furrows dike in the arid and semi-arid areas, the damage reduction due to drought is estimated by 50-55%, because it valorizes a greater quantity of water from the rainfall and distributes the uniform of water, for its use by agricultural crops.
The machine was made in two constructive variants and was tested in 2017, in Romania, in row crops, vines and fruit trees.
During the period 29-30 / 05.2018, the machine was opened to furrows dike in the sunflower, in Field 67, Physical Block 270, at SC AGROMEC SA Cranguri-Calugareni, Giurgiu county and the machine + technology is known in the BRIGAID project under the symbolic name “WATER + FURROW DIKER ”.
The soil had an area of about 17 ha, with uneven terrain, small depressions and different slopes that favour soil erosion and the uneven distribution of water, the soil was also compacted to a humidity that allowed the mechanical works to be performed and the sunflower crop, variety P64LE99, had very variable height: 2-45 cm due to the late germination of sunflower seeds and the density of plants was 55,000-60,000 plants / ha.
The main phases of culture technology were the following:
1. Plow at 30-32 cm, fall.
2. Fertilized with 18-46-0, 200kg / ha, spring.
3. Discussed at 10-12 cm.
4. Frontier herbicide, before sowing (pre-emergent).
5. Incorporated herbicide and finishing the land with the combiner.
6. Sowing on 8 rows at 70 cm distance between rows, 55-60,000 plants / ha.
7. Tillage at 8-10 cm and incorporated 150 kg / ha nitrocalcar.
8. Furrow dike with 5 sections per interval.
9. Harvested with combine with equipment for 8 rows.

The machine worked in aggregate with the tractor with 65 HP, with an average speed of 3 km / h and a gear of II R. The machine made furrows dike on each row, including those between the drill passages due to the high sowing accuracy of the sunflower.
During the tests, the furrows were compartmentalized in an area with uneven surface and the neighboring surface was used as a control area. The machine was tested in a tillage area, on 30 consecutive rows, 866 m long, working width 3.5 m, the area worked on a passage was 0.3031 ha / passage, the depth was variable 12-15 cm depending on the height of the plant, the speed of work and the degree of soil settlement.

In order to know the texture, the humidity and other parameters of the soil it was collaborated with ICPA and in order to know the terrain orography, the longitudinal profile of the land was realized by the compartment TOPO from AQUAPROIECT. The slope of the land was up to 10%.
Due to the uneven emergence of the plants (phenomenon due to the drought from April to May) the size of the plants was variable and the small plants no longer fruited and diminished their production.
The rainfall during the period June 15 - July 6 was 70 l / m^2 and between July 5 and August 30 were 24 l / m^2. The temperature in the same period ranged from 32^0 C to 38^0 C.
The production price for the sunflower crop was 1.02 lei / kg and the sale price was 1.30 lei / kg.
The area where the experimentation was carried out was arid, poor in precipitation, with hills and depression areas, with a medium textured (clay) soil that does not accumulate much water, with coastal springs that develop a specific vegetation and fauna.

3. Furrow dike computing elements

3.1 Calculation of the distance between dikes

The furrows dike retains the eroded soil and the water by forming dikes on the furrows at certain distances, creating collecting micro basins. The distance between the dikes should be chosen so as to reduce soil loss through erosion and to avoid the passage of surface water over the dikes.

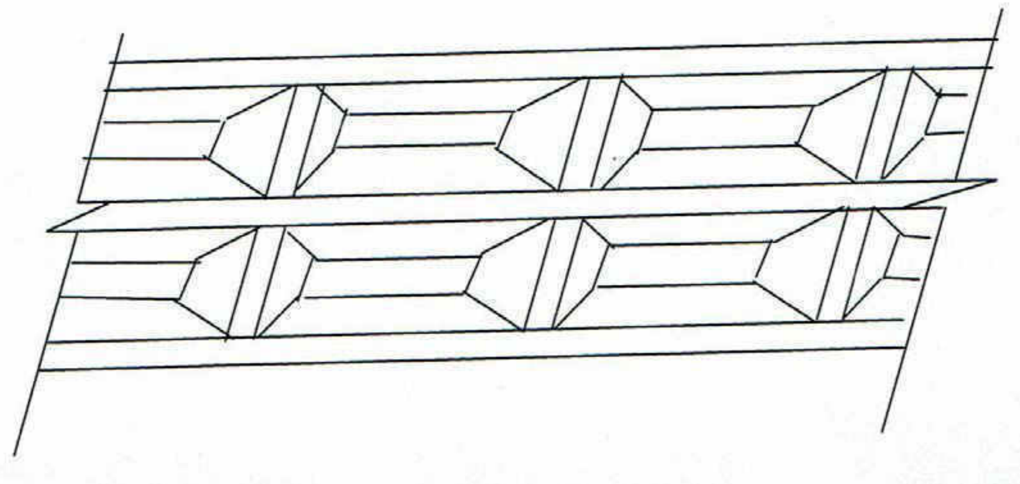

Fig. 1. Top view furrows dike

The calculation elements of the furrows dike consist mainly in determining the optimal distance between two consecutive dikes. If the distance is too large it will collect too much water in each micro basin, a micro basin that does not have enough resistance to store a large volume of water, volume of water that will exert pressure on the downstream dikes and start a chain reaction that would probably produce a channel (soil erosion); in this case, the expenses for combating soil erosion and exploitation will increase.
Based on the principle of water balance, this article proposes the design method according to which the rainwater catchment area must collect water in the micro basin and allow it to infiltrate into the soil.
The trapezoidal section of the furrow is considered to be trapezoidal and the slope of the terrain does not influence the measurement of the dimensions along the furrow.

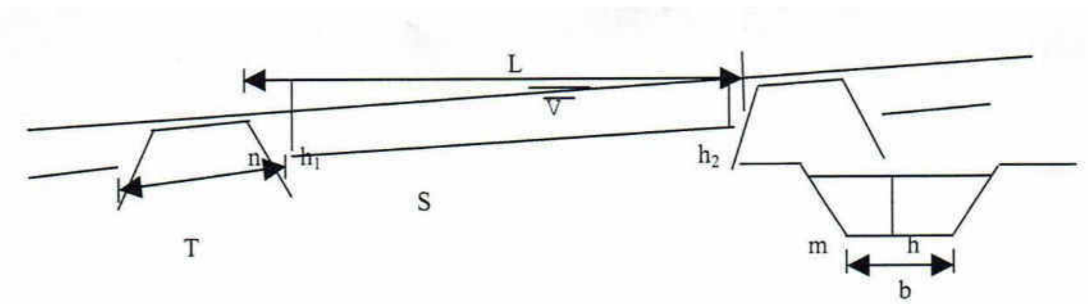

Fig. 2. The profile of the furrow dike Cross section through the furrow

3.2 Calculation of the distance between dikes

Micro basin - the volume of water stored in the furrow between two consecutive dikes.
As shown in the figure above, the water storage formula can be established using the geometric method, as follows:

$$V_S = (A_b + A_B) \times h/2 \tag{1}$$

In which: VS - volume of stored water body, m^3;
Ab - the surface of the bottom of the water body, m^2;
AB - water surface, m^2;
h - average depth water body, m.
$h = (h_1 + h_2) / 2$.

$$A_b = bxS \tag{2}$$

$$A_b= [(b+2mh_1)+(b+2mh_2)]\, L/2, \tag{3}$$

In which: S - the distance between two consecutive dikes,
b- width of the bottom of the furrow
m- slope of the furrow,
h_1-the height of the water downstream,
h_2- the height of the water upstream,
h- average water height.

$$V_S = (A_b + A_B) \times (h_1+h_2)/4 \tag{4}$$

In which: L - the distance between two consecutive dikes, at the surface of the water,
D - the distance between two consecutive dikes at the base of the dikes.
$L = D + nh_1 + nh_2$, and it take: $m = n$

It takes: $D \approx S$ și: $h_2 = h_1 - Si$

Therefore: $L= S+nh_1 +nh_2 =S+nh_1 +n(h_1 -Si)= S+ n(2h_1 -Si)$

$A_b= [(b+2mh_1)+(b+2mh_2)] L/2 = 1/2 [(b+2nh_1)+(b+2nh_2)] [S+ n(2h_1 -Si)]=$

$=1/2 [b+2nh_1+b+2n(h_1 -Si)] [S+ n(2h_1 -Si)]= 1/2 (2b+4nh_1 - 2nSi)] [S+ n(2h_1 -Si)]=$

$=[b+n(2h_1 - Si)] [S+ n(2h_1 -Si)]=bS + nb(2h_1 -Si)+nS(2h_1 - Si)+n^2(2h_1 - Si)^2$

and: $h_1+h_2 = h_1+ h_1 -Si=2h_1 -Si$

From relations (2), (3) and (4) it follows:

$V_S = 1/4[bS + bS + nb(2h_1 -Si)+nS(2h_1 - Si)+n^2(2h_1 - Si)^2] (2h_1 -Si)=$

$=1/4[2bS + n(S+ b)(2h_1 - Si)+n^2(2h_1 - Si)^2] (2h_1 -Si)$

The volume of the water body is calculated by the formula:

$$V_S = 0.25 \times [2bS(2h_1 - Si) + n(S+ b)(2h_1 - Si)^2 + n^2(2h_1 - Si)^3] \quad (5)$$

In which: i = slope of the land
n = slope of the dike

3.3 Calculation of the quantity of stored water, W

The amount of water (precipitation) stored in a micro basin (furrow dike) is equal to the amount of water dropped over a period of time and has the following calculation formula:

$$W = RB_f (S+T) = RB_f S + RB_f T \quad (6)$$

In which: R-amount of net water dropped per unit area, mm / m^2;

$$R = P - I_0 - f t_c - P^` \quad (7)$$

And: S-distance between two consecutive dikes, m;
T - the width of the dike at the surface of the ground, m;
Bf - the distance between two consecutive furrows, m;
I_0 - depth of water in soil (amount of water infiltrated into soil during rain), mm;
P - total quantity of water dropped, mm;
P` - the amount of water remaining in the furrow dike at the end of the rain, mm,
f - velocity of infiltration of water in soil, mm / h;
t_c - the time interval in which the precipitation fell, h.

3.4 Calculation of the distance between two consecutive dikes, S

The conditions imposed by the water balance through the relation: W = VS
From formulas (5) and (6) is shown the distance between two consecutive dikes, S.

4. Conclusions and recommendations

During the vegetation were monitored: the size and the fruiting of the plant, the furrows dike, the phenomenon of watering or sprinkling of surface water, the growth of the crop, the humidity of the soil and the production obtained per hectare.
In the plots where there were furrow dikes the size of the plant was higher and the fructification was better compared to the areas without ferns. The bilonation phenomenon (plant row cover) reduces the evaporation of the water from the root zone and by covering the weeds the water was better conserved in the soil, being used for a longer period by the plant.
The shape of the compartmentalized fences was kept until harvest, the dimensions were reduced and the coppers were not destroyed due to the foliage of the plant which mitigated the impact of the drops on the soil when the precipitation had increased intensity. During the harvest there were no problems due to the furrows dike.
Due to the small rainfall, there was no phenomenon of water trickling or splashing except in the area of coastal springs where no furrows dikes were made. The obtained production was 3000kg / ha and the maximum production obtained in previous years was 3600 kg / ha. In the parceled areas a 10% increase was obtained in furrows dike compared to the parcels without furrows dike.
The main advantages of using furrow dike are the following:
1. The tillage makes use of the water from precipitation by increasing the amount of water in the root zone.
2. The tillage replaced the second mechanical seedbed and destroyed the weeds in the root zone.
3. The tillage contributes to reducing soil erosion.
4. The tillage achieves a better distribution of water on the surface of the soil.
5. The tillage contributes to maintaining a higher humidity in the root zone.
6. Agricultural production increased by 10%.

The work cannot be applied in “NO TILLAGE” technologies, technologies that do not include tillage system.

Furrows dike performed in a sunflower crop

References

[1] Biolan, Ilie, et al. *Irrigation of agricultural crops-Technologies*. Bucharest, AGIR Publishing House, 2016.
[2] Biolan, Ilie, et al. *Irrigation of crops within farms - Application Guide*. Bucharest, AGIR Publishing House, 2018.
[3] Ma, Yongsheng, and Tiayu Wei. „One method of ridged - furrow design.” *The Journal of American Science* 1, no. 1 (2005): 75-77.

ISSN 1454 - 8003
Proceedings of 2019 International Conference on Hydraulics and Pneumatics - HERVEX
November 13-15, Băile Govora, Romania

ELECTROHYDRAULIC CONTROL DEVICES

Petrin DRUMEA[1], Ioan BĂLAN[1], Marian BLEJAN[1], Radu RĂDOI[1]

[1] Hydraulics and Pneumatics Research Institute INOE 2000-IHP, ihp@fluidas.ro

Abstract: *The article refers to the history of the theoretical and practical development, in Romania, of a sub-domain of great interest in the automation process, which is based on the hydraulic elements. The grouping of these equipments in the category of electro-hydraulic control devices was due to the fact that they are hydraulic, that they are adjustable, and the control is electronic. Specifically, these are electro-hydraulic servovalves and proportional electro-hydraulic directional valves.*

Keywords: *Servovalve, proportional valve, controller, PID controller*

1. Introduction

This material tries to remind the specialists in Romania that the field has been approached seriously and with theoretical [1, 2], but also industrial achievements, from 1965-1968 by some research units but also by some precision mechanics factories as well as by a specialized factory in production of hydraulic equipment. Sometime later, after 1974, the research, design and manufacturing activities of these equipments were intensively developed by the hydraulics team from the Institute of Machine Building led by PhD eng. Marin Virgil [3]. About the same period, only theoretical preoccupations began at University Politehnica of Bucharest at the Department of Automation (S. Florea, I. Dumitrache and Ilie Catana). At a certain time, the works from the aviation research units were also of great interest; those were projects carried out by several researchers including Ion Ionescu and C. Mares; also the servosystems and even servovalve achievements of the AEROTEH Bucharest factory were important.

2. Electrohydraulic servovalves

The first servovalves were developed at the level of experimental model and prototype by the engineers Mihai Popescu and Sergiu Medar who also called upon the team of precision engineering from the hydraulics factory in Ramnicu Valcea led by the foreman Popa. During this period, the SV60 servovalve was developed; it unfortunately also had some elements from the MOOG valves and did not exceed the maximum working frequency of 30Hz. About the same time, Prof. Patrut, together with the young specialists David and Tonciu, as well as with two precision engineering foremen, developed the first models of larger flow valves needed for applications with servo cylinders required for a seismic platform. Unfortunately, these achievements, although interesting and quite close to the international level, remained at the stage of experimental or functional models. The first industrial results in the country were obtained after passing the issue from the Institute for Machine-Tools to the Institute of Machine Building, team of proportional hydraulics. Here, engineers among which we mention Petrin Drumea, Mihai Stefan, Ioan Balan and Ion Moldoveanu, created a family of sevovalves, the SD series, sizes 60, 150 and 240 which recorded working frequency of 60Hz. During this period intense work was carried out in collaboration with the Institute of Physics in Iasi which, through the team of PhD. Chiriac, managed to solve the problem of the components made of permalloy, a material with high magnetic permeability qualities. One of the interesting industrial achievements was the servovalve pilot (SV00) developed at Electrotimis in Timisoara, used mainly in spark erosion machines (EDM) of their own manufacture. The same type of servovalve was also developed at IEH Ramnicu Valcea for general purpose industrial applications.

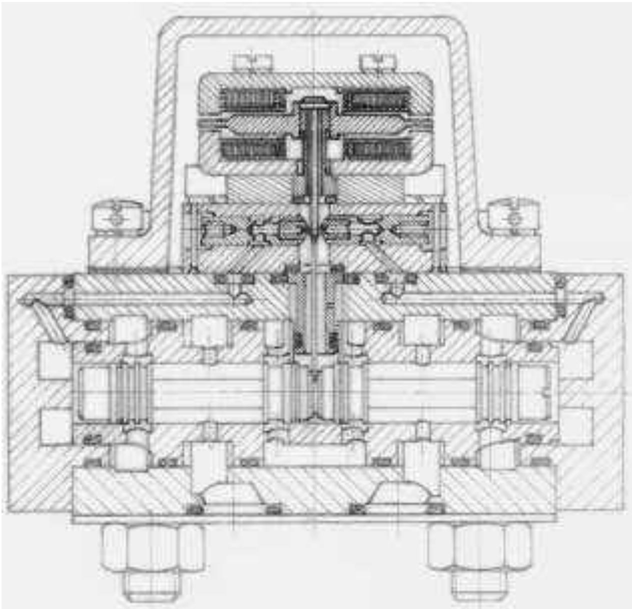

Fig. 1. SD60 hydraulic servovalve

3. Electrohydraulic proportional valves

Proportional hydraulic devices appeared in the 60-70s, many years after the servovalves, due to two important economic factors. The first factor was that the price of the valves was extremely high; thus the entire hydraulic automation system became prohibitive. The second factor was that the number of hydraulic applications with the dynamics offered by servovalves was at most 20% of the total industrial hydraulic automation installations, the rest requiring much lower performance, and consequently the luxury of using servovalves was difficult to sustain. The solution of proportional hydraulic equipment was quickly found, and in this way the transition to industrial manufacturing was made at a rapid pace. The general solution is that in which the standard directional control valves, existing in manufacturing, for which there were standard technologies, have undergone small changes, especially in the control part, and have been transformed into proportional directional control valves, or proportional hydraulic valves [4]. Thus, by replacing manual or electrical controls with proportional force or stroke electromagnets, proportional hydraulic devices were obtained. Initially the team from ICTCM led by Dipl. Eng. Petrin Drumea, which also included the engineers Mihai Stefan and Ioan Balan, as well as the electronics team, led by Dipl. Eng. Mircea Comes, achieved the first force proportional electromagnet with which both directional control valves and hydraulic valves were equipped [5]. Proportional hydraulic equipment with proportional force electromagnets was introduced in series production at the hydraulics factory in Ramnicu Valcea where the proportional hydraulics group was quickly created within the servovalve team led by the foreman Popa [6, 7]. An important step in the direction of improving the manufacturing was taken with carrying out the first serious projects on an electromagnet, by Dipl. Eng. Mircea Comes, and making a manufacturing technology, by the foreman Ion Oprea, by which the axial alignment of the component elements was achieved [8, 9].

The force proportional electromagnet is an electrical device which develops, at the level of a central translation axis, an axial force proportional to the value of the electric current with which it is supplied.

A typical constructive solution of force proportional electromagnet is shown in figure 2.
The device consists of a magnetic circuit provided with a coil which is the magnetic field source. The magnetic circuit consists of a series of fixed cores and a plunger - mobile magnetic core which can move axially under the action of a magnetic field.

The axial displacement of the mobile core and implicitly of the translation axis is relatively small (usually between 1 ... 2 mm); on the other hand, the developed force is relatively important. In general, work is performed with electromagnets that develop a maximum force (at the maximum supply current of the coil) of the order of 8 daN. Characteristic force curve as a function of axial displacement, at constant supply current, F=f(c) for i_c =ct is shown in figure 3.

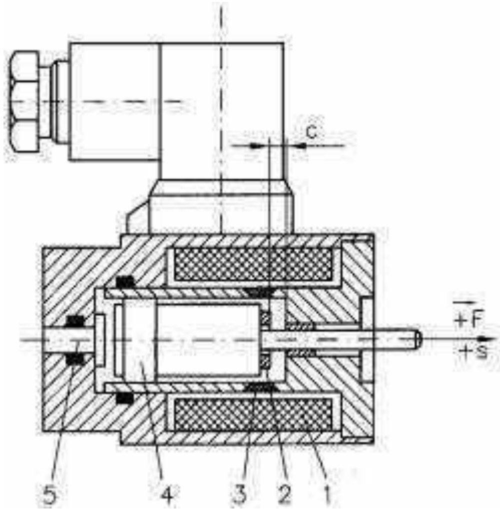

1 – coil; 2 – diamagnetic spacer; 3 – diamagnetic coil; 4 – plunger; 5 – plunger manual release piston

Fig. 2. Force proportional electromagnet

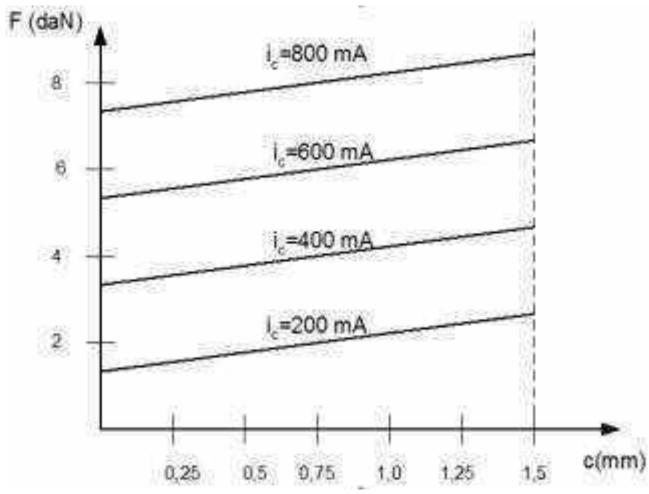

Fig. 3. The characteristic F =f (c), for i_c = ct of the force proportional electromagnet

The proportional hydraulic directional control valve performs its function through a translation slide valve, receiving control pressures at both ends, and from the difference in these pressure values a force of translation occurs. This force is balanced by the antagonistic force of an elastic system consisting of springs, after covering a displacement. Thus, proportionality is established between the displacement of the slide valve and the difference of the control pressures, implicitly the drive current of the actuator. By the construction of the device body, this movement of the slide valve causes progressive variations of the flow sections towards consumers. As one can see on the symbol, the device is provided with four hydraulic ports, namely:

- P - pressurized fluid supply port
- A,B - ports for hydraulic consumers
- T- return port
- The function of the device is to select the direction of flow to one consumer or the other and determine the flow rate to the selected consumer.

Depending on how the flow is, two categories of proportional directional control valves can be distinguished:

- Proportional directional control valves with progressive variation of the flow section (throttling). The flow varies proportionally with the control current in the situation when a constant pressure drop is maintained on the flow section through the device.
- Proportional directional control valves with embedded pressure regulator. The flow varies proportionally with the control current, for pressure drops on the flow section which may vary within relatively wide limits.

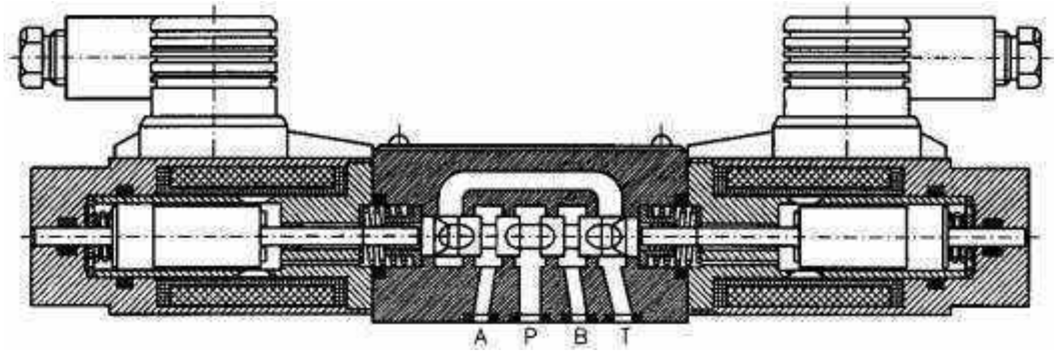

Fig. 4. Single stage proportional directional valve

4. Electronic control units

In the first years of interest of the Romanian specialists in the field the development of electronic control blocks was performed by hand, without a clear conception, and most of the time they were imported from the countries where there is already a mass production of this type of equipment. The first arranging of the subdomain and the transition to manufacture typification has been carried out by the Dipl. Eng. Mircea Comes, within the specialized group led by Dipl. Eng. Petrin Drumea. In time, the team has increased by hiring the engineers Adrian Grozea, Marian Blejan, Marian Neacsu and S. Smarandache. In 1981-1989, the electronic control blocks were standardized both for proportional equipment and for servovalves [10].

Servocontroller for electrohydraulic proportional valves

This servocontroller was designed to have a small printed circuit board that can be easily adjustable and can be used in as many applications. The diagram of fig. 5 is good for automatic control modules, intended for control of positioning systems, which use proportional hydraulic elements. It contains the following blocks: error amplifier, electronic PID controller, polarity separator for control with signal ± 10 V and a dual final power stage in switching mode for electromagnets A and B. In fig. 6 one can see the servocontroller assembly made on a printed circuit board which was mounted in an enclosure.

Servocontroller for servovalves

Servocontrollers for servovalves control have a structure similar to the servocontrollers for proportional elements. In this sense they contain the error amplifier and the PID type controller. Because the valves are equipped with bipolar electromechanical converters, the polarity separator block is no longer needed. Also, since the torque motor coils are usually connected in series or in parallel, a single output stage is required to generate the required servovalve current. Servovalves require a relatively low control current, up to 50mA on the coil, i.e. maximum 100mA. Therefore, the current voltage conversion stage does not need to be of the PWM type, the dissipated energy is much lower than in the case of proportional elements. Based on these considerations, the diagram of a servocontroller (fig. 7) for the control of electro-hydraulic servovalves has been developed.

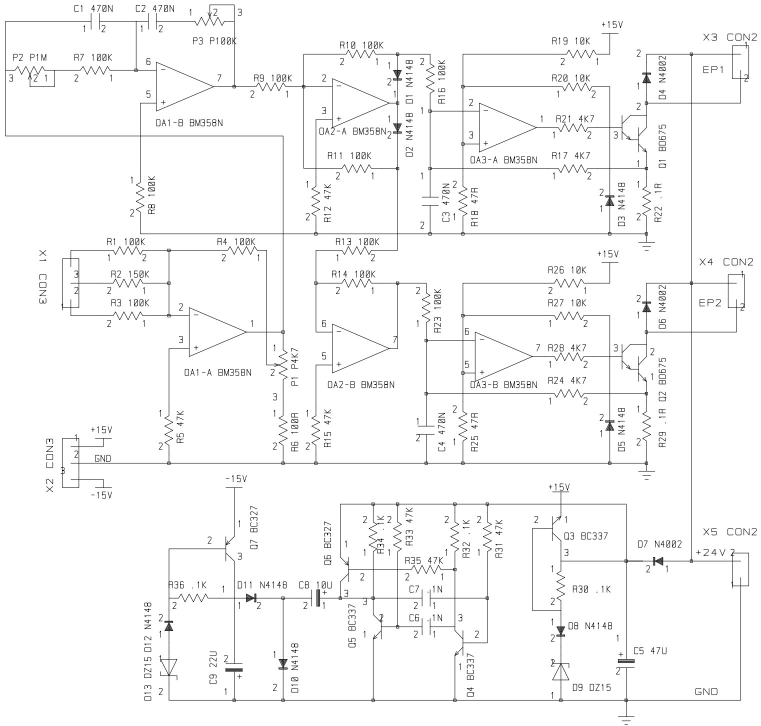

Fig. 5. PID controller diagram for proportional elements

Fig. 6. Mode of manufacturing for the controller for proportional elements

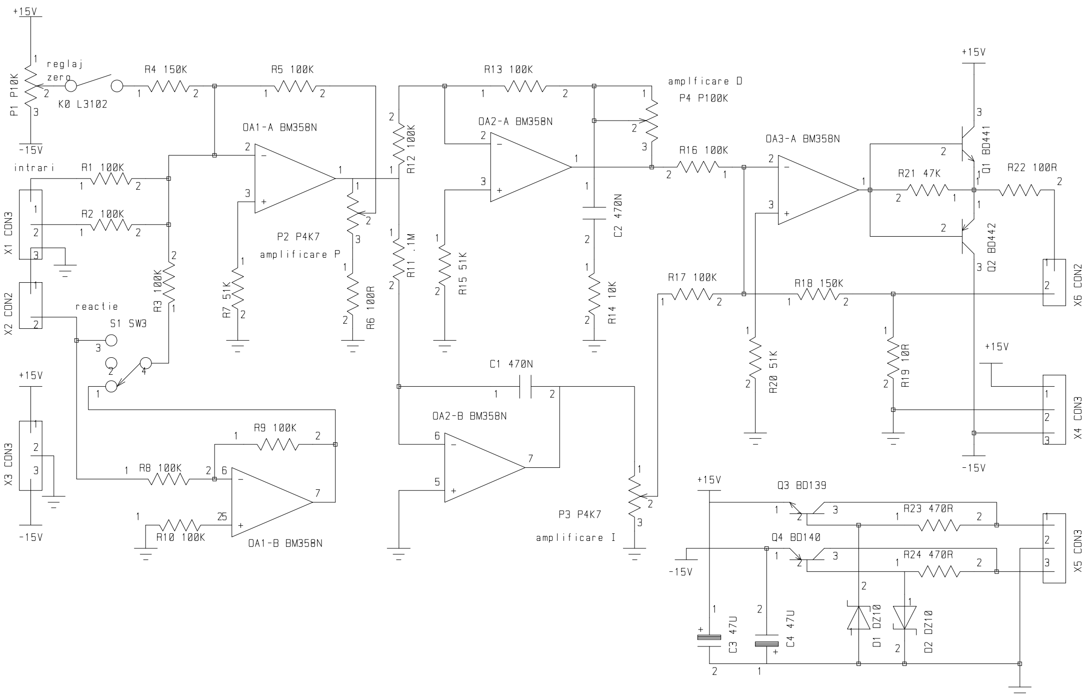

Fig. 7. Electronic diagram of servovalve controller

5. Conclusions

The field of electro-hydraulic control equipment has been approached at the same time with many of the industrially advanced countries. Unfortunately, the poor facilities of the hydraulics factories and the lack of specific materials, sometimes even special ones, prevented the realization of an intense manufacture.

Given the novelty of the field, the number of specialists using these equipments was quite small and as a result the demand for the industry for such products was kept low, so the size of the manufacture remained at the order of tens of pieces per year.

In the last 30 years, this sub-domain has also been abandoned, as is the case with most of the fields in the area of hydraulic drives.

Acknowledgments

This work was done under the scientific Programme NUCLEU 2019, Contract PN 19-18.01.01, Stage 21/2019.

References

[1] Blackburn, J.F. *Fluid Power Control*. Boston, MIT Press, 1969.
[2] Merritt, H. *Hydraulic Control systems*. John Wilez and Sons, 1967.
[3] Marin, V., and R. Moscovici. *Sisteme hidraulice de acţionare şi reglare automată, Probleme practice*. / *Hydraulic systems for automatic actuation and control. Practical problems*. Bucharest, Technical Publishing House, 1981.
[4] Deacu, L., D. Banabic, M.M. Radulescu, and C. Ratiu. *Tehnica hidraulicii proporţionale*. / *The technique of proportional hydraulics*. Cluj- Napoca, Dacia Publishing House, 1989.
[5] Comes, M., P. Drumea, A.V. Mirea, and M. Blejan. "Electronic module for the force proportional electromagnets testing." Paper presented at the 4th International Symposium for Informatics and Tehnology in Electronic Modules Domain, Bucharest, Romania, September 22 - 24, 1998.
[6] Drumea, P., N. Ionita, et. al. "Normally Open High Flow Proportional Hydraulic Valve." Patent No. RO121971 / 2008-09-30.
[7] Drumea, P., and I. Balan. "Distributeur Hydraulique Proportionnel." Patent No. RO88862 / 1986-04-30.
[8] Drumea, P., and I. Balan. "Diviseur Hydraulique Proportionnel." Patent No. RO88861 / 1986-04-30.
[9] Drumea, P., and I. Balan. "Regulateur Hydraulique Proportionnel." Patent No. RO88860 / 1986-04-30.
[10] Dutu, I., and G. Matache. "Computer assisted electro-hydraulic stand for testing servovalves." *Hidraulica Magazin*e, no.3-4 (December 2012): 73-77.

LIFT OF HYDRAULIC POWERED MATERIALS AND DRIVEN BY A PROGRAMMABLE AUTOMATIC

Ionel NICOLAE[1], Traian DORDEA[2]

[1] Prof., Ovidius University of Constanta, inicolae@univ-ovidius.ro

[2] Retired Dipl. eng., traiandordea@yahoo.com

Abstract: *The paper presents the stages of designing a lift for materials, hydraulically driven by a programmable automatic. The introduction presents the history of the lift, the advantages and disadvantages of the hydraulic lift compared to the mechanical lift with drums, rollers and cables.*

***Keywords**: Lift, hydraulic, regime dynamic, automatic programmer.*

In 1867 Leon Edoux presents at the Universal Exhibition in Paris "the first safe direct action hydraulic lifts". The four cast iron guide columns of the elevator were also containers for four counterweights, fastened by chains that rolled down over the rollers, ensuring passenger safety. In 1868 Waygood manufactured the first hydraulic lift.

Operating principle: The operating principle of a hydraulic lift is incredibly simple, it's just a cab attached to a lift system.

Of course, modern passenger and freight elevators are much more elaborate. They need advanced mechanical and electronic systems to manage the substantial weight of the lift cab and its cargo. In addition, they have there is a need for safety and control mechanisms so that everything works smoothly when passengers use them.

The most commonly used models of elevators are hydraulic lifts with direct drive and hydraulic lifts with an indirect drive.

Hydraulic lifts use a hydraulic cylinder operated from the inside by a fluid. You can see this in the sketch below.

2. The operating principle

The cylinder is connected to a hydraulic source (usually hydraulic systems use high-pressure resistant oil). The hydraulic system has the following components:
- a tank (fluid reservoir);
- hydraulic pump, powered by an electric motor;
- safety valve;
- hydraulic track regulator;
- a solenoid valve between the cylinder and the tank;
- reinforcements and pipes.

The hydraulic pump generates sub pressure fluid which through the valves and pipes act the cylinder vertically. When the valve opens the fluid will return to the tank (control unit) and the elevator will descend. When the valve is closed, the liquid under pressure has nowhere to go except in the cylinder. Thus, the fluid collected in the cylinder pushes the piston upward by lifting the elevator cab. To lower the lift, the control system sends a signal to the valve. When the electrical system opens the valve, the fluid that is collected in the cylinder can flow into the liquid reservoir. The weight of the machine and load pushes down the piston that drives the fluid into the tank. The car slowly descends. To stop the cabin on a lower floor, the control system closes the valve again.

2.1 Advantages and disadvantages of the hydraulic lift

• This system is simple and extremely efficient but has some disadvantages.

• In most cases, hydraulic lifts are used where no speed greater than 1 m / s is required.

• There is no limit to high weight. For hydraulic lifts, the normal run goes up to 25 m, and with some special constructions, it can go up to 35 m.

• Maintenance cost - in general, less maintenance work is required on hydraulic lifts, because the pump-engine system works in the oil and has a longer life (lower usage, high reliability).

• To the hydraulic lifts, the engine is running only on the way up, that is, it works half the time compared with the engine at the electric lifts.

• The machine room - the well - to the hydraulic lifts the static and dynamic loads press on the foundation of the building, which by its construction is very resistant. At the electric lifts, the respective loads are taken from the roof of the building that must be specially strengthened.
• Emergency - at hydraulic lifts, the evacuation (at power failure) is very simple, the cab descends to the station below without the need for engine (control unit) operation.

3. The mathematical model of a hydraulic lift equipped with the valve
3.1. Analysis and simulation of the hydraulic system

We will analyze the numerical simulation using the Mathcad environment. Dynamic simulation has two objectives: one is to investigate the dynamic characteristics of the system when climbing and to analyze the existing problems, as well as to adjust the system parameters. A second objective is to compare the dynamic characteristics of the solenoid valve and the downstream hydraulic regulator.

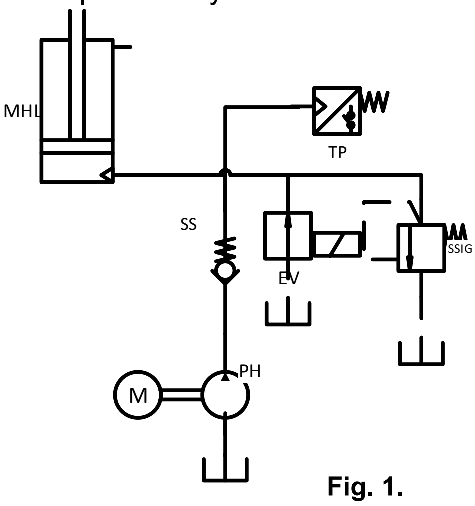

Fig. 1.

3.2 The mathematical model

An elevator is a machine used to lift goods vertically to one or more floors

The lifting mechanism of a lift (figure 1) consists of the metal frame on which a platform slides through which the load is lifted. The load is driven by an MHL hydraulic cylinder. For high productivity, it is necessary to optimize the lifting or lowering of the lifting mechanism. The acceleration (deceleration) process must be evaluated as a whole (hydraulic pump - solenoid valve). In figure 1 the hydraulic circuit is classic: the MHL hydraulic cylinder is fed by the PH pump through the sense valve.

For lifting shall be connected the electric motor E. For lowering is actuated the solenoid valve EV. The braking is provided by the hydraulic resistance of the pipes. The descent is made under the weight of the platform and the load.
- mechanical system analysis.

$$\text{when lifting} \quad F=2*F_f \tag{1}$$
$$\text{when descent} \quad F=2*S \tag{2}$$

The mechanical parameters of the hydraulic cylinder (space, speed, acceleration) change according to the physical process [2]. They may exceed the limit values of:
- maximum pressure of the hydraulic source
- full speed

$$v_{max} = \frac{Q_a}{A_a} = \frac{Q_p}{A_a} \tag{3}$$

- maximum acceleration

$$a_{max} = \frac{p_0 \cdot A_a - F_{max}}{m} \tag{4}$$

but the pump continues to introduce liquid into the space between the pump and the cylinder leading to increased acceleration. (F=ct)

$$\frac{\partial q}{\partial t} = ke \frac{\partial p}{\partial t} \tag{5}$$

or can be expressed through the relationships:

$$a = \frac{pA_a - F}{m} \tag{6}$$

provided that p satisfies:

$$p = \frac{E\Delta V}{V} = \frac{EQ_d \cdot t}{V_a + V_S} = \frac{MQ_d}{V_a + A_a \cdot S} \cdot t \tag{7}$$

and result :

$$a = \frac{A_a}{m} \cdot \frac{EQ_d}{V_a + A_a \cdot S(t)} \cdot t - \frac{F}{m} \tag{8}$$

where: S - lift load; Ff - the frictional forces of the sled and the pulley;

- the coefficient of friction; s, a, v - the space, speed and acceleration of the stem; t - time; Aa - the area of the cylinder; E - the modulus of elasticity; V - total volume of fluid; - volume of liquid due to compression; Qd, Qp-flow through the respective pump distributor.
From the expression (8) the acceleration increases linearly with time until either the maximum pressure or the maximum speed (3) is reached.
The process equations are:
where: S - lift load; Ff - the frictional forces of the sled and the pulley;
μ - the coefficient of friction; s, a, v - the space, speed and acceleration of the stem; t - time; Aa - the area of the cylinder; E - the modulus of elasticity; V - total volume of fluid; ΔV - volume of liquid due to compression; Qd, Qp- flow rate through the distributor respectively of the pump
From the expression (8) the acceleration increases linearly with time, until either the maximum pressure or the maximum speed (3)
The process equations are:

$$p_0 = \frac{F}{A_a} \tag{9}$$

it is the moment of beginning the displacement at which the acceleration is zero:

$$t_0 = \frac{V_a \cdot p_0}{E \cdot Q_d} = \frac{V_a \cdot F}{A_a \cdot E \cdot Q_d} \tag{10}$$

if : $$k_1 = \frac{A_a \cdot E \cdot Q_d}{m \cdot V_a} \quad \text{and} \quad k_2 = \frac{F}{m} \tag{11}$$

then : $$a = k_1 \cdot t - k_2 \tag{12}$$

again $$v = \int a(t)dt = \frac{k_1}{2} \cdot t^2 - k_2 \cdot t \tag{13}$$

$$s = \int v(t)dt = \frac{k_1}{6}t^3 - \frac{k_2}{2}t^2 \tag{14}$$

and pressure $$p = \frac{ma + F}{A_a} = \frac{m(k_1 t - k_2) + F}{A_a} \tag{15}$$

In conclusion, the speed becomes constant (no increases) when it is reached $Q_{max}=Q_p$ or $p_{max}=p_s$.

1) Evolution of the parameters of the system where it is reached $Q_{max}=Q_p$

$$p_{01} = F / A_a \tag{16}$$

$$t_{01} = \frac{V_a}{E \cdot Q_p} \cdot \frac{F}{A_a} \tag{17}$$

if $v_{max} = Q_d / A_a$ results from the equation (13)

$$\frac{k_1}{2} t_{a1} - k_2 t_{a1} = Q_1 / A_a \tag{18}$$

where it can express itself $$t_{a1} = \frac{k_2 + \sqrt{k_2^2 - 2k_1 Q_p / A_a}}{k_1} \tag{19}$$

$$a_{a1} = k_1 \cdot t_{a1} - k_2 \tag{20}$$

and after the time $t_{01} + t_{a1}$ acceleration $Qa = 0$

$$v_{a1} = v_{max} = Q_p / A_a \tag{21}$$

$$s_{a1} = \frac{k_1}{} t_a^{\,3} - \frac{k_2}{2} t_a^{\,2} \tag{22}$$

$$p_{a1} = \frac{m \cdot a_{a1} - F}{A_a} = \frac{m\left(k_1 \cdot t_{a1} - k_2\right) + F}{A_a} \tag{23}$$

Finally, they can be written $s(t), v(t), a(t), p(t), Q(t)$ dpending on time:

$$t = 0{,}001 \ldots t_{01} + t_{a1} + 0{,}1 \quad [s] \tag{24}$$

$$(t)=\frac{t_{01}{}^{2}}{3}\left(\frac{t_{a1}}{2}-k_2\right) \tag{25}$$

$$v_1(t)=\begin{cases}\frac{k_1}{2}t^2-k_2\cdot t \quad daca\ t\le t_{01}+t_{a1}\\ v_{a1} \quad daca\ t>t_{a1}+t_{01}\end{cases} \tag{26}$$

$$a_1(t)=\begin{cases}\frac{k_1}{2}-k_2 \quad daca\ t\le\left(t_{01}+t_{a1}\right)\\ 0 \quad daca\ t>\left(t_{a1}+t_{01}\right)\end{cases} \tag{27}$$

$$p_1(t)=\begin{cases}\frac{p_{a1}}{t_{01}+t_{a1}} \quad daca\ t\le t_{a1}+t_{01}\\ p_s \quad daca\ t>t_{a1}+t_{01}\end{cases} \tag{28}$$

$$Q_1(t)=\begin{cases}0 \quad daca \quad t\le\frac{\Delta V}{Q_{\max}}\\ Q_p \quad daca\ t>\frac{\Delta V}{Q_{\max}}\end{cases} \tag{29}$$

Lift – Hydraulic circuit

Initial dates :

$s = 700\ daN$ $\quad D = 5cm$ $\quad 1daN = 10N$ $\quad 1bar = 10^5Pa$

$a = 15\ deg$ $\quad d = 3{,}6cm$ $\quad V_a = 5000cm^3$

$Q_p = 4000\frac{cm^3}{s}$ $\quad h = 70cm$ $\quad V_b = 3000cm^3$

$\Delta p = 10bar$ $\quad E = 1{,}5\cdot 10^4 bar$

$m = \frac{S}{g}$ $\quad m = 713{,}801kg$ $\quad G = S\cdot\sin\alpha$ $\quad G = 1{,}812\cdot 10^3 N$

$A_a = \frac{\pi D^2}{4}$ $\quad A_b = \frac{\pi(D^2-d^2)}{4}$ $\quad A_a = 19{,}635cm^2$ $\quad A_b = 9{,}456cm^2$

$p_s = 3\cdot\left(\frac{G}{A_a}+\ \Delta p\right)$ $\quad p_s = 57{,}681bar$ $\quad$ or : $\quad p_s = 100bar$

1.The acceleration phase of the mechanism assuming that $p_a < p_s \quad F = 0\ N$

$p_{01} = \frac{G+F}{A_a}$ $\quad p_{01} = 9{,}227bar$ $\quad t_{01} = \frac{V_a}{E\cdot Q_p}\cdot\frac{G+F}{A_a}$ $\quad t_{01} = 7{,}689\cdot 10^{-4}s$

$k_1 = \frac{A_a\cdot E\cdot Q_p}{m\cdot V_a}$ $\quad k_1 = 3{,}301\cdot 10^5\ cm/s^3$ $\quad k_2 = \frac{G+F}{m}$ $\quad k_2 = 253{,}815\ cm/s^2$

$t_{a1} = \frac{k_2+\sqrt{k_2^2\frac{2k_1\cdot Q_p}{A_a}}}{k_1}$ $\quad t_{a1} = 0{,}036\ s$

$a_{a1} = k_1\cdot t_{a1} - k_2$ $\quad a_{a1} = 115{,}998\ m/s^2$ $\quad$ *very high volume* !!!

$\Delta V = 1\cdot 10^2\cdot cm^3$

$v_{a1} = \frac{Q_p}{A_a}$ $\quad v_{a1} = 2.307\, m/s$ $\quad q_1 = \frac{\Delta V}{Q_p}$

$s_{a1} = \frac{k_1}{6} \cdot t_{a1}^3 - \frac{k_2}{6} \cdot t_{a1}^2$ $\quad s_{a1} = 2{,}384 cm$ $\quad q_1 = 0{,}025 s$

$p_{a1} = \frac{m \cdot a_{a1} - (G+F)}{A_a}$ $\quad p_{a1} = 412{,}468\ bar$ $\quad$ *very high volume* !!!

$t = 0 \cdot s, 0{,}001 \cdot s \dots t_{01} + t_{a1} + 0{,}1 \cdot s$ $\quad s(t) = \cdots \frac{t^2}{3} \cdot \left(\frac{k_1}{2} \cdot t - k_2\right)$

$$p_1(t) = \left| \begin{matrix} \frac{p_{a1}}{t_{01}+t_{a1}} \cdot t & if \ \ t \le t_{a1} + t_{01} \\ p_{01} \quad if & t > t_{a1} + t_{01} \end{matrix} \right. \qquad v_1(t) = \left| \begin{matrix} \frac{k_1}{2} \cdot t^2 - k_2 \cdot t & if \ \ t \le t_{a1} + t_{01} \\ v_{01} \quad if & t > t_{a1} + t_{01} \end{matrix} \right.$$

$$v_1(t) = \left| \begin{matrix} \frac{k_1}{2} \cdot t^2 - k_2 \cdot t & if \ \ t \le t_{a1} + t_{01} \\ 0 \quad if & t > t_{a1} + t_{01} \end{matrix} \right. \qquad Q_1(t) = \left| \begin{matrix} 0 & if \ \ t < q_1 \\ Q_p & if \ \ t > q_1 \end{matrix} \right. \qquad \begin{matrix} Q_p = 4 \cdot 10^{-3}\, m/s \\ q_1 = 0{,}025\ s \end{matrix}$$

2. The acceleration phase of the mechanism in the event that $p_a > p_s$

$p_{02} = p_{01}$ $\quad t_{02} = t_{01}$

$a_{a2} = \frac{p_s \cdot A_a - (G+F)}{m}$ $\quad a_{a2} = 24{,}969\, m/s^2$ $\quad t_p = \frac{a_{a2} + k_2}{k_1}$ $\quad t_p = 8{,}333 \cdot 10^3\ s$

$v_p = \frac{k_1}{2} \cdot t_p^2 - k_2 \cdot t_p$ $\quad v_p = 0{,}093\, m/s$ $\quad s_p = \frac{k_1}{6} \cdot t_p^3 - \frac{k_2}{2} \cdot t_p^2$ $\quad s_p = 0{,}023\ cm$

$t_s = \frac{v_{a1} - v_p}{a_{a2}}$ $\quad t_s = 0{,}078\ s$ $\quad t_{a2} = t_p + t_s$ $\quad t_{a2} = 0{,}086$ s

$s_s = \frac{a_{a2} \cdot t_s^2}{2}$ $\quad s_s = 0{,}076\ m$

$s_{a2} = s_p + s_s$ $\quad s_{a2} = 0{,}076\ m$

$p_{a2} = \frac{m \cdot a_{a2} - (G+F)}{A_a}$ $\quad p_{a2} = 81{,}546\ bar$ $\quad$ *and is* $< p_{a1}$

3. Calculation of working parameters in the acceleration period of the mechanism

$$h_k = \frac{\frac{A_b \cdot h}{10 \cdot \sqrt{A_b^3}} + \frac{V_a}{\sqrt{A_b^3}} - \frac{V_b}{\sqrt{A_a^3}}}{10 \cdot \frac{1}{\sqrt{A_a}} + \frac{1}{\sqrt{A_b}}} \qquad h_k = 25{,}368\ cm$$

$C_1 = \frac{A_a^2 \cdot E}{A_a \cdot h_k + V_a}$ $\quad C_2 = \frac{A_b^2 \cdot E}{A_b \cdot (h - h_k) + V_a}$ $\quad C_1 = 1{,}052 \cdot 10^3\ daN/cm$ $\quad C_2 = 247{,}378\ daN/cm$

$f_{0_{min}} = \frac{1}{2\pi} \cdot \sqrt{\frac{C_1 + C_2}{m}}$ $\quad f_{0_{min}} = 6{,}79\ Hz$

$a_{a_{dm}} = \frac{2\pi \cdot f_{0_{min}} \cdot v_{a1}}{18}$ $\quad a_{a_{dm}} = 4{,}828\, m/s^2$ $\quad t_{a_{dm}} = \frac{18}{2\pi \cdot f_{0_{min}}}$ $\quad t_{a_{dm}} = 0{,}422\ s$

$\Delta V_3 = \frac{p_s \cdot V_a}{E}$ $\quad \Delta V_3 = 3{,}333 \cdot 10^{-5}\ \ m^3$

$$p_2(t) = \left| \begin{matrix} \frac{p_{a2}}{t_{01}+t_p} \cdot t \quad if \ \ t \le t_p + t_{01} \\ p_{a2} \ \ if \ \ (t_{01} + t_p) < t \le (t_{01} + t_{a2}) \\ p_{01} \quad if \ \ t > (t_{01} + t_{a2}) \end{matrix} \right. \qquad v_1(t) = \left| \begin{matrix} \frac{k_1}{2} \cdot t_2 - k_2 \cdot t & if \ \ t \le t_{a1} + t_{01} \\ v_{a1} \quad if & t > t_{a1} + t_{01} \end{matrix} \right.$$

$$a_2(t) = \begin{vmatrix} \frac{k_1}{2} \cdot t - k_2 \quad if \quad t \leq \quad if \quad t + t_{01} \\ a_{a2} \quad if \quad t_{01} + t_p < t \leq t_{01} + t_p + t_s \\ o \quad if \quad t > t_{a2} + t_{01} \end{vmatrix} \qquad Q_1(t) = \begin{vmatrix} 0 \quad if \quad t \leq q_1 \\ Q_p \quad if \quad t > q_1 \end{vmatrix}$$

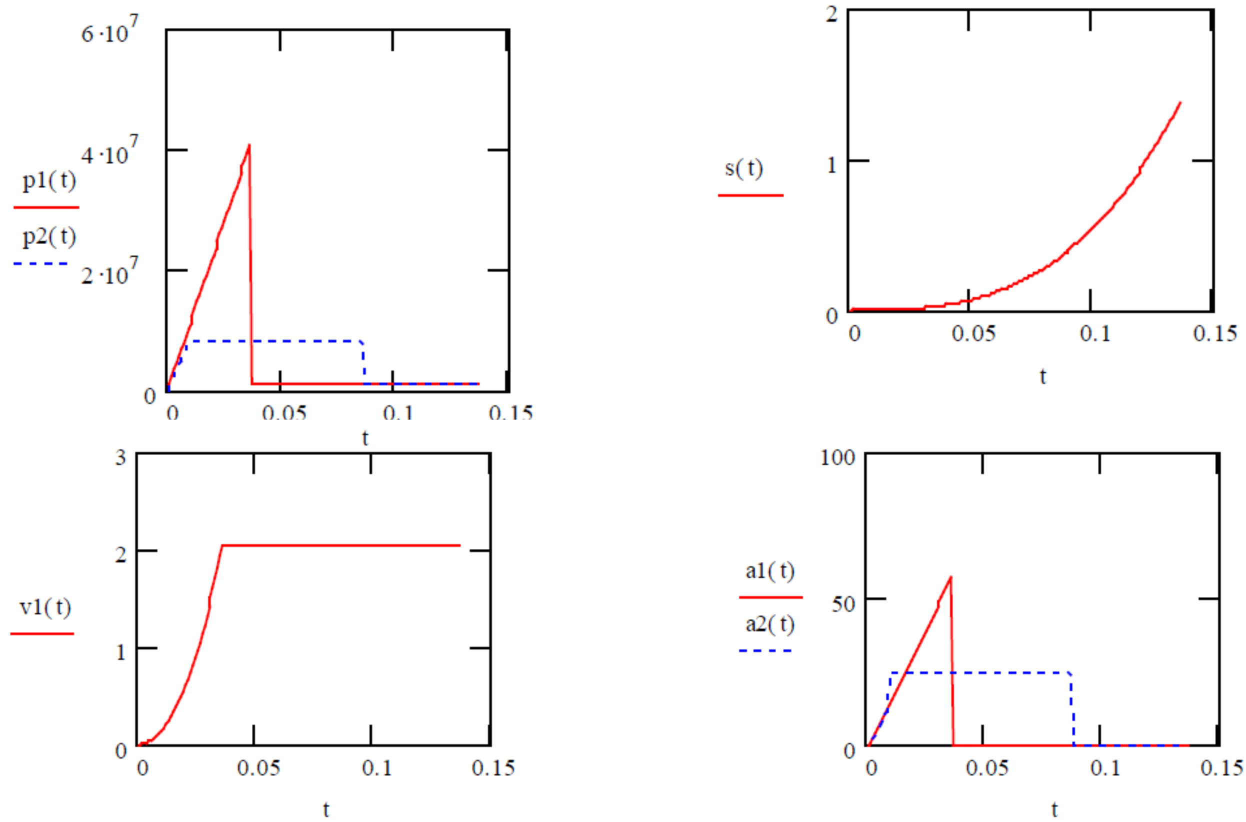

4. Conclusions

The evolution of the process is influenced by three factors: the time, space and frequency of the lifting mechanism:

a) Time t_a must be chosen from 0.1 ... 0.5 (s) because its decrease does not lead to a significant increase in acceleration, and its increase leads to a decrease in productivity.

b) Space must be chosen in the range 1.7 ... 10 cm which correlates with the acceleration through the formula: $s_a = v^2 / 2a$. A smaller space requires an acceleration over 10m/s^2 and the larger space is inadmissible for the mechanism.

c) c) The influence of its own frequency can be presented as follows: a low value of its own frequency leads to intermittent operation. Companies specialized in hydraulic systems recommend that their own frequency should not be less than 3 Hz. In order to increase its frequency, the surface of the hydraulic cylinder must be increased and the oil volume must be as small as possible. The numerical simulation study was performed for a load totaling 700 kg. We observe that in the case of lifting the lift to the maximum load the maximum extreme point of pressure is realized around 4.9 Mpa in a time of t = 0.35s, while in the case of the minimum load the maximum extreme point is obtained at half the value for the maximum load in - a long time t = 0.39s. In the case of lowering the hydraulic lift with the maximum load the maximum pressure reached is 3.8 Mpa in a time of 0.31s, and in the case of the minimum load, it is 3.80 Mpa reached in a time of 0.32s. The study may be extended to other masses, but the essential characteristics have been highlighted in the ranks above.

References

[1] Pătruț, P., and I. Nicolae. *Acţionări hidraulice şi automatizări: Teorie, aparate, sisteme automate şi aplicaţii industriale / Hydraulic drives and automation: Theory, devices, automatic systems and industrial applications*. Bucharest, Nausicaa Publishing House, 1998.
[2] Marin, Virgil, and Al. Marin. *Sisteme hidraulice automate – Construcţie, reglare, exploatare / Automatic hydraulic systems - Construction, adjustment, operation*. Bucharest, Technical Publishing House, 1987.
[3] Oprean, A. *Hidraulica maşinilor unelte / Hydraulics of machine tools*. Bucharest, Didactic and Pedagogical Publishing House, 1983.
[4] http://www.rasfoiesc.com/inginerie/tehnica-mecanica/Structura-unui-sistem-de-actio47.php.
[5] http://www.anc.edu.ro/uploads/SO/Montator.depanator.ascensoare.pdf
[6] https://kleemannlift.wordpress.com/2009/12/09/comparatie-hidraulic-electric/
[7] http://www.ascensoradv.ro/lifturi-hidraulice-principii-de-functionare/
[8] http://stiintasiinginerie.ro/wp-content/uploads/2016/07/29-20-DESPRE-ASCENSOARE-LIFTURI..pdf.

VIBRATING PLATFORMS WITH HYDRAULIC ACTUATION

Petrin DRUMEA[1], Ioan PAVEL[1], Bogdan TUDOR[1], Ștefan-Mihai ȘEFU[1], Alexandru HRISTEA[1]

[1] Hydraulics and Pneumatics Research Institute INOE 2000-IHP Bucharest, ihp@fluidas.ro; pavel.ihp@fluidas.ro; btudor.ihp@fluidas.ro; sefu.stefan93@gmail.com; hristea.ihp@fluidas.ro

Abstract: *The article refers to the need to train the population for rational behavior in the case of earthquakes with a high degree of danger. An efficient training can be performed with the help of vibrating platforms to model the oscillations of the bark that occur in the case of an earthquake with a magnitude of 5-7 degrees on the Richter scale. A large part of the population did not experience an earthquake of more than 5.5 degrees during life and as a result, in such cases, panic will develop, which will easily lead to an increase in the destructive effects. Within the article some schematic solutions of mobile vibrating platforms, hydraulically operated and a solution completed with a patent application will be presented.*

Keywords: *Mobile vibrating platform, servo cylinder, earthquake, oscillatory movements*

1. Introduction

The earthquake represents an oscillatory movement, usually abrupt and of internal origin, of the tectonic plates in the earth's bark, which releases a large amount of kinetic energy. This energy creates seismic waves, thus producing extremely strong oscillations at ground level resulting in significant material damage and loss of human life. The situation at national level is quite disappointing, if in the case of the buildings there were improvements of design, execution and consolidation of the old buildings, in the case of the population nothing was implemented in the field of population preparation in case of earthquake. During the great earthquakes, such as those of 1681, 1738, 1802, 1838, 1940 and 1977, there were a high number of victims, which could have been reduced if mass training of the population had been carried out previously, thus managing to be saved numerous lives. And now this danger persists especially in crowded areas or with intense traffic. Although the earthquakes last several seconds, their effects are catastrophic.
Following the analysis of the usual earthquakes that take place in our country, the following phases of a seismic movement result: - the initial phase with oscillations of the order a = 0.001 g - 0.002 g (0.5 g) with a duration of 2-18 s (g = gravity acceleration); - the main phase, with major oscillations of over 0.05 g, but especially with accelerations a = 0.1 - 0.2 g and a duration of 10 - 50 s (for magnitudes M = 5.5 - 8); - the final phase of gradual amortization of the oscillations, up to the limit of perception, with a duration of 17 - 30s.

2. Simplified solutions of hydraulic vibrating platforms

Figure 1 shows a simple variant of vibrating platform consisting of:
- Servo cylinder 1
- The point of support and articulation
- Pulse attenuator 3.

By actuating the servo cylinder 1 with a frequency of up to 30 Hz, a vibrational movement occurs on the vertical axis around the point of articulation 2. The role of cylinder 3 in this scheme is to dampen the oscillation or to induce a load by drilling it, so it will oppose the movement generated by the cylinder 1 and will decrease the amplitude of the vibrations.

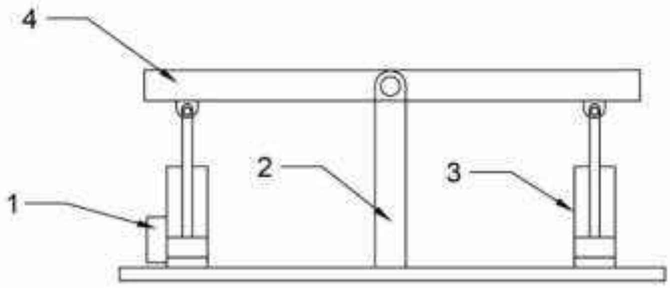

Fig. 1.

In Figure 2 is represented another variant of the vibrating platform, but this time without a pulse attenuator.

The platform consists of:

- Servo cylinder 1
- The support point and joints 2
- The platform itself 3.

Unlike the previous figure, the cylinder with the role of pulsation damper was replaced with a hinged point and we reset, so that the movements performed by the servo cylinder 1 are directly transmitted to the platform 3.

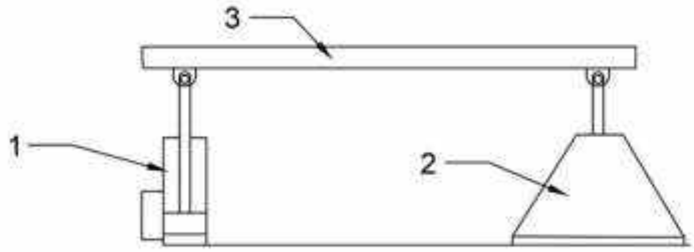

Fig. 2.

Figure 3 shows a simple variant of a horizontal vibrating platform consisting of:

- Servo cylinder 1
- Plate 2
- And the point of articulation 3.

Unlike the platforms in Figures 2 and 3, which generate an oscillatory movement along the z axis, the platform shown in Figure 3 produces an oscillatory movement in the horizontal plane x, y. By actuating the cylinder 1, there is an oscillation movement around the joint point 3. The movement transmitted by the cylinder to the platform 3 is an unamortized one.

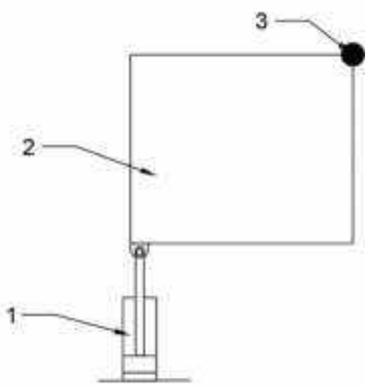

Fig. 3.

3. Solutions of mobile vibrating platforms worldwide

Figure 4 shows a mobile platform called Big Shaker, made by the company QUAKEHOLD from America and is able to simulate earthquakes up to 8 degrees on the Richter scale.

Fig. 4.

Figure 5 [1] shows a mobile earthquake simulation platform in Alaska, which is included in a governmental population training program on the state of seismic production in that state.

Fig. 5.

Figure 6 shows a mobile earthquake simulation platform "called Quake Cottage" [2] and can simulate earthquakes up to 9.5 degrees on a Richter scale. The platform is equipped with various elements of furniture and equipment to be able to observe what happens to them during the production of a large earthquake and the importance of securing some of them.

Fig. 6.

Figure 7 shows another type of mobile earthquake simulation platform used in Japan. As can be seen from the pictures near adults, children are also trained to acquire appropriate behavior in the event of an earthquake.

Fig. 7.

4. Presentation of the vibration platform solution placed on a car trailer

The mobile vibrating platform presented in figure 8, is placed on a car trailer, which gives us the possibility to tow it where it is needed and has been the subject of a patent application, requested by specialists from the National Institute for Research and Development INOE 2000-IHP .
The vibrating mobile platform according to the invention, is made up of a trailer platform (2) which is equipped with a folding hydraulic servo cylinder (fig. 8 pos. 6), located on the small rear side, mounted on the ground in the working position and two folding classic hydraulic cylinders (figs 8, 4 and 5), with a patina on the head of the rod which in the working position have a distance of 50-100 mm from the ground. They are fed from a hydraulic station (fig. 8 pos. 3) through distribution devices and are commanded to execute movements with the help of a controller that allows manual control or after preset programs. The servo cylinder exerts on the platform vibrational movements controlled in vertical direction in the range 0-50 mm and 1-30 Hz. Cylinders located on the side periodically crash into the ground and print to the platform a lateral swing movement in both directions. From this combination of movements you can obtain oscillatory movements of the platform similar to the real situations created by the production of an earthquake.
During the simulation, the wheels are tightened and the trailer is mounted in the front (fig. 8, picture 1) or remains fixed on the tractor head. The amplitude of the movement is taken up by the platform springs and the deformation of the tires which during the simulation remain permanently in contact with the ground.
The hydraulic station (fig. 8 pose 3), is located under the platform, and the three cylinders are foldable with clamping and fastening under the platform so that it can be transported safely on the roads. Depending on the consumption and location, the power supply can be done from the network or from a power generator.

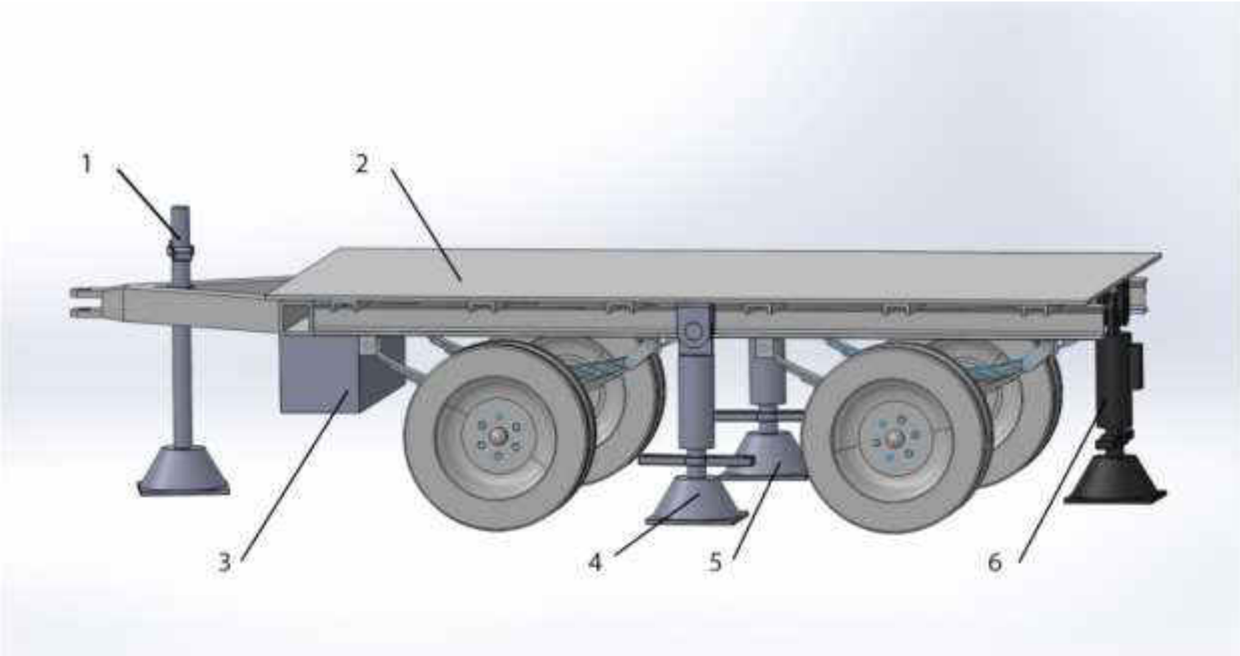

Fig. 8.

The hydraulic diagram shown in Figure 9 performs all the movements necessary for the simulation in real conditions of production of an earthquake.

The hydraulic system shown in Figure 9 is an open system consisting of a basin, on which is filled the filling filter 11, the submersible pump 12 and the electric motor 13 attached to the pump and located on the tank cover, return filter 14 which contains a clogging indicator and the level indicator 15.

Considering that the pump 12 is a fixed flow pump, which is not adjustable, as a protection element against its start-up, the distributor 10 is provided, which at the time of start-up is in the open position, thus making the direct connection between the pump and tank refueling. After starting the pumps, the electromagnet of the distributor 10 is actuated and the pump delivers flow into the system. Also on the discharge route of the pump is provided the manometer 8 to be able to read the pressure in the system, as well as the safety valve 9 that protects the pump in case of overpressure in the system, releasing the pressure to the tank.

On the supply path of the solenoid valve 3 there is also a filter 7 for the protection of the solenoid valve, because it is sensitive to impurities in the system.

Hydraulic cylinders from position 4 and 5 are operated by distributors 1 and 2 to create periodic shocks on the side of the platform, in order to obtain the lateral oscillations. Distributors 1 and 2 in the closed position keep the cylinder stem retracted, remaining prepared for a new balance impulse that should be applied to the platform according to the scheduled scenario.

The vibrations of the servo cylinder - the frequency and the amplitude - are controlled by the solenoid valve 3, also according to the programmed scenario.

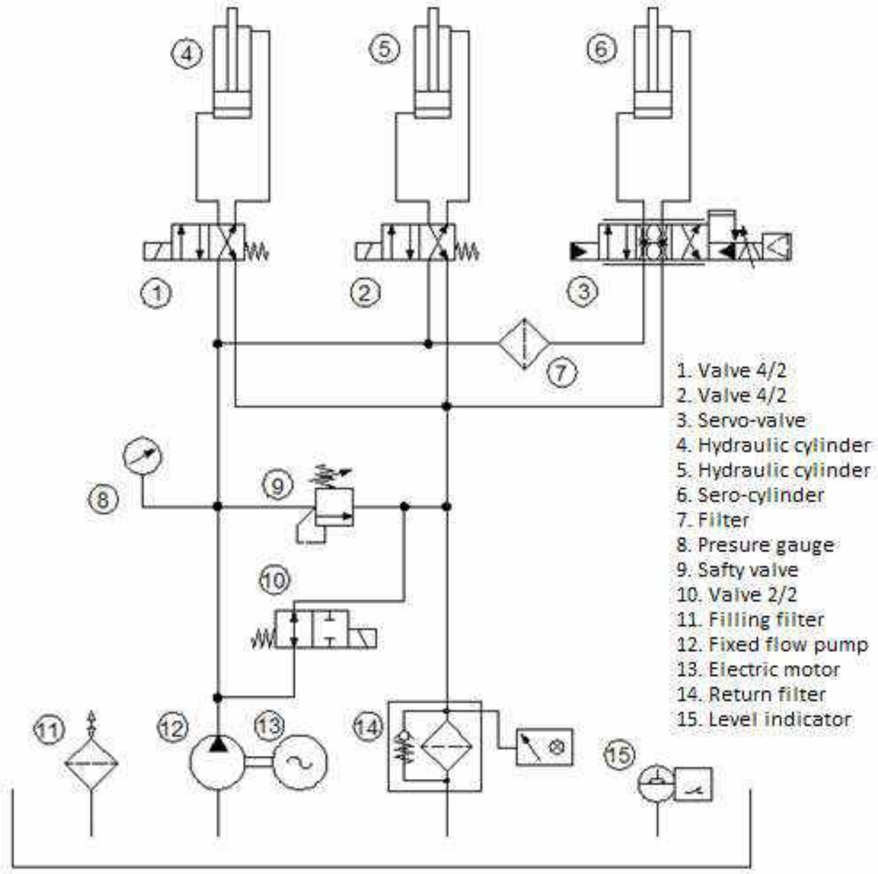

Fig. 9.

5. Conclusions

Romania is among the few countries affected by the intense seismic activity, which has not implemented a program to prepare the population for appropriate behavior in case of a large magnitude earthquake. This population preparation program should be implemented especially in areas with high population density in order to control the effects of panic among the population.
The implementation of such programs also implies the development of such indigenous platforms to support the training programs.
The authors of the article will try to develop such a mobile platform for training the population in case of earthquakes, by applying to different national and European competitions for project submission, but also by seeking beneficiaries from the state institutions that want such equipment.

References

[1] http://www.bigshaker.com/.
[2] https://ready.alaska.gov/Preparedness/Outreach/QuakeCabin.
[3] https://www.quakecottage.com/photos/.
[4] https://selcukcabar.wordpress.com/2011/10/21/erdbebensimulator-earthquake-simulator/.
[5] Radoi, Radu, Ioana Ilie, and Marian Blejan. “Hydraulic drive system for a training simulator of flight attendants.” Paper presented at the 2014 International Conference of Hydraulics and Pneumatics – Hervex, Calimanesti-Caciulata, Romania, November 5-7, 2014.
[6] Drumea, Petrin, Ioan Pavel, and Bogdan Alexandru Tudor. “Simulator for training in case of earthquake.” Patent application no. A/00640 – 09.10.2019.
[7] Marin, V., and Al. Marin. *Sisteme hidraulice automate - Constructie, reglare, exploatare / Automated Hydraulic Systems – Construction, regulation, operation*. Bucharest, Technical Publishing House, 1987.

ISSN 1454 - 8003
Proceedings of 2019 International Conference on Hydraulics and Pneumatics - HERVEX
November 13-15, Băile Govora, Romania

METHOD AND DEMONSTRATING INSTALLATION FOR RECOVERY OF TITANIUM AND TUNGSTEN OXIDES FROM SPENT SCR CATALYST PART I – SCALING OF HYDRODINAMIC CAVITATION METHOD

Adrian CIOCĂNEA[1], Radu SAUCIUC[2], Ioan LEPĂDATU[2], Sanda BUDEA[1], Ștefan-Mihai ȘEFU[2], Ștefan-Mugur SIMIONESCU[1]

[1] University POLITEHNICA of Bucharest, adrian.ciocanea@upb.ro

[2] INOE 2000 – IHP Bucharest, sauciuc.ihp@fluidas.ro

Abstract: *Selective catalyst reduction (SCR) catalysts provided excellent results for the reduction of nitrogen oxide (NOx) emissions in diesel exhaust, due to a large range of operating temperatures, durability of deactivation and high conversion rate of NOx. Due to technological developments is unlikely to be replaced in automotive applications. As a result, the commercial efficiency of recovering critical materials is further sought in the context of reducing energy consumption and environmental impact. A hydrodynamic cavitation method is proposed in order to maximize the effect of destructuration of honeycomb monolithic support of SCR catalyst -* V_2O_5 *–* WO_3/TiO_2 *type - for extracting the crystalline titanium and tungsten oxides from the cordierite surface. High relative inlet pressure of 25 MPa is applied to a divergent nozzle for obtaining cavitation jets. In order to design the dedicated installation, the characteristics of the cavitation jets are analyzed: pressure drop in relation to the length and core diameter of the jet. The data are useful for settling down the optimum distance between the nozzle output and the target i.e. the honeycomb monolithic support of SCR catalyst. Best results are reported for 25 MPa where the ratio between jet core diameter and jet length is d/l=0.115. An inlet pressure at the nozzle input below 16MPa seems to be ineffective since no jet core is recorded.*

Keywords: *Selective catalyst reduction, diesel exhaust, hydrodynamic cavitation, submerged jet*

1. Introduction

Selective catalyst reduction (SCR) catalysts provided excellent results for the reduction of nitrogen oxide (NOx) emissions in diesel exhaust, due to a large range of operating temperatures, durability of deactivation and high conversion rate of NOx [1, 2]. Their advantages recommended them for integration in some diesel-powered light and heavy-duty vehicles [3-6]. SCR catalyst are composed primarily of anatase TiO_2 used as catalyst carrier, V_2O_5 as the active component and WO_3 acting as a promoter for thermal stability of the catalyst and offering resistance to sulfur contamination. The honeycomb - type monolithic support for the metal oxide species in the SCR catalyst is usually made of cordierite ($2MgO \cdot 2Al_2O_3 \cdot 5SiO_2$). The oxides of vanadium and tungsten contribute with about 40% at the total cost of the SCR catalyst [7]. The commercial V_2O_5 – WO_3/TiO_2 catalyst present a high tungsten (W) content, of about 7-10 wt% WO_3 by comparing with vanadium (V) content of only 0.5 – 1.5 % V_2O_5 [1, 8]. Chemical lifetime for the SCR is usually about 3 years and regeneration processes involving chemical and/or heat treatment is often considered in order to extend this lifetime, often doubling it. At the end of lifetime the deactivated SCR catalyst, after several regeneration cycles end up as waste and is disposed of in landfills. In order to avoid the soil contamination a strategy based on the recovery of valuable metals and regeneration of the rest of the spent catalyst must be considered [9]. In this paper a hydrodynamic cavitation method is scaled with the aim to include it in a demonstrator installation in order to maximize the effect of destructuration of honeycomb monolithic support of spent Selective Catalyst Reduction (SCR) catalyst - V2O5 – WO3/TiO2 type - for extracting the crystalline titanium and tungsten oxides from the cordierite surface.

2. Methods for recovering valuable metals from spent catalysts

The classical methods of recovering precious metals from car catalysts with ceramic base structure are of hydro-metallurgical type [10, 11] and of pyro-metallurgical type [10, 12]. From the point of view of the energy and environmental impact, each of the methods described raises specific problems: the hydro-metallurgical method involves wastewater treatment, while the pyro-metallurgical method involves high energy consumption and lower extraction rates.
Another class of methods refers to the mechanical ones: by friction and flotation or by ultrasonic cavitation. In the first method, the extraction is done in containers in which rotors with teeth are placed. They are calibrated such that between the rotors surface and the bottom of the vessel, an interstice of up to 0.3 ÷ 0.5 mm is formed [13, 14]. The grinding of the mixture, by means of the shear forces that appear between the particles, is carried out under conditions of flotation that facilitate a separation of the components.
The efficiency of the process is influenced by the residence time of the mixture in the container in the working range, the liquid/solid ratio and the size of the initial particles introduced into the device. The results reported in the literature [14] show that in fractions smaller than 300 μm the recovery percentage reached 81.2% for a residence time of approximately 60 min, the percentage being higher for the case where the introduced particles had larger dimensions – figure 1.

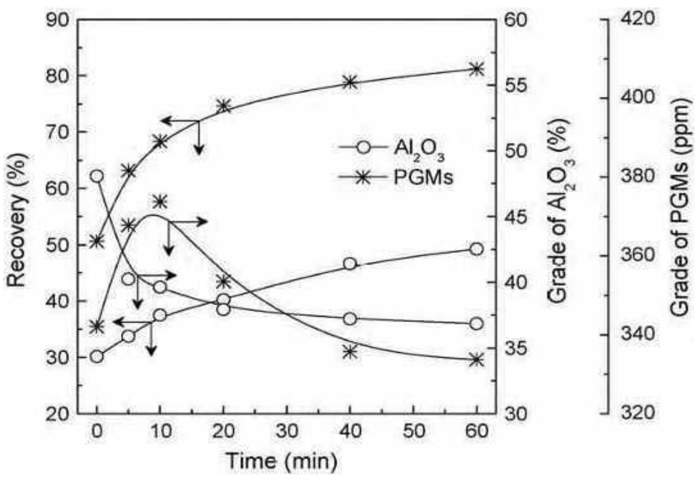

Fig. 1. The degree of recovery of Al_2O_3 and Platinic Metal Group (PMGs) for different time intervals (fractions below 300 μm) [14]

In the second method, the valuable metal extraction takes place by exposing the catalytic converter placed in an ultrasonic washing bath to the effects of (ultrasonic) cavitation [15]. The effects of cavitation are manifested by the detachment of catalytic material from the monolithic support that remains undamaged. Selective powders are obtained by adjusting a frequency in the range 10 ÷ 1000 kHz. There are no known studies in the literature to verify experimentally the above procedure.
A method that combines the two mechanical procedures described above is the hydrodynamic cavitation: (a) the mechanical effect of the cavitational jet produces high shear stresses between the particles of the mixture subjected to the procedure; (b) increasing the concentration of oxygen and free radicals in the biphasic liquid creates higher premises of oxidation reactions with metals.
Hydrodynamic cavitation, respectively the creation of cavitational jets, can be achieved by at least two methods: (a) by using an intermediate fluid (ex. N_2) [16] or (b) by using a high-pressure volumetric pump [17]. By increasing the inlet pressure in a nozzle, the cavitation phenomenon becomes more active. For different working pressures and shapes of the nozzle, the jet is characterized by the appearance of vapors and/or air bubbles, i.e. by the manifestation of cavitation with vapor bubbles and air bubbles. The two types of cavitation appear simultaneously if the liquid is not degassed. It is known that only the bubble cavitation has an erosion effect [18] and

therefore it is desirable that the shape of the nozzle, the ratio of upstream/downstream pressures and the degree of oxygenation of the liquid ensure its occurrence. The existence of the gas bubble cavitation has a mechanical role, since the bubble cloud is destroyed only at the impact with a solid boundary or at a distance if there is enough space available for the pressure to play this role. Experimental studies have revealed the connection between the liquid and nozzle parameters and the two types of cavitation [17].

3. Experimental set-up

The experimental stand was built using a pressure source i.e a volumetric piston pump that provided a maximum pressure of 25 MPa. The pump was mounted to a device with a divergent nozzle with a minimum diameter of 0.5 mm. The working pressure was monitored in real time by means of a digital pressure gauge connected through a data acquisition board to a computer. It was thus possible to determine the number of cavitation cycles that the pump induced in the work room. In figure 2 (a, b, c) the elements of the experimental stand and of the divergent nozzle are presented.

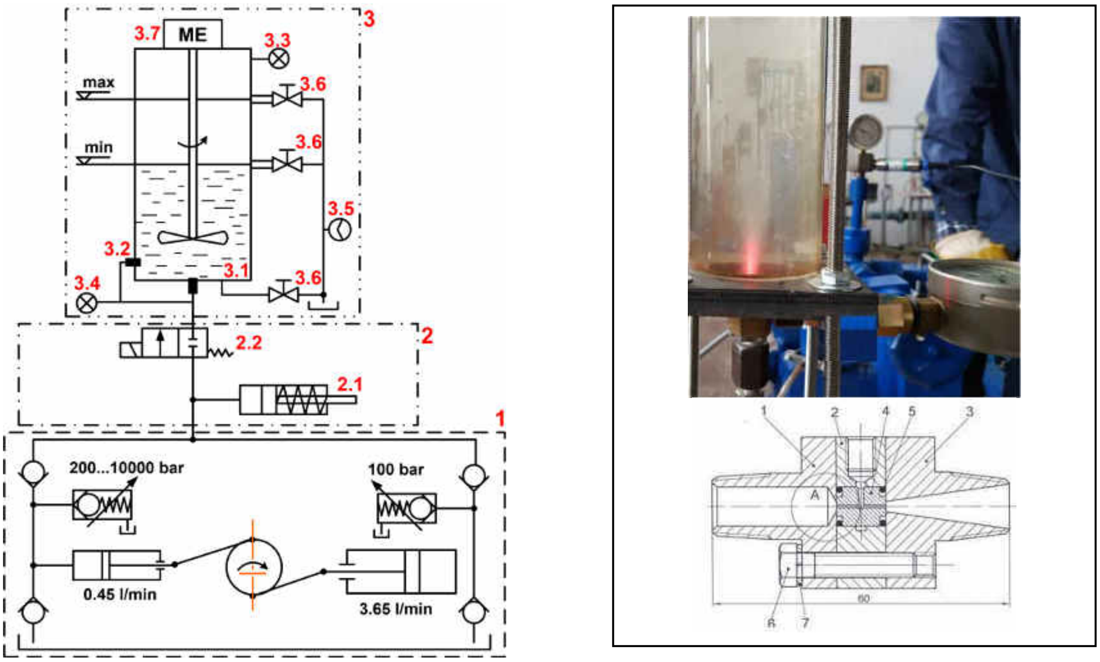

a. b. c.

Fig. 2. Experimental set-up: (a) Cavitation jet system (1. Plunger pump system; 2. Pressure distribution system: 2.1. Accumulator, 2.1. Electric distributer; 3. Test chamber: 3.1., 3.2. Nozzle, 3.3. Low pressure transducer, 3.4. High pressure transducer, 3.5. Flow indicator, 3.6. Valves, 3.7. D.C. motor and propeller) and (b, c) Cavitation nozzle (transparent cylinder, nozzle $\phi = 0.5$ mm)

The pressure drop in the nozzle was measured by using a digital pressure gauge (3.4), as well as the downstream pressure (3.3). The cavitational jet was highlighted with the help of a red-light planar laser that allowed the determination of the jet dimensions.

4. Results

The plunger pump was used in order to deliver three fixed upstream pressures in the nozzle: 250, 160 and 80 MPa. The pressure drop in the divergent nozzle was measured for each inlet pressure at downstream pressure values of 0.0, 0.05 and 0.1 MPa respectively. For each case, the geometry of the cavitational jet was assessed by analyzing a group of photos obtained with a frequency of 1/300 s. The results are presented in figure 3 (a, b, c), where the core diameter and length of the cavitational jet are related with the pressure drop in the nozzle.

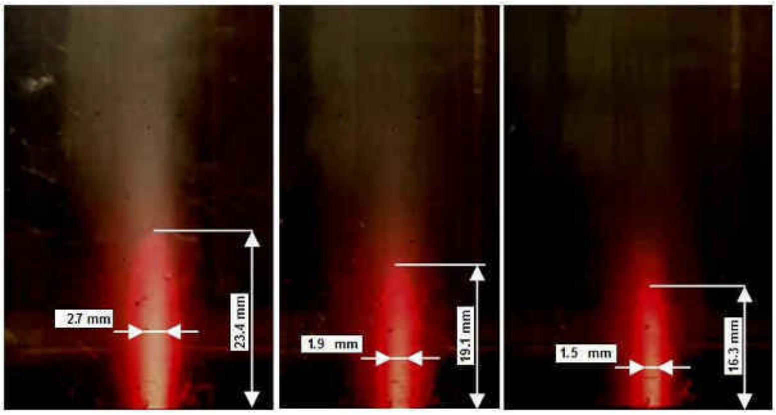

a.

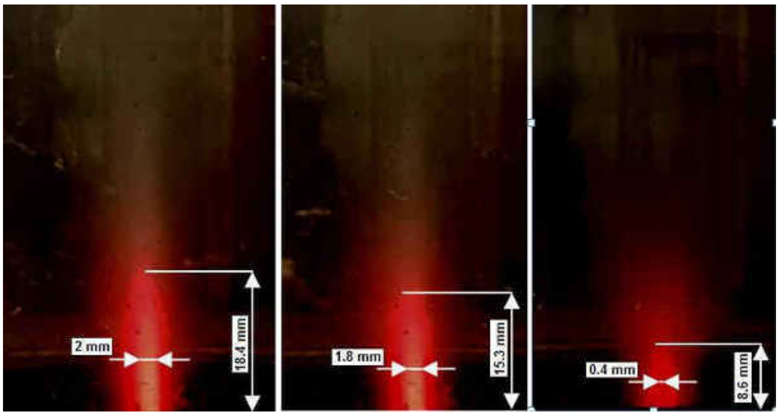

b.

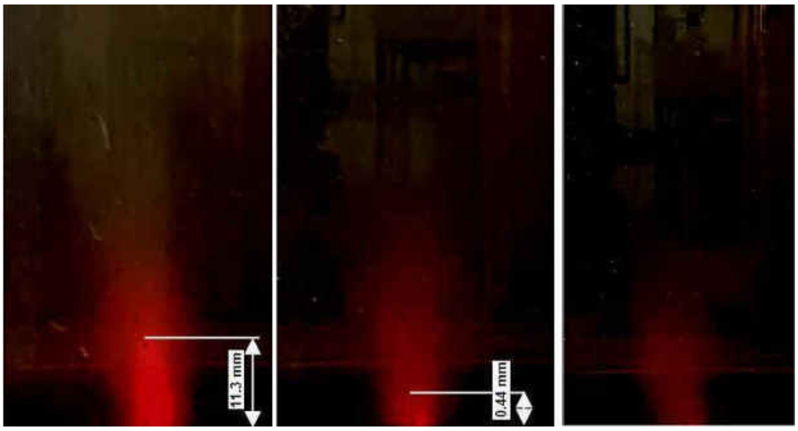

c.

Fig. 3. The geometry of the cavitational jet

a) upstream pressure – 25 MPa and downstream pressure 0.0 MPa, 0.05 MPa and 0.1 MPa;

b) – 16 MPa and downstream pressure 0.0 MPa, 0.05 MPa and 0.1 MPa;

c) – 8 MPa and downstream pressure 0.0 MPa, 0.05 MPa and 0.1 MPa;

Table 1 presents the pressure drop in the nozzle and the *d*/*l* ratio, where *d* is the jet core diameter and *l* is the jet length.

Table 1: Pressure drop in the nozzle and *d*/*l* ratio

Upstream Pressure MPa	**Downstream pressure MPa**	**Pressure drop MPa**	***d* mm**	***l* mm**	***d/l* -**
25	0.00	0.85	2.7	23.4	0.115
25	0.05	0.72	1.9	19.1	0.099
25	0.10	0.56	1.5	16.3	0.092
160	0.00	0.75	2.0	18.4	0.110
160	0.05	0.30	1.8	15.3	0.110
160	0.10	0.16	0.4	8.6	0.046
80	0.00	0.63	-	11.3	-
80	0.05	0.16	-	4.4	-
80	0.10	0.00	-	-	-

The best results are reported for the case where the value for upstream pressure is 25 MPa with no downstream pressure and the ratio has the highest value, *d/l* = 0.115. The maximum length of the cavitational jet is 23.4 mm. For the upstream pressure of 16 MPa the ratio *d/l* = 0.110 – close to the best result reported – but the length of the cavitation jet is shorter, *l* = 18.4 mm. Therefore, when designing the demonstrator installation, the optimum distance from the nozzle outlet to the honeycomb monolithic support of SCR catalyst as target should be in the range of 18÷20 mm in order to maximize the cavitation effect.

5. Conclusions

A hydrodynamic cavitation method is proposed in order to maximize the effect of destructuration of honeycomb monolithic support of SCR catalyst. An upstream pressure of 25 MPa is applied to a divergent nozzle for obtaining cavitation jets and various downstream pressures were settled down in order to assess the impact on jet geometry. The best results of the study will be used for optimizing a dedicated installation i.e. settling down the distance between the nozzle outlet and the honeycomb target. The characteristics of the cavitation jets are analyzed: pressure drop in relation to the length and core diameter of the jet. Best results are reported for 25 MPa where the ratio between jet core diameter and jet length is *d/l*=0.115. An inlet pressure at the nozzle input below 16 MPa seem to be ineffective since no jet core is recorded.

Acknowledgment

This work has been funded by the Romanian Ministry of Research and Innovation under Programme I - Development of national R&D system, Subprogramme 1.2 – Institutional performance – Projects financing excellence in R&D+I, Financial Agreement no. 19PFE/17.10.2018, while the scientific results have been obtained under the PN-III-1.2-PCCDI-2017-0185 Project ECOTECH-GMP – No. 76PCCDI/2018.

References

[1] Adrian, M., E. Martin, F. Davide, and K. Oliver. “VOx surface coverage optimization of V_2O_5-WO_3/TiO_2 SCR catalysts by variation of the V loading and by aging.” *Catalyst* 5 (2015): 1704-1720.

[2] Li, J., H. Chang, L. Ma, J. Hao, and R.T. Yang. “Low temperature selective catalytic reduction of NO_x with NH_3 over metal oxide and zeolite catalysts-A review.” *Catal. Today* 175, 147e156 (2011).
[3] Zielińska, Katarzyna, and Agnieszka Haratym. “Environmental benefits of the SCR systems: a case study of the Lublin city transport.’ *Journal of Ecological Engineering* 18, no. 3 (May 2017): 202–207.
[4] Hosoya, M., Y. Kawada, S. Satao, and M. Shimoda. “The study of NO_x and PM reduction using urea selective catalytic reduction system for heavy duty Diesel engine.” *SAE Technical Paper* 2007-01-1576 (2007). https://doi.org/10.4271/2007-01-1576.
[5] Jaworski, Piotr, Sebastian Jarosiński, Azael Cortes Capetillo, Łukasz Jan Kapusta, Adam Ziółkowski, and Robert Grzywnowicz. “SCR systems for NO_x reduction in heavy and light duty vehicles.” *Combustion Engines* 164, no. 1 (2016): 32-36.
[6] Koebel, M., M. Elsener, and M. Kleemann. “Urea, SCR: a promising technique to reduce NOx emissions from automotive diesel engines.” *Catal. Today* 59, no. 3 (2000): 335–345.
[7] Kim, J.W., W.G. Lee, I.S. Hwang, J.Y. Lee, and C. Han. “Recovery of tungsten from spent selective catalytic reduction catalysts by pressure leaching.” *J. Ind. Eng. Chem.* 28 (2015): 73–77.
[8] Marberger A., M. Elsner, D. Ferrri, and O. Kröcher. “VOx surface coverage optimization of V2O5/WO3-TiO2 SCR catalysts by variation of the V loading and by aging.” *Catalyst* 5 (2015): 1705-1720.
[9] Lia, Meng, Biao Liu, Xinran Wang, Xiaobin Yu, Shili Zheng, Hao Dub, David Dreisinger, and Yi Zhang. “A promising approach to recover a spent SCR catalyst: Deactivation by arsenic and alkaline metals and catalyst regeneration.” *Chemical Engineering Journal* 342 (2018): 1–8.
[10] Dong, Haigang, Jiachun Zhao, Jialin Chen, YuedongWu, and Bojie Li. “Recovery of platinum group metals from spent catalysts: A review.” *International Journal of Mineral Processing* 145 (2015): 108–113.
[11] Jha, Manis Kumar, Jae-chun Lee, Min-seuk Kim, Jinki Jeong, Byung-Su Kim, and Vinay Kumar. “Hydrometallurgical recovery/recycling of platinum by the leaching of spent catalysts: A review.” *Hydrometallurgy* 133 (2013): 23–32.
[12] Liu, S.J. *Metallurgy of Platinum Group Metals*. Central South University Press, Changsha, 2013.
[13] Fornalczyk, A., J. Cebulski, M. Saternus, and J. Willner. “Possibilities of platinum recovery from metal supported spent auto catalysts.” *Metalurgia* 53, no. 4 (2014): 609-612.
[14] Kim, Wan-Tae, Hyung-Seok Kim, Sung-Baek Cho, Jae-chun Lee, and Sang-Bae Kim. “Selective recovery of catalyst layer from supporting matrix of ceramic-honeycomb-type automobile catalyst.” *Journal of Hazardous Materials* 183 (2010): 29–34.
[15] Dobos, Gábor. “Method for recovering precious metals from waste catalyst.” Patent WO2010084364A1, 2010-07-29, 2010.
[16] Wright, M.M. *Cavitation of a Water Jet in Water*. MSc. Thesis. Department of Mechanical Engineering, Brigham Young University, 2012.
[17] Ali, Ezddin, Farag Hutli, and Miloš S. Nedeljković. “Investigation of a Submerged Cavitating Jet Behaviour: Part Two – Influences of Operating Conditions, Geometrical Parameters and Arrangements of Detection System.” *FME Transactions* 35 (2007): 121-128.
[18] Vijay, M.M., C. Zou, and S.A. Tavoularis. “Study of the Characteristics of Cavitating Water Jets by Photography and Erosion Jet Cutting Technology.” *Proceedings of 10th International Conference, 37-67*, Elsevier 1991.

ISSN 1454 - 8003
Proceedings of 2019 International Conference on Hydraulics and Pneumatics - HERVEX
November 13-15, Băile Govora, Romania

EXPERIMENTAL MODEL OF A COMBINED SYSTEM OF THERMAL ENERGY PRODUCTION, BASED ON SOLAR AND BIOMASS ENERGY

Petrin DRUMEA[1], Liliana DUMITRESCU[1], Corneliu CRISTESCU[1]

[1] National Institute for Optoelectronics, INOE 2000-IHP Bucharest, drumea.ihp@fluidas.ro

Abstract: *The article presents a combination of solar energy with energy obtained from biomass, quite often found in the world economy to achieve the thermal energy in the desired quantity and delivered at the right time. The solution includes as basic elements a regular solar panel, existing on the market and a gas generator made by the authors themselves. The assembly is well structured and by proper choosing of the components size, an amount of permanent and sufficient heat is obtained for a small household.*

Keywords*: Experimental model, thermal combined system, solar energy, biomass energy*

1. Introduction

The development of mankind is based on the quantity and quality of the energy used throughout history. At the level of current knowledge it is accepted as the primary source, essential of terrestrial energy is solar energy, which has been stored in fossil fuels or in plant resources, mainly forestry and which is easily accessible by humans and as such is widely used. At the level of the sun there is a permanent activity of nuclear fusion, which creates energy, which reaches the earth transmitted as electromagnetic energy. The amount of energy generated by the sun is huge, well above the level required on earth, but so far people have used very little light and heat provided by nature. Instead they used it without hesitation wood, coal, oil and natural gas, even without discernment, without restrictions and without a perspective of the future, getting in the situation that the resources of this type have diminished and the danger of the energy crisis has increased.
Moreover, all of a sudden, humanity has scientifically found, which has long been known, that the burning of these types of resources has led, and unfortunately still leads, to serious pollution of the environment [1]. The simple and handy solution of all countries was o switch to the production of energy from clean sources, renewable sources, to replace as much as possible the use of fossil fuels. One of the most important problems that should be quickly solved is the one regarding the production of hot water and heat. The first industrially applied method was the use of solar thermal panels through which hot water is produced by direct conversion of solar energy. Only in 2017 is it appreciated in the in international scientific materials that 35 GWth have been added, which provides almost 80% of the hot water and heat needs in the cold season, while in the summer almost all the hot water needs can be provided [2, 3].
The solar thermal panels are divided into two classes, some with vacuum tubes and some with flat solar panels consisting of copper plates. We must admit that solar thermal energy is not permanent 24 hours a day and therefore it should be stored during the day so it can be consumed at night. Storage is a difficult process in the current technical conditions and as a result the efficiency and the price forced the specialists to recourse to alternative solutions, the simplest and cheapest being the solution by combining the thermal panel with a gas tank. The technical and economic advantages of this combined system are obvious, they are major and especially easy to use and maintain.
Given the novelty of the solution, the realization of a combined system at the prototype level that can be introduced in manufacturing must go through an experimental model phase.
The experimental model must respect the structure of the final product, being composed of 2 sources of thermal energy, namely:
- system for converting solar energy into thermal energy using solar thermal panels with vacuum tubes;

- the biomass energy conversion system using an energy module based on a gas generator through the TLUD process and a burner.

The main categories of biomass that can be used for this purpose are wood matter, vegetable residues from agriculture and animal residues from zootechnics, as well as crops and plantations dedicated to energy recovery. The basic process is pyrolysis which consists in the thermochemical decomposition of solid biomass, a process that takes place at temperatures of 300-800 °C and in the absence of oxygen [4]. From this process results heat, which we add to that provided by solar thermal panels, as well as different gases (hydrogen, methane, carbon monoxide, etc.), bio-oil and coal. Through the thermochemical gasification process, solid biomass is transformed into gas at temperatures of 800-1300 °C. The gas obtained is called synthetic or singas gas and is a mixture.

2. The solution chosen

The scheme of the combined system, which includes the 2 conversion systems, is shown in fig.1. The main components of the system are: electric pump, thermal solar panel, thermal burner, boiler, expansion vessel.

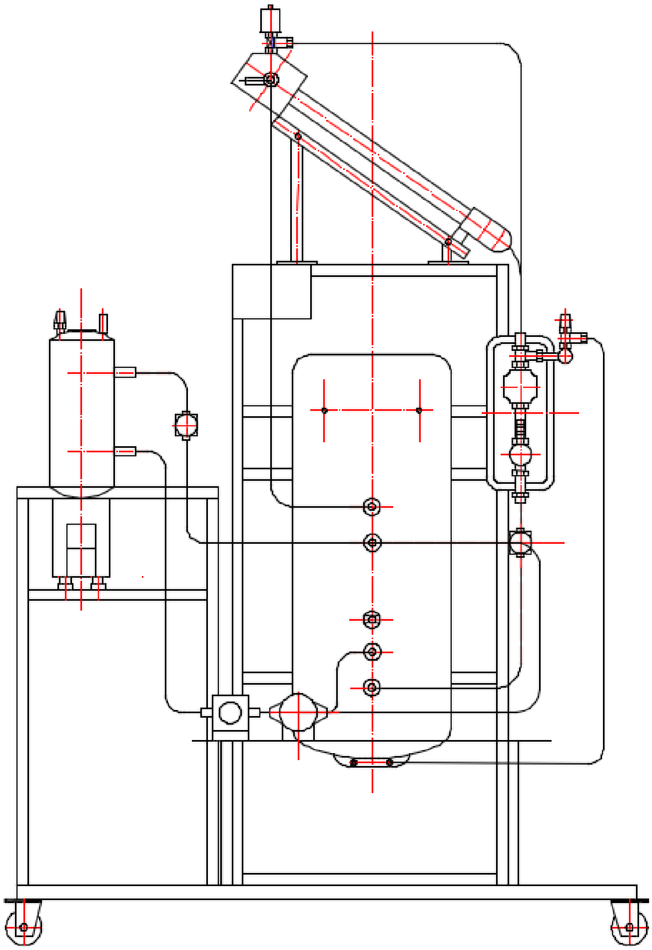

Fig. 1. Schematic of the combined system

Two systems were executed for reduced powers, their role being to validate through the experiment the possibility of cumulating the thermal energy from 2 sources.

The main components of the combined system are the solar thermal panel and the gas generator. Their main features are presented below.

For the conversion of solar energy, a medium-performance solar panel, with vacuum tubes, with the following main characteristics will be used:

Table 1: The main characteristics of the thermal solar panel

Item	Value
Number of tubes	10
Panel width	890 mm
Panel length	2030 mm
Total area	1,81 m^2
The effective surface of absorption	0,94 m^2
Material for tubes	Borosilicate glass
Material for the collector	Al / Cu / Glass / Mineral wool

2.1. Thermal panels

The panels use Heat Pipe technology; the vacuum tubes of the panel consist of 2 concentric glass tubes between which is vacuum. The inner tube is surrounded by a dark absorbent surface that transmits the heat energy to the copper pipe through which a thermal agent circulates. The vacuum between the two tubes contributes to the increase of the efficiency and the temperature, reducing the losses.

The main dimensions of the vacuum tube are the diameter D_t = 58 mm and the length L = 1812 mm. According to the technical data provided by the manufacturer, at an average solar radiation value of 1000 W /m^2, a tube heats 10 liters of water per day, from 15 to 50°C.

Therefore, the amount of heat transferred to the water will be:

$$Q_t = m \cdot c \cdot \Delta t = 10 \cdot 4180 \cdot 35 = 1.463 \cdot 10^6 J \quad (1)$$

where c = 4180 J / kg·K is the specific heat of the water.

For a panel with 10 elements, the energy produced will be:

$$Q_p = Q_t \cdot 10 = 1.463 \cdot 10^6 \cdot 10 = 14.63 \cdot 10^6 J \quad (2)$$

If the energy is expressed in kWth, then we will have:

$$Q_p = \frac{14630000}{3600000} = 4{,}06\ kWth \quad (3)$$

2.2. The TLUD generator

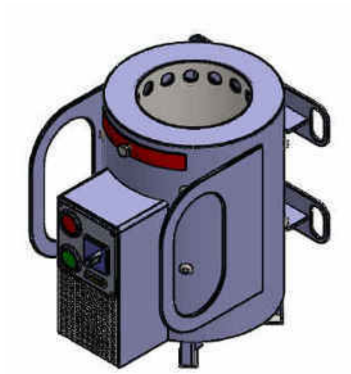

Fig. 2. TLUD type generator

The main dimensions of the generator are: Reactor diameter: $D_r = 10\ cm$

Biomass layer height (loading height): $H_{rbm} = 15\ cm$

Reactor section: $S_r = \frac{\pi \cdot D_r^2}{4} = \frac{\pi \cdot 10^2}{4} = \frac{314}{4} = 78.5\ cm^2$

Biomass volume in the reactor: $V_{rbm} = H_{rbm} \cdot S_r = 0.15 \cdot 78.5 = 1178\ cm^3$

Biomass layer density: 600 kg /m^3 (pellets).
Initial mass in the reactor: $M_{bm0} = 600\ \cdot 0.1178 = 706.5\ g.$
The specific hourly consumption of gasified biomass is 85 kg / m^2·h; therefore, for the reactor surface we will have a specific consumption of:
C_{hbmg} = 85 · 0.00785 = 0,667 kg/h
The operating time will be: $T_g = \frac{600}{667} = 0.9\ h\ (\sim 54\ min.)$
Energy from gas biomass:
$E_{bmg} = M_{bmo} \cdot P_{Cibm}$ = 0.7065 · 17 = 12 MJ
The thermal power [5, 6] of the hot gases: $P_g = \frac{E_{bmg}}{T_f \cdot 3.6} \cdot \eta_{gTLUD} = \frac{12 \cdot 0.93}{0.9 \cdot 3.6} = 3.44\ kWth$ and the thermal power at the burner, which takes into account the fuel combustion efficiency (η_{ard} = 0.95) and the insulation efficiency (outward losses – η_{izol} = 0.96), will be:

$$P_{arz} = P_g \cdot \eta_{ard} \cdot \eta_{izol} = 3.44 \cdot\ 0.95\ \cdot 0.96 = 3.13\ kWth \tag{4}$$

3. Realization of the combined system at the level of Experimental Model

The solar energy conversion system also contains a solar regulator and a pumping unit, which achieves the transfer of the heated fluid from the solar thermal panel to the tank, through one of the 2 coils. With the help of the coil, the fluid transfers thermal energy to the cold water which turns into domestic hot water. Similarly, the thermal energy generated by the combustion of the gas is transferred to a fluid in the closed circuit, which flows through the second coil of the tank.
The combined system [7, 8, 9] is designed to be based on the solar thermal panel, and the energy module, which has a limited operation in time (in this case of about 1 hour), brings additional energy supply during periods when the solar radiation is insufficient. In the experimental model phase, the energy module enters in function when the solar radiation decreases, that is indicated by a cell which measures the light radiation, and the water temperature from the tank, measured with a sensor located at the top of the tank.
The role of this experimental model is to validate the feasibility of the idea of obtaining and using thermal energy from two renewable sources; the following activities provide for the development of a calculation methodology for the quantities of thermal energy produced by each source, as well as the amount of useful energy accumulated in the bivalent boiler during a cycle carried out during a day. During the day, when there is solar radiation, the boiler will store thermal energy produced from this first source; When the solar radiation no longer has the effect of heating the water in the boiler, the energy module enters into action, which by burning an amount of biomass equal to the load capacity for a batch, produces an amount of thermal energy that is added to the initial one.
In this phase it is predicted that the energy produced from biomass will represent approx. 75% of the energy produced by the vacuum tubes (10 tubes); If it is found that the energy produced by the solar panel exceeds the estimated quantity (if the experiment takes place on a day with solar radiation above the annual average taken into account), the number of active tubes will be reduced by removing them from the hydraulic circuit.
The energy produced from the 2 sources, without taking into account at this stage the thermal losses, represents the sum of the energies produced by the 2 energy conversions:

$$Q_T = Q_P + Q_{bmg} = 14.63 + 12 = 26.63 \text{ MJ} \tag{5}$$

Considering that the boiler has a capacity of 80 l, the increase of the water temperature in the boiler will be:

$$\Delta t = 26{,}63 \times 10^6 / (80 \times 4180) = 79.6^\circ\text{C} \tag{6}$$

If the water temperature at the boiler inlet is considered approx. t_i = 15 °C, the final temperature of the water in the boiler will be, at the end of the day:

$$T_F = t_i + \Delta t = 15 + 79.6 = 94.6\ ^\circ\text{C}, \tag{7}$$

which recommends the use of a smaller number of vacuum tubes, in order not to reach the boiling temperature of the water.
In principle, the experimental model of combined thermal system groups, in one place, a solar

thermal panel and an energy module for low power biomass (3 kW), which is a TLUD-type thermal power station, to which are added the necessary components to control the operation, in good condition of the combined system, fig. 3.

Fig. 3. The experimental model of combined thermal system

The principle composition of the experimental model of combined thermal system, for solar energy and biomass, as well as the main technical characteristics, are the following:

- 1 mini solar thermal panel, type with 4 vacuum tubes of 400/500 mm, pressure of 6 bar, fig. 4;
- 1 energy module for biomass, composed mainly of a thermal power plant on biomass (TLUD type gas of 3 kW and a hot water tank), fig. 5;
- 1 hot water circulation electro-pump, with flow rate 05-06 l /min, fig. 6;
- 1 mixed boiler of 120 liters, at 10 bar, with two coils and electrical resistance, fig. 7;
- 1 electro-pump panel for water circulation with adjustment and safety elements, fig.8;
- 1 electrical control and control system with temperature sensors, flow transducers and hot water volume meter, fig. 9.

Fig. 4. Mini solar thermal panel

Fig. 6. Hot water circulation elecro-pump

Fig. 5. Energy module for biomass

Fig. 7. Boiler

Fig. 8. Electro-pump panel

Fig. 9. Electric command and control system

The experimental model of combined thermal system for the generation of thermal energy from renewable sources, solar thermal energy and thermal energy from biomass, ensures the achievement, under laboratory conditions, of the following main functions:
- the functioning in separate mode of water heating only with solar thermal panel;
- the functioning in separate water heating regime only with the thermal power plant based on the biomass burning;
- the combined operation by the simultaneous utilization of the two equipments;
- control of operating regimes;
- adaptation and maintenance of thermal parameters for safe operation.

Only after completing the experimental model and conducting the experimental research, based on the obtained results, will the design of the combined system prototype be obtained for obtaining the thermal energy from two sources: solar energy and biomass.

4. Conclusions

The proposed system at the experimental model level aims to validate the possibility of accumulating thermal energy from 2 sources: solar radiation and biomass, the conversion being made using a solar thermal panel with vacuum tubes, respectively with an energy module based on the TLUD principle. The exploitation of the two sources is managed in this experimental phase by a control and warning block, which warns about when the solar radiation can no longer increase the water temperature in the boiler, and therefore it is necessary to start the biomass-based energy module in operation. It is limited in time due to the small amount of biomass it can be loaded with. Increasing the amount of gas biomass would lead to a significant expansion of the total thermal energy quantity, competing to obtain a combined system capable of ensuring the energy autonomy of a consumer.

Acknowledgments

This paper has been developed in INOE 2000-IHP, as part of a project co-financed by the European Union through the European Regional Development Fund, under Competitiveness Operational Programme 2014-2020, Priority Axis 1: Research, technological development and innovation (RD&I) to support economic competitiveness and business development, Action 1.1.4 - Attracting high-level personnel from abroad in order to enhance the RD capacity, project title: Establishing a high level proficiency nucleus in the field of increasing renewable energy conversion efficiency and energy independence by using combined resources, project acronym: CONVENER, Financial agreement no. 37/02.09.2016.

References

[1] Gudîma, A. ”Tehnologia de obținere a peleților ENPlus din reziduuri agricole în condițiile Republicii Moldova.” PhD. Thesis. Chișinău, 2018.
[2] ***. “Renewables 2018 Global Status Report.” ISBN 978-3-9818911-3-3, www.ren21.net.
[3] Murad, E., E. Maican, C. Dumitrescu, and S.St. Biris. ”Extending the use of hothouses through heating with residual agricultural biomass.” Paper presented at the 2nd International Conference of Thermal Equipment, Renewable Energy and Rural Development TE-RE-RD 2013, Baile Olanesti, June 20 - 22 2013, pp. 209-214.
[4] Murad, E. ”Power production a negative carbon balance with CHAB concept.” Paper presented at the International Conference on Hydraulics and Pneumatics, Băile Govora, Romania, November 9-11, 2016.
[5] Grîu (Dobrev), T.B. ”Evaluarea şi mărirea puterii calorice a biomasei lemnoase.” PhD. Thesis. Transilvania University of Braşov, 2014.
[6] Voicea, I.F. ”Cercetări privind optimizarea procesului de compactare a biomasei.” PhD. Thesis. Politehnica University of Bucharest, 2016.
[7] Cristescu, C., C. Dumitrescu, V. Dulgheru, L. Dumitrescu, and A.-M. Popescu. ”Combined systems for generating electrical and thermal energy from renewable sources, with storage of it through conversion to other energy forms, for use in isolated places.” Paper presented at the 17th International Multidisciplinary Scientific GeoConference (SGEM 2017), Albena, Bulgaria, 29 June - 5 July 2017.
[8] Dumitrescu, L., C. Cristescu, V. Barbu, and M. Mateescu. ”Combined system for the production of thermal energy using solar and biomass energy.” Paper presented at ISB-INMA TEH' 2018 International Symposium, Bucharest, Romania, November 1 - 3, 2018.
[9] Maican, Edmond. *Sisteme de Energii Regenerabile / Renewable Energy Systems*. Bucharest, Printech Publishing House, 2015.

ISSN 1454 - 8003
Proceedings of 2019 International Conference on Hydraulics and Pneumatics - HERVEX
November 13-15, Băile Govora, Romania

IMPROVING THE FLOW VARIATION OF EXTERNAL GEAR HYDRAULIC PUMP

Alina SPÂNU[1], Mihai AVRAM[1]

[1] University Politehnica of Bucharest, Mechatronics and Precision Engineering Department, spanu_alina@yahoo.com, mavram02@yahoo.com

Abstract: *The paper concerns with the theoretical aspects regarding the improvements on the flow ripple for the external hydraulic gear pumps. During the last decades, there are many research activities for increasing the efficiency by using the hydraulic pumps as suppliers for system with variable or constant loads. A better solution could be the external hydraulic gear pump, whether the flow has a continuous variation, so that it could be controlled by the rotational speed of the electric motor.*

Keywords: *Hydraulic system, external gear pump, control, constant flow.*

1. Introduction

Nowadays, there are many concerns regarding the new solutions for designing hydraulic system with lower level consumption of energy. The hydraulic systems work with very high power, so these issues now assumes even greater importance than before. The choosing of the hydraulic supplier system has to be done very carefully based on a technical and economic analysis.
It is very well known that the life cycle cost of the technical system has the following structure:

- 5 – 20 % for investments;
- 80 – 90 % for maintenances, especially for implementation, service, for training, for taxes, assurance, energy.

Regarding the hydraulic actuation systems, where there are higher power levels, the cost of energy is the mainspring of this aspect.
Almost all the hydraulic systems have hydraulic pumps with constant flow as supplier elements of their structure. The constant hydraulic flow of the pump is an useful feature even for the hydraulic systems where we have to accomplish the load variation of the motor. This has to be done because of the lower price of these pumps comparing with the variable flow pumps. More often, the hydraulic system for flow variation implying the variation of the working load has a valve placed before or after the motor. Even though the solution is very simple, the efficiency is very low finally.
The functioning of the volumetric pump is based on the continuous variation of the volume of some internal chambers due to the relative motion of a piston, blade or slider relative to the grounded part. Some technical clearances have to be designed in order to provide the movements. Due to this reason, there are some leaks from the chambers with high pressure to the chambers with low pressure, so the viscous friction forces are working. Meantime, on these parts there are acting pressure forces implying kinetic frictions. A well designed hydraulic pump means a compromise between minimum loss of flow and minimum values of friction.
So, we may conclude we have to choose the hydraulic supplier based on a very carefully analysis made from technical and economical point of view.
The gear hydraulic pump is one of the most used pumps for the systems working with medium power, because of its technical simplicity, the lower price and easily maintenance. We have to specify it is a constant flow pump.
These pumps have the following parts (Fig. 1):

- Cylindrical external gear made of the wheels 1 and 2, most often with teeth’s involute profile;

- The main part comprising the central body 3, and two plates placed on the extremities 4 and 5. Inside the main body, where the minimal clearance was designed around the gear, there are two holes A and R directly tied to the two rooms for flow aspiration and expulsion.
- The rod 6 fastened to one of gear wheel;

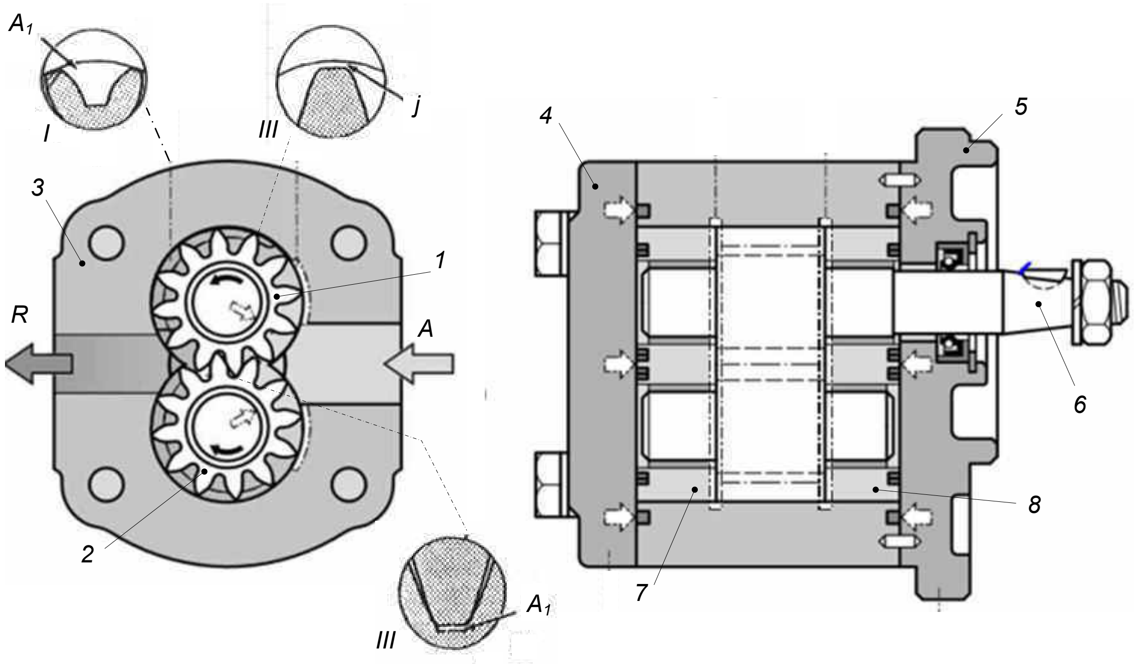

Fig. 1. The main parts of the hydraulic gear pump.

- Two bearings numbered 7 and 8.

When the gear wheels are rotating around the gear axis following the clockwise and counter-clockwise arrows (Fig. 1) the teethes placed nearby the suction chamber are sorting out from the gear space, so that a supplementary room may be functional. Inside this room it is a low level pressure, so the flow coming from the supplier will be filled in. The well-known volume of oil, named “trapped volume” is closed between two consecutive teeth pairs in contact, so it is carried out through the expulsion.
There are two unwished phenomena during the working process: loss of flow and the action of asymmetric forces having higher values whether the pressure increases. The flow is lost between the pump body and external peak of the teeth, the external surfaces of the gear and the parts numbered 7 and 8 (Fig. 1). There are some solutions for reducing these leaks by designing an internal pipe for bringing the expulsion pressure on the external surfaces of the parts 7 and 8, so that there are pushed toward the gear.
The paper [1] presents an improved formulation of the pressure evolution of the external gear pump, highlighting the phenomena such as axial flow, the accurate description of the trapped volume and its connection with input and output chambers. There are pointed out some genuine ideas regarding the simulation for force and torque based on the numerically description of flow areas inside the complex groove designed.
The paper [2] describes the work, which has been done by using HYGESim (Hydraulic Gear Simulation) tool, for modelling the external gear pump functioning with non-Newtonian fluids, like plastics, polymers, paints. The main concern was the modelling of flow through orifices. The results were discussed with respect to the angular position of the gear starting from the suction to the delivery zone, showing the progression of the tooth space. The geometry model can give an idea of how areas of different orifice connections vary with angle.
The work presented in paper [3] is about the 3D numerical simulation of an external gear pump performed for more realistic prediction of pump performance and internal flow phenomena by

considering leakage in the lateral gap. The research was focused on the effects of the designed parameters on the flow rate and flow characteristics. The result validation was done for a pump with high rotational speed.
The paper aims to propose a method for improving the flow variation of an external gear hydraulic pump, by controlling the speed of the electrical motor. The solution is useful and could be used for the systems with constant or variable load.

2. The flow variation for the external gear pump

The external gear pumps used for the hydraulic systems provide the well-known advantages such as higher efficiency, compactness and safety. There are internal and external gear pumps depending on the meshing shape inside the gear, but the latter ones are preferred for high pressures. Due to its working principle, meaning the fluid is passing periodically from inlet port to outlet port there are some disadvantages comprising the flow and pressure ripples as well as the attention we have to pay to the pressure level. The pressure value has to be inside a well-known range, because of malfunction avoidance. If it is lower, we may expect the cavity phenomenon inside and if it is higher, the gear is over-loaded, so the mechanical assembly will be affected by losses, vibration and noise.
The meshing flow that provides the trapped volume is influenced by the tooth profile and it has to be designed very carefully. The entrance shape of this volume is generated by the circle; it is followed by the teeth lateral surface governed by the involute and finally another surface having the circle as generative curve. Because of making the understanding process of the phenomena a little bit easier, we may assume that the instantaneous points along the line of action separate the high pressure from the low pressure at each value of the angular position described by β.
In order to compute the flow variation, we may start from the equality between the hydraulic power and the mechanical power given by the electrical motor:

$$P \cdot dq = M \cdot d\beta \tag{1}$$

P- hydraulic power; dq – elementary flow variation; M – mechanical torque; dβ – elementary rotational movement due to the electrical motor actuation.
The mechanical torque is given by the equation [4]:

$$M = F_1 \cdot \frac{r_a}{2} - F_2 \cdot \frac{\rho_1}{2} + F_3 \cdot \frac{r_a}{2} - F_4 \cdot \frac{\rho_2}{2} = p \cdot \frac{b}{2} \cdot (2 \cdot r_a^2 - \rho_1^2 - \rho_2^2) \tag{2}$$

As it is shown in Fig. 3, there are the following meanings for the notations: F_1, F_2, F_3 and F_4 – pressure forces acting on the lateral teeth surface having the thickness b and p – the pressure value; r_a – value of addendum radius of the gear; ρ_1 and ρ_2 – the radii of points along the tooth profile.

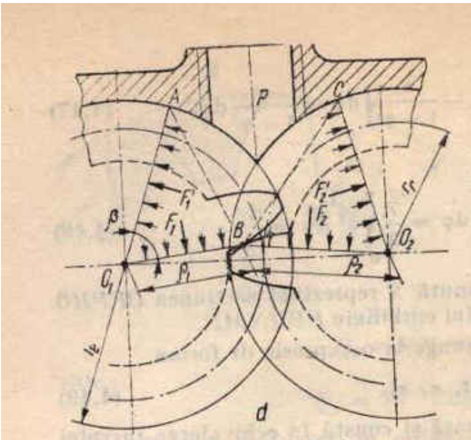

Fig. 2. The geometrical elements of the gear.

Taking into account that:

$$\rho_1^2 + \rho_2^2 = 2 \cdot (r_r^2 + x^2) \tag{3}$$

We may compute the external gear pump torque:

$$M = p \cdot b \cdot (r_a^2 - r_r^2 - x^2) \tag{4}$$

where x – the position of contact point along the line of action.
Finally, as we have started from equation (1) we may find the relationship between the displacement of contact point along the gear line during the process and the rotational movement of driving gear:

$$\frac{dq}{d\beta} = b \cdot (r_a^2 - r_r^2 - x^2) \tag{5}$$

$$\frac{dx}{dt} = r_r \cdot \frac{d\beta}{dt} \tag{6}$$

We use the mathematical equation characterising the geometrical dimensions of the involute gears, so we may assume that: $b = \psi \cdot m$ [mm] the face width of the gear, where m – modulus and ψ – the thickness coefficient; $r_b = \frac{m \cdot z \cdot \cos(\alpha_0)}{2}$ the base circle radius; r_r – the radius of rolling circle; z – the number of teeth for the involute gear and $\alpha_0 = 20^o$ the gear angle.
Taking into account all the mathematical relations presented above, we have computed the flow variation depending on time and rotational speed of the motor by using MATLAB for solving the following first order differential equation system:

$$\begin{cases} \frac{dq}{dt} = \frac{4 \cdot \psi \cdot (r_a^2 - r_r^2 - x^2)}{z \cdot \cos(\alpha_0)} \cdot \left(-2 \cdot x \cdot \frac{dx}{dt}\right) \\ \frac{dx}{dt} = r_r \cdot \omega_m \end{cases} \quad \text{if} \quad 0 <= x < p_b - l/2 \tag{7}$$

$$\begin{cases} \frac{dq}{dt} = \frac{2 \cdot \psi \cdot (r_a^2 - r_r^2 - x^2)}{z \cdot \cos(\alpha_0)} \cdot \left(-2 \cdot x \cdot \frac{dx}{dt}\right) \\ \frac{dx}{dt} = r_r \cdot \omega_m \end{cases} \quad \text{if} \quad p_b - l/2 <= x < l \tag{8}$$

Where ω_m – the electrical motor rotational speed; p_b – the gear pitch along the base circle; l – the length of line of action.

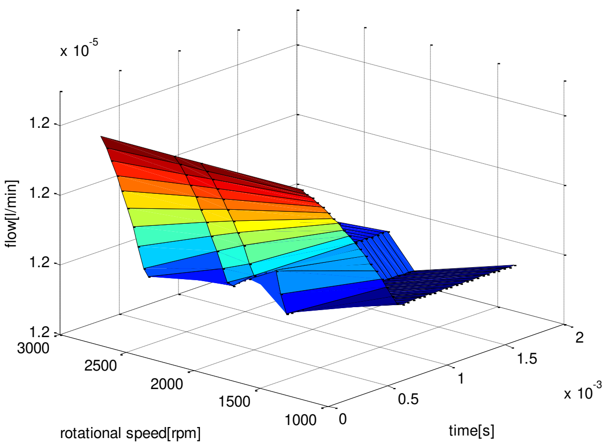

Fig. 3. The computed results.

We have solved this first order differential system by using Runge-Kutta method and imposing the condition for the solutions nearby starting point of time. The numerical set-up was done with the values reported below: m = 1.5 [mm]; z = 13 ; r_a = 23.4 [mm]; r_r = 9.749 [mm]; for the electrical motor we have taking into account the following values: $(n_m)_1$ = 2700 [rot/min] ; $(n_m)_2$ = 2150 [rot/min] ; $(n_m)_3$ = 1950 [rot/min] ; $(n_m)_4$ = 1200 [rot/min] .
The results are presented in Fig. 3 for the flow variation over time and rotational speed of the AC motor, so that we may infer the shape of this dependence and proportionality. As we have expected, the main conclusion is that we may control the flow law variation by controlling the rotational speed of AC motor.

3. Conclusions

The paper aims to point out the main advantages of using the external gear pump for the hydraulic systems with variable or constant flow, as a better solution for improving the efficiency. The choosing of the hydraulic supplier system has to be done very carefully based on a technical and economic analysis. There are two unwished phenomena during the working process: loss of flow and the action of asymmetric forces having higher values whether the pressure increases. The flow variation may appear due to the leaks through the clearance, for instance. The presented theoretical method could be used in order to control the flow according to the electrical motor rotational speed.

References

[1] Mucchi, E., G. Dalpaz, and A. Fernandez del Ricon. "Elasto-dynamic analysis of a gear-pump Part IV: Improvement in the pressure distribution modeling." *Mechanical Systems and Signal processing,* no. 50-51 (2015): 193-213.
[2] Rituraj, Fnu, and Andrea Vacca. “External gear pumps operating with non-Newtonian fluids: Modeling and experimental validation.” *Mechanical Systems and Signal processing,* no. 106 (2018): 284-302.
[3] Yoon, Yonghan, Byung-Ho Park, Jaesool Shim, Yong-Oun Han, Byeong-Joo Hong, and Song-Hyun Yun. “Numerical Simulation of three-dimensional external gear pump using immersed solid method.” *Applied Thermal Engineering,* no. 118 (2017): 539-550.
[4] Oprean, Aurel. *Hydraulics for Tools/Hidraulica masinilor unelte.* Bucharest, Technical Publishing House, 1983.
[5] Devendran, R.S., and Andrea Vacca. “Theoretical analysis for variable delivery flow external gear machines based on asymmetric gears.” *Mechanism and Machine Theory Journal,* no. 108, (2017): 123 – 141.

MECHANICAL-HYDRAULIC CONTROL MECHANISM FOR DIFFERENTIAL PISTON INJECTION DEVICES

Gheorghe ȘOVĂIALĂ[1], Gabriela MATACHE[1], Sava ANGHEL[1], Alina Iolanda POPESCU[1], Carmen NECULA[1], Dragoș MANEA[2]

[1]Hydraulics and Pneumatics Research Institute INOE 2000-IHP, sovaiala.ihp@fluidas.ro

[2]National Institute of Research-Development for Machines and Installations Designed to Agriculture and Food Industry – INMA, manea_dragos_05@yahoo.com

Abstract: *In the development of the injection device of the primary solutions used for underground fertilization of agricultural crops, which is the object of project 5 within the complex project "Innovative technologies for irrigations of agricultural crops in arid, semi-arid and dry sub-humid climate", contract no. 27 PCCDI / 2018- PN III, we started from the D3 Green Line dosing device produced by Dosatron - France. Compared to the D3 Green Line device, in which the direction of movement of the drive piston - piston injection pump with simple effect mobile assembly is achieved with the help of a spring tilting mechanism, an innovative solution of mechanical-hydraulic mechanism with spring and piloted valves was designed and implemented in the device developed within the project. The differential drive piston dosing device and the piston injection pump have major advantages compared to the volumetric dosing devices with membranes used in agriculture: the volume of the injected fertilizer solution is strictly proportional to the volume of water entering the unit, regardless of the variations of flow or pressure that may occur in the main pipe; the water used as a drive fluid mixes with the primary solution inside the device, forming the fertilizing solution; it is introduced into the pipeline of the localized irrigation plant and diluted to an optimum concentration, which eliminates the risk of crop over-fertilization, thus contributing to the protection of plants, consumer and environment health.*

Keywords: *Fertigation, injection device, differential piston*

1. Introduction

The sandy soils of Romania occupy 460 thousand hectares, most of which, 208 thousand ha, are located in a true "Bermuda Triangle", with the peak in the southern border of Craiova and base - on the Danube, in the counties Dolj, Olt and Mehedinți [1]..The sandy soils belong to the group of soils with a more pronounced manifestation of the extreme phenomena (atmospheric drought, pedological and agricultural drought, strong burns and a major deficit in precipitations with uneven distribution during the vegetation period of the plants). All these lead in the vast majority of the years of culture to the drastic diminution of the production on the plants of the big culture, of the orchards of the trees and the vines, often going to compromise the crops in question.
The thermal resources, the strong insulation and the irrigation during the drought periods can favorably influence the agricultural crops on the sandy soils. The possibility of using these poorly fertile soils and the early production (7-10 days in advance of other areas) are some arguments for the development of horticulture in these areas in particular.
On the sandy soils, the stone fruit species (peach tree, apricot tree, cherry tree, sour cherry tree) give the best results.
The methods used to reduce the action of stressors for agricultural crops on the sands are:
• Selection of species with short vegetation period (potato, melons);
• Selection of tolerant and drought resistant varieties based on physiological criteria (rate of transpiration, rate of photosynthesis, water forms);
• Management of agrotechnical factors in order to increase the efficiency of plant metabolism (irrigation, fertilization, disease control and pests).
Irrigation and fertilization of crops on sandy soils, in arid climatic conditions is achieved by the multi-phase application with reduced norms of water and fertilizer, in order to avoid their

evaporation and percolation under the root layer, taking into account the high temperatures during the vegetation period and the reduced sand soil capacity of water retaining.
Under these conditions, fertigation is the most efficient method of water and fertilizer administration [2].

2. Material and method

The differential piston injection device, fig. 1, [3] can be located both on the main hydraulic circuit of the irrigation system (full flow), and on a circuit parallel to it (by-pass), and it uses irrigation water as a drive fluid. The device consists of two functional subassemblies: the subassembly acting as linear hydraulic motor and the subassembly acting as single-effect piston volumetric pump.
The motor subassembly consists of two bodies, assembled together by threading and sealed with O-ring.
The body 1 consists of two concentric tubes: in the inner tube, of cylindrical form, the part of diameter d1 of the motor piston is displaced, while the outer liner is provided with the inlet connections for the water used as a motor fluid and the discharge connections for the fertilizing solution (formed by mixing the primary solution with water).
The body 2 is of cylindrical shape inside; inside of it the motor piston part of diameter d_2 ($d_1 < d_2$) moves.

Fig. 1. Schematic presentation of the injection device with DOSATRON differential piston

Inside the motor assembly, fig. 2, three work chambers are made: chamber A, delimited by the outer surface of the inner cylindrical tube of the body 1, the inner surface of the liner of the body 1, the inner surface of the body 2 and the lower part of the motor piston, in the area of diameter d_2; chamber B, delimited by the upper part of the motor piston in the area of diameter d_2 and the inside of the body 2; chamber C, delimited by the lower part of the motor piston in the zone of diameter d_1 and the inside of the cylindrical tube of the body 1.
The pressurized water supply connection pipe communicates with chamber A, and the fertilizer solution discharge connection pipe - with chamber C.

The subassembly of the volumetric pump with piston is connected by threading to the lower part of the body 1.

During operation, the motor piston and the volumetric pump piston (which form the mobile assembly of the injection device) move in the same direction, as they are joined by a rod.

The water acts on the motor piston of the injection device. The change of direction of movement of the mobile assembly is controlled by the tilting mechanism, located in the motor piston, which by actuating two blocks of valves on the cone allows the access of water acting as drive fluid below or above the piston.

Pressurized water enters through the inlet connection in chamber A. If the valve train 2.4 in the motor piston 2.1 is moved up (see the left side of fig. 2) then the valves 2.2 close the connection between the chambers A and B and the valves 2.3 open the connection between the chambers B and C. Between A and B the liquid forms a pressure difference that acts on the annular surface of the motor piston and produces an upward movement of it. The fluid from chamber B is evacuated through the open valve 2.3 in chamber C where it is mixed with the primary solution arrived from the dosing area and then directed to the discharge. If the valve train is moved down (see right side of fig. 2), the valves between the chambers A and B are opened and the valves between the chambers B and C are closed. The pressure in the chambers A and B is uniformed; the pressurized fluid passes into the chamber B, and acts on the cylindrical surface of the drive piston between B and C and moves the piston down.

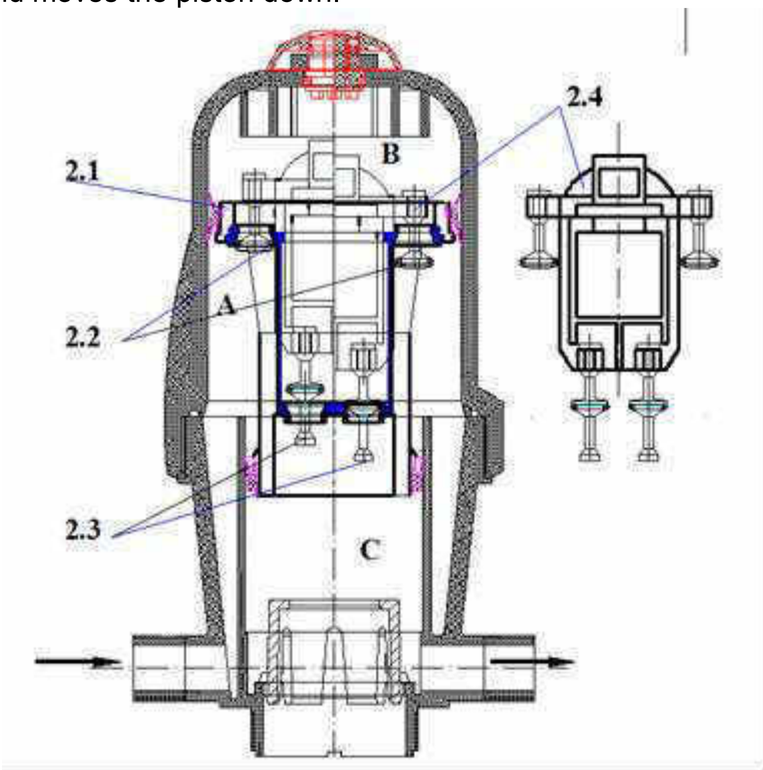

Fig. 2. Cross section through the motor assembly of the injection device with DOSATRON differential piston
Section to the left of the axis of symmetry-ascending stroke of the drive piston; Section to the right of the axis of symmetry-descending stroke of the drive piston

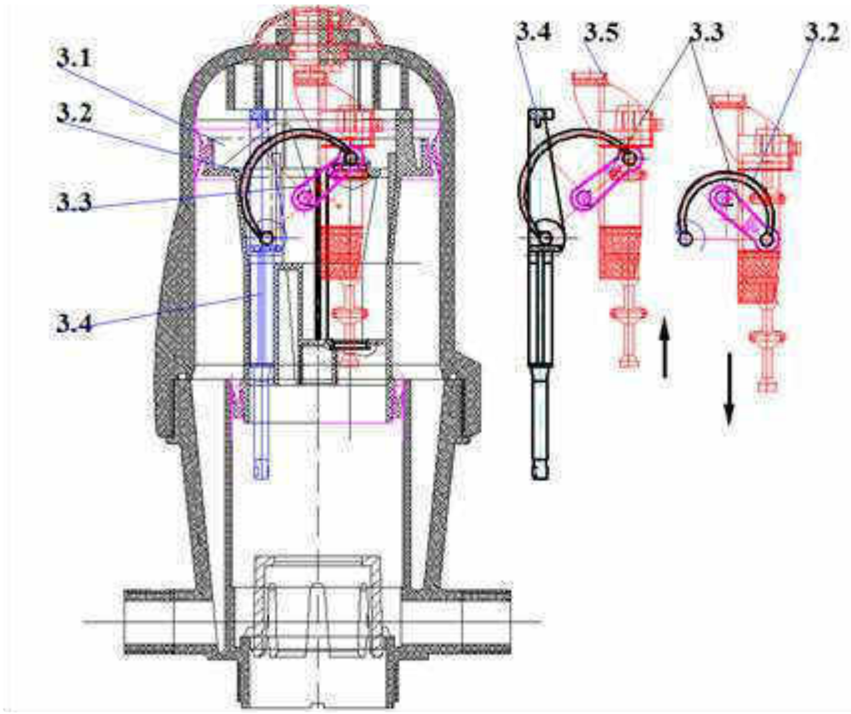

Fig. 3. Tilting mechanism of the of the injection device with DOSATRON differential piston

The tilting mechanism, located in the motor piston 3.1, controls the valve train; it has the following structure:
- the probe 3.4, which moves in a fit in the motor piston 3.1;
- a plastic spring 3.2 hinged to the probe, forming the probe-spring joint;
- the other end of the spring is hinged to the oscillating rod 3.3, forming the spring-rod joint;
- the oscillating rod 3.3 is connected to the motor piston 3.1 through the rod-piston joint.

Approaching the ends of the stroke, the probe 3.4, by leaning on the housing, changes the position of the spring-probe joint, with respect to the motor piston 3.1, respectively the positions of the rod-piston and spring-rod joints.
Under the action of spring 3.2, the joint assembly is unbalanced, tilting the mechanism up or down, depending on the displacement of the probe relative to the motor piston. By tilting, the mechanism hits the valve train 3.5, which it pushes up or down, closing or opening the connections between the chambers A, B, C.
The change of the displacement direction of the motor piston is made mechanically, the stroke being fixed (preset, in terms of construction, by the geometrical dimensions of the tilting mechanism).

3. Results and discussions

In the constructive version of the drive piston made by INOE 2000-IHP, the valves on the cone, actuated by the tilting mechanism with spring were replaced by hydraulic piloted valves [4], which establish the connections between the chambers A and B, respectively between the chambers B and C.

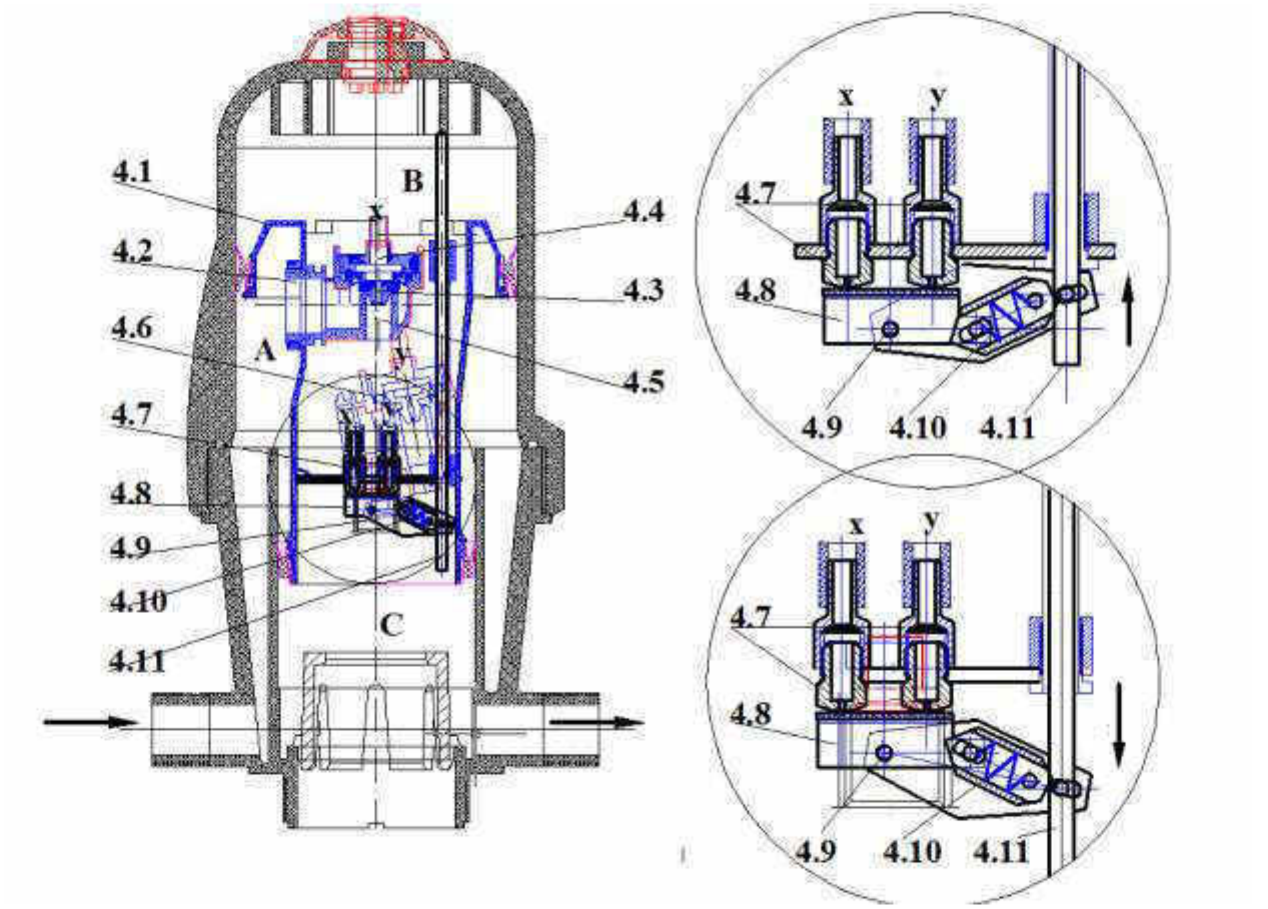

Fig. 4. Constructive variant of the motor piston made by INOE 2000-IHP

The piloting is done with the help of a piece 4.8 (on the surface of which a rubber tape is applied by gluing), which by tilting around the shaft 4.9 alternately closes one of the two nozzles 4.7, thus piloting the two hydraulic valves through the connections x-x or y-y.
The hydraulic valve consists of the tubular part 4.5, which in the inactive state is closed by membrane 4.3. The membrane, the surface of which is larger than the surface of the tubular part, is mounted in the valve housing.
The water enters behind the membrane through the port 4.2 and closes the pilot chamber 4.4, acting on the active surface formed from the sum of the cross-sections of the tubular part 4.5 and annular section delimited by the outer diameters of the membrane and the tubular part.
In the membrane there are ports (nozzles) that establish the communication between the inlet port 4.2 and the pilot chamber. If the tilting device 4.8 closes the nozzle 4.7 related to the valve, then the pilot chamber 4.4 is closed, the pressurized water from the entrance entering the pilot chamber through the ports in the membrane; under the action of the water, the membrane presses on the tubular part 4.5 and closes the path between the chambers A and B. The pressure in the pilot chamber acts on the whole surface and creates a force greater than the same pressure exerted only on the annular surface.
By tilting the pilot device at the stroke end (through the probe 4.11, which drives the compression spring-guide assembly 4.10 and tilts the part 4.8 on the nozzles 4.7), the pilot chambers of the two valves are opened alternately; by opening the ports of the pilot chambers the pressure in the chambers decreases, the membranes are raised and the communication between the chambers A and B (for the upper valve) and B and C (for the lower valve) is established.
The dosing piston, pos. 1.5- fig. 4, joined with the drive piston through a rod, is provided with a sleeve-type translation seal, which in the upward stroke sits on the lower seat, ensures perfect

sealing with the dosing cylinder and creates the depression required to lift the disc valve with the spring from the seat, thus allowing access of the primary solution under the piston and causing driving of the primary solution volume from above, existing inside the piston from the previous stroke, in the drive fluid-primary solution mixing chamber (motor piston cylinder).

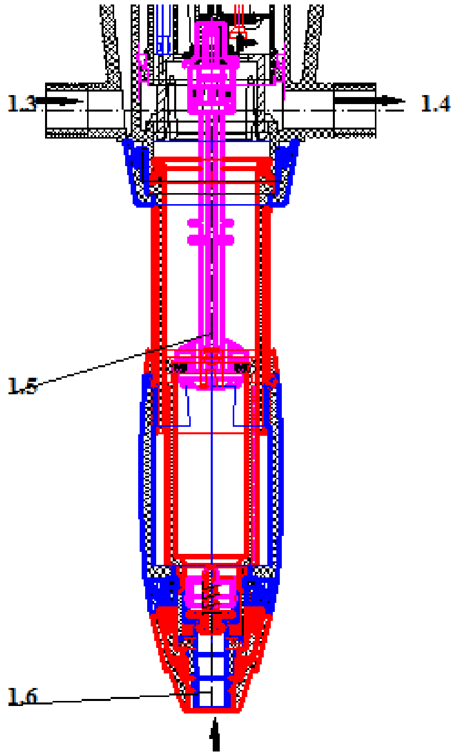

Fig. 5. Injection device dosing pump

In the downward stroke, the sealing piston of the dosing piston is placed on the upper seat of the piston and allows the access of the volume of primary solution already introduced in the dosing cylinder above it during the previous stroke, through the longitudinal slots on the external generators; by continuously varying the volume of the mixing chamber, in order to reduce it, the fertilizing solution is injected by the pump discharge connection into the irrigation system. During this time the inlet valve of the primary solution is placed on the seat, under the action of the spring.

The laboratory tests, carried out on the test stand for devices and equipment that use water as working fluid, from the infrastructure of the Environmental Protection laboratory of INOE 2000-IHP, have demonstrated the functionality of the injection device in the version designed and developed under the component project 5 “Innovative fertigation technology in fruit and vine plantations specific to arid and dry sub-humid climate” within the complex project “Innovative technologies for irrigation of agricultural crops in arid, semi-arid and dry sub-humid climate – SMARTIRRIG”, contract no. 27PCCDI / 2018.

To highlight the way in which the pressure varies, during a functioning cycle, in the connection points of the device to the localized irrigation system, its installation on a circuit parallel to the main circuit of the system (bye-pass) was done. The pressure sensors, located at the mentioned points, were connected to a programmable logic controller which, based on dedicated software, allowed real-time monitoring of the investigated parameters and data acquisition.

Fig. 6 shows the stand for conducting tests on the device in laboratory conditions, and fig. 7 depicts a screen instance of the computer with which data acquisition was made.

Fig. 6. Testing the injection device with differential piston under laboratory conditions

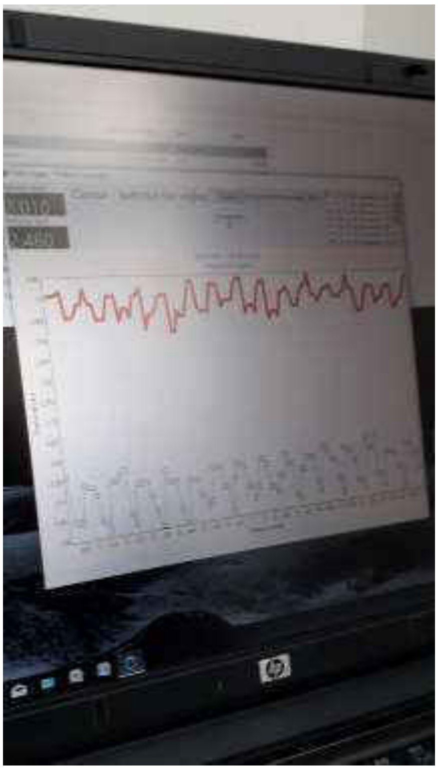

Fig. 7. Acquisition of data regarding the variation of pressures in the connection points of the device to the main pipe of the stand (the equivalent of the main pipe of the localized irrigation system)

The tests were performed with both constructive variants of the drive piston. Fig. 8 shows variation of pressures at the connection points for the drive piston with valve train on mechanically operated cone, belonging to the device DOSATRON D3 Green Line 3 m^3/h, and fig. 9 – the same, for the drive piston with hydraulic piloted valves.

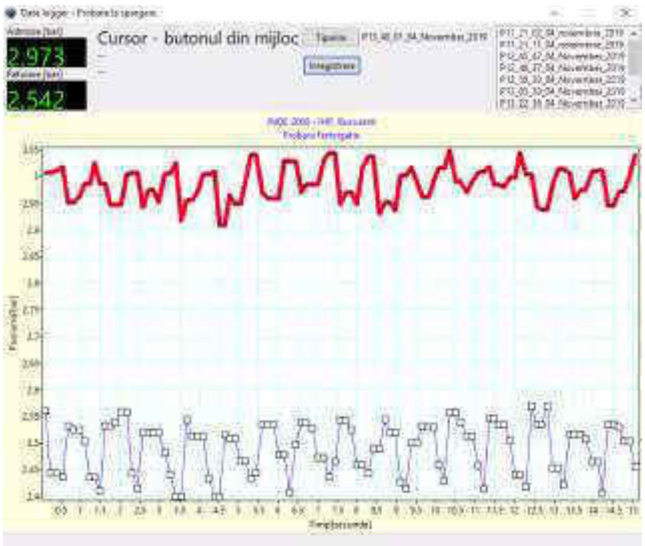

Fig. 8. Variation of pressures at the connection points for the drive piston with valve train on mechanically operated cone

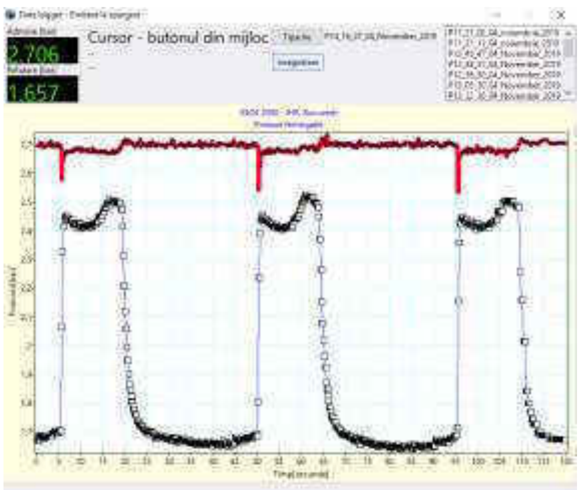

Fig. 9. Variation of pressures at the connection points for the drive piston with hydraulic piloted valves

4. Conclusions

1. The laboratory tests have demonstrated the functionality of the primary solution injection device developed under the component project 5 “Innovative fertigation technology in fruit and vine plantations specific to arid and dry sub-humid climate” within the complex project “Innovative technologies for irrigation of agricultural crops in arid, semi-arid and dry sub-humid climate – SMARTIRRIG”, contract no. 27PCCDI / 2018.
2. For similar working pressures (around 3 bar upon the device inlet port), the primary solution flow rate injected by the Dosatron device is 3000 l/h, for a switching frequency (change of the direction of movement of the drive piston - dosing piston assembly) of 10 s, while the primary solution flow rate injected by the experimental model (EM) developed by INOE 2000 under the mentioned project is 600 l/h, for a switching frequency of 45 s; primary solution flow injected by the EM meets the technical parameters of the fertigation process conducted for horticultural crops on sandy soils, which requires fragmented administration of liquid fertilizers; at a phase fertilization, an amount of 150-200 l /ha of primary solution is usually administered.
The switching frequency of the drive piston can be adjusted through the diameter of the nozzles 4.7, fig. 4.
3. The switching frequency of the motor piston can be adjusted by the diameter of the nozzles 4.7, fig. 4.
4. The tilting mechanism of the motor piston injection device with piloted valves requires an actuating force 5 times smaller than that of the mechanically actuated motor piston device.
5. The injection device realized within the project responds to the requirements of the fertilization of agricultural crops on sandy soils under arid climatic conditions, having the possibility of administering fertilizer norms in accordance with the agricultural technologies practiced in this category of soils.

Acknowledgements

This work was supported by a grant of the Romanian Ministry of Research and Innovation CCDI - UEFISCDI, Project INNOVATIVE TECHNOLOGIES FOR IRRIGATION OF AGRICULTURAL CROPS IN ARID, SEMIARID AND SUBHUMID-DRY CLIMATE, project number PN-III-P1-1.2-PCCDI-2017-0254, Contract no. 27PCCDI / 2018, within PNCDI III.

References

[1] Lăcătuș, Victor, “Fruit growing in the "triangle" of sandy soils.” *FERMA magazine* (May 25 2016).
[2] Biolan, I., I. Serbu, Gh. Sovaiala, and F. Mardare. *Fertilization techniques and technologies for agricultural crops*. Bucharest, AGIR Publishing House, 2010.
[3] www.dosatron.com - Dosatron: Water-powered proportional dosing pumps.
[4] Anghel, Sava, Gheorghe Sovaiala, Gabriela Matache, Dragos Manea. “Mechano-hydraulic control mechanism.” Patent application no. A / 00692 / 29.10.2019.

ISSN 1454 - 8003
Proceedings of 2019 International Conference on Hydraulics and Pneumatics - HERVEX
November 13-15, Băile Govora, Romania

GRID RESOLUTION INFLUENCE ON SMOKE SIMULATION ACCURACY

Dan BURLACU[1], Ștefan-Nicolae TRACHE[2]

[1] Technical University of Civil Engineering Bucharest, burlacudan92@gmail.com

[2] ”Alexandru Ioan Cuza” Police Academy Bucharest, tkstefan@gmail.com

Abstract: *Given the destructive nature of fire, experimental research in fire safety engineering can be a particularly difficult endeavor, characterized by low repeatability, high risk for the researchers and test subjects, and high cost of materials, due to the destructive nature of fire. Numerical simulation provides a way to bypass these shortcomings, offering a faster, safer, cheaper and repeatable solution for the studying of fire related phenomena. One key aspect of numerical simulation is accuracy and fidelity to real life situations, and this can be achieved by proper validation of numerical simulations with the help of experimental testing. This paper validates a numerical simulation of a real life experiment regarding the determination of the optical properties of non-toxic, artificially generated smoke and evaluates its accuracy for different computational cell sizes, in relation with the experimentally determined values. For this purpose, the Computational Fluid Dynamics numerical simulation software PyroSim is used for simulating the experimental setup and applying different mesh resolutions to the computational domain in order to evaluate the relation between mesh refinement and results accuracy regarding optical properties of smoke.*

Keywords*: Fire safety, smoke, visibility, CFD simulation, mesh*

1. Introduction

The destructive nature of fire makes research in fire safety engineering and training of fire safety professionals a particularly dangerous and hardly repeatable endeavor. Minimizing the risks during experimental research is of paramount importance, both for the health of the researchers and that of the test subjects. In this regard, there is a continual search for methods of recreating in experimental conditions certain aspects of a fire that will not influence the health of the participants. One such method of recreating the visibility reduction caused by smoke in enclosed spaces is using non-toxic smoke produced by fog machines. This kind of smoke can be used for research regarding people evacuation from smoke filled environments, firefighter intervention techniques, ventilation tactics and smoke exhaust system testing, without having to expose test subjects and researchers to the toxic components of flame generated smoke, or the heat of an actual fire.
A repeatable experimental evaluation of fire and its various components is hard to achieve given the high number of factors that influence fire behavior and the high cost of replacing experimental materials and sometimes tools that are rendered useless after utilization in harsh conditions such as those that are developed during a fire. To help address this problem, there have been developed fire simulation computer programs that offer the possibility of using numerical simulations to conduct research that would be either more expensive or unrepeatable in an actual experimental environment. One such program is the Fire Dynamics Simulator developed and offered freely by the National Institute of Standards and Technology of the United States and PyroSim, a graphical user interface for the Fire Dynamics Simulator program, offered by Thuderhead engineering under a free for academic use license for the purpose of this research.
This paper proposes an evaluation of grid resolution influence on the accuracy of the simulation of smoke optical properties, namely the optical smoke extinction coefficient and visibility. To this end, the results from a full scale experiment that determine said properties are used as a benchmark for establishing an adequate grid resolution in a numerical simulation of the experiment, in an effort to provide a correlation between grid resolution and accurate smoke properties representation.
The terms used in this paper are defined by the Fire Safety Vocabulary Standard [1] as follows:

- Optical smoke extinction coefficient - natural logarithm of the ratio of incident light intensity to transmitted light intensity, per unit light path length (the typical unit is m^{-1}).

- Smoke transmittance - ratio of transmitted light intensity through smoke to incident light intensity, under specified conditions. It is reciprocal of opacity of smoke and is usually expressed as a percentage. In practice, the transmittance usually measures the obscuration of smoke, which causes a reduction in visibility.

The importance of this kind of study is that it provides information on whether a certain grid resolution is adequate to use in a numerical simulation in which the optical properties of smoke need to be rendered accurately. The delicate balance between using a finer grid and the increase in computational time, which also depends on the performances of the computer the software is used on, while aiming for greater accuracy is tough to achieve. Thus, this paper seeks to provide a comparison of results obtained using different mesh cell sizes in a numerical simulation designed to emulate the optical properties of smoke so that researchers in fire safety engineering can get a sense of the impact that grid resolution in numerical simulations has on results accuracy.
In fire safety engineering, the optical properties of smoke provide information regarding smoke behavior in terms of visibility reduction in case of fires. The visibility reduction, also known as the opacity of the smoke produced by a fire influences the speed at which people evacuate during a fire [2], thus being an important factor to be considered in prescriptive fire safety standards. For example, the National Fire Protection Association standard 130 (NFPA 130) mentions that a tenable environment during fires is one that is characterized by a smoke obscuration level that renders an 80 lx illuminated sign discernable at 30 meters and doors and walls discernible at 10 meters [3].

2. Methodology

In the full scale experiment a fog machine was used to produce increasing amounts of non-toxic smoke in an enclosed space over time. The optical smoke extinction coefficient was determined through the measurement of the decrease in intensity of a laser beam that crossed the smoke filled environment. For the measurement of the light intensity of the laser beam, a luminance meter was used to provide measurements before the activation of the smoke machine, value that was set as the initial light intensity, and during the experiment, as the quantity of smoke in the room increased. A representation of the light source and luminance meter can be seen in figure 1.

Fig. 1. Light source and luminance meter

The experiment was repeated for different distances of the luminance meter from the light source, respectively 5 meters, 7.5 meters and 10 meters. The target upon which the luminance meter was placed served as a visual aid for the comparison of calculated visibility and perceived visibility. The experimental setup was recreated in the simulated environment, with the exception of using three targets at the same time, set at the established distances, thus providing the possibility of simultaneous measurements. An actual image from the experiment can be compared with an image from the numerical simulation in figure 2.

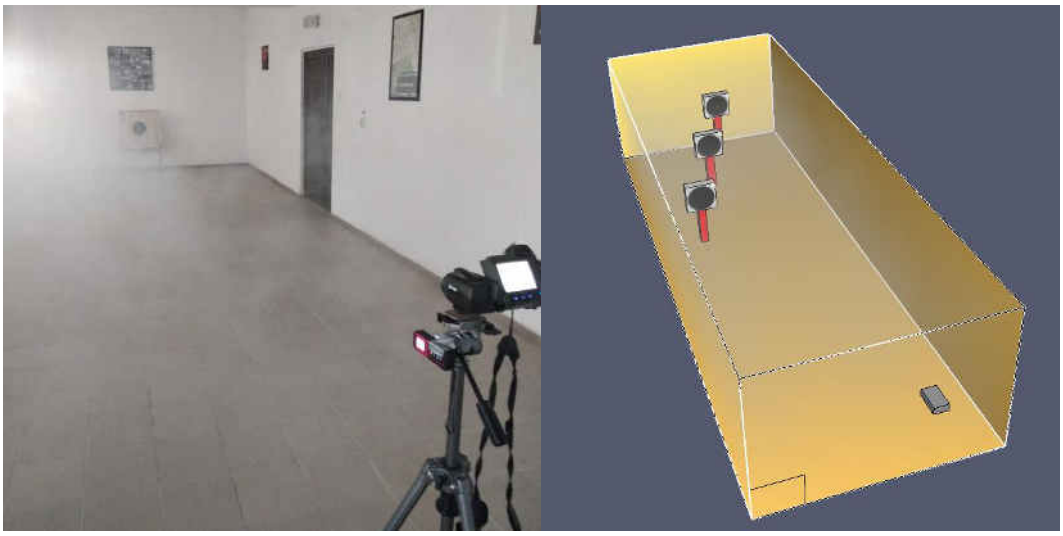

Fig. 2. Simulation of the experiment

For the purposes of this paper, the measured values from target number 2, the one situated at 7.5 meters from the light source were compared with the ones calculated by simulation for the same distance from the observation point, for each of the three simulations involving different coarseness of the calculation grid. During the simulation, the smoke extinction coefficient and visibility for each target were being measured and their values logged for each incremental time step through the use of gas-phase devices positioned in the simulation environment that measure the user specified quantity, be it either visibility (m) or smoke extinction coefficient (m^{-1}).

In the experimental setup, the fog machine was activated for short, timed bursts of about 9 seconds after which the atmosphere was left to settle for ensuring the proper measurement of the analyzed parameters in a calm environment. To replicate the experimental conditions, the simulation time has been set to be 480 seconds, and the simulated vent that produces smoke has been programmed with a timed start/stop control logic that mimics the behavior of the fog machine during the experiment. Table 1 presents a correlation of experimental and simulation chronology.

Table 1: Simulation timetable

No.	Cumulative time of fog machine use (s)	Smoke liquid used (ml)	Simulation time (with pauses for atmospheric stability) (s)	Smoke to room volume ratio
1.	0	0	0	0
2.	5	6	5	0.061
3.	9	11	69	0.109
4.	18	22	138	0.218
5.	27	32	207	0.327
6.	36	43	276	0.436
7.	45	54	345	0.545
8.	54	65	414	0.654

The simulation was repeated for three different sizes of the computational cells that comprise the mesh which fills the simulated domain. The coarsest mesh had a number of 22,080 almost cubic cells with the average linear dimension of 20 centimeters. For the next two simulations the mesh was refined for an average of 15, respectively 10 centimeters average linear dimension resulting in a number of cells of 51,600, respectively 156,000. The visual difference between the three cases can be seen in figure 3. The increase in the number of cells in the domain has led to a significant increase of the time needed for the simulation to complete.

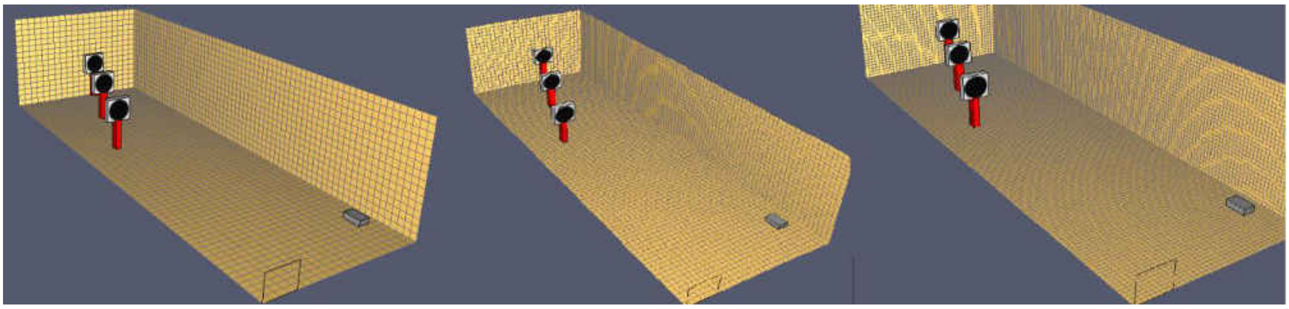

Fig. 3. Visual comparison of grid cells size

3. Results and discussion

This study sought to assess the influence that grid resolution has on the accuracy of the simulation of smoke optical properties by comparison of the values obtained by simulation using three degrees of coarseness of the simulation mesh with the results that were obtained by full scale experimenting. The optical smoke extinction coefficient, the first of the two optical properties of smoke that were analyzed in the present study, provides a measure of light attenuation as it passes through the smoke, or a measure of the capacity of the smoke to diminish the intensity of light as it passes through it, regardless of the nature of the smoke, be it generated by the burning of solid or liquid fuels [4]. The result obtained during the experiment and the simulations have been charted out on the same graph, as presented in figure 4.

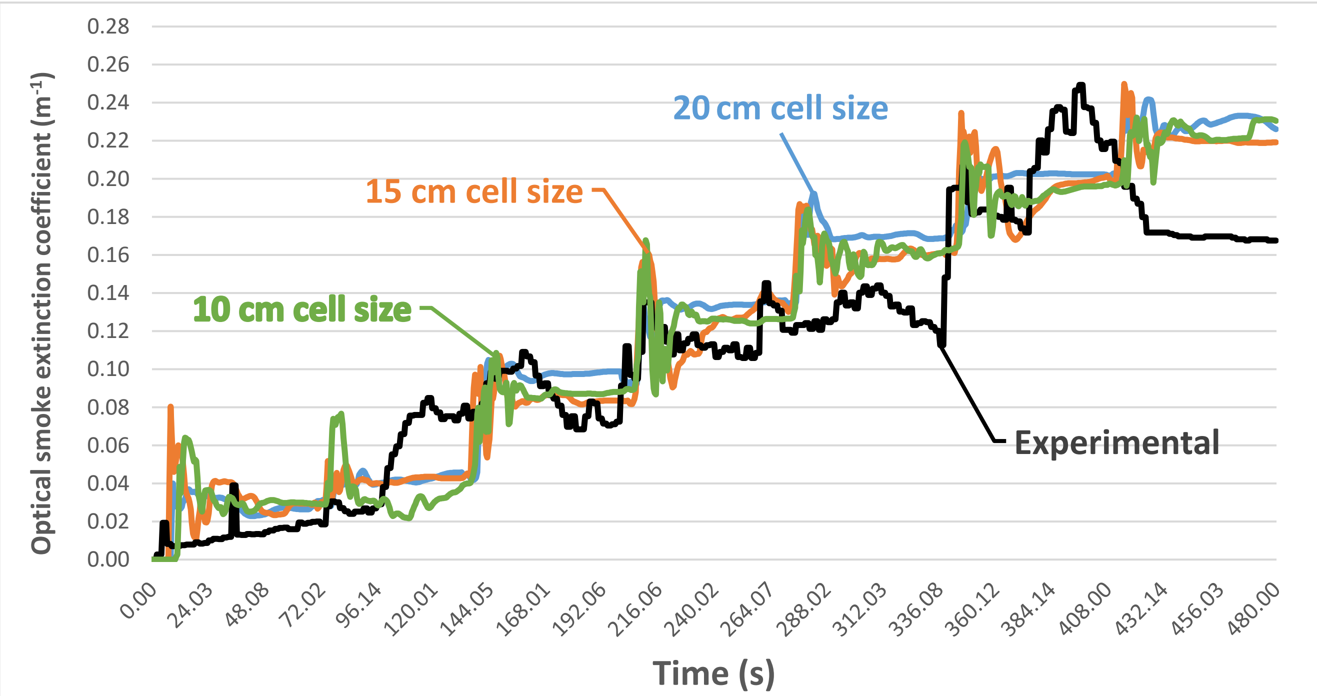

Fig. 4. Optical smoke extinction coefficient comparison for all grid sizes

The average difference between the values for the experiment and the 20 cm cell size simulation is 6.46%, which is a reasonable level of accuracy given the low computational grid resolution. For a better comparison of the differences, the values for the two instances are compared in figure 5, the difference between the higher values and the lower ones being highlighted in the color that corresponds to the higher values method of determination, be it experimental or by simulation.

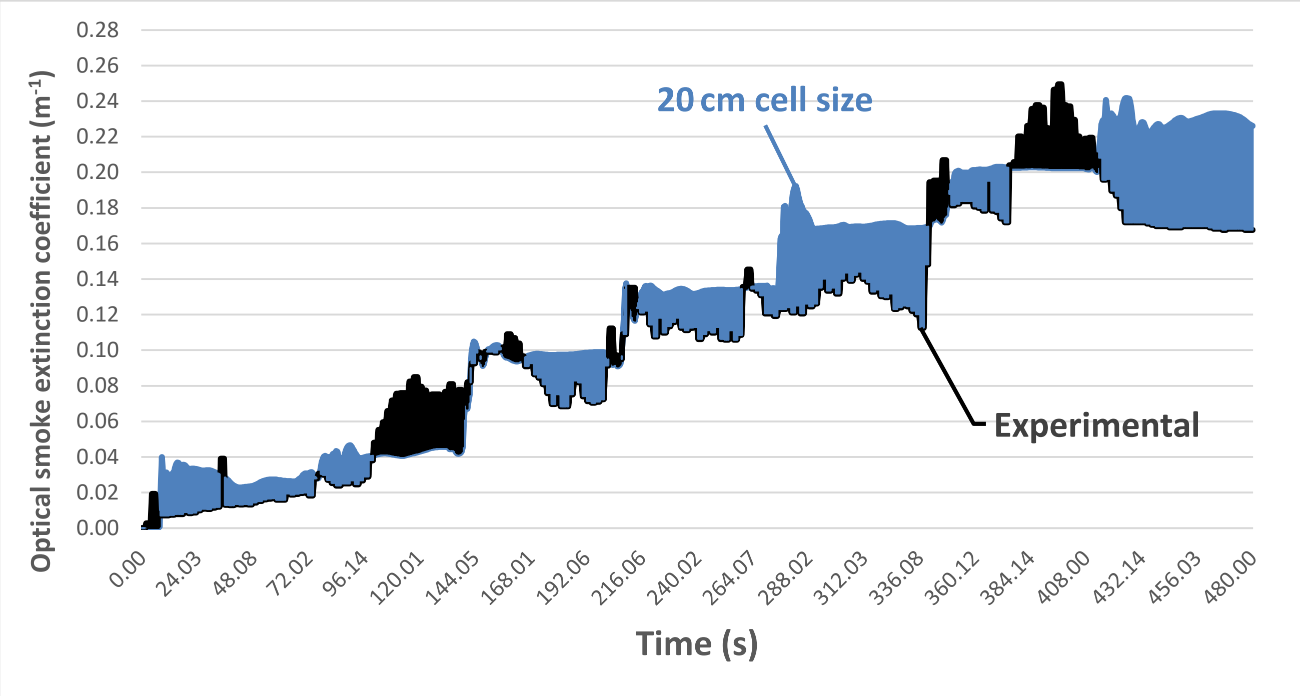

Fig. 5. Optical smoke extinction coefficient comparison 20 cm cell size

The values for the 15 cm cell size simulation differ with those obtained experimentally by an average difference of 4.21%, and the comparison of the two sets of data can be seen in figure 6.

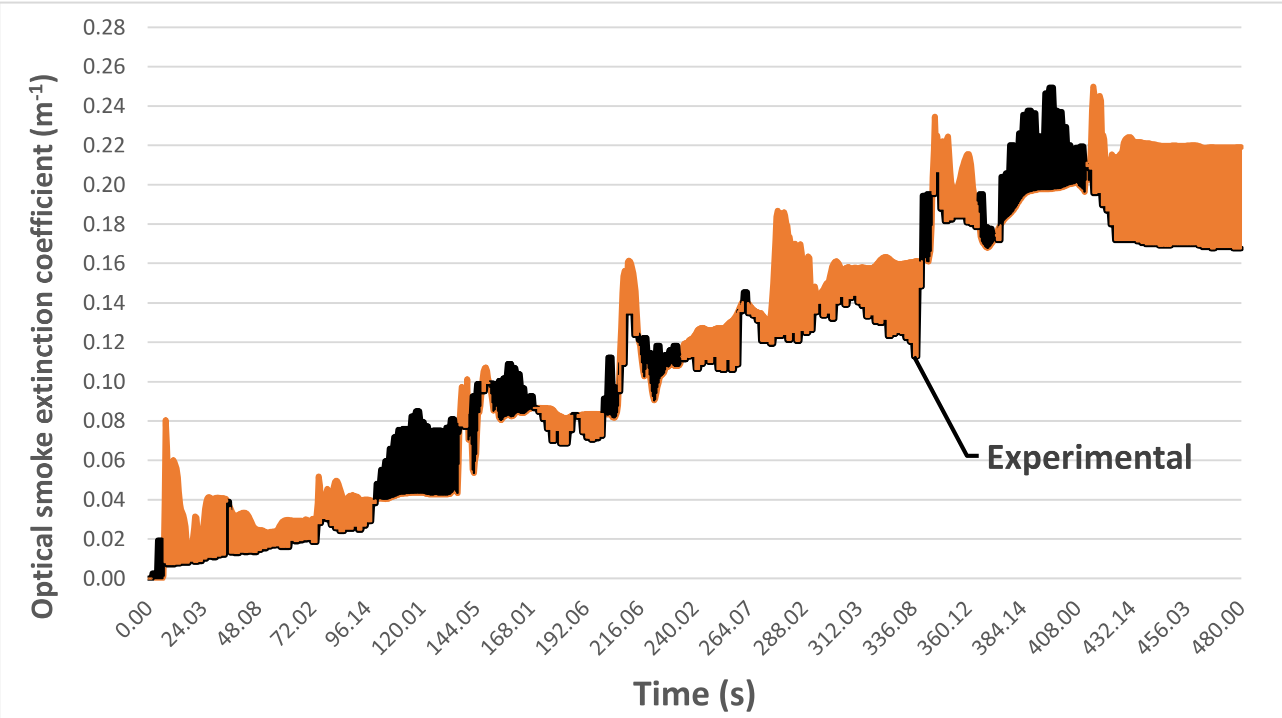

Fig. 6. Optical smoke extinction coefficient comparison 15 cm cell size

With the values obtained by running the simulation with an average linear dimension of 10 cm for the computational grid, there has been obtained an average difference of 4.16%. The comparison of the said values is represented in figure 7.

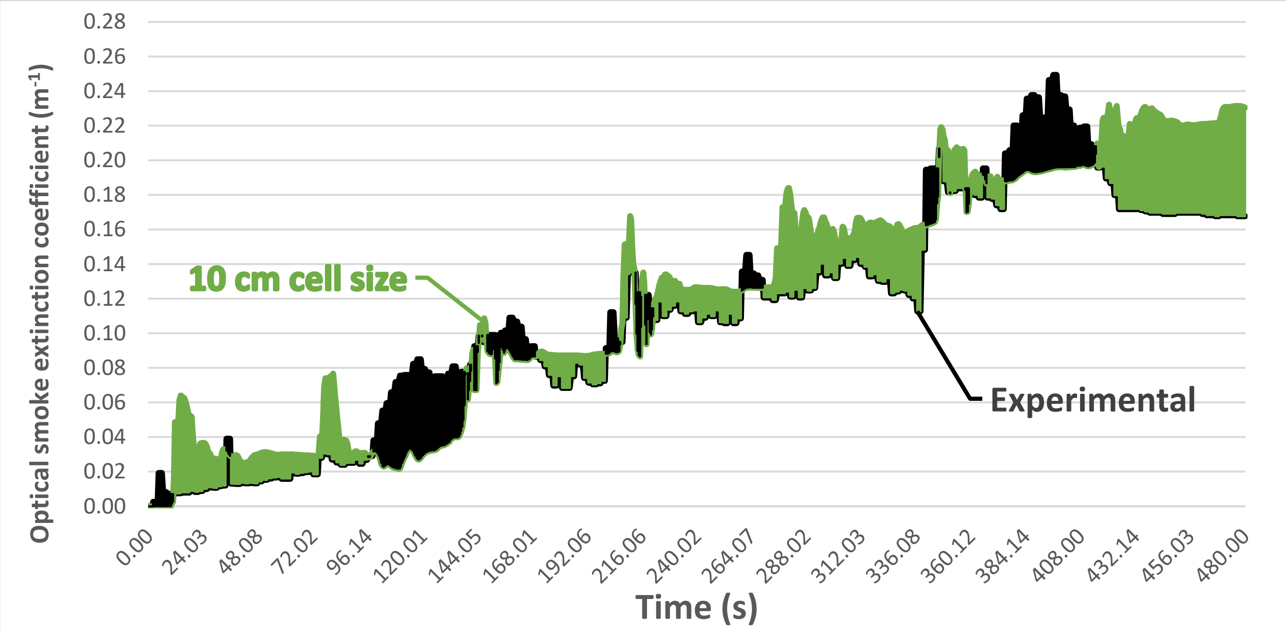

Fig. 7. Optical smoke extinction coefficient comparison 10 cm cell size

Visibility was also measured during the simulation and the results were compared with those obtained by calculation of the amount of light reduction as it passed through the smoke during the experiment. The maximum visibility in the simulation program is considered to be 30 meters [5] and so the reduction in visibility in both the experimental case and the simulations were calculated as percentages. The comparative chart for the visibility in experimental and simulations can be viewed in figure 8.

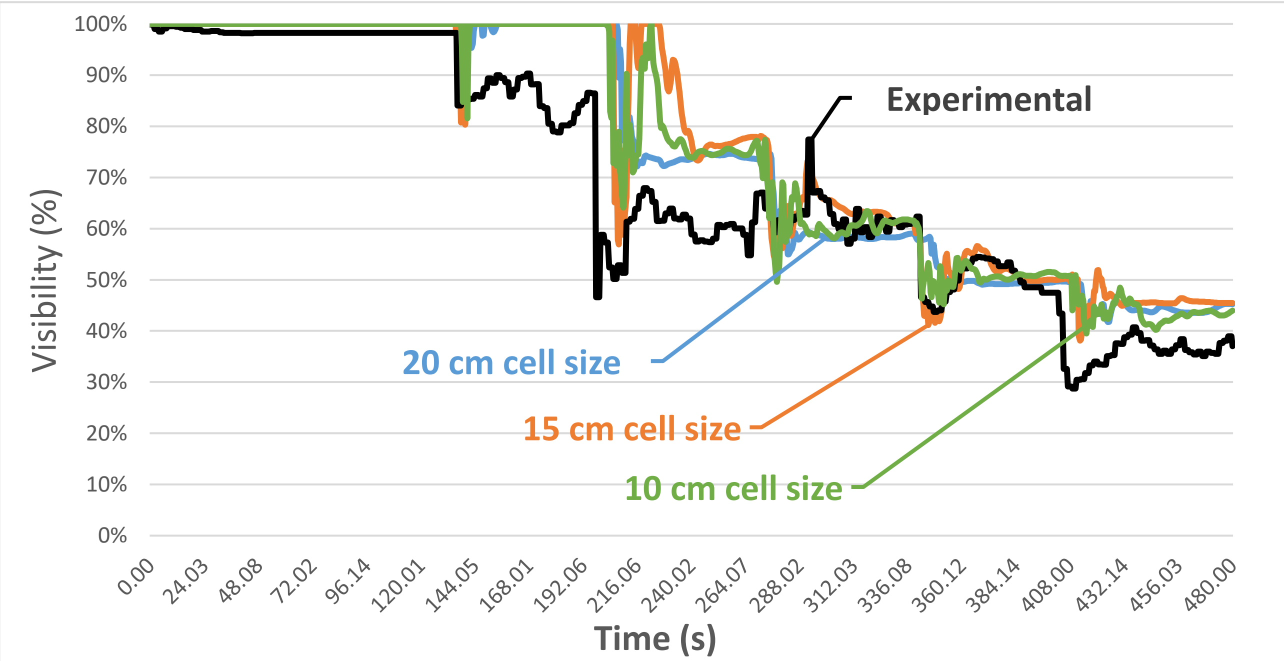

Fig. 8. Visibility comparison for all grid sizes

The average difference between the 20 cm cell size simulation and the experimental values in terms of visibility is 7.96%. For a better comparison of the differences, the values for the two instances are compared in figure 9, the difference between the higher values and the lower ones being highlighted in the color that corresponds to the higher values method of determination, be it experimental or by simulation.

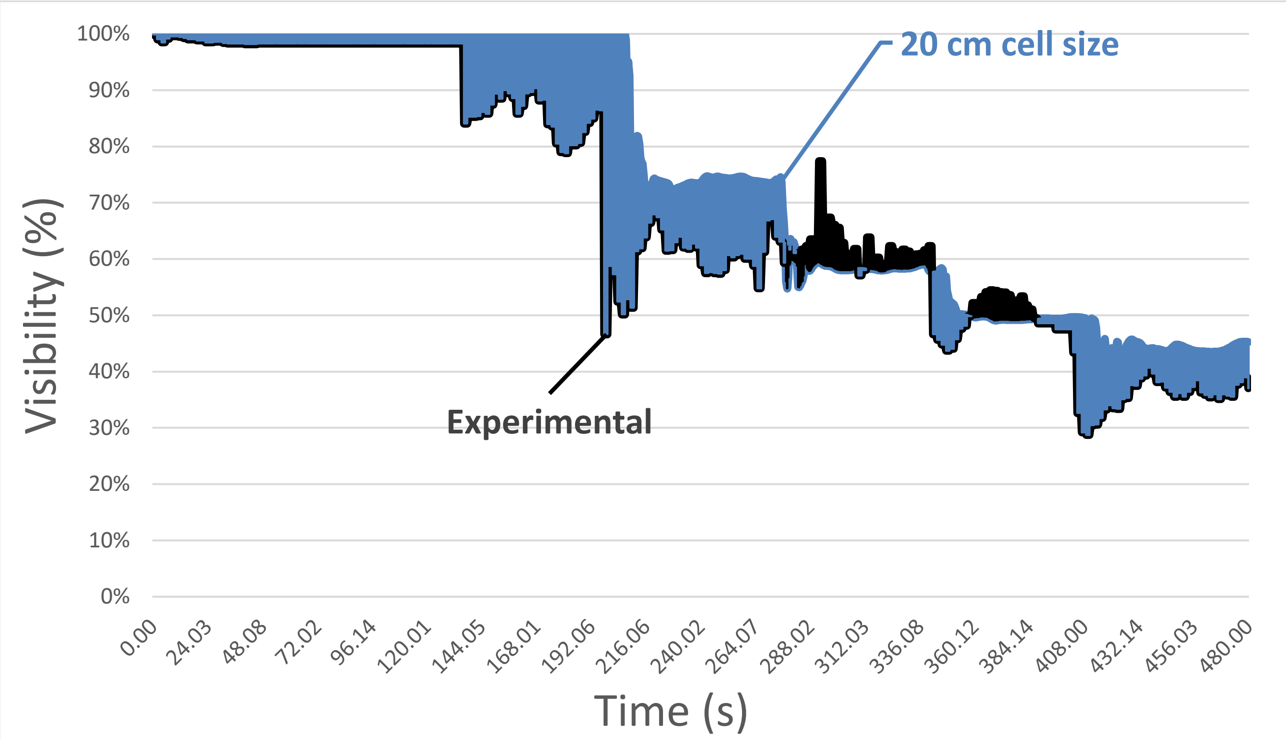

Fig. 9. Visibility comparison 20 cm cell size

The values for the 15 cm cell size simulation differ with those obtained experimentally by an average difference of 7.80%, and the comparison of the two sets of data can be seen in figure 10.

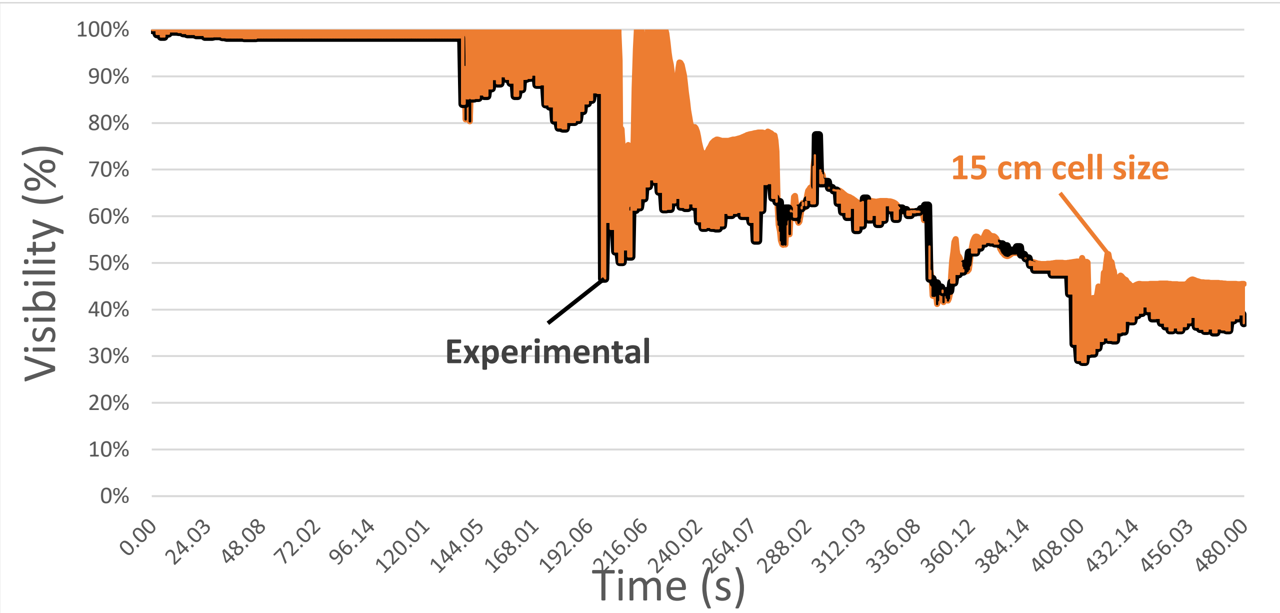

Fig. 10. Visibility comparison 15 cm cell size

With the values obtained by running the simulation with an average linear dimension of 10 cm for the computational grid, there has been obtained an average difference of 7.51%. The comparison of the said values is represented in figure 11.

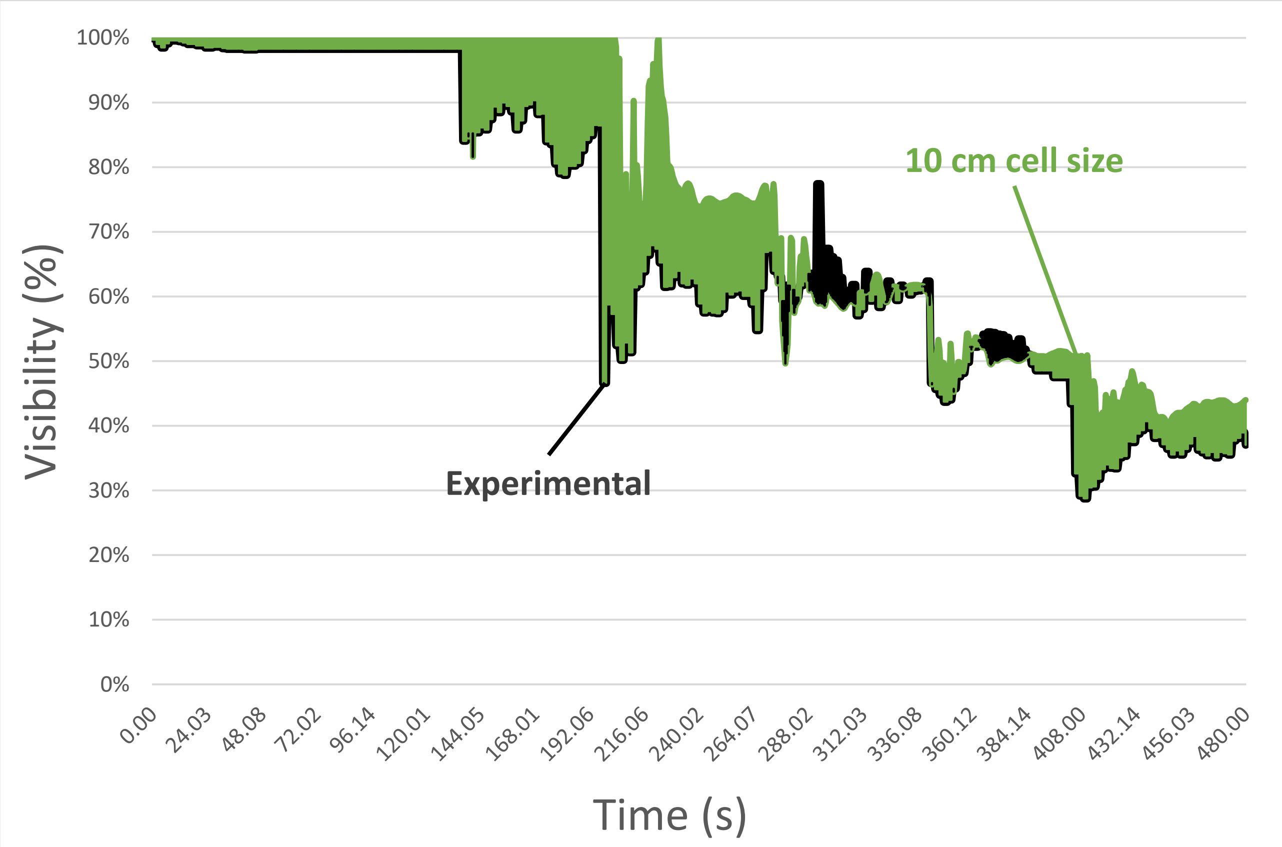

Fig. 11. Visibility comparison 10 cm cell size

A great influence in accuracy can be seen from the 20 cm cell average dimension to the 15 cm cell average dimension in terms of optical smoke extinction coefficient, of about 2.25%. further increasing the number of cells has a much lesser impact, of only 0.05%, thus leading to the conclusion that for the given dimensions of the simulated space, a cell size of 15 x 15 x 15 cm is sufficient for ensuring an accuracy under 5%. In terms of visibility, a greater improvement in accuracy can be seen in lowering the computational cell average dimension from 15 cm to 10 cm, with an 0.29% improvement, which is not that significant, but still greater than the 0.16% improvement gained from decreasing the average cell dimension from 20 cm to 15 cm. Table 2 offers a detailed look at the improvements in accuracy from each incremental adjustment of the average dimension of the cells in the computational mesh.

Table 2: Accuracy improvement

No.	**Average dimension of cells**	**Average difference**	
		Optical extinction coefficient	**Visibility**
1.	20 cm	6.46 %	7.96 %
2.	**Improvement**	**2.25 %**	**0.16 %**
3.	15 cm	4.21 %	7.80 %
4.	**Improvement**	**0.05 %**	**0.29 %**
5.	10 cm	4.16 %	7.51 %

4. Conclusions

For the simulation of a full scale experiment involving smoke optical properties in a compartment or building, for a relatively good accuracy, cells with a size of 0.001 m^3 can be used, meaning that the average dimension of one of their sides can be 10 cm in length. Improvement in simulation accuracy of the optical properties of smoke has been shown to be rather insignificant with the further refinement of the mesh beyond this size. Further research can apply this knowledge to numerical simulations involving smoke generated by burning items, in cases where the optical properties of smoke are evaluated, such as people evacuation from buildings during fire, smoke exhaust systems performance, or firefighter training scenarios in buildings or compartments. Numerical simulations provide a cheaper, faster, more repeatable and less dangerous alternative to experimental research and choosing the right size of the computational cells ensures faster computational time and an adequate accuracy level that meets the needs of the fire safety engineer.

Acknowledgments

This work was supported by a grant of the Romanian Ministry of Research and Innovation, CCCDI - UEFISCDI, project number PN-III-P1-1.2-PCCDI-2017-0350/ 38PCCDI within PNCDI III.

References

[1] International Organization for Standardization. 2017 “ISO 13943:2017 Fire Safety-Vocabulary.” https://www.iso.org/standard/63321.html.
[2] Truchot, B., C. Willmann, and J. Guivarch. “People Evacuation in Tunnel Fires: A Cross Evaluation of Two Methodologies.” *IOP Conf. Series: Journal of Physics: Conf. Series* 1107 (2018) https://doi.org/10.1088/1742-6596/1107/7/072004.
[3] “NFPA 130 Standard for Fixed Guideway Transit and Passenger Rail Systems 2000 Edition An International Codes and Standards Organization.” n.d. Accessed May 21, 2019 www.nfpa.org,.
[4] Ouf, François-Xavier, Alexis Coppalle, Jerome Yon, and Jacques Vendel. “Measurement of the Mass Specific Extinction Coefficient of Acetylene, Toluene and Polymethyl Methacrylate Soot Particles In Visible and Near-Infrared Wavelengths.” (2008) https://doi.org/10.3801/IAFSS.FSS.9-231.
[5] Mcgrattan, Kevin, Randall Mcdermott, Simo Hostikka, and Jason Floyd. n.d. “Fire Dynamics Simulator (Version 5) User’s Guide.” Accessed November 17, 2018 http://fire.fsv.cvut.cz/ifer/2014-Training_school/FDS_5_User_Guide.pdf.

OPTIMIZATION OF THE STRUCTURE OF A MULTIFUNCTIONAL SOIL TILLAGE EQUIPMENT IN AGRICULTURAL HOLDINGS

Gabriel GHEORGHE[1], Gheorghe GANEA[2], Cătălin PERSU[1], Carmen VASILACHI[1]

[1] INMA Bucharest, gabrielvalentinghe@yahoo.com

[2]SC ARTECOM SRL, office@artecom.ro

Abstract: *The heavy operating conditions exposed, raise very severe restrictions and require a rigorous selection of the components of the hydraulic systems that correspond to the requirements imposed on them. The paper analyzes the calculation and selection algorithm according to the standard of the "secondary" component of the hydraulic drive system - the linear hydraulic motor. The dimensioning and resistance calculations of the piston rod are elementary calculations for the optimization of a linear hydraulic motor within the multifunctional soil tillage equipment in agricultural holdings. This system of cylinders has been added to optimize the structure by modifying the center of gravity and reducing the occurrence of the buckling at the connection between the tie rods of the tractor and the equipment.*

Keywords*: Predimensioning, resistance calculation, tensile test*

1. Introduction

Usually solution of different engineering problems requires design of various objects or systems. Basically, there are three general approaches to solving engineering problems: an experimental approach, a computational approach and a computational-experimental approach, which combines both of the mentioned. Each of the first two approaches has advantages and disadvantages, while the last one joins the advantages and avoids the disadvantages of the other two. In this work will be performed a computational approach. When selecting the most suitable computational code for solving a problem, it is obligatory to mind that each computational code is based on a mathematical model of the governing physical processes, expressed in the form of a set of equations derived from physical laws, including semi-empirical and empirical constants or relationships. Consequently, an appropriate method for solving these equations is also required.
For problems which solution is based on Finite Volume Method (FVM) the equations of the mathematical model aresolved in a discrete form on a computational mesh. The solution of the mathematicalproblem is obtained with a certain degree of accuracy, depending on the method ofdiscretising the differential and/or integral equations and on the method of solving theobtained discrete equations. Of course, the solution also depends on the introduced initialdata. It is known that higher accurate solution requires finer computational mesh, providedthrough rather substantial computer memory and CPU time. [1]

2. Pre-dimensioning the linear hydraulic motor

The heavy operating conditions exposed, raise very severe restrictions and require a rigorous selection of the components of the hydraulic systems that correspond to the requirements imposed on them. The paper analyses the calculation and selection algorithm according to the standard of the "secondary" component of the hydraulic drive system - the linear hydraulic motor. Hydraulic motors are used for energy conversion purposes hydrostatic fluid in mechanical energy. In order to approach the calculation of a hydraulic system, namely the hydraulic motor, we must take into account the technical-functional characteristics of the hydraulic cylinder.[2].The hydraulic cylinder subjected to dimensioning, theoretical simulation with Flow Simulation from SolidWorks and resistance calculations using finite element analysis is part of the multifunctional soil working equipment in agricultural operations, fig.1.

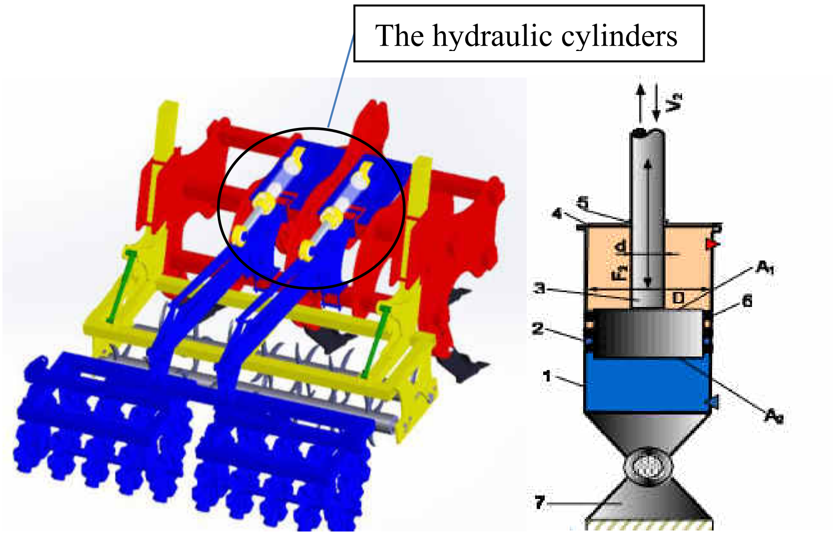

Fig. 1. The multifunctional soil working equipment in agricultural operations, with the highlight of the cylinder who will be analysed (1 - cylinder; 2 - piston; 3 - single or bi-lateral rod; 4 - the lid cylinder; 5 - sealing the piston rod to the cap; 6 - segments of piston seal; 7- cylinder clamping system)

Dimensional characteristics: L = mounting length; S = the maximum race; Lmax = the maximum length; A1 = the piston surface (cm^2).; A2 = small surface of piston (cm^2).

Functional characteristics: pn = the nominal pressure; Pmax = maximum pressure; p_0 = working pressure (210 bar).

For hydraulic cylinders with double effect and unilateral rod, the theoretical forces developed by them, for the two senses of displacement of the piston, are:

$$F_1 = A_2 \cdot p_0 = \frac{\pi \cdot D^2}{4} \cdot p_0, \qquad \text{[daN]} \tag{1}$$

$$F_2 = A_1 \cdot p_0 = \frac{\pi \cdot (D^2 - d^2)}{4} \cdot p_0, \qquad \text{[daN]} \tag{2}$$

From the given forums resulted F_1=299450 and F_2= 514970 N.

The material used in the construction of the rod is 42CrMo with its properties specified in fig. 2.

Property	Value	Units
Elastic Modulus	2.100000031e+11	N/m^2
Poisson's Ratio	0.28	N/A
Shear Modulus	7.9e+10	N/m^2
Mass Density	7800	kg/m^3
Tensile Strength	1000000000	N/m^2
Compressive Strength		N/m^2
Yield Strength	750000000	N/m^2
Thermal Expansion Coefficient	1.1e-05	/K
Thermal Conductivity	14	W/(m·K)

Fig. 2. Properties of the material from which the rod of the hydraulic cylinder is subjected to FEM analysis

3. Traction test of the piston rod material

The tensile test is performed by applying the calculated axial force to the rod, after application, being a very small assembly, the interferences were checked and they do not exist, after this step the boundary conditions (the support of the structure) and their loading with the axial force F_2 and pressure of 210 bar (21 N / mm^2) in different directions for observing the results of the linear-elastic structural analysis: the values of the reactions in the supports, the distribution of the vector field of the relative-resultant displacement in the structure, the distribution of the tensor fields of the specific deformation and the Cauchy tension in the same structure. Also, an important result for the safety of the structure is the distribution of the safety factor; these results are presented in table 1.

Table 1: Results of structural linear elastic analysis

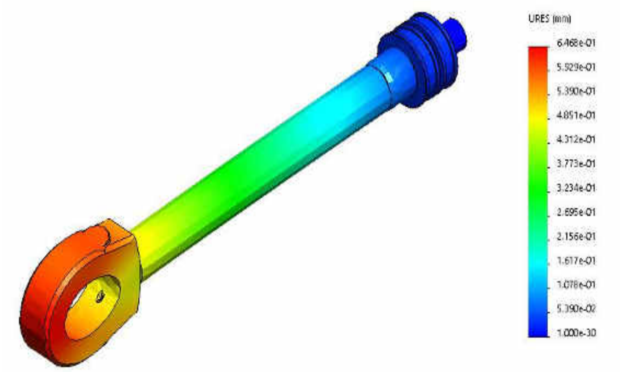

a) The distribution of the values of the resulting relative displacement field on the structure boundary

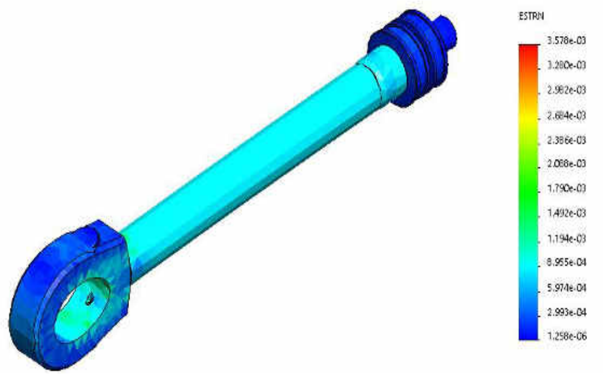

b) Distribution of total specific deformation field values on the structure boundary

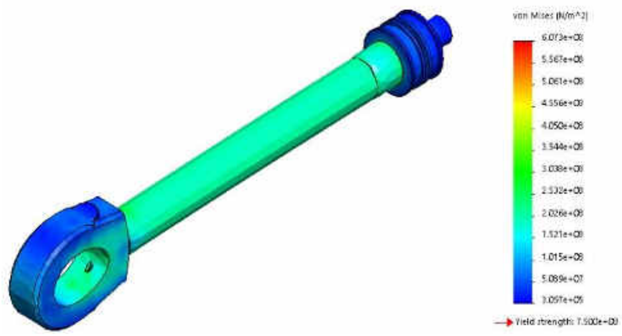

c) Representation of the von Mises Stress on the structure boundary

d) Distribution of the safety factor at the border of the structure

At the maximum value of the force calculated according to the dimensions of the cylinder and the working pressure, a safety factor of 1.2 can be observed. As the force acting within the system is much smaller than the mass of the structure being 1044 kg, it turns out that the cylinder rod will have no problems and the cylinder is over dimensioned and can be optimized in order to choose an optimal cylinder for our structure. As the operating parameters cannot be changed, the optimization will be carried out in the two dimensions D and d. When the force exerted by the real system was introduced, a safety factor of 7.8 was obtained (fig. 3). An optimization will be done to reach a safety factor of 1.2 with this force.

Fig. 3. The safety factor at the actual force of the studied system

An *objective* in optimization is a parameter of the design that the designer seeks to optimize (i.e., either minimize or maximize).

The objective is usually not a parameter the designer can control directly. Instead, it is a function of the design variables that the designer specifies or controls directly. Examples of objective:
- mass, volume, surface area, stress, cost, etc. (for minimization)
- usable container volume, surface area, natural frequency, etc. (for maximization)

You can define only one objective in SW Simulation optimization analysis.
The objective is a function of the design variables; that is, changing the values of the design variables leads to change of value of the objective. In fact, this is the very point of optimization – *change things under your control (design variables) to achieve an objective that is not directly under your control (Factor of Safety).The settings for performing the optimization were made according to figure 4, with the constraint that the safety factor should be between 1 and 1.2 according to the settings from the previous simulation (Static 1).*

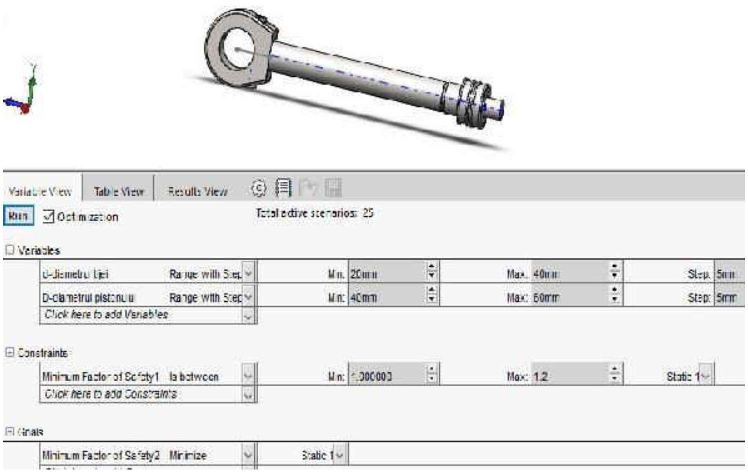

Fig. 4. The settings made to optimize the piston rod

After making the settings, the optimization analysis was run and resulted for the actual force introduced into the system by the weight of the assembly, from the point of view of the safety factor a rod thickness of even 20 mm can be used, the piston diameter remaining the same. it will not yield to this force and to the pressure of 210 bar in the cylinder, as F_2 is inversely proportional to d, the cylinder will generate a maximum force greater than the previous one.

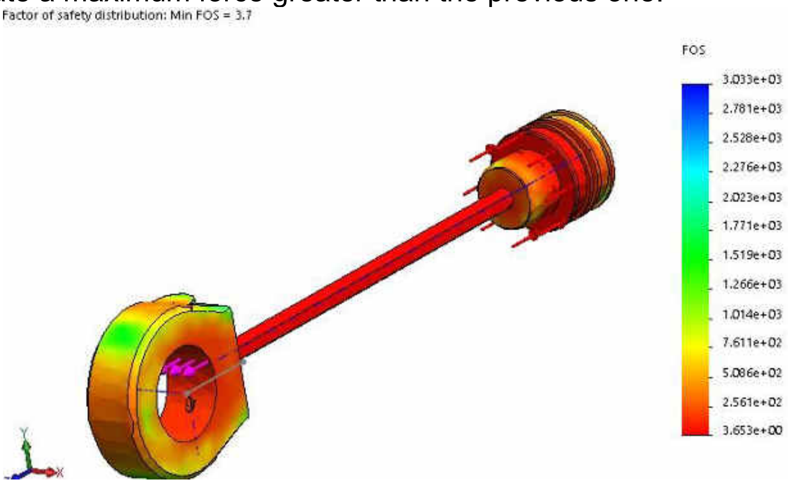

Fig. 5. The safety factor from FEM analysis for d = 20.

Conclusions

Following this first structural study on the cylinder within the equipment, some important conclusions can be drawn for further investigations.

For a normal request, calculated according to the criteria set out in the work, the load-bearing structure of the hydraulic cylinder, is overestimated, abstraction making of possible accidents in the ground, of a use in improper conditions or of shocks produced in transport

Given the maximum values of the equivalent voltage, there is no danger of yielding the structure material.

The high value of the safety coefficient (7.8), compared to its usual values in the practice of designing and manufacturing hydraulic cylinders, shows that the choice in the first phase of the execution of the experimental model was wrong and this will be remedied by the execution of the prototype for cost reduction of production.

Acknowledgments

This work was supported by the European Regional Development Fund under the Competitiveness Operational Program 2014-2020, Project “Rapid knowledge transfer and technical-scientific support in developing competitive products and technologies in enterprises specific to the field of bioeconomy and the production of bioresources” - contract 80/08.09.2016, MySMIS 105551, subsidiary contract 251/21.02.2018 “MULTIFUNCTIONAL EQUIPMENT FOR WORKING THE SOIL IN AGRICULTURAL HOLDINGS and by a grant of the Romanian Research and Innovation Ministry, through Programme 1 – Development of the national research-development system, subprogram 1.2 –Institutional performance – Projects for financing excellence in RDI, contract no. 16PFE.

References

[1] Petrova, Radostina, and Sotir Chernev. “Integrated Technology for CAD Modeling and CAE Analysis of a Basic Hydraulic Cylinder.” Book chapter. *Finite Volume Method - Powerful Means of Engineering Design*. Radostina Petrova (Ed.), ISBN: 978-953-51-0445-2. Rijeka, Intech, 2012.

[2] Balan, Daniel, and Vasile Javgureanu. *Predimensioning the linear hydraulic engine in hydraulic action systems*. Technical University of Moldova, 2013.

[3] Braess, D. *Finite Elements: Theory, Fast Solvers, and Applications in Solid Mechanics – Third Edition*. Cambridge University Press, UK, 2007.

[4] Singiresu, S.R. *The Finite Element Method in Engineering – Fourth Edition*. Elsevier Inc., USA, 2005.

[5] Hurst, William E. *Piezo-Hydraulic actuator Design, and Modeling Using Lumped Parameter Approach*. M.S Thesis, Virginia Polytechnic Institute and State University, 2002.

[6] Egüz, Izzettin Osman. *Hydraulic Press Construction for Fitting the Bearing to a Housing*. Diploma work. Vaxjo University, School of Technology and Design, Växjö, Sweden, 2008.

[7] Ashby, F.M., and R.B.H. Jones. *Engineering Material: An introduction to their properties and application (2nd Edition)*. Oxford Butter Worth Heinmann, 2002.

[8] Parker Hannifin Corporation. *Series of MH Hydraulic Heavy Duty Mill Cylinder*. Catalog HY08-1117-1/NA, Milton, 2008.

[9] Durfee, William, Zongxuan Sun, and James Van de Ven. *Fluid Power System Dynamics*. Center for Compact and Efficient Fluid Power, University of Minnesota Minneapolis, USA, 2015.

[10] Chen, Luo, and Ji-zhao Liang. "Application of complex method in optimal design of hydraulic cylinder supported with flange [J]." *Machinery Design & Manufacture* 3 (2010): 038.

[11] Tenali, V.S. *Simulation of Electro Hydraulic Servo Actuator*. M S. thesis. Department of Mechanical Engineering, National Institute of Technology, Rourkela, 2012.

[12] Ravishankar, N. ”Finite Element Analysis of Hydraulic Cylinders.” *Journal Mech. Des* 103, no. 1 (1981): 239-243.

[13] Ţălu, D.L. Mihai, and Ştefan D.L. Ţălu. ”A Finite Element Analysis Of Hydraulic Cylinder Of Linear Hydraulic Motor From Horizontal Hydraulic Press – 2 Mn.” *Journal of Engineering Studies and Research* 16, no. 4 (2010): 59-62.

[14] Sirohi, Jayant, and Inderjit Chopra. ”Design and Development of a High Pumping Frequency Piezoelectric Hydraulic Hybrid Actuator.” *Journal of Intelligent Material Systems and Structures* 14, no. 3 (March 2003): 135-147.

[15] Henderson, Ross. ”Design, simulation, and testing of a novel hydraulic power take-off system for the Pelamis wave energy converter.” *Renewable Energy* 31 (2006): 271–283.

ISSN 1454 - 8003
Proceedings of 2019 International Conference on Hydraulics and Pneumatics - HERVEX
November 13-15, Băile Govora, Romania

RESEARCH ON METHODS OF DEPOLLUTION OF CONTAMINATED HEAVY METAL SOILS

Nicoleta-Alexandra VANGHELE[1], Valentin VLĂDUȚ[1], Iulian VOICEA[1], Augustina PRUTEANU[1]

[1] INMA Bucharest, vanghelelrc@gmail.com

Abstract: *Heavy metal soil contamination is a major environmental problem resulting from global industrialization in recent years. Therefore, it is very important to decontaminate soil contaminated with heavy metals, reduce the associated risks and maintain environmental health and ecological restoration. Soil contamination is the most serious because it has a significant impact on humans and all ecosystems. Metals in very small quantities are needed for all vital forms, but in large quantities they become toxic.*
This paper aims to highlight the best decontamination techniques that are efficient, not costly and environmentally friendly.

Keywords: *Heavy metals, contamination, de-pollution*

1. Introduction

Heavy metals can be grouped into essential and non-essential classes. Essential heavy metals include Co, Cr, Cu, Fe, Mn, Ni and Zn and are considered to be essential micronutrients, but become poisonous when taken in excessive amounts. Non-essential heavy metals include Pb, Cd and Hg and are highly toxic to living organisms [1].
Heavy metals are natural components of the soil; due to human activities they have increased their concentration. Sources of heavy metals from the soil include excessive application of agrochemicals, waste sludge, industrial wastewater, biosolids and manure [2]. Also, anthropic and geological activities can be sources through which heavy metals enter the soil.
In contrast toorganic contaminants, heavy metals are somewhat unique in that they are highly resistant to biologically or chemically induced degradation. Therefore, the total heavy metal content in the soil persists for a long time after it has been introduced into the soil which causes serious environmental problems, which makes the land resource unavailable and which causes risk to human health, because soil is the main resource to increase part of human food [3].Thus, remediation of soil contaminated with heavy metals is necessary to reduce the associated risks, to make the land resources available for agricultural production, to increase food security and to scale up land use problems [4].
The paper presents a short summary of some methods of decontamination of the soil contaminated with heavy metals, considered to be the most reliable in terms of costs but also without endangering the health of the population.

2. Materials and methods

Techniques for remediation of contaminated soil in heavy metals
Decontamination of soils contaminated with heavy metals is the main concern of environmental legislation. There are two approaches used to decontaminate the affected soils, namely ex-situ (fig.1) and in-situ (fig.2) [5].

Fig.1. Ex-situ decontamination [7]

Fig. 2. In-situ decontamination [7]

Ex-situ procedures involve extracting the soil and treating it in the same site or in another location where the treatment technology is available. The costs of this process depend very much on the amount of material to be evacuated and the distance to which the soil must be transported. Most ex-situ procedures are based on the same principles as in-situ procedures, their main advantages being the shorter period required for decontamination, the possibility of homogenizing the soil which results in more uniform results.
Many of the technologies applied ex-situ can be in the form of mobile installations, which can be easily transported near the contaminated site. [6]

The ex-situ methods (fig. 3) are:

- **biological** - the use of biocells in which the decontamination is carried out with the help of microorganisms, new cultures of microorganisms are added, possibly nutrients air;
- **incineration** - destruction of the pollutants by exposure to high temperatures, it is necessary to have special incendiary installations (furnaces) that must be equipped with an adequate purification and filtration system in order not to generate toxic residues;
- **thermal desorption** - is a decomposition process that involves the volatilization of pollutants by heating the substrate, purifying and filtering waste gases, it is a method that has lower installation and exploitation costs than incineration because the substrate is not burned but only heated the decontaminated space can be reused the least expensive desorption is microwave; [8]
- **treatment / filtration** stations - the contaminated material is driven in these stations where techniques (mechanical / chemical / thermal) are applied for decanting, filtering and inactivating the contaminants.

a) biolgical

b) incineration

c) thermal desorption

d) treatment / filtration

Fig. 3. The ex-situ methods

The in-situ process represents the executionof neutralization directly in the environment affected by pollution, without excavating or moving the contaminated soil.

By applying this method, the simultaneous depollution of soil and groundwater is sought and is generally applied in areas where there are constructions and no excavation operations are possible. In-situ treatment is applied until the limits set in the regulatory acts are reached (specific legislation, environmental authorization / agreement) [7].The most well-known in-situ techniques presented in Figure 4 (a-g) are:

• **isolation of the area with screens / hydraulic insulation** - the isolation of the area contaminated by impermeable screens (covering, creating a wall or insulating layer) does not have the role of decontamination only of prevention, isolation and limitation of pollution, and hydraulic insulation builds an extraction well In front of the pollutant front, from which the polluted water is pumped (which can be purified or transported), an injection well, located upstream of the polluted area, can be built in order to increase the hydraulic gradient;

• **decontamination screens / reactive permeable barriers** - isolation of the contaminated area by impermeable screens with gates / treatment areas, isolation of the contaminated area or substrate by insulating walls that treat / inactivate pollutants;

• **systems pump and treat / volatilize** - the contaminated water is pumped from the underground and treated to the surface using procedures appropriate to the type of pollutant, the purified water can be re-injected into the aquifer to increase the efficiency of the method and reduce the decontamination time, the design of the pump system must be it ensures high pumping rates and possibly re-injection (for rapid decontamination). The method cannot be applied to all types of pollutants. A variant of the type of pumping and treatment is the volatilization method used to extract volatile pollutants (e.g. benzene, toluene, xylene, ammonia) from the water, the exhaust air must often be filtered prior to discharge;

• **SVE systems - underground vapor extraction** - reduce the concentration of volatile compounds absorbed underground, apply a negative pressure underground to have a suction force that collects vapors by suction. A typical EVS system comprises: extraction / suction wells, vacuum pump (for vapor extraction), pipeline treatment system + particle filter [9];

• **air bubbling, steam injection** - a technique that aims to reduce the concentration of volatile contaminants by injecting air into the contaminated substrate;

• **thermal remediation** - thermal remediation theology from the range of EVS techniques (combined with them) is performed almost complete decontamination 95-99%, the efficiency of the decontamination operation increases due to the fact that the weakly volatile compounds, compounds with high boiling temperature are mobilized [10];

• **chemical methods** - it involves immobilizing the polluting compounds at the site of contamination by oxidizing or reducing them into more stable, non-toxic forms, usually using the injection of strong oxidants (hydrogen peroxide, ozone, peroxone, potassium permanganate, oxygen) or some reducing substances (sulfites, sulfur dioxide),but washing techniques can also be used (mobilization and extraction of NAPL - liquids not immiscible with water). Chemical methods include, among other things, soil washing, for less harmful washes, organic acids and chelating agents are often suggested as alternatives to the use of straight mineral acid [4], the most commonly used and studied chelating agents are: EDTA (acid) ethylenediaminetetraacetic), NTA (nitrilotriacetic acid) and DTPA (diethylenetriaminepentaacetic acid) due to their reduced efficiency and cost;

• **stabilization and solidification** - Stabilization - addition of aggregate materials to pollutants to produce more stable compounds and Solidification - addition of aggregate materials to pollutants to increase their stability and isolation in solid products (eg not to be mobilized by water from rain) cement is usually used in different combinations, it is an expensive method, applicable only to certain contaminating products, it requires a complex technique, the durability of insulation is uncertain and the toxic products are not destroyed or extracted but stabilized / cemented at the site of contamination [11];

• **bioremediation techniques** - Biotechnology consisting of the use of living organisms and their metabolic peculiarities - or of some natural processes in the action of removing contaminants from the environment. Oxygen and nutrients are usually injected to accelerate the metabolic capacity of microorganisms, fungi, bacteria to produce enzymes that will enzymatically break down contaminating materials into subcompounds with reduced toxicity.

Bioremediation is a modern technology for treating pollutants that uses biological factors (microorganisms) to transform certain chemicals into less harmful / dangerous final forms, ideally to CO_2 and H_2O, which are non-toxic and released into the environment without altering substantially the balance of ecosystems. Bioremediation is based on the ability of some chemical compounds to be biodegraded.

Classification of decontamination biotechnologies:

• Bioremediation - Bioremediation
• Mycoremediation - Mycoremediation
• Phytoremediation – Phytoremediation [12].

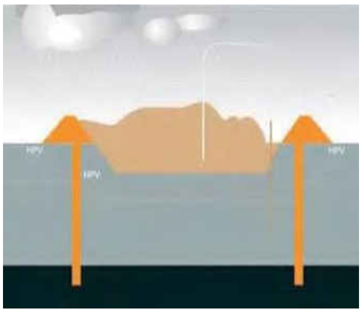

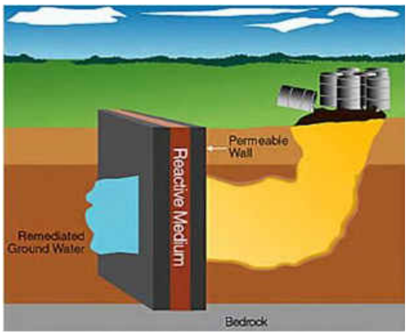

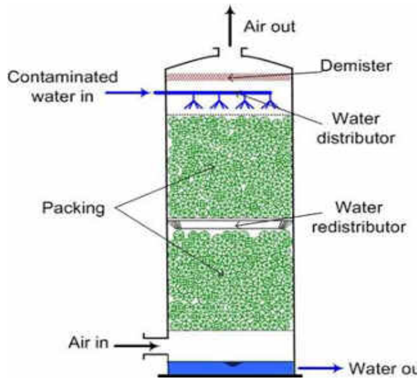

a) Isolation with screens

b) decontamination screens / reactive permeable barriers

c) systems pump and treat / volatilize

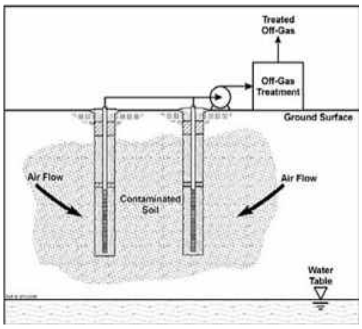

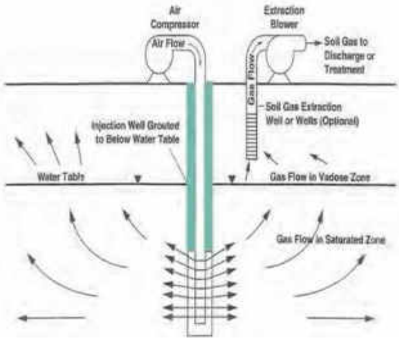

d) EVS - underground vapor extraction systems

e) air bubbling, steam injection

f) chemical methods

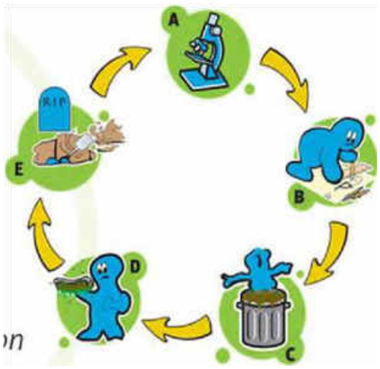

g) bioremediation

Fig. 4. The in-situ methods

3. Results

The remediation techniques currently available for metal-contaminated soil have different advantages and disadvantages. The applicability of these individual techniques in a specific soil remediation project is mainly determined by the geography of the place of contamination, the characteristics of the contamination, the objective of the remediation, the cost efficiency, the financial budget, the availability of the implementation, the time requirement, etc. [14].
All of these factors need to be considered and evaluated comprehensively to select the best techniques for a particular soil remediation project. Integrated uses of two or more available soil remediation techniques may be required at different stages and locations of a project. For example, chemical stabilization can be performed at severely contaminated sites to reduce the bioavailability and toxicity of heavy metals in high concentration in the soil and to allow plants to

settle, followed by phytoremediation to gradually restore the ecosystem functions of the contaminated soil.
Table 1 presents the mechanisms, advantages, disadvantages and the state of application of the remediation techniques available for soils contaminated with heavy metals.

Table 1: Mechanisms, advantages, disadvantages and application status of remediation techniques available for heavy metal contaminated soils [15]

Remediation technique	**Applicability**	**Working mechanisms**	**Advantages**	**Disadvantages**	**Application status**
Surface capping	In-situ, high contamination	Physical containment	Easy to install, low in cost, high security	Limited to small areas and certain geographic locations, loss of land cropping function	Widely practiced
Encapsulation	In-situ, high contamination	Physical containment and isolation	High security, fast to install	Limited to small, shallow contamination areas, high cost, loss of land cropping function	Remediation of radionuclide and mixed waste contamination
Electrokinetics	In-situ, fine soil, moderate to high contamination	Contaminant removal by electricity	Contaminant removal, minimal soil disturbance	Time consuming, low efficiency, best for fine-textured soils with low permeability	Under development with pilot demonstrations
Soil flushing	In-situ, coarse soil, moderate to high contamination	Contaminant removal by chemical solutions	Contaminant removal, minimal soil disturbance, low cost, simple to install	Best for coarse-textured soils with high permeability, potential groundwater pollution	Limited number of applications to mixed waste remediation
Immobilization /stabilization	In-situ, high contamination	Contaminant deactivation by physiochemical transformation	Affordable, easy to implement, immediate effects	Metal-specific, temporary effectiveness, contaminants remaining in soil	Temporary remediation, not officially approved
Phytoremediation	In-situ, low to moderate contamination	Contaminant removal and/or stabilization by plants	High public acceptance, low cost, easy to implement, suitable for large, low contamination areas	Limited to shallow contamination, metal-specific, time-consuming, low efficiency	Under development with pilot demonstrations
Bioremediation	In-situ, low to moderate contamination	Contaminant transformation by	Low cost, simple to implement,	Low efficiency, merely supplemental to	Not practiced for heavy

		microorganisms	minimal soil disturbance	principal remediation techniques	metal remediation
Vitrification	n-situ and ex-situ, high contamination	Contaminant deactivation by thermally vitrifying soil	High efficiency	High cost, limited to small soil area/volume, treated land and soil losing environmental functions	Regularly practiced
Solidification	In-situ and ex-situ, high contamination	Contaminant deactivation by physically solidifying soil	Fast to implement, high efficiency	High cost, treated land and soil losing environmental functions	Regularly practiced
Landfilling	Ex-situ, high contamination	Physical containment and isolation	Immediate cleanup, high security	High cost, requiring additional land for waste storage	Widely practiced
Soil washing	Ex-situ, moderate to high contamination	Contaminant removal by mechanical separation and chemical extraction	High efficiency, fast effects	Extreme soil disturbance	Regularly practiced

4. Conclusions

Following the research conducted over the years in different countries and on different soil types, it has been found that no decontamination method can be declared as the most effective.
To determine the appropriate decontamination method, account must be taken of the geographical location, the degree and characteristics of heavy metal soil pollution, the costs of decontamination, the time allotted for decontamination, the qualification of the decontamination personnel and other factors that may change from a project to another.

Acknowledgement

This work was supported by a grant of the Romanian Research and Innovation Ministry, through Programme 1 – Development of the national research-development system, subprogramme 1.2 – Institutional performance – Projects for financing excellence in RDI, contract no. 16PFE.

References

[1] Sandeep, G., K.R. Vijayalatha, and T. Anitha. "Heavy metals and its impact in vegetable crops." *Int. J. Chem. Stud.* 7, no. 1 (2019): 1612–1621.
[2] Maimon, A., J. Khairiah, R. Ahmad Mahir, A. Aminah, and B.S. Ismail. "Comparative accumulation of heavy metals in selected vegetables, their availability and correlation in lithogenic and nonlithogenic fractions of soils from some agricultural areas in Malaysia." *Adv. Environ. Biol.* 3 (2009): 314–321.
[3] Khalid, S., M. Shahid, N.K. Niazi, B. Murtaza, I. Bibi, and C. Dumat. "A comparison of technologies for remediation of heavy metal contaminated soils." *J. Geochem. Explor.* 182 (2017):247–268.
[4] Wuana, R.A., and F.E. Okieimen. "Heavy metals in contaminated soils: a review of sources, chemistry, risks and best available strategies for remediation." *ISRN Ecol.* (2011): Article ID 402647.

[5] Zhou, Q.X., and Y.F. Song. “Remediation of contaminated soils: principles and methods.” *Sci. Press* 7 (2004): 345–346.
[6] www.scribd.ro- Marian Pen -Jun23,2015.
[7] http://silvic.usv.ro/cursuri/reed.pdf.
[8] Nistor, S., B. Nistor, and D. Strat. “Decontamination through thermal decoration of waste polluted with hydrocarbons in the Suplacu de Barcau (Bihor County) petroliferous area.”/”Decontaminarea prin desorbtie termica a deseurilor poluate cu hidrocarburi in arealul petrolifer Suplacu de Barcau (Jud. Bihor).” Paper presented at INCD ECOIND SIMI 2011 - International Symposium “The Environment and Industry”, Bucharest, Romania, November 16-18, 2011.
[9] https://ro.scribd.com/document/343183285/Metode-Si-Tehnologii-de-Remediere-a-Solurilor-Poluate.
[10]https://rtpime.files.wordpress.com/2010/03/cap-5.pdf.
[11] Simule, Codruța Violeta, and M. Dobrin. “Remedial measures for the contaminated site Post Rât – Turda."/”Măsuri de Remediere a Sitului Contaminat Posta Rât – Turda.” *ProEnvironment* 3, no. 5 (2010): 163 – 169.
[12] Malschi, Dana. *Biotechnologies and the depollution of ecological systems*./ *Biotehnologii si depoluarea sistemelor ecologice*. Online handbook. Cluj-Napoca, Bioflux Publishing House, 2014.
[13]https://images2.bizoo.eu/image/img360/sale/2012/4/12/Statie-de-desorbtie-termica-SDT-30_9145851_1334662132.jpg.
[14] USEPA. “Superfund Remedial Investigation/Feasibility Study (Site Characterization).” U.S. Environmental Protection Agency, Washington, DC, 2017. Accessed January 31, 2018. https://www.epa.gov/superfund/superfund-remedial-investigationfeasibility-study-site-characterization.
[15] Liu, Lianwen, Wei Li, Weiping Song, and Mingxin Guo. “Remediation techniques for heavy metal-contaminated soils: Principles and applicability.” *Science of the Total Environment* 633 (August 2018): 206-219.

ISSN 1454 - 8003
Proceedings of 2019 International Conference on Hydraulics and Pneumatics - HERVEX
November 13-15, Băile Govora, Romania

MATHEMATICAL MODELING IN RENEWABLE ENERGY CONVERSION SYSTEMS

Viorel BOSTAN[1], Ion BOSTAN[1], Valeriu DULGHERU[1], Oleg CIOBANU[1], Marin GUȚU[1]

[1]Techical University of Moldova, valeriu.dulgheru@bpm.utm.md

Abstract: *Research and elaboration of the systems for conversion of renewable energy sources (RES) as a research objective present great interest and importance. Wind and hydraulic energy currently are the most used, cheap and clean renewable energy sources. The main goal of this paper consists in the mathematical modeling of the aero/hydrodynamic profiles of blades and individualized orientation of the hydrodynamic blades. Using a high order panel method, the potential flow analysis is performed in order to compute the hydrodynamic lift and moment coefficients. The drag coefficient is computed through a boundary layer analysis. Increased efficiency is achieved by an optimum position of the blades with hydrodynamic profile.*
In order to increase the lift and reduce the drag forces for a blade segment with aerodynamic profile, a groove was created on its surface. The optimum location of the groove was determined by means of CFD analysis. Simulation results were compared to test results and the CFD analysis model was validated.
A new design and functional concept of a wind and hydraulic flow turbine with orientation of the hydrodynamic blades was proposed and elaborated.

Keywords*: Aero/hydrodynamic profile, wind and hydraulic turbine, water kinetic energy*

1. Introduction

Can you imagine life without television, cars or computers, without being able to prepare your food every day, without lighting in the house, without heating during the cold seasons of the year, etc.? But all this is the result of creative activity of scientists and inventors, especially during the last two hundred years. All this may disappear during the first half of the present century, following the drastic depletion of natural reserves of fossil fuels. Increased energy consumption leads to a continuous increase in the volume of extracting fossil fuels, which provides more than 85% of energy use today.
What energy sources are able to meet these requirements? Increasing power generation by burning traditional fossil fuels would further endanger the ecological impact. Expectancy of power engineering professionals is based on finding new solutions and processes that would meet the energy needs of mankind in the coming decades or centuries. At the forefront, nuclear energy solutions have been related to, but after the power failures (the U.S. Three Miles Island and Chernobyl in Ukraine), the need to develop alternative solutions environmentally friendly, has become an imperative.
One of the greatest challenges of the 21st century is to ensure the access of every citizen of the Planet to sustainable, non-polluting energy, which according to the UN Commission, means „*a development that meets the needs of the present, without compromising the capacities of future generations to satisfy their own n needs*". Looking visionary into the future, Freeman Dyson of the University of Oxford argues that technological changes fundamentally alter our ethical and social arrangements and that three new, rapidly developing technologies - renewable energy, genetic engineering and global communication - today have the potential to create more uniform distribution of global health.
The concept of energy efficiency (or energy optimization) became, at present, one of the main concerns of mankind on the whole world. With the first oil crisis of the early '70s, human society began to realize more than ever the need for a sustainable strategy by increasing the efficiency of energy use and implementing energy efficiency programs taking into account the depletion of fossil fuel reserves on Earth. Today, we speak of a global energy policy and a concerted strategy to reduce harmful emissions into the atmosphere, based on concrete economic and technical

solutions for rational use of fossil fuel reserves (which still have the main share of energy production) and valorization of renewable energy resources on a large scale, the so-called „*clean*" energy or non-conventional energy, as an alternative to the current system of fuel reserves on Earth. Renewable energies (solar, wind, hydro, etc.) are environmentally friendly but today they are not able to meet these ever-growing needs.

2. Mathematical modeling of wind and hydraulic rotors

Hydraulic and wind energies are the oldest form of renewable energy used by man and has become the most currently used renewable energy sources, being also one of the best, cheap and clean energy sources. The problem of the engineers is to develop hydraulic and wind energy conversion systems with higher efficiency, close to the theoretical limit of Betz (0,593).
The emergence of increasingly efficient computers and modern specialized software has made mathematical modeling an indispensable tool for researchers in various fields. Renewable energy conversion systems are one of these areas. In the Center for the Development of Renewable Energy Conversion Systems (CESCER) within the department „*Fundamentals of Machine Design*", extensive scientific research is carried out regarding the optimization of the performance of the working bodies of the wind and hydraulic kinetic energy conversion systems, in particular, in the optimization of the profile of blades for wind and hydraulic rotors. A modern research has the following structure (fig. 1):

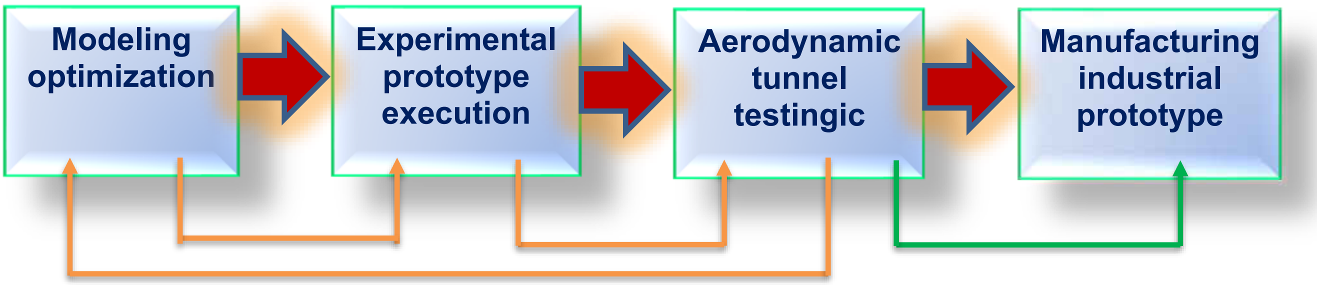

Fig. 1. The structure of modern research

CESCER is equipped with (fig. 2, 3): modern Workstations and performance simulation software ANSYS; 3D printers; aerodynamic laboratory tunnel GUNT HM 170; manufacturing laboratory; human potential.

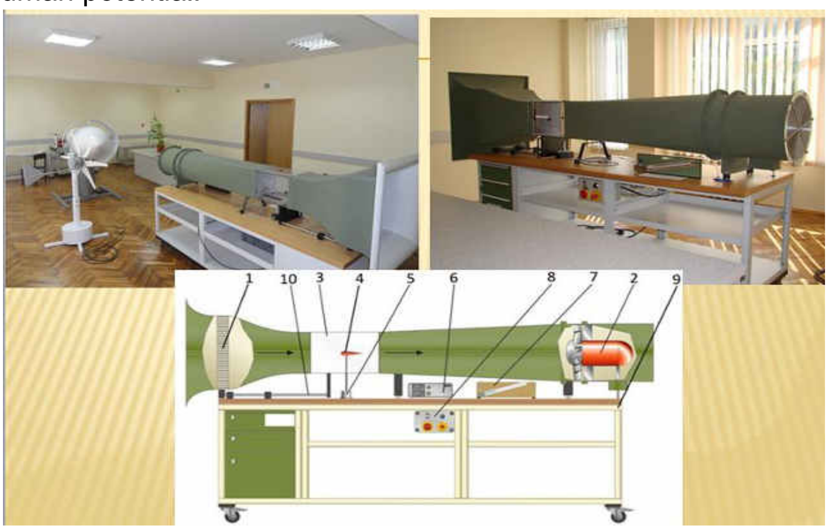

Fig. 2. Aerodynamic tunnel *GUNT HM 170*

Fig. 3. 3D printers for manufacturing

The stages of CFD simulation of the wind and hydraulic rotors are shown in ANSYS Workbench Project schematic (fig. 4).

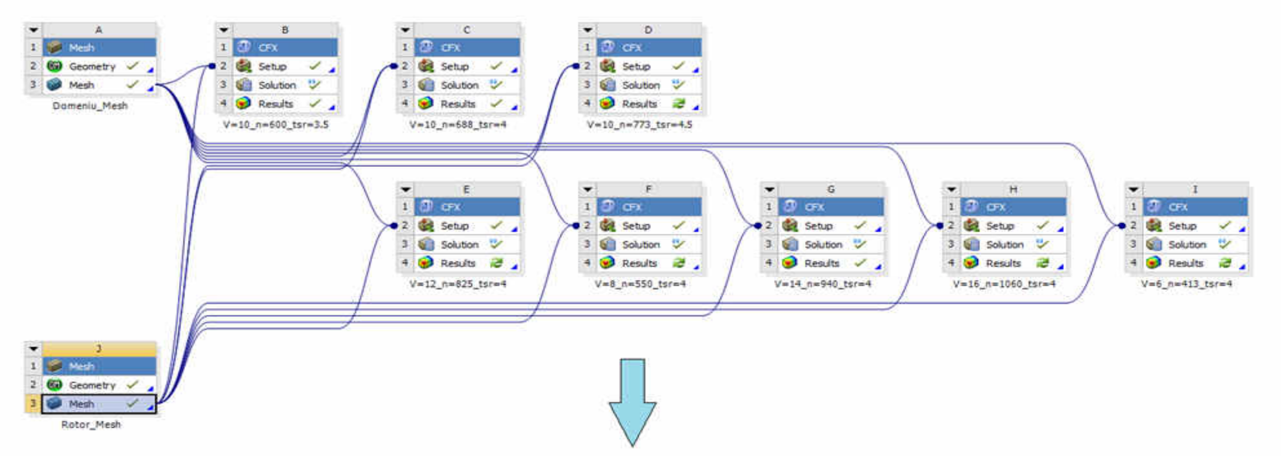

Fig. 4. ANSYS Workbench Project schematic

2.1 Mathematical modelling of hydraulic rotor

Hydraulic energy as a renewable energy source can be captured in two extra power forms:
- potential energy (of the natural water fall);
- kinetic energy (of the water stream running).

Both extra power forms can be captured at different dimensional scales. Thus, the mechanical power of running water can be considered one of the oldest tools. Floating micro hydro power plants are of special interest. In terms of costs, floating micro hydro power plants are efficient because they do not include essential costs related to civil engineering [1,6].

In a classical hydraulic wheel horizontal axle (Fig. 3) [1] the maximum depth at which one of blades is sunk makes approximately 2/3 of the blade height h. Namely, only this area participates in the transformation of water kinetic energy into mechanical one. As well, the prior blade covers approximately 2/3 of the blade surface sunk utmost in the water (h''≈ 2/3h'). This fact reduces significantly the water stream pressure on the blade.

The insistent searches of authors lead to the elaboration and patenting of some advanced technical solutions for floatable micro-hydro power stations, based on the hydrodynamic effect, generated by the hydrodynamic profile of blades, and their orientation at optimum positions concerning the water streams with account of energy conversion in each phase of the turbine rotor rotation (Fig. 4) [1-4,6].

A very important aspect in the functional optimization of micro-hydro power plants is the selection of optimum hydrodynamic profile of the blades which allows increasing the conversion coefficient (Betz coefficient). Therefore, it was necessary to perform a large volume of multi-criteria theoretical research concerning the selection of optimum hydrodynamic profile of the blades and the design of the orientation mechanism towards the water streams.

The adopted technical solutions have resulted in an ample theoretical and experimental research carried out at the Centre for Renewable Energy Conversion Systems Design, Department of the Theory of Mechanisms and Machine Parts. To justify the constructive and functional parameters, supplementary digital modelling and simulation have been carried out by utilizing ANSYS CFX5.7 software. Subprograms developed by authors for the MathCAD, AutoDesk MotionInventor, etc. software, have been utilized, namely simulation of the interaction „flow-blade" of the floatable steadiness and also the optimization of blades hydrodynamic profile, with the purpose to increase the river water kinetic energy conversion efficiency for different velocities by using 3,

ISSN 1454 - 8003
Proceedings of 2019 International Conference on Hydraulics and Pneumatics - HERVEX
November 13-15, Băile Govora, Romania

4 and 5 blade rotors. In the process of micro-hydro power plants design, the experience gained at research-design-manufacturing of the pilot plant was utilized.

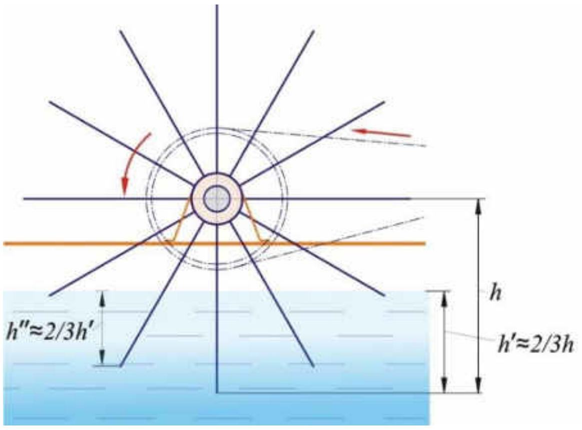

Fig. 5. Conceptual diagram of the water wheel with rectilinear profile of blades.

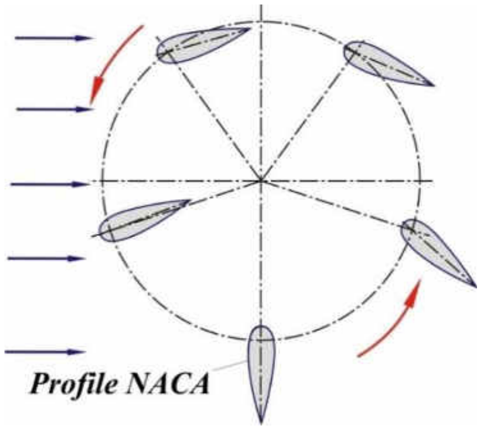

Fig. 6. Conceptual diagram of the rotor with hydrodynamic profile of adjustable blades concerning the water streams

Theoretical argumentation of the hydrodynamic blades profile in normal section

The geometric parameters of the hydrodynamic blades with profile NACA (0012, 0014, 0016, 0018, 63012, 63015, 63018, 66015, 66018, 67015 - about 40 profiles) was optimized [5]. It is considered the symmetrical profile of the blade, which is in a fluid current that moves evenly with speed V_∞ (Fig. 7) [1,2,6]. At the point of fixation *O′* of the symmetrical blade with the arm *OO′* we consider two coordinate systems, namely: the *O′xy* system with the *O′y* axis oriented in the direction of the vector speed V_∞, and the *O′x* axis normal in this direction; the *O′x′y′* system with the *O′y′* axis oriented in the direction of the *O′O* arm, and the *O′x′* axis normal in this direction. Point *A* corresponds to the flight board, and point *B* - the attack board. The angle of attack *α* is the angle between the rope *AB* of the profile and the direction of the velocity vector V_∞, and the positioning angle φ is the angle between the direction of the velocity vector and the *O′O* arm.
The hydrodynamic force *F* has the components in the *O′x* and *O′y* directions, called the load (lift) force F_L and strength (drag) force F_D:

$$F_D = \frac{1}{2} C_D \rho V^2 C_p, \quad (1)$$

$$F_L = \frac{1}{2} C_L \rho V^2 C_p,$$

(2)

where: *ρ* is the density of the fluid, *V* is the velocity of the current, $S_p = ch$ (*c* is the length of the cord *AB*, *h* is the height of the blade) represents the area of the lateral surface of the blade; C_L and C_D are the dimensionless hydrodynamic coefficients, called the lift coefficient (lift) and the coefficient of resistance (drag). The hydrodynamic coefficients C_L and C_D are functions of the angle of attack *α*, the Reynolds number *Re* and the hydrodynamic shape of the blade profile.
The components of the hydrodynamic force in the *O′x′y′* coordinate system are:

$$F_{x'} = - F_L \sin\varphi + F_D \cos\varphi, \quad (3)$$

$$F_{y'} = F_L \cos\varphi + F_D \sin\varphi. \quad (4)$$

Torque moment produced by one blade:

$$T_{r,i} = F_{x'} \cdot |OO'| \tag{5}$$

and total:

$$T_{r\Sigma} = \sum_{i=1}^{Nbl} T_{ri} \ , \tag{6}$$

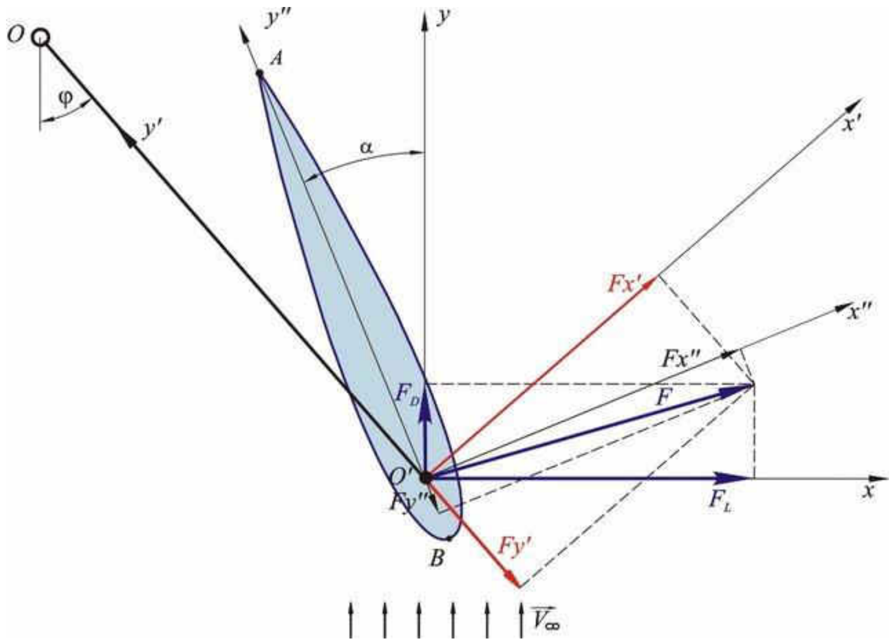

Fig. 7. Symmetrical profile of the blade in fluid current with speed $V\infty$

where: N_{bl} -number of blades.
Determination of the hydrodynamic lift C_L and moment C_M coefficients.

$$C_L = - F_x \sin\alpha + F_y \cos\alpha, \tag{7}$$

$$C_M = \sum_{j=1}^{N} C_{m.j.} \tag{8}$$

We apply the numerical calculation methods described above to calculate the coefficients C_L and C_D for the symmetrical profiles in the NACA aerodynamic profile library (0012, 0016, 63018 and 67015) with the chord length = *1,3 m*. The blade with computational domain was limited (fig. 8) and the streamlines and velocity distribution for angle of attack 18° was determined (fig. 9). Based on the obtained numerical modeling results were determined: drag and lift coeficients as function of the attack angle *α* (fig. 10); hydrodynamic force *F* wich acting on the blade (fig. 11); torque moment *T* produced by 1 blade as function of the position angle (fig. 12) by all blade for 3 values of water flow speed (fig. 13).

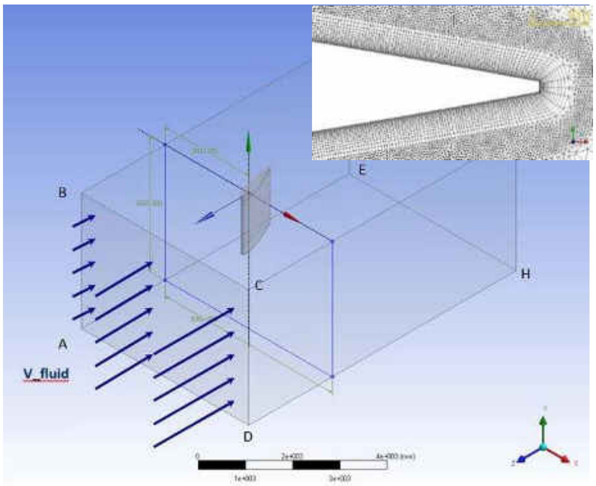

Fig. 8. Computational domain

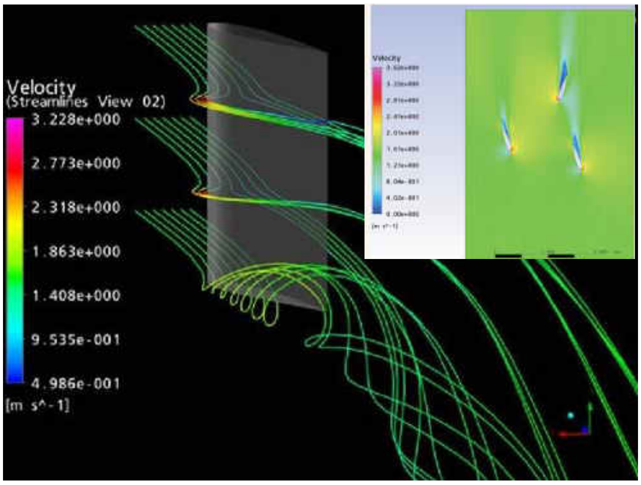

Fig. 9. Streamlines and velocity distribution for angle of attack 18° .

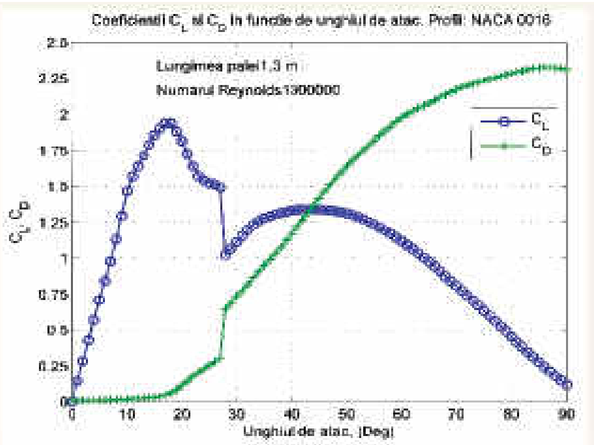

Fig. 10. Drag and lift coeficients as function of the attack angle *α*.

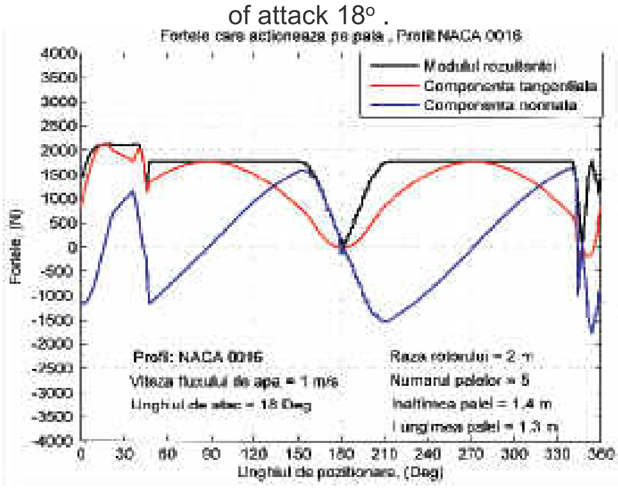

Fig. 11. Hydrodynamic force *F* wich acting on the blade.

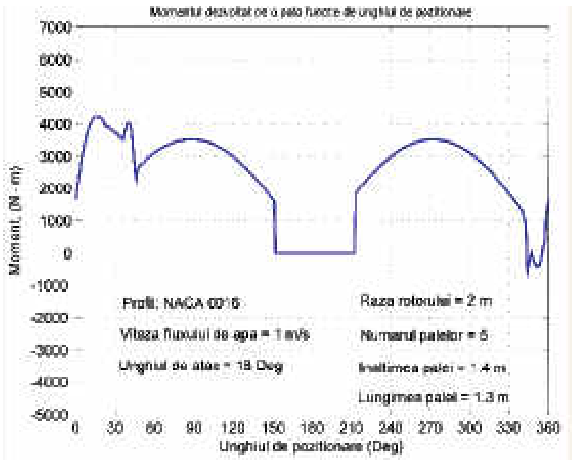

Fig. 12. Torque moment *T* produced by 1 blade as function of the position angle

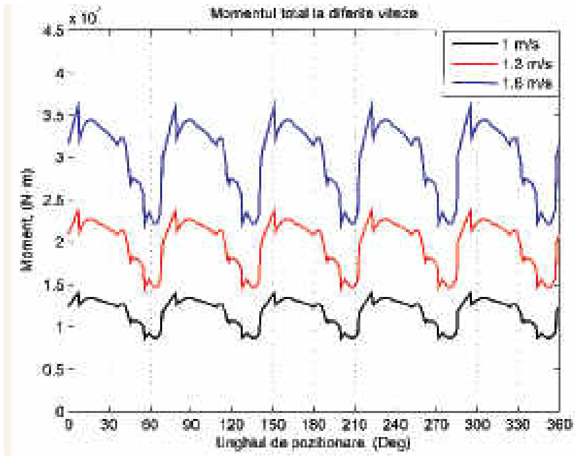

Fig. 13. Torque moment *T* produced by all blade for 3 values of water flow speed

Based on the results of the numerical modelling and the obtained patents [3,4], 3 types of micro-hydroelectric power stations with 3 and 5 blades rotor have been developed, designed, manufactured and tested [1, 5-6].

2.2 Mathematical modelling of wind rotor

In general, the mathematical modelling of the wind rotor is performed similar to the hydraulic one. Mathematical modelling included:

- aspects regarding the optimization of the aerodynamic profile of the blades;
- aspect regarding blade resistance.

2.2.1. Optimization of the aerodynamic profile of the blades

The velocity field around of the profile NACA4412 at the attack angle and Reynolds number given by:

$$Re = \frac{\rho c \vec{V}}{\eta} = \frac{c \vec{V}}{\nu}, \tag{8}$$

CFD modelling of the turbulence. An important problem in horizontal axis rotors is the reduction of the level of turbulence, which reduces the conversion efficiency. The results of measurements of air currents velocity and turbulence intensity in the field around the NACA 4412 profile are presented in fig. 14.

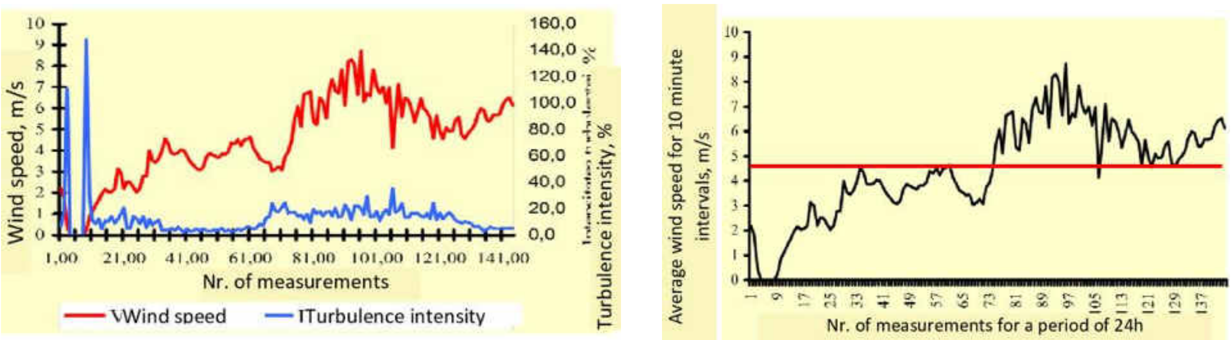

Fig. 14. Wind speed and turbulence intensity

Wind turbine blade segment and domain was designed in SolidWorks and then imported into the ANSYS Workbench software. The dimensions of the blade segment were chosen taking into account the dimensions of the available wind tunnel measuring section (100 mm span and 100 mm chord). The size of the groove opening was accepted by 2.5% of the chord length as recommended in the paper [2]. Several CFD analyzes were performed in order to determine the optimum distance *x* from the leading edge to the center of the channel. Figure 15, *a* show the parameters of the simulated blade segment with airfoil NACA 4412. The dimensions of the computational fluid domain were chosen taking into account good practices and recommendations [3] so as to ensure free flow without influencing the boundaries of the field. Figure 15, *b* show considered fluid domain. Mesh was generated in the ANSYS Meshing Workbench integrated program. After importing the geometric model, the following regions required for computing were defined: (Inlet), (Outlet), (Walls) [5]. The basic dimensions of the mesh are specified by means of the minimum dimension Minimal size=0.22 mm and Maximum Max Size = 30 mm of the faces of the elements and the adjacent volumes. The surface of blade segment was meshed as *Mapped Face* with the mesh size 0.5 mm (Figure 15,*c*). The entire domain was meshed into approx. 1859600 finite elements. For a better understanding of the results the velocity contour and turbulence kinetic energy around the blade segment section was analyzed, Figure 16 and 17. From Figure 16, *b* we can see the delay effect of separating the boundary layer on the surface of the blade section with groove. In order to detect the influence of geometrical factors on blade's performance, turbulence kinetic energy is one of the indicators that helps identifying the regions of major turbulence that cause important energy flow losses.

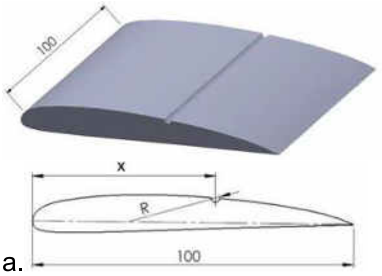

a.

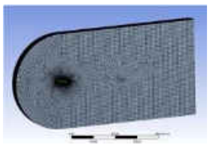

b. c.

Fig. 15. Parameters of the simulated blade segment (a) meshed fluid domain (b) and around the blade (c)

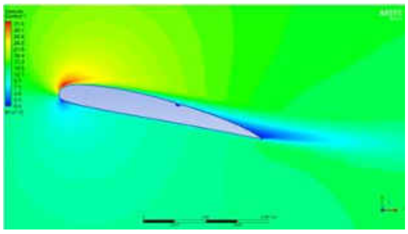

a.

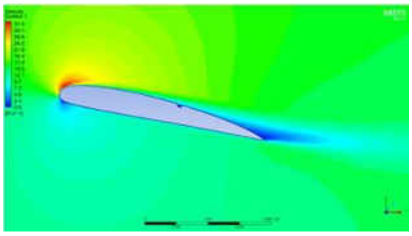

b.

Fig. 16. Velocity contour: *a* - smooth surface blade section; *b* - blade section with groove

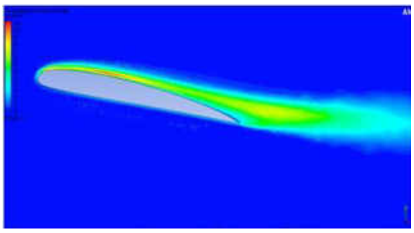

a.

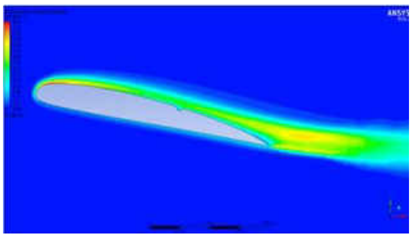

b.

Fig. 17. Turbulence kinetic energy: *a* - smooth surface blade section; *b* - blade section with groove

Physically turbulence kinetic energy is produced due to the mean flow gradients, and is dissipated by viscous effects. For smooth energy is 10.5 J/kg (fig. 17,*a*). For blade with groove the maximum velocity is 31.5 m/s and turbulence kinetic energy is 8 J/kg (fig. 17,*b*).surface blade section the maximum velocity is 29 m/s and turbulence kinetic

2.2.2. Numerical analysis of blade resistance

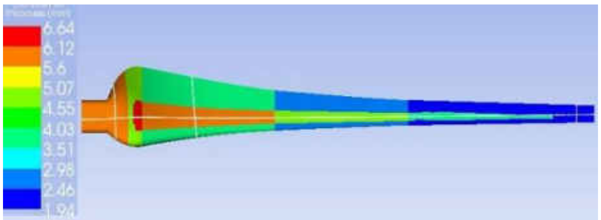

a.

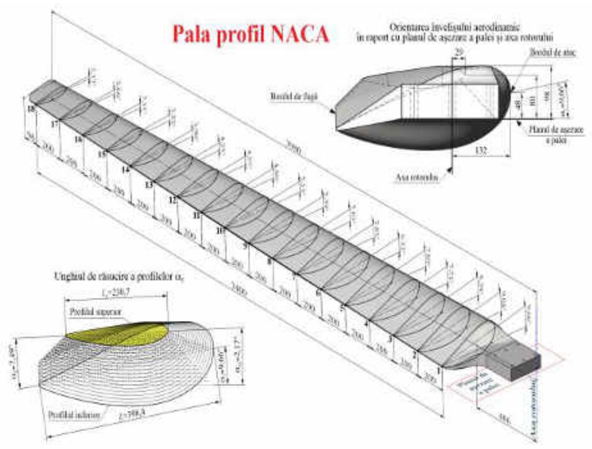

b.

Fig. 18. The composite layer thickness (a) and components in layer schedule (b).

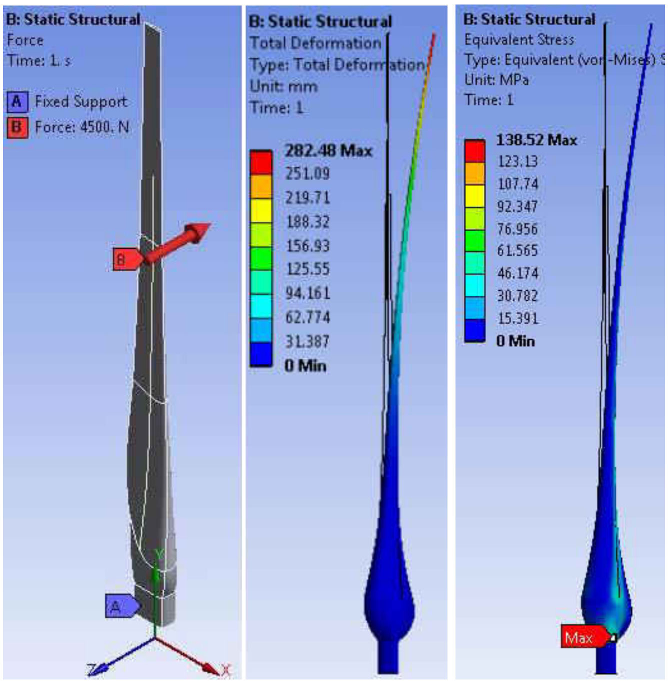

a. *b.* *c.*

Fig. 19. Flapwise bending: *a - axial loading, b – total deformation, c - equivalent stress*.

Along with the development of computer aided design (CAD) tools, design, analysis and manufacturing of wind turbine blades were made very cost effective and feasible. The following criteria have taken into account in the process of optimal blade design: minimize blade weight, does not exceed allowable stresses, minimize blade vibration and obtaining its modal frequency out of resonance. Blade mass and cost is mutually dependent and is related on the blade shell thickness. If the composite layer thickness for different blade section is at optimal level then we obtain the improvement of these parameters.
The load analysis of the blade consists of a 3D CAD model analyzed using the FE method (fig. 18). Regarding the dynamic behavior of the blade and the entire assembly of the wind turbine are imposed the following conditions: 1) the natural frequencies of the blade at 8 m/s wind speed must be above the ~2.5 Hz frequency of the turbine rotor (130 rpm) and 2) the natural frequency of the blade should be separated from the harmonic vibration of the tower (~1.16 Hz estimated first mod).
The blade was meshed entirely with 7539 layered shell elements and 7697 nodes in ANSYS Workbench. ANSYS Composite PrepPost (ACP) was used as a preprocessor for composite layups modeling as well as for post processing to check the stresses and the failure criteria that occur in the composite layers (Fig.18, *b*). To evaluate flapwise rigidity of the blade, this was constrained at the root end surface by fixing all six degrees of freedom and an axial force of 4.5 kN was applied on the blade surface as indicated in Fig. 19, *a*. The resultant deflection profile is illustrated in Fig. 19, *b*, from which it can be seen that the peak tip deflection is 282 mm (the distance from the blade tip to the tower is 480 mm) and the maximum compressive stress is 138 MPa, Fig. 19, *c*. To estimate the mode shapes and natural frequencies of the blade, a modal analysis was conducted in ANSYS Workbench. For a stopped rotor, the fundamental flapwise and edgewise vibrational modes occurred at frequencies of 7.5 and 15.23 Hz, respectively.

3. Conclusions

In conclusion, we state that micro hydropower plants ensure the transformation of 70...86 % of the flowing water potential energy into useful electrical energy transmitted to the hydrodynamic rotor. The basic advantages of micro-hydro power stations are as follows:

- small impact on the environment; it is not necessary to carry out civil constructions;
- the river does not change its natural course;
- the possibility to utilize local knowledge in order to produce floatable turbines;
- the possibility to mount a series of micro-hydro stations at small distances (approximately 30-50 m) because the influence of turbulence provoked by the adjacent installations can be excluded.

The value of the lift force of the blade segment fitted with groove was obtained approximately 6% lower than for the smooth blade segment. And drag force is decreasing with about 18% for blade segment fitted with groove.

References

[1] Bostan, Ion, Adrian Gheorghe, Valeriu Dulgheru, Ion Sobor, Viorel Bostan, and Anatol Sochirean. *Resilient Energy Systems. Renewables: Wind, Solar, Hydro*. Springer, VIII, 507p. 2013. ISBN 978-94-007-4188-1.
[2] Bostan, Viorel, Oleg Ciobanu, Valeriu Dulgheru, and Anatol Sochireanu (MD). BI 4235 C1 (MD), F03B3/12; F03B3/14; F03B7/00; F03B13/00; F03B13/18. “Hydraulic turbine” (“Turbină hidraulică”). Publ. 30.06.2013, BOPI no. 6/2013.
[3] Bostan, Ion, Valeriu Dulgheru, Viorel Bostan, Anatol Sochireanu, Oleg Ciobanu, Radu Ciobanu, and Ion Dicusară (MD). BI 3845 F1, MD, F03B13/00; F03B7/00; F03B13/18; F03B13/22; F03B 17/06. “Hydraulic station” (“Staţie hidraulică”). Publ. 28.02.2009, BOPI no. 2/2009.
[4] Bostan, Ion, Valeriu Dulgheru, Viorel Bostan, Anatol Sochireanu, Oleg Ciobanu, Radu Ciobanu, and Ion Dicusară (MD). BI 3104 G2, MD, F03B7/00; F16H1/00. “Hydraulic station” (“Staţie hidraulică”).

Publl. 31.07.2006, BOPI no. 7/2006.
[5] Bostan, Viorel. *Mathematical models in engineering: Contact problems; Modeling and numerical simulations in aero-hydrodynamics* / *Modele matematice în inginerie: Probleme de contact; Modelări și simulări numerice în aero-hidrodinamică*. Chișinău, BonsOffices, 2014, 470p.
[6] Bostan, Ion, Valeriu Dulgheru, Viorel Bostan, and Anatol Sochirean. *Conversion systems for renewable energies* / *Sisteme de conversie a energiilor regenerabile.* Chişinău, Techn. Univ. of Moldova, Tehnica-Info Publishing House, 2007, 665 p.

CONSIDERATIONS ON MONITORING THE STATE OF SOIL AND VEGETATION POLLUTION IN THE AFFECTED AREAS

Ancuța-Alexandra PETRE[1], Valentin VLĂDUȚ[1], Iulian VOICEA[1], Laurențiu VLĂDUȚOIU[1]

[1]INMA Bucharest, ancapetre28@gmail.com

Abstract: *Soil pollution by organic and inorganic contaminants has been recognized as an important issue in many industrial areas of the nations. In addition, naturally all occurring contaminants from radiological Earth sources and human and animal wastes (nutrients and pathogenic bacteria) impact soil and sediments.*
There is a wide range of types of soil contamination, and an equally large scale of methods and approaches to soil monitoring. This paper will present practical considerations such as how the data will be used, the data's required accuracy and precision, staff, and instrumentation available for the analysis also play a part in the selection of appropriate soil contamination monitoring using automated equipments.

Keywords*: Soil, pollution, vegetation*

1. Introduction

Soil pollution has enormously increased during the last decades due to the intensive use of biocides and fertilizers in agriculture, industrial activities, urban waste and atmospheric deposition. Its occurrence is related to the degree of industrialization and intensity of chemical usage. Soil pollution causes decrease in soil fertility, alteration of soil structure, disturbance of the balance between flora and fauna residing in the soil, contamination of the crops, and contamination of groundwater, constituting a threat for living organisms. [1]
The soil is the place where all pollutants, air powders, the toxic gases transformed by rain into the atmosphere are met, so that the soil is most exposed to the negative effects of these substances. The infiltration waters impregnate the soil with pollutants by training deep, polluted rivers infect flooded or irrigated surfaces, and almost all solid residues are stored by agglomeration or only discarded on the ground.
The soil can be polluted directly through waste spilds on urban or rural land, or from fertilizers and pesticides dumped on farmland and indirectly, by filing polluting agents initially ejected into the atmosphere, the water of the rains contaminated with pollutant agents "washed" from the contaminated atmosphere, the transport of pollutant agents by the wind from one place to another, the soil infiltration of water contaminated.
Soil pollution is closely linked to: atmospheric pollution, hydrosphere, due to the natural circulation of matter in the ecosystem. The irrational methods of soil administration have severely degraded its quality, caused its pollution and accelerated erosion. [2]
Nowadays, soil degradation includes a number of processes, ranging from soil erosion to soil contamination, which reduce the capability of soil to work as a base for vegetation roots.[3]
Environmental remediation and restoration focus on the development and implementation of strategies geared to reverse negative environmental impacts. Anthropogenic activities often perturb environments and severely limit their capacity for regeneration.
Recently, environmental monitoring has become even more critical as human populations increase, adding ever-increasing strains on the environment. There are numerous examples of deleterious environmental changes that result from population increases and concentrated human activities. [4]

2. Materials and methods

Based on the analysis of soil samples, statements regarding the soil quality, soil pollution, biological activity of the soil, the expected behavior of a soil and its suitability for a particular purpose are possible. Physical and chemical parameters can be determined based on the samples which give direct or indirect information on the specific question. The comparison of the parameters in various depths provides information on the soil stratification and also on the distribution of water and nutrients or pollutants in the soil, as well as the depth of anthropogenic influences. [5]

Typical aims are:
- Receiving information about soil structure / the soil stratification
- Information on nutrient and humus content of a soil
- Information on occurrence, frequency, and activity of soil organisms including pests
- pH-value determination of the soil
- Determination of the particle size distribution for the basic characterization of a soil
- Determination of parameters of the water and air balance (for example pore volume, hydraulic and pneumatic conductivity, retention curve)
- Determination of mechanical soil parameters to evaluate the stability of the soil (e.g. pressure sensitivity or shearing resistance)
- Chemical analysis for the detection of harmful and hazardous substances in soil

The possibilities for the analysis of soil samples are very diverse. Accordingly, diverse is the application range for soil sampling within the scientific and economical sector.
- Agriculture
- Forestry
- Soil science includes soil ecology
- Geology
- Hydrology
- Monitoring, evaluation and remediation of legacies of pollution
- Building sector [5]

Several approaches to soil contamination monitoring include chemical, geophysical, and biological techniques. Chemical techniques are used to measure specific organic, inorganic, or radioactive contaminants in the soil using instruments, such as a gas chromatograph, atomic absorption spectrometer, or mass spectrometer. Geophysical techniques examine changes in physical properties of the soil and the contaminants to address large areas of soil contamination. [6]

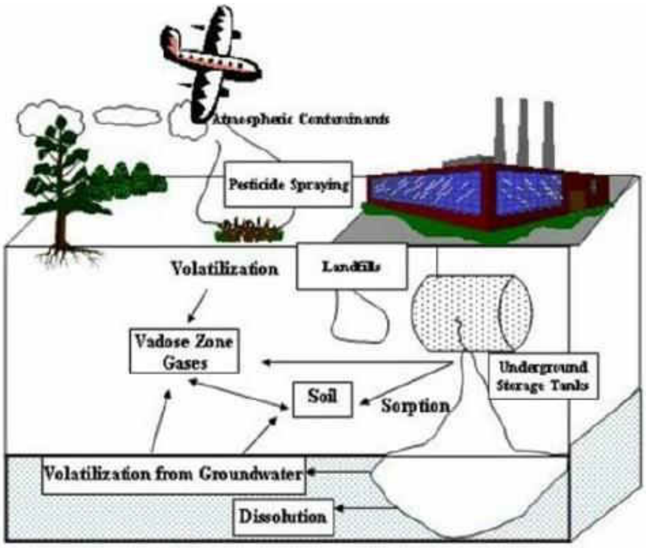

Fig. 1. Soil contamination comes from multiple sources and is impacted by processes such as sorption to soil particles and volatilization into the vadose zone

Soil can be become contaminated with a wide range of pollutants from various sources other than land disposal of waste. Contaminants may be applied directly to the soil, as is the case with pesticides. Alternatively, chemicals in the soils can occur as a result of air pollutants that fall out as wet or dry deposition and settle on aquatic or land surfaces. An example is shown in figure 1 is the contamination of aquatic sediments from the deposition of hydrophobic chemicals emitted from hazardous waste incinerators. These pollutants fall out of the air onto lakes and are eventually trapped on the aquatic sediments where they can reside for many years.[6]

Environmental monitoring using aptamer-based biosensors has grown attention due to unique advantages originated from aptamers which could specifically bind to the diverse target molecules from small molecules to bacteria shown in figure 2. By employing various sensing methodologies and platforms, application of aptasensors in real samples exhibited promising results. There are many challenges, however, that need to be overcome for commercial application. This paper provides the most recent updates on the application of aptasensors in real samples, including water and soil samples for various target molecules. Additionally, challenges yet to be addressed for practical applications of aptasensors have been discussed.[7]

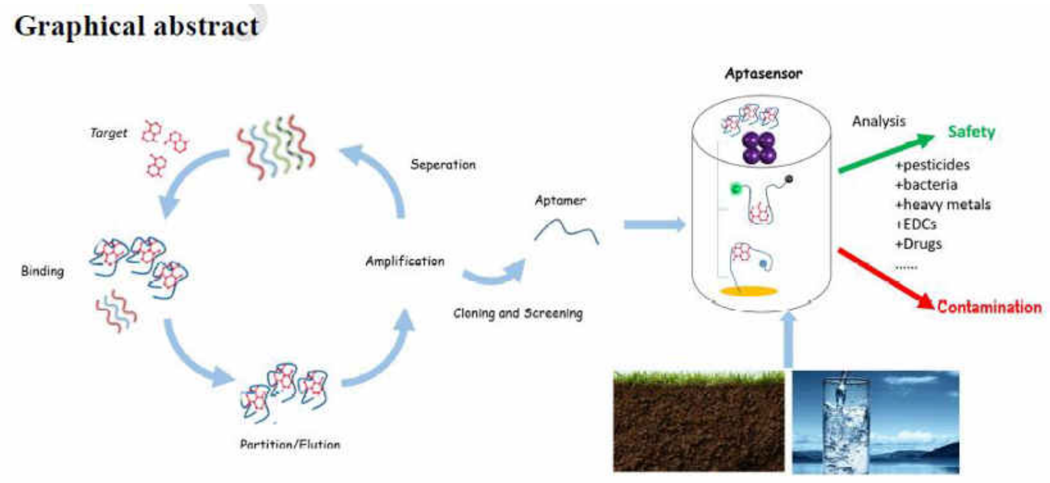

Fig. 2. Graphical abstract Aptamer-based environmental biosensors: from selection aptamer to detection samples

3. Results

The company ZigBee produces one device with the development and implementation of a grid of self-powered multi-functional probes (MFPz) for small-scale measurements of different soil properties, as being part of a wireless sensor network presented in figure 3. The measurement principle is based on the heat-pulse method for soil moisture and water flux measurements and in a Wenner array for soil electrical conductivity. To promote the deployment of these sensing devices across large areas, such as irrigation fields, the ZigBee standard has been adopted as a multi-hop, ad-hoc network enabler. The core of the MFPz device is a wireless microcontroller (with a built-in ZigBee stack) that builds upon an IEEE 802.15.4 radio device. A 7.2Ah NiHM battery that is charged by a solar panel powers the MFPz device. Experimental results have proofed the reliability of the MFPz, regarding power consumption, connectivity and data agreement with known soil samples, as a cost-effective solution for environment monitoring.[8]

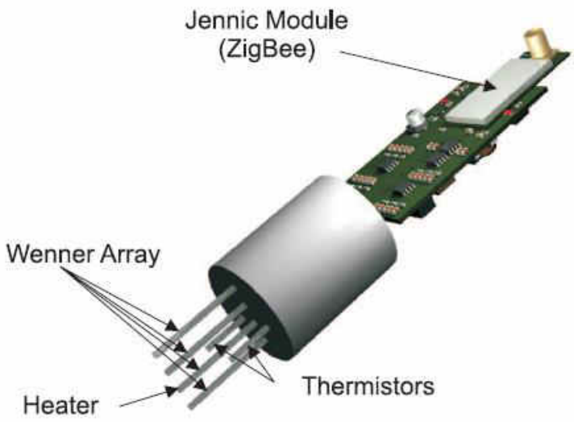

Fig. 3. The MFPz device: At bottom the probe with heater needle, thermistors needles, and Wenner array needles. In the upper part the electronic circuit with RF module (ZigBee)

The company Avigse presents the hydraulic sampling system represented in figure 4 that is designed to collect 0-6” and 6-24” soil samples. The system is powered by an electric over hydraulic power system. The full cycle time for the system is 10-12 seconds (down and up). This sampling system includes the 12-volt power system with control box and power cables, a 30” hydraulic cylinder attached to a channel iron presented in figure 5, 2 stainless steel probe bodies (one slotted and one solid), two quicktatch collars and three replaceable tips (5/8”, 3/4“ and wet tip), 2 heavy duty (Chromoly) probe bodies (one slotted and one solid), quicktatch collars and two replaceable tips (wet and dry tip). Spare parts and accessories included are 1 electric solenoid, 1 spare hydraulic solenoid and 1 control box along with a probe cleaning brush and handle shown in figure 6.

Fig. 4. Electric-hydraulic power system

Fig. 5. Hydraulic cylinder bolted to channel iron

Fig. 6. Spare parts and accessories – 1 electric solenoid, 1 hydraulic solenoid and 1 control box, 1 probe cleaning brush and handle

The inventors Keith W. Wendte and Brian T. Adams are invented the soil monitoring system which is provided with a sensing shank, and a first sensor coupled to a leading edge of the sensing shank. The first sensor is configured to output first signals indicative of a pressure exerted on the first sensor by soil as the sensing shank is driven through the soil along a direction of travel. The soil monitoring system also includes a frame forming a channel oriented in a substantially vertical direction relative to a surface of the soil, and a carrier coupled to the sensing shank and disposed within the channel. The soil monitoring system further includes an actuator extending between the frame and the carrier. The actuator is configured to linearly drive the carrier in a reciprocating motion to vary a penetration depth of the sensing shank within the soil.[9]

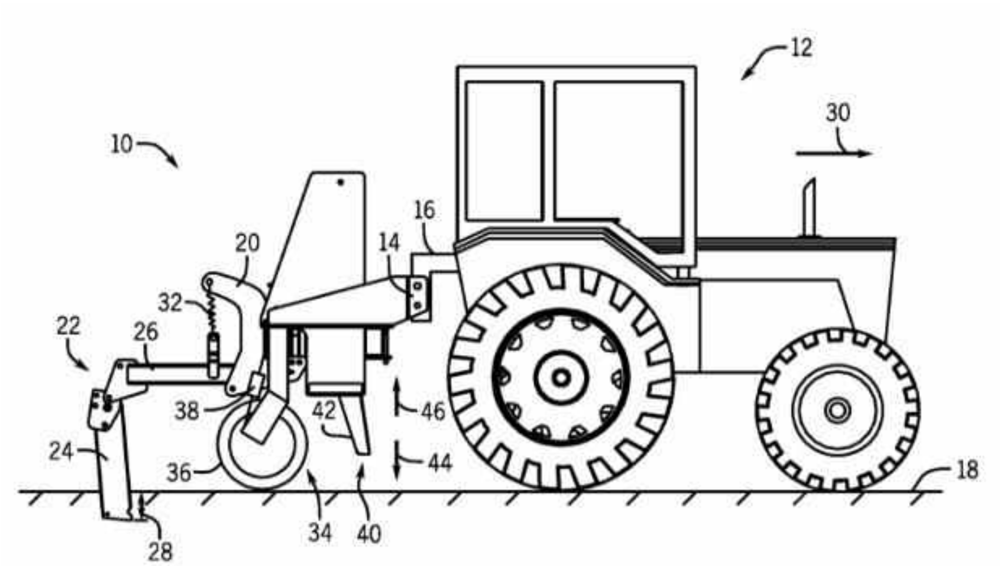

Fig. 7. A side view of an exemplary agricultural implement system, including a tow vehicle and an agricultural implement

Gilson Company produces hydrometer analysis of soil which is widely used in testing distribution of soil particle sizes. Testing is performed with specific products and required sedimentation methods to determine silt and clay fractions. Basic equipment needed for hydrometer analysis in conformance with ASTM D7928, ASTM D422 and AASHTO T 88 standards include Stirring Apparatus, Soil Hydrometers, Hydrometer Sedimentation Cylinder, Sodium Hexametaphosphate, and a Constant Temperature Bath. Soil specimens are mixed in a solution of water and sodium hexametaphosphate.

- **Sodium Hexametaphosphate** is a dry powder dispersion agent used in mixing soil sample solutions.
- **Dispersion Cup** for Soil Dispersion Mixer with 1L capacity to hold soil samples for testing.
- **Soil Dispersion Mixer** thoroughly mixes soil samples with mixing blade.
- **Sedimentation Cylinder**, also called a hydrometer jar, is used with the soil hydrometers for testing suspended solids.
- **Soil Hydrometers** measure suspended solids during testing. Select from models with range of 0.995— 1.038 or -5—+60 g/L.
- **Constant Temperature Bath** maintains uniform temperature in hydrometer testing. [10]

Fig. 8. Hydrometer analysis of soil

The ACE company EmS produces fully automatic Oedometer soil consolidation testing machine that comes loaded with the new environmentally Electro-mechanical Servoactuation (EmS) technology. Silent, compact and highly performing, the ACE EmS testing system can be run with ingenious software that can connect up to 60 units with just one PC, enabling to expand laboratory gradually and seamlessly. The Oedometric test determines the rate and magnitude of soil consolidation when restrained laterally and loaded axially. The ACE EmS can complete the whole test in fully automatic mode by selecting the load (stress), offering a practical and accurate way to obtain reliable results without any need for manual intervention, reducing the risk of human error.

- Can pilot up to 60 ACE EmS units from one single PC with user able to select single or multiple unit batches.
- Once the software is installed and linked to the first ACE EmS, it is easy to add more units by enabling the associated LAN communication (IP address) without complications or costs.
- Calibrations of displacement transducers and load cells are stored as txt file and easy to recall, up to 10 calibration points can be recorded for each channel.[11]

Fig. 9. Oedometer soil testing machine

4. Conclusions

Soil analyses lead to more informed fertiliser decisions, reducing risks and increasing farm profitability in the long term and reveal the amount of plant-available macro-nutrients in the soil and where soil nutrients are in the soil profile, which nutrients could be yield limited.

Acknowledgments

This work was supported by a grant of the Romanian Research and Innovation Ministry, through Programme 1 – Development of the national research-development system, subprogramme 1.2 – Institutional performance – Projects for financing excellence in RDI, contract no. 16PFE.

References

[1] Lionetto, Maria Giulia, Antonio Calisi, and Trifone Schettino. *Soil Health and Land Use Management.* Chapter 16 *"*Earthworm Biomarkers as Tools for Soil Pollution Assessment." London, IntechOpen, 2012*.*
[2] Munteanu, Constantin, Mioara Dumitrascu, and Alexandru Iliuță. "Ecology and Environmental Protection" / "Ecologie şi protecția calitãții mediului" (Course). Bucharest, Balneară (Resort) Publishing House, 2011.
[3] Gholizadeh, Asa, Mohammadmehdi Saberioon, Eyal Ben-Dor, and Luboš Borůvka. "Monitoring of selected soil contaminants using proximal and remote sensing techniques: Background, state-of-the-art and future perspectives." *Critical Reviews in Environmental Science and Technology (CRIT REV ENV SCI TEC)* 48, no. 3 (2018): 243-278.
[4] Aritola, J.F., I.L. Pepper, and M.L. Brusseau. *Environmental Monitoring and Characterization*. San Diego, Elsevier Academic Press, 2004.
[5] http://www.ugt-online.de/en/products/soil-science/soil-sampling/ueber-bodenproben/.
[6] Aelion, C.M. *Environmental Monitoring* – Vol. II – "Soil Contamination Monitoring". Columbia, University of South Carolina, 2009.
[7] Kim, Sang Hoon, Tran Thi Thanh Thoa, and Man Bock Gu. "Aptasensors for Environmental Monitoring of Contaminants in Water and Soil." *Current Opinion in Environmental Science & Health* 10 (2019): 9-21.
[8] Valente, António, Raul Morais, Carlos Serôdio*,* Pedro Mestre, Salviano Pinto, and Manuel Cabral. "A ZigBee Sensor Element for Distributed Monitoring of Soil Parameters in Environmental Monitoring." Paper presented at the 6th Annual IEEE Conference on Sensors IEEE SENSORS 2007 Conference, Atlanta, Georgia, USA, October 28 - 31, 2007.
[9] https://patents.google.com/patent/US8827001B2/en.
[10] https://www.globalgilson.com/soil-testing-equipment.
[11] https://www.controls-group.com/eng/soil-mechanics-testing-equipment/automatic-computerized-oedometer-ace-ems.php.

ISSN 1454 - 8003
Proceedings of 2019 International Conference on Hydraulics and Pneumatics - HERVEX
November 13-15, Băile Govora, Romania

ARGUMENTATION OF THE GEOMETRIC PARAMETERS OF THE WIND ROTOR WITH VERTICAL AXIS

Valeriu DULGHERU[1, 2], Liliana DUMITRESCU[2], Corneliu CRISTESCU[2], Eugeniu GUȚIU[3]

[1]Technical University of Moldova, valeriu.dulgheru@bpm.utm.md

[2]Hydraulics and Pneumatics Research Institute INOE 2000-IHP Bucharest, lilianad.ihp@fluidas.ro

[3]Techical University of Cluj-Napoca

Abstract: *Wind energy currently are the most used, cheap and clean renewable energy sources. The variety of existing wind energy conversion systems can be grouped into two distinct classes: horizontal (HAWTs) and vertical (VAWTs) wind turbines. The main goal of this paper consists in the mathematical modeling of the aerodynamic profiles of VAWTs blades. This paper describes the steps of elaboration of calculation model for dynamic simulation of a small vertical axis wind turbine rotor. The calculation model is based on the finite element analysis ANSYS CFX software. The CFD model is used to determine the performance of the wind turbine rotor. A new design and functional concept of VAWTs was proposed, patented and elaborated.*

Keywords*: Aerodynamic profile, wind turbine with vertical axis (VAWT)*

1. Introduction

One of the greatest challenges of the 21st century is to ensure the access of every citizen of the Planet to sustainable, non-polluting energy. Today, we speak of a global energy policy and a concerted strategy to reduce harmful emissions into the atmosphere. As climate change is a problem of global concern nowadays, renewable energy is considered an important link from the chain of solutions that are to be applied for tackling this problem. Wind energies are the oldest form of renewable energy used by man and has become the most currently used renewable energy sources, being also one of the best, cheap and clean energy sources.
Wind is environmentally friendly but today they are not able to meet these ever-growing needs. The variety of existing wind energy conversion systems can be grouped into two distinct classes: horizontal (HAVT) and vertical (VAVT) wind turbines. HAWTs have been heavily researched and developed until high efficiency has been achieved for the largest ones [1]. Compared to HAVT, vertical axis wind turbines (VAVT) have a number of advantages: they do not require a wind direction orientation mechanism; lightly servicing the generator and multiplier (if applicable) located at the bottom of the turbine; reduced (comparable to HAVT) turbine tower demand; ensures relatively high conversion efficiency in turbulent areas of air currents (urban and suburban areas).
An important tool in engineering that generally lead to cost and time savings during product development are simulations [2]. Finite element analysis serves as a base for the present work. Besides choosing the appropriate mathematical model behind physics of the simulated system, it is important to choose the right shape and size of the finite elements. It is also important that the elements are well adapted for the specific system to be analyzed.
A modern research has the following structure (fig. 1). IHP is equipped with modern Workstations

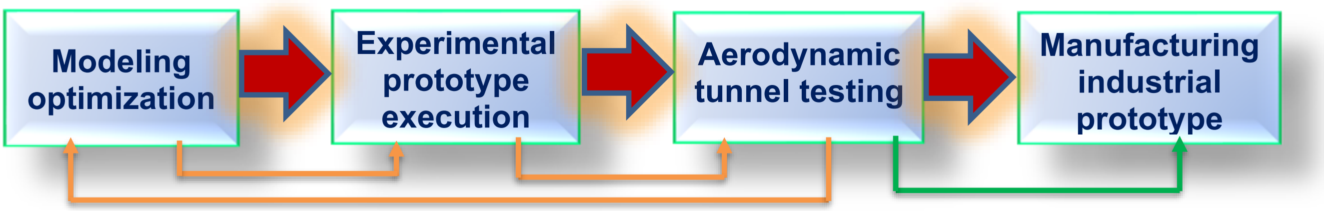

Fig. 1. The structure of modern research

and performance simulation software ANSYS; 3D printer (fig. 2); human potential.

This work presents a CFD model created for determining the performances of a vertical axis wind turbine. The CFD model is made using ANSYS CFX software. The CFD model is used to determine the power curve of a 0.5 kW modeled wind turbine. For this power there are wind turbines developed by several companies. Comparison of the simulated wind turbine power output with real wind turbines power output is considered as validation of the CFD model.

The stages of CFD simulation of the wind and hydraulic rotors are shown in ANSYS Workbench Project schematic (fig. 3).

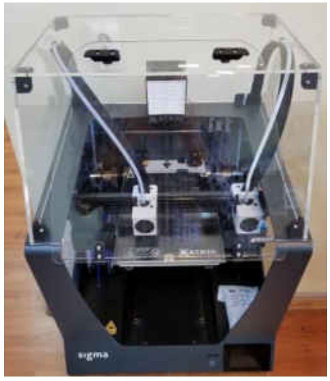

Fig. 2. 3D printers for manufacturing

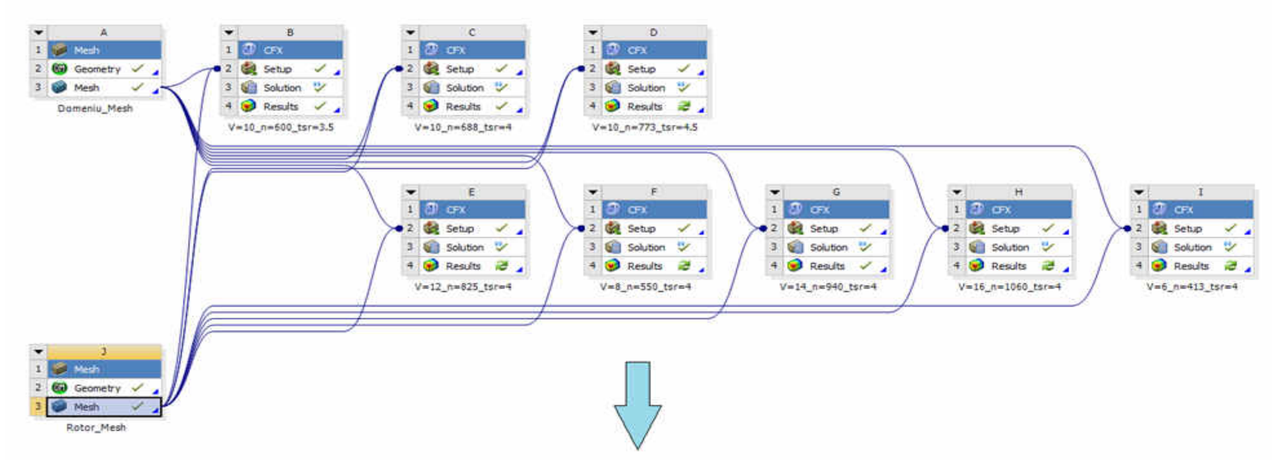

Fig. 3. ANSYS Workbench Project schematic

2. Rotor's geometry and fluid domain modeling and meshing

The general formula for calculating the power output of a wind turbine is expressed as follows:

$$P = \frac{1}{2} C_P \rho A V^3 \qquad (1)$$

where *P* is the output power of the wind turbine;
V – the wind speed before the interaction with the turbine;
ρ – the air density;
A – the swept area of the turbine;
C_P – the performance coefficient of the turbine.

C_P ranges from 0 to 1 with a theoretical maximum of 0.593 called Betz limit. Big modern HAWTs can reach a value of about 0.5 whereas VAWTs a maximum of 0.4. Nevertheless, professor Ion Paraschivoiu from Ecole Polytechnique de Montreal unknown specialist in the field of VAVTs, writes that for VAWTs a maximum of 0.64 can be theoretically reached [3]. The chord of the turbine blade is 0.11m, though more chord lengths were analyzed. The helical angle of the blades is 60°. The rotor geometry, designed using SolidWorks (fig. 4), was then imported into the ANSYS DesignModeler software. The

Fig. 4. The rotor geometry

dimensions of the computational fluid domain were chosen taking into account the recommendations of [4] so that the boundaries of the field do not influence the free flow of the air. The simulated fluid domain was divided into two subdomains: the Stator (static) subdomain and the Rotor subdomain inside of it (of cylindrical form, which rotates around its axis). Figure 5,*a* shows the considered fluid domains. The mesh used for finite element analysis of the rotor fluid domain (fig. 5,*b*) and of the blade (fig. 5,*c*) was generated using the ANSYS Meshing Workbench.

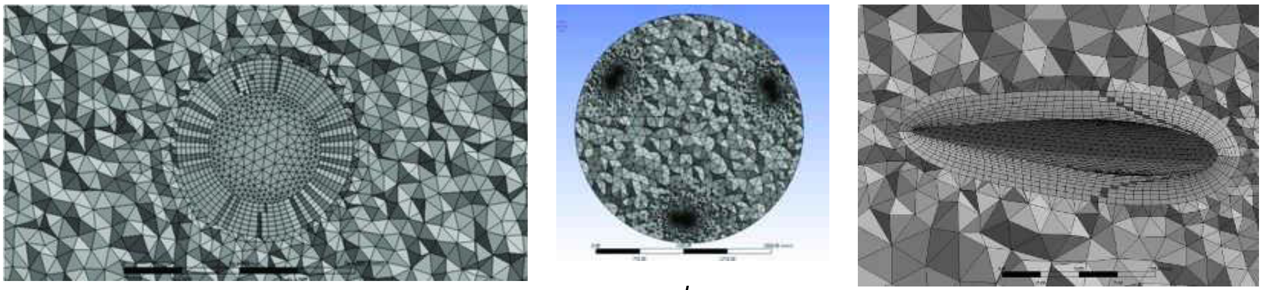

a. *b.* *c.*

Fig. 5. Mesh used for finite element analysis

The basic dimensions of the mesh are as follow: the minimal size of the inflation around the blade = 0.5 mm and the maximum size of the side of one face = 110 mm. The transition from the fine-meshed areas to the gross meshed ones was done by specifying the Growth Rate = 1.15 expansion factor. The maximum variation of the characteristic dimensions of two adjacent elements is not bigger than 4%. The entire domain was meshed into approx. 2 800 000 finite elements.
Very important are the effects formed on the blades' surfaces where it is formed the lift and drag, also the boundary layer separation occurs and other important effects take place. The boundary layer forms, rectangular finite elements have been generated by expanding them from the surface of the blade outwards. This was done using Inflation Layer technique around blades' surfaces: number of layers = 10, the Growth Rate = 1.15 (relative thickness between two adjacent layers), and Growth Rate Type = Geometric. Figure 5, *c* shows the mesh details around the blade.
In order to verify the conversion efficiency of the turbine, several modes have been simulated. There were considered four different airfoils (NACA 0021, NACA 0018, NACA 0015, E168) with different parameters. Each chord length is simulated under different tip speed ratios. The wind speed considered for simulations is 12 m/s.
Surfaces of the Stator fluid domain (fig. 6) are subjected to Walls boundary conditions with the free-slip specification that simulates a zero- adhesion virtual wall. Blades surfaces are subject to Walls boundary conditions with no slip specification which does not allow mass or energy transfer. The surfaces at the intersection of the two Stator and Rotor subdomains (fig. 6) are interface surfaces of the two subdomains through the GGI method. At this stage more attention is required to certain details such as the direction of rotation of the rotor and wind direction, which can be changed with the (-) sign.
The simulations were carried out and the results are presented in figures 6-8. As a result of the multicriteria simulations performed, the distribution of air flow velocities in the middle area of the rotor (CFX–Post 12.1) was established (fig. 7,a). Also, the degree of turbulence of the air currents developed by the blades in the middle area of the rotor was established (fig. 7,a).
Turbulence developed (CFX–Post 12.1). Distribution of pressure on the rotor blades and 3-D visualization of the flow lines for the case of the wind speed of 12 m/s are presented in Figure 8 and 9,*a* (CFX – Post 12.1). The analysis of the obtained distribution of pressure and the flow lines allows the optimization of the blade's geometric parameters and their angle of inclination. The interaction of the blades with the air flow lines generate lift forces that actuate the rotor in rotational motion (fig. 9,*b*). The analysis of the diagram shows that the intensity of the power lines increases towards the middle of the turbine.
Due to the fact that the preliminary results of the numerical analysis of the rotor performance are

better for NACA 0018 airfoil (fig. 10), this airfoil has been selected for subsequent simulations. The solving of discretized equations was performed in parallel using all 16 logical cores. The goal is to obtain 0.4 – 0.5 kW of power at a wind speed of 12 m/s. First of all, optimal airfoil chord length was determined. The optimal chord length for this rotor is 0.11 m.

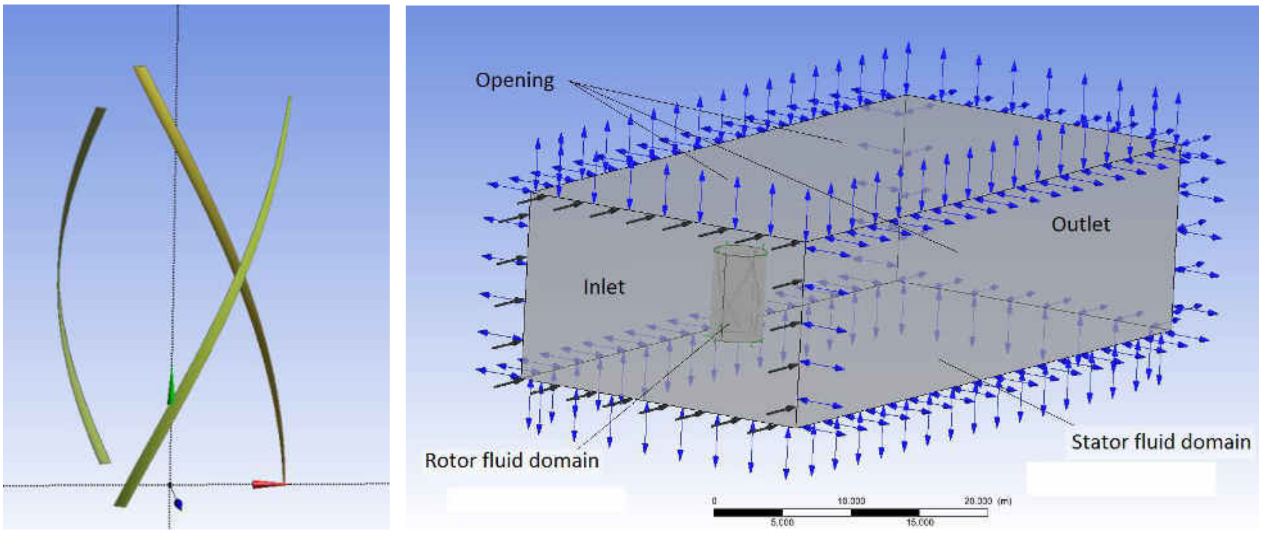

a. *b.*

Fig. 6. Rotor geometrical model (a) and fluid domains (rotor and stator) (b).

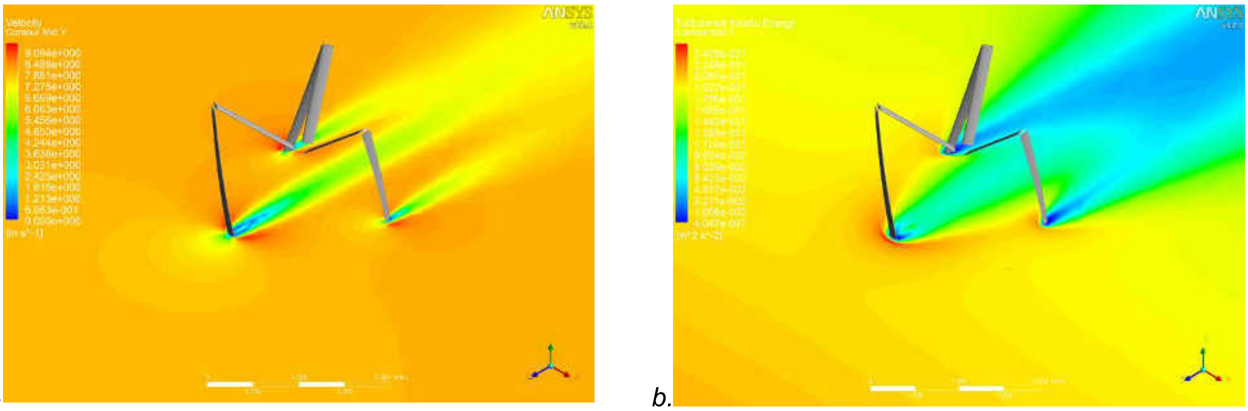

a. *b.*

Fig. 7. Distribution of air flow velocities (a) and turbulence (b) developed by the blades in the middle area of the rotor (CFX–Post 12.1)

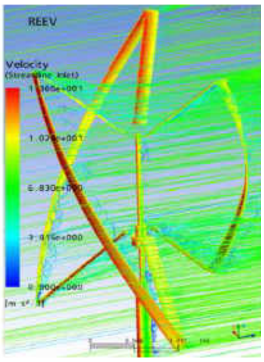

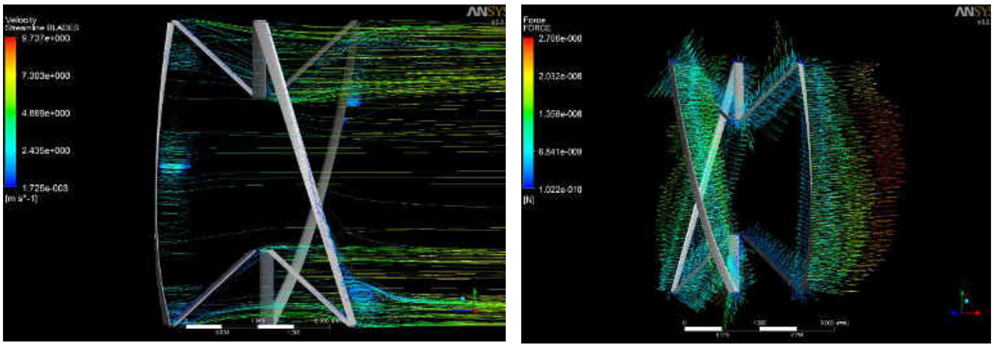

a. *b.*

Fig. 8. Distribution of pressure and the flow lines for wind speed of 12 m/s

Fig. 9. Air lines flowing through the rotor (a) and the forces acting on the rotor (b) (CFX – Post 12.1)

The next stage was the design and manufacture by additive technologies (3D printing) of a blade segment with aerodynamic profile NACA 0018 and its testing at different wind speeds in the aerodynamic tunnel GUNT 170 from the Aerodynamics Laboratory of the Technical University of Moldova. The tests were performed for different wind speeds and different angles of attack, the ratio between the lift and drag forces (F_L/F_D) being determined. The results of the testing are synthetized in the figure 11. It can be noticed from the figure that this profile NACA0018 provides an optimal *Fl/Fd = 5* ratio practically constant for the values of the angle of attack *8 - 16°* at the wind speeds V=10-24 m/s.

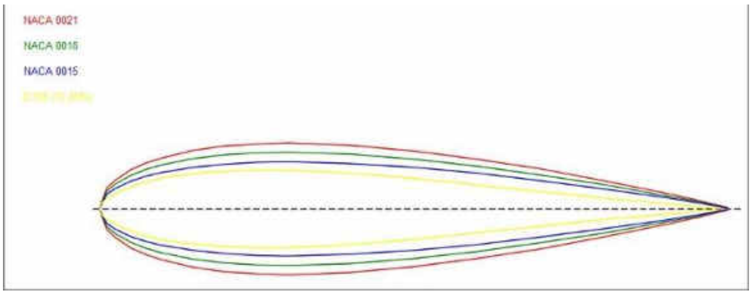

Fig. 10. Comparing airfoils.

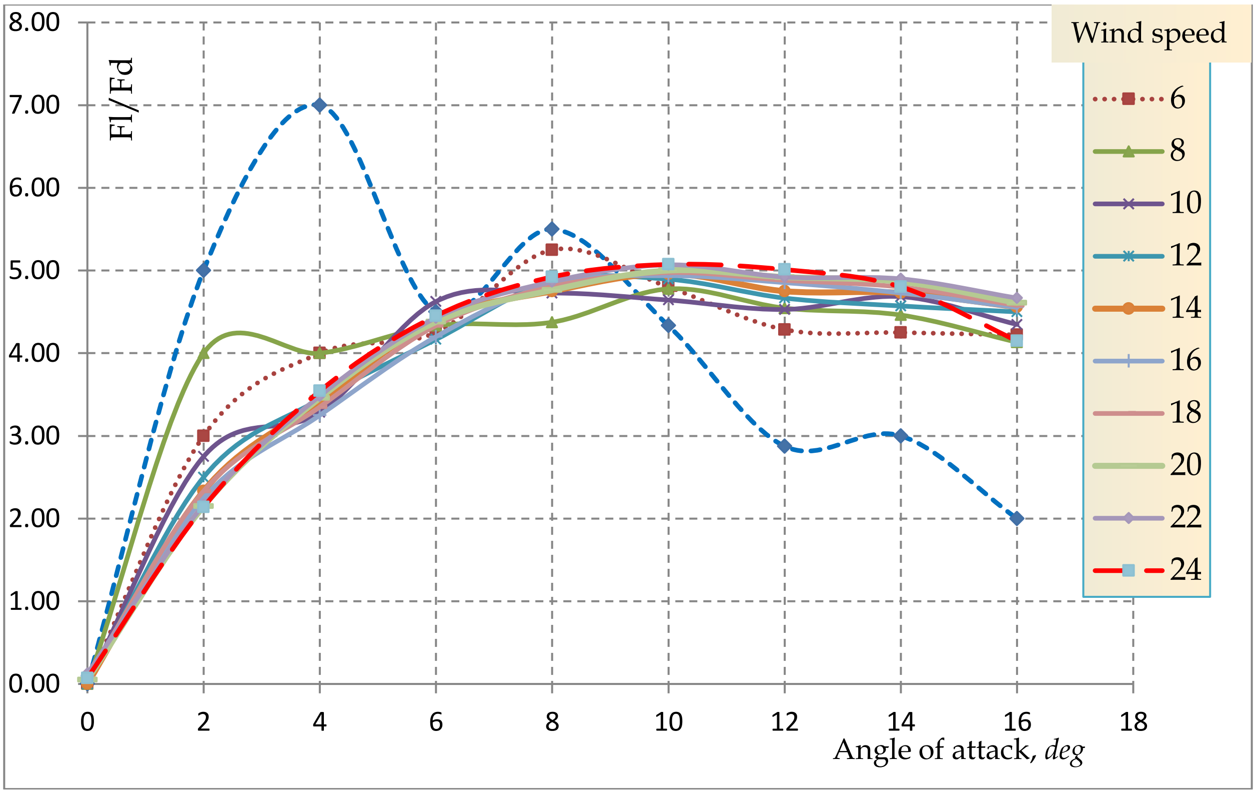

Fig. 11. Blade segment performance determined in the wind tunnel

3. Elaboration of the hybrid wind rotor with vertical axis

Based on the results of the multicriteria simulations and experimental tests performed in the aerodynamic tunnel, the optimum aerodynamic profile NACA 0018 was chosen for this rotor and the attack angle of 12°. These parameters were taken as the basis for designing the experimental prototype of the vertical axis wind turbine (fig. 4). The helical blades (the helicoidal angle - 18°) were manufactured by additive technologies in the Composite Materials Laboratory from Faculty of Machine Construction, Technical University of Cluj-Napoca. To increase the efficiency of conversion of the wind turbine with vertical axis at low wind speeds, the Darrieus rotor was supplemented with a Savonius rotor, which has the starter function. The experimental prototype of the vertical-axis hybrid wind turbine is shown on Figure 12.

Fig. 12. Experimental prototype of the vertical-axis hybrid wind turbine

Also, the stand of natural tests, the program of tests and the necessary equipment for the measurement and processing of the data were developed. The experimental prototype is to be tested in winter conditions with better wind energy potential. Based on the scientific results that will be obtained, the industrial prototype of the hybrid vertical-axis wind turbine will be designed.

4. Conclusions

1. The CFD simulation is applied on the downscaled wind rotor in order to determine the aerodynamic performances.
2. It can be noticed that profile NACA0018 provides an optimal *Fl/Fd = 5* ratio practically constant for the values of the angle of attack 8 - 16^o at the wind speeds V=10-24 m/s.
3. By experimental research there were determined the performances of the downscaled blade segment based on NACA 0018 airfoil in terms of Lift over Drag forces for different wind speeds and for different angles of attack.
4. The technical documentation of the downscaled wind rotor and rotor's stand was realized.
5. Experimental research on the built downscaled wind rotor is to be carried out in the real conditions in order to determine the aerodynamic performances. The results are to be compared with the ones obtained by CFD simulation using ANSYS CFX in order to validate the CFD model used for simulating the wind rotor.

Acknowledgments

This paper has been funded by the Romanian Ministry of Research and Innovation under Programme I - Development of national R&D system, Subprogramme 1.2 – Institutional performance – Projects financing excellence in R&D+I, Financial Agreement no. 19PFE/17.10.2018, while the scientific results have been obtained in the framework of a project co-financed by the European Union through the European Regional Development Fund, under Competitiveness Operational Programme 2014-2020, Priority Axis 1: Research, technological development and innovation (RD&I) to support economic competitiveness and business development, Action 1.1.4 - Attracting high-level personnel from abroad in order to enhance the RD capacity, project title: ESTABLISHING A HIGH LEVEL PROFICIENCY NUCLEUS IN THE FIELD OF INCREASING RENEWABLE ENERGY CONVERSION EFFICIENCY AND ENERGY INDEPENDENCE BY USING COMBINED RESOURCES, project acronym: CONVENER, Financial agreement no. 37/02.09.2016.

References

[1] Hau, E. *Wind turbines, Fundamentals, Technologies, Application, Economics*. 2nd edition. New York, Springer, 2006.

[2] Bostan, Viorel. *Mathematical models in engineering: Contact problems; Modeling and numerical simulations in aero-hydrodynamics / Modele matematice în inginerie: Probleme de contact; Modelări și simulări numerice în aero-hidrodinamică*. Chișinău, BonsOffices, 2014, 470p.

[3] Paraschivoiu, Ion. *Wind turbine design with emphasis on Darrieus concept*. Montreal, Ecole Polytechnique de Montréal, 2002.

[4] Mohamed, M.H., A.M. Ali, and A.A. Hafiz. “CFD analysis for H-rotor Darrieus turbine as a low speed wind energy converter.” *Engineering Science and Technology, an International Journal* 18, no. 1 (March 2015): 1-13.

[5] Bostan, Ion, Valeriu Dulgheru, Viorel Bostan, and Rodion Ciupercă. *Anthology of Inventions: renewable energy conversion systems: theoretical foundations, constructive concepts, technological aspects, descriptions of inventions / Antologia invenţiilor. Sisteme de conversie a energiilor regenerabile: fundamente teoretice, concepte constructive, aspecte tehnologice, descrieri de invenţii*. Vol. 3. Chișinău, Bons Offices, 2009, 432p. ISBN: ISBN 978-995-63-076-4.

[6] Bostan, Ion, Ion Vișa, Valeriu Dulgheru, Viorel Bostan, and Rodion Ciupercă. “Combined Vertical Axis Wind Turbine” / “Turbină de vânt combinată cu ax vertical”. Patent no. 127909 (RO). Publ.: 30.12.2012.

[7] Dulgheru, Valeriu, Cătălin Dumitrescu, and Liliana Dumitrescu. "Hybrid wind - solar heating system for domestic water” / “Sistem hibrid eolian – solar de încălzire a apei menajere”. Patent application no. A/00579. 10.08.2018.

ISSN 1454 - 8003
Proceedings of 2019 International Conference on Hydraulics and Pneumatics - HERVEX
November 13-15, Băile Govora, Romania

CONSIDERATIONS ON THE HYDRAULIC INSTALLATION OF THE EQUIPMENT FOR HARVESTING GREEN HEMP STALKS

Gabriel BOGDANOF[1], Anişoara PĂUN[1], Carmen BRĂCĂCESCU[1], Gheorghe STROESCU[1]

[1] National Institute for Research-Development of Machines and Installations Designed for Agriculture and Food Industry INMA Bucharest, Romania, gbogdanof@gmail.com; ani_paun@yahoo.com; carmenbraca@yahoo.com; gigistroescu@gmail.com

Abstract: *Considering that raw materials that meet the needs of the different areas of the economy with the lowest costs are sought, the reactivation of the hemp culture in Romania must be taken into consideration as well, because hemp (Cannabis Sativa L. - industrial hemp) is the industrial plant most widely used in the industry, and from this plant everything is used. The products obtained from hemp are of a great variety, from the common rope to the medicinal or cosmetic substances, textiles, automotive or construction materials. The fibres content in the stalks have a number of properties that are particularly valuable as (traction, torsion, friction, rot) resistance, extensibility (elastic and plastic), spinning capacity. In this paper we introduce an experimental model of towed technical equipment for harvesting green hemp stalks with hydraulic drive, designed, manufactured and tested by the specialists from INMA Bucharest. The paper presents the constructive-functional scheme, the functional description and the technical and functional characteristics of the Equipment for harvesting green hemp stalks ERCV-0. The ERCV-0 equipment is provided with a hydraulic installation with which the cutting devices, consisting of two knives placed at different heights and offset horizontally are operated, with the possibility of folding during transport. This equipment performs sequential harvesting of hemp stalks leaving them organised on the ground and it is intended for small and medium-sized farms, as required by many farmers who grow industrial hemp and they want the further processing of the stalks.*

Keywords: *Green hemp stalks, harvesting, hydraulic installation*

1. Introduction

Hemp (Canabis Sativa L. - industrial hemp) is the industrial plant most widely used in the industry. The products obtained from hemp are of a great variety, from the common rope to the medicinal or cosmetic substances, textiles, automotive or construction materials.

Considering that raw materials that meet the needs of the different areas of the economy with the lowest costs are sought, the reactivation of the hemp culture in Romania must be taken into consideration as well, because from this plant everything is used. Also, hemp is an unpretentious plant because, apart from the fact that it wants a neutral pH and soils without excess moisture, no maintenance work should be done and no extra care should be given, and the costs per hectare are below the costs of other well-known crops such as rape or wheat [1, 2, 3].

The fibre content in the stalks is influenced by the variety, by the technological and pedoclimatic conditions. Industrial hemp fibres have a number of properties that are particularly valuable as (traction, torsion, friction, rot) resistance, extensibility (elastic and plastic), spinning capacity [4, 5].

As demands for fibre appeared on the hemp market, farmers and researchers from research centres in our country want to make machines that allow them to harvest and process the stalks while green. Also, it is expected that in Romania the areas cultivated with hemp will grow in the next years, gradually becoming a basic culture also through the development of an adequate processing industry.

In this paper we introduce an experimental model of towed technical equipment for harvesting green hemp stalks with hydraulic drive, designed, manufactured and tested by the specialists from INMA Bucharest.

2.Material and methods

The hemp stalks, the component part that constitutes the object of the harvesting operation, is grassy at the beginning of the vegetation, green in colour, covered with rough hairs; at maturity, it is lignified and reaches heights of 1-7 m (depending on the origin, crop area and pedoclimatic conditions of the year), it has 5-25 internodes (depending on the origin), with the base diameter of 0.5-6 cm and is not branched in fibre crops and weakly branched in seed crops (depending on crop form, variety and nutrition space).
The main characteristics of hemp stalks are: length, thickness, colour, resistance to diseases and pests' attack, resistance to mechanical injuries (hail, broken or crushed stalks), breaking load. Knowing the importance of each characteristic allows predicting, to a large extent, according to the outer appearance of the stalks, their behaviour in the technological process of primary processing, as well as the probable results of the processing, both quantitatively and qualitatively. The quantity and especially the resistance of the fibres can be appreciated by the mechanical characteristics of the stalks, respectively by their resistance to breaking [6]. In cases of serious injuries (rotting, retting in the field, severe disease attack), the stalks have a low resistance, they can be easily broken, even by hand. The fibre hemp is harvested at technical maturity, when the male plants shake their last pollen traces, and the stalks have a greenish-yellow colour and the leaves fallen to the ground.
The industrial hemp harvesting is done by cutting both mature male plants and female plants that are in the vegetation phase. The production of stalks is on average 5-6 t/ha, but can reach up to 10-12 t/ha dry stalks. The amount of fibres obtained per hectare, after processing the stalks, represents 16-30% of the stalk production. Usually, the stalks are cut in mid-August and left lying on the ground for 4 to 6 weeks, depending on the weather.
INMA Bucharest comes to the aid of the farmers who cultivate industrial hemp, by designing and realizing the Equipment for harvesting green hemp stalks ERCV-0, of trailed type (figure 1: a, b).

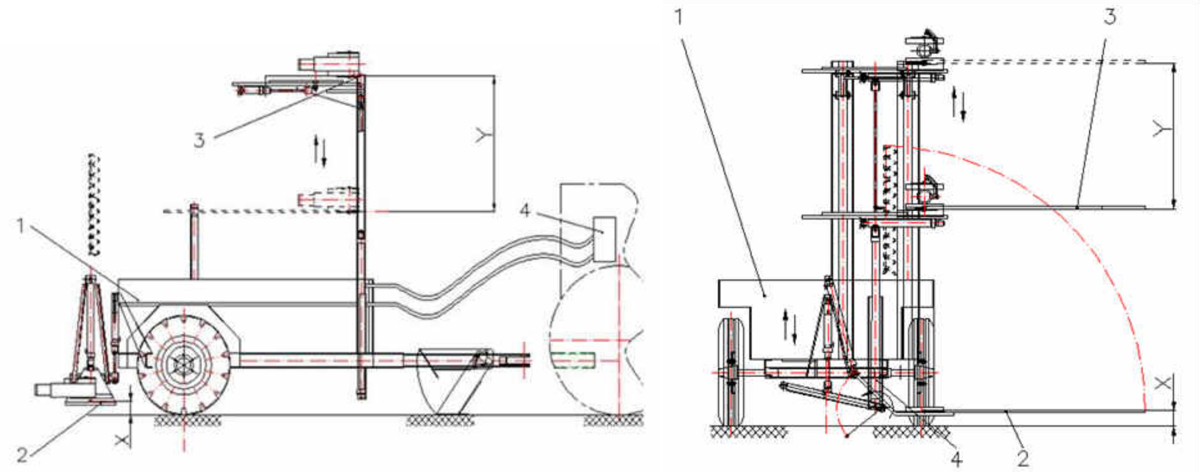

a) b)

Fig. 1. Equipment for harvesting green hemp stalks ERCV-0- experimental model [7]
a) –lateral view; b)–rear view
1-assembled mobile platform; 2,3 knives; 4-hydraulic installation

The assembled mobile platform (pos. 1), is a metallic construction, towed semi-trailer type, on which are mounted 2 movable arms, components that support the two sequential cutting knives and the hydraulic drive system. When moving, the platform is supported by two wheels, and in the stationary position, a support leg on the platform is also used. The platform is coupled to the tractor by means of a tow hitch.
The knife 1 (pos. 2), is mounted on the back of the platform and cuts the stalks at a height of 100 mm from the ground in the working position. In the transport position, the knife folds and rises vertically by using two hydraulic cylinders (see figure 2). The knife 1 is a subassembly that constitutes

the cutting machine and is of the double-knife type, in which the role of the fingers and the counter-cutting plates is fulfilled by the second knife which moves at an equal speed and in the opposite direction with the first.

Knife 2 (pos. 3), is mounted horizontally offset to the first, in the front of the platform and performs cutting of hemp plants' inflorescence. Since the height of the hemp varieties' inflorescences varies, this knife has the possibility to adjust the cutting height in a wide range of values with the help of a vertical cylinder. The second hydraulic cylinder works at the ends of the travel in the working or transport position of the equipment. In transport this knife can be folded 90 degrees backwards on a support, with the help of the hydraulic system (fig.1, pos. 4). This knife is a double-knife cutting machine like the first knife. Each knife is moved by a hydraulic motor through a distributor, operated from the hydraulic system of the equipment (see figure 2).

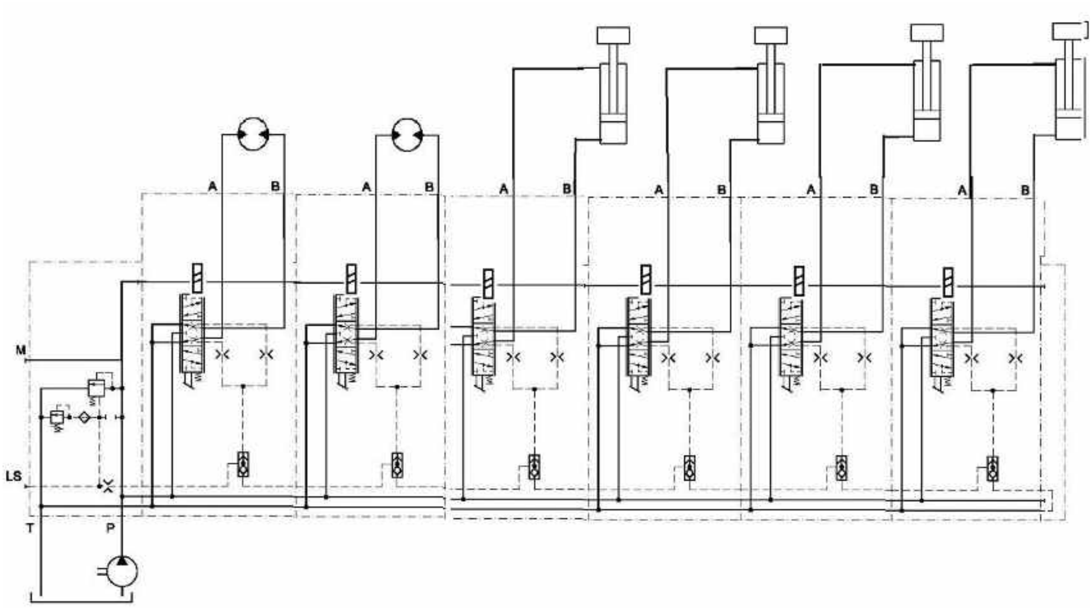

Fig. 2. Hydraulic scheme of the Equipment for harvesting green hemp stalks ERCV-0

The hydraulic system (fig. 1, pos. 4), ensures the independent functioning of the two knives in operation and comprises: a hydraulic motor driven by the tractor, a hydraulic pump, a reservoir for hydraulic oil and connecting elements. The two knives are operated from the tractor cabin.

3. Results

Table 1: General technical characteristics of ERCV-0

Characteristic	Value
Machine type	trailed
Energy source	65 HP tractor
Type of cutting machine	Double-knife
Cutting height: -rear cutting machine -front cutting machine	 100 mm 1500-2500 mm

During the work, the following forces action the cutting machine's knife: the resistance to cutting the plants, the force of inertia and the friction force that appears between the knife and the fixed parts of the machine.

Applying the principle of work conservation, results the resistance R_t, [N] to plant cutting on space x_t, as formula (1) [8]:

$$R_t = \frac{\mathrm{Bh_a\,L_t}}{\mathrm{x_t}} \quad 1)$$

where: B - the working width of the knife, in m;
h_a - supply space, in m;
L_t - the work required for cutting the plants on a surface unit, in Nm/m^2.

The force of inertia F_t, [N] that appears due to the alternative translational motion of the knife is calculated with formula (2):

$$F_t = ma \quad (2)$$

where: m- knife mass, in kg;
a – knife acceleration, in m/s^2.
The acceleration a has the maximum value in the dead points, respectively, the maximum value of the force of inertia, F_i, [N] will be:

$$F_{i_{max}} = m\omega^2\gamma \quad (3)$$

At the half stroke, the acceleration is zero; at this point, the force of inertia is also zero.
The friction force F_f, [N], that appears between the knife and the fixed parts of the machine is calculated with formula (4):

$$F_f = \mu G = \mu B g_0 \quad (4)$$

where: μ–the coefficient of friction between the fixed parts of the machine;
G – knife weight, in N;
B – the working width of the knife, in m;
g_0 – linear weight of the knife; g_0 = 20 – 25N/m.
The power P_{at} required to operate the knife of the cutting machine can be determined approximately by the formula (5) [8]:

$$P_{at} = BP_0 \quad (5)$$

where: P_0– specific power, in kw/m;

Following the specific adjustments of the culture, variety and stage of development, the Equipment for harvesting green hemp stalks ERCV-0 performs the fractional cutting of the stalks as follows:
- rendering uniform the length of the stalks by removing the inflorescence with the upper cutting machine (fig. 1 pos. 3);
- effective cutting of the useful stalks with the lower cutting machine (fig. 1, pos. 2) and leaving them organized on the ground for a period necessary to change colour.

4. Conclusions

Knowing the importance of each characteristic of hemp stalks allows estimating, to a large extent, according to the external appearance of the stalks, their mode of behaviour in the technological process of primary processing, as well as after the probable results of the processing, both quantitatively and qualitatively.
The Equipment for harvesting green hemp stalksERCV-0 is hydraulically operated trailed equipment and is intended for the fractional harvesting of green hemp stalks on small and medium-sized farms, for their further processing.
The main advantages of *ERCV-0 are:*
- low cost exploitation, being recommended for industrial hemp crops on small surfaces;
- simple construction and easy to maintain;

- during operation, the cutting height of the knives can be controlled from the tractor cabin according to the size of the harvested hemp crop;
- during transport the two knives can be folded.

Acknowledgments

This research work was supported by:
- A grant of the Romanian Research and Innovation Ministry, PN 19 10 01 03-Substantion of the technology for harvesting and primary processing green hemp stalks, contract no. 5N/07.02.201;
- A grant of the Romanian Research and Innovation Ministry, through Programme 1 – Development of the national research-development system, subprogramme 1.2 – Institutional performance – Projects for financing excellence in RDI, contract no. 16PFE.

References

[1] Carus, M., S. Karst, and A. Kauffmann. *The European Hemp Industry: Cultivation, Processing and Applications for Fibres, Shives and Seeds.* Cologne: EIHA, pp. 1–9, 2013.
[2] Amaducci, S., A. Zatta, F. Pelatti, and G. Venturi. "Influence of agronomic factors on yield and quality of hemp (Cannabis sativa L.) fibre and implication for an innovative production system." *Field Crops Res.* 107 (2008): 161–169.
[3] Struik, P.C., X. Yin, C. Thouminot, M. Bjelková, V. Stramkale, et al. "Comparing hemp (Cannabis sativa L.) cultivars for dual-purpose production under contrasting environments." *Ind. Crops Prod.* 87 (2016): 33–44.
[4] Ranalli, P., and G. Venturi. "Hemp as a raw material for industrial applications." *Euphytica* 140 (2004): 1–6.
[5] Sheychenko, V., I. Marynchenko, I. Dudnikov, and M. Korchak. "Development of technology for the hemp stalks preparation." *Independent journal of management & production* (2019): 687-701.
[6] Salentijn, E.M.J., J. Petit, and L.M. Trindade. "The Complex Interactions between Flowering Behaviour and Fibre Quality in hemp." *Frontiers in plant science* 10 (2019): 613.
[7] Păun, Anişoara, Gabriel Bogdanof, Ioan Ganea-Christu, Radu Ciupercă, and Mihai Matache. Patent application no. A-00426/04.07.2019 *Equipment for harvesting green hemp / Echipament de recoltat cânepă verde*. OSIM, Romania, 2019.
[8] Neculăiasa, V., and I. Dănilă. *Working processes and agricultural machines for harvesting/Procese de lucru şi maşini agricole de recoltat*. A92 Publishing House, Iaşi, 1995.

ISSN 1454 - 8003
Proceedings of 2019 International Conference on Hydraulics and Pneumatics - HERVEX
November 13-15, Băile Govora, Romania

CONSIDERATIONS REGARDING THE USE OF WATER JET MACHINES IN ORDER TO REALIZE THE EXPERIMENTAL MODELS IN AGRICULTURE

Dragoş DUMITRU[1], Iuliana GĂGEANU[1], Iulian VOICEA[1], Remus OPRESCU[1], Dan CUJBESCU[1], Cătălin PERSU[1], Gabriel GHEORGHE[1]

[1] National Institute for Research-Development of Machines and Installations Designed for Agriculture and Food Industry INMA Bucharest, Romania, dumitrudragos.nicolae@gmail.com

Abstract: *This paper presents the importance of using water jet machines, the principle of operation of hydraulic drive systems in order to realize experimental models in the field of research, innovation and agriculture.*

Keywords: *Industry, water jet cutting, agriculture*

1. Introduction

In the last 25 years in the research and industry of cutting machines, modern solutions have been created to optimize experimental models for agriculture.
Cutting or cutting is the technological operation by which the total or partial detachment of a part of a material is intended, for the purpose of processing it. The classification of the cutting procedures is shown in Figure 1.
Mechanical cutting (cutting) is performed by mechanical means, such as: scissors, pliers, stamps, saws, machines - tools, abrasive stones, chisels. It is particularly applicable in locksmith operations. The choice of the cutting process is made according to the precision imposed on the cut pieces, the hardness of the material, its quality and the energy consumption of the process. It can be done with or without loss of material. For the individual production, a process with low productivity can be adopted, but which requires a cheaper machine. For mass or mass production, highly competitive processes are chosen, compensating for the higher cost of the equipment or installation which is higher.
The cutting operation must ensure:
- small roughness of the separate surfaces;
- high accuracy of the volume or length of the piece;
- lack of deviations from the geometric shape of the piece;
- realization of semi-finished products larger than the cross-section;
- preservation of material characteristics in the separation zone.

According to the nature of the cutting, they are distinguished:
- cutting (cutting the ends of the bars);
- actual cutting (cutting the blank into several pieces);
- splitting (cutting, total or partial, in length, from the outside to the inside);
- excision (cutting to remove a portion from inside a semi-finished product).

In general, cutting is a preparatory work for other cutting, plastic deformation operations. For this reason, the control of the cut semi-finished products is executed from a dimensional point of view. The tools used are meter, slide rule, graded ruler, report and template. Another objective in control is the quality of the processed surfaces. In order to determine whether or not the processed surfaces have marked differences, the verification rule is used. The receipts that are recorded at the cut can be caused by the failure to comply precisely with the prescribed dimensions or process parameters (speed, temperature, electrical parameters). If the cut has been made after the drawing, the rejection may be due to the wrong drawing or the operator's inattention.

2. Material and methods

High pressure water jet cutting was first used by Dr. Norman Franz in the 1950s. He was a forest engineer who was looking for an easier way to cut wood, his experiments helped make this technology work. develop into what it is today.
Two decades later, Dr. Mohamed Hashish discovered a way to add abrasive material to the water jet. Using this a high-pressure water jet cutting machine can cut any type of material.
The high-pressure water jet cutting process is based on the erosive effect of the water on the materials, amplified effect due to the extremely high pressures and speeds with which the water jet acts on small surfaces.
It uses the kinetic energy of water particles, designed at very high speed on the surface of the cutting material. The speed is of the order of 800 - 1000 m / s depending on the working pressure, the section of the jet, the presence or absence of the abrasive.
The equipment required to obtain this jet includes: a hydraulic unit, a pressure multiplier, a battery, a workstation supply circuit and a cutting tube.
The functional principle of a water jet cutting plant is realized by the fact that high pressure water starts from the pump and is first driven to a pressure multiplier and then to the working head for pressure water jet cutting. high.
For the case of processing involving the use of abrasive particles here the system of supplying the abrasive material introduces a liquid under pressure the abrasive material necessary for the process of cutting with water jet with abrasive particles.
After the water jet comes out of the nozzle the energy is dissipated in the liquid collection tank which is usually filled with water and debris from previous cuts.
The movement of the cutting head takes place, usually in the X-Y plane. Motion control is performed using numerically controlled equipment that follows the profile of a CAD model.
The machines can also be equipped with some auxiliary systems such as: automatic cleaning tank, water recycling system, specially inclined ends, Z axis monitoring system, etc.
Ideally, you want a precise cutting in the shortest time and at the least cost. The cutting speed depends on the material to be processed, the geometry of the model, the software and the controller of the movement system, the power and efficiency of the pressure pump and other factors such as the abrasive material used.
The water used is network water, which passes through several filter floors (2 or 3), the last one by a micron, in some cases it has to be softened. To be brought under very high pressure, the water is considered to have the following maximum values:

- Dissolved materials: 500 mg/l
- Hardness (CACO3): 25 mg/l
- Fe: 2 mg/l
- Mn: 1 mg/l
- Chloride (In Cl): 100 mg/l
- Silica (in Si): 15mg/l
- Clor biber: 1 mg/l
- Turbidity: 5 mg/l
- Acidity

3. Results

The hydraulic environment, the engine agent or the working fluid are names commonly assigned to the fluid used in hydraulic drive systems. This fluid is subjected, during the operation of the system, to very difficult working conditions for transmitting movement and effort, such as: variation in a wide range of working temperature, pressure and speeds, conditions in which it must maintain its physical properties. chemical and mechanical for a given period.

The heavy working conditions exposed raise particularly severe restrictions and require a rigorous selection of the fluid categories that correspond to most of the requirements imposed on them. Among the most important requirements that are imposed and based on which these working liquids are chosen, the following are mentioned:
- good lubricating properties and high mechanical strength of the liquid film;
- high resistance and chemical and thermal stability to prevent its oxidation, decomposition and degradation;
- minimum variation of viscosity with temperature;
- not to release vapors at normal operating temperatures and to not contain impurities that facilitate vapor release;
- not to contain, absorb or release air over the quantity allowed by the technical prescriptions;
- not to cause corrosion and deterioration of the sealing elements;
- have a high flash point and low freezing rate;
- minimum content of mechanical and technical impurities.

Mineral oils are the liquids that best meet these requirements and have a wide spread. In addition, a series of synthetic liquids are used as well as other environments, under special operating conditions.

A model of a water jet machine is presented (Figure 2) in order to obtain experimental models and the advantages of using it are presented.

The main features and advantages of a water jet cutting machine (Figure 3) are the following:
- complex abrasive cutting system with 3 or 5 axis water jet, high pressure intensifier (60,000 psi), software and a wide range of options, specially designed to optimize
- the process of cutting metal and non-metal materials, such as: stainless steel, aluminium, copper, bronze, titanium, composite material, as well as other materials such as glass, stone, granite, plastics;
- makes it possible to cut into thick materials, regardless of the type of material;
- the cutting speed management allows the song to be realized to the highest quality standards
- PLC monitoring system for monitoring the entire activity of the pump with pressure sensors, temperature monitoring and consumables life (Figure 4);
- Sand storage tank with pneumatic anti-reflux valve and low pressure required for sand pumping;
- automatic greasing of the treads and self-cleaning bearings;
- system for collecting abrasive matter and draining water from the tank;

water filtration system and water deionization system;

Figure 5 shows a graph that shows the cutting thickness of a CNC water jet cutting machine, respectively in Figure 6 the cutting speed compared to other cutting machines such as laser and oxygen.

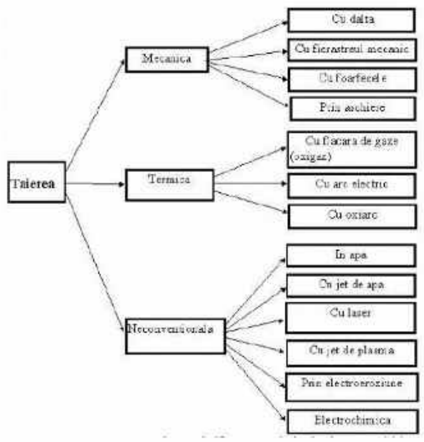

Fig. 1. Classification of cutting procedures

Fig. 2. CNC model with water jet

Fig. 3. CNC machining cutting with water jet

Fig. 4. PLC monitoring system

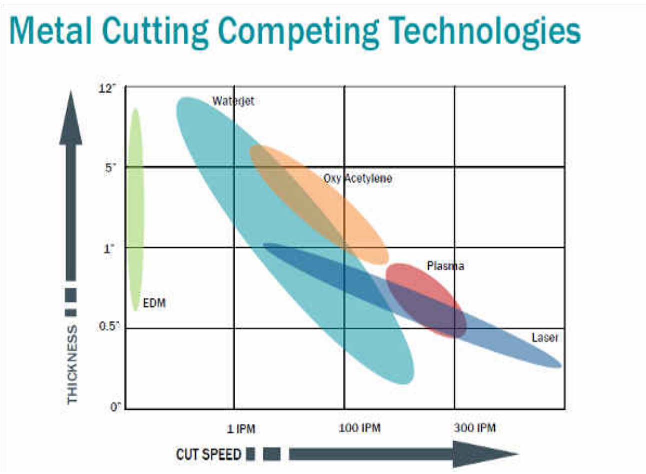

Fig. 5. Cutting thickness

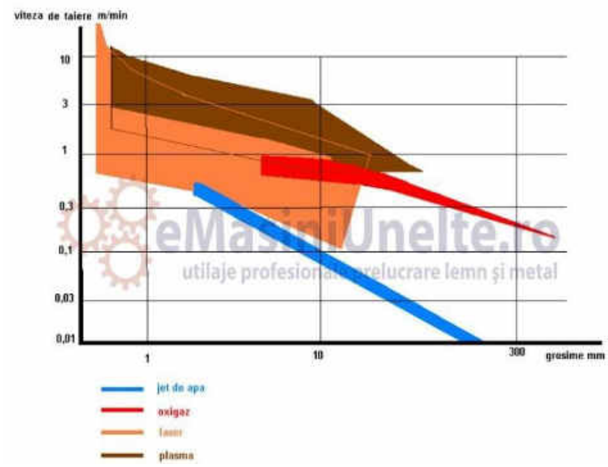

Fig. 6. Cutting speed

Conclusions

In conclusion, water jet cutting machines are an advantage for their use in the field of research because they offer great flexibility, do not generate toxic gases, UV radiation or other harmful substances for the operator, do not thermally influence the material, thus no slag is generated.
The texture / quality of the surface of the material is no longer a critical factor in the cutting process and the quality of the surfaces obtained from the cutting is very high and therefore no further processing is required.

Acknowledgments

This work was supported by a grant of the Romanian Research and Innovation Ministry, through Programme 1 – Development of the national research-development system, sub-programme 1.2 – Institutional performance – Projects for financing excellence in RDI, contract no. 16PFE."

References

[1] Momber, A.W., and R. Kovacevic. *Principles of abrasive water jet machining*. Berlin, Springer, 1998.
[2] Borkowski, J., and P. Borkowski. *High-pressure hydro-jet technologies/Wysokociśnieniowe technologie hydrostrumieniowe*. Koszalin, Wydawnictwo Uczelniane Politechniki Koszalińskiej, 2008.
[3] Akkurt, A. "Surface properties of the cut face obtained by different cutting methods from AISI 304 stainless steel materials." *Indian Journal of Engineering & Materials Sciences* 16 (December 2009): 373-384.
[4] Borkowski, J., and M. Sutowska. "The quality of surface cut after high-pressure abrasive-water cutting.“ *Journal of Machine Engineering* 7, no. 3 (2007): 19-28.
[5] Birtu, C., and V. Avramescu. "Abrasive water jet cutting - technique, equipment, performances." *Nonconventional Technologies Review* 16, no. 1 (March 2012): 40-46.
[6] Chen, L., E. Siores, and W.C.K. Wong. "Optimising abrasive waterjet cutting of ceramic materials.“ *Journal of Materials Processing Technology* 74, no. 1-3 (1998): 251-254.
[7] Chithirai, Pon Selvan M., and N. Mohanna Sundaru Raju "Abrasive Waterjet Cutting Surfaces of Ceramics – An Experimental Investigation." *International Journal of Applied Science, Technology and Engineering Research* 1, no. 3 (June 2012): 52-59.
[8] Miranda, R.M., and L. Quintino. "Microstructural study of material removal mechanisms observed in abrasive waterjet cutting of calcareous stones.“ *Materials Characterization* 54, no. 4 (2005): 370-377.
[9] Wang, J., and W.C.K. Wong. "A study of abrasive waterjet cutting of metallic coated sheet steels." *International Journal of Machine Tools and Manufacture* 39, no. 6 (1999): 855-870.
[10] http://www.kmt-waterjet.com. "Cutting metals with water jet”, 2013.

http://hervex.ro